HORIZONTAL GENE TRANSFER MEDIATED MULTIDRUG RESISTANCE: A GLOBAL CRISIS, 2nd Edition

EDITED BY: Dongchang Sun, Katy Jeannot, Yonghong Xiao and Charles W. Knapp

PUBLISHED IN: Frontiers in Microbiology

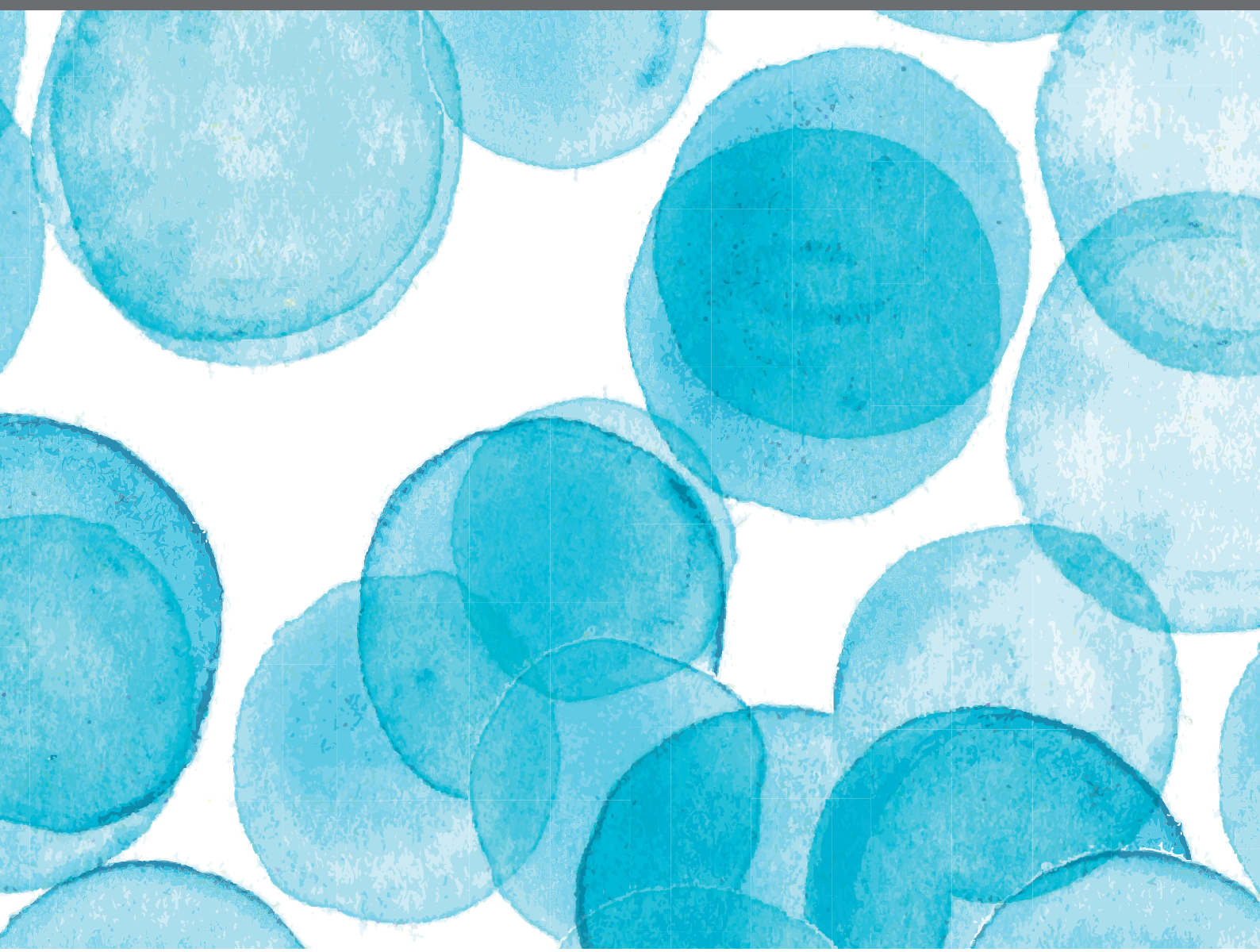

frontiers Research Topics

frontiers

ISSN 1664-8714
ISBN 978-2-88963-880-2
DOI 10.3389/978-2-88963-880-2

About Frontiers

Frontiers is more than just an open-access publisher of scholarly articles: it is a pioneering approach to the world of academia, radically improving the way scholarly research is managed. The grand vision of Frontiers is a world where all people have an equal opportunity to seek, share and generate knowledge. Frontiers provides immediate and permanent online open access to all its publications, but this alone is not enough to realize our grand goals.

Frontiers Journal Series

The Frontiers Journal Series is a multi-tier and interdisciplinary set of open-access, online journals, promising a paradigm shift from the current review, selection and dissemination processes in academic publishing. All Frontiers journals are driven by researchers for researchers; therefore, they constitute a service to the scholarly community. At the same time, the Frontiers Journal Series operates on a revolutionary invention, the tiered publishing system, initially addressing specific communities of scholars, and gradually climbing up to broader public understanding, thus serving the interests of the lay society, too.

Dedication to Quality

Each Frontiers article is a landmark of the highest quality, thanks to genuinely collaborative interactions between authors and review editors, who include some of the world's best academicians. Research must be certified by peers before entering a stream of knowledge that may eventually reach the public - and shape society; therefore, Frontiers only applies the most rigorous and unbiased reviews.
Frontiers revolutionizes research publishing by freely delivering the most outstanding research, evaluated with no bias from both the academic and social point of view. By applying the most advanced information technologies, Frontiers is catapulting scholarly publishing into a new generation.

What are Frontiers Research Topics?

Frontiers Research Topics are very popular trademarks of the Frontiers Journals Series: they are collections of at least ten articles, all centered on a particular subject. With their unique mix of varied contributions from Original Research to Review Articles, Frontiers Research Topics unify the most influential researchers, the latest key findings and historical advances in a hot research area! Find out more on how to host your own Frontiers Research Topic or contribute to one as an author by contacting the Frontiers Editorial Office: researchtopics@frontiersin.org

HORIZONTAL GENE TRANSFER MEDIATED MULTIDRUG RESISTANCE: A GLOBAL CRISIS, 2nd Edition

Topic Editors:
Dongchang Sun, Zhejiang University of Technology, China
Katy Jeannot, Centre National de Référence de la Résistance aux Antibiotiques, France
Yonghong Xiao, Zhejiang University, China
Charles W. Knapp, University of Strathclyde, United Kingdom

Throughout history, human life has been seriously threatened by bacterial infectious diseases. After the discovery of antibiotics, humanity thought it had won the fight against infectious bacteria. However, considering the rapid evolution of bacterial multidrug resistance and exhausted pipeline of antibiotics for fighting bacterial infectious diseases, we are approaching the 'post-antibiotic' era. Unlike eukaryote, bacteria are proficient in exchanging their genetic materials with others by means of horizontal gene transfer (HGT). As a vehicle for antibiotic resistance gene (ARG), plasmid is self-replicable and transferable in a wide range of host bacteria. Moreover, ways of HGT-mediated ARGs spreading are highly diverse among different species, implicating complex evolution routes for the development of multidrug resistance in bacteria. In recent years, multidrug resistance plasmids have been widely found in bacteria not only from clinical patients, but also from animals, birds and plants, as well as from natural environmental settings including soil and water – heralding that the 'post-antibiotic' era is much closer than we previously thought.

The global crisis of multidrug resistance calls for a closer collaboration among people of different professions in different regions, countries and continents, which will help us recognize the current situation and eventually find effective and long-lasting solutions for fighting against infectious bacteria.

Publisher's note: In this 2nd edition, the following article has been updated: LaBreck PT, Rice GK, Paskey AC, Elassal EM, Cer RZ, Law NN, Schlett CD, Bennett JW, Millar EV, Ellis MW, Hamilton T, Bishop-Lilly KA and Merrell DS (2018) Conjugative Transfer of a Novel Staphylococcal Plasmid Encoding the Biocide Resistance Gene, *qacA*. *Front*. *Microbiol*. 9:2664. doi: 10.3389/fmicb.2018.02664

Citation: Sun, D., Jeannot, K., Xiao, Y., Knapp, C. W., eds. (2020). Horizontal Gene Transfer Mediated Multidrug Resistance: A Global Crisis, 2nd Edition. Lausanne: Frontiers Media SA. doi: 10.3389/978-2-88963-880-2

Table of Contents

frontiers in Microbiology

EDITORIAL
published: 27 August 2019
doi: 10.3389/fmicb.2019.01933

Editorial: Horizontal Gene Transfer Mediated Bacterial Antibiotic Resistance

Dongchang Sun[1], Katy Jeannot[2]*, Yonghong Xiao[3]* and Charles W. Knapp[4]**

[1] College of Biotechnology and Bioengineering, Zhejiang University of Technology, Hangzhou, China, [2] Laboratoire de Bactériologie, Centre National de Référence (CNR) de la Résistance aux Antibiotiques, Centre Hospitalier Universitaire (CHRU) de Besançon, Besançon, France, [3] State Key Laboratory for Diagnosis & Treatment of Infectious Diseases, The First Affiliated Hospital, School of Medicine, Zhejiang University, Hangzhou, China, [4] Department of Civil and Environmental Engineering, Centre for Water, Environment, Sustainability, and Public Health, University of Strathclyde, Glasgow, United Kingdom

Keywords: horizontal gene transfer, antibiotic resistance gene, multidrug resistance, plasmid, transformation, conjugation, transposition

OPEN ACCESS

Edited by:
Peter Mullany, University College London, United Kingdom

Reviewed by:
Christopher Morton Thomas, University of Birmingham, United Kingdom

****Correspondence:***
Dongchang Sun
sundch@zjut.edu.cn
Katy Jeannot
katy.jeannot@univ-fcomte.fr
Yonghong Xiao
xiaoyonghong@zju.edu.cn
Charles W. Knapp
charles.knapp@strath.ac.uk

Specialty section:
This article was submitted to Antimicrobials, Resistance and Chemotherapy, a section of the journal Frontiers in Microbiology

Received: *14 June 2019*
Accepted: *06 August 2019*
Published: *27 August 2019*

Citation:
Sun D, Jeannot K, Xiao Y and Knapp CW (2019) Editorial: Horizontal Gene Transfer Mediated Bacterial Antibiotic Resistance. Front. Microbiol. 10:1933. doi: 10.3389/fmicb.2019.01933

Editorial on the Research Topic

Horizontal Gene Transfer Mediated Bacterial Antibiotic Resistance

Bacterial antibiotic resistance, especially multidrug resistance (MDR), has become a global challenge, threatening human and animal health, food, and environment safety. The number of human deaths accounted for by MDR was estimated to increase to 10 million by 2050, exceeding the number of deaths arising from cancer (WHO, 2014). Although a bacterium is able to establish antibiotic resistance through spontaneous mutation (Salverda et al., 2017), development of MDR in the bacterium would take a long time if it only relies on self-adaptive mutation. Horizontal gene transfer (HGT) allows bacteria to exchange their genetic materials (including antibiotic resistance genes, ARGs) among diverse species (Le Roux and Blokesch, 2018), greatly fostering collaboration among bacterial population in MDR development. Recent studies reveal emergence of "superbugs" that carry a number of HGT-transferred ARGs on plasmids and tolerate almost all antibiotics (Mathers et al., 2015; Wang and Sun, 2015; Malhotra-Kumar et al., 2016). These MDR plasmids are able to be further transferred to different bacterial species, creating new "superbugs" that grow in different environments. Global emergence of "superbugs" carrying MDR plasmids (e.g., NDM-1 and MCR-1) in various environmental niches (e.g., patients, animals, and soil) indicates rapid propagation of MDR among bacterial populations. Although HGT and MDR were found to be tightly linked in "superbugs," as revealed by surveillance studies, our knowledge about how and to what extent HGT propels development of MDR under different environmental conditions remain inadequate. The 22 publications collected in the topic "Horizontal Gene Transfer Mediated Bacterial Antibiotic Resistance" show new discoveries and recent advances concerning this issue in a wide range of fields, providing a basis for collaboratively controlling MDR in the future.

ARGs have been identified in not only human (Fang et al.; LaBreck et al.; Zeng et al.) and animals, including macaques (Mannion et al.), mealworms (Osimani et al.), ducks (Sun et al.), pigs (Chi et al.), and companion animals (Wang et al.), but also plants (Chi et al.). These ARGs include *bla* variants that encode β-lactamases for degrading the newest generation of β-lactam antibiotics (Huang et al.; Chi et al.; Zeng et al.), and *mcr*-1 that confers resistance to colistin, the last line of defense (Wang et al.). Plasmids play an important role as vehicles in transferring multiple ARGs from one MDR bacterial host to another simultaneously. Reports in

this collection revealed that ARGs were often identified in plasmids from MDR bacteria living in different niches (Barrón et al.; Fang et al.; Huang et al.; LaBreck et al.; Chi et al; Mannion et al.; Sun et al.; Wang et al.; Zeng et al.). To understand how plasmids have evolved, Liang et al. and Zhang et al. reported the diversification and evolution history of a certain type of plasmid (IncHI5). One study reports an example of direct fusion of two plasmids through illegitimate recombination in the host, which produced a new plasmid with ARGs derived from the two ancestor plasmids (Chi et al.). Plasmids are generally considered to be transferred through either conjugation that requires a type IV secretion system for pushing DNA from a donor cell to a recipient cell, or natural transformation that requires a DNA uptake system for pulling DNA into a recipient cell (Sun). In this topic, two reviews revealed new ways of plasmid transfer that do not use canonical DNA pulling or pushing machineries (Hasegawa et al.; Sun), highlighting diversity of HGT mechanisms in nature. Of note, both the traditional and non-traditional natural transformation mediated plasmid transfer are physiologically controlled, although different DNA uptake machineries and competence regulation circuits are employed (Sun). Moreover, in both kinds of HGT, DNA uptake is triggered by environmental stresses, which induce expression of transcriptional regulators for activating expression of DNA uptake genes (Sun). ARGs were also found in other mobile genetic elements on bacterial chromosomes (Fang et al.; Chi et al.), especially in the integrative and conjugative elements (ICEs, also known as conjugative transposons; Fang et al.).

Transposons (Tn) and Insertion Sequences (IS) are mobile genetic elements in plasmids and chromosomes. They were frequently identified in clinical settings (Sun et al.; van der Zee et al.). In this collection, transposition-mediated transfer of carbapenem and carbapenicillin resistance genes and colistin resistance gene *mcr*-1 was documented (He et al.; van der Zee et al.). A novel mobile transposon Tn6242, which contains ARGs and is flanked by IS26, was characterized in multidrug-resistant uropathogenic *Escherichia coli* ST405 (Chowdhury et al.). Besides moving ARGs, transposons can exacerbate antibiotic resistance on a different layer. By inserting into the promoter region, a transposon activates transcription of genes associated with conjugation and significantly improved conjugation frequency (Poidevin et al.). Another study revealed that insertion of the ISCR1 (Insertion Sequence Common Region) element improved expression of downstream ARGs, providing an explanation for the frequent presence of ISCR1 in the clinical setting (Lallement et al.).

ARGs were found not only in bacteria parasitizing in higher organisms, but also in basic components of our planet earth, such as soil (Chi et al.) and water (Barrón et al.; Fang et al.; Chi et al.). Although transfer of the ARG vehicle (plasmids) has been intensively investigated under laboratory conditions, it remains unclear how plasmid disseminated in our natural environment. By monitoring the dynamic of plasmid transfer in natural soil, researchers investigated transmission of a broad host range plasmid RP4 marked by *gfp* in a natural setting (Fan et al.). Their work showed that RP4 is likely to be transferred into soil bacteria of 15 phyla within 75-day (Fan et al.), providing a foundation for estimating the impact of plasmid-mediated transfer of ARGs in the soil ecosystem. To know the distribution of ARGs in the aquatic ecosystem, another study quantified the abundance of IncP-1 plasmids in samples from Orne River (Barrón et al.). Their work concluded that plasmid-mediated adhesion to particles is one of the main contributors in the formation of MGE-reservoirs in sediments, which contributes to selective enrichment process of ARGs (Barrón et al.). These studies reveal that the impact of ARG transfer to the ecosystem could be more profound than previously thought. Exploring mechanisms of plasmid-mediated ARG spread in soil and water would be crucial for controlling antibiotic resistance in the ecosystem.

In summary, articles presented in this Research Topic demonstrate benefits of using multidisciplinary approaches to deepen our knowledge about HGT-mediated bacterial MDR. These articles analyzed the formation of bacterial MDR as a result of HGT under different settings, highlighting the importance of collaboration among different fields in fighting against MDR. We thank all participating authors for their contributions and reviewers for their constructive comments, which will be the foundation for future surveillance, investigations into mechanisms and controlling strategies of HGT-mediated MDR.

AUTHOR CONTRIBUTIONS

All authors listed have made a substantial, direct and intellectual contribution to the work, and approved it for publication.

FUNDING

This work was supported by the National Natural Science Foundation of China (Grant No. 31670084, 31100071) and the Zhejiang Provincial Natural Science Foundation of China (Grant No. LY16C010003, Y3110237) awarded to DS.

ACKNOWLEDGMENTS

We would like to acknowledge Prof. Yunfeng Yan for critical reading of the manuscript.

REFERENCES

Le Roux, F., and Blokesch, M. (2018). Eco-evolutionary dynamics linked to horizontal gene transfer in Vibrios. *Annu. Rev. Microbiol.* 72, 89–110. doi: 10.1146/annurev-micro-090817-062148

Malhotra-Kumar, S., Xavier, B. B., Das, A. J., Lammens, C., Butaye, P., and Goossens, H. (2016). Colistin resistance gene mcr-1 harboured on a multidrug resistant plasmid. *Lancet Infect. Dis.* 16, 283–284. doi: 10.1016/S1473-3099(16)00012-8

Mathers, A. J., Peirano, G., and Pitout, J. D. (2015). The role of epidemic resistance plasmids and international high-risk clones in the spread of multidrug-resistant Enterobacteriaceae. *Clin. Microbiol. Rev.* 28, 565–591. doi: 10.1128/CMR.00116-14

Salverda, M. L. M., Koomen, J., Koopmanschap, B., Zwart, M. P., and De Visser, J. (2017). Adaptive benefits from small mutation supplies in an antibiotic resistance enzyme. *Proc. Natl. Acad. Sci. U.S.A.* 114, 12773–12778. doi: 10.1073/pnas.1712999114

Wang, B., and Sun, D. (2015). Detection of NDM-1 carbapenemase-producing *Acinetobacter calcoaceticus* and *Acinetobacter junii* in environmental samples from livestock farms. *J. Antimicrob. Chemother.* 70, 611–613. doi: 10.1093/jac/dku405

WHO (2014). *Antimicrobial Resistance Global Report on Surveillance*. World Health Organization. Available online at: https://www.who.int/antimicrobial-resistance/publications/en/

Conflict of Interest Statement: The authors declare that the research was conducted in the absence of any commercial or financial relationships that could be construed as a potential conflict of interest.

frontiers in Microbiology

ORIGINAL RESEARCH
published: 02 February 2018
doi: 10.3389/fmicb.2018.00130

Mutation in ESBL Plasmid from *Escherichia coli* O104:H4 Leads Autoagglutination and Enhanced Plasmid Dissemination

*Mickaël Poidevin[1], Mari Sato[2], Ipek Altinoglu[1,3], Manon Delaplace[1,4], Chikara Sato[2] and Yoshiharu Yamaichi[1]**

[1] Institute for Integrative Biology of the Cell, Université Paris-Saclay, CEA, CNRS, Université Paris-Sud, Gif-sur-Yvette, France, [2] Biomedical Research Institute, National Institute of Advanced Industrial Science and Technology, Tsukuba, Japan, [3] Graduate School of Structure and Dynamics of Living Systems, Université Paris-Sud, Orsay, France, [4] Master of Science and Technology, University Pierre and Marie Curie, Paris, France

Conjugative plasmids are one of the main driving force of wide-spreading of multidrug resistance (MDR) bacteria. They are self-transmittable via conjugation as carrying the required set of genes and *cis*-acting DNA locus for direct cell-to-cell transfer. IncI incompatibility plasmids are nowadays often associated with extended-spectrum beta-lactamases producing Enterobacteria in clinic and environment. pESBL-EA11 was isolated from *Escherichia coli* O104:H4 outbreak strain in Germany in 2011. During the previous study identifying transfer genes of pESBL-EA11, it was shown that transposon insertion at certain DNA region of the plasmid, referred to as Hft, resulted in great enhancement of transfer ability. This suggested that genetic modifications can enhance dissemination of MDR plasmids. Such 'superspreader' mutations have attracted little attention so far despite their high potential to worsen MDR spreading. Present study aimed to gain our understanding on regulatory elements that involved pESBL transfer. While previous studies of IncI plasmids indicated that immediate downstream gene of Hft, *traA,* is not essential for conjugative transfer, here we showed that overexpression of TraA in host cell elevated transfer rate of pESBL-EA11. Transposon insertion or certain nucleotide substitutions in Hft led strong TraA overexpression which resulted in activation of essential regulator TraB and likely overexpression of conjugative pili. Atmospheric Scanning Electron Microscopy observation suggested that IncI pili are distinct from other types of conjugative pili (such as long filamentous F-type pili) and rather expressed throughout the cell surface. High transfer efficiency in the mutant pESBL-EA11 was involved with hyperpiliation which facilitates cell-to-cell adhesion, including autoagglutination. The capability of plasmids to evolve to highly transmissible mutant is alarming, particularly it might also have adverse effect on host pathogenicity.

Keywords: horizontal gene transfer, multidrug resistant, ESBL, conjugation, atmospheric scanning electron microscopy

OPEN ACCESS

Edited by:
Dongchang Sun,
Zhejiang University of Technology, China

Reviewed by:
Yeshi Yin,
Hunan University of Science and Engineering, China
Xiangdong Chen,
Wuhan University, China

***Correspondence:**
Yoshiharu Yamaichi
yoshiharu.yamaichi@i2bc.paris-saclay.fr

Specialty section:
This article was submitted to Antimicrobials, Resistance and Chemotherapy, a section of the journal Frontiers in Microbiology

Received: *05 October 2017*
Accepted: *18 January 2018*
Published: *02 February 2018*

Citation:
Poidevin M, Sato M, Altinoglu I, Delaplace M, Sato C and Yamaichi Y (2018) Mutation in ESBL Plasmid from Escherichia coli O104:H4 Leads Autoagglutination and Enhanced Plasmid Dissemination. Front. Microbiol. 9:130. doi: 10.3389/fmicb.2018.00130

Abbreviations: ASEM, atmospheric scanning electron microscopy; ESBL, extended-spectrum β-lactamase; FE-SEM, field emission scanning electron microscopy; Hft, high frequency transfer; LB, lysogeny broth; M.U., Miller unit; MDR, multidrug resistance; MFP, mating pair formation; SEM, scanning electron microscopy; T4SS, type IV secretion system; WT, wild type.

INTRODUCTION

Worldwide dissemination of antibiotic resistance (and in many cases, MDR) is one of the most important issues in public health. MDR is often associated with (re-)emerging infectious diseases and epidemics, and in many cases, the determinants for the MDR are encoded on the conjugative plasmid which is capable of its cell-to-cell transmission via conjugation. In the devastated outbreak of enterohemorrhagic/enteroaggregative *Escherichia coli* O104 in Germany (and other European countries) in 2011, the causative strain harbored a plasmid encoding two ESBL genes, pESBL-EA11 (hereafter referred to as pESBL) (Frank et al., 2011; Rasko et al., 2011; Rohde et al., 2011).

pESBL belongs to IncI incompatibility group of plasmid and encodes sufficient set of genes and *cis*-elements for its conjugational transfer, hence it can be transmitted between enterobacteria such as *E. coli* and *Klebsiella pneumoniae* (Yamaichi et al., 2015). Despite the diversity of conjugative plasmids found in natural or clinical environments, fundamental steps of conjugational transfer are conserved among different plasmids. Conjugative (sex) pili exported by MPF systems, also known as T4SS, is required for cell-to-cell contact which eventually fuse membranes or allow DNA transfer through the pili, whereas DNA processing (MOB) systems create a nick at origin of transfer (*oriT*) and subsequently strip a single-stranded DNA for the entire plasmid (Smillie et al., 2010). Essentially, MPF/T4SS and MOB systems can be classified into only a few systems (four and six, respectively), and IncI conjugative plasmids consist MPF_I type of MPF/T4SS system (Smillie et al., 2010). In classic prototype of IncI plasmids, R64, transfer genes were identified by brute force approach including knocking out of each gene (Komano et al., 2000 and references therein). By contrast, transfer genes of pESBL have been recently addressed by genome-wide approach, transposon insertion site sequencing (Tnseq) (Yamaichi et al., 2015). Nevertheless, list of transfer genes of these two plasmids are parallel and consists of 4 clusters: *oriT* and *nikAB* genes corresponding to MOB system, *tra/trb* gene cluster for conjugation in general corresponding to MPF/T4SS system, *pil* gene cluster for synthesis of pili, and *traABCD* regulatory gene cluster (of which *traBC* are essential for conjugation, and *traD* is not present in pESBL) (Sampei et al., 2010; Yamaichi et al., 2015). For clarity, genes with same name but in different MPF/T4SS systems do not necessary mean they are homologous (for example, TraA from F plasmid encodes prepropilin and has no similarity to TraA from pESBL).

Remarkably, Tnseq revealed that the short DNA region (dubbed as Hft for high frequency transfer) upstream of *traABC* regulates transfer efficiency of pESBL (**Figure 1A**). Transposon insertion in the region resulted in highly (>10-fold) elevated transfer efficiency (Yamaichi et al., 2015), which is alarming as a simple transposition event can dramatically increase the transmission of already highly transmittable conjugative plasmids. Such 'superspreader' mutants could evolve any time in various ways. For instance, widespread plasmid pOXA-48a has a transposon inserted in the *tir* gene, and the disruption of Tir results in elevated transfer efficiency by unknown mechanism (Poirel et al., 2012; Potron et al., 2014). *stbA* mutation in broad-host-range R388 increased transfer efficiency of the plasmid by 50-fold, although exhibiting instability in the host cell in exchange (Guynet et al., 2011). In fact, mutants of resistance plasmids with increased transfer rates have already been described and isolated several decades ago (Meynell and Datta, 1967). As ability of transfer is considered to be repressed by regulatory genes in normal state, these mutants were called 'derepressed' and have been widely used in research. *E. coli* fertility factor (F plasmid) which presents high transfer efficiency can be also considered as 'derepressed', since it has authentic mutation in *finO* repressor (Frost et al., 1994). As derepressed plasmids exhibit elevated transfer efficiency, they often express more pili (Meynell et al., 1968; Bradley, 1980a), and presumably in a consequence of cell-to-cell adhesion, promote development of biofilm (Ghigo, 2001).

Due to their characteristics, visualization of pili is not easy and has mainly done with Electron Microscopy (EM) using derepressed plasmid but pili were detached from cells followed by enrichment *in vitro*. Antibodies or bacteriophages targets particular conjugative pili were also used for specific labeling. Initial morphological and serological observations by EM in early 80's classified conjugative pili in 3 classes: thin flexible, thick flexible and rigid (Bradley, 1980a,b, 1983, 1984). Since then, researches have mainly focused on F-type pili (represented by F plasmid) which is flexible and can be extended up to 20 μm (Meynell et al., 1968). IncI plasmids were reported to possess two different kinds of pili: thick and thin ones (Bradley, 1980b, 1983). In R64, *pil* operon, which encodes proteins homologous to type IV pilus, was shown to be involved in liquid but not on solid-surface conjugation (Kim and Komano, 1997; Yoshida et al., 1999). While *pil* genes considered to encode 'thin' pilus in R64 (Kim and Komano, 1997; Yoshida et al., 1999), 5 *pil* genes in pESBL are classified as essential for conjugational transfer on solid surface (Yamaichi et al., 2015). Nonetheless, distinguishing the two kinds of pili attached to the host cell has not been successful. P-type conjugative pili (represented by RP4 and R388 plasmids, not confused by P-pili/fimbriae from uropathogenic *E. coli*) were expedited by MPF_T type of MPF/T4SS system (Lawley et al., 2003; Smillie et al., 2010). Bradley originally reported them to be shorter and more rigid (Bradley, 1980b), however, controversial morphology was also described from *Agrobacterium tumefaciens* Ti plasmid (Fullner et al., 1996).

Although EM provides sub-nanometer resolution, biological samples require unidealistic pretreatment such as dehydration and under vacuum. Recent innovation of ASEM, however, allows visualization of nanostructures in aqueous solution at atmospheric pressure. In bacteria, extracellular proteins such as pili and flagella, and biofilm matrices have been successfully observed by ASEM using immunogold labeling with specific antibody or rather non-specific labeling with positively and/or negatively charged Nanogold (Sato et al., 2012; Nishiyama et al., 2014; Sugimoto et al., 2016).

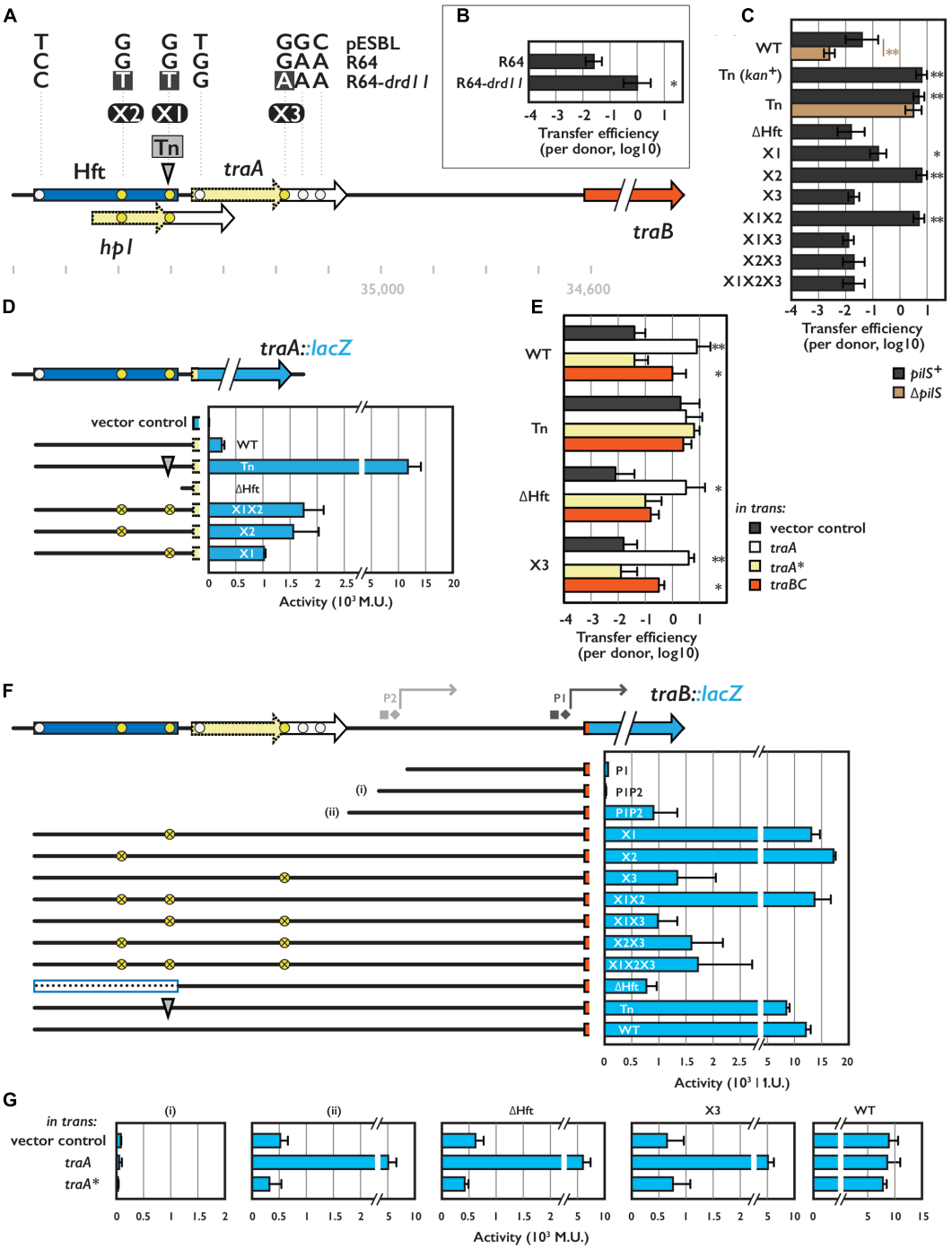

FIGURE 1 | Hft and its flanking region involved in transcriptional regulation for conjugative transfer. **(A)** Schematic representation of the Hft (shown in blue box) and flanking *tra* genes. Arrows with solid and broken line indicate coding sequences and its truncated variants, respectively. Transposon insertion site for the Tn mutant is shown by the gray arrowhead. Single nucleotide polymorphisms among pESBL, R64 and R64-*drd11* are also indicated (see text). Coordinates shown below are obtained from NC_018659.1. **(B)** Transfer efficiencies of R64 and R64-*drd11*. From **(B)** through **(G)**, the mean and standard deviations of at least three independent experiments are shown. **(C,E)** Transfer efficiencies of various pESBL variants. In **(E)**, donor cells harbor an extra plasmid for overexpression of indicated gene. **(D,F,G)** Reporter assay for TraA **(D)** and TraB **(F,G)** with indicated construct. β-galactosidase activities were shown in Miller Unit (M.U.). In **(G)**, cells harbor an extra plasmid for overexpression of indicated gene. In **(F)**, square and diamond indicate predicted –35 and –10 sequence, respectively. *Indicates $p < 0.05$ and ** indicates $p < 0.01$, respectively.

MATERIALS AND METHODS

Plasmids and Strains

Plasmids and strains used in this study were listed in Supplementary Tables S1, S2, respectively.

kan gene cassette from pESBL::Tn1 transposon insertion mutant (Yamaichi et al., 2015) was removed by *in vivo* expression of FRT recombinase using pCP20 (Datsenko and Wanner, 2000; Chiang and Rubin, 2002).

Δ*fliA* mutation was introduced by P1 transduction from JW1907 (KEIO collection, Baba et al., 2006), and the mutation was confirmed by antibiotic resistance and motility phenotype.

Gene deletions (Δ*oriT* and Δ*pilS*) and introduction of point mutation(s) in pESBL were carried out by conventional double-crossovers with pDM4-based plasmids as previously described (Milton et al., 1996; Yamaichi et al., 2015). To introduce point mutation(s) in the Hft region, Hft and its flanking regions were amplified and cloned into pDM4 vector, resulting in pEYY39. Nucleotide substitutions were subsequently introduced by QuickChange II XL site-directed mutagenesis kit (Agilent Tech, Santa Clara, CA, United States). In some cases, two allelic exchanges were performed to facilitate introducing and following validation of point mutation(s). Essentially, the Hft region was first replaced by a gene cassette containing *kan* and *rpsL*$^+$ which screened by resistance to Kanamycin, then second allelic exchange to introduce point mutation(s) were selected by resistance to Streptomycin. *kan-rpsL*$^+$ gene cassette, which was amplified with primers oYo417 and oYo421, was inserted in pEYY39 *in vivo* by λ Red recombination technique (Datsenko and Wanner, 2000). Gene replacements in pESBL were carried out by conventional double-crossovers as previously described (Yamaichi et al., 2015). For the second step of the two steps replacement strategy, β2163 (Demarre et al., 2005) was used for the donor instead of conventional SM10 λ *pir* so that exconjugants can be selected by growth on LB plate without diammonium phosphate. Inherited ability of conjugative transfer was used to move pESBL and its derivatives between different *E. coli* strains.

For the cloning of plasmids for β-galactosidase assay, DNA fragments were amplified from corresponding pESBL mutant and cloned into pCB192-YY (Yamaichi et al., 2011) linearized by *Eco*RI-*Hin*dIII, either by conventional restriction cloning or Gibson Assembly (Gibson et al., 2009).

Unless specified, clonings were done by Gibson Assembly. When necessary, nucleotide sequence was verified by Sanger sequencing (GATC biotech, Germany). oYo170 and oYo171 were used for sequencing of Hft and its flanking region of R64. Oligo nucleotides used in this study were listed in Supplementary Table S3.

Cell Growth

Otherwise specified, cells were grown in LB in liquid or on agar (1.5%) plate at 37°C. Supplements were used in following concentrations when appropriate; Ampicillin 100 μg/mL, Chloramphenicol 25 μg/mL, Kanamycin 25 μg/mL, Streptomycin 100 μg/mL, Tetracycline 10 μg/mL, Arabinose 0.1%, diammonium phosphate 300 μM.

To measure growth rate, overnight culture of cells were backdiluted in 50 mL of LB in 250-mL Erlenmeyer and grown at 37°C with orbital shaking at 180 rpm. OD 600 nm and colony forming units were measured every 30–60 min of incubation. Alternatively, a microplate reader (Tecan Infinite M200 Pro, Tecan Group, Switzerland) was used. In a conventional flat-bottom, 96-well cell culture plate, 150 μL of LB medium was aliquoted then the overnight culture was inoculated at 1:500 dilution. OD 600 nm was measured every 15 min during the 12-h growth at 37°C with orbital shaking (4 mm pitch). For each experiment, samples were prepared in triplicate.

To measure sedimentation, 25-mL overnight culture in a 100-mL Erlenmeyer was settled at room temperature and 100∼1000 μL of supernatant was carefully taken for the measurement of OD 600 nm every 1 h.

To measure mobility/chemotaxis, overnight culture was diluted 10 times then 1 μL was inoculated in LB motility plate containing 0.3% agar. After incubating at room temperature for overnight, X and Y diameters of the zone cells expanded were measured. For the reference, each test plate included parental *E. coli* strain without plasmid.

Susceptibility to β-lactam antibiotics were tested by ETEST (bioMérieux) with supplier's instruction.

Bacterial Conjugation and Transfer Efficiency

For the conventional surface mating, 100 and 10 μL of overnight cultures of recipient and donor cells, respectively, were washed once with LB to remove antibiotics then mixed and spun down in Eppendorf tube. Cells were then resuspended in 50 μL of LB and placed on a 0.45-μm HAWP filter (EMD Milipore, Billerica, MA, United States) on LB agar plate. After incubation at 37°C for 2 h, cells were recovered in 1 mL of LB in a 50-mL centrifuge tube then plated on LB agar plates containing relevant antibiotics with appropriate dilutions.

For 'snap conjugation' assay, overnight cultures of recipient and donor cells were backdiluted and grown for 2.5 h without antibiotic selection. No loss of pESBL or F plasmid was detected after the 2.5 h of growth. In an Eppendorf tube, 890 μL of LB, 100 μL of recipient cells and 10 μL of donor cells were added sequentially. The tube was immediately vortexed for 3 s followed by plating the cells on LB agar containing appropriate antibiotics.

Transfer efficiencies were $\log_{10}$ transformed then the average and standard deviations were calculated. Student's *t*-test (heteroscedastic test with two-tailed distribution) was performed in Microsoft Excel for significance analysis.

β-galactosidase Assay

Assays were performed as previously described (Miller, 1992). A microplate reader (Tecan) was used to measure OD 420, 550, and 600 nm.

Biofilm Assay

Cells were allowed to form biofilm in LB or M9 medium supplemented with glucose (0.2%) and casamino acid (0.1%), in a flat-bottom 96-well cell culture plate. After 24 h of incubation at 37°C without agitation, biofilms were stained by crystal violet (Sigma–Aldrich, St. Louis, MO, United States) followed by optical quantification (Tecan) as previously described (O'Toole, 2011). *Pseudomonas aeruginosa* strain (PA14) was used for the positive control and the standard. Each sample used 3–4 replicate wells and was examined by at least 3 independent experiments.

ASEM

Δ*fliA* mutants harboring WT or mutant pESBL were grown in LB medium without agitation then gently placed on poly-L-lysine (Sigma–Aldrich) coated ASEM dish with 8 SiN film windows (Memtily et al., 2015). After 10 min of incubation, cells were fixed by fixing solution (2.5% glutaraldehyde and 1% paraformaldehyde in 0.1 M phosphate buffer pH 7.4) for 15 min. Unattached cells were flushed by miliQ water then the dish was filled by phosphate-buffered saline for transport and storage. The bacterial cells were labeled and observed as described (Nishiyama et al., 2014; Sugimoto et al., 2016). In brief, for the charged Nanogold-labeling, bacteria on the ASEM dish were incubated with 6 μM positively charged 1.4 nm Nanogold solution (Nanoprobes, Yaphank, NY, United States) for 20 min at room temperature. After washing with double-distilled water, the size of the gold particles was increased by gold enhancement using GoldEnhance-EM (Nanoprobes) for 10 min at room temperature, followed by washing with double-distilled water. Bacterial cells immersed in 10 mg/mL ascorbic acid were imaged by ASEM at an acceleration voltage of 20 kV with × 20,000 magnification using backscattered electrons. The electron dose was 6 $e^{-}/Å^{2}$, which is 13% of the dose permitted in low-dose cryo-EM aiming at atomic-resolution single-particle reconstructions.

Intensity profile was measured with 'Plot Profile' function in ImageJ version 1.51k (Schneider et al., 2012). Fixed length (200 pixels) perpendicular to the long axis was taken approximately one quarter of the cell length position and each profile was recorded by 'ROI Manager' in ImageJ. Analysis of data including subtraction of the background intensity and graph drawing was done with MATLAB version 2013a with Statistics and Machine Learning Toolbox (MathWorks, Natick, MA, United States).

Field Emission Scanning EM (FE-SEM)

Traditional Pt-coated FE-SEM was performed by modification of the method described in Nishiyama et al. (2014). Briefly, *E. coli* cells were cultured on SiN layer on Si chip, fixed by the fixing solution at room temperature for 15 min, washed with phosphate buffer, dehydrated with alcohol gradient series, and dried using the critical point drying technique (Leica CPD300, Leica Camera, Germany). The cells were sputter coated with platinum (∼3 nm thickness) (Quick cool coater SC701MC, Sanyu Co., Ltd., Japan), and observed with a FE-SEM, JSM 7400F (JEOL Ltd., Japan) using secondary electrons. The acceleration voltage of the FE-SEM was 1.5 kV and the working distance was 8 mm.

RESULTS

Comparison of the Hft Region in Different Plasmids and Their Superspreader Derivatives

To address the regulation of conjugational transfer by the Hft region in pESBL, we first engineered a superspreader mutant pESBL::Tn1 isolated in the previous work (Yamaichi et al., 2015). Using Flp-*FRT* site-specific recombination, kanamycin resistant cassette was removed which resulted in 199 bp scar inserted in the Hft region flanked with duplication of TA dinucleotide. While the resulting plasmid (hereafter referred to as Tn mutant) is now sensitive to kanamycin and eliminated potential polar effect, it retained all the phenotypes including elevated transfer efficiency from parental pESBL::Tn1 (**Figures 1A,C** and Supplementary Figures S1A,C).

Next, we tried to determine nucleotide substitution(s) that can elevate transfer efficiency. To do so, we compared the nucleotide sequence of the Hft region to the similar IncI conjugative plasmid, R64. In fact, the R64 sequence registered in the Genbank (AP005147.1, Sampei et al., 2010) is not *bona fide* R64, but a derivative *drd11* which presents derepressed/superspreader phenotype. Enhancement of transfer efficiencies from pESBL WT to Tn mutant and from R64 to R64 *drd11* were somewhat similar (**Figures 1B,C**). Therefore, we sequenced the ∼600 bp region encompassing Hft and its downstream *traA* gene of the WT and *drd11* of R64. To this end, we identified seven mismatched bases among three plasmids of which three were located in the Hft region. Particular interest was gathered in three of the seven mismatches that are specific to R64-*drd11*, while the other four appeared to be divergence between pESBL and R64 (**Figure 1A**, yellow and white circles, respectively). To elucidate the impact of the three mutations highlighted in R64-*drd11*, nucleotide substitutions (dubbed X1, X2, and X3, see **Figure 1A**) were introduced in pESBL and resulting mutant plasmids were subjected to conjugational transfer experiments. As shown in **Figure 1C**, X2 showed increased transfer efficiency that was comparable to the Tn mutant. In contrast, X3 exhibited rather decreased transfer efficiency. Furthermore, X3 mutation was epistatic to X2: neither X2X3 double nor X1X2X3 triple mutant showed increased transfer efficiency (**Figure 1C**). These results suggest that not only transposition but also nucleotide substitution in the Hft region can result in enhanced conjugational transfer. Even though they are very similar, pESBL X1X2X3 triple mutant did not show elevated transfer efficiency as seen in R64-*drd11*. Thus it is possible that pESBL and R64 may not possess exact regulatory mechanism, or R64-*drd11* includes further mutations than the three nucleotide substitutions to manifest its higher transfer ability. This suggests that there could be multiple ways for plasmid to evolve to superspreader.

Regulators of Conjugational Transfer of pESBL

In the Hft region, there is an open reading frame encoding hypothetical protein Hp1, and X1 and Tn harbor mutation in its coding region (**Figure 1A**). Lines of evidence suggested that Hp1 protein does not involve in conjugational transfer. Notably, overexpression of Hp1 *in trans* in the donor cell did not affect transfer efficiency of pESBL (data not shown).

Besides X1/Tn disrupting Hp1, nucleotide substitution at X3 position results in truncation of TraA protein (hereafter truncated TraA will be denoted as TraA*). Previous results showed that neither *traA* of pESBL nor *traA** of R64-*drd11* is essential for conjugation (Kim et al., 1993; Yamaichi et al., 2015). However, we found that overexpression of TraA in the donor cell increased the transfer efficiency of WT pESBL comparable to the Tn mutant (**Figure 1E**). Consistent to the transfer efficiency assay, transposon insertion at Hft resulted in huge (∼50-fold) increase of *traA::lacZ* expression level compared to the WT context. On the other hand, deletion of the entire Hft region abolished the expression of *traA::lacZ* (**Figure 1D**). Providing intact TraA *in trans* in ΔHft or X3 pESBL rescued the transfer efficiency that is comparable to the WT pESBL with TraA overexpression (**Figure 1E**). These results indicated that TraA is directly or indirectly involved in pESBL transfer.

In contrast to *traA* and *traA**, downstream *traBC* genes were previously classified as essential for transfer in both pESBL and R64-*drd11* (Kim et al., 1993; Yamaichi et al., 2015). When TraBC was overexpressed *in trans* in the donor cell, enhanced transfer efficiency of pESBL was also observed (**Figure 1E**). It is noteworthy that extent of the enhancement of transfer efficiency by TraBC overexpression was somewhat lower than by overexpression of TraA. Particularly in case of Tn and ΔHft, there were no significant increase compared to the vector control (*p*-value 0.71 and 0.07, respectively) (**Figure 1E**). Next, we investigated *traBC* expression level. Even though two potential promoters (P1 and P2 in **Figure 1F**) for *traB* were predicted by BPROM[1], these two sites were not sufficient for *traB::lacZ* expression (**Figure 1F**). Considerable expression of TraB::LacZ was observed when additional 54 bp upstream to P2 was included, but it was significantly increased when the reporter plasmid contained the Hft region (**Figure 1F**). Deletion of Hft or introduction of X3 nucleotide substitution in the reporter plasmid alleviated the enhancement, suggesting that TraA could activate TraB expression. Consistent to the idea, expression of *traA in trans* boosted the TraB::LacZ expression when the reporter plasmid contains additional 54 bp upstream to the P2 (**Figure 1G**, ii). Since TraA did not affect the transcription level of P1P2 context (**Figure 1G**, i), this 54 bp region would contain essential regulatory elements of *traBC* expression. Unlike TraA::LacZ expression, significant increment of TraB::LacZ expression level was not observed in many of Tn, and X1 and/or X2 constructs, even though they remained to show very high (**Figure 1F**). Because these assays were based on high-copy-number plasmid, it is possible that TraA expression was saturated. We also tested whether truncated TraA* retains functionality or not. TraA* overexpression appeared to have no effect on both transfer efficiency of WT pESBL and TraB::LacZ expression (**Figures 1E,G**). Therefore, TraA* is not likely functional at least for the TraB activation.

Other Phenotypes of the Tn Mutant

Escherichia coli harboring the Tn mutant showed other phenotypes than elevated transfer efficiency including growth defect and sedimentation. While harboring WT pESBL did not cause significant difference in growth rate, Tn mutant showed moderate growth defect (**Figure 2A**). It is noteworthy that this growth defect can be overrated when growth rate was measured by OD in an automated plate reader (**Figure 2A**), presumably because of sedimentation phenotype which will be discussed below. When the overnight cultures of *E. coli* harboring different pESBL was settled on the bench, sedimentation of cells were apparent in the Tn mutant, while harboring WT or ΔHft pESBL did not cause host *E. coli* to sediment over the 4 h of time-course experiments (**Figure 2B**). Furthermore, *E. coli* cells harboring Tn mutant was found to be particularly non-motile in motility plate assay (**Figure 2D**) as well as under microscope (data not shown).

It is known that *Vibrio cholerae* culture autoaggultinates when the expression of toxin-coregulated pili was induced (Taylor et al., 1987), and many non-motile *V. cholerae* mutants exhibited the toxin-coregulated pili overexpressed (Gardel and Mekalanos, 1996). Taking them into account, we hypothesized that this sedimentation/autoagglutination phenotype is reflecting the increased cell-to-cell contact which is caused by overexpression of (conjugative) pili encoded on pESBL.

Altered Cell Surfaces by pESBL

Enhanced cell-to-cell attachment in the Tn mutant was also evident under microscopes as clumps, however, visualization of conjugative pili of pESBL that are associated with *E. coli* cells has been hardly successful. First we transferred test plasmids into Δ*fliA* mutant of *E. coli* (Macnab, 1996) to avoid contamination of flagella. The Tn mutant in Δ*fliA* host showed comparable phenotypes as in the flagellated host, including elevated transfer efficiency and sedimentation (Supplementary Figures S1A,E). Then we carried out experiments to observe pilliation by different plasmids. Our microscopic investigations included traditional FE-SEM with Pt-coated samples. Any particular structures associated to the WT or Tn mutant pESBL samples were not observed in multiple examinations (Supplementary Figure S1F). Therefore, we concluded that conjugative pili would not have been preserved during the sample preparation including dehydrating and vacuum procedures. To overcome potential sample preparation issues, we sought ASEM. In ASEM, aldehyde-fixed cells were treated with positively charged Nanogold particles, which means that negatively charged extracellular structures will be visualized. Somewhat similar to the observation of bacterial cells under fluorescent microscope with membrane dye such as FM4-64, the perimeter of the cells showed highest signal intensities and lesser signals were observed inside the outline, or cell surfaces (**Figure 3**). While we did not see any extracellular structures from negative control cells without

[1]http://www.softberry.com

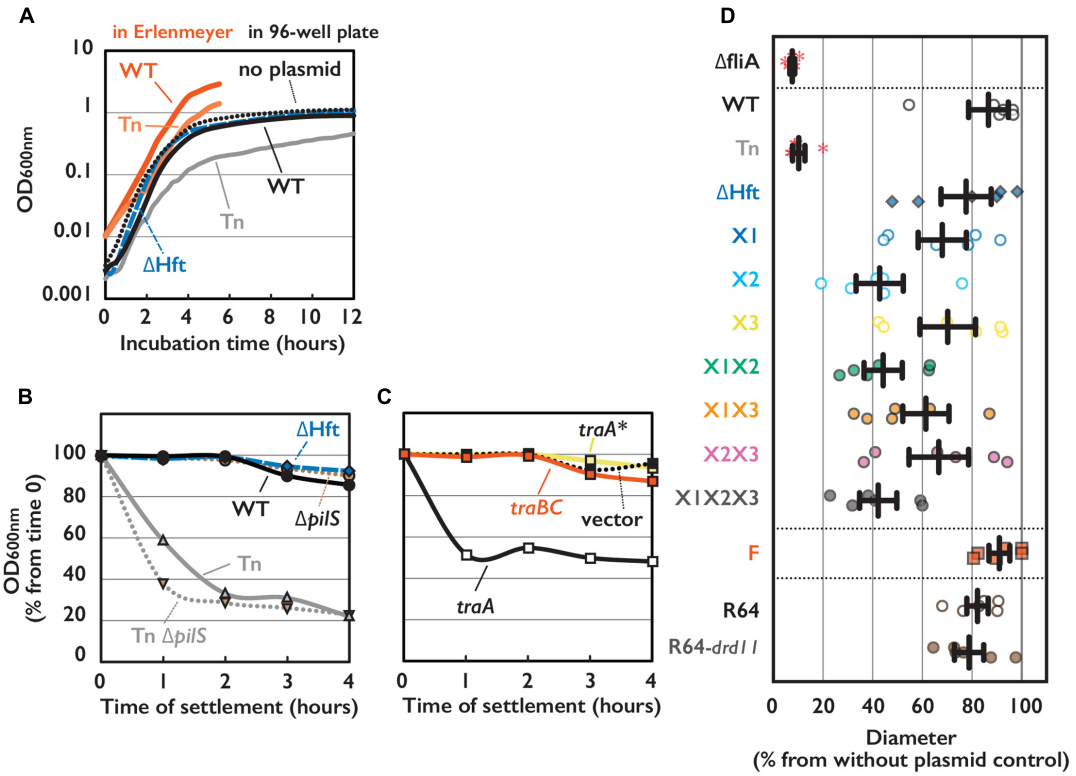

FIGURE 2 | Phenotypes of *E. coli* cells harboring conjugative plasmid. **(A)** Cell growth of *E. coli* strain harboring indicated plasmid measured by OD 600 nm with either conventional spectrometer or 96-well plate reader. **(B,C)** Sedimentation phenotype measured by OD 600 nm of culture supernatant settled on bench for indicated time. *E. coli* cells harboring WT or mutant of pESBL as indicated **(B)** or WT pESBL and an extra plasmid indicated for overexpression **(C)**. Average of at least 3 independent experiments were shown. **(D)** Motility phenotype measured by diameter of expansion on soft agar plate. Results of 6 independent experiments along with the mean and standard deviations were shown. Δ*fliA* mutant without plasmid was used for the negative control. Red asterisks indicate no motility.

plasmid, thin and long filamentous structure was readily detected from cells harboring the F plasmid (**Figures 3A,D**). As this resembled well-known F pili (Brinton et al., 1964; Clarke et al., 2008), we believe that sample preparation for ASEM was capable to maintain conjugative pili attached to the cell. Yet, we did not see any appendages from cells harboring either WT or Tn mutant of pESBL. However, we noticed that they showed different intensities at the cell surfaces (**Figure 3**). To clarify the difference, perpendicular intensity profiles were obtained from more than 100 cells from each sample. As shown in **Figure 3G**, *E. coli* cells harboring WT pESBL showed increased intensity in the cell body, and this was more profound in case of cells possessing the Tn mutant. In contrast, harboring F plasmid did not appear to alter the intensity profile from without plasmid control. These results suggest that pESBL, and possibly other IncI plasmids, exhibit their conjugative pili in a distinct manner to previously described F- and P-types of pili (Christie, 2014). Early EM works by Bradley illustrated pili from IncI plasmids as thick rigid and thin pili (Bradley, 1980b, 1983).

To distinguish plausible thick and thin pili, we deleted *pilS* gene which encodes major subunit of Type IV pili (Kim and Komano, 1997; Horiuchi and Komano, 1998) in WT and Tn pESBL. Increase of intensities in the cell body of *E. coli* cells harboring Tn pESBL was alleviated by introduction of Δ*pilS* (**Figures 3E–G**). Yet we are unsuccessful to gain evidence that two different kinds of pili are appended from the cell, it is suggested that Type IV pili contributed major part of extracellular structures.

Autoagglutination Phenotype May Facilitate Conjugation in Liquid

Although Tn mutants of pESBL and F plasmid led marked difference in host *E. coli* cells, both showed very high transfer ability. ASEM results suggested that pESBL does not likely produce long pili that believed to facilitate cell-to-cell attachment. Furthermore, in our transfer efficiency assay conjugation events were occurred on solid surfaces in which cell-to-cell contacts were rather enforced. In some IncI plasmids, Type IV pili were shown to contribute conjugative transfer in liquid condition (Kim and Komano, 1997; Yoshida et al., 1999; Dudley et al., 2006). These made us wondered to test transfer efficiency of pESBL mutants in liquid condition. **Figure 4** shows transfer efficiency in liquid, and in particular, donor and recipient cells were mixed only a few seconds before plating to isolate exconjugants. Tn mutant of pESBL remained to show extreme efficiency for conjugational transfer in this 'snap conjugation' condition, and notably it was about 10 times better than the transfer efficiency of the F plasmid. Deletion of *pilS* weaken the transfer efficiency of WT pESBL

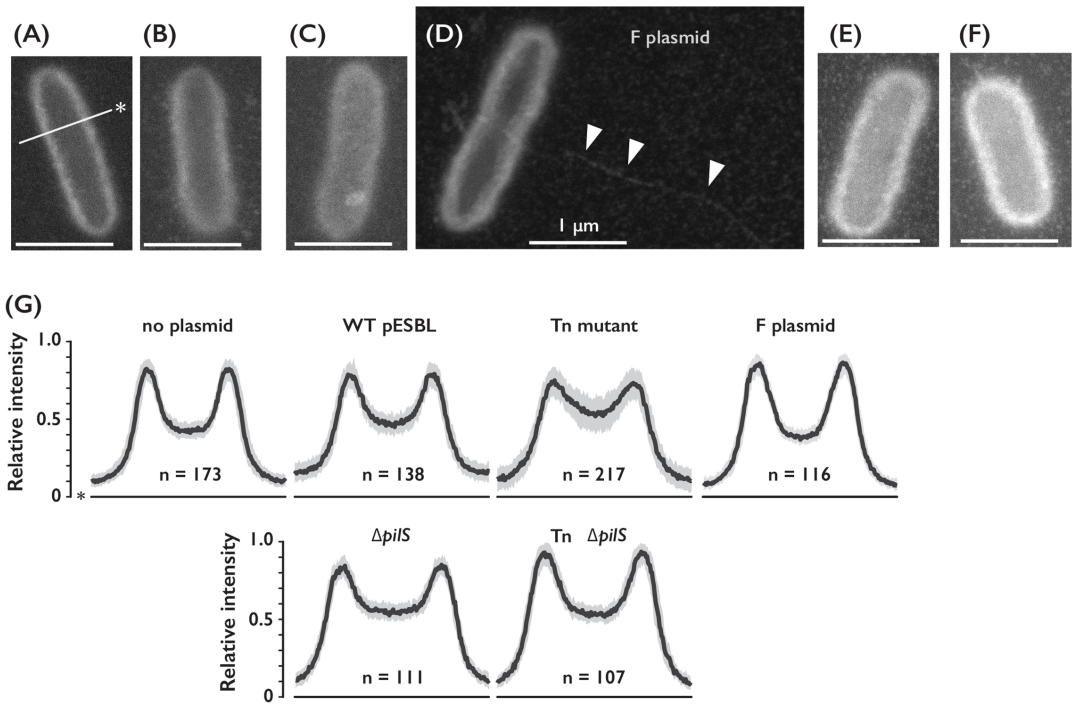

FIGURE 3 | Cell surfaces of *E. coli* cells harboring different conjugative plasmids. **(A–D)** Representative ASEM images of *E. coli* cells without plasmid **(A)**, or harboring either WT **(B)**, Tn **(C)** Δ*pilS* **(E)** or Tn Δ*pilS* mutant **(F)** of pESBL, and F plasmid **(D)**. Arrowheads indicate presumable F pilus. Line with an asterisk indicates perpendicular axis for the intensity profile analysis. Bar = 1 μm. **(G)** Intensity profile of *E. coli* cells with or without plasmids as indicated. Among number of cells analyzed shown as n, median was drawn by the solid line and the gray area represents between the first and third quartiles.

significantly but the effect was modest and not significant in Tn background (**Figure 4A**). Furthermore, *E. coli* cells harboring ΔTn *pilS* pESBL remained to show sedimentation phenotype (**Figure 2B**). Very efficient cell-to-cell attachment is likely one of the biggest factor to endorse high transfer efficiency of the Tn mutant of pESBL. Interestingly, while the Tn mutant induced cells to autoaggregate and sediment, it does not well promote cells to develop biofilm. In our biofilm assay, only moderate and inconstant biofilm formation was observed with Tn mutant grown in M9 media, and biofilm was barely detected with WT pESBL or when cells were grown in LB (Supplementary Figure S1G). On the other hand, F plasmid does not induce cells to sediment (Supplementary Figure S1D) but was shown to induce formation of thick biofilm (Ghigo, 2001).

DISCUSSION

Here we showed that TraA as a new positive regulator for conjugational transfer of pESBL. TraA exceeded TraBC in enhancement of transfer efficiency when overexpressed (**Figures 1E**, **4B**). Furthermore, TraA, but not TraBC overexpression induced WT pESBL harboring cells to sediment (**Figure 2C**). These lines of evidence suggested that some transfer genes are under control of TraBC, and TraA could regulate not only *traBC* but also its own downstream genes. *traA* was not identified as essential gene for conjugation in previous Tnseq analysis (Yamaichi et al., 2015), probably because expression of essential transfer factor TraB is not fully dependent on TraA. Alternatively, it is possible that *traB* expression level could be retained by polar effect of transposon insertion at *traA*. On the other hand, R64-*drd11* possesses silent mutation in *traA* thus expresses TraA* rather than intact TraA. Supplying TraA* did not show significant effect neither on transfer efficiency nor *traB* expression, it is reasonable that inactivation of *traA** did not have effect on transfer efficiency in previous study on R64 (Kim et al., 1993).

It is still elusive for full understanding of the regulation mechanism for conjugational transfer. Most puzzling thing is that X1X2 mutations led TraA to be overexpressed, but X3 mutation resulted in expression of truncated TraA*. Yet, R64-*drd11* showed superspreader phenotype in contrast to corresponding pESBL X1X2X3 which presented even little lower transfer efficiency than the WT. Furthermore, sedimentation phenotypes in different point mutants of pESBL as well as R64 variants were not fully explained by TraA and TraBC regulon (Supplementary Figures S1B,D). Protein folding and topology predictions (Käll et al., 2004; Kelley et al., 2015) suggested that TraA has structural similarity to transcriptional regulators. It is also predicted that the C-terminal of the TraA possibly include transmembrane domain, thus TraA and TraA* might show different protein localization in the cell. So far we do not have direct evidence that TraA regulates transcription of *traBC* for example binding to the upstream 54 bp region. Besides, our preliminary results

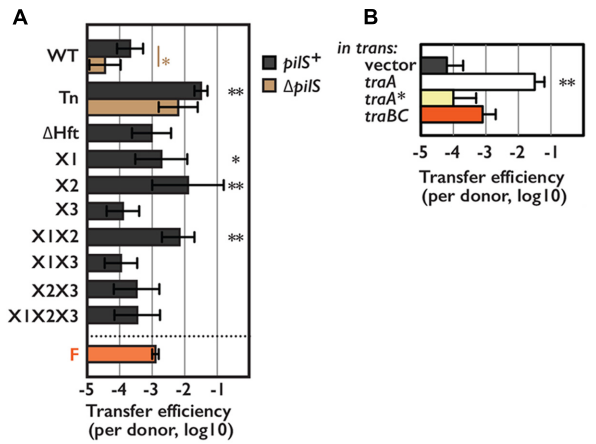

FIGURE 4 | Transfer efficiency of pESBL in snap conjugation. Transfer efficiencies of various pESBL variants **(A)** or WT pESBL harboring an extra plasmid for overexpression of indicated gene **(B)**. F plasmid was used for comparison. Average and standard deviation of at least 3 independent experiments were shown. *Indicates $p < 0.05$ and ** indicates $p < 0.01$, respectively.

with Δ*hfq E. coli* host suggested involvement of small RNAs in multiple steps including expression of *traA* as well as *traBC* (data not shown). Biochemistry and cell biology of TraA variants are awaiting.

In addition to the Hft∼*traABC* regulation, there could be other layer(s) of regulatory circuit to control transfer efficiency of pESBL. One of such mechanism would be DNA processing that is also an important step for successful conjugational transfer. For instance Δ*oriT* totally abolished the transfer efficiency of pESBL (data not shown), yet Tn Δ*oriT* double mutant showed sedimentation phenotype (Supplementary Figure S1A). Another possible mechanism includes small RNA, and they are scope of future investigations.

In combination with positively charged Nanogold-labeling, ASEM was able to visualize delicate hydrophilic nano-structures on *E. coli* cells (**Figure 3**), and the required pretreatment is just aldehyde fixation and staining. The pili-like structure which was labeled on a small population of *E. coli* cells using positively charged Nanogold (Nishiyama et al., 2014) is similar to the protrusions on cells with F plasmid (**Figure 3D**), and it could be F-type Pili. These results suggest the applicability of this cutting-edge technique to diverse bacterial filaments, as shown for flagella (Nishiyama et al., 2014; Sugimoto et al., 2016). As ASEM also allowed visualization of various eukaryotic cells and host-microbe interaction of mouse stomach (Nishiyama et al., 2010, 2014; Maruyama et al., 2012; Memtily et al., 2015), it could be useful to study the roles and mechanisms for microbial appendages such as pili and flagella interaction with both prokaryotic and eukaryotic cells.

Studies of *pil* operon in R64 suggested that it encodes thin pili that is predicted to belong to the type IVB family (Kim and Komano, 1997). *pilS* deletion in WT pESBL resulted in significant reduction of transfer efficiency in both liquid and solid conjugation. However, in superspreader pESBL Tn background the effect was modest (**Figures 1C**, **4A**). It is possible that thin pili is also required for solid conjugation in the WT and not derepressed mutant of R64. Nevertheless, our data suggest that pESBL, and potentially other IncI conjugative plasmids, do not exhibit long filamentous structure but rather possess distinct class of pili that resemble to 'Velcro.' Since Δ*pilS* also did not affect sedimentation phenotype of pESBL Tn, 'thick' conjugative pili could be sufficient for cell-to-cell adhesion and collision of cells seems enough to establish MPF and following conjugational transfer of the DNA. This characteristic could account for superspreader pESBL mutant's higher transfer efficiency than F plasmid in snap conjugation. It could also allow mutant pESBL to have fitness advantage in certain niches for the expansion of the plasmid, although transforming cells non-motile and reducing the growth rate. Furthermore, some enteroaggregative *E. coli* strains are shown not to possess canonical genes for its characteristic aggregative adherence. Instead, an IncI plasmid harbored in a such atypical enteroaggregative *E. coli* strain was shown to contribute cell adhesion (Dudley et al., 2006). Thus, it is possible that IncI plasmids not only provide MDR but also enhance host cell ability to adhere which in turn associate to the pathogenicity of the host cell.

Considering the less potency to induce biofilm, it is possible that pESBL pili are more specialized to bacteria-to-bacteria interaction. R64, pESBL, and other IncI plasmids possess shufflon, site-specific recombination mechanism supposed to create variability on the tip of pili (Komano, 1999). Shufflon has been proposed to alter the specificity of recipient in liquid conjugation (Komano et al., 1994), and in R64 and another IncI plasmid ColIb-P9, certain version of PilV shown to be involved in aggregation phenotype (Yoshida et al., 1998). Our preliminary results suggested that *rci* which encodes shufflon-specific DNA recombinase was much higher expressed in Tn and X1X2 mutants than in WT pESBL (data not shown). It is intriguing to see if each of the cells harboring superspreader mutant of pESBL exhibit wider variety of 'crochet' to achieve cell-to-cell attachment. Closely related pESBL-305 isolated from chicken cecum has transposon inserted in the shufflon region (Brouwer et al., 2014), although biological consequences are not understood thus far.

Lastly, resistance to antimicrobial reagents is arguably the most important phenotype pESBL provides to the host cell. Even though Tn and ΔHft mutation resulted in increased and decreased transcripts of the two β-lactamase genes, respectively (data not shown), these mutations did not alter minimum inhibitory concentrations of β-lactams we tested; all WT, Tn and ΔHft pESBL led cells resistant against > 256 μg/mL of Amoxicillin and >32 μg/mL of Cefotaxime. It is still possible that these mutations could modify susceptibility to other β-lactam antibiotics.

Altogether, here we showed that mutations in Hft can lead strong TraA overexpression which resulted in overexpression of conjugative pili. Subsequently, hyperpiliation facilitates cell-to-cell adhesion thus promote plasmid transfer efficiency. Potential emergence of superspreader mutant plasmids is threatening, particularly it could make adverse consequence in terms of

epidemic of host pathogen. Further investigations could shed light on curbing devastating dissemination of MDR.

AUTHOR CONTRIBUTIONS

YY conceived and designed the overall research project. Molecular and genetic experiments were performed by MP, MD, and YY. Biochemical experiments were performed by MP. Microscopy experiments were carried out by MS, CS, and YY, and following image analysis was done by IA. All authors contributed to analyzing data and editing the manuscript. The paper was written by CS and YY.

FUNDING

This research was supported by I2BC (to YY), a Grant-in-Aid for Scientific Research on Innovative Areas, Sparse modeling (to CS), CREST (to CS), a Grant-in-Aid for Scientific Research from JSPS (15K14499) (to CS), grants from the Ministry of Education, Culture, Sports, Science, and Technology (MEXT) (to CS), a Grant-in-Aid from CANON (to CS), a strategic grant to NISP from AIST (to CS) and a Grant-in-Aid from AIST (to CS).

ACKNOWLEDGMENTS

The authors are grateful to Drs. Nobuhisa Furuya and Teruya Komano for R64 plasmids and sharing unpublished data, Dr. Christian Lesterlin for the F plasmid, Drs. Slamti Leyla and Isabelle Vallet-Gely for help on biofilm assay, and Dr. Matthew Waldor for the discussion on the project. *E. coli* strain JW1907 was provided, as a part of the KEIO collection, by The National Bioresource Project, National Institute of Genetics, Japan. They thank Drs. S. Leyla, Vicky Lioy and Elena Espinosa for critical reading the paper. They also thank Bahmann Amir Moezzi, Alice Gamelin and Eric Disdero for technical assistance for molecular and genetic experiments.

SUPPLEMENTARY MATERIAL

The Supplementary Material for this article can be found online at: https://www.frontiersin.org/articles/10.3389/fmicb.2018.00130/full#supplementary-material

REFERENCES

Baba, T., Ara, T., Hasegawa, M., Takai, Y., Okumura, Y., Baba, M., et al. (2006). Construction of *Escherichia coli* K-12 in-frame, single-gene knockout mutants: the Keio collection. *Mol. Syst. Biol.* 2, 2006.0008. doi: 10.1038/msb4100050

Bradley, D. E. (1980a). Determination of pili by conjugative bacterial drug resistance plasmids of incompatibility groups B, C, H, J, K, M, V, and X. *J. Bacteriol.* 141, 828–837.

Bradley, D. E. (1980b). Morphological and serological relationships of conjugative pili. *Plasmid* 4, 155–169.

Bradley, D. E. (1983). Derepressed plasmids of incompatibility group I1 determine two different morphological forms of pilus. *Plasmid* 9, 331–334. doi: 10.1016/0147-619X(83)90011-2

Bradley, D. E. (1984). Characteristics and function of thick and thin conjugative pili determined by transfer-derepressed plasmids of incompatibility groups I1, I2, I5, B, K and Z. *J. Gen. Microbiol.* 130, 1489–1502. doi: 10.1099/00221287-130-6-1489

Brinton, C. C. Jr., Gemski, P. Jr., and Carnahan, J. (1964). A new type of bacterial pilus genetically controlled by the fertility factor of e. *coli* k 12 and its role in chromosome transfer. *Proc. Natl. Acad. Sci. U.S.A.* 52, 776–783. doi: 10.1073/pnas.52.3.776

Brouwer, M. S., Bossers, A., Harders, F., van Essen-Zandbergen, A., Mevius, D. J., and Smith, H. E. (2014). Complete genome sequences of IncI1 plasmids carrying extended-spectrum -lactamase genes. *Genome Announc.* 2, e859–e814. doi: 10.1128/genomeA.00859-14

Chiang, S. L., and Rubin, E. J. (2002). Construction of a mariner-based transposon for epitope-tagging and genomic targeting. *Gene* 296, 179–185. doi: 10.1016/S0378-1119(02)00856-9

Christie, P. J. (2014). "Conjugative pili," in *Bacterial Pili: Structure, Synthesis and Role in Disease*, eds M. A. Barocchi and J. L. Telford (Boston, MA: CABI), 17–35. doi: 10.1079/9781780642550.0017

Clarke, M., Maddera, L., Harris, R. L., and Silverman, P. M. (2008). F-pili dynamics by live-cell imaging. *Proc. Natl. Acad. Sci. U.S.A.* 105, 17978–17981. doi: 10.1073/pnas.0806786105

Datsenko, K. A., and Wanner, B. L. (2000). One-step inactivation of chromosomal genes in *Escherichia coli* K-12 using PCR products. *Proc. Natl. Acad. Sci. U.S.A.* 97, 6640–6645. doi: 10.1073/pnas.120163297

Demarre, G., Guérout, A. M., Matsumoto-Mashimo, C., Rowe-Magnus, D. A., Marlière, P., and Mazel, D. (2005). A new family of mobilizable suicide plasmids based on broad host range R388 plasmid (IncW) and RP4 plasmid (IncPalpha) conjugative machineries and their cognate *Escherichia coli* host strains. *Res. Microbiol.* 156, 245–255. doi: 10.1016/j.resmic.2004.09.007

Dudley, E. G., Abe, C., Ghigo, J. M., Latour-Lambert, P., Hormazabal, J. C., and Nataro, J. P. (2006). An IncI1 plasmid contributes to the adherence of the atypical enteroaggregative *Escherichia coli* strain C1096 to cultured cells and abiotic surfaces. *Infect. Immun.* 74, 2102–2114. doi: 10.1128/IAI.74.4.2102-2114.2006

Frank, C., Werber, D., Cramer, J. P., Askar, M., Faber, M., an der Heiden, M., et al. (2011). Epidemic profile of Shiga-toxin-producing *Escherichia coli* O104:H4 outbreak in Germany. *N. Engl. J. Med.* 365, 1771–1780. doi: 10.1056/NEJMoa1106483

Frost, L. S., Ippen-Ihler, K., and Skurray, R. A. (1994). Analysis of the sequence and gene products of the transfer region of the F sex factor. *Microbiol. Rev.* 58, 162–210.

Fullner, K. J., Lara, J. C., and Nester, E. W. (1996). Pilus assembly by *Agrobacterium* T-DNA transfer genes. *Science* 273, 1107–1109. doi: 10.1126/science.273.5278.1107

Gardel, C. L., and Mekalanos, J. J. (1996). Alterations in *Vibrio cholerae* motility phenotypes correlate with changes in virulence factor expression. *Infect. Immun.* 64, 2246–2255.

Ghigo, J. M. (2001). Natural conjugative plasmids induce bacterial biofilm development. *Nature* 412, 442–445. doi: 10.1038/35086581

Gibson, D. G., Young, L., Chuang, R. Y., Venter, J. C., Hutchison, C. A., and Smith, H. O. (2009). Enzymatic assembly of DNA molecules up to several hundred kilobases. *Nat. Methods* 6, 343–345. doi: 10.1038/nmeth.1318

Guynet, C., Cuevas, A., Moncalián, G., and de la Cruz, F. (2011). The stb operon balances the requirements for vegetative stability and conjugative transfer of plasmid R388. *PLOS Genet.* 7:e1002073. doi: 10.1371/journal.pgen.1002073

Horiuchi, T., and Komano, T. (1998). Mutational analysis of plasmid R64 thin pilus prepilin: the entire prepilin sequence is required for processing by type IV prepilin peptidase. *J. Bacteriol.* 180, 4613–4620.

Käll, L., Krogh, A., and Sonnhammer, E. L. (2004). A combined transmembrane topology and signal peptide prediction method. *J. Mol. Biol.* 338, 1027–1036. doi: 10.1016/j.jmb.2004.03.016

Kelley, L. A., Mezulis, S., Yates, C. M., Wass, M. N., and Sternberg, M. J. (2015). The Phyre2 web portal for protein modeling, prediction and analysis. *Nat. Protoc.* 10, 845–858. doi: 10.1038/nprot.2015.053

Kim, S. R., Funayama, N., and Komano, T. (1993). Nucleotide sequence and characterization of the traABCD region of IncI1 plasmid R64. *J. Bacteriol.* 175, 5035–5042. doi: 10.1128/jb.175.16.5035-5042.1993

Kim, S. R., and Komano, T. (1997). The plasmid R64 thin pilus identified as a type IV pilus. *J. Bacteriol.* 179, 3594–3603. doi: 10.1128/jb.179.11.3594-3603.1997

Komano, T. (1999). Shufflons: multiple inversion systems and integrons. *Annu. Rev. Genet.* 33, 171–191. doi: 10.1146/annurev.genet.33.1.171

Komano, T., Kim, S. R., Yoshida, T., and Nisioka, T. (1994). DNA rearrangement of the shufflon determines recipient specificity in liquid mating of IncI1 plasmid R64. *J. Mol. Biol.* 243, 6–9. doi: 10.1006/jmbi.1994.1625

Komano, T., Yoshida, T., Narahara, K., and Furuya, N. (2000). The transfer region of IncI1 plasmid R64: similarities between R64 tra and legionella icm/dot genes. *Mol. Microbiol.* 35, 1348–1359. doi: 10.1046/j.1365-2958.2000.01769.x

Lawley, T. D., Klimke, W. A., Gubbins, M. J., and Frost, L. S. (2003). F factor conjugation is a true type IV secretion system. *FEMS Microbiol. Lett.* 224, 1–15. doi: 10.1016/S0378-1097(03)00430-0

Macnab, R. M. (1996). "Flagella and motility," in *Escherichia coli and Salmonella: Cellular and Molecular Biology*, 2nd Edn, ed. F. C. Neidhardt (Washington, DC: ASM Press), 123–145.

Maruyama, Y., Ebihara, T., Nishiyama, H., Suga, M., and Sato, C. (2012). Immuno EM-OM correlative microscopy in solution by atmospheric scanning electron microscopy (ASEM). *J. Struct. Biol.* 180, 259–270. doi: 10.1016/j.jsb.2012.08.006

Memtily, N., Okada, T., Ebihara, T., Sato, M., Kurabayashi, A., Furihata, M., et al. (2015). Observation of tissues in open aqueous solution by atmospheric scanning electron microscopy: applicability to intraoperative cancer diagnosis. *Int. J. Oncol.* 46, 1872–1882. doi: 10.3892/ijo.2015.2905

Meynell, E., and Datta, N. (1967). Mutant drug resistant factors of high transmissibility. *Nature* 214, 885–887. doi: 10.1038/214885a0

Meynell, E., Meynell, G. G., and Datta, N. (1968). Phylogenetic relationships of drug-resistance factors and other transmissible bacterial plasmids. *Bacteriol. Rev.* 32, 55–83.

Miller, J. H. (1992). *A Short Course in Bacterial Genetics - A Laboratory Manual and Handbook for Escherichia coli and Related Bacteria*. New York, NY: Cold Spring Harbor Laboratory Press.

Milton, D. L., O'Toole, R., Horstedt, P., and Wolf-Watz, H. (1996). Flagellin A is essential for the virulence of *Vibrio anguillarum*. *J. Bacteriol.* 178, 1310–1319. doi: 10.1128/jb.178.5.1310-1319.1996

Nishiyama, H., Suga, M., Ogura, T., Maruyama, Y., Koizumi, M., Mio, K., et al. (2010). Atmospheric scanning electron microscope observes cells and tissues in open medium through silicon nitride film. *J. Struct. Biol.* 169, 438–449. doi: 10.1016/j.jsb.2010.01.005

Nishiyama, H., Teramoto, K., Suga, M., and Sato, C. (2014). Positively charged nanogold label allows the observation of fine cell filopodia and flagella in solution by atmospheric scanning electron microscopy. *Microsc. Res. Tech.* 77, 153–160. doi: 10.1002/jemt.22322

O'Toole, G. A. (2011). Microtiter dish biofilm formation assay. *J. Vis. Exp.* 47, 2437. doi: 10.3791/2437

Poirel, L., Bonnin, R. A., and Nordmann, P. (2012). Genetic features of the widespread plasmid coding for the carbapenemase OXA-48. *Antimicrob. Agents Chemother.* 56, 559–562. doi: 10.1128/AAC.05289-11

Potron, A., Poirel, L., and Nordmann, P. (2014). Derepressed transfer properties leading to the efficient spread of the plasmid encoding carbapenemase OXA-48. *Antimicrob. Agents Chemother.* 58, 467–471. doi: 10.1128/AAC.01344-13

Rasko, D. A., Webster, D. R., Sahl, J. W., Bashir, A., Boisen, N., Scheutz, F., et al. (2011). Origins of the *E. coli* strain causing an outbreak of hemolytic-uremic syndrome in Germany. *N. Engl. J. Med.* 365, 709–717. doi: 10.1056/NEJMoa1106920

Rohde, H., Qin, J., Cui, Y., Li, D., Loman, N. J., Hentschke, M., et al. (2011). *E. coli* O104:H4 genome analysis crowd-sourcing consortium open-source genomic analysis of shiga-toxin-producing *E. coli* O104:H4. *N. Engl. J. Med.* 365, 718–724. doi: 10.1056/NEJMoa1107643

Sampei, G., Furuya, N., Tachibana, K., Saitou, Y., Suzuki, T., Mizobuchi, K., et al. (2010). Complete genome sequence of the incompatibility group I1 plasmid R64. *Plasmid* 64, 92–103. doi: 10.1016/j.plasmid.2010.05.005

Sato, C., Manaka, S., Nakane, D., Nishiyama, H., Suga, M., Nishizaka, T., et al. (2012). Rapid imaging of mycoplasma in solution using atmospheric scanning electron microscopy (ASEM). *Biochem. Biophys. Res. Commun.* 417, 1213–1218. doi: 10.1016/j.bbrc.2011.12.111

Schneider, C. A., Rasband, W. S., and Eliceiri, K. W. (2012). NIH Image to ImageJ: 25 years of image analysis. *Nat. Methods* 9, 671–675. doi: 10.1038/nmeth.2089

Smillie, C., Garcillán-Barcia, M. P., Francia, M. V., Rocha, E. P., and de la Cruz, F. (2010). Mobility of plasmids. *Microbiol. Mol. Biol. Rev.* 74, 434–452. doi: 10.1128/MMBR.00020-10

Sugimoto, S., Okuda, K., Miyakawa, R., Sato, M., Arita-Morioka, K., Chiba, A., et al. (2016). Imaging of bacterial multicellular behaviour in biofilms in liquid by atmospheric scanning electron microscopy. *Sci. Rep.* 6:25889. doi: 10.1038/srep25889

Taylor, R. K., Miller, V. L., Furlong, D. B., and Mekalanos, J. J. (1987). Use of *phoA* gene fusions to identify a pilus colonization factor coordinately regulated with cholera toxin. *Proc. Natl. Acad. Sci. U.S.A.* 84, 2833–2837. doi: 10.1073/pnas.84.9.2833

Yamaichi, Y., Chao, M. C., Sasabe, J., Clark, L., Davis, B. M., Yamamoto, N., et al. (2015). High-resolution genetic analysis of the requirements for horizontal transmission of the ESBL plasmid from *Escherichia coli* O104:H4. *Nucleic Acids Res.* 43, 348–360. doi: 10.1093/nar/gku1262

Yamaichi, Y., Gerding, M. A., Davis, B. M., and Waldor, M. K. (2011). Regulatory cross-talk links *Vibrio cholerae* chromosome II replication and segregation. *PLOS Genet.* 7:e1002189. doi: 10.1371/journal.pgen.1002189

Yoshida, T., Furuya, N., Ishikura, M., Isobe, T., Haino-Fukushima, K., Ogawa, T., et al. (1998). Purification and characterization of thin pili of IncI1 plasmids ColIb-P9 and R64: formation of PilV-specific cell aggregates by type IV pili. *J. Bacteriol.* 180, 2842–2848.

Yoshida, T., Kim, S. R., and Komano, T. (1999). Twelve pil genes are required for biogenesis of the R64 thin pilus. *J. Bacteriol.* 181, 2038–2043.

Conflict of Interest Statement: The authors declare that the research was conducted in the absence of any commercial or financial relationships that could be construed as a potential conflict of interest.

frontiers in Microbiology

ORIGINAL RESEARCH
published: 05 March 2018
doi: 10.3389/fmicb.2018.00311

Plasmid-Mediated Quinolone Resistance in *Shigella flexneri* Isolated From Macaques

*Anthony J. Mannion, Heather R. Martin†, Zeli Shen, Ellen M. Buckley, JoAnn L. Dzink-Fox, Alexis Garcia, Robert P. Marini, Mary M. Patterson and James G. Fox**

Division of Comparative Medicine, Massachusetts Institute of Technology, Cambridge, MA, United States

OPEN ACCESS

Edited by:
Yonghong Xiao,
Zhejiang University, China

Reviewed by:
Zhi Ruan,
Sir Run Run Shaw Hospital, China
Remy A. Bonnin,
Université Paris-Saclay, France

***Correspondence:**
James G. Fox
jgfox@mit.edu

†Present Address:
Heather R. Martin,
Sloan Kettering Institute, New York, NY, United States

Specialty section:
This article was submitted to Antimicrobials, Resistance and Chemotherapy, a section of the journal Frontiers in Microbiology

Received: *10 October 2017*
Accepted: *09 February 2018*
Published: *05 March 2018*

Citation:
Mannion AJ, Martin HR, Shen Z, Buckley EM, Dzink-Fox JL, Garcia A, Marini RP, Patterson MM and Fox JG (2018) Plasmid-Mediated Quinolone Resistance in Shigella flexneri Isolated From Macaques. Front. Microbiol. 9:311. doi: 10.3389/fmicb.2018.00311

Non-human primates (NHPs) for biomedical research are commonly infected with *Shigella* spp. that can cause acute dysentery or chronic episodic diarrhea. These animals are often prophylactically and clinically treated with quinolone antibiotics to eradicate these possible infections. However, chromosomally- and plasmid-mediated antibiotic resistance has become an emerging concern for species in the family *Enterobacteriaceae*. In this study, five individual isolates of multi-drug resistant *Shigella flexneri* were isolated from the feces of three macaques. Antibiotic susceptibility testing confirmed resistance or decreased susceptibility to ampicillin, amoxicillin-clavulanic acid, cephalosporins, gentamicin, tetracycline, ciprofloxacin, enrofloxacin, levofloxacin, and nalidixic acid. *S. flexneri* isolates were susceptible to trimethoprim-sulfamethoxazole, and this drug was used to eradicate infection in two of the macaques. Plasmid DNA from all isolates was positive for the plasmid-encoded quinolone resistance gene *qnrS*, but not *qnrA* and *qnrB*. Conjugation and transformation of plasmid DNA from several *S. flexneri* isolates into antibiotic-susceptible *Escherichia coli* strains conferred the recipients with resistance or decreased susceptibility to quinolones and beta-lactams. Genome sequencing of two representative *S. flexneri* isolates identified the *qnrS* gene on a plasmid-like contig. These contigs showed >99% homology to plasmid sequences previously characterized from quinolone-resistant *Shigella flexneri* 2a and *Salmonella enterica* strains. Other antibiotic resistance genes and virulence factor genes were also identified in chromosome and plasmid sequences in these genomes. The findings from this study indicate macaques harbor pathogenic *S. flexneri* strains with chromosomally- and plasmid-encoded antibiotic resistance genes. To our knowledge, this is the first report of plasmid-mediated quinolone resistance in *S. flexneri* isolated from NHPs and warrants isolation and antibiotic testing of enteric pathogens before treating macaques with quinolones prophylactically or therapeutically.

Keywords: plasmid-mediated quinolone resistance, enrofloxacin resistance, multi-drug antibiotic resistance, *Shigella flexneri*, non-human primates, zoonotic risk

INTRODUCTION

Shigella spp., particularly *Shigella flexneri*, are common enteric pathogens isolated from non-human primates (NHPs), including macaques, that can cause acute dysentery and are associated with chronic episodic diarrhea. In addition to the lower bowel, *Shigella* spp. can also colonize the inflamed gingival mucosa (McClure et al., 1976; Armitage et al., 1982). Clinically, animals may not appear ill, but *Shigella* spp. can be cultured from normally formed, but blood-streaked feces. These animals represent *Shigella* spp. reservoirs capable of transmitting the pathogen to other colony-maintained NHPs and pose important zoonotic risks to research, veterinary, and zoo personnel (Fox, 1975; Tribe and Fleming, 1983; Kennedy et al., 1993).

Because of the high incidence of diarrhea in newly imported NHPs, antibiotics are often given prophylactically to reduce its clinical severity. Enrofloxacin, a fluoroquinolone antibiotic, is commonly prescribed because of its efficacy in treating gram-negative pathogens and its convenience of a once-daily parenteral treatment. In addition, enrofloxacin has also been used to successfully eradicate *Shigella* spp. from a variety of NHP species housed in a laboratory and zoological setting (Line et al., 1992; Banish et al., 1993). However, widespread and prophylactic use of enrofloxacin and other antibiotics act as selective pressures for the emergence of antibiotic resistant organisms.

Quinolone resistance is typically chromosomally-mediated; however, an increasing finding among species in the family *Enterobacteriaceae* is plasmid-mediated quinolone resistance due to *qnr* genes. While several homologs of *qnr* genes have been discovered, the best characterized are the *qnrA*, *qnrB*, and *qnrS* genes (Strahilevitz et al., 2009; Redgrave et al., 2014). These genes encode a ∼218 amino acid protein that protects bacterial DNA gyrase and topoisomerase from quinolone and fluoroquinolone inhibition, thus resulting in low-level quinolone resistance (Tran and Jacoby, 2002; Tran et al., 2005a,b; Redgrave et al., 2014). Since first being reported in 1998 from a clinical isolate of *Klebsiella pneumoniae* (Martinez-Martinez et al., 1998), plasmid-mediated quinolone resistance has been reported in other *Enterobacteriaceae* species throughout the United States (Wang et al., 2004) and elsewhere in the world (Hata et al., 2005; Mammeri et al., 2005; Strahilevitz et al., 2009; Karczmarczyk et al., 2012).

Plasmids encoding *qnr* often harbor other antibiotic resistance genes and can be transferred to other bacterial species by conjugation (Martinez-Martinez et al., 1998). For example, the ∼47 kb, conjugative plasmid pAH0376 was discovered in *S. flexneri* 2b isolates that caused a food poisoning outbreak and harbors both a TEM-1 β-lactamase gene and *qnrS* gene (Hata et al., 2005). Thus, plasmid-mediated quinolone resistance represents a significant public health concern because they act as vectors that propagate multi-drug antibiotic resistant pathogens.

Given the frequent use of quinolones and potential for zoonotic transmission, the purpose of this report is to describe the isolation of plasmid-mediated multiple-antibiotic resistant *S. flexneri* strains recovered from three colony-maintained macaques, and the successful eradication of these drug-resistant *S. flexneri* isolates.

MATERIALS AND METHODS

Case History

Macaques (*Macaca mulatta*), obtained from a United States-based vendor in 2005, underwent physical examination and routine diagnostic evaluations during quarantine and thereafter at quarterly intervals. Macaques were routinely pair-housed and maintained in an AAALAC International-accredited animal facility. They were fed specified amounts of primate chow (Purina Lab Diet® 5038, St. Louis, MO) twice daily and provided water *ad libitum*. Housing conditions were maintained between 20 and 22°C, 30–70% humidity, 10–15 non-recirculated air changes per hour, and a light cycle of 12 h light, 12 h of dark per day.

During a quarterly physical and diagnostic evaluation, macaque 05-18 presented with fresh blood in its feces. Fecal samples were collected directly from the rectum and submitted for culture and antibiotic sensitivity. Shortly after the initial fecal sample was collected, macaque 05-18 and its cagemate underwent antibiotic treatment with enrofloxacin (5 mg/kg IM every 24 h for 10 days) following research-related surgical procedures. *S. flexneri* variant Y (strain 06-2384) was cultured from the original submission and found sensitive to trimethoprim-sulfamethoxazole, but resistant to ampicillin, amoxicillin-clavulanic acid, cephalothin, gentamicin, and enrofloxacin using Kirby-Bauer antibiotic testing. The two clinically normal monkeys were placed in quarantine together and a set of rectal and gingival swabs were submitted for culture. The second culture sample, as well as fecal samples collected twice more at 2-week intervals, were negative for *Shigella* spp. Following treatment with enrofloxacin, multiple follow-up fecal cultures were negative for *Shigella* spp.

Fecal samples were collected from all macaques ($N = 24$) and submitted for culture and antibiotic susceptibility testing during the same time interval the shigella-positive macaque, 05-18, was found. Two additional macaques, 05-15 and 05-16, housed in the adjacent cage to macaque 05-18, had fecal cultures positive for *S. flexneri* type 5b, designated 06-2835 and 06-2836, respectively. This serotype also showed multiple-antibiotic resistance, with intermediate sensitivity to enrofloxacin and sensitivity to trimethoprim-sulfamethoxazole. The second pair was moved to quarantine and treated with enrofloxacin (5 mg/kg IM every 24 h for 10 days). However, follow-up fecal cultures from the cage pan were still positive for *S. flexneri* type 5b, designated strain 06-3102. Subsequently, the pair was treated with trimethoprim-sulfadiazine (30 mg/kg SQ every 24 h for 10 days); all subsequent cultures were negative for *Shigella* spp.

Shigella Isolation

Cage pan feces and rectal swabs collected from macaques were swabbed onto XLD (xylose, lysine, deoxycholate) and HE (hektoen-enteric) agar media, and the samples were then placed into selenite broth (Remel, Inc., Lenexa, KS.). All media were incubated at 37°C for 18 to 24 h, after which the selenite broth was sub-cultured onto the same media and re-incubated. Isolates that were transparent on the XLD and HE agars were sub-cultured on BAP (Trypticase Soy Agar with 5% Sheep Blood; Remel) and identified as *Shigella* spp. by API 20E (bioMerieux,

Inc., Hazelwood, MO). Isolates were submitted to the Texas Department of State Health Services lab for serotyping.

Antimicrobial Agents

Antibiotics used for broth microdilution assays (ampicillin, azithromycin, cefazolin, cefoxitin, ceftazidime, ceftriaxone, cephalothin, ciprofloxacin, clarithromycin, enrofloxacin, gentamicin, imipenem, levofloxacin, nalidixic acid, and tetracycline powders) were purchased from the Sigma Chemical Company (St. Louis, MO). Amoxicillin-clavulanic acid and trimethoprim-sulfamethoxazole were obtained as E-test strips from bioMerieux (Durham, NC.). Disks of ampicillin (10 μg), cephalothin (30 μg), enrofloxacin (5 μg), nalidixic acid (30 μg), tetracycline (30 μg), amoxicillin-clavulanic acid (30 μg), and trimethoprim-sulfamethoxazole (25 μg) were obtained from Remel (Lenexa, KS.).

Antimicrobial Susceptibility Testing

Antimicrobial susceptibility tests were initially performed by disk diffusion in accordance with the Clinical Laboratory Standards Institute (2010). In addition, to determine the level of sensitivity, antibiotic mean inhibitory concentrations (MICs) were determined by the broth microdilution method using 2-fold serial dilutions, as recommended by CLSI (Clinical Laboratory Standards Institute, 2012, 2014). MIC is defined as the lowest concentration of an antimicrobial agent that inhibits visible growth. *Escherichia coli* (ATCC25922) was used as the standard reference strain. Experiments were performed in triplicate from two or more independent experiments.

DNA Extraction

Whole DNA (includes both chromosomal and plasmid DNA) from the five *S. flexneri* isolates was extracted using the High Pure PCR Template Preparation Kit (Roche Molecular Biochemicals, Indianapolis, IN). Plasmid DNA was extracted using the QIAprep Spin Miniprep Kit (QIAGEN Inc. Valencia, CA).

Screening of *qnr* Antimicrobial-Resistance Genes

Screening for the *qnrA*, *qnrB*, and *qnrS* genes was performed on whole and plasmid DNA using the primers and PCR conditions described previously (Robicsek et al., 2006). PCR products were concentrated and purified with the QIAquick PCR purification kit (Qiagen, Valencia, CA) for sequencing with an ABI Prism cycle sequencing kit (BigDye Terminator cycle sequencing kit) on an ABI 3100 genetic analyzer (Applied Biosystems, Foster City, CA). Sequences were analyzed by BLAST hosted by the National Center for Biotechnology Information (NCBI) to identify homologous genes and calculate percent identity.

Conjugation and Transformation Assays

Conjugation experiments were performed using the *S. flexneri* isolates as donors and *E. coli* J53 Az^r as the recipients (Wang et al., 2004). Cultures of donor and recipient cells were grown in 3 mL of fresh Luria Bertani (LB) broth (BBL®) at 37°C with shaking for 3 h. The conjugation assay was then performed in 3 mL of fresh LB broth using the donor and recipient cells in logarithmic phase (0.5 mL each) and incubated at 37°C for 3 h without shaking. Transconjugants were selected on trypticase soy agar plates (TSA; BBL®) containing sodium azide (100 μg/mL: Sigma-Aldrich Corporation, St. Louis, Mo.) for counter-selection, and ampicillin (50 μg/mL; Sigma-Aldrich Corp.) for selection of plasmid-encoded resistance (Fox, 1975; Mammeri et al., 2005; Cattoir et al., 2007). Colonies were also plated on TSA plates containing sodium azide (100 μg/mL) and nalidixic acid (16 μg/mL). The transconjugants were plated onto MacConkey agar plates, and their identities were reconfirmed as *E. coli* using with API 20E.

For transformation experiments, 5 μL of plasmid DNA from four donor strains was heat shocked at 42°C for 30 s into chemically component *E. coli* Top10 cells. The cells were then incubated in 250 μL of S.O.C. (super optimal broth with catabolic repressor) for 1 h at 37°C, followed by overnight growth on LB plates supplemented with ampicillin (50 μg/mL; Sigma-Aldrich Corp.) for selection of antibiotic-resistant transformants. Colonies were screened by PCR for the *qnrS* gene. MICs for the donors, recipient, transconjugants, and transformants were measured as described above.

Whole Genome Sequencing of Representative *S. flexneri* Isolates

Whole DNA was extracted from two representative *S. flexneri* isolates, 06-2384 and 06-3102, using the High Pure PCR Template Preparation Kit (Roche Molecular Biochemicals, Indianapolis, IN). These isolates were chosen in order to represent all infected animals (06-2384 cultured from monkey 05-18; 06-3102 cultured from co-housed monkeys 05-15 and 05-16) as well as the potential genetic diversity of both serotypes (variant Y and 5b, corresponding to 06-2384 and 06-3102, respectively). DNA was then prepared into libraries using the SMRTbell Template Prep Kit 1.0 and the DNA/Polymerase Binding Kit P6 v2 (Pacific Biosciences, Menlo Park, CA). DNA libraries were size-selected for fragments $\geq\sim$5kb and then were sequenced on a single SMRT cell per genome using a Pacific Biosciences RSII sequencer at the University of Massachusetts Deep Sequencing Core Facility (Worchester, MA). Sequencing reads were quality filtered and trimmed for *de novo* assembly using the Hierarchical Genome Assembly Process (HGAP 3.0) workflow hosted on the SMRT Portal 2.3. Resulting contigs were annotated using RASTtk (Aziz et al., 2008) hosted by Pathosystems Resource Integration Center (PATRIC) (Wattam et al., 2014, 2017). VirulenceFinder 1.5 (Joensen et al., 2014), ResFinder 2.1 (Zankari et al., 2012), and PlasmidFinder 1.3 (Carattoli et al., 2014) were used to identify virulence factors, antibiotic resistance genes, and plasmids, respectively. *In silico* multi-locus sequencing type (MLST) was determined using MLST-1.6 (Larsen et al., 2012) against the *E. coli* #1 allelic profile database. Average nucleotide identity (ANI) was calculated with OrthoANIu (Lee et al., 2016), and digital DNA-DNA hybridization (dDDH) was calculated with Genome-to-Genome Distance Calculator (GGDC) 2.1 (Auch et al., 2010). Graphical circular maps of chromosome and plasmid sequences were generated using the CGView Server (Grant and Stothard, 2008).

RESULTS

Shigella spp. Identification

S. flexneri isolates were identified using selective agar and API 20E strips and were also serotyped by the Texas Department of State Health Services. *S. flexneri* variant Y strain 06-2384 was isolated in the index case (*i.e.,* monkey 05-18). *S. flexneri* type 5b strains 06-2835 R1 and 06-2835 R2, which had different colony morphologies and API codes, were isolated from monkey 05-15. Strain 06-2836 was cultured from monkey 05-16. Following unsuccessful enrofloxacin treatment of paired monkeys 05-15 and 05-16, feces were collected from the cage pan and strain 06-3102 was cultured. These *S. flexneri* isolates were then analyzed for antibiotic susceptibility, the presence of *qnr* genes by PCR, and the ability to transfer plasmid-encoded antibiotic resistance genes to *E. coli* recipients by conjugation and transformation.

qnrS1 Gene Detected in *S. flexneri* Strains Isolated From Macaques

PCR detected *qnrS*, but not *qnrA* or *qnrB*, in both whole and plasmid DNA from all five *S. flexneri* isolates (Supplementary Figure 1). BLAST analysis of three representative *qnrS* PCR product sequences against the nr/nt database determined they were 100% identical to the plasmid-encoded *qnrS1* genes found in other *Enterobacteriaceae* species, including pAH0376 from *Shigella flexneri* 2b and pVQS1 from *Salmonella enterica*, indicating these novel *S. flexneri* strains harbor the *qnrS1* variant.

Antimicrobial Resistance Transferrable by Plasmid Conjugation and Transformation

Antimicrobial susceptibility testing of four *S. flexneri* isolates by microdilution indicated multi-drug resistance to ampicillin, cephalothin, ceftazidime, ceftriaxone, cefazolin, gentamicin (except strain 06-2835), nalidixic acid, and tetracycline and decreased susceptibility to amoxicillin-clavulanic acid, ciprofloxacin, enrofloxacin, and levofloxacin compared to the *E. coli* control strain ATCC25922 (**Table 1**). The *S. flexneri* isolates were in general susceptible to azithromycin, imipenem, cefoxitin, trimethoprim-sulfamethoxazole (**Table 1**).

Plasmid DNA from these *S. flexneri* isolates were successfully conjugated and transformed into the *E. coli* recipient strains J53 Az^r and Top10, respectively. Plasmid DNA isolated from all the transconjugants and transformants were PCR-positive for the *qnrS* gene (Supplementary Figure 2). Likewise, plasmid profiles were similar between the donor *S. flexneri* isolates and the *E. coli* transconjugants and transformants, indicating successful transfer of plasmid DNA to the recipients (**Figure 1**). The *S. flexneri* isolates have several bands in the plasmid profile, indicating they may harbor multiple different plasmids.

Compared to the naïve *E. coli* recipient strains J53 Az^r and Top10, the transconjugants and transformants demonstrated increased resistance to all quinolone antibiotics tested (**Table 1**). The MIC of the fluoroquinolones was 8- to 32-fold higher in the transconjugants and transformants, while nalidixic acid showed a 2- to 8-fold increase versus their naïve *E. coli* recipient strains (**Table 1**). The transconjugants and transformants also had increased resistance to amoxicillin-clavulanic acid as compared to the naïve *E. coli* recipient strains. All transconjugants and transformants were highly resistant to ampicillin and several cephalosporins, characteristic of beta-lactamase activity. The transconjugants and transformants demonstrated similar susceptibility to azithromycin, clarithromycin, gentamicin, tetracycline, and trimethoprim-sulfamethoxazole compared to their naïve *E. coli* recipient strains. Interestingly, when compared to the *S. flexneri* donor isolates, the transconjugants and transformants in general had about 2- to 8-fold lower MIC levels for some of the quinolones tested. This result suggests the novel *S. flexneri* isolates may have additional mechanisms to resist quinolones not harbored on the plasmid(s) transferred to the transconjugants and transformants.

Whole Genome Analysis of *S. flexneri* Strains Isolated From Macaques

To corroborate antibiotic resistance phenotypes, whole genome sequences of two representative *S. flexneri* isolates, 06-2384 and 06-3102, were obtained (summarized in **Table 2** and Supplementary Table 1). The genomes for *S. flexneri* 06-2384 and 06-3102 were assembled into 5 and 8 contigs, respectively. The largest contig for both isolates was ∼4.7 Mb with a G+C content of ∼50.9%, which is consistent with the chromosomal sequence of other *S. flexneri* genomes (Jin et al., 2002; Wei et al., 2003; Shen et al., 2017). Using PlasmidFinder-1.2, plasmid replicon sequences were detected in the remaining contigs, suggesting they are plasmids. Additionally, the top 5 BLAST hits for these contigs corresponded to plasmids sequences from *Shigella* spp., *E. coli*, *S. enterica*, *K. pneumoniae*, and *Citrobacter freundii* (Supplementary Table 2). Thus, *S. flexneri* 06-2384 and 06-3102 strains both appear to harbor several different plasmids in addition to their chromosome. This agrees with **Figure 1** in that several bands were apparent after separating plasmid DNA. Despite representing the serotype variants Y and 5b, both 06-2384 and 06-3102 were identified as ST245 by *in silico* MLST and had an ANI of 99.95% and a dDDH of 99.80%, indicating substantial genetic similarity. However, the difference in serotypes as well as the number/size of plasmids (**Figure 1** and **Table 2**) suggests more than one strain variant was present in the NHP colony.

Antibiotic Resistance Genes Detected by Whole Genome Analysis

ResFinder-2.1 identified several antibiotic resistance genes in the chromosome and plasmid sequences (**Table 2**). Aminoglycosides (*aadA1*, *aac(3)-IId*), beta-lactams (*blaOXA-1*), quinolones (*oqxA*, *oqxB*), chloramphenicol (*catA*), and tetracycline (*tet(B)*) resistance genes were detected in the chromosomes of both strains. In both genomes, *oqxA*, *oqxB*, and *aac(3)-IId* and *aadA1*, *blaOXA-1*, *catA1*, and *tet(B)* clustered together in separate regions. Both of these gene clusters were flanked by several mobile element protein, transposase, and integrase gene annotations. Mutations in the genes for DNA gyrase and topoisomerase subunits A and B were not identified in either of the genomes. Colistin resistance genes (*mcr-1*, *mcr-2*, and *mcr-3*) were also not identified.

TABLE 1 | MIC (μg/mL)[†].

Antibiotic class		*Shigella flexneri* donor (origin)				*E. coli* J53 transconjugants					*E. coli* Top10 transformants					Control *E. coli*	
		06-2384	06-2835	06-2836	06-3102	Naïve strain	06-2384	06-2835	06-2836	06-3102	Naïve strain	06-2384	06-2835	06-2836	06-3102	*E. coli* ATCC 25922	Breakpoint resistance
Macrolide	Azithromycin	1–2	1–2	2	2	8	8	8	8	8-16	4–8	4	4–8	8	4	4–8	N/A
	Clarithromycin	64	32–64	32–64	32–64	64–128	128	128	64	64–128	64–128	128	32–64	>128	64–128	64–128	N/A
Cephalosporin	Cephalothin	32–64	>128	>128	>128	16	32–64	32–64	>128	64	32	32	64–128	>128	32–64	32	≥32
	Ceftazidime	16	128	128	128	N/T	N/T	N/T	N/T	N/T	N/T	N/T	N/T	N/T	N/T	0.125	≥16
	Ceftriaxone	8	>128	>128	>128	N/T	N/T	N/T	N/T	N/T	N/T	N/T	N/T	N/T	N/T	0.06	≥4
	Cefazolin	32	>128	>128	>128	N/T	N/T	N/T	N/T	N/T	N/T	N/T	N/T	N/T	N/T	2	≥8
	Cefoxitin	4	4	4	4	N/T	N/T	N/T	N/T	N/T	N/T	N/T	N/T	N/T	N/T	4	≥32
Aminoglycoside	Gentamicin	>128	0.5–1	>128	>128	2	1–2	2	2	2–4	0.5–1	1	0.5–1	1–2	1–2	1–2	≥16
Tetracycline	Tetracycline	128	128	128	128	2	2	2	2	2–4	2–4	2	2–4	2	2–4	1–2	≥16
Quinolone	Nalidixic Acid	32	32–64	32–64	32	4–8	32	16	16	16	1–2	4–16	8–32	8	4–8	2–4	≥32
	Ciprofloxacin	1–2	1–2	1–2	1–2	0.015	0.5–1	0.5–1	0.5	0.5–1	<0.015	0.25–0.5	0.25–0.5	0.5	0.25–0.5	<0.015	≥4
	Enrofloxacin	1–4	1–4	1–4	1–4	0.03–0.06	1–2	0.125–2	1	1–2	<0.015	0.125–1	0.25–2	0.125–0.5	0.125–0.5	<0.015	≥4
	Levofloxacin	0.5–1	0.5–2	0.5–1	1–2	0.03–0.06	0.5–1	0.25–0.5	0.5–1	0.5–1	<0.015	0.125–0.25	0.25–0.5	0.25	0.125–0.25	<0.015	≥8
Beta-Lactam	Ampicillin	>256	>256	>256	>256	4	>256	>256	>256	>256	4–8	>256	>256	>256	>256	2–4	≥32
	Imipenem	0.03	0.03	0.03	0.03	N/T	N/T	N/T	N/T	N/T	N/T	N/T	N/T	N/T	N/T	0.03	≥4
	Amoxicillin-Clavulanic Acid	16	12	12–16	12	4	6–8	8–12	12	12	4	16	16	16	16	4–6	≥32
Sulfonamide	Trimethoprim-Sulfamethoxazole	0.064	0.064	0.064–0.094	0.064	0.064	0.19	0.064	0.064	0.064	0.032	0.032	0.047	0.047	0.032	0.19	≥4

[†] *N/A, not available; N/T, not tested.*

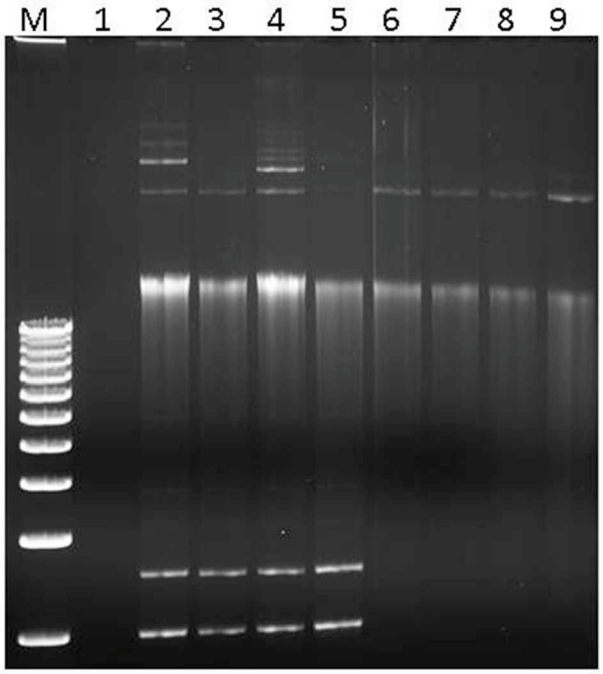

FIGURE 1 | Plasmid separation profiles of the donor *S. flexneri* isolates, naïve *E. coli* recipient strain, and *E. coli* transformants. Lane 1: naïve *E. coli* Top10 recipient. Lanes 2–5: *S. flexneri* isolates 06-3102, 06-2384, 06-2835, 06-2836. Lanes 6–9: *E. coli* transformants t-06-3102, t-06-2384, t-06-2835, t-06-2836. Similar results were obtained for the transconjugants (not shown).

The *qnrS* gene and beta-lactam resistance gene *blaTEM-1B* were detected on the 60 and 52 kb plasmid contigs for *S. flexneri* 06-2384 and 06-3102, respectively. BLAST analysis found these plasmid contigs were homologous to the completely-sequenced ∼40 kb, conjugative plasmid pVQS1 from *S. enterica* (Karczmarczyk et al., 2012) and the partially-sequenced ∼47 kb, conjugative plasmid pAH0376 from *Shigella flexneri* 2b (Hata et al., 2005), both of which harbor functional *blaTEM-1B* and *qnrS1* resistance genes. The annotated *qnrS* genes from the novel *S. flexneri* isolates showed 100% sequence identity and coverage to the *qnrS1* genes found in pAH0376 and pVQS1. In general, the resistance genes and flanking mobile element protein genes from *S. flexneri* 06-2384 and 06-3102 showed >98% identity and similar synteny to pVQS1 and pAH0376, except for the transposase genes *tinR* vs. *tnpA*, which had 31%, identify homology (**Figure 2**). Bidirectional BLASTP analysis using PATRIC's proteome comparison tool indicated >90% of the annotated genes in pVQS1 shared >97% identity to those of the *S. flexneri* 06-2384 and 06-3102 plasmid sequences, including homologs for replication and conjugation genes. This suggests these plasmid sequences from *S. flexneri* 06-2384 and 06-3102 have the potential for self-replication and ability to transfer to new hosts. The *S. flexneri* 06-2384 and 06-3102 plasmid sequences were identical to each other, except 06-3102 appears to contain a duplication of the region encoding *qnrS* and associated mobile element proteins. This second *qnrS* gene is truncated into a predicted 106 amino acid product and is likely non-functional as a result.

S. flexneri 06-3102 also contained the beta-lactam resistance gene *blaCTX-M-14* on a ∼86 kb plasmid contig. BLAST analysis of this plasmid contig detected >99% identity to the ∼74 kb IncFII2 plasmid pAC2901 from *C. freundii* strain AC290 that also encodes the *blaCTX-M-14* resistance gene. The remaining plasmid contig sequences from *S. flexneri* 06-2384 and 06-3102 showed BLAST homology to plasmids from *Enterboacteriaceae* species (Supplemental Table 2). These plasmid sequences were typed as ColRNAI using PlasmidFinder1.2, primarily contained hypothetical proteins, and some encoded phage-related gene annotations. Interestingly, the 15 and 19 kb plasmids from *S. flexneri* 06-2384 and 06-3102, respectively, were enriched for ferric enterobactin uptake protein *FepE* (8/17 and 9/25 annotations for *S. flexneri* 06-2384 and 06-3102, respectively), suggesting a role in iron acquisition.

Virulence Factor Genes Detected by Whole Genome Analysis

Using VirulenceFinder1.5, virulence factor genes were detected on the chromosome and ∼210 kb plasmid sequences from both isolates (**Table 2**). Additional potential virulence factor genes were also identified by BLASTP from the VFDB, Victors, and PATRIC_VF databases using the specialty genes feature hosted by PATRIC. This included 998 and 1,009 virulence factor genes detected in *S. flexneri* 06-2384 and 06-3102, respectively, with functions ranging from host adherence and invasion to biofilm formation and iron acquisition (Supplemental Table 3).

Of particular note, several serine protease autotransporters of *Enterobacteriaceae* (SPATE) enterotoxin genes were identified, which are implicated in diarrheal illness and gastrointestinal cytotoxicity by pathogenic *Shigella* spp. and *E. coli* infection (Dautin, 2010; Mattock and Blocker, 2017). For both *S. flexneri* 06-2384 and 06-3102, these include the chromosomally-encoded *Shigella* enterotoxin 1 (*ShET1*), protease involved in intestinal colonization (*Pic*), and *Shigella* extracellular protein A (*SigA*) genes, which have been shown to exert cytotoxicity to epithelial cells, mediate serum resistance, induce fluid secretion, and degrade mucus/mucin (Dautin, 2010; Faherty et al., 2012; Mattock and Blocker, 2017). Two paralogs for *ShET2* along with type III secretion system (T3SS) components and conjugative transfer genes were identified on the ∼210 kb, IncFII plasmids in both *S. flexneri* 06-2384 and 06-3102. These *ShET2* paralogs are T3SS effector proteins that induce secretory activity by the gastrointestinal epithelium to cause fluid-laden diarrhea (Farfan et al., 2011; Faherty et al., 2012; Mattock and Blocker, 2017).

DISCUSSION

In this study, five novel, multiple-antibiotic resistant *S. flexneri* isolates were cultured from the feces of three macaques maintained in a biomedical research colony. MIC testing demonstrated these *S. flexneri* isolates were resistant or have decreased susceptibility to beta-lactam, cephalosporin, aminoglycoside, tetracycline, and quinolone, but were susceptible

TABLE 2 | Genomic characteristics of representative *Shigella flexneri* isolates.

Isolate	Contig No.[a]	Contig size (bp)	G+C content (%)	Protein coding sequences	Antibiotic resistance genes[b]	Virulence genes[c]	Plasmid type[d]	GenBank accession
S. flexneri 06-2384	1	4,687,966	50.88	5,092	*aadA1*, *aac(3)-IId, blaOXA-1, oqxA, oqxB, catA, tet(B)*	*ipaH9.8, gad* (2 copies), *sigA, pic, lpfA*	–	NXME00000000
	2	214,255	45.89	314	–	*capU, ipaD, virF*	IncFII	
	3	87,520	48.39	119	–	–	ColRNAI	
	4	60,354	50.64	86	*blaTEM-1B, qnrS1*	–	IncN	
	5	15,063	45.43	17	–	–	ColRNAI	
S. flexneri 06-3102	1	4,731,519	50.87	5,182	*aadA1*, *aac(3)-IId, blaOXA-1, oqxA, oqxB, catA, tet(B)*	*ipaH9.8, gad* (2 copies), *sigA, pic, lpfA*	–	NXMF00000000
	2	211,922	44.65	299	–	*capU, ipaD, virF*	IncFII	
	3	86,076	51.83	108	*blaCTX-M-14*	–	IncFII	
	4	6,2689	48.22	81	–	–	IncN	
	5	52001	50.82	75	*blaTEM-1B, qnrS1*	–	ColRNAI	
	6	19,452	45.33	25	–	–	ColRNAI	
	7	12,688	48.84	17	–	–	ColRNAI	
	8	9,913	53.04	23	–	–	ColRNAI	

[a] *Graphical circular maps of the chromosome and plasmid sequences available in Supplementary Figure 3.*
[b] *Antibiotic resistance genes detected using ResFinder 2.1.*
[c] *Virulence factor genes detected using VirulenceFinder 1.5.*
[d] *Plasmid type predicted using PlasmidFinder 1.3.*

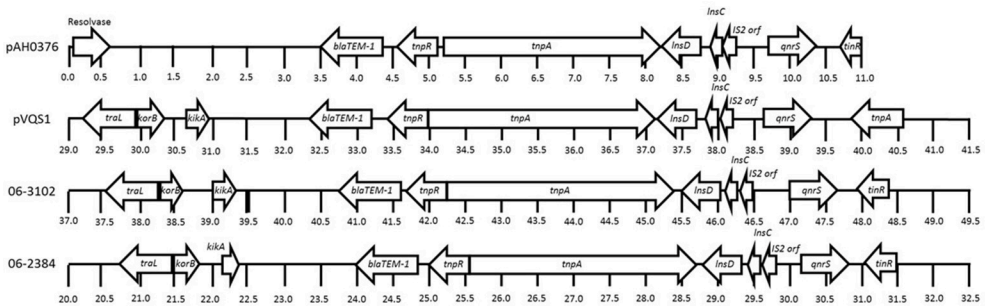

FIGURE 2 | Comparative alignment showing the *blaTEM-1B*, *qnrS*, and flanking mobile element protein genes from the plasmid sequences of pAH0376 (*Shigella flexneri* 2b; GenBank: AB187515.1), pVQS1 (*Salmonella enterica*; GenBank: JQ609357.1), and *Shigella flexneri* 06-2384 and 06-3102 have nearly identical homology and synteny. Arrowheads represent annotated protein coding sequences and direction of their transcription. Numbers below each sequence represent distance expressed in kilobases.

to macrolide and sulfonamide antibiotic classes. Treatment with trimethoprim-sulfadiazine successfully eradicated *S. flexneri* infection in two of these animals, while infection in the third appeared to be self-limiting after post-surgical use of enrofloxacin. The purpose of this study was to understand the potential mechanisms of multi-drug resistance in these novel *S. flexneri* isolates.

PCR of plasmid-enriched DNA detected the *qnrS*, but not *qnrA* or *qnrB*, in all of the *S. flexneri* isolates. The sequences of the *qnrS* genes had 100% homology to the plasmid-encoded *qnrS1* genes from *S. flexneri* and other *Enterobacteriaceae* species with quinolone resistance phenotypes. This suggested quinolone resistance in the novel *S. flexneri* isolates was mediated by a plasmid-encoded *qnrS1* gene. To test this, quinolone-susceptible *E. coli* strains were introduced with plasmid DNA from the novel *S. flexneri* isolates via conjugation or transformation and then tested for antibiotic resistance. Plasmid DNA isolated from the transconjugants and transformants was PCR-positive for the *qnrS* gene. The transconjugants and transformants demonstrated decreased susceptibility to quinolones and resistance to beta-lactam antibiotics compared to their respective naïve *E. coli* recipient strains. When compared to their respective *S. flexneri*

donor isolates, the transconjugants and transformants in general had lower resistance to the quinolones.

To further support that the novel *S. flexneri* isolates harbored plasmid-encoded *qnrS* genes and to identify other mechanisms for quinolone resistance, whole genome sequences were obtained for two representative isolates. Consistent with the MIC results, antibiotic resistance genes for aminoglycosides (*aadA1*, *aac(3)-IId*), beta-lactams (*blaOXA-1*), quinolones (*oqxA*, *oqxB*), and tetracycline (*tet(B)*) were detected in their chromosomes. The *catA* was also detected in the chromosomes, suggesting these isolates have the potential for chloramphenicol resistance, although this was not experimentally confirmed. The *oqxA* and *oqxB* genes have been previously identified in *E. coli*, *K. pneumoniae*, and *K. oxytoca* isolates and encode multi-drug efflux pumps against quinolones that yield low-level resistance (Poirel et al., 2012; Andres et al., 2013; Rodriguez-Martinez et al., 2013).

In both *S. flexneri* genomes, *qnrS* was co-associated with *blaTEM-1B* on plasmid-like sequences that had identical homology and synteny to pAH0376 and pVQS1 from *S. flexneri* 2b and *S. enterica*, respectively. Additionally, as observed for pAH0376 and pVQS1, these plasmids could be experimentally transferred to *E. coli*, conferring the recipients with quinolone and beta-lactam resistance (Hata et al., 2005; Karczmarczyk et al., 2012). The activity of *oqxA* and *oqxB* combined with *qnrS* may enhance overall quinolone resistance in these *S. flexneri* isolates and may explain why the *E. coli* recipients demonstrated less resistance to quinolones compared to their donor counterparts.

A recently published study surveyed the prevalence of antimicrobial resistance in zoonotic pathogens cultured from NHPs across several different biomedical research institutions in the United States (Kim et al., 2017). The authors found that enrofloxacin is the primary antibiotic chosen by veterinarians for treating diarrhea and gingivitis caused by presumptive *S. flexneri* infection, and while diagnostic labs commonly screen *S. flexneri* isolates for enrofloxacin resistance, no resistant strains were reported. A major caveat of this study is the small number of participating institutions; only seven institutions participated, and antibiotic resistance data was obtained from just three. Likewise, the methods used to detect and characterize antibiotic resistance potential were inconsistent between institutions. Therefore, estimations of resistance to enrofloxacin and other quinolones by *S. flexneri* could have been underreported or missed.

The World Health Organization (WHO) classifies quinolones as the highest priority of clinically important antibiotics based on it being a limited available therapy option to treat serious bacterial infections with a high risk of zoonosis and an ability to acquire antibiotic resistance genes (WHO, 2017). The Centers for Disease Control and Prevention (CDC) recognizes that *Shigella* spp. are becoming increasingly resistant to fluoroquinolones and other antibiotics (CDC, 2017). The CDC recommends that fluoroquinolones should be avoided when the MIC for ciprofloxacin is $\geq$0.12 μg/mL, even though this is classified as "susceptible" according to CLSI criteria. The novel *S. flexneri* isolates and their *E. coli* transconjugants/transformants in this study had MICs for ciprofloxacin of 0.25–2 μg/mL, which though below the CLSI criteria for resistance, meet the CDC's standard for excluding fluoroquinolones to treat *Shigella* spp.

According to the latest report by the National Antimicrobial Resistance Monitoring System (2016), as well as the survey by Kim et al. (2017), *S. flexneri* isolates from humans and NHP's frequently demonstrate resistance to more than one class of antibiotics. *Shigella* spp. can also exhibit multi-drug resistance with substantial diversity observed in their resistance profiles. As observed for the *S. flexneri* isolates in this study, resistance or decreased susceptibility to beta-lactam, cephalosporin, aminoglycoside, and tetracycline antibiotic classes, along with quinolones, was noted. The co-association of *qnrS1* and *blaTEM-1B* and other antibiotic resistance gene clusters poses a particular risk in predicting successful eradication strategies. Therefore, culture for *Shigella* spp. and other enteric pathogens followed by antibiotic testing should be perform prior to initiation of treatment.

The finding of quinolone-resistant *S. flexneri* in this study may reflect the common use of enrofloxacin to preemptively treat suspected shigella-induced diarrheal disease commonly encountered in newly imported macaques from Asia (Fox, 1975; Tribe and Fleming, 1983; Line et al., 1992; Banish et al., 1993). Macaques co-housed or maintained in groups can also readily acquire *Shigella* spp. infections from other infected monkeys via fecal/oral or oral/oral routes (Shipley et al., 2010). Cross-transmission of *Shigella* spp. could have occurred in our colony because animals were co-housed in adjacent cages within the same animal facility. In two of the three rhesus monkeys, a standard enrofloxacin regimen failed to eradicate the *S. flexneri* infection, but trimethoprim-sulfadiazine treatment was successful. Trimethoprim-sulfamethoxazole has been reported to successfully eradicate *Shigella* spp. infection in a colony of wild-caught rhesus monkeys (Pucak et al., 1977). *S. flexneri* in the third rhesus was eliminated during a 10-day course of enrofloxacin treatment. Shigellosis in humans is known to typically resolve within 5–7 days without antibiotic treatment (Hale and Keusch, 1996), so it is possible infection was self-limiting in this individual.

Humans can become infected with *Shigella* spp. through contact with NHPs in research or zoo setting or maintained as pets (Fox, 1975; Tribe and Fleming, 1983; Kennedy et al., 1993). *Shigella* spp. infection in humans can readily transmit from person-to-person or through contaminated food or water (Scallan et al., 2011). Additionally, ciprofloxacin has continued to be one of the most commonly prescribed antibiotics for treating shigellosis in human patients despite the discovery of ciprofloxacin-resistant *Shigella* spp. and plasmid-mediated quinolone resistant strains of *S. flexneri* (Bowen et al., 2015; CDC, 2017). Therefore, *S. flexneri* isolates with the capacity to spread and acquire quinolone resistance genes represent not only an institutional concern when treating NHPs, but also a public health concern considering the zoonotic potential of these pathogens. Strict hygienic principles should also be implemented and always followed by personnel in contact with NHPs in order to reduce risk of acquiring infection.

In conclusion, this study demonstrates for the first time the discovery of plasmid-mediated quinolone resistance

genes in multiple-antibiotic drug resistant *S. flexneri* isolated from research macaques. Given that antibiotic treatments, such as enrofloxacin, are often prescribed empirically and prophylactically, the findings of this study stress the need to test for antibiotic susceptibility in NHPs with suspected *Shigella* spp. infection beforehand in order to appropriately treat these animals and reduce zoonotic risk.

ETHICS STATEMENT

All procedures were performed under animal protocols approved by the Massachusetts Institute of Technology Committee on Animal Care (CAC) and in accordance with the guidelines for animal care at Massachusetts Institute of Technology. Animals were cared for in an AAALAC International-accredited animal facility at MIT under federal, state, local and NIH guidelines for animal care.

AUTHOR CONTRIBUTIONS

AM, HM, ZS, JD-F, and AG characterized novel Shigella isolates. EB cultured novel Shigella isolates. HM, RM, and MP provided veterinary clinical work up of non-human primates, including sample collection. AM, HM, JD-F, and JF wrote and/or reviewed manuscript.

FUNDING

This study was supported by NIH grants T32-OD010978-26 (JF), P30-ES002109 (JF).

SUPPLEMENTARY MATERIAL

The Supplementary Material for this article can be found online at: https://www.frontiersin.org/articles/10.3389/fmicb.2018.00311/full#supplementary-material

REFERENCES

Andres, P., Lucero, C., Soler-Bistue, A., Guerriero, L., Albornoz, E., Tran, T., et al. (2013). Differential distribution of plasmid-mediated quinolone resistance genes in clinical enterobacteria with unusual phenotypes of quinolone susceptibility from Argentina. *Antimicrob. Agents Chemother.* 57, 2467–2475. doi: 10.1128/AAC.01615-12

Armitage, G. C., Newbrun, E., Hoover, C. I., and Anderson, J. H. (1982). Periodontal disease associated with *Shigella flexneri* in rhesus monkeys. Clinical, microbiologic and histopathologic findings. *J. Periodontal Res.* 17, 131–144. doi: 10.1111/j.1600-0765.1982.tb01139.x

Auch, A. F., Klenk, H. P., and Goker, M. (2010). Standard operating procedure for calculating genome-to-genome distances based on high-scoring segment pairs. *Stand. Genomic Sci.* 2, 142–148. doi: 10.4056/sigs.541628

Aziz, R. K., Bartels, D., Best, A. A., DeJongh, M., Disz, T., Edwards, R. A., et al. (2008). The RAST Server: rapid annotations using subsystems technology. *BMC Genomics* 9:75. doi: 10.1186/1471-2164-9-75

Banish, L. D., Sims, R., Sack, D., Montali, R. J., Phillips, L. Jr., and Bush, M. (1993). Prevalence of shigellosis and other enteric pathogens in a zoologic collection of primates. *J. Am. Vet. Med. Assoc.* 203, 126–132.

Bowen, A., Hurd, J., Hoover, C., Khachadourian, Y., Traphagen, E., Harvey, E., et al. (2015). Importation and domestic transmission of *Shigella sonnei* resistant to ciprofloxacin - United States, May 2014-February 2015. *Morbid. Mortal. Week. Rep.* 64, 318–320.

Carattoli, A., Zankari, E., Garcia-Fernandez, A., Voldby Larsen, M., Lund, O., Villa, L., et al. (2014). *In silico* detection and typing of plasmids using *PlasmidFinder* and *plasmid multilocus* sequence typing. *Antimicrob. Agents Chemother.* 58, 3895–3903. doi: 10.1128/AAC.02412-14

Cattoir, V., Weill, F. X., Poirel, L., Fabre, L., Soussy, C. J., and Nordmann, P. (2007). Prevalence of qnr genes in *Salmonella* in France. *J. Antimicrob. Chemother.* 59, 751–754. doi: 10.1093/jac/dkl547

CDC (2017). *CDC Recommendations for Diagnosing and Managing Shigella Strains with Possible Reduced Susceptibility to Ciprofloxacin*. Atlanta, GA: U.S. Department of Health and Human Services.

Dautin, N. (2010). Serine protease autotransporters of enterobacteriaceae (SPATEs): biogenesis and function. *Toxins* 2, 1179–1206. doi: 10.3390/toxins2061179

Faherty, C. S., Harper, J. M., Shea-Donohue, T., Barry, E. M., Kaper, J. B., Fasano, A., et al. (2012). Chromosomal and plasmid-encoded factors of *Shigella flexneri* induce secretogenic activity *ex vivo*. *PLoS ONE* 7:e49980. doi: 10.1371/journal.pone.0049980

Farfan, M. J., Toro, C. S., Barry, E. M., and Nataro, J. P. (2011). Shigella enterotoxin-2 is a type III effector that participates in Shigella-induced interleukin 8 secretion by epithelial cells. *FEMS Immunol. Med. Microbiol.* 61, 332–339. doi: 10.1111/j.1574-695X.2011.00778.x

Fox, J. G. (1975). Transmissible drug resistance in *Shigella* and *Salmonella* isolated from pet monkeys and their owners. *J. Med. Primatol.* 4, 165–171. doi: 10.1159/000459850

Grant, J. R., and Stothard, P. (2008). The CGView Server: a comparative genomics tool for circular genomes. *Nucleic Acids Res.* 36, W181–W184. doi: 10.1093/nar/gkn179

Hale, T. L., and Keusch, G. T. (1996). "Shigella," in *Medical Microbiology, 4th edn*, ed S. Baron (Galveston, TX: University of Texas Medical Branch at Galveston).

Hata, M., Suzuki, M., Matsumoto, M., Takahashi, M., Sato, K., Ibe, S., et al. (2005). Cloning of a novel gene for quinolone resistance from a transferable plasmid in *Shigella flexneri* 2b. *Antimicrob. Agents Chemother.* 49, 801–803. doi: 10.1128/AAC.49.2.801-803.2005

Jin, Q., Yuan, Z., Xu, J., Wang, Y., Shen, Y., Lu, W., et al. (2002). Genome sequence of *Shigella flexneri* 2a: insights into pathogenicity through comparison with genomes of *Escherichia coli* K12 and O157. *Nucleic Acids Res.* 30, 4432–4441. doi: 10.1093/nar/gkf566

Joensen, K. G., Scheutz, F., Lund, O., Hasman, H., Kaas, R. S., Nielsen, E. M., et al. (2014). Real-time whole-genome sequencing for routine typing, surveillance, and outbreak detection of verotoxigenic *Escherichia coli*. *J. Clin. Microbiol.* 52, 1501–1510. doi: 10.1128/JCM.03617-13

Karczmarczyk, M., Stephan, R., Hachler, H., and Fanning, S. (2012). Complete nucleotide sequence of pVQS1 containing a quinolone resistance determinant from *Salmonella enterica* serovar Virchow associated with foreign travel. *J. Antimicrob. Chemother.* 67, 1861–1864. doi: 10.1093/jac/dks158

Kennedy, F. M., Astbury, J., Needham, J. R., and Cheasty, T. (1993). Shigellosis due to occupational contact with non-human primates. *Epidemiol. Infect.* 110, 247–251. doi: 10.1017/S0950268800068163

Kim, J., Coble, D. J., Salyards, G. W., Bower, J. K., Rinaldi, W. J., Plauche, G. B., et al. (2017). Antimicrobial use for and resistance of zoonotic bacteria recovered from nonhuman primates. *Comp. Med.* 67, 79–86.

Larsen, M. V., Cosentino, S., Rasmussen, S., Friis, C., Hasman, H., Marvig, R. L., et al. (2012). Multilocus sequence typing of total-genome-sequenced bacteria. *J. Clin. Microbiol.* 50, 1355–1361. doi: 10.1128/JCM.06094-11

Lee, I., Ouk Kim, Y., Park, S. C., and Chun, J. (2016). OrthoANI: an improved algorithm and software for calculating average nucleotide identity. *Int. J. Syst. Evol. Microbiol.* 66, 1100–1103. doi: 10.1099/ijsem.0.000760

Line, A. S., Paul-Murphy, J., Aucoin, D. P., and Hirsh, D. C. (1992). Enrofloxacin treatment of long-tailed macaques with acute bacillary dysentery due to multiresistant *Shigella flexneri* IV. *Lab. Anim. Sci.* 42, 240–244.

Mammeri, H., M., Van De Loo, Poirel, L., Martinez-Martinez, L., and Nordmann, P. (2005). Emergence of plasmid-mediated quinolone resistance

in *Escherichia coli* in Europe. *Antimicrob. Agents Chemother.* 49, 71–76. doi: 10.1128/AAC.49.1.71-76.2005

Martinez-Martinez, L., Pascual, A., and Jacoby, G. A. (1998). Quinolone resistance from a transferable plasmid. *Lancet* 351, 797–799. doi: 10.1016/S0140-6736(97)07322-4

Mattock, E., and Blocker, A. J. (2017). How do the virulence factors of shigella work together to cause disease? *Front. Cell. Infect. Microbiol.* 7:64. doi: 10.3389/fcimb.2017.00064

McClure, H. M., Alford, P., and Swenson, B. (1976). Nonenteric *Shigella* infections in nonhuman primates. *J. Am. Vet. Med. Assoc.* 169, 938–939.

National Antimicrobial Resistance Monitoring System (2016). *National Antimicrobial Resistance Monitoring System for Enteric Bacteria (NARMS): Human Isolates Surveillance Report for 2014.* Final Report, U.S. Department of Health and Human Services, Atlanta, GA.

Poirel, L., Cattoir, V., and Nordmann, P. (2012). Plasmid-mediated quinolone resistance; interactions between human, animal, and environmental ecologies. *Front. Microbiol.* 3:24. doi: 10.3389/fmicb.2012.00024

Pucak, G. J., Orcutt, R. P., Judge, R. J., and Rendon, F. (1977). Elimination of the Shigella carrier state in rhesus monkeys (*Macaca mulatta*) by trimethoprim-sulfamethoxazole. *J. Med. Primatol.* 6, 127–132. doi: 10.1159/000459732

Redgrave, L. S., Sutton, S. B., Webber, M. A., and Piddock, L. J. (2014). Fluoroquinolone resistance: mechanisms, impact on bacteria, and role in evolutionary success. *Trends Microbiol.* 22, 438–445. doi: 10.1016/j.tim.2014.04.007

Robicsek, A., Strahilevitz, J., Sahm, D. F., Jacoby, G. A., and Hooper, D. C. (2006). *qnr* prevalence in ceftazidime-resistant *Enterobacteriaceae* isolates from the United States. *Antimicrob. Agents Chemother.* 50, 2872–2874. doi: 10.1128/AAC.01647-05

Rodriguez-Martinez, J. M., Diaz de Alba, P., Briales, A., Machuca, J., Lossa, M., Fernandez-Cuenca, F., et al. (2013). Contribution of OqxAB efflux pumps to quinolone resistance in extended-spectrum-β-lactamase-producing *Klebsiella pneumoniae*. *J. Antimicrob. Chemother.* 68, 68–73. doi: 10.1093/jac/dks377

Scallan, E., Hoekstra, R. M., Angulo, F. J., Tauxe, R. V., Widdowson, M. A., Roy, S. L., et al. (2011). Foodborne illness acquired in the United States–major pathogens. *Emerging Infect. Dis.* 17, 7–15. doi: 10.3201/eid1701.P11101

Shen, P., Fan, J., Guo, L., Li, J., Li, A., Zhang, J., et al. (2017). Genome sequence of Shigella flexneri strain SP1, a diarrheal isolate that encodes an extended-spectrum β-lactamase (ESBL). *Ann. Clin. Microbiol. Antimicrob.* 16:37. doi: 10.1186/s12941-017-0212-2

Shipley, S. T., Panda, A., Khan, A. Q., Kriel, E. H., Maciel, M. Jr., Livio, S., et al. (2010). A challenge model for *Shigella dysenteriae* 1 in cynomolgus monkeys (*Macaca fascicularis*). *Comp. Med.* 60, 54–61.

Clinical and Laboratory Standards Institute (2010). *Performance Standards for Antimicrobial Disk Susceptibility Tests, Approved Standard, 10th Edn*. Wayne, PA.

Clinical and Laboratory Standards Institute (2012). *Methods for Dilution Antimicrobial Susceptibility Tests for Bacteria that Grow Aerobically, Approved Standard, 9th Edn*. Wayne, PA.

Clinical and Laboratory Standards Institute (2014). *Performance Standards for Antimicrobial Susceptibility Testing; Twenty-Fourth Informational Supplement (M100-S24).* Wayne, PA.

Strahilevitz, J., Jacoby, G. A., Hooper, D. C., and Robicsek, A. (2009). Plasmid-mediated quinolone resistance: a multifaceted threat. *Clin. Microbiol. Rev.* 22, 664–689. doi: 10.1128/CMR.00016-09

Tran, J. H., and Jacoby, G. A. (2002). Mechanism of plasmid-mediated quinolone resistance. *Proc. Natl. Acad. Sci. U.S.A.* 99, 5638–5642. doi: 10.1073/pnas.082092899

Tran, J. H., Jacoby, G. A., and Hooper, D. C. (2005a). Interaction of the plasmid-encoded quinolone resistance protein Qnr with *Escherichia coli* DNA gyrase. *Antimicrob. Agents Chemother.* 49, 118–125. doi: 10.1128/AAC.49.1.118-125.2005

Tran, J. H., Jacoby, G. A., and Hooper, D. C. (2005b). Interaction of the plasmid-encoded quinolone resistance protein QnrA with *Escherichia coli* topoisomerase IV. *Antimicrob. Agents Chemother.* 49, 3050–3052. doi: 10.1128/AAC.49.7.3050-3052.2005

Tribe, G. W., and Fleming, M. P. (1983). Biphasic enteritis in imported cynomolgus (*Macaca fascicularis*) monkeys infected with *Shigella*, *Salmonella* and *Campylobacter* species. *Lab. Anim.* 17, 65–69. doi: 10.1258/002367783781070957

Wang, M., Sahm, D. F., Jacoby, G. A., and Hooper, D. C. (2004). Emerging plasmid-mediated quinolone resistance associated with the qnr gene in *Klebsiella pneumoniae* clinical isolates in the United States. *Antimicrob. Agents Chemother.* 48, 1295–1299. doi: 10.1128/AAC.48.4.1295-1299.2004

Wattam, A. R., Abraham, D., Dalay, O., Disz, T. L., Driscoll, T., Gabbard, J. L., et al. (2014). PATRIC, the bacterial bioinformatics database and analysis resource. *Nucleic Acids Res.* 42, D581–D591. doi: 10.1093/nar/gkt1099

Wattam, A. R., Davis, J. J., Assaf, R., Boisvert, S., Brettin, T., Bun, C., et al. (2017). Improvements to PATRIC, the all-bacterial bioinformatics database and analysis resource center. *Nucleic Acids Res.* 45, D535–D542. doi: 10.1093/nar/gkw1017

Wei, J., Goldberg, M. B., Burland, V., Venkatesan, M. M., Deng, W., Fournier, G., et al. (2003). Complete genome sequence and comparative genomics of *Shigella flexneri* serotype 2a strain 2457T. *Infect. Immun.* 71, 2775–2786. doi: 10.1128/IAI.71.5.2775-2786.2003

WHO (2017). *Critically Important Antimicrobials for Human Medicine, 5th Edn*. Geneva: World Health Organization.

Zankari, E., Hasman, H., Cosentino, S., Vestergaard, M., Rasmussen, S., Lund, O., et al. (2012). Identification of acquired antimicrobial resistance genes. *J. Antimicrob. Chemother.* 67, 2640–2644. doi: 10.1093/jac/dks261

Conflict of Interest Statement: The authors declare that the research was conducted in the absence of any commercial or financial relationships that could be construed as a potential conflict of interest.

frontiers in Microbiology

ORIGINAL RESEARCH
published: 11 May 2018
doi: 10.3389/fmicb.2018.00920

Distribution and Genetic Characteristics of SXT/R391 Integrative Conjugative Elements in *Shewanella* spp. From China

*Yujie Fang[1,2,3], Yonglu Wang[4], Zhenpeng Li[1,2], Zongdong Liu[5], Xinyue Li[1,2], Baowei Diao[1,2], Biao Kan[1,2] and Duochun Wang[1,2,3]**

[1] State Key Laboratory of Infectious Disease Prevention and Control, National Institute for Communicable Disease Control and Prevention, Chinese Center for Disease Control and Prevention, Beijing, China, [2] Collaborative Innovation Center for Diagnosis and Treatment of Infectious Diseases, Hangzhou, China, [3] Center for Human Pathogen Collection, Chinese Center for Disease Control and Prevention, Beijing, China, [4] Ma'anshan Center for Disease Control and Prevention, Ma'anshan, China, [5] Laizhou Center for Disease Control and Prevention, Laizhou, China

OPEN ACCESS

Edited by:
Yonghong Xiao,
Zhejiang University, China

Reviewed by:
Michael P. Ryan,
University of Limerick, Ireland
Maria Soledad Ramirez,
California State University,
United States

***Correspondence:**
Duochun Wang
wangduochun@icdc.cn

Specialty section:
This article was submitted to Antimicrobials, Resistance and Chemotherapy, a section of the journal Frontiers in Microbiology

Received: 17 October 2017
Accepted: 20 April 2018
Published: 11 May 2018

Citation:
Fang Y, Wang Y, Li Z, Liu Z, Li X, Diao B, Kan B and Wang D (2018) Distribution and Genetic Characteristics of SXT/R391 Integrative Conjugative Elements in Shewanella spp. From China. Front. Microbiol. 9:920. doi: 10.3389/fmicb.2018.00920

The genus *Shewanella* consists of facultatively anaerobic Gram-negative bacteria, which are regarded as potential agents of food contamination and opportunistic human pathogens. Information about the distribution and genetic characteristics of SXT/R391 integrative conjugative elements (ICEs) in *Shewanella* species is limited. Here, 91 *Shewanella* strains collected from diverse samples in China were studied for the presence of SXT/R391 ICEs. Three positive strains, classified as *Shewanella upenei*, were obtained from patients and water from a local mill. In light of their close clonal relationships and high sequence similarity, a representative ICE was selected and designated ICE*Sup*CHN110003. The BLASTn searches against GenBank showed that ICE*Vch*Ban5 was most closely related to ICE*Sup*CHN110003, with the coverage of 76% and identity of 99%. The phylogenetic tree of concatenated core genes demonstrated that ICE*Sup*CHN110003 formed a distinct branch outside the cluster comprising ICE*Val*A056-1, ICE*Pmi*CHN2410, and ICE*Pmi*Chn1. Comparison of the genetic structures revealed that ICE*Sup*CHN110003 encoded uncommon genes in hotspots, such as specific type III restriction-modification system, conferring adaptive functions to the host. Based on the low coverage in the sequence analysis, independent clade in the phylogenetic tree, and unique inserted fragments in hotspots, ICE*Sup*CHN110003 represented a novel SXT/R391 element, which widened the list of ICEs. Furthermore, the antibiotic resistance genes *floR*, *strA*, *strB*, and *sul2* in ICE*Sup*CHN110003 and resistance to multiple drugs of the positive isolates were detected. A cross-species transfer capability of the SXT/R391 ICEs was also discovered. In summary, it is necessary to reinforce continuous surveillance of SXT/R391 ICEs in the genus *Shewanella*.

Keywords: distribution, genetic characteristics, SXT/R391, integrative conjugative elements, *Shewanella*, China

INTRODUCTION

In the last two decades, it has become known that horizontal gene transfer (HGT) plays a leading role in the evolutionary and environmental adaptation of bacteria (Hacker and Kaper, 2000; Juhas et al., 2009). The significance of HGT is ascribed to mobile genetic elements (MGEs) (Wozniak and Waldor, 2010). In essence, MGEs are discrete DNA segments involved in the transmission of various genes and constitute a crucial driving force in bacterial evolution. Previously described conjugative transposons, prophages, and integrative conjugative elements (ICEs) are members of the MGE family (Juhas et al., 2009). Among them, ICEs comprise a large number of self-transmissible elements, which can integrate into bacterial chromosomes, excise from their host chromosome, form a transient circular intermediate, transfer to another cell and reintegrate into the new host's chromosome at the target site (Burrus et al., 2006; Wozniak and Waldor, 2010).

SXT/R391 elements belong to an ICE family, and to date, at least 89 ICEs from the SXT/R391 family have been identified[1] (Bi et al., 2012). SXT/R391 ICEs have been found in different sources, including clinical, food, and environmental samples, and they share a conserved integrase that mediates the integration into the 5′ end of the *prfC* gene in the host chromosome (Burrus et al., 2006; Wozniak et al., 2009). SXT is an ∼100 kb ICE, which was originally detected in *Vibrio cholerae* O139 (Waldor et al., 1996), and R391 (89 kb) was identified in *Providencia rettgeri* in 1972 (Coetzee et al., 1972). SXT and R391 have been grouped in an ICE family containing 52 nearly identical core genes. Some of them are involved in the process of integration/excision, conjugative transfer, and regulation, while other core genes may encode functions that enhance ICE fitness to the environment. In addition to the core modules, five hotspots (HS1–5) and four variable regions (VRI–VRIV) have been reported, which contain inserted variable genes conferring resistance to antibiotics and heavy metals (Wozniak et al., 2009; Lei et al., 2016).

The genus *Shewanella* includes motile Gram-negative bacilli, which are widely distributed in marine habitats (Ronconi et al., 1999; Dikow, 2011). Currently, more than 60 species of *Shewanella* have been recognized[2]. They have been isolated from diverse samples and identified as potential agents of food contamination and opportunistic pathogens of humans. Among them, four species have been reported to cause human infections, i.e., *Shewanella putrefaciens*, *Shewanella algae*, *Shewanella haliotis*, and *Shewanella xiamenensis*. The majority of *Shewanella*-associated syndromes involve skin and soft-tissue infections (Pagani et al., 2003; Goyal et al., 2011; Rouzic et al., 2012), followed by blood borne illnesses (Dominguez et al., 1996) and infections of the biliary tree (Liu et al., 2013; Janda and Abbott, 2014).

The first complete SXT/R391 ICE reported in *Shewanella* species was a novel R391-like element, ICE*Spu*PO1, derived from *S. putrefaciens* W3-18-1, which was isolated from the Pacific Ocean 10 years ago (Pembroke and Piterina, 2006). SXT/R391 ICEs in the genus *Shewanella* have also been detected in *S. haliotis* in Portugal (Rodriguez-Blanco et al., 2012) and *S. fidelis* in Japan (Nonaka et al., 2012). ICE*Sha*Por1 of *S. haliotis*, available in GenBank, is only an amplified fragment of specific hotspot regions. The SXT/R391 element from the species *S. fidelis* has merely been documented by Nonaka et al. (2014), and the lack of public submission makes it impossible to compare. Recently, several novel SXT/R391 ICEs have been reported among *Vibrio* (Song et al., 2013; Wang et al., 2016) and *Proteus* (Lei et al., 2016; Li et al., 2016) species in China. However, little information is available on the distribution and genetic characteristics of SXT/R391 ICEs from *Shewanella* species in China. In this study, we screened 91 *Shewanella* strains, which were isolated between 2007 and 2016 in China, by targeting the int_{SXT} gene. We also investigated the sequence similarities, evolutionary relationships and genetic structures of novel SXT/R391 ICEs from *Shewanella* species. Further, antibiotic susceptibility of the positive isolates and the transfer capability of the SXT/R391 ICEs were determined.

MATERIALS AND METHODS

Bacterial Isolation, Taxonomic Identification, and PFGE Characterization of *Shewanella* Strains

In this study, a total of 91 *Shewanella* isolates obtained from diverse sources were included. The collections of *Shewanella* isolates comprised of fecal specimens of diarrhea patients (n = 45), food samples (n = 39), and environments (n = 7) from four provinces (Anhui, Hainan, Liaoning, and Shandong) in China during the years 2007–2016. Pure bacterial cultures with pink–orange colored colonies were obtained on LB agar according to standard procedures described previously (Lei et al., 2016; Li et al., 2016). The taxonomy of *Shewanella* isolates was identified by the amplification and sequencing of 16S rRNA with universal primers 27F and 1492R (Lane, 1991). The *Shewanella* isolates were further characterized by pulsed field gel electrophoresis (PFGE) after the genomic DNA digestion of *Xba*I (Fermentas, United States) (Cooper et al., 2006). The results of PFGE were analyzed by Bionumerics software (Applied Maths, Belgium) to estimate the clonal relationships between different *Shewanella* isolates.

PCR Screening, Genome Sequencing, and Assembly of SXT/R391-Harboring *Shewanella* Isolates

All *Shewanella* isolates were subjected to a PCR screen for SXT/R391 ICEs by targeting the int_{SXT} gene, which is regarded as a conserved integrase-coding gene among members of the ICE family. The PCR primers designed for the int_{SXT} gene were used as previously described (McGrath et al., 2006). Genomic DNA of SXT/R391-positive *Shewanella* isolates was extracted by the Wizard Genomic DNA Purification kit (Promega, United States) in line with the manufacturer's protocols. The whole genomes were sequenced on the Illumina HiSeq 2000 platform, employing

[1] http://db-mml.sjtu.edu.cn/ICEberg/

[2] http://www.bacterio.net/shewanella.html

two paired-end libraries with average insert lengths of 500 and 2000 bp, respectively. The clean paired-end read data were assembled by means of SOAPdenovo v2.04 (Li et al., 2010). Genomic similarities of the SXT/R391-positive isolates were estimated by the average nucleotide identity (ANI) service[3].

Extraction, Annotation, and Submission of SXT/R391 ICEs

The SXT/R391 ICEs of the *Shewanella* isolates were identified and extracted by the alignment with the reference ICE sequence of SXT^{MO10} (AY055428.1). The complete ICEs of the isolates were assembled and obtained by PCR linkage of the gaps between separate scaffolds. Putative coding sequences of the SXT/R391 ICEs were predicted by Glimmer and annotated by the RAST (Rapid Annotation using Subsystem Technology) server (Aziz et al., 2008; Overbeek et al., 2014; Brettin et al., 2015). The integrated SXT/R391 ICE sequence and annotation of the representative *Shewanella* isolate were deposited in GenBank.

Sequence Similarities and Phylogenetic Analysis of SXT/R391 Elements

The genetic and evolutionary relationships between the novel SXT/R391 of typical *Shewanella* isolate and the recognized SXT/R391 ICEs were determined by BLASTn search and phylogenetic analysis. The BLASTn tool was employed to obtain the similarities in nucleotide sequences of SXT/R391 elements and seek out the known ICEs with high homology. Based on blast results, 24 representative ICEs were selected with different sequences scores and distinct evolutionary origins to construct the phylogenetic tree of core genes (Supplementary Table S1). The concatenated sequences of core genes identified by OrthoMCL software were included and aligned in phylogenetic analysis. Phylogenetic tree was constructed by the maximum-likelihood method and evaluated with 1000 bootstrap replications.

Comparative Analysis and Genetic Organization of the Novel SXT/R391 and Closely Related ICEs

The SXT/R391 sequence of the *Shewanella* isolate was further evaluated by comparison with classical and related SXT/R391 ICEs, i.e., SXT^{MO10} (*V. cholerae* MO10; AY055428.1), R391 (*P. rettgeri* R391; AY090559.1), ICE*Vch*Ban5 (*V. cholerae* Ban5; GQ463140.1), ICE*Spu*PO1 (*S. putrefaciens* W3-18-1; CP000503.1), and ICE*Sha*Por1 (*S. haliotis* AC6; HE577620.1). The sequence visualization of BLASTn analysis with four reference sequences listed above, except for ICE*Sha*Por1, which was assembled as PCR fragments of hotspot regions, was performed by the Artemis Comparison Tool (ACT) (Carver et al., 2008). Genetic structures of the novel SXT/R391 element from the *Shewanella* isolate and the five related ICEs were indicated for conserved and variable regions to distinguish unique genes among the SXT/R391 ICEs.

[3]http://www.ezbiocloud.net/tools/ani

Antibiotic Susceptibility Testing

The broth microdilution method was employed to determine the susceptibility of SXT/R391-harboring *Shewanella* isolates to 16 antibiotics, including amoxicillin/clavulanic acid, ampicillin, azithromycin, cefixime, cefoxitin, ceftriaxone, chloramphenicol, ciprofloxacin, doxycycline, gentamicin, imipenem, kanamycin, streptomycin, sulfamethoxazole, tetracycline, and trimethoprim-sulfamethoxazole. The standards of the Clinical and Laboratory Standards Institute (2015) were followed to carry out the antibiotic tests and identify the susceptibility of isolates.

Conjugation Assays

The ability to transfer of the positive *Shewanella* isolates was estimated by the mating assays according to previous description (Mata et al., 2011). The streptomycin-resistant SXT/R391-positive *Shewanella* isolates were used as the donor isolates and the kanamycin-resistant *E. coli* SM10 served as the recipient isolate. Transconjugants were discerned from the selective media, which contained 100 μg/ml streptomycin and 100 μg/ml kanamycin. The transfer frequency of ICEs was determined by calculating the number of transconjugants per recipient cell. The transconjugants were further verified by the amplification of int_{SXT} gene and antibiotic resistance genes in the SXT/R391-harboring *Shewanella* isolates as previously described (Li et al., 2016).

RESULTS

Distribution and Characterization of SXT/R391-Positive *Shewanella* Isolates

The *Shewanella* strains in China belonged to seven species, including *S. algae*, *S. chilikensis*, *S. haliotis*, *S. indica*, *S. seohaensis*, *S. upenei*, and *S. xiamenensis*. SXT/R391-like ICEs were detected in 3 out of 91 *Shewanella* isolates, which belonged to the species *S. upenei* (Supplementary Figure S1 and Supplementary Table S2). Among the SXT/R391-harboring isolates, two were obtained from stool samples of diarrhea patients, and the third one was isolated from washing water. Interestingly, the three SXT/R391-positive isolates were derived from a local mill of soybean products in Dangtu county, Anhui province, China, on September 8, 2011. In the mill, another six *Shewanella* isolates were obtained from the brine and bean curd; however, these isolates were negative for SXT/R391 elements and were confirmed as strains of *S. haliotis* (Supplementary Figure S1). Based on the PFGE analysis, which revealed the clonal relationships of the nine isolates from Dangtu county, the three SXT/R391-harboring isolates of *S. upenei* had similar profiles, and the six SXT/R391-negative isolates of *S. haliotis* shared identical patterns, traced to the same origin, respectively (**Figure 1**).

Sequence Analysis and ICE Features of SXT/R391 in *Shewanella* Isolates

The assembled genomes of the three SXT/R391-positive isolates showed high similarity values (99.9%), as estimated by ANI. Analysis of the three complete SXT/R391 elements showed that

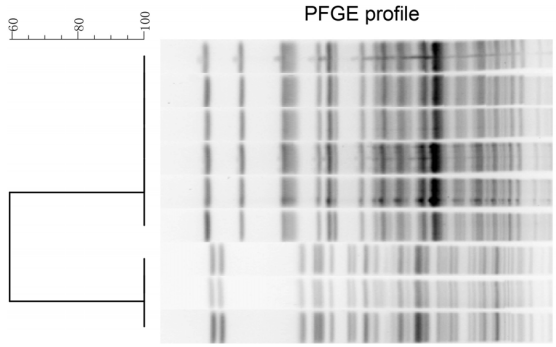

PFGE profile	Strain	Species	Sample source	SXT/R391 ICE
	11MAS2077	*S. haliotis*	Brine	-
	11MAS2078	*S. haliotis*	Brine	-
	11MAS2079	*S. haliotis*	Brine	-
	11MAS2080	*S. haliotis*	Brine	-
	11MAS2083	*S. haliotis*	Bean curd	-
	11MAS2084	*S. haliotis*	Bean curd	-
	110003	*S. upenei*	Stool of patient	+
	11dtj4	*S. upenei*	Stool of patient	+
	11MAS2081	*S. upenei*	Water	+

FIGURE 1 | PFGE profile characterization of nine *Shewanella* strains isolated simultaneously from a local mill in Dangtu county, Anhui province, China. PFGE were performed with CHEF-DR III system under the following conditions: voltage gradient, 6 V/cm; run time, 20 h; initial switch time, 1 s; final switch time, 15 s.

the ICE sequences were almost identical, with only several different bases in variable regions. Given that the three ICE-harboring isolates shared identical PFGE profiles, high genomic similarities, and nuances of SXT/R391 elements, strain 110003 was selected as the representative SXT/R391-positive *Shewanella* isolate. The corresponding SXT/R391 element was designated ICE*Sup*CHN110003 following the nomenclature for the ICE family. The sequence of ICE*Sup*CHN110003 was 91,669 bp in length, with 46.3% GC content, included 82 coding genes (Supplementary Table S3) and was submitted in GenBank under accession number MG014393.

BLAST Results for ICE*Sup*CHN110003 and ICEs Available in GenBank

The nucleotide sequence of ICE*Sup*CHN110003 was aligned with those of the ICEs available in the GenBank database to evaluate its homology with the recognized ICEs. Comparison between ICE*Sup*CHN110003 and the reported ICEs showed a query coverage from 40 to 76%, the identity from 96 to 99%, the total score from 64,604 to 1.89E+05 and the max score from 15,189 to 46,405. The most closely related ICE was ICE*Vch*Ban5 carried by *V. cholerae* strain Ban5, with the query coverage of 76% and identity of 99%. However, the novel SXT/R391 element from the *Shewanella* isolate exhibited relatively low homology to classical ICEs, i.e., SXT^{MO10} and R391, with 70 and 54% query coverages as well as 97 and 98% identities, respectively. Comparison between ICE*Sup*CHN110003 and ICE*Spu*PO1 from *S. putrefaciens* showed that the query coverage and identity were 57 and 97%, respectively.

Taxonomic Position of ICE*Sup*CHN110003

The phylogenetic tree of concatenated core genes demonstrated that ICE*Sup*CHN110003 formed an independent branch outside the cluster comprising of ICE*Val*A056-1 (Guangdong, China, 2003), ICE*Pmi*CHN2410 (Anhui, China, 2009), and ICE*Pmi*Chn1 (Hubei, China, 2013) (**Figure 2** and Supplementary Table S1). The strains in the cluster involving *Vibrio alginolyticus* and *Proteus mirabilis* species were isolated from various sources including shrimp, chicken, and stool specimen of patient. The phylogenetic analysis indicated that the ICE*Sup*CHN110003 as a novel SXT/R391 element was evolutionarily related to the three ICEs discovered in China.

Overall Comparison Between ICE*Sup*CHN110003 and Representative Related ICEs

By and large, collinear relationships among the five ICEs were detected in conserved regions and variable region III (**Figure 3**). ICE*Sup*CHN110003 with a complete core backbone exhibited 94–97% similarity with the reference ICEs in conserved regions. Higher similarities among the ICE sequences (98–99%) could be found in variable region III, which existed in ICE*Sup*CHN110003, SXT^{MO10}, and ICE*Vch*Ban5. Inverted areas were also observed in this region, corresponding to several genes of mobile elements. Unmatched areas were concentrated in specific inserted variable regions with low homology, making ICE*Sup*CHN110003 a novel SXT/R391 element that could be distinguished from the recognized ICEs.

Genetic Structure of Hotspots and Variable Regions in SXT/R391 ICEs

Analysis of genetic organization was performed among the aforementioned SXT/R391 sequences, with the addition of ICE*Sha*Por1 from *S. haliotis*, which was amplified in specific inserted loci (**Figure 4**). The genetic structure of ICE*Sup*CHN110003 in inserted regions indicated that the novel SXT/R391 element from the *Shewanella* isolate comprised five hotspots (HS1–5) and two variable regions (II and III).

The five intergenic hotspot regions were identified by locating the boundaries, as described previously (Wozniak et al., 2009). In HS1, a conserved hypothetical gene of 588 bp in length was identified in ICE*Sup*CHN110003, which shared 94.7–96.6% similarity with the reference ICEs, with the exception of SXT^{MO10}, consistent with the graphical alignment generated by the ACT software (**Figure 3**). In HS2, mosA/T toxin–antitoxin systems, which support ICE maintenance, or heavy metal efflux gene clusters, which protect against heavy metal toxicity, were identified in four reference ICEs apart from R391. Whereas,

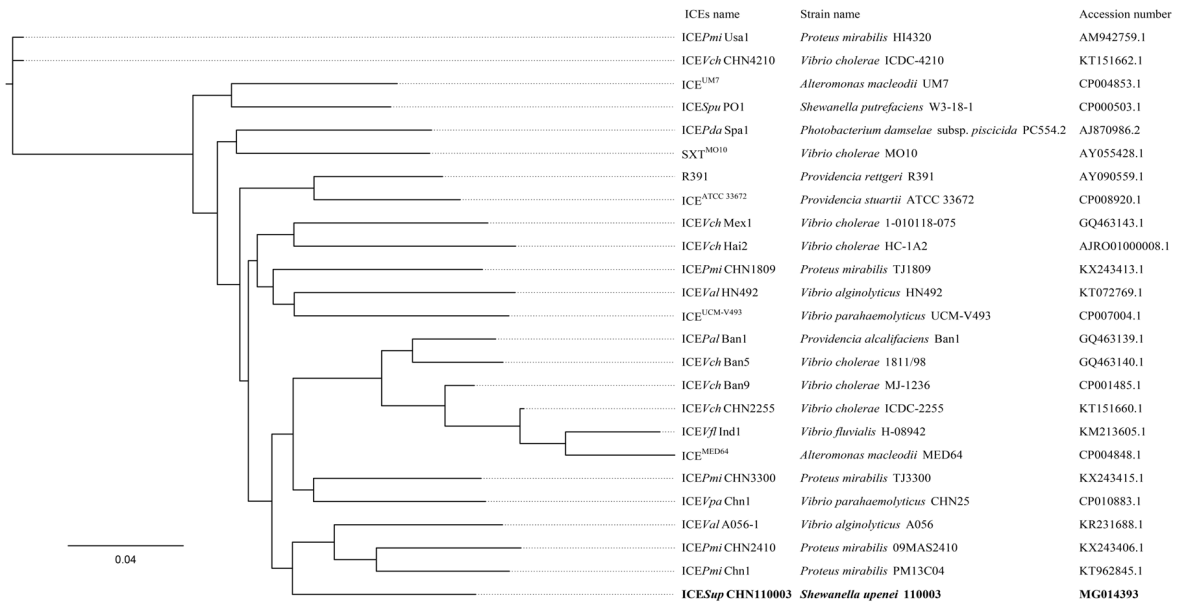

FIGURE 2 | Phylogenetic analysis based on the concatenated core genes between ICE*Sup*CHN110003 and 24 representative ICEs. The phylogenetic tree was constructed by maximum-likelihood methods. Bootstrap values were evaluated with 1000 replications. Bold font indicated the ICE*Sup*CHN110003.

ICE*Sup*CHN110003 encoded a distinct gene exhibiting high homology to ICE*Vsc*Spa2 with only 2-bp difference, indicating their close evolutionary origin. This gene was found to share 49% similarity with the ProP osmoprotectant transporter gene from *Francisella tularensis* subsp. *holarctica* (Rodriguez-Blanco et al., 2012). In HS3, a large DNA fragment of approximately 5.7 kb, only discovered in ICE*Pmi*Chn2, was inserted in this region and annotated as a serine protease-like protein by RAST (Supplementary Table S3). Gene clusters encoding endonuclease, helicase, methyl-accepting chemotaxis protein, restriction-modification (RM) system and the *mrr* restriction system were identified in HS4 and HS5. Among the reference ICEs, a type I RM system was detected in ICE*Spu*PO1, and a type II RM system was discovered in SXT^{MO10}, R391, and ICE*Vch*Ban5. On the other hand, the novel SXT/R391 ICE*Sup*CHN110003 encoded a type III RM system, which was differentiated from those of closely related ICEs. The type III RM system, comprising the R (restriction) subunit and the M (modification) subunit and conferring resistance to phage infection, was delineated in ICE*Vsp*Por3 and ICE*Val*Spa1 among the recognized ICEs (Balado et al., 2013). However, only few ICE*Sup*CHN110003 areas were aligned with those, indicating a distant relationship and diversity among the type III RM systems in SXT/R391 elements. The BLASTn results for the type III RM system of ICE*Sup*CHN110003 showed its higher homology with several complete genome and plasmid sequences, except for the M subunit, which had a nucleotide coverage of only approximately 50%. Because of the low similarities in type III RM systems among SXT/R391 elements and the half coverage of the M subunit in public databases, the RM system found in ICE*Sup*CHN110003 served as a distinct type III RM system in ICEs.

Two inserted variable regions (II and III) were identified in ICE*Sup*CHN110003, conferring adaptive functions and multidrug resistance to the isolate. The high level of homology (99%) in these regions between ICE*Sup*CHN110003 and ICE*Vch*Ban5, as shown by ACT, made ICE*Vch*Ban5 the most closely related ICE. Variable region II, located between the *xis* and *int* genes, included a DNA mismatch repair gene, *mutL*, which is involved in the process of DNA replication, recombination, and repair. Variable region III, disrupting the *rumB* gene, was detected in SXT^{MO10}, ICE*Vch*Ban5, and ICE*Sup*CHN110003. A putative transposon cassette harboring multidrug resistance genes was present in this region, which tends to accumulate and disseminate antibiotic resistance, as previously described (Wozniak et al., 2009). In ICE*Sup*CHN110003, variable region III comprised four antibiotic resistance genes, including *floR*, *strA*, *strB*, and *sul2*, which mediate resistance to chloramphenicol, streptomycin, and sulfamethoxazole, respectively. By comparison, ICE*Vch*Ban5 possessed an extra copy of *floR*, and SXT^{MO10} carried the *dhfR* gene conferring resistance to trimethoprim. In general, the acquisition and recombination of genes, frequently occurring in hotspots and variable regions of ICEs, lead to the emergence of novel SXT/R391 elements such as ICE*Sup*CHN110003, stably maintained in a rapidly changing environment.

Antibiotic Resistance of SXT/R391-Harboring *Shewanella* Isolates

The three SXT/R391-positive *Shewanella* isolates, 110003, 11dtj4, and 11MAS2081, were subjected to antibiotic susceptibility tests and found to share similar multidrug resistance profiles. All isolates were resistant to 9 out of 16 drugs, including

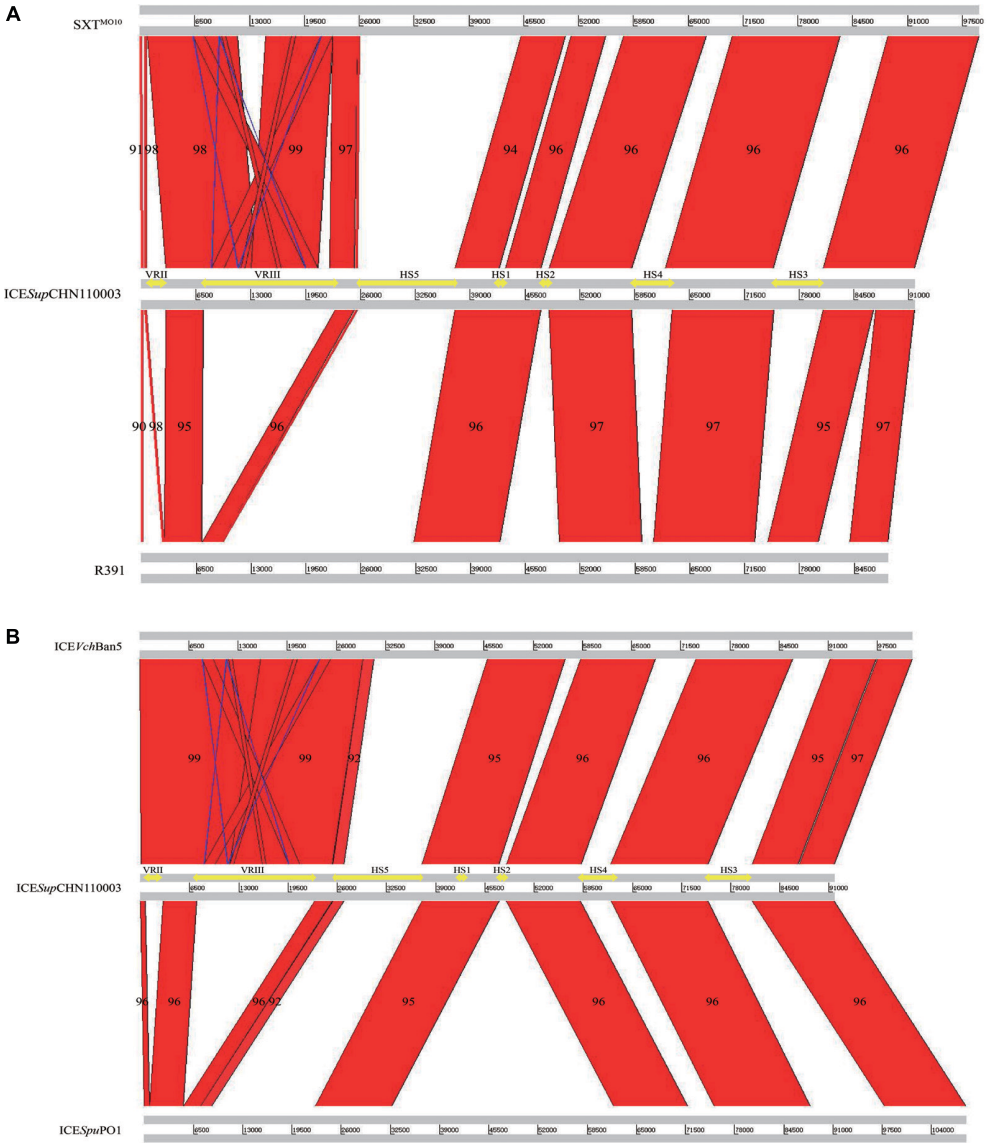

FIGURE 3 | General comparisons presented by ACT software of ICE*Sup*CHN110003 with: **(A)** SXT^{MO10} and R391; **(B)** ICE*Vch*Ban5 and ICE*Spu*PO1. Red areas indicated homologous regions. Blue areas indicated inverse regions. Yellow arrows indicated hotspots and variable regions in ICE*Sup*CHN110003. Numbers in areas indicated the similarity (%) of the compared regions.

amoxicillin/clavulanic acid, cefixime, cefoxitin, chloramphenicol, imipenem, streptomycin, sulfamethoxazole, tetracycline, and trimethoprim-sulfamethoxazole, except for intermediate resistance of isolate 110003 to tetracycline. The phenotype of multidrug resistance to chloramphenicol, streptomycin, sulfamethoxazole, and trimethoprim-sulfamethoxazole could be attributed to the presence of the SXT/R391 element, which carried the antibiotic resistance genes *floR*, *strA*, *strB*, and *sul2*.

Transfer Ability of SXT/R391 Elements in *Shewanella* Isolates

A conjugation assay was employed to investigate the transfer ability of the three SXT/R391-harboring *Shewanella* isolates. The mobility of ICEs was detected, with a transfer frequency ranging from 9.5×10^{-8} (11dtj4) to 5×10^{-7} (110003) per recipient cell, indicating the possibility of gene dissemination via horizontal transfer of SXT/R391 ICEs. The transconjugants were further confirmed by PCR-based amplification targeting the int_{SXT} gene and antibiotic resistance genes (*floR*, *strA*, *strB*, and *sul2*) harbored by the SXT/R391-positive *Shewanella* isolates.

DISCUSSION

Until now, SXT/R391 ICEs have been investigated in the genera *Vibrio* (Wang et al., 2016), *Providencia* (Coetzee et al., 1972), *Photobacterium* (Nonaka et al., 2012), *Proteus* (Lei et al., 2016;

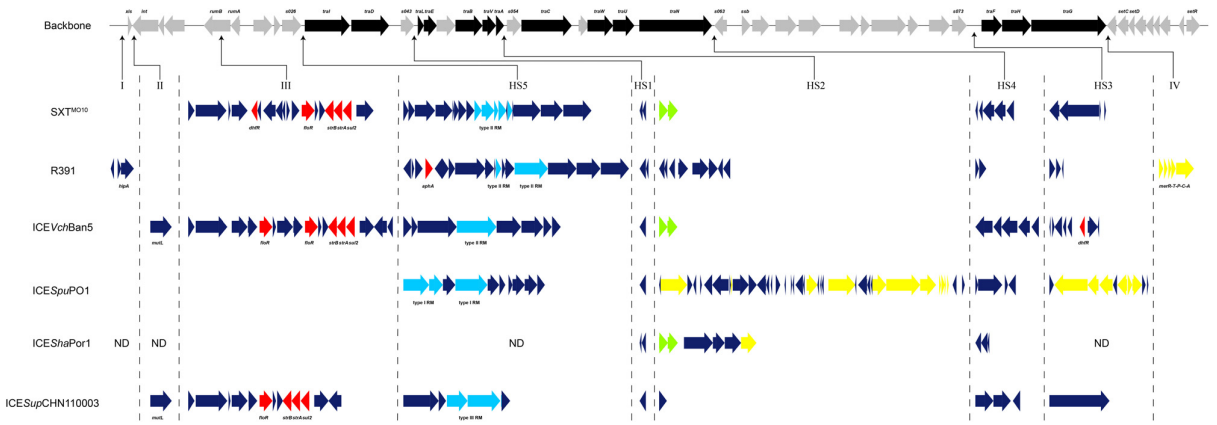

FIGURE 4 | Genetic structure of ICE*Sup*CHN110003 and five representative ICEs: SXT^{MO10}, R391, ICE*Vch*Ban5, ICE*Spu*PO1, and ICE*Sha*Por1. The upper line demonstrated the backbone of 52 core genes in SXT/R391 ICEs. Black arrows indicated the coding genes involved in conjugative transfer process. Gray arrows indicated other genes in conserved regions. Under the backbone, the inserted genes of six SXT/R391 ICEs in five hotspots (HS1–5) and four variable regions (I–IV) were shown. Red arrows indicated antibiotic resistance genes. Light blue arrows indicated restriction-modification system. Green arrows indicated toxin–antitoxin system. Yellow arrows indicated heavy metals resistance genes. Dark blue arrows indicated other genes in hotspots and variable regions. Several distinct genes in these regions were marked. ND, not determined.

Li et al., 2016), *Alteromonas* (Badhai and Das, 2016), *Enterovibrio* (Taviani et al., 2009; Song et al., 2013; Luo et al., 2016), and *Shewanella*. *S. putrefaciens*, *S. haliotis*, and *S. fidelis* in the genus *Shewanella*, which were obtained from the Pacific Ocean, Portugal, and Japan, respectively, were reported to harbor SXT/R391 elements (Pembroke and Piterina, 2006; Rodriguez-Blanco et al., 2012; Nonaka et al., 2014). In this study, we discerned seven *Shewanella* species, including *S. algae*, *S. chilikensis*, *S. haliotis*, *S. indica*, *S. seohaensis*, *S. upenei*, and *S. xiamenensis*, among 91 strains isolated from four provinces in China, whereas only the species *S. upenei* from Anhui province was found to carry SXT/R391 elements. This was the first time when SXT/R391 elements were detected in the genus *Shewanella* in China, and a novel multidrug-resistant ICE, ICE*Sup*CHN110003, was characterized in *S. upenei*. Three SXT/R391-positive strains of *S. upenei*, with similar PFGE profiles, were simultaneously isolated from fecal samples of diarrhea patients and from washing water. The existence of SXT/R391-harboring *Shewanella* isolates among patients and in an aquatic environment from an inland city raises risks of contaminating water sources and causing diseases. Six isolates of *S. haliotis*, which was reported to have the potential to acquire ICEs, were also obtained from commercial food at the same place and time. The SXT/R391 ICE*Sup*CHN110003 present in positive isolates as a self-transmissible element, was proven to have the ability to transfer via conjugation. It is likely that the ICEs harbored by *S. upenei* could transmit to *S. haliotis* isolates in food and to other aquatic bacteria in water and confer multidrug resistance to the hosts. As a consequence, it is urgent to reinforce continuous and widespread surveillance for ICEs in the genus *Shewanella*. Meanwhile, more attention should be paid to preventing the occurrence and dispersion of SXT/R391-harboring isolates.

The sequence relationships between ICE*Sup*CHN110003 and known ICEs available in public databases were evaluated by BLASTn, and the results showed that the nucleotide query coverage was less than 76% and the sequence similarity ranged from 96 to 99%. However, the graphical alignment generated by the ACT software demonstrated high levels of similarity with typical ICEs in conserved backbone genes, with 94–97% homology, and in variable region III, encoding multidrug resistance genes, with 98–99% similarity. The low coverage values were attributed to the unique genes positioned in hotspot regions of ICE*Sup*CHN110003, which were rarely discovered among recognized ICEs. Based on a comprehensive consideration of multiple indicators, the novel ICE shared a higher homology with ICE*Vch*Ban5 (Wozniak et al., 2009) from the genus *Vibrio* than with the previously reported ICEs from *Shewanella* species, indicating a low correlation within the genus.

The phylogenetic tree based on core genes demonstrated that ICE*Sup*CHN110003 formed a distinct clade separated from other representative ICEs. This evolutionary analysis revealed that ICE*Sup*CHN110003 was a novel ICE, adding to the members of the SXT/R391 family. The closely related ICEs were harbored by the species *V. alginolyticus* and *P. mirabilis*, indicating those as possible ancestors, rather than the SXT/R391 elements previously described in *Shewanella* species (Nonaka et al., 2014). Phylogenetic neighbors of ICEs were isolated from different provinces in China during a long time span, from 2003 to 2013. The discovery of ICE*Sup*CHN110003, emerged in 2011, reveals the evolution and dispersion of SXT/R391 ICEs in China. Notably, the related ICE*Pmi*CHN2410 (Li et al., 2016) was identified in *P. mirabilis* from the same province, Anhui, as the novel ICE. The close geographical distribution suggests an extensive local transfer of ICEs among diverse bacterial species. Therefore, a wide-ranging monitoring of ICEs is necessary to prevent the spread of related mobile elements in China.

Comparative genetic structure analysis was employed to elucidate the gene organization in hotspots and variable regions of the novel SXT/R391. The unique genes detected

in five hotspots of ICE*Sup*CHN110003 had few counterparts in the NCBI database. For instance, the novel SXT/R391 harbored uncommon coding genes in the HS2 and HS3 regions, exclusively corresponding to those in ICE*Vsc*Spa2 and ICE*Pmi*Chn2, respectively. The distinct type III RM system found in ICE*Sup*CHN110003 showed low homology with those in recognized ICEs, whereas only partial fragments were discovered in genome and plasmid sequences. A novel functional gene cluster detected in ICE*Sup*CHN110003 endowed the hosts with adaptive abilities to the changing environment. Specific genes found in SXT/R391 elements from diverse origins indicate that the acquisition and recombination of foreign genes are common among ICEs, as previously described (Wozniak et al., 2009). Although unique accessory genes were detected in ICEs, genomes, and plasmids, none of the SXT/R391 elements were completely identical to ICE*Sup*CHN110003, owing to their mosaicism. Comparative analysis provided further evidence supporting characterization of ICE*Sup*CHN110003 as a novel SXT/R391 element distinguished from other ICEs.

An inserted fragment in variable region III contributed to the high level of homology between ICE*Sup*CHN110003 and ICE*Vch*Ban5, which was identified as the most closely related ICE. A multidrug resistance cassette was discovered in this region of the novel SXT/R391, conferring multiple resistance to antibiotics. The SXT/R391-positive *Shewanella* isolates exhibited a wide range of phenotypic resistance to more than half of the tested drugs. The antibiotic resistance determinants, including *floR*, *strA*, *strB*, and *sul2*, detected in ICE*Sup*CHN110003, are considered to confer resistance to chloramphenicol, streptomycin, and sulfamethoxazole. In addition, drug resistance genes located on the chromosome or a plasmid may endow the hosts with resistance to the remaining antibiotics. In addition, ICEs served as carriers for multidrug resistance clusters and transposase genes frequently occurred in variable region III. These transposable genetic elements in ICE*Sup*CHN110003 would promote HGT of antibiotic resistance determinants in clinical and aquatic environments.

CONCLUSION

In conclusion, our study describes, for the first time, SXT/R391 elements detected in *Shewanella* species in China, which were isolated from the clinic, environment, and food. Three *Shewanella* isolates were found to harbor SXT/R391 elements, and ICE*Sup*CHN110003 was designated a representative ICE among the positive isolates. Given its low alignment coverage with recognized ICEs, independent clade in a phylogenetic tree of conserved core genes and uncommon inserted fragments in hotspots regions, ICE*Sup*CHN110003 represents a novel SXT/R391, thus enhancing the knowledge of ICEs. Resistance to multiple antibiotics and a cross-species transfer ability were discovered in these SXT/R391-positive *Shewanella* isolates from patients and water, posing a deep threat to public health and natural environments. Hence, it is imperative to increase our awareness of the emergence of ICEs in *Shewanella* species and take actions to prevent dissemination of SXT/R391 ICEs.

ETHICS STATEMENT

This study was carried out in accordance with the recommendations of the Ethics Committee of National Institute for Communicable Disease Control and Prevention, Chinese Center for Disease Control and Prevention with written informed consent from all subjects. All subjects gave written informed consent in accordance with the Declaration of Helsinki. The protocol was approved by the Ethics Committee of National Institute for Communicable Disease Control and Prevention, Chinese Center for Disease Control and Prevention.

AUTHOR CONTRIBUTIONS

DW designed the work. YF, ZhL, BD, and XL performed the experiments. YW and ZoL collected the sample and isolated the strain. YF, ZhL, DW, and BK analyzed the data. YF and DW wrote the paper.

FUNDING

This work was supported by the NSFC of China (31570134) and the Priority Project on Infectious Disease Control and Prevention from National Health Commission of China (2018ZX10102001 and 2017ZX10104002).

SUPPLEMENTARY MATERIAL

The Supplementary Material for this article can be found online at: https://www.frontiersin.org/articles/10.3389/fmicb.2018.00920/full#supplementary-material

REFERENCES

Aziz, R. K., Bartels, D., Best, A. A., Dejongh, M., Disz, T., Edwards, R. A., et al. (2008). The RAST server: rapid annotations using subsystems technology. *BMC Genomics* 9:75. doi: 10.1186/1471-2164-9-75

Badhai, J., and Das, S. K. (2016). Characterization of three novel SXT/R391 integrating conjugative elements ICE*Mfu*Ind1a and ICE*Mfu*Ind1b, and ICE*Mpr*Chn1 identified in the genomes of *Marinomonas fungiae* JCM 18476T and *Marinomonas profundimaris* strain D104. *Front. Microbiol.* 7:1896. doi: 10.3389/fmicb.2016.01896

Balado, M., Lemos, M. L., and Osorio, C. R. (2013). Integrating conjugative elements of the SXT/R391 family from fish-isolated *Vibrios* encode restriction-modification systems that confer resistance to bacteriophages. *FEMS Microbiol. Ecol.* 83, 457–467. doi: 10.1111/1574-6941.12007

Bi, D., Xu, Z., Harrison, E. M., Tai, C., Wei, Y., He, X., et al. (2012). ICEberg: a web-based resource for integrative and conjugative elements found in Bacteria. *Nucleic Acids Res.* 40, D621–D626. doi: 10.1093/nar/gkr846

Brettin, T., Davis, J. J., Disz, T., Edwards, R. A., Gerdes, S., Olsen, G. J., et al. (2015). RASTtk: a modular and extensible implementation of the RAST algorithm for

building custom annotation pipelines and annotating batches of genomes. *Sci. Rep.* 5:8365. doi: 10.1038/srep08365

Burrus, V., Marrero, J., and Waldor, M. K. (2006). The current ICE age: biology and evolution of SXT-related integrating conjugative elements. *Plasmid* 55, 173–183. doi: 10.1016/j.plasmid.2006.01.001

Carver, T., Berriman, M., Tivey, A., Patel, C., Bohme, U., Barrell, B. G., et al. (2008). Artemis and ACT: viewing, annotating and comparing sequences stored in a relational database. *Bioinformatics* 24, 2672–2676. doi: 10.1093/bioinformatics/btn529

Clinical and Laboratory Standards Institute (2015). *Performance Standards for Antimicrobial Susceptibility Testing: Twenty-Fifth Informational Supplement. CLSI document M100-S25*. Wayne, PA: CLSI.

Coetzee, J. N., Datta, N., and Hedges, R. W. (1972). R factors from *Proteus rettgeri*. *J. Gen. Microbiol.* 72, 543–552. doi: 10.1099/00221287-72-3-543

Cooper, K. L., Luey, C. K., Bird, M., Terajima, J., Nair, G. B., Kam, K. M., et al. (2006). Development and validation of a PulseNet standardized pulsed-field gel electrophoresis protocol for subtyping of *Vibrio cholerae*. *Foodborne Pathog. Dis.* 3, 51–58. doi: 10.1089/fpd.2006.3.51

Dikow, R. B. (2011). Genome-level homology and phylogeny of *Shewanella* (Gammaproteobacteria: lteromonadales: Shewanellaceae). *BMC Genomics* 12:237. doi: 10.1186/1471-2164-12-237

Dominguez, H., Vogel, B. F., Gram, L., Hoffmann, S., and Schaebel, S. (1996). *Shewanella alga* bacteremia in two patients with lower leg ulcers. *Clin. Infect. Dis.* 22, 1036–1039. doi: 10.1093/clinids/22.6.1036

Goyal, R., Kaur, N., and Thakur, R. (2011). Human soft tissue infection by the emerging pathogen *Shewanella algae*. *J. Infect. Dev. Ctries.* 5, 310–312. doi: 10.3855/jidc.1436

Hacker, J., and Kaper, J. B. (2000). Pathogenicity islands and the evolution of microbes. *Annu. Rev. Microbiol.* 54, 641–679. doi: 10.1146/annurev.micro.54.1.641

Janda, J. M., and Abbott, S. L. (2014). The genus *Shewanella*: from the briny depths below to human pathogen. *Crit. Rev. Microbiol.* 40, 293–312. doi: 10.3109/1040841X.2012.726209

Juhas, M., Van Der Meer, J. R., Gaillard, M., Harding, R. M., Hood, D. W., and Crook, D. W. (2009). Genomic islands: tools of bacterial horizontal gene transfer and evolution. *FEMS Microbiol. Rev.* 33, 376–393. doi: 10.1111/j.1574-6976.2008.00136.x

Lane, D. J. (1991). "16S/23S rRNA sequencing," in *Nucleic Acid Techniques in Bacterial Systematics*, eds E. Stackebrandt and M. Goodfellow (New York, NY: Wiley), 115–175.

Lei, C. W., Zhang, A. Y., Wang, H. N., Liu, B. H., Yang, L. Q., and Yang, Y. Q. (2016). Characterization of SXT/R391 integrative and conjugative elements in *Proteus mirabilis* isolates from food-producing animals in China. *Antimicrob. Agents Chemother.* 60, 1935–1938. doi: 10.1128/AAC.02852-15

Li, R., Zhu, H., Ruan, J., Qian, W., Fang, X., Shi, Z., et al. (2010). De novo assembly of human genomes with massively parallel short read sequencing. *Genome Res.* 20, 265–272. doi: 10.1101/gr.097261.109

Li, X., Du, Y., Du, P., Dai, H., Fang, Y., Li, Z., et al. (2016). SXT/R391 integrative and conjugative elements in Proteus species reveal abundant genetic diversity and multidrug resistance. *Sci. Rep.* 6:37372. doi: 10.1038/srep37372

Liu, P. Y., Lin, C. F., Tung, K. C., Shyu, C. L., Wu, M. J., Liu, J. W., et al. (2013). Clinical and microbiological features of *Shewanella* bacteremia in patients with hepatobiliary disease. *Intern. Med.* 52, 431–438. doi: 10.2169/internalmedicine.52.8152

Luo, P., He, X., Wang, Y., Liu, Q., and Hu, C. (2016). Comparative genomic analysis of six new-found integrative conjugative elements (ICEs) in *Vibrio alginolyticus*. *BMC Microbiol.* 16:79. doi: 10.1186/s12866-016-0692-9

Mata, C., Navarro, F., Miro, E., Walsh, T. R., Mirelis, B., and Toleman, M. (2011). Prevalence of SXT/R391-like integrative and conjugative elements carrying blaCMY-2 in *Proteus mirabilis*. *J. Antimicrob. Chemother.* 66, 2266–2270. doi: 10.1093/jac/dkr286

McGrath, B. M., O'halloran, J. A., Piterina, A. V., and Pembroke, J. T. (2006). Molecular tools to detect the IncJ elements: a family of integrating, antibiotic resistant mobile genetic elements. *J. Microbiol. Methods* 66, 32–42. doi: 10.1016/j.mimet.2005.10.004

Nonaka, L., Maruyama, F., Miyamoto, M., Miyakoshi, M., Kurokawa, K., and Masuda, M. (2012). Novel conjugative transferable multiple drug resistance plasmid pAQU1 from *Photobacterium damselae* subsp. *damselae* isolated from marine aquaculture environment. *Microbes Environ.* 27, 263–272. doi: 10.1264/jsme2.ME11338

Nonaka, L., Maruyama, F., Onishi, Y., Kobayashi, T., Ogura, Y., Hayashi, T., et al. (2014). Various pAQU plasmids possibly contribute to disseminate tetracycline resistance gene tet(M) among marine bacterial community. *Front. Microbiol.* 5:152. doi: 10.3389/fmicb.2014.00152

Overbeek, R., Olson, R., Pusch, G. D., Olsen, G. J., Davis, J. J., Disz, T., et al. (2014). The SEED and the rapid annotation of microbial genomes using subsystems technology (RAST). *Nucleic Acids Res.* 42, D206–D214. doi: 10.1093/nar/gkt1226

Pagani, L., Lang, A., Vedovelli, C., Moling, O., Rimenti, G., Pristera, R., et al. (2003). Soft tissue infection and bacteremia caused by *Shewanella putrefaciens*. *J. Clin. Microbiol.* 41, 2240–2241. doi: 10.1128/JCM.41.5.2240-2241.2003

Pembroke, J. T., and Piterina, A. V. (2006). A novel ICE in the genome of *Shewanella putrefaciens* W3-18-1: comparison with the SXT/R391 ICE-like elements. *FEMS Microbiol. Lett.* 264, 80–88. doi: 10.1111/j.1574-6968.2006.00452.x

Rodriguez-Blanco, A., Lemos, M. L., and Osorio, C. R. (2012). Integrating conjugative elements as vectors of antibiotic, mercury, and quaternary ammonium compound resistance in marine aquaculture environments. *Antimicrob. Agents Chemother.* 56, 2619–2626. doi: 10.1128/AAC.05997-11

Ronconi, M., Merino, L., Usandizaga, G. B., Camargo, M. C., Irigoyen, B. I., Presti, S., et al. (1999). Non fermentative gram negative bacilli isolated in a hospital laboratory. *Enferm. Infecc. Microbiol. Clin.* 17, 269–273.

Rouzic, N., Hery-Arnaud, G., Jaffuel, S., Garo, B., Payan, C., and Garre, M. (2012). Soft tissue infection associated with bacteremia caused by *Shewanella putrefaciens*. *Pathol. Biol.* 60, e27–e29. doi: 10.1016/j.patbio.2011.04.005

Song, Y., Yu, P., Li, B., Pan, Y., Zhang, X., Cong, J., et al. (2013). The mosaic accessory gene structures of the SXT/R391-like integrative and conjugative elements derived from *Vibrio* spp. isolated from aquatic products and environment in the Yangtze River Estuary, China. *BMC Microbiol.* 13:214. doi: 10.1186/1471-2180-13-214

Taviani, E., Grim, C. J., Chun, J., Huq, A., and Colwell, R. R. (2009). Genomic analysis of a novel integrative conjugative element in *Vibrio cholerae*. *FEBS Lett.* 583, 3630–3636. doi: 10.1016/j.febslet.2009.10.041

Waldor, M. K., Tschape, H., and Mekalanos, J. J. (1996). A new type of conjugative transposon encodes resistance to sulfamethoxazole, trimethoprim, and streptomycin in *Vibrio cholerae* O139. *J. Bacteriol.* 178, 4157–4165. doi: 10.1128/jb.178.14.4157-4165.1996

Wang, R., Yu, D., Yue, J., and Kan, B. (2016). Variations in SXT elements in epidemic *Vibrio cholerae* O1 El Tor strains in China. *Sci. Rep.* 6:22733. doi: 10.1038/srep22733

Wozniak, R. A., Fouts, D. E., Spagnoletti, M., Colombo, M. M., Ceccarelli, D., Garriss, G., et al. (2009). Comparative ICE genomics: insights into the evolution of the SXT/R391 family of ICEs. *PLoS Genet.* 5:e1000786. doi: 10.1371/journal.pgen.1000786

Wozniak, R. A., and Waldor, M. K. (2010). Integrative and conjugative elements: mosaic mobile genetic elements enabling dynamic lateral gene flow. *Nat. Rev. Microbiol.* 8, 552–563. doi: 10.1038/nrmicro2382

Conflict of Interest Statement: The authors declare that the research was conducted in the absence of any commercial or financial relationships that could be construed as a potential conflict of interest.

frontiers in Microbiology

ORIGINAL RESEARCH
published: 02 July 2018
doi: 10.3389/fmicb.2018.01443

Suspended Materials in River Waters Differentially Enrich Class 1 Integron- and IncP-1 Plasmid-Carrying Bacteria in Sediments

*Magali De la Cruz Barrón[1], Christophe Merlin[1], Hélène Guilloteau[1], Emmanuelle Montargès-Pelletier[2,3] and Xavier Bellanger[1]**

[1] LCPME, CNRS, Université de Lorraine, Nancy, France, [2] LIEC, CNRS, Université de Lorraine, Nancy, France, [3] LTSER France, Zone Atelier du Bassin de la Moselle, Nancy, France

OPEN ACCESS

Edited by:
Katy Jeannot,
UMR6249 Chrono Environnement, France

Reviewed by:
Edgardo Sepulveda,
Centro de Investigación Científica y de Educación Superior de Ensenada, Mexico
Arnaud Dechesne,
Technical University of Denmark, Denmark

***Correspondence:**
Xavier Bellanger
xavier.bellanger@univ-lorraine.fr

Specialty section:
This article was submitted to Antimicrobials, Resistance and Chemotherapy, a section of the journal Frontiers in Microbiology

Received: 01 March 2018
Accepted: 11 June 2018
Published: 02 July 2018

Citation:
De la Cruz Barrón M, Merlin C, Guilloteau H, Montargès-Pelletier E and Bellanger X (2018) Suspended Materials in River Waters Differentially Enrich Class 1 Integron- and IncP-1 Plasmid-Carrying Bacteria in Sediments. Front. Microbiol. 9:1443. doi: 10.3389/fmicb.2018.01443

Aquatic ecosystems are frequently considered as the final receiving environments of anthropogenic pollutants such as pharmaceutical residues or antibiotic resistant bacteria, and as a consequence tend to form reservoirs of antibiotic resistance genes. Considering the global threat posed by the antibiotic resistance, the mechanisms involved in both the formation of such reservoirs and their remobilization are a concern of prime importance. Antibiotic resistance genes are strongly associated with mobile genetic elements that are directly involved in their dissemination. Most mobile genetic element-mediated gene transfers involve replicative mechanisms and, as such, localized gene transfers should participate in the local increase in resistance gene abundance. Additionally, the carriage of conjugative mobile elements encoding cell appendages acting as adhesins has already been demonstrated to increase biofilm-forming capability of bacteria and, therefore, should also contribute to their selective enrichment on surfaces. In the present study, we investigated the occurrence of two families of mobile genetic elements, IncP-1 plasmids and class 1 integrons, in the water column and bank sediments of the Orne River, in France. We show that these mobile elements, especially IncP-1 plasmids, are enriched in the bacteria attached on the suspended matters in the river waters, and that a similar abundance is found in freshly deposited sediments. Using the IncP-1 plasmid pB10 as a model, *in vitro* experiments demonstrated that local enrichment of plasmid-bearing bacteria on artificial surfaces mainly resulted from an increase in bacterial adhesion properties conferred by the plasmid rather than an improved dissemination frequency of the plasmid between surface-attached bacteria. We propose plasmid-mediated adhesion to particles to be one of the main contributors in the formation of mobile genetic element-reservoirs in sediments, with adhesion to suspended matter working as a selective enrichment process of antibiotic resistant genes and bacteria.

Keywords: class 1 integrons, IncP-1 plasmids, environmental reservoirs of antibiotic resistance genes, river water column, suspended matter, sediments, biofilm, horizontal gene transfer

INTRODUCTION

Predictions of future scenarios regarding the consequences associated with the burden of antibiotic resistant bacteria (ARB) in the forthcoming years are still a matter of debate (de Kraker et al., 2016), but there is no doubt that this burden is already impairing our ability to treat common infectious diseases (Cosgrove, 2006). Natural environments, especially soils and aquatic ecosystems, are believed to play a key role in the emergence and dissemination of ARB. Indeed, being the final recipient of wastewater discharges or solid wastes from animal husbandry, such environments are often exposed to anthropogenic chemical pollutants such as antibiotics and biocides, as well as microbial pollutants such as ARB (Baquero et al., 2008; Knapp et al., 2010; Heuer et al., 2011). Considering the ever-increasing occurrence of ARB in the anthropogenic-impacted environments, these bacteria and their antibiotic resistance genes (ARGs) are now considered as environmental contaminants of emerging concern (Pruden et al., 2006).

Several studies have shown that, globally, the environment can act as a reservoir of ARGs and that many Gram-positive and Gram-negative pathogens have acquired new resistance traits originating from this huge gene pool (Martinez, 2009; Wright, 2010; Perry and Wright, 2013). Part of the problem arises from the association of ARGs with so-called mobile genetic elements (MGEs) that allow them to be horizontally transferred between environmental and/or clinical bacteria. MGEs represent a rather large variety of elements including conjugative plasmids, integrative and conjugative elements, transposons, and integrons (Frost et al., 2005), some of them being more often associated with ARGs than others. As a consequence, instead of monitoring the occurrence of a large panel of clinically relevant ARGs, some authors prefer focusing on selected MGEs frequently associated with ARGs. Among them, class 1 integrons, and to a lesser extent, IncP-1 conjugative plasmids, have been widely studied as proxies to assess the global ARG content of environmental matrices (Stalder et al., 2012; Rizzo et al., 2013; Gillings et al., 2015; Jechalke et al., 2015). Class 1 integrons are genetic platforms able to capture and express resistance gene cassettes, thus promoting genotypic/phenotypic diversity and adaptation of bacteria (Mazel, 2006). They are minimally constituted of an *intI1* gene encoding a site-specific recombinase and of a recombination site *attI* where IntI1 catalyzes the gene cassette insertions. Class 1 integrons usually carry 1–4 of more than 130 different resistance gene cassettes that have been described to date, which makes them integrated indicators of ARGs (Partridge et al., 2009; Stalder et al., 2014; Cury et al., 2016). The plasmids of the IncP-1 incompatibility group are broad host range conjugative elements (Adamczyk and Jagura-Burdzy, 2003). These plasmids, found in clinical and environmental contexts, often carry multiple antibiotic resistance determinants suggesting that they also play a significant role in ARG dissemination (Popowska and Krawczyk-Balska, 2013).

It has been demonstrated that ARGs tend to accumulate over time in environmental microbial communities as a probable consequence of anthropogenic pressure (Knapp et al., 2010). Their association with MGEs can explain the persistence of ARGs in the environment as MGEs allow them to be transferred from unfit bacteria originating from the animal/human microbiome to more locally adapted bacteria (Frost et al., 2005; Martinez, 2009). Surprisingly, MGEs are not equally distributed in heterogeneous matrices, with specific enrichment of some MGEs on suspended particles in marine waters, as demonstrated by Ganesh and collaborators (Ganesh et al., 2014). This suggests that MGE-bearing bacteria can selectively and locally be enriched. The reason for such local and selective enrichment of MGEs is not fully elucidated but it has been known for some time that, besides their ability to transfer genes, MGEs, such as conjugative plasmids, also influence surface properties of bacterial cells (Van Houdt and Michiels, 2005). Indeed, the conjugation of plasmids implies the synthesis of external cell appendages (conjugative pili or adhesins in either Gram-negative or Gram-positive bacteria) that have been demonstrated *in vitro* to promote cell adhesion to solid surface and biofilm formation (Ghigo, 2001; Bhatty et al., 2015, 2017). On the principle, bacterial adhesion thanks to plasmid pili and conjugative transfer of plasmids are two phenomena that might contribute to the formation of local reservoirs of enriched plasmid occurrence, but their relative contributions in a context as complex as a river remain to be elucidated.

In the present work, we investigated the relative occurrence of two MGE proxies for ARGs, namely class 1 integrons and IncP-1 plasmids, in the water column and surface sediments of the Orne River (France) by analyzing raw waters, suspended materials (SMs), and sediments. The results obtained tend to show that bacteria carrying IncP-1 plasmids, and to a lesser extent class 1 integrons, selectively attached on SMs that finally settle to form sediments. *In vitro* experiments were further used to assess the contribution of IncP-1 plasmids to the binding of plasmid-bearing bacteria to artificial supports, and the contribution of bacterial adhesion to plasmid dissemination. All in all, our results demonstrate the major contribution of plasmid-mediated adhesion to particles to the formation of MGE reservoirs in sediments.

MATERIAL AND METHODS

Bacterial Strains and Growth Conditions

The bacterial strains and plasmids used in this work are presented in **Table 1**. Bacteria were grown aerobically in LB medium (LB Broth Miller, Difco^{TM}) at 30°C, with agitation at 160 rpm for liquid cultures. Solid medium was prepared by adding 15 g/L of agar. When required, antibiotic selection was applied at the following concentrations: ampicillin at 100 mg/L, rifampicin at 20 mg/L, and tetracycline at 10 mg/L.

Study Site and River Material Sampling

The Orne is an 86 km long river flowing in Lorraine, tributary of the Moselle in northeastern France, and sub-tributary of the Rhine. The Orne is one of the rivers of the area strongly impacted by ancient mining and iron- and steel-making plants during the 20th century. The Orne River takes its source in a forest area, flows through countryside consisting of fields and meadows, then

TABLE 1 | Bacteria and plasmids used in this study.

Name/species	Genotype/characteristics[a]	References
Plasmids		
pB10	Wild type IncP-1 plasmid isolated from activated sludge	Schlüter et al. (2003)
pBELX	pEX-A derivative (pUC18-based) containing qPCR target sequences for *trfA* of IncP-1 plasmids, the Eubacterial 16S rRNA gene	Bellanger et al. (2014b)
pNORM1	pEX-A derivative (pUC18-based) containing the qPCR target sequences for *intI* of class 1 integron, the Eubacterial 16S rRNA gene	Gat et al. (2017)
Bacillus subtilis		
LMG 7135^T	ATCC 6051, Type strain	BCCM/LMG[b]
CM291	Rif^R derivative of LMG 7135^T	This work
CM295	CM291(pB10), Rif^R, Amx^R, Str^R, Sul^R, Tet^R	This work
Cupriavidus metallidurans		
AE815	plasmid free and Rif^R derivative of wild type strain CH34	Springael et al. (1993)
CM124	AE815(pB10), Rif^R, Amx^R, Str^R, Sul^R, Tet^R	Bellanger et al. (2014a)
Delftia acidovorans		
CM122	*Delftia acidovorans*, Rif^R, Kan^R	Eva Top lab strain collection
CM294	CM122(pB10), Rif^R, Kan^R, Amx^R, Str^R, Sul^R, Tet^R	This work
Escherichia coli		
DH5α	ϕ80*lacZ*ΔacZ*erecA1endA1gyrA96* (Nal^R) *thi-1 hsdR17*($r_K^- m_K^+$) *supE44 relA1 deoR* Δ*(lacZYAargF) U169*	Sambrook et al. (1989)
MG1655	Sequenced λ$^-$ and F$^-$derivative of strain K-12	Blattner et al. (1997)
CM102	DH5α(pB10), Nal^R, Amx^R, Str^R, Sul^R, Tet^R	Schlüter et al. (2003)
CM125	Nal^R derivative of MG1655	Bellanger et al. (2014a)
CM278	CM125(pB10), Nal^R, Amx^R, Str^R, Sul^R, Tet^R	This work
Pseudomonas fluorescens		
CIP 69.13^T	ATCC 13525, Type strain	ATCC[c]
CM292	Rif^R derivative of wild type strain CIP 69.13^T	This work
CM297	CM292(pB10), Rif^R, Amx^R, Str^R, Sul^R, Tet^R	This work
Pseudomonas putida		
SM1443	KT2442 (Rif^R) with a mini-Tn*5-lacI^q* insertion	Christensen et al. (1998)
CM236	SM1443(pB10), Rif^R, Amx^R, Str^R, Sul^R, Tet^R	This work
Shewanella oneidensis		
CM87	Rif^R derivative of wild type strain MR-1^T	Schwalb et al. (2003)
CM293	CM87(pB10), Rif^R, Amx^R, Str^R, Sul^R, Tet^R	This work

[a]*Antibiotic resistance phenotype: Amx^R, amoxicillin; Kan^R, kanamycin; Nal^R, nalidixic acid; Rif^R, rifampicin; Str^R, streptomycin; Sul^R, sulfamides; Tet^R, tetracycline.* [b]*Belgian coordinated collections of microorganisms.* [c]*American Type Culture Collection.*

a highly urbanized and ancient industrialized area before joining the Moselle River. The latter part represents about one fourth of the river linear and, based on geographical data, it is assumed that the river waters drain between 86 and 100% of the watershed surface (1276 km^2), depending on the sampling site considered in this study (see Supplementary Figure 1). The riverbed was strongly modified for industrial purposes. Indeed, two dams were built in the 1958–1965 period and the river was calibrated and channeled in the very last kilometers (Abuhelou et al., 2017; Kanbar et al., 2017). Fifteen pairs of river raw water and SM samples were collected along the last 23 km of the Orne River and over an 11-month period from November 2014 to October 2015 (four pairs on 2014/11/04, three pairs on 2015/02/02, two pairs on 2015/02/03, three pairs on 2015/05/05, and three pairs on 2015/10/06). As previously described (Le Meur et al., 2016), the river water was pumped and sent to a continuous flow field CEPA Z-41 centrifuge (20,000 RPM, equivalent to 17,000 × *g*, with a 600 L/h flow rate), which was used to collect a representative SM-enriched fraction from [*ca.*] 1–2 m^3 of raw water. Raw water samples were collected from the pumping outlet (excess flow). The top surface sediments were collected along the same Orne River section at five different places from January 2014 to July 2015. Sediment samples were collected (on 2014/03/18 and 2015/02/19) as short cores using a piston corer or simple coring tubes (diameter of 6 cm or 9 cm). Coring was preferred to grabbing in order to preserve the layered structure of sediments. The collected sediments were sealed from air and transported in a vertical position. The upper 2 cm layer, referred to as surface sediments, was separated from the core using a single use spatula and into an N_2-filled glove bag to avoid oxidation. The surface layer is highly hydrated, and loosely attached to the underneath material. Different aliquots were prepared for distinct purposes. For geochemical analyses, an aliquot was freeze-dried and ground using an agate mortar and pestle. For DNA extraction, all samples were kept frozen at −20°C (short term storage of SMs and raw waters) or −80°C (long term storage of sediments).

Geochemical Analyses on Sediments and Suspended Materials

Major elements were detected by inductively coupled plasma optical emission spectrometry (ICP-OES). These analyses were performed at SARM (Service d'Analyse des Roches et des Minéraux – CRPG, Vandœuvre-lès-Nancy, France) and all analytical methods were subject to QC/QA procedures using certified reference materials (Carignan et al., 2001). Grain size distribution of SMs and bottom sediments was obtained using laser diffraction (SYMPATEC) with two distinct lenses corresponding to two distinct size ranges (0.45–87.5 μm and 4.5–875 μm). Samples were systematically ultrasonicated for 20 s before measurement, and each measurement was duplicated or triplicated. Mineralogy of sediment and SM samples was investigated using X-ray Diffraction and Transmission Electron Microscopy (like in Kanbar et al., 2017). A synthesis of those analyses is available in Supplementary Table 1 and Supplementary Figures 2, 3.

DNA Extraction

Recombinant plasmid DNAs pBELX and pNORM1, used as qPCR standards, were extracted using the "Wizard® Plus SV Minipreps DNA Purification System" (Promega) according to the recommendations provided by the manufacturer. The plasmids were linearized by *Bam*HI (Promega) before being purified with the "QIAquick PCR DNA purification kit" (Qiagen). Total environmental DNAs were extracted using the "PowerWater DNA Isolation Kit" (MO BIO laboratories Inc). Briefly, 50 mg of sediments or SMs were thawed before being dispersed in 100 mL of non-pyrogenic sterile water (Aqua B-Braun) by vortexing for 30 s followed by 15 min stirring at 160 rpm and 25°C. These sediment/SM suspensions (or 100 mL of sample for raw waters) were filtered on polycarbonate filters (Whatman Nuclepore filter, pore size 0.22 μm, diameter 47 mm) using a filtration apparatus (Combisart 6-branch Manifold, Sartorius). Total DNAs were directly extracted from the filters according to the recommendations provided by the manufacturer and were eluted from silica columns with 100 μL of PCR grade water (RNase-Free Water, Qiagen). Plasmid and total DNA concentration and purity were estimated by spectrophotometry according to standard procedures, and all DNAs were stored at −20°C until use.

Quantitative PCR Assays

The abundance of class 1 integrons and IncP-1α/β plasmids were quantified by qPCR in total environmental DNAs using "Power SYBR® Green PCR Master Mix" (Applied Biosystems) with the primers listed in **Table 2**. Quantitative PCRs were performed in triplicate using "Step One Plus Real-Time PCR System" (Applied Biosystems, driver: StepOne Software v2.2) in a 25 μL reaction volume with 1 μM of each primer, and with thermocycling conditions set as follows: 10 min at 95°C followed by 45 cycles of 15 s at 95°C and 1 min at 60°C. The quality of the PCR products was subsequently checked by melting curve analyses, for which the temperature was ramped between 60 and 95°C in increments of 0.3°C. IncP-1α/β plasmid and class 1 integron quantitative results were normalized to the amount of eubacterial 16S rRNA gene, also quantified by qPCR with the 331F/518R universal primers and using the cycling conditions described above. For quantifications of 16S rRNA gene and IncP-1α/β plasmids and of class 1 integrons, plasmids pBELX and pNORM1, linearized with *Bam*HI, were used as standards, respectively (**Table 1**). The absence of residual inhibitors in the DNA extracts was checked by qPCR by comparing amplifications from serially diluted DNA templates.

Crystal-Violet Staining of Adhering Biomass

Two milliliters of LB was inoculated with a single colony picked from a fresh plate, containing tetracycline for pB10-carrying bacteria, and then incubated for 16 h. One hundred microliters of this culture was mixed with 10 mL of fresh medium and placed in a 55 mm petri dish containing a 47 mm-diameter flat polyethylene disk (Kaldnes Biochip Media) that are originally dedicated to the colonization of bacteria in moving bed biofilm reactors in wastewater treatment processes. The plates were incubated at 30°C under agitation (80 rpm) for 18 h. The quantity of biomass adhering to Kaldnes polyethylene disks was determined by classical crystal-violet staining (Chavant et al., 2007). First, the total amount of planktonic bacteria surrounding the polyethylene disks was estimated by measuring broth turbidity (OD_{600nm}). Second, the polyethylene disks were transferred into new petri dishes where they were successively washed three times with 10 mL of sterile water for removing poorly adherent bacteria. The polyethylene disks were then air-dried for 1.5 h before being incubated in 10 mL of a 0.1% v/v crystal violet solution in H_2O (Biomérieux) for 45 min at room temperature (20°C ± 1°C). The stained disks were then gently washed six times with sterile water to remove excess of crystal violet. Finally, the biomass-associated crystal violet was dissolved with 10 mL of glacial acetic acid and quantified by UV-Vis spectrophotometry at 540 nm (OD_{540nm}). Polyethylene disks without exposure to bacterial cells were used as control.

Bacterial Mating Assays

Mating assays were performed in liquid medium either containing or not a 47 mm polyethylene disk (Kaldnes Biochip Media). Donor (CM102) and recipient bacteria (AE815) were grown for 16 h in broth, supplemented or not with antibiotics, then washed by centrifugation and re-suspended in one volume of sterile $MgSO_4$ (10 mM). For mating assays with a polyethylene disk, 10 mL of LB broth containing a 1:100 dilution of both strains, prepared from the washed cell suspensions, were introduced in an empty 55 mm petri dish and incubated for 18 h at 30°C under agitation (80 rpm). At the end of the incubation period, broth and polyethylene disks were recovered separately for bacterial strain enumeration. Beforehand, the polyethylene disks were washed three times with sterile water and adhering bacteria were re-suspended by vigorous vortexing in 20 mL of $MgSO_4$ (10 mM). Donor (CM102), recipient (AE815), and transconjugant bacteria [AE815(pB10)] were enumerated on selective plates containing either tetracycline (Tet), rifampicin

TABLE 2 | Primers used in qPCR.

Name	Sequence	Targeted gene	Product size (bp)	Referencec
331F	5′-TCCTACGGGAGGCAGCAGT-3′	16S rRNA	197 bp	Muyzer et al., 1993; Nadkarni et al., 2002
518R	5′-ATTACCGCGGCTGCTGG-3′			
intI1-LC1	5′-GCCTTGATGTTACCCGAGAG-3′	*intI1* (class 1 integrons)	196 bp	Barraud et al., 2010
intI1-LC5	5′-GATCGGTCGAATGCGTGT-3′			
trfA2-1	5′-CGAAATTCRTRTGGGAGAAGTA-3′	*trfA* (IncP-1 plasmids)	241 bp	Götz et al., 1996
trfA2-2	5′-CGYTTGCAATGCACCAGGTC-3′			

(Rif), or both antibiotics (Tet Rif), respectively. For the control mating assays between planktonic cells, the incubations of donor and recipient cells were performed as described above but the polyethylene disks were omitted.

Statistical Analyses

Statistical analyses were performed using the R software and presented according to Cumming and collaborators (Cumming et al., 2007). The normality of the data was verified using the Shapiro-Wilks test before performing other statistical tests. The potential pairing between data was also taken into account before carrying out the analyses. For statistical analyses of the data, Wilcoxon signed-rank test, Wilcoxon rank-sum test, Kruskal–Wallis rank-sum test, Student's *T*-test, and Spearman correlation test were independently chosen according to the circumstances, as justified in the corresponding Result subsections.

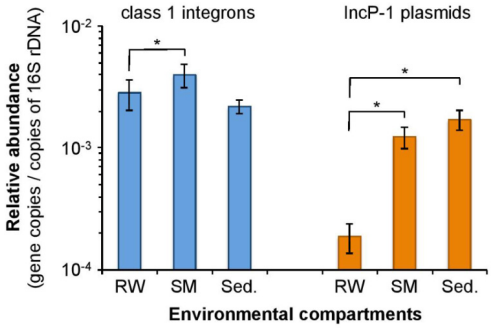

FIGURE 1 | Relative abundance of class 1 integrons and IncP-1α/β plasmids in compartments from the Orne River. RW, Raw waters; SM, Suspended materials; Sed., Sediments. Error bars indicate the standard error of the mean (n = 15 for RW and SM; n = 8 for Sed.). Asterisks indicate statistical differences between relative abundances ($p < 10^{-3}$).

RESULTS

Occurrence of Class 1 Integrons and IncP-1 Plasmids in the Orne River

The distribution of class 1 integrons and IncP-1α/β plasmids in the different physical compartments of the Orne River was first investigated so as to point out any selective/specific partitioning. Total community DNA was extracted from 15 raw water samples, 15 corresponding SM samples, and eight surface sediment samples collected over an 11-month period. Their contents in class 1 integrons and IncP-1α/β plasmids were determined by qPCR and then further normalized to the corresponding 16S rRNA gene content, also determined by qPCR. The relative abundance of each MGE in the three compartments is presented in **Figure 1**.

Globally, the relative abundance of class 1 integrons and IncP-1α/β appeared to be 2.2 ± 0.4 and 13.3 ± 4.0 times higher in SMs than in the corresponding raw water samples, respectively. This trend was observed in all but 1 of the 15 paired samples. Wilcoxon signed-rank test further confirmed the statistical significance of the MGE enrichment on SM-associated microbial communities with p-values of 3.10^{-4} and 6.10^{-5} for class 1 integrons and IncP-1α/β plasmids, respectively. Despite being both significant, the enrichment effect observed for MGE-bearing bacteria on SMs remains higher for IncP-1α/β plasmids than for class-1 integrons (Wilcoxon signed rank test; $p = 2.10^{-4}$), which already points out two different bacterial populations with different MGE content characteristics.

The statistical comparison of the MGE abundances obtained for top surface sediments with those obtained for the other compartments requires using a Wilcoxon rank-sum test as sediments were sampled independently from raw waters and SMs, and data were not normally distributed. In this respect, the relative abundance of class 1 integrons in surface sediments did not seem to differ significantly from those of raw waters or SMs ($p = 0.39$ and $p = 1$, respectively). For IncP-1α/β plasmids though, the relative abundance was 9.1 and 1.4 higher in sediments than in raw waters and SMs, respectively. If these relative abundances were statistically different between sediments and raw waters ($p = 5.10^{-4}$), they remained non-significantly different between surface sediments and SMs ($p = 0.18$). The latter result raises the question of whether plasmid-bearing bacteria from raw waters could selectively be enriched on SMs, which could then settle in the riverbed to form fresh sediments that exhibit a similar IncP-1 plasmid richness, as we shall discuss in subsection 3.2.

The different distributions observed between IncP-1 plasmid- and class 1 integron-bearing bacteria show that MGEs influence their own compartmentalization in aqueous media. Two hypotheses can be made to explain the specific enrichment of IncP-1 plasmids on SMs. First, IncP-1 plasmids are conjugative elements for which it has been suggested that the promiscuity encountered in biofilms favors gene transfer compared to the planktonic bacteria life style (Molin and Tolker-Nielsen, 2003). Considering the fact that conjugative transfer is a replicative event (Lanka and Wilkins, 1995), it can be argued that bacterial

adhesion to SMs leads to biofilm formation, which then favors plasmid transfer and, therefore, results in an increase in its relative abundance. Alternatively, Ghigo (2001) showed that conjugative plasmids themselves could promote the formation of biofilms as they encode for a conjugative pili, a cell appendage also considered as an adhesion substrate. In such a case, the IncP-1 plasmid-bearing fraction of the bacterial population should be more likely to bind to the organo-mineral particles constituting SMs than the plasmid-free bacteria, which should lead to a compartmentalization of the plasmid-bearing bacteria over time. The two hypotheses, "adhesion-promoted plasmid transfer" and "plasmid-promoted adhesion" are not exclusive, but their relative contributions remain to be elucidated.

Mineral Relationship Between Sediments and SMs of the Orne River

If IncP-1 plasmid-bearing bacteria were to be selectively enriched on SMs before particles settle and form sediments, a parent-like relationship between SMs and surface sediments is to be expected. In such a case, SMs and top surface sediments should share common mineral properties demonstrating their relationship in terms of size distribution, element composition, and mineral constituents (Supplementary Table 1 and Supplementary Figures 2, 3). SMs and sediments are predominated by silicates, in particular clay minerals. SM particles are relatively fine with a grain size distribution centered below 10 μm, and the decile (D50) of Orne River suspended particles was estimated to be 12 ± 3 μm. The grain size distribution measurements evidenced that sediments are coarser than SMs, suggesting a size sorting upon settling and/or a post-settlement modification of the grain size distribution, as reported elsewhere (Lartiges et al., 2001; Droppo et al., 2009). This modification can be linked to a slightly higher carbon content in sediments ($4.3 \pm 2\%$ and $4.9 \pm 0.7\%$ for SMs and sediments, respectively) as organic matter is known to enhance particle aggregation. All in all, the element composition and the mineralogy clearly draw a parent-like relationship between SMs and surface sediments. Although slight differences remain, they can be attributed to both successive settling events and post-settlement modifications. Yet, a parental-like relationship between SMs and sediments can be interpreted as particle settling, as sediment mobilization, or as both.

Due the locations of the sampling stations (Supplementary Figure 1), the SMs transported by the Orne River are likely to be alternatively predominated by runoff-generated particles during rain events (or high water discharge periods), and by urban inputs and primary production in the water column during low-water discharge periods. The relative contribution of sediment remobilization as SMs is driven by different parameters including hydroclimatic conditions and river characteristics (class, width, flood bed status, sediment flow rate, etc.). This contribution is considered to be significant during specific periods of hydrological sequences, i.e., during the early stages of flood events occurring after a long low-flow period (typically during the fall season). In the studied case, most of the samples were collected in the middle or late stages of flood events (see Supplementary Figure 1), thus it can be considered that the origin of SMs sampled in the water column was predominated by particles resulting from soil leaching. In the Orne watershed, 67% of the surface is dedicated to agriculture, enhancing the generation of suspended particles during rain events (Le Meur et al., 2016). Thus, although we cannot fully demonstrate the absence of sediment remobilization, its contribution is considered to be minor in such water discharge conditions. Mineralogy, particle size distribution, and element contents clearly draw a parental-like link between sediments and SMs. Thus, these similarities are explained by the SM settling process, which mostly occurs at the end of the flood events, i.e., when water flow is decreasing.

The Carriage of an IncP-1 Plasmid Has Contrasted Effects on Bacterial Adhesion

Considering the selective enrichment of IncP-1 plasmid-bearing bacteria on SMs and sediments, we wondered if the mere fact of bearing this kind of MGEs was sufficient to increase cell adhesion to surfaces compared to plasmid-free bacteria. The phenotypic effect of bearing an IncP-1 plasmid was investigated using a series of isogenic bacterial strains from various species carrying or not the natural IncP-1β plasmid pB10 (Schlüter et al., 2003). Bacteria were allowed to grow as biofilm on Kaldnes polyethylene disks immerged in LB medium for 18 h, resulting in a large excess of planktonic cells. The abundance of planktonic bacteria (PB) was estimated at 600 nm (OD_{600}) by spectrometry, while the abundance of the adhering biomass was measured using a classical crystal violet staining method [(CV); OD_{540}] (**Table 3**). The propensity to form biofilms was finally estimated as the relative abundance of adhering cells compared to planktonic bacteria, here given in arbitrary units [(CV)/(PB)]. The results obtained (**Table 3**) showed that the carriage of pB10 significantly increased the relative amount of adhering bacteria on polyethylene surfaces (Student's *T*-test for paired data, $p = 5.10^{-3}$). Apart from the outlier strains *Escherichia coli* MG1655 and *Shewanella oneidensis* MR-1 that seem to have peculiar behaviors, the effect of pB10 carriage on adhesion is stronger when the basal level of biofilm formation is initially low in the absence of plasmid (Spearman correlation without considering strains MG1655 and MR-1: $r = -0.943$, $p = 0.02$) (**Figure 2**). It should be noted that the different adhesion behaviors observed for the different strains could not be attributed to a strain-dependent instability of the plasmid. This was estimated by plating overnight cultures grown without antibiotics on plates selective or not for pB10-bearing bacteria. Plasmid pB10 appeared to be highly stable as no significant loss could be observed in all the bacterial hosts used (Kruskal–Wallis rank sum test, $p = 0.99$), and as it had already be thoroughly assessed before for most of the bacteria and/or strains used in this work (De Gelder et al., 2007). Putting these observations back in the context of the plasmid enrichment observed on the SMs and sediments of the Orne River, it tends to demonstrate that (i) IncP-1 plasmid carriage is sufficient to promote the compartmentalization of plasmid-bearing bacteria on SMs and thus on freshly deposited sediments, and (ii) the gain in adhesion

TABLE 3 | Effect of pB10 carriage on bacterial adhesion properties.

	Planktonic biomass (OD_{600nm})		Adhering biomass (OD_{540nm})		Relative biofilm amount (arbitrary unit: OD_{540nm}/OD_{600nm})		
Strains/species	**Without pB10**	**With pB10**	**Without pB10**	**With pB10**	**Without pB10**	**With pB10**	**Fold increase**
E. coli DH5α	3.205 ± 0.032	3.686 ± 0.038	0.323 ± 0.072	1.101 ± 0.129	0.10 ± 0.02	0.30 ± 0.03	3.18 ± 1.04
E. coli MG1655	4.669 ± 0.219	4.960 ± 0.388	0.254 ± 0.047	0.309 ± 0.065	0.05 ± 0.01	0.06 ± 0.02	1.15 ± 0.09
C. metallidurans	3.251 ± 0.136	3.271 ± 0.313	0.530 ± 0.152	0.898 ± 0.483	0.16 ± 0.04	0.28 ± 0.16	1.70 ± 1.04
B. subtilis	3.988 ± 0.357	3.700 ± 0.056	0.372 ± 0.045	0.864 ± 0.222	0.10 ± 0.02	0.23 ± 0.06	2.53 ± 0.64
P. putida	5.787 ± 0.211	5.047 ± 0.220	2.361 ± 0.405	2.838 ± 0.092	0.41 ± 0.08	0.56 ± 0.03	1.44 ± 0.33
P. fluorescens	3.401 ± 1.238	2.715 ± 1.522	0.513 ± 0.047	0.591 ± 0.026	0.17 ± 0.06	0.30 ± 0.15	1.64 ± 0.38
S. oneidensis	4.985 ± 1.317	4.719 ± 1.142	0.503 ± 0.150	0.419 ± 0.200	0.12 ± 0.08	0.11 ± 0.08	0.82 ± 0.09
D. acidovorans	4.501 ± 0.488	3.634 ± 0.915	2.664 ± 0.384	2.294 ± 0.928	0.60 ± 0.12	0.67 ± 0.21	1.09 ± 0.14

Values are expressed as a mean ± standard error (n = 3).

is not equally distributed among bacterial strains, which should also contribute to compartmentalize bacteria according to their nature.

Adhesion to Polyethylene Disks Does Not Increase the Transfer Frequency of Plasmid pB10

Considering the fact that cell-cell contacts, required for conjugation, may be favored in biofilm and that conjugation is an intercellular mode of DNA replication, an increased frequency of transfer in biofilm may also explain enrichment of IncP-1 plasmid on SMs. This hypothesis was tested by comparing the transfer efficiency of plasmid pB10 among both planktonic bacteria and surface-associated cells. The donor bacteria *E. coli* DH5α(pB10) and the recipient strain *Cupriavidus metallidurans* AE815 were mixed and incubated for 18 h in LB medium in the presence or absence of Kaldnes polyethylene disks. Donor, recipient, and transconjugant cells were then enumerated independently from (i) the disk-free mating experiment for assessing pB10 transfer in planktonic conditions, and (ii) directly from the Kaldnes polyethylene disks for assessing pB10 transfer in biofilm. When comparing the mating conditions (planktonic versus biofilms), transfer frequencies, expressed either as transconjugant per recipient or transconjugant per donor (**Figure 3**), did not appear significantly different (Kruskal–Wallis rank sum test; $p > 0.05$). Moreover, donor, recipient, and transconjugant cells were also enumerated in the liquid medium surrounding the Kaldnes polyethylene disks. The corresponding pB10 transfer frequencies were similar to that observed for the bacteria growing as a biofilm on the disks (Wilcoxon signed rank test; $p > 0.1$). Therefore, it is unlikely that the calculation of transfer frequencies were biased by transconjugants accumulating from the liquid to the biofilm or standing out from the disks to the liquid. All in all, it thus appears that, under the conditions provided by the tests carried out on polyethylene disks, development as biofilm does not promote a higher transfer level of pB10. Therefore, between the two formulated hypotheses, the enrichment of plasmid-bearing bacteria on SMs and sediments is likely to be dominated by the adhesion properties brought by conjugative plasmids and their conjugative pili.

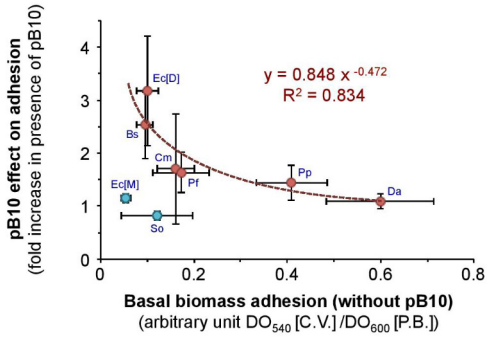

FIGURE 2 | Gain in biofilm formation for pB10-bearing bacteria. Biofilm formation was compared for isogenic strains with and without the IncP-1β plasmid pB10: *B. subtilis* CM291 (Bs); *C. metallidurans* AE815 (Cm); *D. acidovorans* (Da); *E. coli* DH5α (Ec[D]), *E. coli* MG1655 (Ec[M]); *P. fluorescens* CM292 (Pf); *P. putida* SM1443 (Pp); *S. oneidensis* CM87 (So). Error bars indicate the standard error of the means ($n = 3$). The dotted line represents a regression curve related to a Spearman correlation without considering strains MG1655 and MR-1 showing that the effect of pB10 carriage on adhesion is stronger as the basal level of biofilm formation is initially low in the absence of plasmid ($r = -0.943$, $p = 0.02$). The equation of the regression curve is indicated.

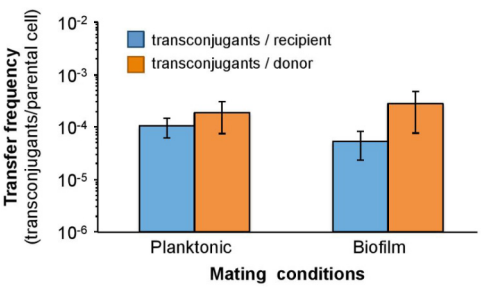

FIGURE 3 | Transfer of pB10 among planktonic and polyethylene disk-adhering bacteria. Error bars indicate the standard error of the means ($n = 4$). There is not any statistical difference between the presented transfer frequencies.

DISCUSSION

With their very close association with ARGs, MGEs undoubtedly play a central role in the dissemination of antibiotic resistance (Frost et al., 2005). Yet, demonstrating such dissemination in environmental settings remains relatively challenging as there is no easy way to evaluate the relative contribution of well-known mechanisms when combined to the complexity and heterogeneity of the environment (Elsas et al., 2002; Bellanger et al., 2014a). Occurrence-based studies have brought to light the existence of environmental reservoirs of ARGs and MGEs, suggesting the existence of environmental hotspots of ARG dissemination (Martinez, 2009; Wright, 2010; Perry and Wright, 2013). Without questioning the simple fact that ARGs can disseminate thanks to MGEs, we demonstrated with plasmid pB10 that physico-chemical interactions of bacteria with particle surfaces could preferentially promote the adhesion of IncP-1 plasmid-bearing bacteria without increasing the plasmid transfer frequency. This also means that, in the environmental context, the biofilm mode of life or adhesion to particles may also act as a "selective enrichment process" for ARGs associated with conjugative plasmids, leading to local reservoirs, even in the absence of any selective antibiotics.

The compartmentalization of IncP-1 plasmid-bearing bacteria observed in the context of the Orne River fits well the spatial clustering reported in a few metagenomic studies showing that numerous genes encoding functions associated with horizontal gene transfer and MGEs, among which type IV secretion systems (conjugation machineries), are statically overrepresented in marine bacteria attached to organo-mineral particles or algae (Burke et al., 2011; Allen et al., 2013; Ganesh et al., 2014). The authors of these works suggest that this enrichment could be due to peculiar conditions encountered in sediments and on SMs (high cell density, probable nutrient richness, shelter effect, etc.) that would promote horizontal gene transfer. In this respect, bacterial biofilms have frequently been described as hot spots of conjugative transfers (Molin and Tolker-Nielsen, 2003; Aminov, 2011; Skippington and Ragan, 2011; Madsen et al., 2012). However, to the best of our knowledge, this alternative has never been challenged experimentally by possible enrichment of plasmid-bearing bacteria due to their adhesion to mineral particles or organo-mineral aggregates.

Slight enrichment in class 1 integrons of environmental bacteria attached on the organo-mineral particles forming SMs from the Orne River by comparison to bacteria from raw waters has also been reported. To our knowledge, such a spatial clustering of class 1 integrons in an environmental compartment had never been reported. Class 1 integrons are frequently described as being hosted by IncP-1 plasmids (Popowska and Krawczyk-Balska, 2013) and as such may then show a similar compartmentalization. However, in complete genome databases, while 67% of integrons could be described as mobile (i.e., integrons associated with MGEs), only 12% of integrons (mostly class 1 integrons) appeared to be plasmid borne (Cury et al., 2016). This moderate association with plasmids could explain why class 1 integron-bearing bacteria of the Orne River do not follow the same distribution as that of the IncP-1 plasmid-bearing bacteria if the adhesion to particles was to play a central role in the compartmentalization of MGEs.

Here, we described one situation, in which the transfer of plasmid pB10 is not significantly enhanced in biofilm compared to planktonic cells. This observation is in line with a few studies showing that the transfer of conjugative plasmids in bacterial populations structured as biofilm is often limited to the donor-recipient interfaces, where bacteria are most physiologically active (Stalder and Top, 2016 and references therein). Thus, even if highly efficient in biofilm, the ability of a plasmid to transfer to the neighboring cells can appear very localized and may go unnoticed if the active recipient-donor interface represents a minute part of a well developed biofilm as it is often the case (Stalder and Top, 2016 and references therein).

With this study, we showed that IncP-1 plasmid-bearing bacteria are significantly enriched on SMs and surface sediments of the Orne River, and we provided a case study with pB10 where the carriage of plasmid can promote the adhesion of bacteria, while the adhesion to surfaces does not seem to promote significantly the transfer of the plasmid. Future efforts will focus on investigating the occurrence of class 1 integrons and IncP-1 plasmids in deeper sediment layers in order to get an insight into their abundance as a function of the local physical chemistry of the sediments, in order to determine the driving parameters associated with local MGE enrichment.

Whatever the main driving phenomenon, i.e., selective attachment of plasmid-bearing bacteria or increase in plasmid transfer in adhering bacteria, enrichment of MGEs on SMs likely means ARG/ARB enrichment as well. Considering that river SMs participate in sediment formation, this work pinpoints the role that sediments could play as ARG, ARB, and MGE reservoirs. Indeed, in the studied case presented here, SMs can be assumed as the finest fraction of sediments, predominated by clay minerals. Clay and other minerals confer to those river materials high potential to bind to organic matter and microorganisms. Thus, studying the ability of various SM physicochemical surfaces such as phyllosilicates or carbonates in being differentially colonized by ARG/MGE-free or -bearing bacteria would be of interest to predicting whether a given environment is likely to be permissive for the enrichment of MGEs and their ARGs. Ultimately, river sediments can be considered as a compartment where ARGs can accumulate and disseminate by means of MGEs to environmental and pathogenic bacteria. Numerous European rivers have been polluted, channeled, and fragmented by dams, sills, hydroelectric power stations, mills, and other obstacles. This leads to a dramatic reduction in biodiversity and water quality as well as massive disappearance of the associated wetlands, essential for the prevention of floods, and excessive sediment accumulation on riverbeds. The EU Water Framework Directive promotes river restoration and improvement of both chemical and biological water quality, notably by removing dams and other hindrances. These removal operations associated with more and more frequent hydroclimatic events and severe floods resulting from climate change will lead to remobilization of sediments and their associated content in chemical and biological pollutants such as ARGs, ARB, and MGEs. The consequences

on public health of these sediment remobilizations remain an open question that should be addressed in future works/research programs.

AUTHOR CONTRIBUTIONS

XB, EM-P, and CM contributed substantially to the conception, the design, and the supervision of the study. MCB and HG performed experiments. MCB, HG, CM, and XB interpreted the results. XB and CM prepared the manuscript with input from the other co-authors.

FUNDING

The present work was part of a larger research project on the Orne River, financially supported by the Agence Nationale de la Recherche ANR (MOBISED project, ANR-14-CE01-0019), the Rhin-Meuse Water Agency (AERM project QUALIORNE), the LTSER-France, and the Lorraine Region through the research network of Zone Atelier Moselle (ZAM). MCB was funded by a Ph.D. studentship from the National Council on Science and Technology of Mexico (CONACYT) Ph.D. scholarship (reference 410720).

ACKNOWLEDGMENTS

The authors wish to thank the members of the MOBISED project Valery COLLIN, Renaud GLEY, and Allan BAUER who performed water and sediment sampling. They are grateful to Claire Delus from Université de Lorraine for helping in describing the Orne watershed. They would also like to thank the Syndicat de Valorisation des Eaux de l'Orne (SVEO) and the city of Moyeuvre-Grande for granting them access to the sampling sites.

SUPPLEMENTARY MATERIAL

The Supplementary Material for this article can be found online at: https://www.frontiersin.org/articles/10.3389/fmicb.2018.01443/full#supplementary-material

REFERENCES

Abuhelou, F., Mansuy-Huault, L., Lorgeoux, C., Catteloin, D., Collin, V., Bauer, A., et al. (2017). Suspended particulate matter collection methods influence the quantification of polycyclic aromatic compounds in the river system. *Environ. Sci. Pollut. Res.* 24, 22717–22729. doi: 10.1007/s11356-017-9840-5

Adamczyk, M., and Jagura-Burdzy, G. (2003). Spread and survival of promiscuous IncP-1 plasmids. *Acta Biochim. Pol.* 50, 425–453.

Allen, A. E., Allen, L. Z., and McCrow, J. P. (2013). Lineage specific gene family enrichment at the microscale in marine systems. *Curr. Opin. Microbiol.* 16, 605–617. doi: 10.1016/j.mib.2013.10.001

Aminov, R. I. (2011). Horizontal gene exchange in environmental microbiota. *Front. Microbiol.* 2:158. doi: 10.3389/fmicb.2011.00158

Baquero, F., Martínez, J.-L., and Cantón, R. (2008). Antibiotics and antibiotic resistance in water environments. *Curr. Opin. Biotechnol.* 19, 260–265. doi: 10.1016/j.copbio.2008.05.006

Barraud, O., Baclet, M. C., Denis, F., and Ploy, M. C. (2010). Quantitative multiplex real-time PCR for detecting class 1, 2 and 3 integrons. *J. Antimicrob. Chemother.* 65, 1642–1645. doi: 10.1093/jac/dkq167

Bellanger, X., Guilloteau, H., Bonot, S., and Merlin, C. (2014a). Demonstrating plasmid-based horizontal gene transfer in complex environmental matrices: a practical approach for a critical review. *Sci. Total Environ.* 493, 872–882. doi: 10.1016/j.scitotenv.2014.06.070

Bellanger, X., Guilloteau, H., Breuil, B., and Merlin, C. (2014b). Natural microbial communities supporting the transfer of the IncP-1β plasmid pB10 exhibit a higher initial content of plasmids from the same incompatibility group. *Front. Microbiol.* 5:637. doi: 10.3389/fmicb.2014.00637

Bhatty, M., Camacho, M. I., Gonzalez-Rivera, C., Frank, K. L., Dale, J. L., Manias, D. A., et al. (2017). PrgU: a suppressor of sex pheromone toxicity in *Enterococcus faecalis*. *Mol. Microbiol.* 103, 398–412. doi: 10.1111/mmi.13563

Bhatty, M., Cruz, M. R., Frank, K. L., Gomez, J. A. L., Andrade, F., Garsin, D. A., et al. (2015). *Enterococcus faecalis* pCF10-encoded surface proteins PrgA, PrgB (aggregation substance) and PrgC contribute to plasmid transfer, biofilm formation and virulence. *Mol. Microbiol.* 95, 660–677. doi: 10.1111/mmi.12893

Blattner, F. R., Plunkett, G., Bloch, C. A., Perna, N. T., Burland, V., Riley, M., et al. (1997). The complete genome sequence of *Escherichia coli* K-12. *Science* 277, 1453–1462. doi: 10.1126/science.277.5331.1453

Burke, C., Steinberg, P., Rusch, D., Kjelleberg, S., and Thomas, T. (2011). Bacterial community assembly based on functional genes rather than species. *Proc. Natl. Acad. Sci. U.S.A.* 108, 14288–14293. doi: 10.1073/pnas.1101591108

Carignan, J., Hild, P., Mevelle, G., Morel, J., and Yeghicheyan, D. (2001). Routine analyses of trace elements in geological samples using flow injection and low pressure on-line liquid chromatography coupled to ICP-MS: a study of geochemical reference materials BR, DR-N, UB-N, AN-G and GH. *Geostand. Newsl.* 25, 187–198. doi: 10.1111/j.1751-908X.2001.tb00595.x

Chavant, P., Gaillard-Martinie, B., Talon, R., Hébraud, M., and Bernardi, T. (2007). A new device for rapid evaluation of biofilm formation potential by bacteria. *J. Microbiol. Methods* 68, 605–612. doi: 10.1016/j.mimet.2006.11.010

Christensen, B. B., Sternberg, C., Andersen, J. B., Eberl, L., Møller, S., Givskov, M., et al. (1998). Establishment of new genetic traits in a microbial biofilm community. *Appl. Environ. Microbiol.* 64, 2247–2255.

Cosgrove, S. E. (2006). The relationship between antimicrobial resistance and patient outcomes: mortality, length of hospital stay, and health care costs. *Clin. Infect. Dis.* 42, S82–S89. doi: 10.1086/499406

Cumming, G., Fidler, F., and Vaux, D. L. (2007). Error bars in experimental biology. *J. Cell Biol.* 177, 7–11. doi: 10.1083/jcb.200611141

Cury, J., Jové, T., Touchon, M., Néron, B., and Rocha, E. P. (2016). Identification and analysis of integrons and cassette arrays in bacterial genomes. *Nucleic Acids Res.* 44, 4539–4550. doi: 10.1093/nar/gkw319

De Gelder, L., Ponciano, J. M., Joyce, P., and Top, E. M. (2007). Stability of a promiscuous plasmid in different hosts: no guarantee for a long-term relationship. *Microbiology* 153, 452–463. doi: 10.1099/mic.0.2006/001784-0

de Kraker, M. E. A., Stewardson, A. J., and Harbarth, S. (2016). Will 10 million people die a year due to antimicrobial resistance by 2050? *PLoS Med.* 13:e1002184. doi: 10.1371/journal.pmed.1002184

Droppo, I. G., Liss, S. N., Williams, D., Nelson, T., Jaskot, C., and Trapp, B. (2009). Dynamic existence of waterborne pathogens within river sediment compartments. Implications for water quality regulatory affairs. *Environ. Sci. Technol.* 43, 1737–1743. doi: 10.1021/es802321w

Elsas, V., Dirk, J., and Bailey, M. J. (2002). The ecology of transfer of mobile genetic elements. *FEMS Microbiol. Ecol.* 42, 187–197. doi: 10.1111/j.1574-6941.2002.tb01008.x

Frost, L. S., Leplae, R., Summers, A. O., and Toussaint, A. (2005). Mobile genetic elements: the agents of open source evolution. *Nat. Rev. Microbiol.* 3, 722–732. doi: 10.1038/nrmicro1235

Ganesh, S., Parris, D. J., DeLong, E. F., and Stewart, F. J. (2014). Metagenomic analysis of size-fractionated picoplankton in a marine oxygen minimum zone. *ISME J.* 8, 187–211. doi: 10.1038/ismej.2013.144

Gat, D., Mazar, Y., Cytryn, E., and Rudich, Y. (2017). Origin-dependent variations in the atmospheric microbiome community in eastern Mediterranean dust storms. *Environ. Sci. Technol.* 51, 6709–6718. doi: 10.1021/acs.est.7b00362

Ghigo, J.-M. (2001). Natural conjugative plasmids induce bacterial biofilm development. *Nature* 412, 442–445. doi: 10.1038/35086581

Gillings, M. R., Gaze, W. H., Pruden, A., Smalla, K., Tiedje, J. M., and Zhu, Y.-G. (2015). Using the class 1 integron-integrase gene as a proxy for anthropogenic pollution. *ISME J.* 9, 1269–1279. doi: 10.1038/ismej.2014.226

Götz, A., Pukall, R., Smit, E., Tietze, E., Prager, R., Tschäpe, H., et al. (1996). Detection and characterization of broad-host-range plasmids in environmental bacteria by PCR. *Appl. Environ. Microbiol.* 62, 2621–2628.

Heuer, H., Schmitt, H., and Smalla, K. (2011). Antibiotic resistance gene spread due to manure application on agricultural fields. *Curr. Opin. Microbiol.* 14, 236–243. doi: 10.1016/j.mib.2011.04.009

Jechalke, S., Broszat, M., Lang, F., Siebe, C., Smalla, K., and Grohmann, E. (2015). Effects of 100 years wastewater irrigation on resistance genes, class 1 integrons and IncP-1 plasmids in Mexican soil. *Front. Microbiol.* 6:163. doi: 10.3389/fmicb.2015.00163

Kanbar, H. J., Montargès-Pelletier, E., Losson, B., Bihannic, I., Gley, R., Bauer, A., et al. (2017). Iron mineralogy as a fingerprint of former steelmaking activities in river sediments. *Sci. Total Environ.* 59, 540–553. doi: 10.1016/j.scitotenv.2017.04.156

Knapp, C. W., Dolfing, J., Ehlert, P. A. I., and Graham, D. W. (2010). Evidence of increasing antibiotic resistance gene abundances in archived soils since 1940. *Environ. Sci. Technol.* 44, 580–587. doi: 10.1021/es901221x

Lanka, E., and Wilkins, B. M. (1995). DNA processing reactions in bacterial conjugation. *Annu. Rev. Biochem.* 64, 141–169. doi: 10.1146/annurev.bi.64.070195.001041

Lartiges, B. S., Deneux-Mustin, S., Villemin, G., Mustin, C., Barrès, O., Chamerois, M., et al. (2001). Composition, structure and size distribution of suspended particulates from the Rhine River. *Water Res.* 35, 808–816. doi: 10.1016/S0043-1354(00)00293-1

Le Meur, M., Montargès-Pelletier, E., Bauer, A., Gley, R., Migot, S., Barres, O., et al. (2016). Characterization of suspended particulate matter in the Moselle River (Lorraine, France): evolution along the course of the river and in different hydrologic regimes. *J. Soils Sediments* 16, 1625–1642. doi: 10.1007/s11368-015-1335-8

Madsen, J. S., Burmølle, M., Hansen, L. H., and Sørensen, S. J. (2012). The interconnection between biofilm formation and horizontal gene transfer. *FEMS Immunol. Med. Microbiol.* 65, 183–195. doi: 10.1111/j.1574-695X.2012.00960.x

Martinez, J. L. (2009). Environmental pollution by antibiotics and by antibiotic resistance determinants. *Environ. Pollut.* 157, 2893–2902. doi: 10.1016/j.envpol.2009.05.051

Mazel, D. (2006). Integrons: agents of bacterial evolution. *Nat. Rev. Microbiol.* 4, 608–620. doi: 10.1038/nrmicro1462

Molin, S., and Tolker-Nielsen, T. (2003). Gene transfer occurs with enhanced efficiency in biofilms and induces enhanced stabilisation of the biofilm structure. *Curr. Opin. Biotechnol.* 14, 255–261. doi: 10.1016/S0958-1669(03)00036-3

Muyzer, G., de Waal, E. C., and Uitterlinden, A. G. (1993). Profiling of complex microbial populations by denaturing gradient gel electrophoresis analysis of polymerase chain reaction-amplified genes coding for 16S rRNA. *Appl. Environ. Microbiol.* 59, 695–700.

Nadkarni, M. A., Martin, F. E., Jacques, N. A., and Hunter, N. (2002). Determination of bacterial load by real-time PCR using a broad-range (universal) probe and primers set. *Microbiology* 148, 257–266. doi: 10.1099/00221287-148-1-257

Partridge, S. R., Tsafnat, G., Coiera, E., and Iredell, J. R. (2009). Gene cassettes and cassette arrays in mobile resistance integrons. *FEMS Microbiol. Rev.* 33, 757–784. doi: 10.1111/j.1574-6976.2009.00175.x

Perry, J., and Wright, G. (2013). The antibiotic resistance "mobilome": searching for the link between environment and clinic. *Front. Microbiol.* 4:138. doi: 10.3389/fmicb.2013.00138

Popowska, M., and Krawczyk-Balska, A. (2013). Broad-host-range IncP-1 plasmids and their resistance potential. *Front. Microbiol.* 4:44. doi: 10.3389/fmicb.2013.00044

Pruden, A., Pei, R., Storteboom, H., and Carlson, K. H. (2006). Antibiotic resistance genes as emerging contaminants: studies in northern Colorado. *Environ. Sci. Technol.* 40, 7445–7450. doi: 10.1021/es060413l

Rizzo, L., Manaia, C., Merlin, C., Schwartz, T., Dagot, C., Ploy, M. C., et al. (2013). Urban wastewater treatment plants as hotspots for antibiotic resistant bacteria and genes spread into the environment: a review. *Sci. Total Environ.* 447, 345–360. doi: 10.1016/j.scitotenv.2013.01.032

Sambrook, J., Fritsch, E. F., and Maniatis, T. (1989). *Molecular Cloning: A Laboratory Manual*. Cold Spring Harbor, NY: Cold Spring Harbor Laboratory Press

Schlüter, A., Heuer, H., Szczepanowski, R., Forney, L. J., Thomas, C. M., Pühler, A., et al. (2003). The 64508 bp IncP-1β antibiotic multiresistance plasmid pB10 isolated from a waste-water treatment plant provides evidence for recombination between members of different branches of the IncP-1β group. *Microbiology* 149, 3139–3153. doi: 10.1099/mic.0.26570-0

Schwalb, C., Chapman, S. K., and Reid, G. A. (2003). The tetraheme cytochrome CymA is required for anaerobic respiration with Dimethyl sulfoxide and nitrite in Shewanella oneidensis. *Biochemistry* 42, 9491–9497. doi: 10.1021/bi034456f

Skippington, E., and Ragan, M. A. (2011). Lateral genetic transfer and the construction of genetic exchange communities. *FEMS Microbiol. Rev.* 35, 707–735. doi: 10.1111/j.1574-6976.2010.00261.x

Springael, D., Kreps, S., and Mergeay, M. (1993). Identification of a catabolic transposon, Tn4371, carrying biphenyl and 4-chlorobiphenyl degradation genes in *Alcaligenes eutrophus* A5. *J. Bacteriol.* 175, 1674–1681. doi: 10.1128/jb.175.6.1674-1681.1993

Stalder, T., Barraud, O., Casellas, M., Dagot, C., and Ploy, M.-C. (2012). Integron involvement in environmental spread of antibiotic resistance. *Front. Microbiol.* 3:119. doi: 10.3389/fmicb.2012.00119

Stalder, T., Barraud, O., Jové, T., Casellas, M., Gaschet, M., Dagot, C., et al. (2014). Quantitative and qualitative impact of hospital effluent on dissemination of the integron pool. *ISME J.* 8, 768–777. doi: 10.1038/ismej.2013.189

Stalder, T., and Top, E. (2016). Plasmid transfer in biofilms: a perspective on limitations and opportunities. *NPJ Biofilms Microbiomes* 2:16022. doi: 10.1038/npjbiofilms.2016.22

Van Houdt, R., and Michiels, C. W. (2005). Role of bacterial cell surface structures in *Escherichia coli* biofilm formation. *Res. Microbiol.* 156, 626–633. doi: 10.1016/j.resmic.2005.02.005

Wright, G. D. (2010). Antibiotic resistance in the environment: a link to the clinic? *Curr. Opin. Microbiol.* 13, 589–594. doi: 10.1016/j.mib.2010.08.005

Conflict of Interest Statement: The authors declare that the research was conducted in the absence of any commercial or financial relationships that could be construed as a potential conflict of interest.

frontiers in Microbiology

ORIGINAL RESEARCH
published: 15 August 2018
doi: 10.3389/fmicb.2018.01908

Characterization of a Novel bla_{KLUC} Variant With Reduced β-Lactam Resistance From an IncA/C Group Plasmid in a Clinical *Klebsiella pneumoniae* Isolate

Pingping Li[1†], Kai Shen[1†], Ying Zhang[1†], Jianchao Ying[1], Tingyuan Zhu[1], Yabo Liu[1], Lei Xu[1], Chaoqing Lin[1], Kaibo Zhang[2], Peizhen Li[1], Junwan Lu[2], Kewei Li[1], Huiguang Yi[1], Qiyu Bao[1] and Teng Xu[1,3*]*

[1] Institute of Biomedical Informatics, School of Laboratory Medicine and Life Science, Wenzhou Medical University, Wenzhou, China, [2] School of Medicine, Lishui University, Lishui, China, [3] Institute of Translational Medicine, Baotou Central Hospital, Baotou, China

OPEN ACCESS

Edited by:
Dongchang Sun, Zhejiang University of Technology, China

Reviewed by:
Nilton Lincopan, Universidade de São Paulo, Brazil
Wei Liu, ZheJiang Academy of Agricultural Sciences, China

***Correspondence:**
Teng Xu
xuteng@wmu.edu.cn
Kaibo Zhang
893286261@qq.com

[†] These authors have contributed equally to this work

Specialty section:
This article was submitted to Antimicrobials, Resistance and Chemotherapy, a section of the journal Frontiers in Microbiology

Received: *09 May 2018*
Accepted: *30 July 2018*
Published: *15 August 2018*

Citation:
Li P, Shen K, Zhang Y, Ying J, Zhu T, Liu Y, Xu L, Lin C, Zhang K, Li P, Lu J, Li K, Yi H, Bao Q and Xu T (2018) Characterization of a Novel bla_{KLUC} Variant With Reduced β-Lactam Resistance From an IncA/C Group Plasmid in a Clinical Klebsiella pneumoniae Isolate. Front. Microbiol. 9:1908. doi: 10.3389/fmicb.2018.01908

Similar to other CTX-M family enzymes, KLUC is a recently identified and emerging determinant of cefotaxime resistance that has been recovered from at least three *Enterobacteriaceae* species, including *Kluyvera cryocrescens*, *Escherichia coli,* and *Enterobacter cloacae*. Whether this extended-spectrum β-lactamase (ESBL) has been disseminated among commonly isolated *Enterobacteriaceae* is worthy of further investigation. In this study, we screened 739 nosocomial *Enterobacteriaceae* isolates (240 *Klebsiella pneumoniae* and 499 *E. coli* strains) and found that one *K. pneumoniae* and four *E. coli* isolates harbored the bla_{KLUC} gene. Three bla_{KLUC} determinants isolated from *E. coli* were entirely identical to a bla_{KLUC-3} gene previously recovered in the same hospital. PFGE of four bla_{KLUC}-harboring *E. coli* strains showed that prevalence of these determinants was most likely mediated by horizontal gene transfer but not clonal dissemination. However, the variant isolated from *K. pneumoniae* belonged to a novel member of the KLUC enzyme group. This newly identified enzyme (KLUC-5) has an amino acid substitution compared with previously identified KLUC-1 (G18S) and KLUC-3 (G240D). Antimicrobial susceptibility tests showed that KLUC-5 significantly reduced resistance activity to almost all the selected antimicrobials compared to previously identified KLUC-3. Site-directed mutagenesis showed that bla_{KLUC-5}-D240G and bla_{KLUC-5}-S18G significantly enhanced the MIC against its best substrate. Conjugation and S1-PFGE indicated that bla_{KLUC-5} was located on a transferable plasmid, which was further decoded by single-molecule, real-time sequencing. Comparative genome analysis showed that its backbone exhibited genetic homology to the IncA/C incompatibility group plasmids. A transposable element, IS*Ecp1*, was detected

256-bp upstream of the bla_{KLUC-5} gene; this location was inconsistent with the previously identified bla_{KLUC-1} but congruent with the variants recovered from *E. coli* in the same hospital. These data provide evidence of the increasingly emerging KLUC group of ESBLs in China.

Keywords: *Klebsiella pneumoniae*, CTX-M, KLUC enzyme, IncA/C group plasmid, IS*Ecp1*

INTRODUCTION

CTX-M β-lactamase nomenclature is derived from their powerful cefotaxime hydrolysis activity, which is a functional indicator of these enzymes. These enzymes were initially reported in the late 1980s, and they have now become one of the most widespread ESBLs. Based on amino acid sequence similarity, the CTX-Ms are divided into at least six groups, including CTX-M-1, CTX-M-2, CTX-M-8, CTX-M-9, CTX-M-25, and KLUC (Bonnet, 2004). An increasing number of novel CTX-M variants has been identified. In addition, certain CTX-M variants have a chimeric structure, such as CTX-M-45, CTX-M-64, CTX-M-123, CTX-M-132, and CTX-M-137 (Zhao and Hu, 2013). In contrast to the many acquired β-lactamases for which the original sources remained unknown, the source of bla_{CTX-M} genes has been identified in certain species of the genus *Kluyvera*. In 2001, a novel chromosomally-encoded ESBL named KLUC-1 was identified from *Kluyvera cryocrescens*, and it shares 77–86% amino acid identity with other CTX-M members (Decousser et al., 2001). KLUC-2, a plasmid-mediated CTX-M family ESBL, was identified from *Enterobacter cloacae*, and it possesses a single amino acid difference compared with KLUC-1, G115R (Petrella et al., 2008). The most recently identified proteins KLUC-3 and KLUC-4 were both demonstrated to be located on plasmids from *Escherichia coli* and *E. cloacae* (Xu et al., 2012), indicating that mobile DNA elements might contribute to the transfer of the bla_{KLUC} gene between chromosomes and plasmids.

Acquired bla_{CTX-M} genes detected in clinical isolates are generally located on conjugative plasmids (Carattoli, 2009). In most cases, acquired bla_{CTX-M} genes are associated with either IS*Ecp1* or IS*CR1*, two different insertion sequences that are able to mobilize flanking DNA segments (Toleman et al., 2006). IS*Ecp1* is composed of an open reading frame (ORF) encoding a transposase with 420 amino acids and two imperfect inverted repeats (Bonnet, 2004). IS*Ecp1* can mobilize downstream-located bla_{CTX-M} genes, such as $bla_{CTX-M-3}$ and $bla_{CTX-M-15}$, and provide promoters for their expression (Dhanji et al., 2011; Ma et al., 2011). The IS*CR1* element is defined by an *orf513* gene encoding a putative recombinase and a recombination crossover site, and it has been identified upstream of several bla_{CTX-M} genes, such as $bla_{CTX-M-2}$ and $bla_{CTX-M-9}$, and can initiate downstream gene expression (Valverde et al., 2006). Four bla_{KLUC} variants have been detected in at least three genera from the family *Enterobacteriaceae*, including *K. cryocrescens*, *E. coli* and *E. cloacae*; thus whether bla_{KLUC} variants have been widely disseminated is worthy of further investigation. In this study, we screened for bla_{KLUC} variants from 240 *K. pneumoniae* and 499 *E. coli* clinical isolates and identified five bacterial strains carrying bla_{KLUC} variants. Among them, one was shown to encode an enzyme which is different from other KLUC group enzymes. We characterized the resistance activity and genetic environment of this new enzyme.

MATERIALS AND METHODS

Bacterial Strains

A total of 739 consecutive, non-duplicated enterobacterial clinical isolates, including 240 *K. pneumoniae* and 499 *E. coli* strains from feces, blood, urine, and pus samples of patients, were collected in the First Affiliated Hospital of Wenzhou Medical University between 2015 and 2016. These strains were identified both by conventional methods and an auto-analysis system (BioMerieux Corporate, Lyon, France). The bla_{KLUC-5}-harboring strain *K. pneumoniae* KP1276 was isolated from a 75-year-old male patient who was suffering upper respiratory tract and treated with cefoxitin before the bacterial strain was isolated.

bla_{KLUC}-Harboring Strains Identification and Conjugation Assay

PCR amplification of 739 consecutive and non-duplicated enterobacterial isolates was performed to screen for bla_{KLUC}-positive strains. The primer sequences were described as previously (Xu et al., 2012). PCR products were sequenced on an ABI 3730XL automated sequencer (Thermo Fisher Scientific, MA, United States). The bla_{KLUC-5}-positive strain and rifampin-resistant *E. coli* EC600 strain were used as the donor and recipient, respectively, to conduct conjugation assays as described elsewhere (Xu et al., 2018). The transconjugant was selected on Mueller-Hinton agar plates containing 1800 μg/ml rifampin and 512 μg/ml ampicillin. Amplification and sequencing of 16S rRNA (Forward: 5′-AGAGTTTGATCCTGGCTCAG-3′ and Reverse: 5′-GGTTACCTTGTTACGACTT-3′) and the bla_{KLUC} gene (Xu et al., 2012) were performed to confirm the positive transconjugants.

PFGE, S1-PFGE and Multi-Locus Sequence Typing (MLST)

Clonal relatedness for four bla_{KLUC}-harboring *E. coli* strains was evaluated by pulsed-field gel electrophoresis (PFGE). Bacterial DNA was extracted and then subjected to complete

digestion with the restriction endonuclease *Xba*I (TaKaRa, Dalian, China). The fragmented DNA then separated in a CHEF Mapper XA system (Bio-Rad, CA, United States) at 120 V for 19 h with pulse time of 5–35 s. The DNA fingerprint patterns were analyzed according to the criteria as previously proposed (Hu et al., 2013). S1-PFGE experiments were conducted on three bacterial strains, including the wild-type KP1276, transconjugant and *E. coli* C600 (EC600). The bacterial isolates were grown on LB plates at 37°C for 16–18 h as previously reported with some modifications (Chang et al., 2013). The S1 Nuclease (TaKaRa, Dalian, China) was used to digest chromosomal DNA. *Xba*I chromosomal digestion of *Salmonella serotype Braenderup* strain H9812 was used as a molecular size marker. The digested DNA was then separated in a 1% SeaKem Gold agarose (LONZA, Rockland, ME, United States) with pulse time of 6–36 s for 18.5 h at 14°C and constant voltage of 6 V/cm. The patterns were analyzed and compared using BioNumerics software version 6.5 (Ashayeri-Panah et al., 2013). Genotyping for KP1276 was determined using 7 housekeeping genes (*gapA*, *infB*, *mdh*, *pgi*, *phoE*, *rpoB*, and *tonB*), and the MLST method was described previously (Diancourt et al., 2005). Alleles and sequence types (STs) were assigned using the MLST database[1].

bla_{KLUC-5} Gene Cloning, Site-Directed Mutagenesis and Antimicrobial Susceptibility Testing

The complete ORFs of the bla_{KLUC} gene from KP1276 (carrying bla_{KLUC-5}) and D2712 (carrying bla_{KLUC-3}) were amplified using the primers 5′-CGGGATCCATG GTTAAAAAATCATTACGCCAGT-3′ and 5′-CGGAATTC CTATAATCCCTCAGTGACGATTTTC-3′ with a pair of flanking restriction endonuclease adapters. Then, the purified PCR products were digested and ligated into the pET-28a(+) vector. The recombinant vectors were further transformed into *E. coli* BL21 using the calcium chloride method and grown on Luria-Bertani agar plates supplemented with kanamycin (50 μg/ml), IPTG (24 μg/ml), and *X*-Gal (40 μg/ml). The recombinant plasmids were verified by *BamH*I and *EcoR*I (TaKaRa, Dalian, China) digestion and sequencing. To further validate the key role of the amino acid at position 18 and 240, site-directed mutagenesis was performed to generate mutants of bla_{KLUC-3} and bla_{KLUC-5}. PCR was conducted by using mutagenic primers (**Table 1**) and the recombinant clones carrying bla_{KLUC-3} and bla_{KLUC-5} as the templates which was amplified with *TransStart FastPfu* DNA Polymerase (TransGen Biotech, Beijing China). Mutagenesis was performed using a Fast Mutagenesis System (TransGen Biotech, Beijing, China). Mutations in the recombinant plasmids were confirmed by DNA sequencing. The primers used for site-directed mutagenesis were listed in **Table 1**. Bold nucleotide in the primers indicated the site-directed mutagenic base pair. A total of nine strains were subjected to minimum inhibitory concentration (MIC) detection against 17 β-lactams or their compounds. Antimicrobial susceptibility testing of selected antibiotics was performed by the agar dilution method according to the recommendations of the Clinical and Laboratory Standards Institute [CLSI] (2017) documents. The standard *E. coli* ATCC25922 was used as the quality control strain.

TABLE 1 | Primers used for site-directed mutagenesis.

Mutagenesis	Direction of primer	Primer sequence (5′–3′)	Annealing temp (°C)
bla_{KLUC-5}D240G	Forward	TAAAACCGGCAG CGGTG**G**TTACGGCACC	63
	Reverse	**C**CACCGCTGCCGGTTTT ATCGCCCACCA	
bla_{KLUC-5}S18G	Forward	TTCCGCTG CTGGCA**G**GCAGCGTATCG	63
	Reverse	**C**TGCCAGCAGCGGAA AGACCGTCGCG	
bla_{KLUC-3}G240D	Forward	AACCGGCA GCGGTG**A**TTACGGCACCA	63
	Reverse	**T**CACCGCTGCCGGTTTT ATCGCCCACC	

bla_{KLUC}-Harboring Plasmid Sequencing and Bioinformatic Analyses

The plasmid KP1276 was extracted using an alkaline lysis method as previously described (Nicoletti and Condorelli, 1993). A 20-kb library was generated using the SMRTbell Template Prep Kit (Pacific Biosciences, Menlo Park, CA, United States) according to the PacBio standard protocol and sequenced on a PacBio RS II instrument. In addition, a paired-end library with 300-bp insert sizes was constructed and sequenced from both ends using Illumina technology (Illumina, CA, United States). The PacBio long reads were initially assembled using Canu software (Koren et al., 2017). The Illumina reads were then mapped onto the assembled contigs to correct the primary assembly by using Bwa and the Genome Analysis Toolkit (McKenna et al., 2010). The potential ORFs were predicted using Glimmer software and annotated against a non-redundant protein database using the BLASTX program. The neighbor-joining phylogenetic tree of five bla_{KLUC} genes was constructed using MEGA6 with 1000 bootstrap replications. $bla_{CTX-M-10}$ was used as an outgroup to root the tree. As mutation and selection have different effects on synonymous (K_s) and non-synonymous (K_a) substitution rates, the complete coding sequence of five bla_{KLUC} genes were pairwise alignment by using MAFFT software (bla_{KLUC-1} as the reference), and the K_a/K_s were further measured by $K_a\_K_s$ calculator to understand molecular sequence evolution (Zhang et al., 2006). The three-dimensional structure of KLUC-3 and KLUC-5 was constructed via homology modeling method by using SWISS-MODEL[2] based on the crystal structure of CTX-M-15 (Lahiri et al., 2013). The complete nucleotide sequence of the

[1]https://pubmlst.org/mlst/

[2]https://www.swissmodel.expasy.org/

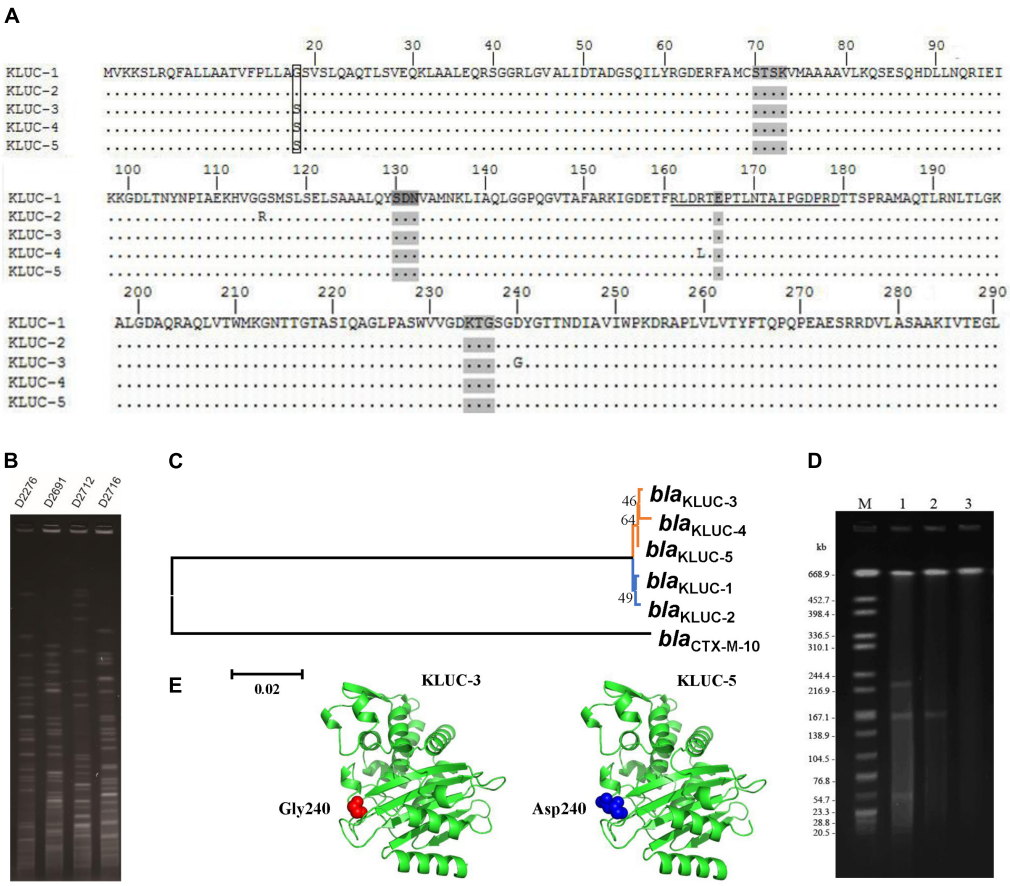

FIGURE 1 | Sequence comparison, transferability and phylogenetic analyses of bla_{KLUC-5}. **(A)** Alignment of KLUC-5 with four other KLUC subtypes. Amino acids are numbered according to the standard numbering scheme for the class A β-lactamases. Ellipses indicate identical amino acid residues. The amino acids composing the omega loop are underlined. Four structural elements characteristic of class A β-lactamases are shaded (70SXXK73, 130SDN132, 166E and 234KTG236). The substituted amino acids between KLUC-5 and KLUC-1 are boxed. The four KLUC subtypes, KLUC-1, KLUC-2, KLUC-3, and KLUC-4, were retrieved from the NCBI under accession numbers AAK08976, ABM73648, JX185316, and JX185317, respectively. **(B)** PFGE analysis of four bla_{KLUC}-harboring *E. coli* clinical isolates. **(C)** Phylogenetic analysis of five bla_{KLUC} genes. Branches with the same color indicate that the genes were isolated from the same district. **(D)** S1-PFGE patterns of KP1276, transconjugant, and EC600. Lane M is the size marker strain *Salmonella serotype Braenderup* H9812 digested with *Xba*I. Lanes 1–3 are the genomes of strain KP1276, transconjugant, and EC600 digested with S1 Nuclease. **(E)** The three-dimensional structure of KLUC-3 and KLUC-5. The atoms belonging to amino acid at position 240 of KLUC-3 and KLUC-5 are indicated.

pIA/C-KLUC has been deposited to GenBank under accession number MH476540.

RESULTS

bla_{KLUC} Gene Identification

We screened the bla_{KLUC} gene in 240 *K. pneumoniae* and 499 *E. coli* strains via PCR. One *K. pneumoniae* (Strain No. KP1276) and four *E. coli* strains (Strain No. D2276, D2691, D2712, and D2716) were bla_{KLUC} positive. Sanger sequencing showed that D2276, D2691, and D2712 all harbored the bla_{KLUC-3} gene. In addition to bla_{KLUC-3}-harboring strains, *E. coli* D2716 contained a bla_{KLUC-3}-like gene that contained a stop codon at position 153. However, the bla_{KLUC} gene isolated from *K. pneumoniae* KP1276 belonged to a novel subtype of the bla_{KLUC} group enzymes. This determinant possessed 1 (S18G), 2 (S18G and G115R), 1 (D240G) and 1 (R164L) amino acid differences compared with KLUC-1, KLUC-2, KLUC-3, and KLUC-4, respectively (**Figure 1A**). Therefore, we sequentially named this new subtype as KLUC-5.

Since bla_{KLUC-3} has been previously identified in a clinical *E. coli* strain in the same area, the potential epidemiology of bla_{KLUC-3} in recently identified *E. coli* isolates would be of interest. We performed PFGE for those *E. coli* isolates which carried bla_{KLUC-3} (D2276, D2691, and D2712) and bla_{KLUC-3}-like (D2716) determinants. Results showed that the genomes of four isolates exhibited distinct fingerprint among each other (**Figure 1B**), indicating that prevalence of bla_{KLUC-3} or its close relatives in this area is transmitted by horizontal gene transfer.

Phylogenetic analyses of five known bla_{KLUC} variants showed that bla_{KLUC-1} and bla_{KLUC-2}, which were both isolated from Paris (France), were clustered together (**Figure 1C**), while the

TABLE 2 | MICs of 17 antimicrobials for 9 strains.

Antibiotics	MIC (mg/L)								
	KP1276	**EC600 [pIA/C-KLUC]**	**EC600**	**BL21**	**BL21 [pET28a::** ***bla*** $_{KLUC-5}$**]**	**BL21 [pET28a::** ***bla*** $_{KLUC-3}$ **G240D]**	**BL21 [pET28a::** ***bla*** $_{KLUC-3}$**]**	**BL21 [pET28a::** ***bla*** $_{KLUC-5}$ **D240G]**	**BL21 [pET28a::** ***bla*** $_{KLUC-5}$ **S18G]**
Ampicillin	>512	>512	8	1	64	64	256	256	128
Meropenem	0.06	0.06	0.06	0.06	0.06	0.06	0.06	0.06	0.06
Imipenem	0.5	0.5	0.5	0.5	0.5	0.5	0.5	0.5	0.5
Cefotaxime	32	4	0.12	<0.03	<0.03	<0.03	2	2	2
Cefotaxime + CLA[a]	64	8	0.12	<0.03	<0.03	<0.03	2	2	1
Cefotaxime + TZB[b]	2	0.06	0.06	<0.03	<0.03	<0.03	<0.03	<0.03	<0.03
Ceftazidime	8	1	0.5	0.06	0.06	0.06	0.5	0.5	0.06
Ceftazidime + CLA[a]	4	1	0.25	0.06	0.06	0.06	0.25	0.25	0.06
Ceftazidime + TZB[b]	1	0.5	0.25	0.06	0.06	0.06	0.06	0.06	0.06
Cefepime	32	4	0.12	<0.03	0.12	0.12	0.5	0.5	0.25
Cefepime + CLA[a]	32	4	0.12	<0.03	<0.03	<0.03	<0.03	<0.03	<0.03
Cefepime + TZB[b]	4	0.12	0.12	<0.03	<0.03	<0.03	<0.03	<0.03	<0.03
Piperacillin	>1024	128	4	1	16	16	32	32	16
Piperacillin + TZB[b]	64	2	2	0.5	0.5	0.5	0.5	1	0.25
Cefazolin	>512	256	4	2	32	32	64	64	64
Cefoxitin	8	8	8	2	2	2	2	2	2
Ceftriaxone	64	8	0.125	<0.03	<0.03	<0.03	0.25	0.25	0.25

[a]*CLA, clavulanic acid at a fixed concentration of 2 mg/L;* [b]*TZB, tazobactam at a fixed concentration of 4 mg/L.*

three other members, bla_{KLUC-3}, bla_{KLUC-4}, and bla_{KLUC-5} had closer relation and were all derived from the same district (Wenzhou, China). As bla_{KLUC-5} and bla_{KLUC-3} differed by only a single mutation (nucleotide position 725 A->G), it suggested that the presumably same origin of these two determinants.

Transferability of the bla_{KLUC-5}-Harboring Plasmid

Previous study showed that bla_{KLUC-3} was located on a conjugative plasmid. To validate the transferability of bla_{KLUC-5}-harboring plasmid, we performed conjugative assay of wild *K. pneumoniae* KP1276. The result showed that bla_{KLUC-5}-harboring plasmid can transfer from the donor to the recipient cells. This was further confirmed by Sanger sequencing of the PCR products from transconjugants. S1-PFGE showed that the wild-type KP1276 harbored three plasmids (**Figure 1D**). However, only the plasmid with medium size of about 180-kb from the KP1276 wild strain was transferred to the recipient (**Figure 1D**). MLST revealed that the KP1276 wild-type strain belonged to a new sequence type ST1881. These results demonstrated that the bla_{KLUC-5} gene was also located on a conjugative plasmid, which lay the molecular basis for rapid spread of β-lactams resistance phenotype through horizontal gene transfer.

Resistance Activities of bla_{KLUC} Variants

We cloned the complete ORFs of both bla_{KLUC-3} and bla_{KLUC-5} into pET-28a vectors and transformed them separately into the *E. coli* strain BL21. The minimal inhibitory concentrations (MICs) of six strains, including the wild-type KP1276, the transconjugant of KP1276, BL21[pET28a::bla_{KLUC-5}], BL21[pET28a::bla_{KLUC-3}] and two blank controls, were tested against a series of 17 β-lactams or their compounds (**Table 2**). BL21[pET28a::bla_{KLUC-3}] showed a high level of resistance to several selected antibiotics, including ampicillin and cefazolin as well as its best substrate, cefotaxime. The resistance activities of bla_{KLUC-3} were highly consistent with the previous observations (Xu et al., 2012). However, BL21[pET28a::bla_{KLUC-5}] did not show resistance to several antimicrobials, such as aztreonam, ceftazidime, and ceftriaxone, but was still resistance to ampicillin and cefazolin. The resistance activity of the transconjugant of KP1276 against selected antimicrobials was universally stronger than that of the cloned bla_{KLUC-5}, indicating that other determinants were located on the conjugative plasmid.

Since bla_{KLUC-5} had S18G and D240G substitutions with bla_{KLUC-1} and bla_{KLUC-3}, respectively, and the stronger resistance activities of bla_{KLUC-1} and bla_{KLUC-3} were observed when compared to bla_{KLUC-5} (**Table 2**), the amino acid at positions 18 and 240 might be importance for high hydrolytic activity against oxyimino-cephalosporins. To address this concern, mutants of bla_{KLUC-3} and bla_{KLUC-5} were constructed by using site-directed mutagenesis, including mutant of bla_{KLUC-5} at position 240 (bla_{KLUC-5}-D240G), mutant of bla_{KLUC-5} at 18 (bla_{KLUC-5}-S18G) and mutant of bla_{KLUC-3} at position 240 (bla_{KLUC-3}-G240D). The MICs of bla_{KLUC-5}-D240G evoke the resistance activity which was similar to that of bla_{KLUC-3}, whereas opposite mutagenesis of bla_{KLUC-3} at position 240 (bla_{KLUC-3}-G240D) led to the reduced activity against oxyimino-cephalosporins (**Table 2**). This indicated that amino acid at position 240 of KLUC enzyme is a key residue for hydrolytic activity against its best substrate. Homology modeling of KLUC-3 and KLUC-5 indicated that the position 240 was located on the extremity of β3 strand (**Figure 1E**) which was similar to that of CTX-M-15 (Lahiri et al., 2013). Likewise, bla_{KLUC-5}-S18G significantly enhanced the hydrolytic activity against cefotaxime and ceftriaxone for at least 4 MIC dilution, while it slightly enhanced MICs of ampicillin, cefepime, and cefazolin compared to wild bla_{KLUC-5} (**Table 2**), suggesting that Gly18 is also important for KLUC enzymatic activity. Interestingly, we also observed that the resistance activities of bla_{KLUC-5}-D240G against ampicillin, ceftazidime, cefepime and piperacillin were stronger than that of bla_{KLUC-5}-S18G, suggesting that the hydrolytic activities of KLUC-3 against β-lactams were higher than KLUC-1.

We further performed ML estimation of K_a and K_s in pairwise sequence comparisons for five bla_{KLUC} variants. Results showed that all the bla_{KLUC} variants have ω (K_a/K_s) < 1, ranging from 0.09 to 0.27, indicating that purifying selection was adopted in KLUC evolution (**Table 3**). This was also reflected by three variants including KLUC-4, KLUC-5 as well as the bla_{KLUC-3}-like gene (D2716) out of six bla_{KLUC} genes had no or reduced hydrolytic activity against β-lactams.

Complete Sequence of pIA/C-KLUC and Comparative Genome Analyses

To identify the potential mobile genetic element (MGE) associated with bla_{KLUC-5} mobilization and the other antibiotic resistance determinants, we applied SMRT and Illumina technologies to define the complete nucleotide sequence of this conjugative plasmid. The results showed that the plasmid was 182,450 bp which had an average GC content of 51.01%, and was predicted to encode 222 ORFs. A complete nucleotide sequence search against the GenBank nucleotide database showed that the plasmid possessed the highest identity and coverage with plasmids belonging to the IncA/C incompatibility group, such as pIP1202, pP91278, pP99-018, R222, pVC1447, pSRC119-A/C and

TABLE 3 | Maximum likelihood estimation of K_a and K_s in pairwise sequence comparisons for five bla_{KLUC} variants.

Variants	*S*-Substitutions	*N*-Substitutions	*S*-Sites	*N*-Sites	K_a	K_s	K_a/K_s
bla_{KLUC-2}	1.50797	0.500444	190.3	682.7	0.000733	0.0079242	0.093
bla_{KLUC-3}	2.02526	2.00713	190.6	682.4	0.002941	0.0106257	0.277
bla_{KLUC-4}	4.04959	2.00489	249.8	623.2	0.003217	0.0162113	0.198
bla_{KLUC-5}	2.02534	1.00178	190.2	682.8	0.001467	0.0106485	0.138

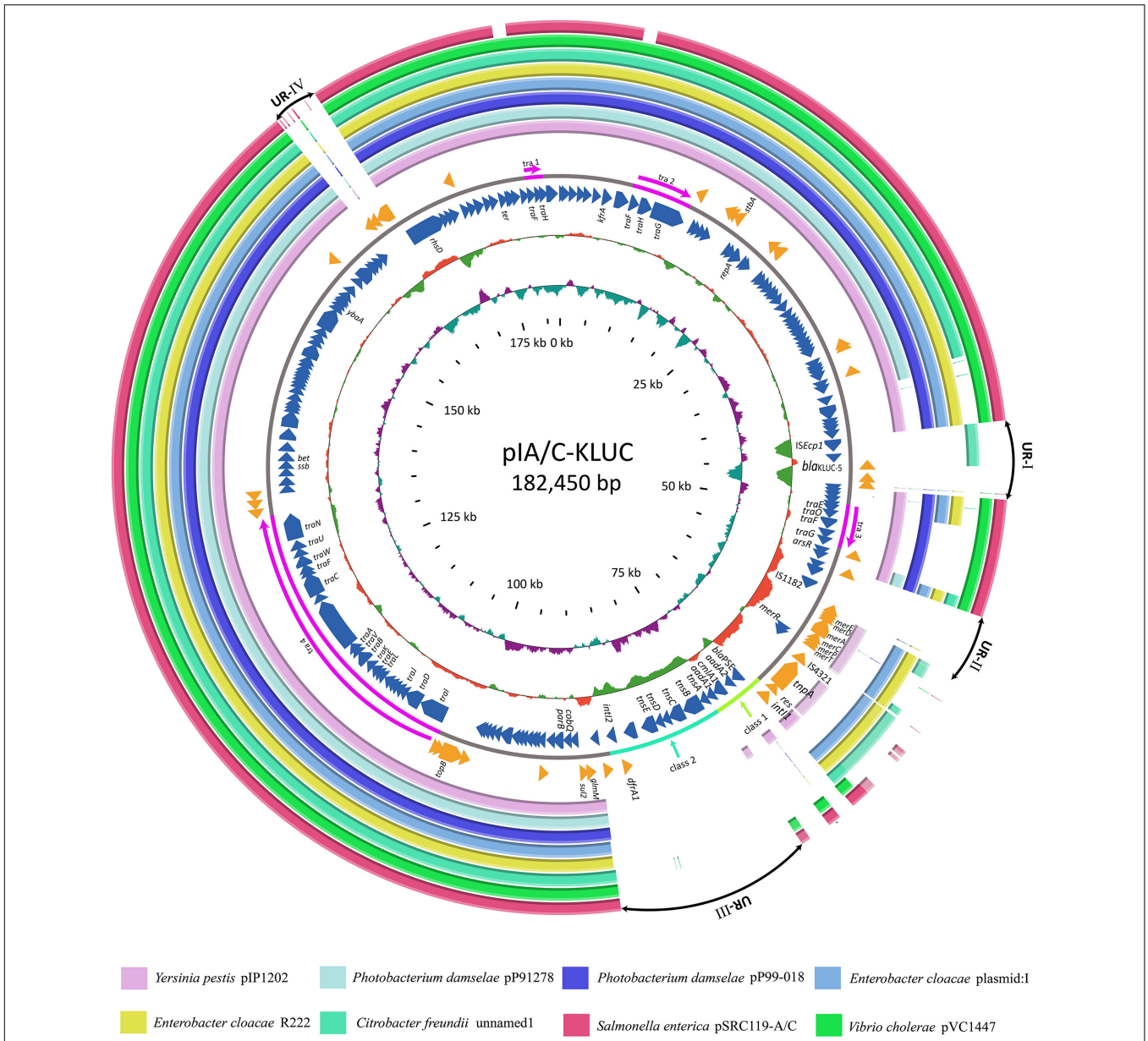

FIGURE 2 | Comparative genome analyses of several IncA/C group plasmids. Structural comparison of pIA/C-KLUC with those of the most similar IncA/C group plasmids. Circles 1-8 (from outside to inside) are homologous regions of pSRC119-A/C (Accession Number KM670336), pVC1447 (KM083064), unnamed1 (CP017058), R22 (KX8697741), plasmid: 1 (LT882699), pP99-018 (AB277723), pP91278 (AB277724), and pIP1202 (CP000603) compared to pIA/C-KLUC, whereas unmatched regions are left blank. Circles 9 and 11 represent the genes encoded by the forward and reverse strands of pIA/C-KLUC. Circles 12–13 are GC content and GC skew maps of pIA/C-KLUC. The four transfer regions of the plasmid (Tra1-4) are marked in pink in circle 10 and further indicated by arrows. UR-I, II, III, and IV are four large unique regions in pIA/C-KLUC compared with the other plasmids. Classes 1 and 2 represent classes 1 and 2 integrons.

two unnamed plasmids. We designated this plasmid as pIA/C-KLUC. Comparative genome analyses showed that pIA/C-KLUC had high genomic collinearity and shared a conserved backbone with the aforementioned IncA/C plasmids (**Figure 2**). Four unique regions (UR) were detected in pIA/C-KLUC, and the genes in two of these regions (UR-II and IV) were not annotated with known functions. Interestingly, UR-III consisted of a class 2 integron which was directly subtended by a class 1 integron. The genomic architecture represented direct connection of class 1 and class 2 integrons had not been observed in recently sequenced bacterial genomes. The bla_{KLUC-5} gene was located 256-bp downstream of the IS*Ecp1* transposase in the UR-I of the plasmid (**Figure 2**). A comparative genome analysis of the genetic environment of several representatives of bla_{CTX-M} genes, including bla_{KLUC-1}, bla_{KLUC-5}, $bla_{CTX-M-62}$, $bla_{CTX-M-3}$, and $bla_{CTX-M-15}$, showed that bla_{KLUC-5}, $bla_{CTX-M-62}$,

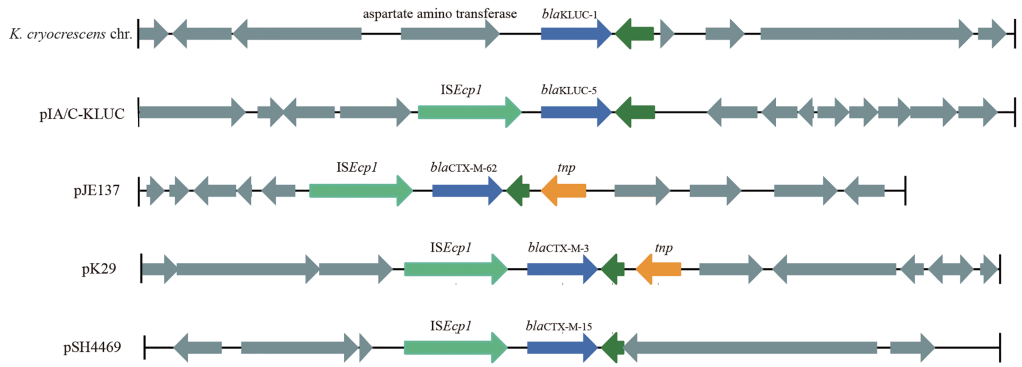

FIGURE 3 | Genetic environments of several *bla*$_{CTX-M}$ family genes. The genes are shown as arrows, with the arrowheads indicating the direction of transcription. The homologous genes are filled with the same color except for those filled with dark green. Regions are drawn to scale from accession numbers BCTM01000044 (local chromosomal fragment of *bla*$_{KLUC-1}$), EF219134 (pJE137), EF382672 (pK29), and KJ406378 (pSH4469).

bla$_{CTX-M-3}$, and *bla*$_{CTX-M-15}$ were located downstream of the IS*Ecp1* transposase, whereas *bla*$_{KLUC-1}$ was sedentarily located on the *K. cryocrescens* chromosome (**Figure 3**). Further PCR screen of IS*Ecp1*-*bla*$_{KLUC}$ in four *bla*$_{KLUC}$-positive *E. coli* strains exhibited positive results, suggesting that mobilization of these *bla*$_{KLUC}$ genes are unanimously mediated by IS*Ecp1* elements which was inconsistent with chromosomally-encoded *bla*$_{KLUC-1}$ (Decousser et al., 2001).

DISCUSSION

This study identified five *bla*$_{KLUC}$-positive strains from 739 enterobacterial isolates. Three determinants recovered from *E. coli* were demonstrated to be KLUC-3, which had been identical to previously isolated from *E. coli* D41 in the same hospital (Xu et al., 2012), indicating nosocomial dissemination of this determinant. PFGE demonstrated that prevalence of *bla*$_{KLUC}$ in this area was transmitted by horizontal gene transfer. In addition, one *K. pneumoniae* strain was found to harbor a novel KLUC subtype, suggesting that *bla*$_{KLUC}$ has been disseminated to the commonly isolated *Enterobacteriaceae* species in the same area. It was obvious that the clinical significance of KLUC-5 is not evident, because it possessed a reduced β-lactams resistance activity compared to previously identified variants and recently had a relative low emergence frequency. However, the epidemiology of KLUC enzyme in the present study (5/739, 0.68%) showed a significant increase in southeast of China compared to previous investigation (0.22%, 2/928) (Xu et al., 2012), and most of the KLUC variants identified in this study was KLUC-3 which was demonstrated to be a strong determinant against many β-lactam antibiotics. The amino acid sequences of five KLUC subtypes showed limited variations and only presented 1–3 substitutions among them (**Figure 1A**). Several key residues in the CTX-M family enzymes have been previously characterized. For example, Ser237 and Arg276 are specific to the CTX-M members and are used to define increased specificity for cefotaxime hydrolysis (Adamski et al., 2015). Moreover, Asn170 and Asp240 are located in the omega loop and β3 strand of the CTX-M enzymes, which are the binding regions of cefotaxime (Delmas et al., 2010). It has also been known that KLUC-1 confer strong resistance to extended β-lactams such as aztreonam and cefotaxime. We demonstrated that KLUC-3 conferred strong resistance to its best substrate, cefotaxime, whereas KLUC-4 did not show any resistance to almost all the selected antimicrobials because of a key substitution in the omega loop (Xu et al., 2012). However, the newly identified KLUC-5 which harbored only one substitution compared to KLUC-1 (G18S) and KLUC-3 (G240D), respectively, reduced the resistance activities to cefotaxime as well as most of antimicrobials. This was also validated by site-directed mutagenesis of *bla*$_{KLUC-3}$ at position 240 (*bla*$_{KLUC-3}$-G240D) which significantly reduced resistance activity against many antimicrobials, whereas opposite mutation of *bla*$_{KLUC-5}$ at position 240 (*bla*$_{KLUC-5}$-D240G) caused the increased MICs of oxyimino-cephalosporins such as cefotaxime, ceftazidime and ceftriaxone compared to wild *bla*$_{KLUC-5}$. Indeed, D240G substitution resulted in elevated hydrolytic activity against extended β-lactams has been previously observed in other CTX-M family enzymes such as introduction of this substitution in CTX-M-14 or CTX-M-9 (Bonnet, 2004; Palzkill, 2018). Interestingly, compared to KLUC-3, KLUC-5 reduced the resistance activities against cefazolin, cefoxitin and piperacillin for no more than 1 MICs dilution, suggesting that glycine at position 240 is not required for hydrolysis of these β-lactams. However, the lack of kinetic characterization of KLUC-5 against β-lactams is a key limitation in this study.

The complete plasmid nucleotide sequence showed that *bla*$_{KLUC-5}$ was embedded in an IncA/C group plasmid and located 256-bp downstream of IS*Ecp1*, suggesting that the movement of *bla*$_{KLUC-5}$ was mediated by this MGE. Interestingly, an IncA/C group plasmid ('unnamed1,' accession: CP017058.1) isolated from *Citrobacter freundii* SL151 also harbored an IS*Ecp1* element-mediated CTX-M enzyme-encoding gene, *bla*$_{CTX-M-15}$ (UR-I, **Figure 2**). The movement of *bla*$_{KLUC-5}$ was similar to that of a number of CTX-M family members, such as *bla*$_{CTX-M-62}$, *bla*$_{CTX-M-3}$, and *bla*$_{CTX-M-15}$, but was dissimilar to *bla*$_{CTX-M-2}$ and *bla*$_{CTX-M-9}$, whose mobilization is mediated by IS*CR1* (Eckert et al., 2006).

In addition to bla_{KLUC-5}, the plasmid pIA/C-KLUC also contained other antibiotic resistance genes that are included in tail-to-tail directly connected class 1 and class 2 integrons. Four antibiotic resistance gene cassettes, which were sequentially arranged as bla_{PSE-1}, *aadA2*, *cmlA1,* and *aadA1*, were embedded in the class 1 integron, which represented a novel cassettes arrangement. This class 1 integron harbored a complete 5′-CS but lacked the entire 3′-CS, which was presumably truncated by a class 2 integron. The acquisition of the class 2 integron into pIA/C-KLUC was most probably involved the Tn*7* transposon encoded by *tnsABCDE* through horizontal transfer, which could be reflected by the biased GC skew in class 2 integrons compared with the flanking regions (UR-III, **Figure 2**), and the class 2 integrons have been illustrated to be most frequently associated with Tn*7* derivatives (Peters and Craig, 2001). In addition, a Tn*3* family transposon was also identified in pIA/C-KLUC. This transposon was possibly truncated by a gene cluster corresponding to mercury resistance flanked by a pair of insertion elements, IS*4321* and IS*1182*, and the typical inverted repeats belonging to the Tn*3* transposon were not identified in this region.

CONCLUSION

Increased emergency of KLUC group enzyme-encoding genes from *Enterobacteriaceae* was observed in the southeast of China. Of them, a new subtype, KLUC-5, was recovered from a clinical *K. pneumoniae* strain and demonstrated to be located on an IncA/C group plasmid. The mobilization of bla_{KLUC-5} was associated with the IS*Ecp1* element, which may be different from that of bla_{KLUC-1} but similar to that of bla_{KLUC-3} from the same district as bla_{KLUC-5}. This new enzyme showed significantly reduced resistance to extended β-lactams presumably ascribed to the two combined amino acids substitution compared to KLUC-1 and KLUC-3.

DATA AVAILABILITY

Data and materials have been provided in the main manuscript. Where necessary additional information of the study can be made available from the corresponding author on request.

AUTHOR CONTRIBUTIONS

TX and QB designed and supervised the study. PPL, KS, YZ, JY, TZ, YL, LX, and CL performed the experiments. TX, JY, and HY analyzed the data. KZ, JL, PZL, and KL contributed the reagents. PPL drafted the manuscript. TX and QB revised the manuscript. All authors read and approved the final manuscript.

FUNDING

This work was financially supported by the National Natural Science Foundation of China (Grant Numbers 81501780, 81501808, 31500109, and 81401702); the Natural Science Foundation of Zhejiang Province, China (Grant Number LQ17H190001); the Nucleic Acids Based Molecular Diagnostics Innovative Discipline, Health and Family Planning Commission of Zhejiang Province; and start-up funds from the Wenzhou Medical University to TX (Grant Number QTJ14002).

REFERENCES

Adamski, C. J., Cardenas, A. M., Brown, N. G., Horton, L. B., Sankaran, B., Prasad, B. V., et al. (2015). Molecular basis for the catalytic specificity of the CTX-M extended-spectrum beta-lactamases. *Biochemistry* 54, 447-457. doi: 10.1021/bi501195g

Ashayeri-Panah, M., Eftekhar, F., Ghamsari, M. M., Parvin, M., and Feizabadi, M. M. (2013). Genetic profiling of *Klebsiella pneumoniae*: comparison of pulsed field gel electrophoresis and random amplified polymorphic DNA. *Braz. J. Microbiol.* 44, 823-828. doi: 10.1590/S1517-83822013005000055

Bonnet, R. (2004). Growing group of extended-spectrum beta-lactamases: the CTX-M enzymes. *Antimicrob. Agents Chemother.* 48, 1–14. doi: 10.1128/AAC.48.1.1-14.2004

Carattoli, A. (2009). Resistance plasmid families in Enterobacteriaceae. *Antimicrob. Agents Chemother.* 53, 2227-2238. doi: 10.1128/AAC.01707-08

Chang, K. M., Huang, W. C., Chiou, C. S., Shen, G. H., Huang, C. C., and Wen, F. S. (2013). Suitable restriction enzyme for standardization of pulsed-field gel electrophoresis protocol and interlaboratory comparison of *Acinetobacter baumannii*. *J. Microbiol. Immunol. Infect.* 46, 195-201. doi: 10.1016/j.jmii.2012.05.011

Clinical and Laboratory Standards Institute [CLSI] (2017). *Performance Standards for Antimicrobial Susceptibility Testing. CLSI Supplement M100 S27*, 27th Edn. Wayne, PA: Clinical and Laboratory Standards Institute.

Decousser, J. W., Poirel, L., and Nordmann, P. (2001). Characterization of a chromosomally encoded extended-spectrum class A beta-lactamase from *Kluyvera cryocrescens*. *Antimicrob. Agents Chemother.* 45, 3595-3598. doi: 10.1128/AAC.45.12.3595-3598.2001

Delmas, J., Leyssene, D., Dubois, D., Birck, C., Vazeille, E., Robin, F., et al. (2010). Structural insights into substrate recognition and product expulsion in CTX-M enzymes. *J. Mol. Biol.* 400, 108-120. doi: 10.1016/j.jmb.2010.04.062

Dhanji, H., Patel, R., Wall, R., Doumith, M., Patel, B., Hope, R., et al. (2011). Variation in the genetic environments of bla(CTX-M-15) in Escherichia coli from the faeces of travellers returning to the United Kingdom. *J. Antimicrob. Chemother.* 66, 1005-1012. doi: 10.1093/jac/dkr041

Diancourt, L., Passet, V., Verhoef, J., Grimont, P. A., and Brisse, S. (2005). Multilocus sequence typing of *Klebsiella pneumoniae* nosocomial isolates. *J. Clin. Microbiol.* 43, 4178-4182. doi: 10.1128/JCM.43.8.4178-4182.2005

Eckert, C., Gautier, V., and Arlet, G. (2006). DNA sequence analysis of the genetic environment of various blaCTX-M genes. *J. Antimicrob. Chemother.* 57, 14-23. doi: 10.1093/jac/dki398

Hu, L., Zhong, Q., Tu, J., Xu, Y., Qin, Z., Parsons, C., et al. (2013). Emergence of blaNDM-1 among *Klebsiella pneumoniae* ST15 and novel ST1031 clinical isolates in China. *Diagn. Microbiol. Infect. Dis.* 75, 373-376. doi: 10.1016/j.diagmicrobio.2013.01.006

Koren, S., Walenz, B. P., Berlin, K., Miller, J. R., Bergman, N. H., and Phillippy, A. M. (2017). Canu: scalable and accurate long-read assembly via adaptive k-mer weighting and repeat separation. *Genome Res.* 27, 722-736. doi: 10.1101/gr.215087.116

Lahiri, S. D., Mangani, S., Durand-Reville, T., Benvenuti, M., De Luca, F., Sanyal, G., et al. (2013). Structural insight into potent broad-spectrum inhibition with reversible recyclization mechanism: avibactam in complex with CTX-M-15 and *Pseudomonas aeruginosa* AmpC beta-lactamases. *Antimicrob. Agents Chemother.* 57, 2496-2505. doi: 10.1128/AAC.02247-12

Ma, L., Siu, L. K., and Lu, P. L. (2011). Effect of spacer sequences between bla(CTX-M) and ISEcp1 on bla(CTX-M) expression. *J. Med. Microbiol.* 60(Pt 12), 1787-1792. doi: 10.1099/jmm.0.033910-0

McKenna, A., Hanna, M., Banks, E., Sivachenko, A., Cibulskis, K., Kernytsky, A., et al. (2010). The genome analysis toolkit: a mapreduce framework for analyzing next-generation DNA sequencing data. *Genome Res.* 20, 1297-1303. doi: 10.1101/gr.107524.110

Nicoletti, V. G., and Condorelli, D. F. (1993). Optimized PEG method for rapid plasmid DNA purification: high yield from "midi-prep". *Biotechniques* 14, 532-534, 536.

Palzkill, T. (2018). Structural and mechanistic basis for extended-spectrum drug-resistance mutations in altering the specificity of TEM, CTX-M, and KPC beta-lactamases. *Front. Mol. Biosci.* 5:16. doi: 10.3389/fmolb.2018.00016

Peters, J. E., and Craig, N. L. (2001). Tn7: smarter than we thought. *Nat. Rev. Mol. Cell Biol.* 2, 806-814. doi: 10.1038/35099006

Petrella, S., Ziental-Gelus, N., Mayer, C., Renard, M., Jarlier, V., and Sougakoff, W. (2008). Genetic and structural insights into the dissemination potential of the extremely broad-spectrum class A beta-lactamase KPC-2 identified in an *Escherichia coli* strain and an *Enterobacter cloacae* strain isolated from the same patient in France. *Antimicrob. Agents Chemother.* 52, 3725-3736. doi: 10.1128/AAC.00163-08

Toleman, M. A., Bennett, P. M., and Walsh, T. R. (2006). ISCR elements: novel gene-capturing systems of the 21st century? *Microbiol. Mol. Biol. Rev.* 70, 296-316. doi: 10.1128/MMBR.00048-05

Valverde, A., Canton, R., Galan, J. C., Nordmann, P., Baquero, F., and Coque, T. M. (2006). In117, an unusual In0-like class 1 integron containing CR1 and bla(CTX-M-2) and associated with a Tn21-like element. *Antimicrob. Agents Chemother.* 50, 799-802. doi: 10.1128/AAC.50.2.799-802.2006

Xu, T., Wang, J., Ying, J., Zhu, T., Liu, Y., Xu, L., et al. (2018). Characterization of class 1 integron associated with the formation of quadruple blaGES-5 cassettes from an IncP-1beta group plasmid in *Pseudomonas aeruginosa*. *Int. J. Antimicrob. Agents* doi: 10.1016/j.ijantimicag.2018.07.002

Xu, T., Ying, J., Yao, X., Song, Y., Ma, P., Bao, B., et al. (2012). Identification and characterization of two novel bla(KLUC) resistance genes through large-scale resistance plasmids sequencing. *PLoS One* 7:e47197. doi: 10.1371/journal.pone.0047197

Zhang, Z., Li, J., Zhao, X. Q., Wang, J., Wong, G. K., and Yu, J. (2006). KaKs_calculator: calculating Ka and Ks through model selection and model averaging. *Genomics Proteomics Bioinformatics* 4, 259-263. doi: 10.1016/S1672-0229(07)60007-2

Zhao, W. H., and Hu, Z. Q. (2013). Epidemiology and genetics of CTX-M extended-spectrum beta-lactamases in gram-negative bacteria. *Crit. Rev. Microbiol.* 39, 79-101. doi: 10.3109/1040841X.2012.691460

Conflict of Interest Statement: The authors declare that the research was conducted in the absence of any commercial or financial relationships that could be construed as a potential conflict of interest.

frontiers in Microbiology

ORIGINAL RESEARCH
published: 21 August 2018
doi: 10.3389/fmicb.2018.01938

Further Spread of a *bla*$_{KPC}$-Harboring Untypeable Plasmid in *Enterobacteriaceae* in China

Jiansheng Huang[1,2,3], *Hui Ding*[1,2,3], *Yang Shi*[1,2,3], *Yunan Zhao*[1,2,3], *Xiaolei Hu*[1,2,3], *Jianmin Ren*[1,2,3], *Guiying Huang*[1,2,3], *Rongzhen Wu*[1,2,3] *and Zhigang Zhao*[1,2,3]*

[1] *Lishui Hospital, Zhejiang University School of Medicine, Lishui, China,* [2] *The Fifth Affiliated Hospital of Wenzhou Medical University, Lishui, China,* [3] *Lishui Municipal Central Hospital, Lishui, China*

The wide spread of *Klebsiella pneumoniae* carbapenemase (KPC)-producing *Enterobacteriaceae* is great threat to public health in China. Plasmids are among the major factors mediating *bla*$_{KPC}$ gene dissemination. A total of 156 carbapenem-resistant *Enterobacteriaceae* (CRE) isolates were identified in a tertiary hospital in China. Six KPC-producing isolates, namely, *E. coli* ($n = 2$), *E. asburiae* ($n = 1$), *C. freundii* ($n = 1$), *C. portucalensis* ($n = 1$), and *C. koseri* ($n = 1$), tested positive for the pCKPC18-1-like untypeable plasmid, which was described recently in *C. freundii*. All 6 plasmids could be easily transferred into *E. coli* by chemical transformation or conjugation and were confirmed by sequencing to harbor *bla*$_{KPC-2}$. Multilocus PCRs and EcoRI-RFLP revealed that the 6 untypeable plasmids belonged to 2 isoforms. High-throughput sequencing of representative plasmids (pCP40 and pEC86) led to the identification of 2 plasmids that shared the common backbone genes *repA*, *DnaJ*, *StpA,* and *yafB*, which were characteristic of the untypeable plasmid, and had similar *bla*$_{KPC-2}$ genetic contexts of the Tn*3*-Tn*4401* chimera. Nucleotide comparison revealed high sequence identity of the 2 plasmids with previously reported *bla*$_{KPC-2}$-carrying untypeable plasmids. In particular, the pCP40 plasmid from *C. portucalensis* and the pHS062105-3 plasmid from *K. pneumoniae* differed by only 20 single-nucleotide polymorphisms (SNPs). To the best of our knowledge, this is the first report of a *bla*$_{KPC}$-harboring untypeable plasmid spread into *E. coli*, *E. asburiae,* and *C. koseri* strains in China.

Keywords: *Enterobacteriaceae*, carbapenemase, *bla*$_{KPC}$, untypeable plasmid, dissemination

OPEN ACCESS

Edited by:
Charles W. Knapp,
University of Strathclyde,
United Kingdom

Reviewed by:
Angela Novais,
UCIBIO Rede de Química e Tecnologia, Portugal
Miklos Fuzi,
Semmelweis University, Hungary

***Correspondence:**
Zhigang Zhao
zjlszzg@163.com

Specialty section:
This article was submitted to Antimicrobials, Resistance and Chemotherapy, a section of the journal Frontiers in Microbiology

Received: *13 May 2018*
Accepted: *31 July 2018*
Published: *21 August 2018*

Citation:
Huang J, Ding H, Shi Y, Zhao Y, Hu X, Ren J, Huang G, Wu R and Zhao Z (2018) Further Spread of a bla$_{KPC}$-Harboring Untypeable Plasmid in Enterobacteriaceae in China. Front. Microbiol. 9:1938. doi: 10.3389/fmicb.2018.01938

INTRODUCTION

Carbapenems are often used as the last effective agents in the treatment of severe infections caused by multidrug-resistant gram-negative bacteria, especially strains expressing high-level AmpC cephalosporinase or extended spectrum β-lactamases (ESBLs). However, the emergence of carbapenem-hydrolyzing enzymes has greatly limited the effectiveness of these agents (Nordmann et al., 2009; Zhang et al., 2017).

Klebsiella pneumoniae carbapenemase (KPC), an Ambler class A enzyme, is a powerful carbapenem-hydrolyzing enzyme and can hydrolyze most of the beta-lactams (Nordmann et al., 2009). Since the first report of the *bla*$_{KPC}$ gene from *Klebsiella pneumoniae* isolated in North Carolina (USA) in 2001 (Yigit et al., 2001), this gene has been identified in multiple genera and

species of *Enterobacteriaceae*, including *K. pneumoniae* (Naas et al., 2008; Gootz et al., 2009; Monteiro et al., 2009; Shen et al., 2009), *Escherichia coli* (Cai et al., 2008; Chen L. et al., 2014), *Salmonella* spp. (Cai et al., 2008), and *Serratia marcescens* (Zhang et al., 2007; Cai et al., 2008), and has even been identified in nonfermenters such as *Acinetobacter* (Robledo et al., 2010) and *Pseudomonas* spp. (Poirel et al., 2010). Rapid spread of the bla_{KPC} gene is of great concern (Nordmann et al., 2009; Zhang et al., 2017).

Plasmids play an important role in the dissemination of the bla_{KPC-2} gene. Only one identified bla_{KPC-18} gene has been determined to be located on the chromosome (Thomson et al., 2016), while nearly all of the other identified bla_{KPC} genes were harbored on plasmids. Plasmids of the incompatibility groups F (IncF), N (IncN), L/M (IncL/M), and X (IncX) have been reported to mediate bla_{KPC-2} gene transfer in *Enterobacteriaceae* (Cuzon et al., 2010; Jiang et al., 2010; Chen et al., 2013; Chen L. et al., 2014; Chen Y. T. et al., 2014).

Recently, a novel bla_{KPC}-harboring untypeable plasmid (pCKPC18-1) encoding a replication protein that could not be assigned to any known incompatibility group was described in China (Zheng et al., 2018). To date, the likely plasmid has only been detected in *Citrobacter freundii*, *Klebsiella pneumonia,* and *Enterobacter cloacae* strains (Jiang et al., 2015; Shen et al., 2016; Zheng et al., 2018). In this study, we provided evidence for the further spread of the bla_{KPC}-carrying untypeable plasmid in *Enterobacteriaceae* in the southwestern Zhejiang province of China.

MATERIALS AND METHODS

Bacterial Strains, Detection of Carbapenem Resistance Genes, and Plasmid Incompatibility Typing

From 2011 to 2016, a total of 156 non-repetitive carbapenem-resistant *Enterobacteriaceae* (CRE) strains were isolated by the VITEK2 Compact system (bioMérieux VITEK, USA) in Lishui Hospital of Zhejiang University, a tertiary hospital in southwestern Zhejiang province of China. Species were further identified using an automated mass spectrometry microbial identification system (MALDI-TOF, Bruker, USA) and re-confirmed by 16S rRNA, *RecN,* and *Hsp60* sequencing (Hoffmann and Roggenkamp, 2003; Ribeiro et al., 2015). Common carbapenemase-encoding genes, including bla_{KPC}, bla_{NDM}, bla_{VIM}, bla_{IMP}, bla_{GES}, bla_{SME}, bla_{IMI}, bla_{SIM}, bla_{GIM}, bla_{SPM}, bla_{OXA-23}, bla_{OXA-24}, and bla_{OXA-58}, from all 156 isolates were amplified, and amplicons were sequenced (Pfeifer et al., 2010; Huang et al., 2012; Zhang et al., 2017, 2018). Plasmids of the untypeable incompatibility group, represented by pCKPC18-1 (CP022276), were screened by specific primers (UTF-TGCATCGATACGTTCCTGCA and UTR-ACTCGCTAGCATGGAACATC) targeting the replication initiator (*repA*). The untypeable *repA*-positive isolates were selected for further studies.

Antimicrobial Susceptibility Testing

Antimicrobial susceptibilities were first determined by the disc diffusion (Kirby-Bauer, K-B) method. The minimum inhibitory concentrations (MICs) of imipenem, ertapenem, ceftazidime, ceftriaxone, cefepime, ampicillin, aztreonam, ciprofloxacin, levofloxacin, trimethoprim/sulfamethoxazole, tobramycin, gentamicin, and amikacin were detected by the VITEK2 Compact system with AST-GN13 cards or *E*-test (bioMérieux, France) according to the manufacturer's instructions. The results were interpreted according to the guidelines of the Clinical and Laboratory Standards Institute (CLSI) (Wayne, 2017). *E. coli* ATCC 25922 was used for quality control.

Determination of Genetic Relatedness

Multilocus sequence typing was performed on the *E. coli* (http://mlst.warwick.ac.uk/mlst/dbs/Ecoli) and *C. freundii* (https://pubmlst.org/cfreundii/) isolates according to the online databases. Pulsed-field gel electrophoresis (PFGE) was performed to further evaluate the relatedness of the *E. coli* strains via XbaI digestion (Huang et al., 2016).

Multilocus PCR and RFLP Analysis of Plasmids

Transformation and conjugation experiments were performed to acquire purified single plasmids as described previously (Jiang et al., 2010, 2015; Shen et al., 2016; Zheng et al., 2018). The bla_{KPC-2}-carrying plasmids were extracted with a Plasmid Miniprep Kit (Transgen Biotech, China) from the transconjugants. Multilocus PCR was performed to evaluate the relationships of the 6 untypeable plasmids discovered in this study. In addition to the *repA* and bla_{KPC} genes, primers (**Table 1**) were designed to target the backbone genes *taxA*, *virB5*, *virB11,* and *repB* and the mobile elements Tn*1721-TnpA* and Tn*1721-TnpR*. Amplicons were analyzed by electrophoresis and sequencing. Meanwhile, plasmids were digested with EcoRI and subjected to restriction fragment length polymorphism (RFLP) by electrophoresis on 1% agarose (Sangon, China) gels in 1×TAE buffer as reported before (Ho et al., 2012).

Plasmid Sequencing and Annotation

Representative plasmids were fragmented by the whole-genome shotgun (WGS) approach and libraries were constructed. Genomic DNA were completely sequenced by next-generation sequencing (NGS) on an Illumina MiSeq platform with 2 × 400 bp paired-end reads. Adapters were removed using AdapterRemoval (ver. 2.1.7), and the high quality reads were screened through SOAPec (v2.0) with a Kmer frequency of 17. Sequences were then assembled with the A5-miseq (v20160825) and SPAdes (v3.9.0) programs. Protein-coding genes were predicted using GeneMarkS (v4.28) software, and coding sequence (CDS) annotations were performed using the BLASTP program with the NR database, followed by manual inspection.

TABLE 1 | Multilocus-PCR primers used in this study.

Target	Primer	Sequence	Size (bp)	References
repA	UTF	TGCATCGATACGTTCCTGCA	841	pCKPC18-1 and pFOS18
	UTR	ACTCGCTAGCATGGAACATC		
bla_{KPC}	KPCF	GCTACACCTAGCTCCACCTTC	989	Shen et al., 2009
	KPCR	ACAGTGGTTGGTAATCCATGC		
taxA	CH1F	GCGTTGAATCCACGTATTGG	752	pCKPC18-1
	CH1R	TATCATGCCCGTATACTCGC		
virB5	CH2F	GCACCTTGTGGTGAAGAACC	779	pCKPC18-1
	CH2R	TGTACGGCATTAGCGGCATC		
virB11	CH3F	CTACGTTCGTCAATTCACTG	772	pCKPC18-1
	CH3R	AGGTGTAGATCACCAACGCG		
Tn*1721-TnpA*	CH4F	CAGGTAGTCGTCGAAGTCGC	815	pCKPC18-1
	CH4R	CCAACTCTCGGCACATGCTG		
Tn*1721-TnpR*	CH5F	TCTGTACCAAGCGACGCAGG	762	pCKPC18-1
	CH5R	CGGCCTCATGGTACATCTGG		
TnpA/repB	CH4F	CAGGTAGTCGTCGAAGTCGC	954 or 2558	pCKPC18-1 and pFOS18
	CH5R	CGGCCTCATGGTACATCTGG		

RESULTS

Bacterial Strains and Antimicrobial Susceptibility Testing

Among all the 156 strains, 6 bla_{KPC-2} producers [2 *E. coli* strains (EC84 and EC86), 1 *E. asburiae* strain (EAK7), 1 *C. freundii* strain (CF111), 1 *C. portucalensis* strain (CP40), and 1 *C. koseri* strain (CK61)] isolated from different patients were positive for the untypeable plasmid (**Supplementary S1**). EAK7, which was isolated from hematology wards in December 2010, was the first untypeable plasmid carrier identified in our hospital. Then it was CP40 in January 2012, CK61 in September 2012, EC84 in May 2013, EC86 in June 2013 and CF111 in October 2014. However, except for the 2 *E. coli* strains isolated from the ICU, all the strains were isolated from different wards. No apparent contact among the patients was validated. None of the other CRE isolates were positive for the untypeable plasmid. All 6 isolates were resistant to carbapenems, third-generation cephalosporins and aztreonam, but were susceptible to colistin (**Table 2**). Notably, *C. portucalensis* CP40 was resistant to sulfonamides and aminoglycosides but was susceptible to quinolones; however, *C. freundii* CF111 was exhibited the opposite resistance and susceptibility. Both *E. coli* EC84 and EC86 were resistant to levofloxacin, ciprofloxacin, trimethoprim/sulfamethoxazole, gentamicin and tobramycin and were susceptible to amikacin. Nevertheless, all the transconjugants showed similar susceptibility profiles that were resistant to the β-lactams but susceptible to quinolones, aminoglycosides and sulfonamides.

Analysis of the Genetic Relatedness

According to the MLST results, both *E. coli* EC84 and EC86 belonged to ST648 and showed identical PFGE patterns (**Supplementary S2**), suggesting the clonal relatedness of the 2 strains. The *C. freundii* CF111 belonged to sequence type ST116.

Multilocus PCR and RFLP Analysis of Plasmids

Single plasmids were successfully obtained via transformation (pCP40, pCF111, pEC84, and pEC86) and conjugation (pEAK7 and pCK61). All the plasmids tested positive for *repA* and bla_{KPC}. Upon amplification of the *TaxA*, *virB5*, *virB11*, Tn*1721-TnpA*, and Tn*1721-TnpR* sequences, positive results, which exhibited 100% sequence identity with pCKPC18-1, were obtained with pEAK7, pCP40, pCK61, and pCF111; however, none of these genes were detected in pEC84 and pEC86 (**Figure 1A**). Interestingly, fragments of different lengths were obtained from all the plasmids with the forward and reverse primers CH4F and CH5R, targeting Tn*1721-TnpA* and *repB*, respectively. The fragment lengths were approximately 2,500 bp from pEAK7, pCP40, pCK61 and pCF111 and 1,000 bp from pEC84 and pEC86. Sequencing analysis revealed that the large and small fragments shared 100% identity with pCKPC18-1 (CP022276) and pKPC-ECN49 (KP726894), respectively. Consistent with the multilocus PCR results, 2 different patterns were observed in the RFLP analysis (**Figure 1B**). The plasmids pEAK7, pCP40, pCK61, and pCF111 yielded identical fragments, which differed from the fragments from pEC84 and pEC86.

Characteristics of the bla_{KPC-2}-Carrying Untypeable Plasmids

The plasmids pCP40 and pEC86, isolated from *C. portucalensis* and *E. coli* strains respectively, were chosen as representative plasmids for complete genome sequencing. The plasmid pCP40 is a 42,848-bp closed circular DNA with an average G+C content of 50.1%. Annotation of the final sequence of pCP40 revealed 50 open reading frames (ORFs), 32 of which encoded homologous proteins with known functions. In the backbone structure, there were genes encoding an untypeable replication protein, the molecular chaperone DnaJ, the type IV secretory pathway

TABLE 2 | Antimicrobial susceptibilities of the six enterobacteriaceae and their transconjugants.

Isolates	Species	IPM		ETP		FEP		CAZ		CRO		AMP		ATM		LEV*		CIP*		SXT		Gm		TM		AMK		PB
		MIC	KB	MIC	KB	MIC	KB	MIC	KB	MIC	KB	MIC	KB	MIC	KB	MIC	KB	MIC	KB	MIC	KB	MIC	KB	MIC	KB	MIC	KB	KB
EAK7	*E. asburiae*	≥16	R	≥8	R	≥64	R	8	R	≥64	R	≥32	R	≥64	R	1	S	0.5	S	≤20	S	≥16	R	≥16	R	≥64	R	S
CP40	*C. portucalensis*	≥16	R	≥8	R	32	R	≥64	R	≥64	R	≥32	R	≥64	R	8	R	4	R	≤20	S	≤1	S	≤1	S	≤2	S	S
CK61	*C. koseri*	2	I	8	R	16	R	16	R	32	R	≥32	R	≥64	R	0.064	S	0.016	S	≤20	S	8	R	≤1	S	≤2	S	S
EC84	*E. coli*	8	R	≥8	R	≥64	R	≥64	R	≥64	R	≥32	R	≥64	R	≥32	R	≥32	R	≥320	R	≥16	R	8	I	≤2	S	S
EC86	*E. coli*	8	R	≥8	R	≥64	R	≥64	R	≥64	R	≥32	R	≥64	R	≥32	R	≥32	R	≥320	R	≥16	R	≥16	R	4	S	S
CF111	*C. freundii*	≥16	R	≥8	R	≥64	R	16	R	≥64	R	≥32	R	≥64	R	2	S	1	I	≥320	R	≥16	R	≥16	R	≥64	R	S
Tc-K7	*E. coli* J53	≥16	R	≥8	R	≥64	R	≥64	R	≥64	R	≥32	R	≥64	R	0.064	S	0.016	S	≤20	S	4	S	≤1	S	4	S	S
Tc-40	*E. coli* DH5α	≥16	R	≥8	R	≥64	R	≥64	R	≥64	R	≥32	R	≥64	R	0.008	S	0.008	S	≤20	S	2	S	2	S	4	S	S
Tc-61	*E. coli* J53	≥16	R	≥8	R	≥64	R	≥64	R	≥64	R	≥32	R	≥64	R	0.064	S	0.016	S	≤20	S	4	S	2	S	4	S	S
Tc-84	*E. coli* DH5α	≥16	R	≥8	R	≥64	R	≥64	R	≥64	R	≥32	R	≥64	R	0.016	S	0.008	S	≤20	S	2	S	2	S	≤2	S	S
Tc-86	*E. coli* DH5α	≥16	R	≥8	R	≥64	R	≥64	R	≥64	R	≥32	R	≥64	R	0.016	S	0.008	S	≤20	S	2	S	2	S	≤2	S	S
Tc-111	*E. coli* DH5α	≥16	R	≥8	R	≥64	R	≥64	R	≥64	R	≥32	R	≥64	R	0.008	S	0.008	S	≤20	S	4	S	≤1	S	4	S	S
J53	*E. coli* J53	≤1	S	≤0.5	S	≤1	S	≤1	S	≤1	S	4	S	≤1	S	0.064	S	0.008	S	≤20	S	≤1	S	≤1	S	≤2	S	S
Trans1-T1	*E. coli* DH5α	≤1	S	≤0.5	S	≤1	S	≤1	S	≤1	S	4	S	≤1	S	0.008	S	0.016	S	≤20	S	≤1	S	≤1	S	≤2	S	S
25922	*E. coli*	≤1	S	≤0.5	S	≤1	S	≤1	S	≤1	S	2	S	≤1	S	0.008	S	0.008	S	≤20	S	≤1	S	≤1	S	≤2	S	S

*Susceptibilities were determined by KB method and MICs (μg/mL) were obtained by VITEK2 compact system with AST-GN13 cards, the results were interpreted according to CLSI guidelines. Tc, transconjugants. J53, azide-resistant E. coli J53Az^R strain; Trans1-T1, E. coli competent cells; 25922, E. coli ATCC25922 strain. IMP, imipenem; ETP, ertapenem; FEP, cefepime; CAZ, ceftazidime; CRO, ceftriaxone; AMP, ampicillin, ATM, aztreonam; LEV, levofloxacin; SXT, trimethoprim/sulfamethoxazole; CIP, ciprofloxacin; Gm, gentamicin; TM, tobramycin; AMK, amikacin. S, susceptible; I, intermediate; R, resistant. *Tested by E-test technique (AB bioMerieux, Sweden).*

(VirB1-10), the DNA-binding protein StpA, the antirestriction protein Klca, and the transcriptional repressor protein KorC. In the variable region, the bla_{KPC-2} gene was embedded in the Tn*3*-Tn*4401* chimera with the gene order Tn*3-TnpA*, Tn*3-TnpR*, IS*Kpn8*, bla_{KPC-2}, IS*Kpn6-like*, Tn*1721-TnpR,* and Tn*1721-TnpA* (**Figure 2**).

The plasmid pEC86 was 24,228-bp in length, possessed an average G+C content of 50.9% and had 37 predicted ORFs. This plasmid contained backbone genes encoding the replicons, DnaJ, StpA, Klca, and KorC, though the type IV secretory system (VirB1-10) was absent. Similar to pCP40, bla_{KPC-2} was the only resistance gene present in pEC86 and was integrated in the same genetic context but without Tn*1721-TnpR* and with a partial Tn*1721-TnpA* (**Figure 2**).

The sequences of 5 bla_{KPC}-harboring plasmids with identical *repA* genes were downloaded from the NCBI database. pCP40 shared 99% sequence similarity with the untypeable plasmids pHS062105-3 (KF623109, 42,848-bp), pP10159-3 (MF072963, 42,763-bp), pCKPC18-1 (CP022276, 47,164-bp), and pKPC-ECN49 (KP726894, 41,317-bp). In particular, with the exception of 20 single-nucleotide polymorphisms (SNPs), pCP40 was identical to the plasmid pHS062105-3 from a *K. pneumoniae* isolate from Shanghai. The overall structure of pEC86 was most similar to that of pFOS18 (KJ653815, 23,939-bp) from *K. pneumoniae* and pKPC-ECN49 from *E. cloacae* (Jiang et al., 2015). However, the *fosA3* gene embedded the IS*26* composite transposon in pFOS18 and the type IV secretory pathway in pKPC-ECN49 was not observed in pEC86.

Nucleotide Accession Numbers

The complete sequences of pCP40 and pEC86 have been deposited in GenBank under the accession numbers MH328006 and MH328007, respectively.

DISCUSSION

Plasmids are one of the major causes responsible for the rapid dissemination of the bla_{KPC} gene (Cuzon et al., 2010; Jiang et al., 2010; Chen et al., 2013; Chen L. et al., 2014; Chen Y. T. et al., 2014). The novel plasmid pFOS18, characterized by backbone genes encoding a replication protein (RepA) that could not be assigned to any known incompatibility group, the molecular chaperone DnaJ, the DNA-binding protein StpA, the antirestriction protein Klca, and the transcriptional repressor protein KorC, was first described in 2015 from a fosfomycin-resistant KPC-producing *K. pneumoniae* strain in Zhejiang province (Jiang et al., 2015). Recently, plasmids containing identical *repA* genes were detected in *Citrobacter freundii* (pCKPC18-1) and *Enterobacter cloacae* (pKPC-ECN49) stains in the Zhejiang and Jiangsu provinces, respectively (Zheng et al., 2018).

In this study, we identified the untypeable plasmids in 6 *Enterobacteriaceae*. Besides *C. freundii* strain, the untypeable plasmid was detected in 2 *E. coli*, 1 *E. asburiae*, 1 *C. portucalensis* and 1 *C. koseri* strains. Although *E. asburiae* was the first strain carrying the untypeable plasmid isolated in our hospital, clonal spread of this strain was not detected. The 2 *E. coli* strains exhibited identical ST types, PFGE profiles and susceptibility patterns, suggesting clonal spread of the *E. coli* strains. However, due to limited information, it is not clear whether the CF111 (ST116) is related to the *C. freundii* strains carrying pCKPC18-1 in Hangzhou or pP10159-3 in Chongqing (Zheng et al., 2018).

Consistent with the previous studies (Jiang et al., 2015; Shen et al., 2016; Zheng et al., 2018), 2 different subtypes of the untypeable plasmids were characterized in the 6 strains according to multilocus-PCR and RFLP analysis. The plasmids pEAK7, pCP40, pCK61, and pCF111 yielded identical multilocus-PCR results matching pCKPC18-1, while the other 2 (pEC84 and pEC86) were more related to pFOS18. Complete sequencing of the 2 representative plasmids, pCP40 and pEC86, showed that they were 42,848 and 24,228-bp in size, respectively. Although they differed in size, identical replication initiators and similar backbone genes and bla_{KPC-2} genetic contexts were observed in the 2 plasmids. Comparative analysis revealed that pCP40 shared high query coverage and identity with untypeable plasmids isolated from *K. pneumoniae*, *C. freundii* and *E. cloacae* in different areas of China. In particular, pCP40 present in the *C. portucalensis* isolate and pHS062105-3 from a *K. pneumoniae* strain differed by only 20 SNPs. Taken together, the high sequence similarity among pCP40, pKPC-ECN49, pHS062105-3, pP10159-3, and pCKPC18-1 suggested that these plasmids evolved from a common plasmid and spread independently (Zheng et al., 2018).

A previous study showed that the *K. pneumoniae* strains could transfer their bla_{KPC-2}-carrying untypeable plasmids to the azide-resistant *E. coli* strain J53, implying the possibility of horizontal transfer of the untypeable plasmid (Shen et al., 2016). Moreover, the transfer regions of these untypeable plasmids also share high identity with the transferable IncN plasmid p1 (CP006657) (Zheng et al., 2018). In our study, 2 strains (EAK7 and CK61) successfully transferred untypeable plasmids to the recipient, thereby reconfirming the horizontal transfer capacity. Take account of the high similarity of pEAK7, pCP40, pCK61, and pCF111, the untypeable plasmid may transfer among *Enterobacteriaceae*, mediating bla_{KPC} dissemination. However, after 5 attempts, the *E. coli* strains (EC84 and EC86) failed in conjugation experiments. Compared with pCP40, complete sequencing revealed the main difference of lacking the type IV secretory system in pEC86. The type IV secretory system has been reported to deliver DNA and protein substrates from donor to target bacterial cells by conjugation (Christie, 2004), implying that it is the factor responsible for the horizontal transferability of the untypeable plasmid.

In summary, this study characterized the epidemiological contexts of 6 CRE isolates carrying the untypeable plasmids in our hospital and identified two plasmids, namely, pCP40 and pEC86. To the best of our knowledge, this is the first description of a bla_{KPC}-harboring untypeable plasmid in *E. coli*, *E. asburiae,* and *C. koseri* strains. This work provided evidence of the spread of this bla_{KPC}-harboring untypeable plasmid in *Enterobacteriaceae* in China and highlights the

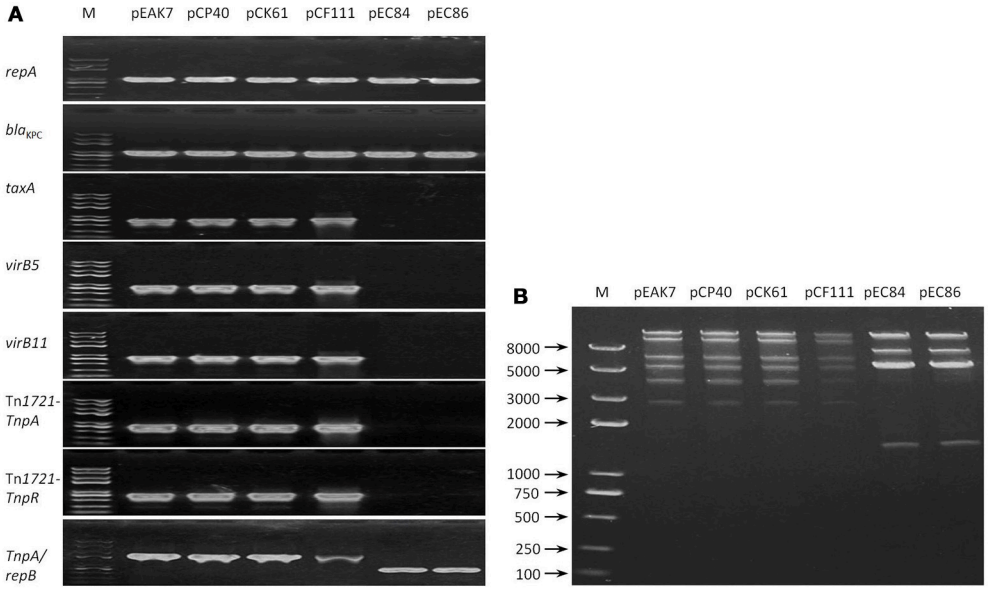

FIGURE 1 | Relatedness of the 6 untypeable plasmids. **(A)** Mutilocus-PCR results. Primers targeting the genes *repA*, bla_{KPC}, *TaxA*, *virB5*, *virB11*, Tn*1721-TnpA*, Tn*1721-TnpR*, and *repB* were designed. Two profiles were obtained after evaluation of the amplicons by electrophoresis. The plasmids pEAK7, pCP40, pCK61, and pCF111 exhibited one pattern, while pEC84 and pEC86 exhibited a different pattern. **(B)** RFLP results. Fragments were separated by electrophoresis on a 1% agarose gel in 1 × TAE buffer. Two different patterns, one for the plasmids pEAK7, pCP40, pCK61, and pCF111 and another for pEC84 and pEC86, were obtained. EA, *E. asburiae*; CP, *C. portucalensis*; CF, *C. freundii*; CK, *C. koseri*; EC, *E. coli*; M, DNA marker.

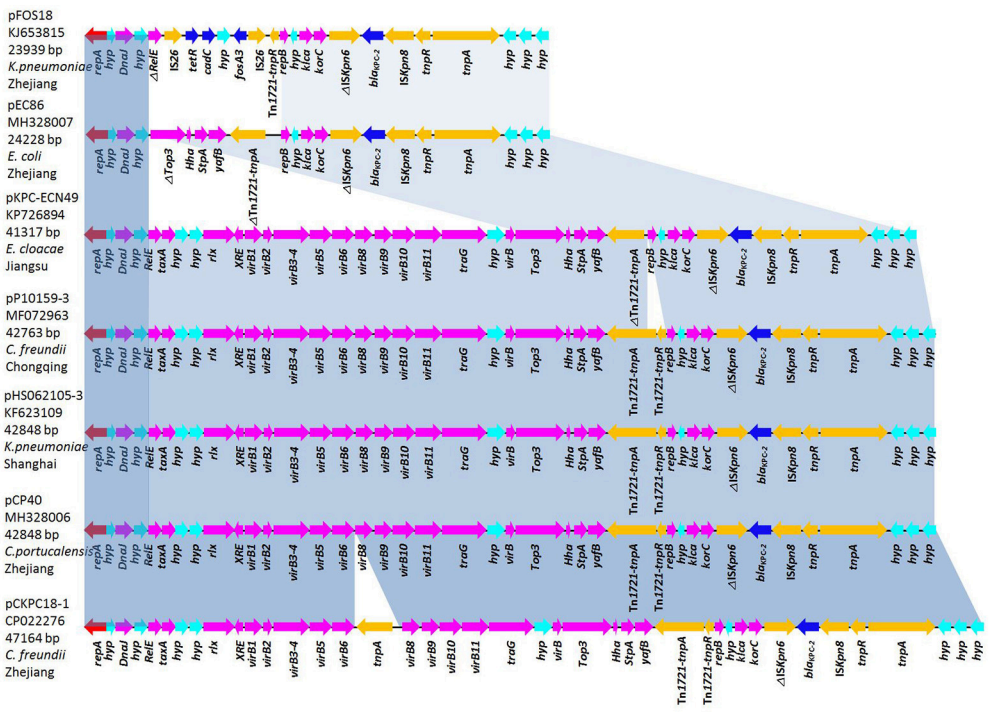

FIGURE 2 | Comparative analysis of the bla_{KPC}-harboring untypeable plasmids pFOS18 (KJ653815), pEC86 (MH328007), pKPC-ECN49 (KP726894), pHS062105-3 (KF623109), pP10159-3 (MF072963), pCP40 (MH328006), and pCKPC18-1 (CP022276). Light-blue shading denotes shared regions of homology in each adjacent plasmid. Notably, the type IV secretory pathway (VirB1-10) present in pKPC-ECN49, pHS062105-3, pP10159-3, pCP40, and pCKPC18-1 is absent in pFOS18 and pEC86. Open reading frames (ORFs) are depicted by arrows and are colored based on predicted gene function. Resistance genes are indicated with deep-blue arrows.

urgent need for effective surveillance of KPC-producing *Enterobacteriaceae* to control rapid bla_{KPC} gene dissemination. A specific nomenclature for the untypeable plasmids is required.

AUTHOR CONTRIBUTIONS

JH and ZZ were responsible for the study design and data interpretation. HD, YZ, XH, and JR collected all the clinical isolates and performed susceptibility tests. YS, GH, and RW carried out PCRs, transformation and conjugation experiments. JH performed RFLP and wrote the report. All authors revised, reviewed, and approved the final report.

FUNDING

This work was supported by the Medical and health technological project of Zhejiang province of China (2018KY935) and the Major Research and Development Project of Lishui City of China (2017ZDYF13).

SUPPLEMENTARY MATERIAL

The Supplementary Material for this article can be found online at: https://www.frontiersin.org/articles/10.3389/fmicb.2018.01938/full#supplementary-material

REFERENCES

Cai, J. C., Zhou, H. W., Zhang, R., and Chen, G. X. (2008). Emergence of *Serratia marcescens*, *Klebsiella pneumoniae*, and *Escherichia coli* Isolates possessing the plasmid-mediated carbapenem-hydrolyzing beta-lactamase KPC-2 in intensive care units of a Chinese hospital. *Antimicrob. Agents Chemother.* 52, 2014–2018. doi: 10.1128/AAC.01539-07

Chen, L., Chavda, K. D., Fraimow, H. S., Mediavilla, J. R., Melano, R. G., Jacobs, M. R., et al. (2013). Complete nucleotide sequences of blaKPC-4- and blaKPC-5-harboring IncN and IncX plasmids from *Klebsiella pneumoniae* strains isolated in New Jersey. *Antimicrob. Agents Chemother.* 57, 269–276. doi: 10.1128/AAC.01648-12

Chen, L., Hu, H., Chavda, K. D., Zhao, S., Liu, R., Liang, H., et al. (2014). Complete sequence of a KPC-producing IncN multidrug-resistant plasmid from an epidemic *Escherichia coli* sequence type 131 strain in China. *Antimicrob. Agents Chemother.* 58, 2422–2425. doi: 10.1128/AAC.02587-13

Chen, Y. T., Lin, J. C., Fung, C. P., Lu, P. L., Chuang, Y. C., Wu, T. L., et al. (2014). KPC-2-encoding plasmids from *Escherichia coli* and *Klebsiella pneumoniae* in Taiwan. *J. Antimicrob. Chemother.* 69, 628–631. doi: 10.1093/jac/dkt409

Christie, P. J. (2004). Type IV secretion: the *Agrobacterium* VirB/D4 and related conjugation systems. *Biochim. Biophys. Acta* 1694, 219–234. doi: 10.1016/j.bbamcr.2004.02.013

Cuzon, G., Naas, T., Truong, H., Villegas, M. V., Wisell, K. T., Carmeli, Y., et al. (2010). Worldwide diversity of *Klebsiella pneumoniae* that produce beta-lactamase blaKPC-2 gene. *Emerging Infect. Dis.* 16, 1349–1356. doi: 10.3201/eid1609.091389

Gootz, T. D., Lescoe, M. K., Dib-Hajj, F., Dougherty, B. A., He, W., Della-Latta, P., et al. (2009). Genetic organization of transposase regions surrounding blaKPC carbapenemase genes on plasmids from *Klebsiella* strains isolated in a New York City hospital. *Antimicrob. Agents Chemother.* 53, 1998–2004. doi: 10.1128/AAC.01355-08

Ho, P.-L., Li, Z., Lo, W.-U., Cheung, Y.-Y., Lin, C.-H., Sham, P.-C., et al. (2012). Identification and characterization of a novel incompatibility group X3 plasmid carrying blaNDM-1 in *Enterobacteriaceae* isolates with epidemiological links to multiple geographical areas in China. *Emerg. Microbes Infect.* 1, 39–45. doi: 10.1038/emi.2012.37

Hoffmann, H., and Roggenkamp, A. (2003). Population genetics of the *Nomenspecies Enterobacter cloacae*. *Appl. Environ. Microbiol.* 69, 5306–5318. doi: 10.1128/aem.69.9.5306-5318.2003

Huang, J., Li, X., Zhu, N., and Li, G. (2012). Genetic characteristics of one highly multi-drug-resistant strain of *Klebsiella ozaenae*. *J. Med. Microbiol.* 61, 1303–1305. doi: 10.1099/jmm.0.044115-0

Huang, Y., Yu, X., Xie, M., Wang, X., Liao, K., Xue, W., et al. (2016). Widespread dissemination of carbapenem-resistant *Escherichia coli* sequence type 167 strains harboring blaNDM-5 in clinical settings in China. *Antimicrob. Agents Chemother.* 60, 4364–4368. doi: 10.1128/AAC.00859-16

Jiang, Y., Shen, P., Wei, Z., Liu, L., He, F., Shi, K., et al. (2015). Dissemination of a clone carrying a fosA3-harbouring plasmid mediates high fosfomycin resistance rate of KPC-producing *Klebsiella pneumoniae* in China. *Int. J. Antimicrob. Agents* 45, 66–70. doi: 10.1016/j.ijantimicag.2014.08.010

Jiang, Y., Yu, D., Wei, Z., Shen, P., Zhou, Z., and Yu, Y. (2010). Complete nucleotide sequence of *Klebsiella pneumoniae* multidrug resistance plasmid pKP048, carrying blaKPC-2, blaDHA-1, qnrB4, and armA. *Antimicrob. Agents Chemother.* 54, 3967–3969. doi: 10.1128/AAC.00137-10

Monteiro, J., Santos, A. F., Asensi, M. D., Peirano, G., and Gales, A. C. (2009). First report of KPC-2-producing *Klebsiella pneumoniae* strains in Brazil. *Antimicrob. Agents Chemother.* 53, 333–334. doi: 10.1128/AAC.00736-08

Naas, T., Cuzon, G., Villegas, M. V., Lartigue, M. F., Quinn, J. P., and Nordmann, P. (2008). Genetic structures at the origin of acquisition of the beta-lactamase bla KPC gene. *Antimicrob. Agents Chemother.* 52, 1257–1263. doi: 10.1128/AAC.01451-07

Nordmann, P., Cuzon, G., and Naas, T. (2009). The real threat of *Klebsiella pneumoniae* carbapenemase-producing bacteria. *Lancet Infect. Dis.* 9, 228–236. doi: 10.1016/S1473-3099(09)70054-4

Pfeifer, Y., Cullik, A., and Witte, W. (2010). Resistance to cephalosporins and carbapenems in Gram-negative bacterial pathogens. *Int. J. Med. Microbiol.* 300, 371–379. doi: 10.1016/j.ijmm.2010.04.005

Poirel, L., Nordmann, P., Lagrutta, E., Cleary, T., and Munoz-Price, L. S. (2010). Emergence of KPC-producing *Pseudomonas* aeruginosa in the United States. *Antimicrob. Agents Chemother.* 54:3072. doi: 10.1128/AAC.00513-10

Ribeiro, T. G., Novais, A., Branquinho, R., Machado, E., and Peixe, L. (2015). Phylogeny and comparative genomics unveil independent diversification trajectories of qnrB and genetic platforms within particular citrobacter species. *Antimicrob. Agents Chemother.* 59, 5951–5958. doi: 10.1128/AAC.00027-15

Robledo, I. E., Aquino, E. E., Sante, M. I., Santana, J. L., Otero, D. M., Leon, C. F., et al. (2010). Detection of KPC in *Acinetobacter* spp. in Puerto Rico. *Antimicrob. Agents Chemother.* 54, 1354–1357. doi: 10.1128/AAC.00899-09

Shen, P., Wei, Z., Jiang, Y., Du, X., Ji, S., Yu, Y., et al. (2009). Novel genetic environment of the carbapenem-hydrolyzing beta-lactamase KPC-2 among *Enterobacteriaceae* in China. *Antimicrob. Agents Chemother.* 53, 4333–4338. doi: 10.1128/AAC.00260-09

Shen, P., Zhang, Y., Li, G., and Jiang, X. (2016). Characterization of the genetic environment of the blaKPC-2 gene among *Klebsiella pneumoniae* isolates from a Chinese Hospital. *Braz. J. Infect. Dis.* 20, 384–388. doi: 10.1016/j.bjid.2016.04.003

Thomson, G. K., Snyder, J. W., McElheny, C. L., Thomson, K. S., and Doi, Y. (2016). Coproduction of KPC-18 and VIM-1 Carbapenemases by Enterobacter cloacae: implications for newer beta-lactam-beta-lactamase inhibitor combinations. *J. Clin. Microbiol.* 54, 791–794. doi: 10.1128/JCM.02739-15

Wayne, P. (2017). *Performance Standards for Antimicrobial Susceptibility Testing [S]: Twenty-Seventh Informational Supplement*. Pennsylvania, PA: Clinical and Laboratory Standards Institute, M100–S27.

Yigit, H., Queenan, A. M., Anderson, G. J., Domenech-Sanchez, A., Biddle, J. W., Steward, C. D., et al. (2001). Novel carbapenem-hydrolyzing beta-lactamase, KPC-1, from a carbapenem-resistant strain

of *Klebsiella pneumoniae*. *Antimicrob. Agents Chemother.* 45, 1151–1161. doi: 10.1128/AAC.45.4.1151-1161.2001

Zhang, R., Liu, L., Zhou, H., Chan, E. W., Li, J., Fang, Y., et al. (2017). Nationwide surveillance of clinical carbapenem-resistant enterobacteriaceae (CRE) strains in China. *EBioMed.* 19, 98–106. doi: 10.1016/j.ebiom.2017.04.032

Zhang, R., Zhou, H. W., Cai, J. C., and Chen, G. X. (2007). Plasmid-mediated carbapenem-hydrolysing beta-lactamase KPC-2 in carbapenem-resistant *Serratia marcescens* isolates from Hangzhou, China. *J. Antimicrob. Chemother.* 59, 574–576. doi: 10.1093/jac/dkl541

Zhang, Y., Wang, Q., Yin, Y., Chen, H., Jin, L., Gu, B., et al. (2018). Epidemiology of carbapenem-resistant enterobacteriaceae infections: report from the China CRE network. *Antimicrob. Agents Chemother.* 62:e01882–17. doi: 10.1128/AAC.01882-17

Zheng, B., Huang, C., Xu, H., Yu, X., Zhang, J., Wang, X., et al. (2018). Complete nucleotide sequences of two KPC-2-encoding plasmids from the same *Citrobacter freundii* isolate. *J. Antimicrob. Chemother.* 73, 531–533. doi: 10.1093/jac/dkx381

Conflict of Interest Statement: The authors declare that the research was conducted in the absence of any commercial or financial relationships that could be construed as a potential conflict of interest.

frontiers in Microbiology

ORIGINAL RESEARCH
published: 05 September 2018
doi: 10.3389/fmicb.2018.02057

Spread of Carbapenem Resistance by Transposition and Conjugation Among *Pseudomonas aeruginosa*

*Anneke van der Zee[1], W. Bart Kraak[1], Arjan Burggraaf[1], Wil H. F. Goessens[2], Walter Pirovano[3], Jacobus M. Ossewaarde[1,2] and Jan Tommassen[4]**

[1] Laboratory of Medical Microbiology, Molecular Diagnostics Unit, Maasstad Hospital, Rotterdam, Netherlands, [2] Erasmus University Medical Center, Rotterdam, Netherlands, [3] BaseClear, Leiden, Netherlands, [4] Section Molecular Microbiology, Department of Biology, Faculty of Science, Utrecht University, Utrecht, Netherlands

The emergence of carbapenem-resistant *Pseudomonas aeruginosa* represents a worldwide problem. To understand the carbapenem-resistance mechanisms and their spreading among *P. aeruginosa* strains, whole genome sequences were determined of two extensively drug-resistant strains that are endemic in Dutch hospitals. Strain Carb01 63 is of O-antigen serotype O12 and of sequence type ST111, whilst S04 90 is a serotype O11 strain of ST446. Both strains carry a gene for metallo-β-lactamase VIM-2 flanked by two *aacA29* genes encoding aminoglycoside acetyltransferases on a class 1 integron. The integron is located on the chromosome in strain Carb01 63 and on a plasmid in strain S04 90. The backbone of the 159-kb plasmid, designated pS04 90, is similar to a previously described plasmid, pND6-2, from *Pseudomonas putida*. Analysis of the context of the integron showed that it is present in both strains on a ∼30-kb mosaic DNA segment composed of four different transposons that can presumably act together as a novel, active, composite transposon. Apart from the presence of a 1237-bp insertion sequence element in the composite transposon on pS04 90, these transposons show > 99% sequence identity indicating that transposition between plasmid and chromosome could have occurred only very recently. The pS04 90 plasmid could be transferred by conjugation to a susceptible *P. aeruginosa* strain. A second class 1 integron containing a gene for a CARB-2 β-lactamase flanked by an *aacA4′-8* and an *aadA2* gene, encoding an aminoglycoside acetyltransferase and adenylyltransferase, respectively, was present only in strain Carb01 63. This integron is located also on a composite transposon that is inserted in an integrative and conjugative element on the chromosome. Additionally, this strain contains a frameshift mutation in the *oprD* gene encoding a porin involved in the transport of carbapenems across the outer membrane. Together, the results demonstrate that integron-encoded carbapenem and carbapenicillin resistance can easily be disseminated by transposition and conjugation among *Pseudomonas aeruginosa* strains.

Keywords: *Pseudomonas aeruginosa*, genome sequence, carbapenem resistance, VIM-2, integron, transposon, conjugation, integrative and conjugative element

OPEN ACCESS

Edited by:
Katy Jeannot, UMR6249 Chrono Environment, France

Reviewed by:
Antonio Oliver, Hospital Universitario Son Dureta, Spain
Josep M. Sierra, University of Barcelona, Spain

***Correspondence:**
Jan Tommassen
J.P.M.Tommassen@uu.nl

Specialty section:
This article was submitted to Antimicrobials, Resistance and Chemotherapy, a section of the journal Frontiers in Microbiology

Received: *17 June 2018*
Accepted: *13 August 2018*
Published: *05 September 2018*

Citation:
van der Zee A, Kraak WB, Burggraaf A, Goessens WHF, Pirovano W, Ossewaarde JM and Tommassen J (2018) Spread of Carbapenem Resistance by Transposition and Conjugation Among Pseudomonas aeruginosa. Front. Microbiol. 9:2057. doi: 10.3389/fmicb.2018.02057

INTRODUCTION

Pseudomonas aeruginosa is an opportunistic gram-negative pathogen causing acute and chronic infections in hospitalized and immune-compromised patients (Kerr and Snelling, 2009). *Pseudomonas* species are known to have evolved from a wide variety of environments and are highly adaptable (Silby et al., 2011). In recent years, extensively drug-resistant *P. aeruginosa* present a globally increasing problem in hospital environments (Edelstein et al., 2013; Wright et al., 2015). *P. aeruginosa* can rapidly become resistant to antibiotics due to various mechanisms (Oliver et al., 2015), including chromosomal mutations leading to inducible hyper-production of chromosomal AmpC β-lactamase, overexpression of efflux pumps, and/or reduced membrane permeability. Such mutations together are referred to as the mutational resistome (López-Causapé et al., 2018). Additionally, horizontal transfer of mobile genetic elements, such as integrons, transposons, or plasmids, can confer resistance mechanisms. The increasing prevalence of metallo-β-lactamases (MBLs), such as VIM or IMP, can be caused by horizontal acquisition of integrons, which are often found to contain also genes encoding aminoglycoside resistance. As a result of frequent acquisition of mobile DNA elements, the genome of *Pseudomonas* can be divided into a core genome and an accessory genome (Battle et al., 2009; Oliver et al., 2015). The population structure therefore was termed non-clonal epidemic, with a high recombination frequency between isolates (Kidd et al., 2012).

Carbapenemase-producing *P. aeruginosa* are often only susceptible to colistin (Edelstein et al., 2013; Kos et al., 2015), thus limiting therapeutic options to treat infected patients. Worldwide, carbapenemase-producing *P. aeruginosa* were assigned to successful clonal complexes (CCs) by multi-locus sequence typing (MLST) and O-antigen serotyping (Thrane et al., 2015). CCs 111 and 235 are considered responsible for the worldwide dissemination of extensively drug-resistant lineages which are of the serotypes O12 and O11, respectively (Thrane et al., 2015). The prevalence of ST111 in the Netherlands was previously described (Van der Bij et al., 2012), and this sequence type was also involved in outbreaks in the United Kingdom (Breathnach et al., 2012). ST235/O11 is more prevalent in Eastern European countries, including Russia (Oliver et al., 2015).

For several years, multidrug-resistant, VIM-producing *P. aeruginosa* were isolated in several hospitals in the Rotterdam area, The Netherlands. In the Erasmus University Medical Centre, two different genotypes predominate (Van der Bij et al., 2011), one of which, an ST111 clone, also dominates in the Maasstad Hospital as well as in many other hospitals in the Netherlands (Van der Bij et al., 2012). Both strains persist and spread through the hospitals via the sinks and drains in spite of hypochlorite treatment. Here, we analyzed representative isolates of both genotypes, which were subjected to whole genome sequencing to study their genetic background. To gain insight into the mobilization of integrons, we analyzed the context of the integrons in detail.

MATERIALS AND METHODS

Ethics Statement

P. aeruginosa strains were selected under designated names and were not related to patients. According to the Dutch regulation for research with human subjects, no medical or ethical approval was required to conduct this study. The regional medical ethics committee (Toetsingscommissie Wetenschappelijk Onderzoek Rotterdam e.o.) waived the need for informed consent and approved the study (L201586), in agreement with national law by the Federation of Dutch Medical Scientific Societies[1].

Strains

P. aeruginosa strain Carb01 63 is a representative of the dominant ST111 genotype isolated from drains and sinks of the Intensive Care Unit at Maasstad Hospital, Rotterdam. Strain S04 90 is a representative of a distinct genotype, i.e., ST446, and was isolated from a patient in Erasmus University Medical Center. Strain PAO1 (Holloway, 1955) was used in conjugation experiments.

Whole Genome Sequencing

Genomic DNA libraries for the Illumina and PacBio platforms were generated and sequenced at BaseClear B.V. (Leiden, Netherlands). For Illumina sequencing, high-molecular-weight genomic DNA was used as input for library preparation using the Illumina TruSeq library preparation kit. Briefly, the genomic DNA was fragmented by nebulization and subjected to end repair, A-tailing, ligation of adaptors including sample-specific barcodes, and size selection. After PCR enrichment, the resultant library was checked on a Bioanalyzer (Agilent) and quantified. The libraries were multiplexed, clustered, and sequenced on an Illumina HiSeq 2000 instrument with paired-end protocol. For PacBio sequencing, high-molecular-weight genomic DNA was sheared to fragments of about 10 kb in length using G-tubes (Covaris) and further processed into a PacBio sequencing library using the standard protocols (Pacific Biosciences). The resulting PacBio library was checked on a BioAnalyzer (Agilent), quantified and sequenced on a PacBio RSII instrument.

Illumina FASTQ sequence files were generated using the Illumina Casava pipeline version 1.8.3. Initial quality assessment was based on data passing the Illumina Chastity filtering. Subsequently, reads containing adapters and/or PhiX control signal were removed using an in-house filtering protocol. The second quality assessment was based on the remaining reads using the FASTQC quality control tool version 0.10.0.

The long read data collected from the PacBio RS instrument were processed and filtered using the SMRT Analysis software suite. The Continuous Long Read (CLR) data were filtered by Read length (>50), Sub read length (>50), and Read quality (>0.75).

The quality of the Illumina FASTQ sequences was enhanced by trimming off low-quality bases using the "Trim sequences" option of the CLC Genomics Workbench version 7.5.1. The

[1] http://www.federa.org

quality-filtered sequence reads were puzzled into a number of contig sequences using the "*De novo* assembly" option of the CLC Genomics Workbench version 7.5.1. The optimal *k*-mer size was automatically determined using KmerGenie (Chikhi and Medvedev, 2014). The contigs were linked and placed into super-scaffolds based on the alignment of the PacBio CLR reads. Alignment was performed with BLASR (Boetzer and Pirovano, 2014). From the alignment, the orientation, order and distance between the contigs were estimated using the SSPACE-LongRead scaffolder version 1.0 (Boetzer and Pirovano, 2014). Final adjustments were manually made based on the assembly graph. The gapped regions within the super-scaffolds were (partially) closed in an automated manner using GapFiller version 1.10 (Boetzer and Pirovano, 2012). The method takes advantage of the insert size between the Illumina paired-end reads.

Genome Analysis

All sequences were automatically annotated using the NCBI Prokaryotic Genomes Automatic Annotation Pipeline (PGAAP)[2] followed by the Rapid Annotations using Subsystems Technology (RAST) server (Aziz et al., 2008). Prophages were assigned by Phage Search Tool (PHAST) (Zhou et al., 2011). The CRISPRFinder (Grissa et al., 2007) was used to search the genomes for possible CRISPR fragments. Restriction-modification systems were analyzed by submission of PacBio data in REBASE (Roberts et al., 2015). Multi-locus sequence types were assigned[3] for both strains. O-antigen types of both strains were determined on the BLAST server of NCBI, where the whole genome sequences were aligned against the different O-antigen sequences of O1-O20. IS finder[4] was used to identify IS elements (Siguier et al., 2006).

Conjugation

Strain PAO1 was consecutively exposed to increasing concentrations of fosfomycin (FOS) to select for mutants with minimum inhibitory concentration (MIC) > 256 μg ml^{-1}, needed for counter selection. After overnight growth, 5 μl of FOS-resistant PAO1 was mixed with 5 μl of strain S04 90. Subsequently, the suspension was plated on MacConkey agar plates containing FOS (150 μg ml^{-1}), and five disks each containing 10 μg meropenem (MER) were placed on the plates. The selected colonies resistant to FOS and MER were investigated for the presence of the VIM gene by PCR (Van der Zee et al., 2014). VIM-positive colonies were typed by amplified fragment length polymorphism (AFLP) to verify if they were PAO1 derivatives. VITEK2 (Biomérieux, Marcy l'Etoile, France) analysis was used to determine antibiotic resistance in donor, recipient and transconjugant strains.

AFLP Typing

Amplified fragment length polymorphism typing was performed essentially as described previously (Van der Zee et al., 2003), except that primers were labeled at the 5′ end with Yakima Yellow. Fragments were analyzed by capillary electrophoresis in an ABI3500 instrument and compared to GeneScan™ 600 LIZ® Size Standard v2.0 (Life Technologies, Bleiswijk, Netherlands). Peak patterns were converted to banding patterns using Bionumerics v7.6 (Applied Maths, St Martens Latem, Belgium). Cluster analysis of the fingerprints was performed by Unweighted Pair Group Method with Arithmetic mean (UPGMA).

Nucleotide Sequence Accession Numbers

The nucleotide sequences of the Carb01 63 chromosome, the S04 90 chromosome, and the pS04 90 plasmid were deposited in Genbank under accession numbers CP011317.1, CP011369.1, and CP011370.1, respectively. Complete assemblies of Carb01 63 and S04 90 are filed under assembly numbers ASM98182v1 and ASM98850v1, respectively.

RESULTS

Bacterial Isolates

Genotyping by multi-locus variable-number tandem-repeat analysis (MLVA) revealed two separate clusters of strains among the VIM-2 MBL-producing *P. aeruginosa* in the hospitals in the Rotterdam area (Van der Bij et al., 2011). MLST revealed that the main cluster consisted of ST111 strains, whilst a minor cluster contains strains of ST446 (Van der Bij et al., 2012). A representative of each of these clusters was elected for genome sequence analysis, i.e., strains Carb01 63 and S04 90 of ST111 and ST446, respectively. VITEK2 analysis showed that both strains are resistant to most antibiotics commonly used to treat *P. aeruginosa* infections but are sensitive for colistin (**Table 1**).

TABLE 1 | Antibiograms of strains Carb01 63, S04 90, PAO1, and a transconjugant of PAO1 carrying pS04 90.

Antibiotics	Carb01 63 MIC[a]	S04 90 MIC[a]	PAO1 MIC[a]	PAO1/pS04 90[b] MIC[a]
Piperacillin/Tazobactam	≥128	≥128	8	≥128
Ceftazidime	16–32	≥64	4	≥64
Gentamicin	≥16	≥16	≤1	≤1
Tobramycin	≥16	≥16	≤1	≥16
Colistin	≤0.5	≤0.5	≤0.5	≤0.5
Ciprofloxacin	≥4	≥4	≤0.25	≤0.25
Meropenem	≥16	8-≥ 16	1	≥16
Imipenem	≥16	≥16	2	≥16
Cefepime	≥64	≥64	2	16
Amikacin	≥64	ND	ND	ND
Fosfomycin	32	64	ND	ND

[a]MIC is given in μg ml^{-1}. [b]Increased MIC values of the transconjugant relative to the recipient strain are marked in gray.

[2]http://www.ncbi.nlm.nih.gov/

[3]http://pubmlst.org/paeruginosa/

[4]http://www-is.biotoul.fr

Genome Analysis

The complete nucleotide sequence of the Carb01 63 genome was recovered by *de novo* hybrid assembly. To overcome sequencing difficulties as a result of large repeats in the genome of S04 90, the sequences were aligned with that of UCBB-PA14 (Lee et al., 2006) which resulted in a single sequence of the chromosome with five gaps of in total 152 bp. This strain was found to contain a large plasmid of 159,187 bp, designated pS04 90. The plasmid has a GC content of 57.7% (**Table 2**), which is substantially lower than the average chromosomal GC content of *P. aeruginosa.* The strains carry different O-antigens, i.e., O12 in Carb01 63 and O11 in S04 90 (**Table 2**). Bacterial defense systems against the uptake of foreign DNA are CRISPR/Cas and restriction-modification systems. No genes for functional CRISPR/Cas systems were observed in the chromosome of either isolate, but the plasmid pS04 90 encodes a putative CRISPR (**Table 2**). Carb01 63 contains type I, II, and III restriction-modification systems, and two unique type I target recognition domains could be identified. S04 90 contains type I and II restriction-modification systems. Plasmid pS04 90 also contains a type II system. Bacteriophage searches revealed the presence of nine prophages, of which four questionable, in Carb01 63 and of 11 prophages, of which four questionable, in S04 90 (**Table 2**). These high numbers of prophages might be related to the absence of CRISPR/CAS systems on the chromosomes of the strains.

Genes for all major virulence factors were found in the genomes of Carb01 63 and S04 90, including alkaline protease AprA, which is a substrate for the type I protein secretion system (T1SS), and elastase LasB, exotoxin A, and the haemolytic and non-haemolytic phospholipases C PlcH and PlcN, which are substrates of the T2SS (Bleves et al., 2010). The T3SS substrates ExoS and ExoU are mutually exclusive and predominantly found in invasive and cytotoxic *P. aeruginosa* strains, respectively (Bleves et al., 2010). Strain Carb01 63 contains an *exoS* gene (locus tag YQ19_07370), whilst an *exoU* gene (locus tag YH69_22740) was found in strain S04 90.

Comparison of the nucleotide sequences of the chromosomes of Carb01 63 and S04 90 revealed 99% identity with query coverage Carb01 63/S04 90 of 88% and S04 90/Carb01 63 of 92% and only minor differences in size and GC content (**Table 2**). Based on the dendrogram generated by genomic BLAST[5], these sequences are quite distinct (**Supplementary Figure S1**). Carb01 63 belongs to a large clade of 152 leaves which is represented by P17_North_West_14_VIM_2_03_10, whilst S04 90 belongs to a clade of 34 leaves which is represented by the lineage of 468_PAER. Both clades contain related strains of medical origin mostly from the United Kingdom and France. Schematic representations of both genomes and of some well-described *P. aeruginosa* genomes were made by progressive Mauve (Darling et al., 2010) to indicate the similarities and differences (**Supplementary Figure S2**).

TABLE 2 | Characteristics of the chromosomes of Carb01 63 and S04 90 and pS04 90.

Characteristics	*P. aeruginosa* Carb01 63	*P. aeruginosa* S04 90	Plasmid pS04 90
Genome size (bp)	7,497,593	7,099,963	159,187
GC (%)	65.60	66.01	57.73
Genome coverage	98x	97x	97x
No. genes	7071	6889	160
Coding sequences	6986	6720	160
rRNAs	12 (5S, 16S, 23S)	12 (5S, 16S, 23S)	0
tRNAs	65	65	0
Non-coding RNAs	8	1	0
Pseudo genes	76	91	-
CRISPR/Cas systems	0	0	1 (putative)
MLST type	ST111	ST446	-
O-antigen	O12	O11	-
Phages (questionable)	9 (4)	11 (4)	0

Characteristics of the Integrons in Strains Carb01 63 and S04 90

Outbreak strains in the Rotterdam area were reported to contain a bla_{VIM-2} gene on an integron (Van der Bij et al., 2011). Consistently, bla_{VIM-2}-containing class 1 integrons were found in the genome sequences of strains Carb01 63 and S04 90 and they were designated In1163 and In1025, respectively (**Figure 1**). In Carb01 63, the integron was found on the chromosome, whilst it was present on the plasmid in S04 90. The sequences of integrons In1025 and ln1163 are closely related (**Figure 1**) and very similar but not identical to that of In59 (Poirel et al., 2001). Small differences were observed in the gene cassette promoter *Pc* and in the *aacA* genes flanking bla_{VIM-2} and conferring aminoglycoside resistance (**Figure 1**). Differences in the *Pc* promoter affect promoter strength and, because the *Pc* promoter is located within the *intI1* coding sequence, also the integron-excision activity of the encoded integrase (Jové et al., 2010). Whilst In1025 contains two *aacA29b* genes, these genes are replaced by *aacA29e* genes in In1163 (**Figure 1**). With respect to the *aacA29* genes, both strains are also different from other analyzed outbreak strains in the Rotterdam area, which were all (n = 25) reported to contain *aacA29a* and *aacA29b* genes upstream and downstream of the bla_{VIM-2} gene, respectively (Van der Bij et al., 2012). The *aacA29e* genes in In1163 are different from previously described *aacA* genes and their products differ from those of the *aacA29b* genes by a single F41L amino-acid substitution. Although the function of the newly found *aacA29e* genes on the integron of Carb01 63 was not determined, *aacA29a* and *-29b* are known to cause decreased susceptibility to amikacin and to tobramycin, but not to gentamicin (Poirel et al., 2001).

Besides the bla_{VIM-2}-containing integron, Carb01 63 contains a second class 1 integron, designated In99, containing a bla_{CARB-2} gene (**Figure 1**). The bla_{CARB-2} gene is flanked by an *aacA4′-8* gene [a.k.a. *aac(6′)-Ib*] encoding an aminoglycoside 6′-*N*-acetyltransferase and an *aadA2* gene encoding an aminoglycoside-3′′-adenylyltransferase, which is associated with resistance to streptomycin and spectinomycin. Class 1 integrons with such cassette composition were previously described in *P. aeruginosa* isolates from Portugal (Caetano et al., 2007).

[5]http://www.ncbi.nlm.nih.gov/genome/187

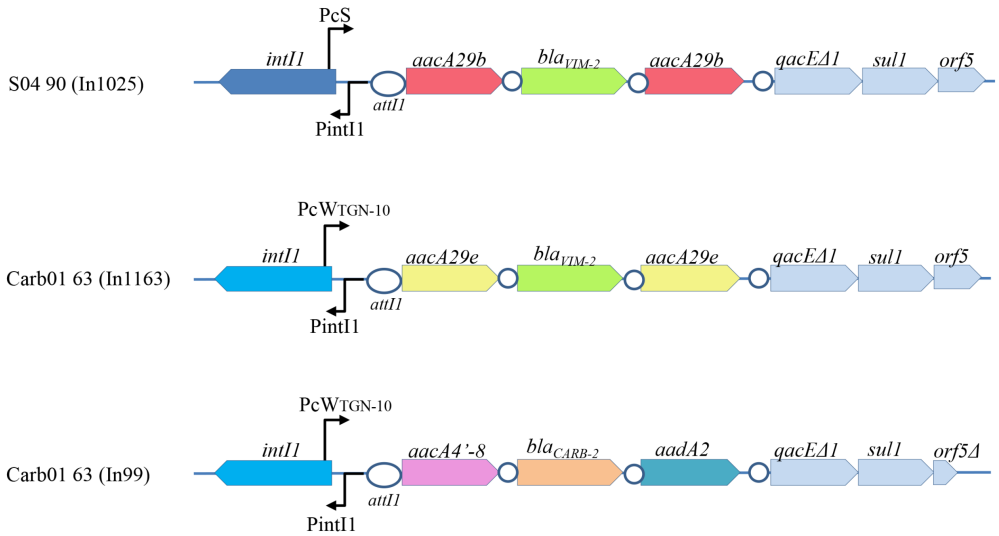

FIGURE 1 | Schematic representation of the integrons of Carb01 63 and S04 90. The gene cassette promoters (Pc) are different. PcS represents a strong promoter, whereas PcW_{TGN-10} represents a promoter that is considerably weaker due to nucleotide substitutions in the –10 and –35 regions, which are, however, partially compensated by a C to G substitution upstream of the –10 region, resulting in an extended –10 motif (Jové et al., 2010). These differences also affect the primary structures of the integrases encoded by the *intI1* genes (dark and bright blue). Cassettes with the same nucleotide sequences are indicated with the same color. No differences were observed in the 3′ conserved sequences, except that *orf5* in In99 is truncated. The integration sites *attI1* and *attC* are indicated by ovals and circles, respectively.

Genetic Context of the bla_{VIM-2} Containing Integrons

In spite of the different genomic location of the bla_{VIM-2}-containing integrons in Carb01 63 and S04 90, i.e., on the chromosome and on a plasmid, respectively, they are both located on a ∼30-kb DNA fragment with very high sequence similarity between the strains. On the 159,187-bp plasmid pS04 90, this segment covers nucleotides 129,245–159,187 plus 1–20 (**Figure 2**). The integron is contained in a Tn*402* transposon (Gillings, 2017) that is bounded by 25-nt inverted repeats (IR) (**Figure 2A**). This transposon is immobilized as the *tni* transposition module is incomplete with *tniQ* and *tniC* genes being absent. The Tn*402* transposon is inserted into a Tn*21*-like transposon between two open reading frames, designated *tnpM* (locus tag YH69_34320) and a truncated *urf2* (locus tag YH69_34365). Presumably, these two open reading frames are derived from a single gene, designated *urf2M* that was split by the Tn*402* insertion (Liebert et al., 1999). Insertion resulted in a 5-nt (5′-TCCAT-3′) duplication of the target site. The Tn*21*-like transposon contains several genes involved in conferring mercury resistance but the locus is incomplete as the essential *merP*, *merT*, and *merR* genes are deleted (**Figure 2A**). This deletion also covers the IRR of the Tn*21* transposon, which is, therefore, immobilized. The Tn*21*-like transposon is contained within a severely disrupted Tn*4661* transposon the remnants of which are an intact 47-nt IRL, the 5′ end of the *tnpA* gene encoding the transposase, and an incomplete IRR that covers only 20 of the 47 nt of a complete IRR (**Figure 2A**). Also inserted in this transposon is a complete Tn*4661* (**Figure 2A**), which has >99% sequence identity with Tn*4661* of *P. aeruginosa* plasmid RMS148 (Yano et al., 2013). Tn*4661* is often found inserted in chromosomes of *P. aeruginosa*, e.g., one copy is found on the chromosome of S04 90, whilst strain S86968 (Genbank accession number CP008865.2) contains two copies. In plasmid pS04 90, this transposon contains an IS*222* insertion element of 1237 bp, containing two overlapping ORFs encoding InsE and the transposase InsM that is generated by translational frameshifting at an $(A)_6G$ site (Kropinski et al., 1994) (**Figure 2A**). This element is inserted with a 3-nt target site duplication (5′-TAC-3′) into codon 11 of the *tnpA* transposase gene of the Tn*4661* transposon and, probably, prevents expression of this gene. The inserted complete Tn*4661* is separated from the *merA* gene of Tn*21* by a 332-bp element that is bounded by 29-nt perfect inverted repeats (5′-GTTGTGGGATGCAAATAAAGTTTCATCCT-3′). Since three copies of this element are found at different positions in the chromosome of strain Carb01 63, it might be a replicative transposable element, but it does not contain a discernible transposase gene. Probably, it represents a hitherto undescribed miniature inverted-repeat transposable element (MITE), which are non-autonomous mobile elements found in both eukaryotes and prokaryotes (Delihas, 2008). The entire 30-kb composite transposon extending from the IRL to the incomplete IRR of the disrupted Tn*4661* transposon is inserted into a plasmid with a core that shows high similarity with the 117-kb plasmid pND6-2 from *Pseudomonas putida* (Li et al., 2013) with a query coverage and sequence identity of 78 and 95%, respectively (**Figure 2B**). The transposon is inserted into a gene corresponding to *orf042* of the pND6-2 plasmid encoding a large hypothetical protein (Li et al., 2013). Consequently, this gene is split into two pseudogenes with locus tags YH69_34300 and YH69_ 33605 on

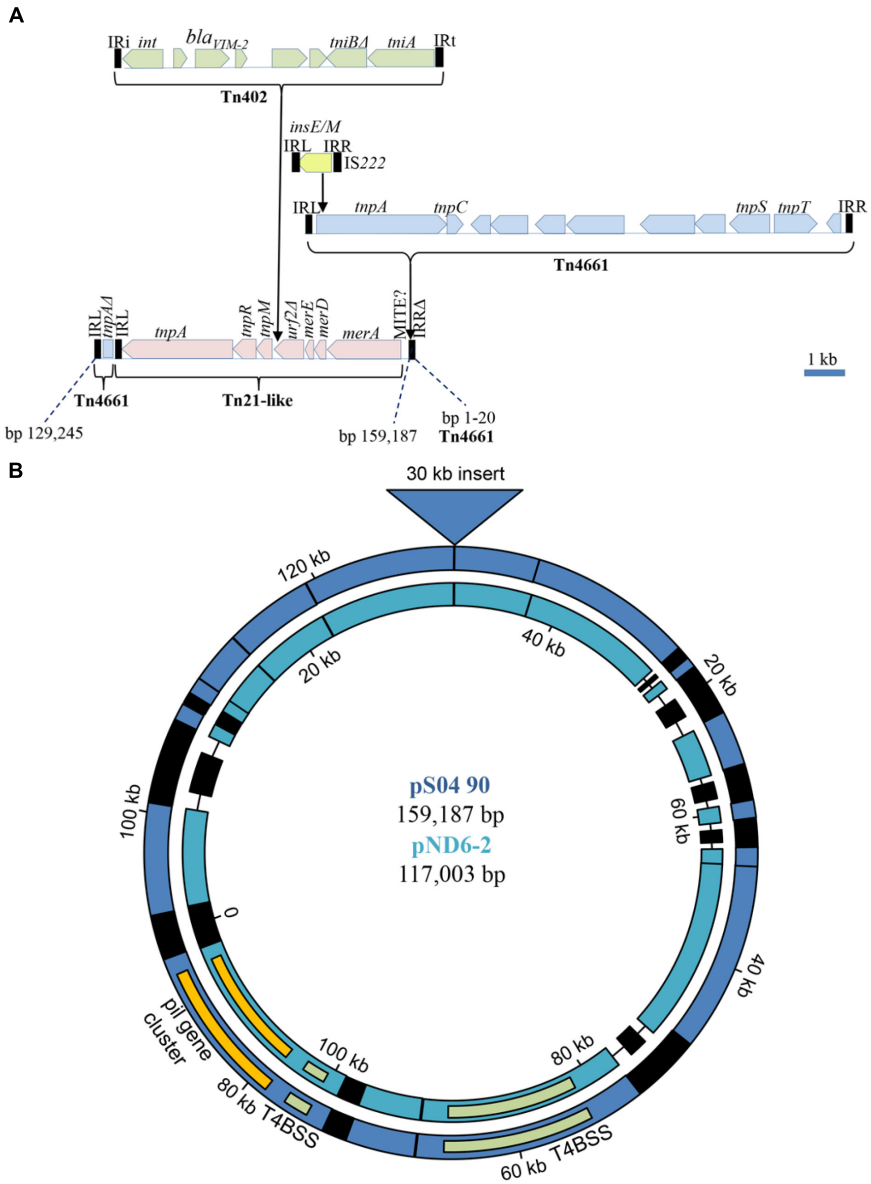

FIGURE 2 | Genetic context of the bla_{VIM-2} containing integron on pS04 90. **(A)** Composition of a mosaic 30 kb transposon containing the integron with the bla_{VIM-2} gene. Open reading frames of different transposable elements are indicated by different colors. MITE?, 332-bp inserted element possibly representing a MITE. **(B)** Comparison of pS04 90 (blue) with pND6-2 (sea-green). Regions of homology are indicated by color. Non-homologous regions are black and deletions are indicated by a line. The positions of the *pil* gene cluster (yellow) and the genes involved in the type IVB secretion system (T4BSS) (green) are indicated in both plasmids. The large insertion, detailed in **(A)**, is indicated by a triangle at the top. The dissimilar regions (black) around 20, 90, and 105 kb in pS04 90, encode, amongst others, a toxin/antitoxin addiction module, an *O*-antigen transacetylase OafA, and CRISPR-related proteins, respectively. Most of the proteins putatively encoded by the dissimilar regions are hypothetical proteins and several transposases/integrases.

pS04 90, and the insertion resulted in a target site duplication of five nucleotides (5′-TGTTC-3′).

In strain Carb01 63, the complete 30-kb fragment described above, except for the inserted IS*222* element and the incomplete IRR of the disrupted Tn*4661*, is present on the chromosome (nt 3,707,795–3,736,497). The IS*222* element is found on six other chromosomal sites in the Carb01 63 chromosome. As the *tnpA* gene of the complete Tn*4661* is not disrupted, an active transposase can be produced and the entire 30-kb element may constitute an active composite transposon extending from the IRL of the disrupted Tn*4661* to the IRR of the complete Tn*4661*. Insertion of this composite transposon into the Carb01 63 chromosome, has split a gene putatively encoding a MOSC domain-containing molybdenum cofactor sulfurase into two pseudogenes, one of which (the 5′ end) was not annotated and the other (the 3′ end) was annotated with locus tag YQ19_17550. Insertion resulted in a 5-nt (5′-ATGGA-3′) duplication of the target site. Thus, it can be inferred that the complete composite

transposon, including the integron with bla_{VIM-2}, was acquired by transposition.

pS04 90 Is a Conjugative Plasmid

pND6-2 is a conjugative plasmid that was reported to mobilize a co-resident plasmid from *P. putida* to *Escherichia coli* (Li et al., 2013). Like pND6-2, pS04 90 carries genes encoding an *icm*/*dot* type IVB secretion system and type IV pili, suggesting it might also be a conjugative plasmid (**Figure 2B**). To investigate whether indeed pS04 90 is transferrable, a conjugation experiment was performed using a FOS-resistant derivative of strain PAO1 as the recipient. After conjugation, seven colonies that were resistant to both MER and FOS were further analyzed. These seven strains, which were all positive for bla_{VIM-2} in PCR analysis, were genotyped by AFLP. Two strains showed a similar AFLP profile as PAO1 (see **Supplementary Figure S3** for an example) and are therefore regarded as transconjugants. The other five strains resembled the AFLP profile of S04 90 (data not shown) and are, therefore, presumably spontaneous FOS-resistant mutants of this isolate. FOS-resistant strain PAO1 and both transconjugants were analyzed by VITEK, which confirmed the susceptibility of the PAO1 strain to most antibiotics tested and multidrug resistance of the transconjugants (**Table 1**). Repeated attempts to transfer the plasmid to *E. coli*, either by conjugation or by electroporation, failed indicating that it has a narrow host range.

Genetic Context of the bla_{CARB-2}-Containing Integron

The In*99* integron with the bla_{CARB-2} gene (**Figure 1**) is contained in a severely disrupted Tn*402* transposon that is bounded by 25-nt inverted repeats (**Figure 3A**). This transposon lacks the entire *tni* transposition module. The *orf5* gene of the integron is disrupted by the insertion of an IS*6100* element (**Figure 3A**). The defective Tn*402* is inserted in a Tn*5051*-like transposon, which, apart from the insertion of the Tn*402* and of the IS*1071* element described below, shows high sequence similarity with other Tn*5051*-like transposons, such as Tn*AO22* from *Achromobacter* sp. AO22 (Ng et al., 2009) with only 15 single-nucleotide polymorphisms (SNPs) over an 8230-bp sequence. Like in the Tn*21* transposon described above, the Tn*402* is inserted in the *urf2M* gene but more toward the 3′ end of the gene, i.e., at a position identical to a previously reported integron-insertion site in Tn*5051* (Toleman et al., 2003). Insertion resulted in a 5-nt (5′-GAGTC-3′) duplication of the target site. The genes that are essential for mercury resistance, i.e., *merR*, *merT*, *merP*, and *merA*, are complete in the Tn*5051* transposon, and they have indeed been shown to confer mercury resistance in the case of Tn*AO22* (Ng et al., 2009). The *tnpA* gene of the Tn*5051* transposon is truncated by the insertion of an IS*1071* element (**Figure 3A**), which probably renders the Tn*5051* TnpA inactive. The Tn*5051* is bounded by 38-nt inverted repeats and inserted into a gene encoding a hypothetical protein with a DUF4158 domain that is thereby split into two pseudogenes with locus tags YQ19_26565 and YQ19_26485. Insertion resulted in a 5-nt (5′-CTCAA-3′) target site duplication. This disrupted gene is situated within an integrative and conjugative element (ICE), which is integrated in a tRNA-*gly* gene (locus tag YQ19_26215). This 89,494-bp ICE is flanked by two 20-bp direct repeats, corresponding to the 3′ end of the tRNA-*gly* gene and representing the *attL* and *attR* sites (**Figure 3B**). With only very few SNPs, the core composition of the ICE is almost identical to that of the *P. aeruginosa* genomic island PAGI-16 of strain KMU11, but the cassette composition of the integron of this Korean ST235 isolate is different (Hong et al., 2016).

Mutational Resistome

Besides by the acquisition of genes by horizontal gene transfer, antibiotic susceptibility can be decreased by mutations in the core genome, together constituting the mutational resistome (Lopéz-Causapé et al., 2018). Several mutations are present in the core genome of strains Carb01 63 and S04 90 that likely contribute to the observed resistance phenotypes. The porin OprD mediates the diffusion of carbapenems across the outer membrane, and disruption of the *oprD* gene or downregulation of its expression represents an important carbapenem-resistance mechanism (Pirnay et al., 2002; Lister et al., 2009; Ruiz-Martínez et al., 2011; Cabot et al., 2016). In strain Carb01 63, the *oprD* gene (locus tag YQ19_24920) is disrupted by an 11-bp deletion leading to a frame-shift. This mutation likely contributes to the high level of resistance of the strain to carbapenems. In strain S04 90, the *oprD* gene contains nine mutations leading to amino-acid substitutions relative to OprD of strain PAO1. This variant is identical to variant T1-IV described previously (Ocampo-Sosa et al., 2012), which is not associated with resistance to carbapenems. In strain S04 90, but not in Carb01 63, the *mexZ* gene (locus tag YH69_17355) is disrupted by a frameshift mutation. Inactivation of MexZ leads to overproduction of the MexXY components of the MexXY-OprM efflux pump and is associated with increased resistance to aminoglycosides, fluoroquinolones, and zwitterionic cephalosporins, such as cefepime, amongst others (Guénard et al., 2014). Both strains carry missense mutations leading to a T83I amino-acid substitution in the GyrA protein and an S87L substitution in ParC, which are associated with resistance to fluoroquinolones (Kos et al., 2015). These mutations explain the observed resistance of the strains to ciprofloxacin (**Table 1**).

DISCUSSION

The two *P. aeruginosa* strains analyzed here belong to two MBL-producing clones that are endemic in Dutch hospitals (Van der Bij et al., 2011). Carb01 63 is a representative of the most prevalent clone. The spread of this ST111 clone among various hospitals in The Netherlands has been demonstrated (Van der Bij et al., 2012), and this type caused the first outbreak (Van der Bij et al., 2011). Carb01 63, which was isolated from drains and sinks in the Maasstad hospital, is closely related to the recently sequenced strain RIVM-EMC2982 (accession number CP016955.1), a patient isolate from the Erasmus University Medical Center in Rotterdam. Carb01 63

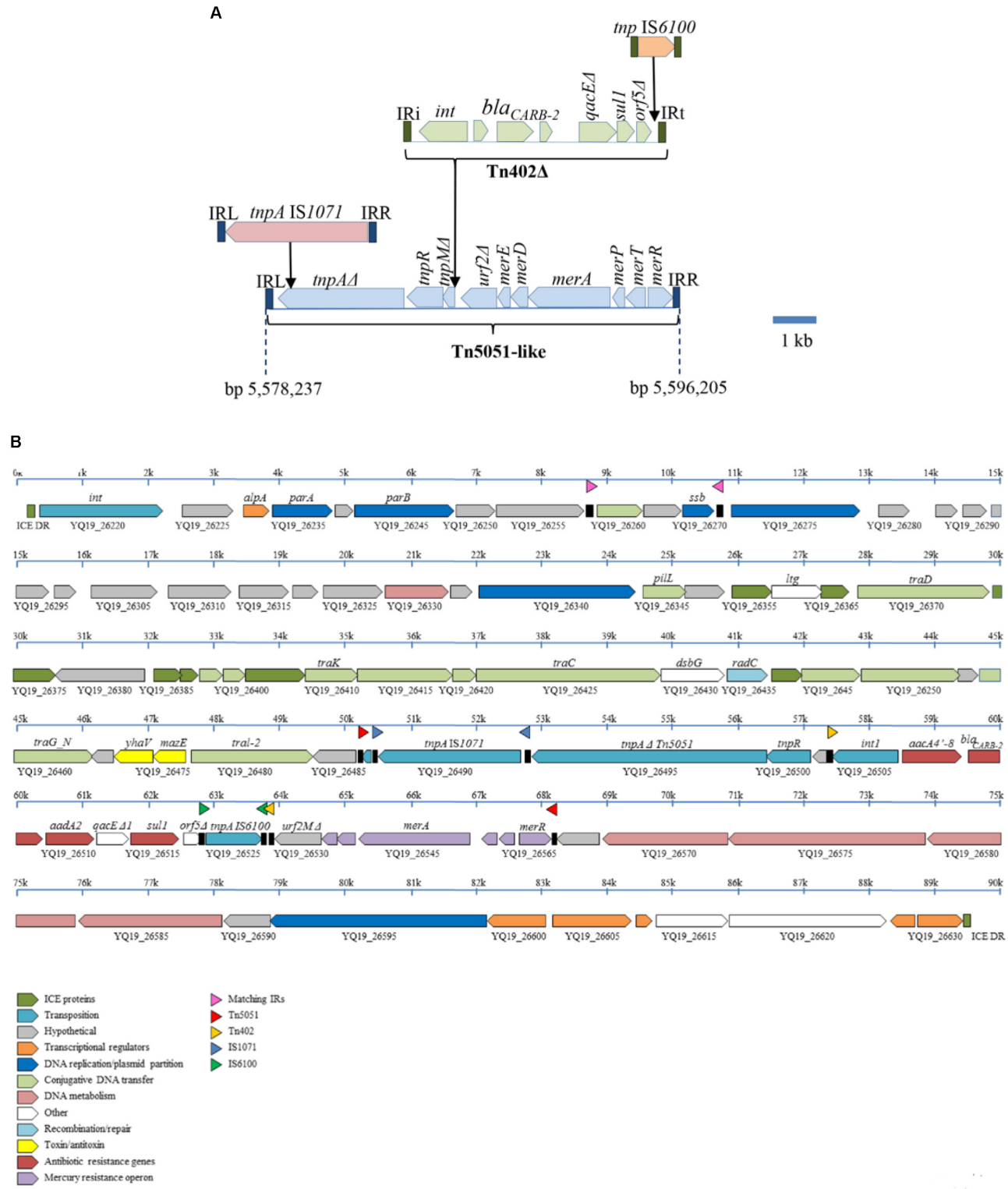

FIGURE 3 | Genetic context of the bla_{CARB-2}-containing integron in Carb01 63. **(A)** Composition of a mosaic 18-kb transposon containing the integron with the bla_{CARB-2} gene. Open reading frames of different transposable elements are indicated by different colors. **(B)** Composition of the ICE into which the composite transposon depicted in **(A)** is inserted. The ICE is bounded by 20-bp direct repeats (ICE DR). ORFs encoding proteins of different functional classes are indicated by different colors as outlined in the inset at the bottom. Inverted repeats are indicated by black boxes in between the ORFs with a colored triangle above.

is also closely related to previously described outbreak strains of the same ST111 and O12 antigen, reported in hospitals in the United Kingdom (Breathnach et al., 2012; Witney et al., 2014; Turton et al., 2015). The most closely related neighbors of strain S04 90 are two clinical ST446 isolates from France, strains AZPAE15043 (Kos et al., 2015) and WH-SGI-V-07172 (van Belkum et al., 2015), which are susceptible to carbapenems.

Both strains are resistant to many antibiotics, and the presence of bla_{VIM-2} and other resistance genes was demonstrated. The presence of bla_{VIM-2} genes in *P. aeruginosa* isolates has been repeatedly described, but how these genes spread among strains is usually not clear because, apart from the cassette composition of the class 1 integrons in which they are located, their genetic context is often not described. In *P. aeruginosa*, bla_{VIM-2}-containing integrons are usually associated with the chromosome as was found in strain Carb01 63, but it is present on a plasmid in strain S04 90. Although plasmid-associated bla_{VIM-2} genes have occasionally been reported before (Poirel et al., 2000; Edelstein et al., 2013; Wright et al., 2015), only in a single case the gene was shown to be present on a conjugative plasmid (Botelho et al., 2017). We have experimentally demonstrated that also pS04 90 is a conjugative plasmid. The plasmid shows high similarity to pND6-2, a previously described plasmid from *P. putida* strain ND6 that was suggested to belong to a new plasmid incompatibility (Inc) group (Li et al., 2013). Nucleotide BLAST searches showed that pS04 90 has high sequence similarity to pND6-2 also in the DNA fragment containing the *oriV* and the *repB* gene, suggesting that pS04 90 belongs to this same new Inc group. DNA segments with high sequence similarity to the plasmid backbone were also found on contigs of several other incomplete *P. aeruginosa* genome sequences (see **Supplementary Figure S4** for an example), indicating that the plasmid is more commonly found in this species. As compared with pND6-2, pS04 90 has acquired a large DNA fragment of ∼30 kb that contains the integron with the bla_{VIM-2} gene. Interestingly, the bla_{VIM-2}-containing integron is located on a very similar DNA fragment on the chromosome of strain Carb01 63 that, apart from the absence of the IS*222* element and the incomplete IRR of the severely disrupted Tn*4661*, deviates from the DNA fragment of pS04 90 in the presence of only 42 SNPs over the entire 29,963 nt sequence. Also the closely related strain RIVM-EMC2982 contains this DNA fragment on the chromosome in the same position as in Carb01 63, and it is even more closely related to that on pS04 90 with only 5 SNPs besides the absence of the IS*222* element and the incomplete IRR. Thus, it appears that the entire ∼30-kb DNA fragment can move position between plasmid and chromosome as a novel, composite transposon, and, in view of the very high sequence identity of these transposons, this could have occurred only very recently. Since pS04 90 is a conjugative plasmid, this illustrates how MBL-encoding integrons can be mobilized and transferred between strains. Interestingly, the entire composite transposon also appears to be present in a *P. aeruginosa* isolate of Czech origin, i.e., strain Pae-31448cz (Papagiannitsis et al., 2017). However, the severely disrupted Tn*4661*, although present in the available nucleotide sequence (Genbank accession number KY860571.1), was not noticed and, therefore, the possibility that entire fragment could function as a composite mobile element was not considered.

Besides the bla_{VIM-2}-containing integron, strain Carb01 63 contains an additional class 1 integron containing *aacA4*, bla_{CARB-2}, and *aadA2* gene cassettes. The integron is located on a composite transposon that is integrated into an ICE. Apart from the cassette composition of the integron, this ICE is very similar to PAGI-16 in the Korean isolate KMU11 (Hong et al., 2016), probably reflecting a common origin of these genomic islands. The presence of the island in strains of different sequence types, i.e., ST111 and ST235 for Carb01 63 and KMU11, respectively, suggests that it may be transferred between strains. Interestingly, in strain RIVM-EMC2982, which is highly related to Carb01 63, the ICE is split into two parts located at different chromosomal positions and each associated with an IS*6100* element. Similarly, PAGI-16 has been reported to be split into two parts in Korean strain BP14 by a large chromosomal inversion resulting from duplication and insertion of the IS*6100* element (Hong et al., 2016). A similar recombination event apparently occurred in strain RIVM-EMC2982, where it disrupted the *oprD* gene, which encodes a porin mediating transport of carbapenems across the outer membrane.

In our hospitals, MBL-producing clones of ST111 are persistent in sinks and drains despite treatment with 10% hypochlorite, and they are spreading to different departments. These unpublished findings oppose previous results that showed successful reduction of extensively drug-resistant strains from these systems (Witney et al., 2014). Further studies into the resistance of the strains to disinfectants will be facilitated by the available genome sequences. The *P. aeruginosa* strains studied are susceptible only to colistin treatment. Recent discovery of widespread colistin resistance in bacteria urges to keep alert of possible colistin resistance of already extensively drug-resistant *Pseudomonas*, which is a major concern for hospitals, since no option is available for adequate disinfection of drains and sinks, while colonization, infection and outbreaks via these routes are difficult to control.

CONCLUSION

The genome sequences of two multidrug-resistant *P. aeruginosa* strains endemic in Dutch hospitals revealed the presence of a novel, large, composite transposon that carries a class 1 integron with a bla_{VIM-2} gene and aminoglycoside-resistance genes. This transposon can apparently move position between chromosome and a conjugative plasmid, with which it can be transferred to other *P. aeruginosa* strains. Besides, the genome sequences revealed other mobile resistance genes and mutations in the core genome that contribute to the multidrug-resistance phenotype.

AUTHOR CONTRIBUTIONS

AZ, JO, and WG initiated the study. WK and AB performed the experimental work. WP performed the whole genome sequencing

and assembly. WK, AZ, and JT performed the bioinformatic analysis and drafted the manuscript. All authors read and approved the final manuscript.

ACKNOWLEDGMENTS

The authors would like to thank Ria van Boxtel for assistance in some of the experiments. Strain PAO1 was kindly provided by Gilles Vergnaud and Christine Pourcel, Université Paris-Sud, Orsay, France.

SUPPLEMENTARY MATERIAL

The Supplementary Material for this article can be found online at: https://www.frontiersin.org/articles/10.3389/fmicb.2018.02057/full#supplementary-material

REFERENCES

Aziz, R. K., Bartels, D., Best, A. A., DeJongh, M., Disz, T., Edwards, R. A., et al. (2008). The RAST server: rapid annotations using subsystems technology. *BMC Genomics* 9:75. doi: 10.1186/1471-2164-9-75

Battle, S. E., Rello, J., and Hauser, A. R. (2009). Genomic islands of *Pseudomonas aeruginosa*. *FEMS Microbiol. Lett.* 290, 70–78. doi: 10.1111/j.1574-6968.2008.01406.x

Bleves, S., Viarre, V., Salacha, R., Michel, G. P. F., Filloux, A., and Voulhoux, R. (2010). Protein secretion systems in *Pseudomonas aeruginosa*: a wealth of pathogenic weapons. *Int. J. Med. Microbiol.* 300, 534–543. doi: 10.1016/j.ijmm.2010.08.005

Boetzer, M., and Pirovano, W. (2012). Toward almost closed genomes with GapFiller. *Genome Biol.* 13:R56. doi: 10.1186/gb-2012-13-6-r56

Boetzer, M., and Pirovano, W. (2014). SSPACE-LongRead: scaffolding bacterial draft genomes using long read sequence information. *BMC Bioinformatics* 15:211. doi: 10.1186/1471-2105-15-211

Botelho, J., Grosso, F., Quinteira, S., Mabrouk, A., and Peixe, L. (2017). The complete nucleotide sequence of an IncP-2 megaplasmid unveils a mosaic architecture comprising a putative novel *bla*VIM-2-harbouring transposon in *Pseudomonas aeruginosa*. *J. Antimicrob. Chemother.* 72, 2225–2229. doi: 10.1093/jac/dkx143

Breathnach, A. S., Cubbon, M. D., Karunaharan, R. N., Pope, C. F., and Planche, T. D. (2012). Multidrug-resistant *Pseudomonas aeruginosa* outbreaks in two hospitals: association with contaminated hospital waste-water systems. *J. Hosp. Infect.* 82, 19–24. doi: 10.1016/j.jhin.2012.06.007

Cabot, G., López-Causapé, C., Ocampo-Sosa, A. A., Sommer, L. M., Angeles Domínguez, M., Zamorano, L., et al. (2016). Deciphering the resistome of the widespread *Pseudomonas aeruginosa* sequence type 175 international high-risk clone through whole-genome sequencing. *Antimicrob. Agents Chemother.* 60, 7415–7423. doi: 10.1128/AAC.01720-16

Caetano, T., Ferreira, S., Mondego, A. P., Correia, A., and Mendo, S. (2007). In99, an In100-related integron, its occurrence and prevalence in clinical *Pseudomonas aeruginosa* strains from a central region of Portugal. *Epidemiol. Infect.* 135, 502–504. doi: 10.1017/S095026880600700X

Chikhi, R., and Medvedev, P. (2014). Informed and automated k-mer size selection for genome assembly. *Bioinformatics* 30, 31–37. doi: 10.1093/bioinformatics/btt310

Darling, A. E., Mau, B., and Perna, N. T. (2010). progressiveMauve: multiple genome alignment with gene gain, loss and rearrangement. *PLoS One* 5:e11147. doi: 10.1371/journal.pone.0011147

Delihas, N. (2008). Small mobile sequences in bacteria display diverse structure/function motifs. *Mol. Microbiol.* 67, 475–481. doi: 10.1111/j.1365-2958.2007.06068.x

Edelstein, M. V., Skleenova, E. N., Shevchenko, O. V., D'souza, J. W., Tapalski, D. V., Azizov, I. S., et al. (2013). Spread of extensively resistant VIM-2-positive ST235 *Pseudomonas aeruginosa* in Belarus, Kazakhstan, and Russia: a longitudinal epidemiological and clinical study. *Lancet Infect. Dis.* 13, 867–876. doi: 10.1016/S1473-3099(13)70168-3

Gillings, M. R. (2017). Class 1 integrons as invasive species. *Curr. Opin. Microbiol.* 38, 10–15. doi: 10.1016/j.mib.2017.03.002

Grissa, I., Vergnaud, G., and Pourcel, C. (2007). CRISPRFinder: a web tool to identify clustered regularly interspaced short palindromic repeats. *Nucleic Acids Res.* 35, W52–W57. doi: 10.1093/nar/gkm360

Guénard, S., Muller, C., Monlezun, L., Benas, P., Broutin, I., Jeannot, K., et al. (2014). Multiple mutations lead to MexXY-OprM-dependent aminoglycoside resistance in clinical strains of *Pseudomonas aeruginosa*. *Antimicrob. Agents Chemother.* 58, 221–228. doi: 10.1128/AAC.01252-13

Holloway, B. W. (1955). Genetic recombination in *Pseudomonas aeruginosa*. *J. Gen. Microbiol.* 13, 572–581. doi: 10.1099/00221287-13-3-572

Hong, J. S., Yoon, E. J., Lee, H., Jeong, S. H., and Lee, K. (2016). Clonal dissemination of *Pseudomonas aeruginosa* sequence type 235 isolates carrying blaIMP-6 and emergence of blaGES-24 and blaIMP-10 on novel genomic islands PAGI-15 and PAGI-16 in South Korea. *Antimicrob. Agents Chemother.* 60, 7216–7223. doi: 10.1128/AAC.01601-16

Jové, T., Da Re, S., Denis, F., Mazel, D., and Ploy, M. C. (2010). Inverse correlation between promoter strength and excision activity in class 1 integrons. *PLoS Genet.* 6:e1000793. doi: 10.1371/journal.pgen.1000793

Kerr, K. G., and Snelling, A. M. (2009). *Pseudomonas aeruginosa*: a formidable and ever-present adversary. *J. Hosp. Infect.* 73, 338–344. doi: 10.1016/j.jhin.2009.04.020

Kidd, T. J., Ritchie, S. R., Ramsay, K. A., Grimwood, K., Bell, S. C., and Rainey, P. B. (2012). *Pseudomonas aeruginosa* exhibits frequent recombination, but only a limited association between genotype and ecological setting. *PLoS One* 7:e44199. doi: 10.1371/journal.pone.0044199

Kos, V. N., Déraspe, M., McLaughlin, R. E., Whiteaker, J. D., Roy, P. H., Alm, R. A., et al. (2015). The resistome of *Pseudomonas aeruginosa* in relationship to phenotypic susceptibility. *Antimicrob. Agents Chemother.* 59, 427–436. doi: 10.1128/AAC.03954-14

Kropinski, A. M., Farinha, M. A., and Jansons, I. (1994). Nucleotide sequence of the *Pseudomonas aeruginosa* insertion sequence IS222: another member of the IS3 family. *Plasmid* 31, 222–228. doi: 10.1006/plas.1994.1024

Lee, D. G., Urbach, J. M., Wu, G., Liberati, N. T., Feinbaum, R. L., Miyata, S., et al. (2006). Genomic analysis reveals that *Pseudomonas aeruginosa* virulence is combinatorial. *Genome Biol.* 7:R90. doi: 10.1186/gb-2006-7-10-r90

Li, S., Zhao, H., Li, Y., Niu, S., and Cai, B. (2013). Complete nucleotide sequence of plasmid pND6-2 from *Pseudomonas putida* ND6 and characterization of conjugative genes. *Gene* 512, 148–156. doi: 10.1016/j.gene.2012.09.065

Liebert, C. A., Hall, R. M., and Summers, A. O. (1999). Transposon Tn21, flagship of the floating genome. *Microbiol. Mol. Biol. Rev.* 63, 507–522.

Lister, P. D., Wolter, D. J., and Hanson, N. D. (2009). Antibacterial-resistant *Pseudomonas aeruginosa*: clinical impact and complex regulation of chromosomally encoded resistance mechanisms. *Clin. Microbiol. Rev.* 22, 582–610. doi: 10.1128/CMR.00040-09

Lopéz-Causapé, C., Cabot, G., del Barrio-Tofiño, E., and Oliver, A. (2018). The versatile mutational resistome of *Pseudomonas aeruginosa*. *Front. Microbiol.* 9:685. doi: 10.3389/fmicb.2018.00685

Ng, S. P., Davis, B., Palombo, E. A., and Bhave, M. (2009). A Tn5051-like mer-containing transposon identified in a heavy metal tolerant strain *Achromobacter* sp. *AO22*. *BMC Res. Notes* 2:38. doi: 10.1186/1756-0500-2-38

Ocampo-Sosa, A. A., Cabot, G., Rodríguez, C., Roman, E., Tubau, F., Macia, M. D., et al. (2012). Alterations of OprD in carbapenem-intermediate and -susceptible strains of *Pseudomonas aeruginosa* isolated from patients with bacteremia in a Spanish multicenter study. *Antimicrob. Agents Chemother.* 56, 1703–1713. doi: 10.1128/AAC.05451-11

Oliver, A., Mulet, X., López-Causapé, C., and Juan, C. (2015). The increasing threat of *Pseudomonas aeruginosa* high-risk clones. *Drug Resist. Updat.* 2, 41–59. doi: 10.1016/j.drup.2015.08.002

Papagiannitsis, C. C., Medvecky, M., Chudejova, K., Skalova, A., Rotova, V., Spanelova, P., et al. (2017). Molecular characterization of carbapenemase-producing *Pseudomonas aeruginosa* of Czech origin and evidence for clonal spread of extensively resistant sequence type 357 expressing IMP-7 metallo-β-lactamase. *Antimicrob. Agents Chemother.* 61, e1811–e1817. doi: 10.1128/AAC.01811-17

Pirnay, J. P., De Vos, D., Mossialos, D., Vanderkelen, A., Cornelis, P., and Zizi, M. (2002). Analysis of the *Pseudomonas aeruginosa* oprD gene from clinical and environmental isolates. *Environ. Microbiol.* 4, 872–882. doi: 10.1046/j.1462-2920.2002.00281.x

Poirel, L., Lambert, T., Türkoglü, S., Ronco, E., Gaillard, J., and Nordmann, P. (2001). Characterization of class 1 integrons from *Pseudomonas aeruginosa* that contain the bla_{VIM-2} carbapenem-hydrolyzing β-lactamase gene and of two novel aminoglycoside resistance gene cassettes. *Antimicrob. Agents Chemother.* 45, 546–552. doi: 10.1128/AAC.45.2.546-552.2001

Poirel, L., Naas, T., Nicolas, D., Collet, L., Bellais, S., Cavallo, J. D., et al. (2000). Characterization of VIM-2, a carbepenem-hydrolyzing metallo-ß-lactamase and its plasmid- and integron-borne gene from a *Pseudomonas aeruginosa* clinical isolate in France. *Antimicrob. Agents Chemother.* 44, 891–897. doi: 10.1128/AAC.44.4.891-897.2000

Roberts, R. J., Vincze, T., Posfai, J., and Macelis, D. (2015). REBASE–a database for DNA restriction and modification: enzymes, genes and genomes. *Nucleic Acids Res.* 43, D298–D299. doi: 10.1093/nar/gku1046

Ruiz-Martínez, L., Lopéz-Jiménez, L., d'Ostuni, V., Fusté, E., Vinuesa, T., and Viñas, M. (2011). A mechanism of carbapenem resistance due to a new insertion element (ISPa133) in *Pseudomonas aeruginosa*. *Int. Microbiol.* 14, 51–58. doi: 10.2436/20.1501.01.135

Siguier, P., Perochon, J., Lestrade, L., Mahillon, J., and Chandler, M. (2006). ISfinder: the reference centre for bacterial insertion sequences. *Nucleic Acids Res.* 34, D32–D36. doi: 10.1093/nar/gkj014

Silby, M. W., Winstanley, C., Godfrey, S. A. C., Levy, S. B., and Jackson, R. W. (2011). *Pseudomonas* genomes: diverse and adaptable. *FEMS Microbiol. Rev.* 35, 652–680. doi: 10.1111/j.1574-6976.2011.00269.x

Thrane, S. W., Taylor, V. L., Freschi, L., Kukavica-Ibrulj, I., Boyle, B., Laroche, J., et al. (2015). The widespread multidrug-resistant serotype O12 *Pseudomonas aeruginosa* clone emerged through concomitant horizontal transfer of serotype antigen and antibiotic resistance gene clusters. *mBio* 6:e01396-15. doi: 10.1128/mBio.01396-15

Toleman, M. A., Biedenbach, D., Bennett, D., Jones, R. N., and Walsh, T. R. (2003). Genetic characterization of a novel metallo-β-lactamase gene, blaIMP13, harboured by a novel Tn5051-type transposon disseminating carbapenemase genes in Europe: report from the SENTRY worldwide antimicrobial surveillance programme. *J. Antimicrob. Chemother.* 52, 583–590. doi: 10.1093/jac/dkg410

Turton, J. F., Wright, L., Underwood, A., Witney, A. A., Chan, Y. T., Al-Shahib, A., et al. (2015). High-resolution analysis by whole-genome sequencing of an international lineage (sequence type 111) of *Pseudomonas aeruginosa* associated with metallo-carbapenemases in the United Kingdom. *J. Clin. Microbiol.* 53, 2622–2631. doi: 10.1128/JCM.00505-15

van Belkum, A., Soriaga, L. B., LaFave, M. C., Akella, S., Veyrieras, J. B., Barbu, E. M., et al. (2015). Phylogenetic distribution of CRISPR-Cas systems in antibiotic-resistant *Pseudomonas aeruginosa*. *mBio* 6:e01796-15. doi: 10.1128/mBio.01796-15

Van der Bij, A. K., Van der Zwan, D., Peirano, G., Severin, J. A., Pitout, J. D. D., Van Westreenen, M., et al. (2012). Metallo-β-lactamase-producing *Pseudomonas aeruginosa* in the Netherlands: the nationwide emergence of a single sequence type. *Clin. Microbiol. Infect.* 18, E369–E372. doi: 10.1111/j.1469-0691.2012.03969.x

Van der Bij, A. K., Van Mansfeld, R., Peirano, G., Goessens, W. H. F., Severin, J. A., Pitout, J. D., et al. (2011). First outbreak of VIM-2 metallo-β-lactamase-producing *Pseudomonas aeruginosa* in The Netherlands: microbiology, epidemiology and clinical outcomes. *Int. J. Antimicrob. Agents* 37, 513–518. doi: 10.1016/j.ijantimicag.2011.02.010

Van der Zee, A., Roorda, L., Bosman, G., and Ossewaarde, J. M. (2014). Screening rectal swabs for carbapenemase genes. *J. Clin. Microbiol.* 52, 4401–4403. doi: 10.1128/JCM.02256-14

Van der Zee, A., Steer, N., Thijssen, E., Nelson, J., van't Veen, A., and Buiting, A. (2003). Use of multienzyme multiplex PCR amplified fragment length polymorphism typing in analysis of outbreaks of multiresistant *Klebsiella pneumoniae* in an intensive care unit. *J. Clin. Microb.* 41, 798–802. doi: 10.1128/JCM.41.2.798-802.2003

Witney, A. A., Gould, K. A., Pope, C. F., Bolt, F., Stoker, N. G., Cubbon, M. D., et al. (2014). Genome sequencing and characterization of an extensively drug-resistant sequence type 111 serotype O12 hospital outbreak strain of *Pseudomonas aeruginosa*. *Clin. Microbiol. Infect.* 20, O609–O618. doi: 10.1111/1469-0691.12528

Wright, L. L., Turton, J. F., Livermore, D. M., Hopkins, K. L., and Woodford, N. (2015). Dominance of international 'high-risk clones' among metallo-β-lactamase-producing *Pseudomonas aeruginosa* in the UK. *J. Antimicrob. Chemother.* 70, 103–110. doi: 10.1093/jac/dku339

Yano, H., Genka, H., Ohtsubo, Y., Nagata, Y., Top, E. M., and Tsuda, M. (2013). Cointegrate-resolution of toluene-catabolic transposon Tn4651: determination of crossover site and the segment required for full resolution activity. *Plasmid* 69, 24–35. doi: 10.1016/j.plasmid.2012.07.004

Zhou, Y., Liang, Y., Lynch, K., Dennis, J. J., and Wishart, D. S. (2011). PHAST: a fast phage search tool. *Nucleic Acids Res.* 39, W347–W352. doi: 10.1093/nar/gkr485

Conflict of Interest Statement: The authors declare that the research was conducted in the absence of any commercial or financial relationships that could be construed as a potential conflict of interest.

frontiers in Microbiology

MINI REVIEW
published: 06 September 2018
doi: 10.3389/fmicb.2018.02154

Pull in and Push Out: Mechanisms of Horizontal Gene Transfer in Bacteria

*Dongchang Sun**

College of Biotechnology and Bioengineering, Zhejiang University of Technology, Hangzhou, China

Horizontal gene transfer (HGT) plays an important role in bacterial evolution. It is well accepted that DNA is pulled/pushed into recipient cells by conserved membrane-associated DNA transport systems, which allow the entry of only single-stranded DNA (ssDNA). However, recent studies have uncovered a new type of natural bacterial transformation in which double-stranded DNA (dsDNA) is taken up into the cytoplasm, thus complementing the existing methods of DNA transfer among bacteria. Regulated by the stationary-phase regulators RpoS and cAMP receptor protein (CRP), *Escherichia coli* establishes competence for natural transformation with dsDNA, which occurs in agar plates. To pass across the outer membrane, a putative channel, which may compete for the substrate with the porin OmpA, may mediate the transfer of exogenous dsDNA into the cell. To pass across the inner membrane, dsDNA may be bound to the periplasmic protein YdcS, which delivers it into the inner membrane channel formed by YdcV. The discovery of cell-to-cell contact-dependent plasmid transformation implies the presence of additional mechanism(s) of transformation. This review will summarize the current knowledge about mechanisms of HGT with an emphasis on recent progresses regarding non-canonical mechanisms of natural transformation. Fully understanding the mechanisms of HGT will provide a foundation for monitoring and controlling multidrug resistance.

Keywords: antibiotic resistance gene, multidrug resistance, DNA transfer, natural transformation, conjugation, *Escherichia coli*

OPEN ACCESS

Edited by:
Peter Mullany,
University College London,
United Kingdom

Reviewed by:
Baltasar Mayo,
Consejo Superior de Investigaciones Científicas (CSIC), Spain
Victor Krylov,
I. I. Mechnikov Research Institute of Vaccines and Sera (RAS), Russia
J. Tony Pembroke,
University of Limerick, Ireland

***Correspondence:**
Dongchang Sun
sundch@zjut.edu.cn

Specialty section:
This article was submitted to Antimicrobials, Resistance and Chemotherapy, a section of the journal Frontiers in Microbiology

Received: *23 March 2018*
Accepted: *22 August 2018*
Published: *06 September 2018*

Citation:
Sun D (2018) Pull in and Push Out: Mechanisms of Horizontal Gene Transfer in Bacteria. Front. Microbiol. 9:2154. doi: 10.3389/fmicb.2018.02154

INTRODUCTION

Horizontal gene transfer (HGT) drives the evolution of bacteria. Transfer of antibiotic resistance genes (ARGs) plays an important role in the development of multidrug resistance (MDR) in bacteria (Forsberg et al., 2012). There are three "classical" methods of DNA transfer in nature: bacterial conjugation, natural transformation, and transduction (von Wintersdorff et al., 2016). Via HGT, exogenous DNA can be transferred from one bacterium to another even if they are only distantly related (Chen et al., 2005; Burton and Dubnau, 2010). With the accumulation of genes involved in different resistance mechanisms from the exogenous DNA, bacteria are able to acquire MDR rapidly. For example, *Acinetobacter* and *Enterobacter* strains carrying the NDM-1 plasmid or *mcr-1* plasmid, which contain a group of resistance genes, can tolerate even last-resort antibiotics (Yong et al., 2009; Wang and Sun, 2015; Liu et al., 2016; Shen et al., 2016; Zheng et al., 2017). Understanding the mechanisms of DNA transfer in bacteria would provide new strategies to help address the ongoing challenge of multi-drug-resistant bacteria in the future.

Natural bacterial transformation and conjugation have been found in bacteria and archaea. Two different membrane protein complexes consisting of conserved proteins are responsible for pulling in and pushing out DNA during natural bacterial transformation and conjugation, respectively (Chen and Dubnau, 2004; Claverys et al., 2009; Burton and Dubnau, 2010; Johnston et al., 2014; Cabezon et al., 2015; Ilangovan et al., 2015, 2017). These DNA transport systems deliver single-stranded DNA (ssDNA) either from the donor cell (for conjugation) or into the recipient cell (for transformation) (Chen and Dubnau, 2004; Claverys et al., 2009; Burton and Dubnau, 2010; Johnston et al., 2014; Cabezon et al., 2015; Ilangovan et al., 2015, 2017). Recent studies have revealed two new types of DNA transfer in *Escherichia coli*. One of these methods has been shown to be independent of the conserved proteins for the transport of ssDNA during natural transformation or bacterial conjugation. Instead, double-stranded DNA (dsDNA) is taken up into the cytoplasm and internalized by *E. coli* cells on solid agar plates (Sun et al., 2006, 2009, 2013; Sun, 2011, 2016; Zhang et al., 2012). The other method of DNA transfer is dependent on cell-to-cell contact and DNA transfer occurs within a colony on agar plates (Maeda et al., 2004, 2006; Etchuuya et al., 2011; Sobue et al., 2011; Kurono et al., 2012; Matsuda et al., 2012; Matsumoto et al., 2016). DNA transfer via this method is sensitive to DNase I, indicating that DNA that is transported into the recipient cell is naked (rather than protein-protected). Although DNA transfer occurs on agar plates via both of the above two transformation methods, no evidence shows similarities between DNA transfer mechanisms of the two methods. In the former transformation method, DNA transfer occurs in the absence of donor cells. Whereas, in the latter transformation method, donor cells are required for DNA transfer in the colony. During bacterial conjugation, physical contact between the donor and the recipient cells is required. Nonetheless, the cell-to-cell contact-dependent plasmid transformation is different from conjugation in that DNA transfer is not mediated by mobile elements (Maeda et al., 2004; Kurono et al., 2012; Matsuda et al., 2012). In this review, we will first discuss the mechanisms of classical natural bacterial transformation and conjugation. Then, the non-canonical DNA transfer on agar plates will be described in detail, with an emphasis on how DNA is pulled into cells.

PULL DNA IN DURING NATURAL TRANSFORMATION

Natural transformation was discovered in *Streptococcus pneumoniae* in 1928 (Griffith, 1928). Induced by a heptadecapeptide pheromone, naturally transformable bacteria show a special physiological state termed "competence", during which they are capable of pulling in exogenous DNA (Berka et al., 2002; Ogura et al., 2002). The mechanism of DNA transfer during natural transformation is well conserved among Gram-positive (G^+) (e.g., *Bacillus subtilis* and *S. pneumoniae*) and Gram-negative (G^-) bacterial species (e.g., *Neisseria gonorrhoeae*, *Haemophilus influenzae*, and *Vibrio cholerae*), as well as archaea (Chen and Dubnau, 2004; Claverys et al., 2009; Burton and Dubnau, 2010; Johnston et al., 2014; Cabezon et al., 2015; Ilangovan et al., 2015, 2017; Veening and Blokesch, 2017). Although conditions for competence induction vary widely among bacterial species (Aas et al., 2002; Berka et al., 2002; Claverys et al., 2006; Veening and Blokesch, 2017), proteins involved in DNA uptake are highly conserved even among distantly related bacteria (Johnston et al., 2014), except for *Helicobacter pylori*, which uses a conjugation-like system for DNA uptake during natural transformation (Smeets and Kusters, 2002). Here, the conserved DNA uptake system in bacteria is described.

G^- bacteria have an outer membrane (OM), whereas G^+ bacteria have not. During natural transformation, G^- bacteria need to pull DNA across both the OM and the inner membrane (IM), whereas G^+ bacteria need to overcome the barrier of the peptidoglycan layer, which is much thicker and denser, and needs to be weakened before translocation of DNA across the IM. In this process, dsDNA is pulled across the OM in G^- bacteria and ssDNA is pulled across the IM in both G^+ and G^- bacteria. The general mechanism underlying DNA transfer during natural transformation is summarized in **Figure 1**.

Crossing the OM

For G^- bacteria, a sophisticated protein complex is assembled in the OM, where the complex binds exogenous DNA and drags it into the periplasm (**Figure 1**). The assembly and

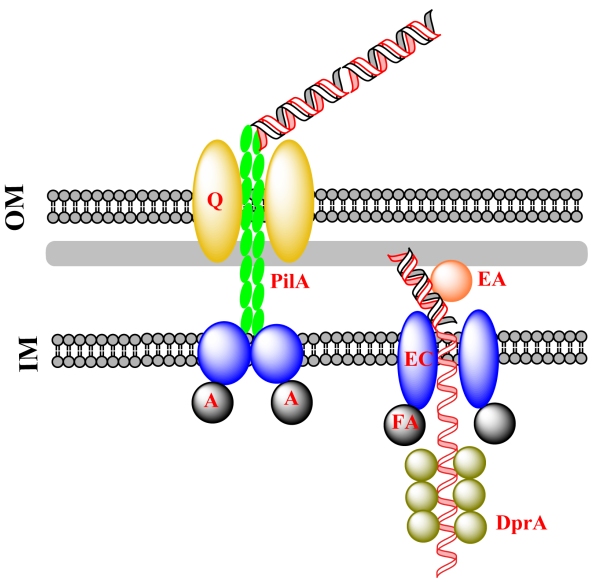

FIGURE 1 | Classical DNA uptake during natural transformation. Exogenous DNA is pulled into the cytoplasm by the extension and retraction of pseudopili, as a consequence of the assembly and disassembly of pseudopilin multimers (PilA). This is followed by the transfer of dsDNA across the OM protein PilQ/HofQ (for G^- bacteria only). The DNA receptor (ComEA) mediates the transfer of one strand of DNA across the IM channel formed by ComEC with the assistance of the ATPase ComFA, accompanied by degradation of the other strand of DNA. The incoming ssDNA is protected by DprA which conveys it to RecA for homologous recombination in the cytoplasm.

disassembly of a type IV pilus causes a fiber-like pseudopilus to be extruded out of and hauled back into the pore-forming OM proteins (Chen and Dubnau, 2004). The pore that accommodates exogenous DNA is 6–6.5 nm in diameter, and is formed by PilQ, a secretin that is 15 nm wide and 34 nm long with five rings and an extraordinary stable "cone" and "cup" structures (Chen and Dubnau, 2004). The pore cavity is large enough to accommodate dsDNA (∼2.4 nm) (Collins et al., 2001; Assalkhou et al., 2007; Burkhardt et al., 2011). Accompanied by the extension and retraction of type IV pili, DNA is transported across the OM through the pore (Laurenceau et al., 2013; Salzer et al., 2014, 2016; Leong et al., 2017). Between the OM and IM (the periplasm), the incoming DNA is bound by the substrate-binding protein ComEA, which prevents DNA from slipping by means of a "Brownian Ratcheting" mechanism (Inamine and Dubnau, 1995; Provvedi and Dubnau, 1999; Berge et al., 2002; Takeno et al., 2012; Seitz et al., 2014; Salzer et al., 2016).

Crossing the IM

Bound by ComEA in the periplasm, exogenous DNA is translocated across the IM via a pore formed by ComEC, also named Rec2 in some G^- bacteria (e.g., *H. influenzae*), a widely conserved IM protein for translocation of DNA across the IM (Barouki and Smith, 1985; Berge et al., 2002; Draskovic and Dubnau, 2005; Sinha et al., 2012; Baker et al., 2016; Salzer et al., 2016). It has been proposed that ComEC acts as both a translocase and nuclease during DNA translocation (Chen and Dubnau, 2004; Claverys et al., 2009; Burton and Dubnau, 2010; Johnston et al., 2014; Veening and Blokesch, 2017). In this process, one strand of the dsDNA is translocated into the cytoplasm, simultaneously the degradation of the other strand occurs (Barouki and Smith, 1985; Berge et al., 2002; Baker et al., 2016). *In silico* analysis of ComEC indicates that the β-lactamase-like domain at the C-terminus may function as a nuclease and Domain of Unknown function 4131 at the N-terminus has a DNA binding domain (Baker et al., 2016). It is possible that the dsDNA that is bound to the N-terminus of ComEC is divided into two strands of ssDNA and one of them is degraded by the nuclease at the C-terminus.

The channel for DNA translocation is assumed to be formed by two ComEC monomers with seven transmembrane segments (Draskovic and Dubnau, 2005). Given that over-expression of ComEC is toxic to the cell, the structure of ComEC remains unresolved (Draskovic and Dubnau, 2005). The driving force for translocation of ssDNA across the IM may be provided by an ATPase (ComFA), which is also widely conserved in bacteria (Londono-Vallejo and Dubnau, 1994; Takeno et al., 2011; Chilton et al., 2017; Diallo et al., 2017). After translocation of ssDNA, DprA, and RecA bind ssDNA and catalyze the formation of joint DNA molecules for homologous recombination (Mortier-Barriere et al., 2007; Dwivedi et al., 2013; Yadav et al., 2013, 2014; Duffin and Barber, 2016; Diallo et al., 2017; Hovland et al., 2017; Le et al., 2017). In this way, the incoming foreign ssDNA displaces one strand of the chromosomal dsDNA (Mortier-Barriere et al., 2007), followed by being converted to homogeneous dsDNA through DNA replication.

THE TRANSFER OF DNA DURING BACTERIAL CONJUGATION

Bacterial conjugation was first discovered in *E. coli* (Lederberg and Tatum, 1946). Relying on cell-to-cell contact, DNA can be pushed out of a donor cell and transported into a recipient cell during bacterial conjugation. A group of modular mobile genetic elements, known as integrative and conjugative elements (ICEs) or conjugative transposons (Franke and Clewell, 1981), has been found in many bacterial genomes (Wozniak and Waldor, 2010; Bi et al., 2012; Cury et al., 2017). ICEs can transfer from one bacterium to another, facilitating the spread of ARGs in environment (Wozniak and Waldor, 2010; Bi et al., 2012; Cury et al., 2017). The transfer of conjugative DNA across the membrane of the donor bacterium relies on a large membrane-associated protein complex, that belongs to the type IV secretion system (T4SS) (Goessweiner-Mohr et al., 2013; Cabezon et al., 2015; Ilangovan et al., 2015; **Figure 2**). Components of the T4SS for conjugation are encoded by genes of either self-replicable conjugative plasmids or ICEs in the chromosomal DNA of the donor bacterium (Cabezon et al., 2015; Ilangovan et al., 2015; Johnson and Grossman, 2015). The mechanism of DNA transfer is summarized in **Figure 2**.

Protein-coated conjugative ssDNA is transported across the IM, periplasm and OM through a membrane channel formed by a group of proteins encoded by the conjugative DNA molecule (Goessweiner-Mohr et al., 2013; Cabezon et al., 2015; Ilangovan et al., 2015). Inside the channel, the conjugative pilus (formed by pilins) is responsible for pushing ssDNA out of membrane. The mechanism of DNA transfer via conjugation has been best exemplified by the Vir system. To export DNA out of the donor cell, a conjugative plasmid encodes a complicated membrane protein complex. During conjugation, a plasmid- or ICE-encoded relaxase creates a nick in one strand of the conjugative DNA at the *oriT* site, followed by ssDNA translocation across the channel formed by components of the T4SS and replication of the remaining strand, either independently from or in concert with conjugation (Ilangovan et al., 2017). During translocation across cell membranes, three ATPases (VirD4, VirB4, and VirB11) provide the energy for DNA transport (Chen et al., 2005; Cabezon et al., 2015; Ilangovan et al., 2015). In natural transformation and conjugation, different types of pili participate in the movement of DNA. Competence pili or pseudopili mediate the transfer of dsDNA across the membrane during natural transformation, whereas conjugative pili mediates the transfer of ssDNA across the membrane during conjugation (Cabezon et al., 2015; Ilangovan et al., 2015). In both cases, the assembly/disassembly of pili drives the movement of transferring DNA. It remains unclear how conjugative DNA is further transported in the recipient cell.

THE UPTAKE OF dsDNA IN *E. coli*

E. coli has long been thought not to be naturally transformable. In this century, the natural transformation of *E. coli* has been observed initially on nutrient-deficient agar plates and later

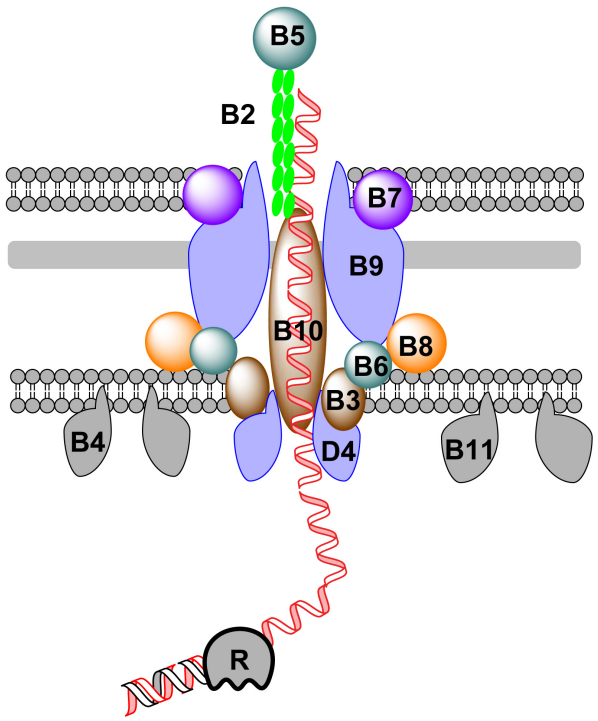

FIGURE 2 | DNA transfer during bacterial conjugation. Conjugative DNA is processed into ssDNA by a relaxase (R) in the cytoplasm of the donor bacterium. To further transport ssDNA, a group of membrane and periplasmic proteins are assembled together to form a large complex, which can be subdivided into four distinct parts: (1) the pilus is formed by the assembly of pilins (VirB2) with adhesins (VirB5) at the distal end; (2) the OM component, which consists of VirB7, VirB9, and the C-terminus of VirB10; (3) the periplasmic component which consists of VirB8, VirB10, and VirB6; and (4) the IM component, formed of VirB3, VirB6, VirB8, and VirB10. Additionally, three hexameric ATPases (VirB4, VirB11, and VirD4) are attached to the IM to provide energy during DNA transfer.

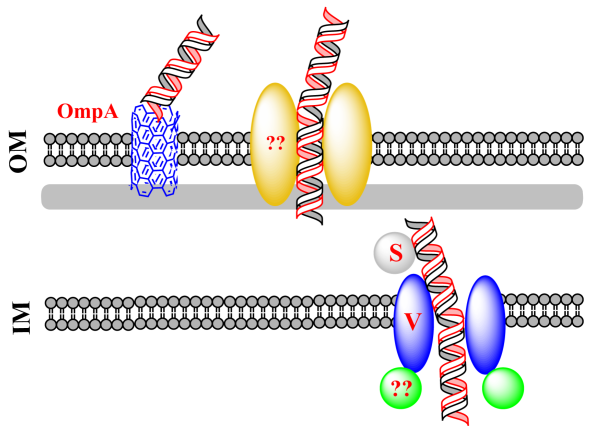

FIGURE 3 | A new route for dsDNA transfer in *Escherichia coli*. Via an unidentified channel, exogenous DNA transfers across the OM. The pore-forming protein OmpA can compete for DNA with the unidentified channel. To pass across the IM, the incoming DNA binds the substrate-binding protein YdcS and is translocated from the periplasm to the cytoplasm via an IM channel formed by YdcV. It remains unclear whether a plasmid enters *E. coli* as intact circular or linear dsDNA.

on nutrient-rich agar plates (Tsen et al., 2002; Sun et al., 2006). Although natural plasmid transformation of *E. coli* shows single-hit kinetics, implying that dsDNA may enter the cell (Sun et al., 2009), there are basic differences between natural and chemical transformation. First, natural transformation is promoted by an increased concentration of agar, whereas chemical transformation relies on high concentrations of divalent ions (i.e., Ca^{2+}, Mg^{2+}, or Mn^{2+}) (Sun et al., 2009). However, the stimulating effect of agar on transformation is not due to an increase in Ca^{2+}, Mg^{2+}, or Mn^{2+} concentration (Sun et al., 2009). It remains unclear whether osmotic pressure and/or any other biological/physical factor(s) contribute to the increase of transformation on plates with a high concentration of agar. Second, an OM protein, OmpA, plays opposite roles in natural and chemical transformation of *E. coli*: it promotes chemical transformation but suppresses natural transformation (Sun et al., 2013). Third, exponentially growing *E. coli* cells are often employed for preparing chemically competent cells with the highest efficiency, and chemical transformation occurs in a liquid, whereas the natural transformation of stationary-phase *E. coli* cells is regulated by the transcriptional regulator RpoS and the cyclic AMP (cAMP) – cAMP receptor protein (CRP), and these cells can acquire exogenous DNA exclusively on agar plates (Zhang et al., 2012; Guo et al., 2015). The functions of RpoS or the cAMP-CRP complex in the chemical transformation of *E. coli* have not been found.

Natural transformation of *E. coli* also differs from that of other naturally transformable bacteria in that the conserved DNA uptake machinery is not required for the uptake of exogenous dsDNA in *E. coli* (Sun et al., 2009). Some components of the conserved DNA uptake machinery are believed to function in using DNA as a nutrient in *E. coli* (Finkel and Kolter, 2001; Palchevskiy and Finkel, 2006). Nevertheless, attempts to confirm these observations in three independent laboratories have not succeeded (Sun, 2011; Johnston et al., 2014). DNA, which has been thought to serve as the sole carbon source could not account for cell growth, implying that other nutrient sources should be present in the culture (Sun, 2011; Johnston et al., 2014). It is possible that degraded DNA in the minimal culture serves as a source of building blocks for the synthesis of new DNA in bacteria. During the natural transformation of *E. coli*, new ABC transporter proteins have been shown to participate in DNA transfer (Sun et al., 2009; Sun, 2016). These transporters are different from the known classical DNA uptake proteins that mediate natural bacterial transformation. The mechanism of this new type of DNA transfer is proposed in **Figure 3**.

Crossing the OM

Escherichia coli has a complete set of genes that potentially encode components of the classical DNA uptake machinery. These genes are homologous to the conserved DNA uptake genes in other naturally transformable bacteria. Comparative genomic analysis predicts that, in *E. coli*, putative DNA uptake genes *hofQ* and *gspD*

may encode proteins forming a channel for transporting DNA across the OM, and *ppdD* may encode pilins for the assembly of the competence pili or pseudopili which pull exogenous DNA in (Finkel and Kolter, 2001; Claverys and Martin, 2003; Sun et al., 2009). However, inactivation of *hofQ*, *gspD*, or *ppdD* does not affect natural transformation with dsDNA, suggesting that the conserved DNA uptake machinery for translocation of ssDNA does not mediate dsDNA transfer across the OM in *E. coli* (Sun et al., 2009). To identify the OM pore used for DNA transport during natural transformation of *E. coli*, the pore-forming protein OmpA was evaluated, considering that OmpA performs functions in bacteriophage infection and bacterial conjugation. Inactivation of *ompA* increases natural transformation by 7- to 60-fold while decreasing chemical transformation by ∼10-fold, suggesting that OmpA blocks DNA transfer during natural transformation but promotes DNA transfer in artificial transformation (Sun et al., 2013). OmpA is unlikely to form an open gate under natural conditions, but can be switched to the open state with the molecular force of electrostatic interaction (i.e., salt-bridge), that drives structural transition of a protein under different conditions (Hong et al., 2006). The closed and open states of the gate are dependent on the formation of salt bridges of Arg138-Glu52 and Lys82-Glu128, respectively (Hong et al., 2006). During natural transformation of *E. coli*, DNA may pass across an unidentified channel that competes with OmpA for transforming DNA. The putative channel may be consisted of OM components (i.e., OM protein and pili/psedopili) of a DNA transport system and pulls DNA into the cell on the LB-agar plate. In the default "gate-closed" state, OmpA traps the transforming DNA, making it unable to reach the right channel for completing transformation. By contrast, during chemical transformation or electroporation, a high concentration of Ca^{2+} or an electric current helps open the gate, allowing DNA to pass across the channel formed by OmpA (Sun et al., 2013).

Crossing the IM

Based on a membrane topology study, the conserved IM protein called ComEC is predicted to mediate the translocation of ssDNA during classical natural transformation (Chen and Dubnau, 2004; Claverys et al., 2009; Johnston et al., 2014). However, inactivation of the ComEC homolog YcaI in *E. coli* does not affect natural plasmid transformation of *E. coli*, suggesting that DNA is translocated into the cytoplasm via a different route (Sun et al., 2009). The single-hit kinetics in natural plasmid transformation of *E. coli* suggest that the establishment of a plasmid in the cytoplasm is mediated not by the annealing of partially overlapping opposite ssDNA derived from two independent plasmid monomers, but by a new route, i.e., the transfer of dsDNA across the IM of bacteria (Sun et al., 2009). Screening of RpoS-targeted transformation-related genes has identified *ydcS* and *ydcV*, which are located in the same ABC-transporter operon (Sun, 2016). Inactivation of *ydcS* and *ydcV* reduces natural transformation 6.7- and 9.5-fold, respectively (Sun, 2016). Chemical transformation is also reduced by Inactivation of *ydcS*, whereas the chemical transformation in a *ydcV* mutant is not reduced as compared to its wild-type counterpart (Sun, 2016). According to the Transporter Classification Database (TCDB[1]), *ydcS* and *ydcV* are predicted to encode proteins for binding a substrate in the periplasm and for translocation of the substrate across IM (Saier et al., 2014). YdcS has been shown as a PHB synthase in the periplasm (Dai and Reusch, 2008). The mutant lacking *ydcT* (a putative ATPase encoding gene) in the same operon as *ydcS* and *ydcV*, is naturally transformed with slightly but obviously reduced frequency (less than 50%) (Sun, 2016), indicating that this gene is also involved in natural plasmid transformation of *E. coli*. Nonetheless, with respect to significantly reduced transformation frequency in the *ydcV* and the *ydcS* mutants, *ydcT* seems to have only a minor effect on DNA transport. It is likely that additional energy source is required for efficient transport of dsDNA across the IM.

CELL-TO-CELL TRANSFER OF NON-CONJUGATIVE PLASMIDS

Cell-to-cell contact is often required for bacterial conjugation. Of note, plasmid transformation of *E. coli* in colonies proceeds on the surface of agar plates and cell-to-cell contact is required for the transfer of plasmids that do not carry conjugative functions (Maeda et al., 2004, 2006). Cell-to-cell contact-dependent plasmid transformation occurs not only within the same genus but also across genera (Wang et al., 2007). In some naturally transformable G^- bacteria (e.g., *H. influenzae* and *N. gonorrhoeae*), a short DNA sequence (named DUS) can increase DNA uptake (Claverys and Martin, 2003; Wang and Sun, 2015; Zheng et al., 2017). During cell-to-cell contact-dependent plasmid transformation of *E. coli*, an 88 bp DNA sequence promotes DNA transfer (Sobue et al., 2011). Screening of the Keio collection (Baba et al., 2006), a comprehensive library of *E. coli* knock-out mutants defective in non-essential genes, has identified *rodZ*, whose product regulates the rod-shape of the cell, as an essential gene for cell-to-cell contact-dependent transformation (Kurono et al., 2012). Because the homologs of DNA uptake genes (e.g., *ycaI*) have not been revealed to be essential genes, conventional DNA uptake machinery is not likely to be involved in cell-to-cell contact-dependent plasmid transformation of *E. coli*. Recently, cell-to-cell contact-dependent transformation is discovered in *B. subtilis* (Zhang et al., 2018). However, inactivation of the competence regulator ComK, that controls the expression of conserved DNA uptake genes, abolishes cell-to-cell DNA transfer (Zhang et al., 2018), indicating that mechanisms of the cell-to-cell DNA transfer in *E. coli* and *B. subtilis* are basically different.

CONCLUDING REMARKS

Classical mechanisms of HGT (i.e., natural transformation and conjugation) share common features in that ssDNA is pushed out

[1]http://www.tcdb.org

or pulled into the cell with the assistance of membrane-associated protein complexes. Recent studies have uncovered new types of DNA transfer, which are independent of the classical DNA uptake or conjugation machineries, suggesting that other therapeutic targets should be considered in the fight against ARGs. The conserved proteins involved in transporting or protecting DNA may serve as targets for limiting the transfer of ARGs and in turn for reducing MDR in bacteria (Goessweiner-Mohr et al., 2013). On the other hand, the discovery of non-classical HGT mechanisms suggests that controlling the spread of ARGs is more complicated than previously thought.

AUTHOR CONTRIBUTIONS

DS conceived the idea and wrote the manuscript.

FUNDING

This research was supported by the National Natural Science Foundation of China (Grant Nos. 31670084, 31100071) and the Zhejiang Provincial Natural Science Foundation of China (Grant Nos. LY16C010003, Y3110237).

REFERENCES

Aas, F. E., Wolfgang, M., Frye, S., Dunham, S., Lovold, C., and Koomey, M. (2002). Competence for natural transformation in *Neisseria gonorrhoeae*: components of DNA binding and uptake linked to type IV pilus expression. *Mol. Microbiol.* 46, 749–760. doi: 10.1046/j.1365-2958.2002.03193.x

Assalkhou, R., Balasingham, S., Collins, R. F., Frye, S. A., Davidsen, T., Benam, A. V., et al. (2007). The outer membrane secretin PilQ from *Neisseria meningitidis* binds DNA. *Microbiology* 153, 1593–1603. doi: 10.1099/mic.0.2006/004200-0

Baba, T., Ara, T., Hasegawa, M., Takai, Y., Okumura, Y., Baba, M., et al. (2006). Construction of *Escherichia coli* K-12 in-frame, single-gene knockout mutants: the Keio collection. *Mol. Syst. Biol.* 2:msb4100050. doi: 10.1038/msb4100050

Baker, J. A., Simkovic, F., Taylor, H. M., and Rigden, D. J. (2016). Potential DNA binding and nuclease functions of ComEC domains characterized in silico. *Proteins* 84, 1431–1442. doi: 10.1002/prot.25088

Barouki, R., and Smith, H. O. (1985). Reexamination of phenotypic defects in rec-1 and rec-2 mutants of *Haemophilus influenzae* Rd. *J. Bacteriol.* 163, 629–634.

Berge, M., Moscoso, M., Prudhomme, M., Martin, B., and Claverys, J. P. (2002). Uptake of transforming DNA in Gram-positive bacteria: a view from *Streptococcus pneumoniae*. *Mol. Microbiol.* 45, 411–421. doi: 10.1046/j.1365-2958.2002.03013.x

Berka, R. M., Hahn, J., Albano, M., Draskovic, I., Persuh, M., Cui, X., et al. (2002). Microarray analysis of the *Bacillus subtilis* K-state: genome-wide expression changes dependent on ComK. *Mol. Microbiol.* 43, 1331–1345. doi: 10.1046/j.1365-2958.2002.02833.x

Bi, D., Xu, Z., Harrison, E. M., Tai, C., Wei, Y., He, X., et al. (2012). ICEberg: a web-based resource for integrative and conjugative elements found in bacteria. *Nucleic Acids Res.* 40, D621–D626. doi: 10.1093/nar/gkr846

Burkhardt, J., Vonck, J., and Averhoff, B. (2011). Structure and function of PilQ, a secretin of the DNA transporter from the thermophilic bacterium *Thermus thermophilus* HB27. *J. Biol. Chem.* 286, 9977–9984. doi: 10.1074/jbc.M110.212688

Burton, B., and Dubnau, D. (2010). Membrane-associated DNA transport machines. *Cold Spring Harb. Perspect. Biol.* 2, a000406. doi: 10.1101/cshperspect.a000406

Cabezon, E., Ripoll-Rozada, J., Pena, A., De La Cruz, F., and Arechaga, I. (2015). Towards an integrated model of bacterial conjugation. *FEMS Microbiol. Rev.* 39, 81–95. doi: 10.1111/1574-6976.12085

Chen, I., Christie, P. J., and Dubnau, D. (2005). The ins and outs of DNA transfer in bacteria. *Science* 310, 1456–1460. doi: 10.1126/science.1114021

Chen, I., and Dubnau, D. (2004). DNA uptake during bacterial transformation. *Nat. Rev. Microbiol.* 2, 241–249. doi: 10.1038/nrmicro844

Chilton, S. S., Falbel, T. G., Hromada, S., and Burton, B. M. (2017). A conserved metal binding motif in the *Bacillus subtilis* vompetence protein ComFA enhances transformation. *J. Bacteriol.* 199:e00272-17. doi: 10.1128/JB.00272-17

Claverys, J. P., and Martin, B. (2003). Bacterial "competence" genes: signatures of active transformation, or only remnants? *Trends. Microbiol.* 11, 161–165. doi: 10.1016/S0966-842X(03)00064-7

Claverys, J. P., Martin, B., and Polard, P. (2009). The genetic transformation machinery: composition, localization, and mechanism. *FEMS Microbiol. Rev.* 33, 643–656. doi: 10.1111/j.1574-6976.2009.00164.x

Claverys, J. P., Prudhomme, M., and Martin, B. (2006). Induction of competence regulons as a general response to stress in gram-positive bacteria. *Annu. Rev. Microbiol.* 60, 451–475. doi: 10.1146/annurev.micro.60.080805.142139

Collins, R. F., Davidsen, L., Derrick, J. P., Ford, R. C., and Tonjum, T. (2001). Analysis of the PilQ secretin from *Neisseria meningitidis* by transmission electron microscopy reveals a dodecameric quaternary structure. *J. Bacteriol.* 183, 3825–3832. doi: 10.1128/JB.183.13.3825-3832.2001

Cury, J., Touchon, M., and Rocha, E. P. C. (2017). Integrative and conjugative elements and their hosts: composition, distribution and organization. *Nucleic Acids Res.* 45, 8943–8956. doi: 10.1093/nar/gkx607

Dai, D., and Reusch, R. N. (2008). Poly-3-hydroxybutyrate synthase from the periplasm of *Escherichia coli*. *Biochem. Biophys. Res. Commun.* 374, 485–489. doi: 10.1016/j.bbrc.2008.07.043

Diallo, A., Foster, H. R., Gromek, K. A., Perry, T. N., Dujeancourt, A., Krasteva, P. V., et al. (2017). Bacterial transformation: ComFA is a DNA-dependent ATPase that forms complexes with ComFC and DprA. *Mol. Microbiol.* 105, 741–754. doi: 10.1111/mmi.13732

Draskovic, I., and Dubnau, D. (2005). Biogenesis of a putative channel protein, ComEC, required for DNA uptake: membrane topology, oligomerization and formation of disulphide bonds. *Mol. Microbiol.* 55, 881–896. doi: 10.1111/j.1365-2958.2004.04430.x

Duffin, P. M., and Barber, D. A. (2016). DprA is required for natural transformation and affects pilin variation in *Neisseria gonorrhoeae*. *Microbiology* 162, 1620–1628. doi: 10.1099/mic.0.000343

Dwivedi, G. R., Sharma, E., and Rao, D. N. (2013). *Helicobacter* pylori DprA alleviates restriction barrier for incoming DNA. *Nucleic. Acids. Res.* 41, 3274–3288. doi: 10.1093/nar/gkt024

Etchuuya, R., Ito, M., Kitano, S., Shigi, F., Sobue, R., and Maeda, S. (2011). Cell-to-cell transformation in *Escherichia coli*: a novel type of natural transformation involving cell-derived DNA and a putative promoting pheromone. *PLoS One* 6:e16355. doi: 10.1371/journal.pone.0016355

Finkel, S. E., and Kolter, R. (2001). DNA as a nutrient: novel role for bacterial competence gene homologs. *J. Bacteriol.* 183, 6288–6293. doi: 10.1128/JB.183.21.6288-6293.2001

Forsberg, K. J., Reyes, A., Wang, B., Selleck, E. M., Sommer, M. O., and Dantas, G. (2012). The shared antibiotic resistome of soil bacteria and human pathogens. *Science* 337, 1107–1111. doi: 10.1126/science.1220761

Franke, A. E., and Clewell, D. B. (1981). Evidence for conjugal transfer of a *Streptococcus faecalis* transposon (Tn916) from a chromosomal site in the absence of plasmid DNA. *Cold Spring Harb. Symp. Quant. Biol.* 45(Pt 1), 77–80. doi: 10.1101/SQB.1981.045.01.014

Goessweiner-Mohr, N., Arends, K., Keller, W., and Grohmann, E. (2013). Conjugative type IV secretion systems in Gram-positive bacteria. *Plasmid* 70, 289–302. doi: 10.1016/j.plasmid.2013.09.005

Griffith, F. (1928). The significance of Pneumococcal types. *J. Hyg.* 27, 113–159. doi: 10.1017/S0022172400031879

Guo, M., Wang, H., Xie, N., and Xie, Z. (2015). Positive effect of carbon sources on natural transformation in *Escherichia coli*: role of low-level cyclic AMP (cAMP)-cAMP receptor protein in the derepression of rpoS. *J. Bacteriol.* 197, 3317–3328. doi: 10.1128/JB.00291-15

Hong, H., Szabo, G., and Tamm, L. K. (2006). Electrostatic couplings in OmpA ion-channel gating suggest a mechanism for pore opening. *Nat. Chem. Biol.* 2, 627–635. doi: 10.1038/nchembio827

Hovland, E., Beyene, G. T., Frye, S. A., Homberset, H., Balasingham, S. V., Gomez-Munoz, M., et al. (2017). DprA from *Neisseria meningitidis*: properties and role in natural competence for transformation. *Microbiology* 163, 1016–1029. doi: 10.1099/mic.0.000489

Ilangovan, A., Connery, S., and Waksman, G. (2015). Structural biology of the gram-negative bacterial conjugation systems. *Trends. Microbiol.* 23, 301–310. doi: 10.1016/j.tim.2015.02.012

Ilangovan, A., Kay, C. W. M., Roier, S., El Mkami, H., Salvadori, E., Zechner, E. L., et al. (2017). Cryo-EM structure of a relaxase reveals the molecular basis of DNA unwinding during bacterial conjugation. *Cell* 169, 708.e12–721.e12. doi: 10.1016/j.cell.2017.04.010

Inamine, G. S., and Dubnau, D. (1995). ComEA, a *Bacillus subtilis* integral membrane protein required for genetic transformation, is needed for both DNA binding and transport. *J. Bacteriol.* 177, 3045–3051. doi: 10.1128/jb.177.11.3045-3051.1995

Johnson, C. M., and Grossman, A. D. (2015). Integrative and conjugative elements (ICEs): what they do and how they work. *Annu. Rev. Genet.* 49, 577–601. doi: 10.1146/annurev-genet-112414-055018

Johnston, C., Martin, B., Fichant, G., Polard, P., and Claverys, J. P. (2014). Bacterial transformation: distribution, shared mechanisms and divergent control. *Nat. Rev. Microbiol.* 12, 181–196. doi: 10.1038/nrmicro3199

Kurono, N., Matsuda, A., Etchuya, R., Sobue, R., Sasaki, Y., Ito, M., et al. (2012). Genome-wide screening of *Escherichia coli* genes involved in execution and promotion of cell-to-cell transfer of non-conjugative plasmids: rodZ (yfgA) is essential for plasmid acceptance in recipient cells. *Biochem. Biophys. Res. Commun.* 421, 119–123. doi: 10.1016/j.bbrc.2012.03.127

Laurenceau, R., Pehau-Arnaudet, G., Baconnais, S., Gault, J., Malosse, C., Dujeancourt, A., et al. (2013). A type IV pilus mediates DNA binding during natural transformation in *Streptococcus pneumoniae*. *PLoS Pathog.* 9:e1003473. doi: 10.1371/journal.ppat.1003473

Le, S., Serrano, E., Kawamura, R., Carrasco, B., Yan, J., and Alonso, J. C. (2017). *Bacillus subtilis* RecA with DprA-SsbA antagonizes RecX function during natural transformation. *Nucleic. Acids. Res.* 45, 8873–8885. doi: 10.1093/nar/gkx583

Lederberg, J., and Tatum, E. L. (1946). Gene recombination in *Escherichia coli*. *Nature* 158, 558. doi: 10.1038/158558a0

Leong, C. G., Bloomfield, R. A., Boyd, C. A., Dornbusch, A. J., Lieber, L., Liu, F., et al. (2017). The role of core and accessory type IV pilus genes in natural transformation and twitching motility in the bacterium *Acinetobacter baylyi*. *PLoS One* 12:e0182139. doi: 10.1371/journal.pone.0182139

Liu, Y. Y., Wang, Y., Walsh, T. R., Yi, L. X., Zhang, R., Spencer, J., et al. (2016). Emergence of plasmid-mediated colistin resistance mechanism MCR-1 in animals and human beings in China: a microbiological and molecular biological study. *Lancet Infect. Dis.* 16, 161–168. doi: 10.1016/S1473-3099(15)00424-7

Londono-Vallejo, J. A., and Dubnau, D. (1994). Mutation of the putative nucleotide binding site of the *Bacillus subtilis* membrane protein ComFA abolishes the uptake of DNA during transformation. *J. Bacteriol.* 176, 4642–4645. doi: 10.1128/jb.176.15.4642-4645.1994

Maeda, S., Ito, M., Ando, T., Ishimoto, Y., Fujisawa, Y., Takahashi, H., et al. (2006). Horizontal transfer of nonconjugative plasmids in a colony biofilm of *Escherichia coli*. *FEMS Microbiol. Lett.* 255, 115–120. doi: 10.1111/j.1574-6968.2005.00072.x

Maeda, S., Sawamura, A., and Matsuda, A. (2004). Transformation of colonial *Escherichia coli* on solid media. *FEMS Microbiol. Lett.* 236, 61–64. doi: 10.1111/j.1574-6968.2004.tb09627.x

Matsuda, A., Kurono, N., Kawano, C., Shirota, K., Hirabayashi, A., Horino, M., et al. (2012). Genome-wide screen for *Escherichia coli* genes involved in repressing cell-to-cell transfer of non-conjugative plasmids. *Biochem. Biophys. Res. Commun.* 428, 445–450. doi: 10.1016/j.bbrc.2012.10.098

Matsumoto, A., Sekoguchi, A., Imai, J., Kondo, K., Shibata, Y., and Maeda, S. (2016). Natural *Escherichia coli* strains undergo cell-to-cell plasmid transformation. *Biochem. Biophys. Res. Commun.* 481, 59–62. doi: 10.1016/j.bbrc.2016.11.018

Mortier-Barriere, I., Velten, M., Dupaigne, P., Mirouze, N., Pietrement, O., Mcgovern, S., et al. (2007). A key presynaptic role in transformation for a widespread bacterial protein: DprA conveys incoming ssDNA to RecA. *Cell* 130, 824–836. doi: 10.1016/j.cell.2007.07.038

Ogura, M., Yamaguchi, H., Kobayashi, K., Ogasawara, N., Fujita, Y., and Tanaka, T. (2002). Whole-genome analysis of genes regulated by the *Bacillus subtilis* competence transcription factor ComK. *J. Bacteriol.* 184, 2344–2351. doi: 10.1128/JB.184.9.2344-2351.2002

Palchevskiy, V., and Finkel, S. E. (2006). *Escherichia coli* competence gene homologs are essential for competitive fitness and the use of DNA as a nutrient. *J. Bacteriol.* 188, 3902–3910. doi: 10.1128/JB.01974-05

Provvedi, R., and Dubnau, D. (1999). ComEA is a DNA receptor for transformation of competent *Bacillus subtilis*. *Mol. Microbiol.* 31, 271–280. doi: 10.1046/j.1365-2958.1999.01170.x

Saier, M. H. Jr., Reddy, V. S., Tamang, D. G., and Vastermark, A. (2014). The transporter classification database. *Nucleic Acids Res.* 42, D251–D258. doi: 10.1093/nar/gkt1097

Salzer, R., Joos, F., and Averhoff, B. (2014). Type IV pilus biogenesis, twitching motility, and DNA uptake in *Thermus thermophilus*: discrete roles of antagonistic ATPases PilF, PilT1, and PilT2. *Appl. Environ. Microbiol.* 80, 644–652. doi: 10.1128/AEM.03218-13

Salzer, R., Kern, T., Joos, F., and Averhoff, B. (2016). The *Thermus thermophilus* comEA/comEC operon is associated with DNA binding and regulation of the DNA translocator and type IV pili. *Environ. Microbiol.* 18, 65–74. doi: 10.1111/1462-2920.12820

Seitz, P., Pezeshgi Modarres, H., Borgeaud, S., Bulushev, R. D., Steinbock, L. J., Radenovic, A., et al. (2014). ComEA is essential for the transfer of external DNA into the periplasm in naturally transformable *Vibrio cholerae* cells. *PLoS Genet.* 10:e1004066. doi: 10.1371/journal.pgen.1004066

Shen, Z., Wang, Y., Shen, Y., Shen, J., and Wu, C. (2016). Early emergence of mcr-1 in *Escherichia coli* from food-producing animals. *Lancet Infect. Dis.* 16:293. doi: 10.1016/S1473-3099(16)00061-X

Sinha, S., Mell, J. C., and Redfield, R. J. (2012). Seventeen Sxy-dependent cyclic AMP receptor protein site-regulated genes are needed for natural transformation in *Haemophilus influenzae*. *J. Bacteriol.* 194, 5245–5254. doi: 10.1128/JB.00671-12

Smeets, L. C., and Kusters, J. G. (2002). Natural transformation in *Helicobacter* pylori: DNA transport in an unexpected way. *Trends. Microbiol* 10, 159–162; discussion 162. doi: 10.1016/S0966-842X(02)02314-4

Sobue, R., Kurono, N., Etchuya, R., and Maeda, S. (2011). Identification of a novel DNA element that promotes cell-to-cell transformation in *Escherichia coli*. *FEBS Lett.* 585, 2223–2228. doi: 10.1016/j.febslet.2011.05.040

Sun, D. (2011). *Etude de la Transformation Plasmidique Naturelle D'escherichia Coli Et De Ses Relations Eventuelles la compétence Programmée Pour la Transformation Génétique et la Compétence Dite Nutritionnelle*. Ph.D. thesis, avec, Toulouse.

Sun, D. (2016). Two different routes for double-stranded DNA transfer in natural and artificial transformation of *Escherichia coli*. *Biochem. Biophys. Res. Commun.* 471, 213–218. doi: 10.1016/j.bbrc.2016.01.137

Sun, D., Wang, B., Zhu, L., Chen, M., and Zhan, L. (2013). Block and boost DNA transfer: opposite roles of OmpA in natural and artificial transformation of *Escherichia coli*. *PLoS One* 8:e59019. doi: 10.1371/journal.pone.0059019

Sun, D., Zhang, X., Wang, L., Prudhomme, M., Xie, Z., Martin, B., et al. (2009). Transforming DNA uptake gene orthologs do not mediate spontaneous plasmid transformation in *Escherichia coli*. *J. Bacteriol.* 191, 713–719. doi: 10.1128/JB.01130-08

Sun, D., Zhang, Y., Mei, Y., Jiang, H., Xie, Z., Liu, H., et al. (2006). *Escherichia coli* is naturally transformable in a novel transformation system. *FEMS Microbiol. Lett.* 265, 249–255. doi: 10.1111/j.1574-6968.2006.00503.x

Takeno, M., Taguchi, H., and Akamatsu, T. (2011). Role of ComFA in controlling the DNA uptake rate during transformation of competent *Bacillus subtilis*. *J. Biosci. Bioeng.* 111, 618–623. doi: 10.1016/j.jbiosc.2011.02.006

Takeno, M., Taguchi, H., and Akamatsu, T. (2012). Role of ComEA in DNA uptake during transformation of competent *Bacillus subtilis*. *J. Biosci. Bioeng.* 113, 689–693. doi: 10.1016/j.jbiosc.2012.02.004

Tsen, S. D., Fang, S. S., Chen, M. J., Chien, J. Y., Lee, C. C., and Tsen, D. H. (2002). Natural plasmid transformation in *Escherichia coli*. *J. Biomed. Sci.* 9, 246–252. doi: 10.1159/000059425

Veening, J. W., and Blokesch, M. (2017). Interbacterial predation as a strategy for DNA acquisition in naturally competent bacteria. *Nat. Rev. Microbiol.* 15, 621–629. doi: 10.1038/nrmicro.2017.66

von Wintersdorff, C. J., Penders, J., Van Niekerk, J. M., Mills, N. D., Majumder, S., Van Alphen, L. B., et al. (2016). Dissemination of antimicrobial resistance in microbial ecosystems through horizontal gene transfer. *Front. Microbiol.* 7:173. doi: 10.3389/fmicb.2016.00173

Wang, B., and Sun, D. (2015). Detection of NDM-1 carbapenemase-producing *Acinetobacter calcoaceticus* and *Acinetobacter junii* in environmental samples from livestock farms. *J. Antimicrob. Chemother.* 70, 611–613. doi: 10.1093/jac/dku405

Wang, X., Li, M., Yan, Q., Chen, X., Geng, J., Xie, Z., et al. (2007). Across genus plasmid transformation between *Bacillus subtilis* and *Escherichia coli* and the effect of *Escherichia coli* on the transforming ability of free plasmid DNA. *Curr. Microbiol.* 54, 450–456. doi: 10.1007/s00284-006-0617-1

Wozniak, R. A., and Waldor, M. K. (2010). Integrative and conjugative elements: mosaic mobile genetic elements enabling dynamic lateral gene flow. *Nat. Rev. Microbiol.* 8, 552–563. doi: 10.1038/nrmicro2382

Yadav, T., Carrasco, B., Hejna, J., Suzuki, Y., Takeyasu, K., and Alonso, J. C. (2013). *Bacillus subtilis* DprA recruits RecA onto single-stranded DNA and mediates annealing of complementary strands coated by SsbB and SsbA. *J. Biol. Chem.* 288, 22437–22450. doi: 10.1074/jbc.M113.478347

Yadav, T., Carrasco, B., Serrano, E., and Alonso, J. C. (2014). Roles of *Bacillus subtilis* DprA and SsbA in RecA-mediated genetic recombination. *J. Biol. Chem.* 289, 27640–27652. doi: 10.1074/jbc.M114.577924

Yong, D., Toleman, M. A., Giske, C. G., Cho, H. S., Sundman, K., Lee, K., et al. (2009). Characterization of a new metallo-beta-lactamase gene, bla(NDM-1), and a novel erythromycin esterase gene carried on a unique genetic structure in *Klebsiella pneumoniae* sequence type 14 from India. *Antimicrob. Agents Chemother.* 53, 5046–5054. doi: 10.1128/AAC.00774-09

Zhang, X., Jin, T., Deng, L., Wang, C., Zhang, Y., and Chen, X. (2018). Stress-induced, highly efficient, donor cell-dependent cell-to-cell natural transformation in *Bacillus subtilis*. *J. Bacteriol.* 200:e00267-18. doi: 10.1128/JB.00267-18

Zhang, Y., Shi, C., Yu, J., Ren, J., and Sun, D. (2012). RpoS regulates a novel type of plasmid DNA transfer in *Escherichia coli*. *PLoS One* 7:e33514. doi: 10.1371/journal.pone.0033514

Zheng, B., Huang, C., Xu, H., Guo, L., Zhang, J., Wang, X., et al. (2017). Occurrence and genomic characterization of ESBL-Producing, MCR-1-harboring *Escherichia coli* in farming soil. *Front. Microbiol.* 8:2510. doi: 10.3389/fmicb.2017.02510

Conflict of Interest Statement: The author declares that the research was conducted in the absence of any commercial or financial relationships that could be construed as a potential conflict of interest.

frontiers in Microbiology

MINI REVIEW
published: 04 October 2018
doi: 10.3389/fmicb.2018.02365

Horizontal Plasmid Transfer by Transformation in *Escherichia coli*: Environmental Factors and Possible Mechanisms

*Haruka Hasegawa, Erika Suzuki and Sumio Maeda**

Graduate School of Humanities and Sciences, Nara Women's University, Nara, Japan

Transformation is one mode of horizontal gene transfer (HGT) in bacteria, wherein extracellular naked DNA is taken up by cells that have developed genetic competence. Sensitivity to DNase, which degrades naked DNA, is the key to distinguishing transformation from the DNase-resistant HGT mechanisms. In general, *Escherichia coli* is not believed to be naturally transformable; it develops high competence only under artificial conditions, including exposure to high Ca^{2+} concentrations. However, *E. coli* can reportedly express modest competence under certain conditions that are feasible in natural environments outside laboratory. In addition, recent data suggest that environmental factors influence multiple routes of transformation. In this mini review, we (1) summarize our studies on transformation-based HGT using *E. coli* experimental systems and (2) discuss the possible occurrence of transformation via multiple mechanisms in the environment and its possible impact on the spread of antibiotic resistance genes.

Keywords: plasmid transformation, horizontal plasmid transfer, *Escherichia coli*, antibiotic resistance, solid-air biofilm

OPEN ACCESS

Edited by:
Dongchang Sun,
Zhejiang University of Technology, China

Reviewed by:
Nathalie J. A. Campo,
UMR5100 Laboratoire de Microbiologie et Génétique Moléculaires (LMGM), France
Rosemary Redfield,
The University of British Columbia, Canada
Radoslaw Pluta,
Institute for Research in Biomedicine, Spain

***Correspondence:**
Sumio Maeda
smaeda@cc.nara-wu.ac.jp

Specialty section:
This article was submitted to Antimicrobials, Resistance and Chemotherapy, a section of the journal Frontiers in Microbiology

Received: *21 June 2018*
Accepted: *14 September 2018*
Published: *04 October 2018*

Citation:
Hasegawa H, Suzuki E and Maeda S (2018) Horizontal Plasmid Transfer by Transformation in Escherichia coli: Environmental Factors and Possible Mechanisms. Front. Microbiol. 9:2365. doi: 10.3389/fmicb.2018.02365

INTRODUCTION

Horizontal gene transfer (HGT) between bacterial cells contributes to bacterial adaptation to various environments and, in the long term, to bacterial evolution (Lorenz and Wackernagel, 1994; Bushman, 2002; Thomas and Nielsen, 2005). However, in human environments, it causes undesirable spread of pathogenicity, antibiotic resistance, or artificially engineered genes (Bushman, 2002; Keese, 2008; Kelly et al., 2009a,b). Three mechanisms of HGT in bacteria are generally accepted: conjugation, transduction, and transformation (Bushman, 2002; von Wintersdorff et al., 2016). Conjugation and transduction involve specific apparatus for DNA transfer from donor to recipient cells; these are conjugative pili and phage virions, respectively. Transformation is primarily a function of recipient cells that express competence to take up extracellular naked DNA.

Transformation competence can be naturally or artificially induced, but not all bacterial species develop natural competence (Lorenz and Wackernagel, 1994; Johnston et al., 2014). In naturally transformable bacteria, competence is usually transient and induced by alterations in the growth state of organism (Johnston et al., 2014). A group of "competence genes" has been identified, and general mechanistic models have been proposed (Chen and Dubnau, 2004), although precise

mechanisms for individual bacterial species have not been sufficiently elucidated (Cameron and Redfield, 2006, 2008; Sinha et al., 2009; Seitz and Blokesch, 2013; Johnston et al., 2014; Jaskólska and Gerdes, 2015). Because transformation requires extracellular naked DNA as the substrate, sensitivity to DNase, which degrades naked DNA, is key in distinguishing transformation from other DNase-resistant HGT mechanisms (Lorenz and Wackernagel, 1994; Giovanetti et al., 2005; Marshall et al., 2010; Rohrer et al., 2012; Blesa and Berenguer, 2015).

In general, *Escherichia coli* is not believed to be naturally transformable; it develops high genetic competence only under artificial conditions, including exposure to high Ca^{2+} concentrations and temperature shock (Mandel and Higa, 1970; Hanahan, 1983; Sambrook et al., 1989), polyethylene glycol treatment (Chung et al., 1989; Sambrook et al., 1989), or electrical shock (Sambrook and Russell, 2006). However, reportedly, *E. coli* can express modest competence under certain conditions that are feasible in its natural environments (Baur et al., 1996, Bauer et al., 1999; Tsen et al., 2002; Woegerbauer et al., 2002). In the following, we define transformation wherein plasmid was added externally as plasmid transformation (PT) and transformation wherein plasmid DNA comes from dead bacterial cells (from the environment) as horizontal plasmid transfer by transformation (HPTT).

Escherichia coli seems to possess multiple DNA-uptake mechanisms, including two popular ones: one that is dependent on the "competence genes," which commonly work in many gram-negative and -positive bacteria (Finkel and Kolter, 2001; Palchevskiy and Finkel, 2006; Sinha et al., 2009; Sinha and Redfield, 2012; Seitz and Blokesch, 2013; Johnston et al., 2014; Jaskólska and Gerdes, 2015). This mechanism is mainly conducted by the specific molecular apparatus formed around the cell surface structure, which pass through the cell membranes only linear single-stranded DNA produced using a specific periplasmic nuclease. In *E. coli*, these genes are not considered to contribute to PT because PT requires the uptake of intact double-stranded circular DNA (Sinha and Redfield, 2012; Johnston et al., 2014). Therefore, it is unlikely that this mechanism contributes to PT in the environment. The second mechanism is that dependent on external environmental factors, such as divalent metal ions, heat shock, and physical stresses (Mandel and Higa, 1970; Hanahan, 1983; Yoshida, 2007; Rodríguez-Beltrán et al., 2013). These stimuli are commonly considered to induce the formation of pore-like structures in cell surface for the passing of intact double-stranded DNA, including circular plasmids, although the details remain unclear (Reusch et al., 1986; Reusch and Sadoff, 1988; Huang and Reusch, 1995; Sun et al., 2013; Asif et al., 2017). Ca^{2+} and Mg^{2+} ions are the most typical competence-inducing factors. Environmental habitats often contain several millimolar of these ions, whose concentrations are sufficient to induce weak but detectable competence in *E. coli* (Baur et al., 1996, Bauer et al., 1999; Maeda et al., 2003). Therefore, this mechanism is possible in the environment outside laboratories. In addition to the above two mechanisms, another mechanism has been proposed by Sun et al. (2006, 2009), Zhang et al. (2012), Guo et al. (2015), and Sun (2016), in which an ABC transporter and specific periplasmic and inner membrane proteins are involved. This mechanism is regulated by internal transcriptional regulators, RpoS and CRP, therefore it was suggested that this mechanism is also a genetically controlled natural process.

In this mini review, we summarize our studies on HGT using *E. coli* experimental systems and discuss the possible occurrence of transformation by multiple mechanisms in natural environments and its possible impact on the spread of antibiotic resistance genes.

PLASMID TRANSFORMATION OF *E. coli* IN CONDITIONS MIMICKING NATURAL ENVIRONMENT

PT in Food Extracts

Human foods are excellent culture media for many bacteria. However, little attention has been paid to the effects of foods on bacterial physiology other than growth and survival. We investigated the possibility that foods act as media for bacterial transformation. Foods often contain millimolar concentrations of divalent metal ions (Ca^{2+} and Mg^{2+}) and are often stored in a refrigerator or freezer followed by rapid warming (i.e., heat shocked). These conditions are conducive to the development of competency in *E. coli* (Mandel and Higa, 1970; Huang and Reusch, 1995; Baur et al., 1996); because *E. coli* is a common food contaminant, it is interesting to determine whether it can be transformed in foods. Certain foods can indeed act as media that induce competency in *E. coli* (Maeda et al., 2003). Of 42 food samples tested, >10 exhibited an ability to induce competency at a frequency of 10^{-7}–10^{-9}. Among these, the supernatant from tofu (a cheese-like food made of curdled soybean milk) exhibited the highest activity (one in 10^{-7}–10^{-8} recipient cells), corresponding to approximately one-half of the efficiency obtained with 100 mM $CaCl_2$. However, there were no clear correlations between transformation frequencies and chemical characteristics of the foods (Ca^{2+} or Mg^{2+} concentrations and pH), suggesting that complex factors within the foods affect competency development. Similar effects of foods in inducing transformation have been reported in *E. coli* (Bauer et al., 1999) and *Bacillus subtilis* (Brautigam et al., 1997; Zenz et al., 1998).

PT in Solid-Air Biofilm

Many bacteria exist as biofilms in natural and artificial environments (Davey and O'Toole, 2000). Biofilms are aggregates of microbes that form at solid-liquid or solid-air (SA) interfaces (Anderl et al., 2000; Carmen et al., 2004). Cells in these high-density cultures interact with one another and express distinctive physiological functions compared with their free planktonic forms. Previous studies on *E. coli* transformation exclusively focused on planktonic cells (Mandel and Higa, 1970; Hanahan, 1983), but we showed that *E. coli* cells within SA biofilms develop competence at a frequency of 10^{-6}–10^{-8} on various solid media, including LB and H_2O agar and various moist foods (Maeda et al., 2004). Living cells generally coexist with dead cells in biofilms, and the latter can release their DNA and certain divalent metal

ions, including Ca^{2+} and Mn^{2+}, into the local microenvironment of the biofilm (Davey and O'Toole, 2000; Whitchurch et al., 2002). These conditions may be conducive for the development of transformation and may not be exclusive to SA biofilms since a similar enhancement in *E. coli* air-liquid biofilms has also been reported (Król et al., 2011).

PT of Wild *E. coli* Strains in Water

Our and others' results suggest that environmental *E. coli* can potentially acquire foreign DNA via transformation. However, there are few previous reports of investigations into the transformability of natural *E. coli* strains (Woegerbauer et al., 2002; Sinha and Redfield, 2012). Therefore, we examined the potential of natural *E. coli* strains to develop competence under environmental conditions. We used a standard *E. coli* collection of reference (ECOR) strains as our model of natural *E. coli* (Ochman and Selander, 1984) because these ECOR strains have been widely used in various studies on the physiology, behavior, and genotypic variation of natural *E. coli* (Tenaillon et al., 2010). We found that some ECOR strains exhibited detectable transformability (10^{-10}–10^{-11}) in natural water (commercially available bottled natural pure water) at constant and varying temperatures between 5 and 35°C and at winter temperatures in a field experiment, suggesting that natural *E. coli* can potentially develop competence under certain conditions that could feasibly occur in the environment (Matsumoto et al., 2016b).

HORIZONTAL PLASMID TRANSFER BY TRANSFORMATION IN *E. coli*

Freeze–Thaw-Induced HPTT in Natural Waters and Food Extracts

In the environment, naked DNA can be naturally supplied from dead cells to neighboring cells within the same habitat or microenvironment. Therefore, it is worth investigating the possibility of HPTT in a closed system under some feasible conditions. Freeze–thaw is a common process in the handling of foodstuffs and also occurs in nature. Freeze–thaw treatment of *E. coli* cells may promote DNA leakage from dead cells and subsequent uptake by surviving cells because they respond to heat shock, resulting in *in situ* transformation (Li et al., 1992; Takahashi et al., 1992). This treatment of condensed suspensions of mixed *E. coli* strains in natural waters and food extracts caused *in situ* lateral transfer of non-conjugative plasmids at a frequency of 10^{-8}–10^{-10} (Ishimoto et al., 2008). This phenomenon also occurred even after 1–2 months of storage at −20°C, and its sensitivity to DNase demonstrated that it was mediated via a transformation mechanism.

Low Frequency of HPTT in SA Biofilms

Biofilms are thought to be suitable environments for *in situ* transformation because living and dead cells coexist in close proximity, and DNA released from dead cells often accumulates around living cells. In addition, as described above, because *E. coli* cells can develop modest competence in SA biofilms (Maeda et al., 2004), both these factors contribute to HPTT in biofilms. By simply co-culturing a plasmid-free strain with one harboring a non-conjugative plasmid in a SA biofilm on antibiotic-free agar media, transformed cells were produced at low frequency (10^{-9}–10^{-10}) within 24–48 h (Maeda et al., 2006). Liquid cultures of the same strains in LB broth produced no or few transformants, suggesting the importance of SA biofilm formation for plasmid transfer. Essentially, the same phenomenon occurred in SA biofilms on food-based media (Ando et al., 2009). This phenomenon also occurred between popular laboratory strains such as DH5, HB101, and MG1655 (Etchuuya et al., 2011), which are lysogenic phage-free and conjugative apparatus-free, suggesting that the low frequency of horizontal plasmid transfer in SA biofilms can occur without the aid of phage or conjugation machinery and, therefore, that this DNA transfer is due to a kind of transformation. However, since *rpoS*$^{-}$ mutation did not affect this HPTT (Maeda et al., 2006), the RpoS-dependent mechanism (Zhang et al., 2012) is unlikely to be involved.

High Frequency of HPTT Induced by P1 Phage

By assessing combinations of several strains and plasmids for horizontal plasmid transfer, the *E. coli* strain CAG18439 was found to act as both a plasmid donor and a plasmid recipient in combination with the plasmid pHSG299 and could frequently transfer the plasmid in a mixed cell culture even in a liquid medium (Etchuuya et al., 2011). This HGT was demonstrated to be a type of transformation because the high frequency plasmid transfer (10^{-5}–10^{-8}) was DNase-sensitive. Further studies revealed that this phenomenon exhibits some specific characteristics: (1) promotion by proteinaceous factor released from CAG18439 (Etchuuya et al., 2011); (2) promotion by an 88-bp sequence on pHSG299 (Sobue et al., 2011); (3) high transfer frequency (Etchuuya et al., 2011; Sobue et al., 2011); and (4) dependence on specific genes (Kurono et al., 2012; Matsuda et al., 2012). With respect to (1), a later study revealed that these proteinaceous factors include a P1*vir* phage particle (or a derivative thereof) and that externally added P1*vir* phage can reproduce horizontal plasmid transfer between *E. coli* cells and the three other major features of CAG18439-dependent HPTT (Sugiura et al., 2017). This phenomenon was also largely DNase-sensitive, suggesting that a large part of this plasmid transfer is due to transformation despite the involvement of P1 phage. The transformation mechanism of P1*vir* phage-induced plasmid transfer may be due to phage infection or spontaneous awakening of lysogenized phage in plasmid-harboring cells, leading to cell lysis and subsequent intracellular plasmid DNA release in a usable form for transformation. Although such a mechanism is generally feasible, there have been few clear demonstrations of it in *E. coli*. A recent study by Keen et al. (2017) using other phage system also demonstrated a similar phage-induced transformation mechanism in *E. coli*. However, HPTT by P1*vir* or CAG18439 cannot be adequately explained only by enhanced DNA supply from phage-induced cell lysis, and it differs from simple transformation in *E. coli* (Hanahan, 1983) in terms of its

distinctive characteristics (2–4). With respect to (2), the 88-bp sequence on pHSG299 is not homologous to the part of the P1 phage genome sequence. This sequence is often found in databases among general cloning vector sequences but not in any natural source. By tracing back the construction process of pHSG299 (Hashimoto-Gotoh et al., 1981; Brady et al., 1984; Takeshita et al., 1987), however, we suspect that the 88-bp sequence originates from R6-5, a conjugative R plasmid. This sequence, and similar DNA elements, may contribute to HPTT of R and other plasmids in the environment. With respect to (3), this high-frequency transfer cannot be explained by the simple PT ability of CAG18439 and other strains used because simple PT in those strains under the equivalent culture condition was 10^5–10^2 times less frequent (Etchuuya et al., 2011). It was, therefore, suggested that a CAG18439-derived proteinaceous factor, with size estimated between 9 and 30 kDa (Etchuuya et al., 2011) could also be involved in promoting HPTT. This factor presumably assists in DNA uptake by recipient cells, probably in combination with the 88-bp sequence on the transforming DNA. Lastly, with respect to (4), later genome-wide screening studies for recipient genes involved in HPTT suggested that multiple genes participate in the mechanism (Kurono et al., 2012; Matsuda et al., 2012; Shibata et al., 2014a). These include those that have not been reported to be involved in natural or artificial transformation in *E. coli* (such as *rodZ*) and a few known competence gene homologs, such as *ybaV* and *yhiR* (Finkel and Kolter, 2001; Palchevskiy and Finkel, 2006), but do not include *rpoS* and other genes related to the RpoS-dependent mechanism (Zhang et al., 2012). Overall, these results point toward an unknown, complex mechanism of phage-induced, high-frequency HPTT that may partly share the pathway of natural transformation.

HPTT Between Natural *E. coli* Strains

To further assess the generality and variety of HPTT in *E. coli* strains, natural strains (the aforementioned ECOR strains) were used in a study of HPTT. Several combinations of ECOR strains were co-cultured in liquid media, resulting in DNase-sensitive horizontal transfer of natural antibiotic resistance genes (Matsumoto et al., 2016a,b). Plasmid isolation from these new transformants demonstrated horizontal plasmid transfer between ECOR strains (Matsumoto et al., 2016a,b). Simple PT experiments using the same ECOR strains revealed that HPTT occurs much more frequently (10^{-6}–10^{-8}) than simple PT (below 10^{-10}) under the same culture conditions, which suggested that HPTT is unique and effective. Moreover, we discovered that 6 of 12 combinations of the ECOR strains, some of which produce no plaque-forming phages (Shibata et al., 2014b), exhibited DNase-sensitive gene transfer, leading us to suspect that HPTT is rather common in natural *E. coli* strains. Overall, these data suggest that some phage- and conjugation-free transformation mechanism(s) also naturally exist in some *E. coli* strains and that HPTT of antibiotic-resistant natural plasmids (such as plasmids of the ECOR24 strain: Accession Nos. AB905284 and AB905285) can be a pathway for producing multidrug-resistant natural *E. coli* cells.

POSSIBLE MECHANISMS AND FEASIBILITY OF PT AND HPTT IN *E. coli* IN THE ENVIRONMENT

Examples of PT and freeze–thaw-induced and low-frequency HPTT introduced in this mini-review are probably more related to the pore-forming mechanism than the competence gene-dependent mechanism because foods and natural waters often contain mM levels of Ca^{2+} and Mg^{2+} ions (Baur et al., 1996, Bauer et al., 1999; Maeda et al., 2003), and the biofilm environment supply living cells with the content of dead cells, including divalent metal ions and transformable plasmid DNA. As we described previously (Maeda et al., 2006), an SA biofilm (diameter, 10–12 mm; thickness, 0.5–0.8 mm) contains approximately 2–5 $\times$ 10^9 cells. In addition, gut bacteria in mammals generally amount to approximately 10^{11} cells/g (Zoetendal et al., 2004; Sekirov et al., 2010). Considering the enormous scale of the environment, even transformation frequencies of 10^{-9}–10^{-10} cannot be underestimated as they will have an impact on the bacteria populations.

High-frequency HPTT described in this article may involve not only the pore-forming mechanism but also a part of the competence gene functions and possibly another unknown mechanism, as mentioned above. Because bacteriophages are one of the most abundant organisms in the biosphere and ubiquitous in the environment (Clokie et al., 2011), phage-induced HPTT is also considered to be feasible in the environment, as well as ordinary transduction and other phage-derived ways of HGT, e.g., gene transfer agents (Lang et al., 2012).

CONCLUSION AND PERSPECTIVE

Overall, our results and related previous data indicate that multiple mechanisms induce transformation-type HGT in *E. coli* based on various environmental and cellular circumstances such as the nature of the media (e.g., water and food), variable temperature from sub-zero to ∼40°C, high cell density in biofilms, and varying genetic backgrounds of the strains involved. The contribution of transformation-type HGT to genetic dynamics in the environment may be underestimated (Bushman, 2002; Thomas and Nielsen, 2005), and our studies indicate that HPTT in *E. coli* occurs at substantial transfer frequencies (10^{-5}–10^{-10}) under the conditions that can be feasibly encountered in the environment. Therefore, transformation-type HGT can contribute to the spread of antibiotic resistance genes and emergence of multidrug-resistant bacteria in the real environment outside laboratories. Further studies are required to understand the precise role and contribution of transformation-type HGT in spreading antibiotic resistance.

AUTHOR CONTRIBUTIONS

HH, ES, and SM wrote the paper.

FUNDING

This work was supported by JSPS KAKENHI (Grant #25292051).

ACKNOWLEDGMENTS

We are grateful to Enago (www.enago.jp) for English editing and proofreading services.

REFERENCES

Anderl, J. N., Franklin, M. J., and Stewart, P. S. (2000). Role of antibiotic penetration limitation in *Klebsiella pneumoniae* biofilm resistance to ampicillin and ciprofloxacin. *Antimicrob. Agents Chemother.* 44, 1818–1824. doi: 10.1128/AAC.44.7.1818-1824.2000

Ando, T., Itakura, S., Uchii, K., Sobue, R., and Maeda, S. (2009). Horizontal transfer of non-conjugative plasmid in colony biofilm of *Escherichia coli* on food-based media. *World J. Microbiol. Biotechnol.* 25, 1865–1869. doi: 10.1007/s11274-009-0070-y

Asif, A., Mohsin, H., Tanvir, R., and Rehman, Y. (2017). Revisiting the mechanisms involved in calcium chloride induced bacterial transformation. *Front. Microbiol.* 8:2169. doi: 10.3389/fmicb.2017.02169

Bauer, F., Hertel, C., and Hammes, W. P. (1999). Transformation of *Escherichia coli* in foodstuffs. *Syst. Appl. Microbiol.* 22, 161–168. doi: 10.1016/S0723-2020(99)80061-7

Baur, B., Hanselmann, K., Schlimme, W., and Jenni, B. (1996). Genetic transformation in freshwater: *Escherichia coli* is able to develop natural competence. *Appl. Environ. Microbiol.* 62, 3673–3678.

Blesa, A., and Berenguer, J. (2015). Contribution of vesicle-protected extracellular DNA to horizontal gene transfer in *Thermus* spp. *Int. Microbiol.* 18, 177–187. doi: 10.2436/20.1501.01.248

Brady, G., Jantzen, H. M., Bernard, H. U., Brown, R., Schütz, G., and Hashimoto-Gotoh, T. (1984). New cosmid vectors developed for eukaryotic DNA cloning. *Gene* 27, 223–232. doi: 10.1016/0378-1119(84)90143-4

Brautigam, M., Hertel, C., and Hammes, W. P. (1997). Evidence for natural transformation of *Bacillus subtilis* in foodstuffs. *FEMS Microbiol. Lett.* 155, 93–98. doi: 10.1016/S0378-1097(97)00372-8

Bushman, F. (2002). *Lateral DNA Transfer. Cold Spring Harbor*. New York, NY: Laboratory Press, Cold Spring Harbor.

Cameron, A. D. S., and Redfield, R. J. (2006). Non-canonical CRP sites control competence regulons in *Escherichia coli* and many other g-proteobacteria. *Nucleic Acids Res.* 34, 6001–6014. doi: 10.1093/nar/gkl734

Cameron, A. D. S., and Redfield, R. J. (2008). CRP binding and transcription activation at CRP-S sites. *J. Mol. Biol.* 383, 313–323. doi: 10.1016/j.jmb.2008.08.027

Carmen, J. C., Nelson, J. L., Beckstead, B. L., Runyan, C. M., Robinson, R. A., Schaalje, G. B., et al. (2004). Ultrasonic-enhanced gentamicin transport through colony biofilms of *Pseudomonas aeruginosa* and *Escherichia coli*. *J. Infect. Chemother.* 10, 193–199. doi: 10.1007/s10156-004-0319-1

Chen, I., and Dubnau, D. (2004). DNA uptake during bacterial transformation. *Nat. Rev. Microbiol.* 3, 241–249. doi: 10.1038/nrmicro844

Chung, C. T., Niemera, S. L., and Miller, R. H. (1989). One-step preparation of competent *Escherichia coli*: transformation and storage of bacterial cells in the same solution. *Proc. Natl. Acad. Sci. U.S.A.* 86, 2172–2175. doi: 10.1073/pnas.86.7.2172

Clokie, M. R., Millard, A. D., Letarov, A. V., and Heaphy, S. (2011). Phages in nature. *Bacteriophage* 1, 31–45. doi: 10.4161/bact.1.1.14942

Davey, M. E., and O'Toole, G. A. (2000). Microbial biofilms: from ecology to molecular genetics. *Microbiol. Mol. Biol. Rev.* 64, 847–867. doi: 10.1128/MMBR.64.4.847-867.2000

Etchuuya, R., Ito, M., Kitano, S., Shigi, F., Sobue, R., and Maeda, S. (2011). Cell-to-cell transformation in *Escherichia coli*: a novel type of natural transformation involving cell-derived DNA and a putative promoting pheromone. *PLoS One* 6:e16355. doi: 10.1371/journal.pone.0016355

Finkel, S. E., and Kolter, R. (2001). DNA as a nutrient: novel role for bacterial competence gene homologs. *J. Bacteriol.* 183, 6288–6293. doi: 10.1128/JB.183.21.6288-6293.2001

Giovanetti, E., Brenciani, A., Vecchi, M., Manzin, A., and Varaldo, P. E. (2005). Prophage association of mef(A) elements encoding efflux-mediated erythromycin resistance in *Streptococcus pyogenes*. *J. Antimicrob. Chemother.* 55, 445–451. doi: 10.1093/jac/dki049

Guo, M., Wang, H., Xie, N., and Xie, Z. (2015). Positive Effect of carbon sources on natural transformation in *Escherichia coli*: role of low-level cyclic AMP (cAMP)-cAMP receptor protein in the derepression of rpoS. *J. Bacteriol.* 197, 3317–3328. doi: 10.1128/JB.00291-15

Hanahan, D. (1983). Studies on transformation of *Escherichia coli* with plasmids. *J. Mol. Biol.* 166, 557–580. doi: 10.1016/S0022-2836(83)80284-8

Hashimoto-Gotoh, T., Franklin, F. C., Nordheim, A., and Timmis, K. N. (1981). Specific-purpose plasmid cloning vectors. I. Low copy number, temperature-sensitive, mobilization-defective pSC101-derived containment vectors. *Gene* 16, 227–235. doi: 10.1016/0378-1119(81)90079-2

Huang, R., and Reusch, R. N. (1995). Genetic competence in *Escherichia coli* requires poly-beta-hydroxybutyrate/calcium polyphosphate membrane complexes and certain divalent cations. *J. Bacteriol.* 177, 486–490. doi: 10.1128/jb.177.2.486-490.1995

Ishimoto, Y., Kato, S., and Maeda, S. (2008). Freeze-thaw-induced lateral transfer of non-conjugative plasmids by in situ transformation in *Escherichia coli* in natural waters and food extracts. *World J. Microbiol. Biotechnol.* 24, 2731–2735. doi: 10.1007/s11274-008-9761-z

Jaskólska, M., and Gerdes, K. (2015). CRP-dependent positive autoregulation and proteolytic degradation regulate competence activator Sxy of. *Escherichia coli*. *Mol. Microbiol.* 95, 833–845. doi: 10.1111/mmi.12901

Johnston, C., Martin, B., Fichant, G., Polard, P., and Claverys, J. P. (2014). Bacterial transformation: distribution, shared mechanisms and divergent control. *Nat. Rev. Microbiol.* 12, 181–196. doi: 10.1038/nrmicro3199

Keen, E. C., Bliskovsky, V. V., Malagon, F., Baker, J. D., Prince, J. S., Klaus, J. S., et al. (2017). Novel "superspreader" bacteriophages promote horizontal gene transfer by transformation. *mBio* 8:e02115-16. doi: 10.1128/mBio.02115-16

Keese, P. (2008). Risks from GMOs due to horizontal gene transfer. *Environ. Biosafety Res.* 7, 123–149. doi: 10.1051/ebr:2008014

Kelly, B. G., Vespermann, A., and Bolton, D. J. (2009a). Gene transfer events and their occurrence in selected environments. *Food Chem. Toxicol.* 47, 978–983. doi: 10.1016/j.fct.2008.06.012

Kelly, B. G., Vespermann, A., and Bolton, D. J. (2009b). Horizontal gene transfer of virulence determinants in selected bacterial foodborne pathogens. *Food Chem. Toxicol.* 47, 969–977. doi: 10.1016/j.fct.2008.02.007

Król, J. E., Nguyen, H. D., Rogers, L. M., Beyenal, H., Krone, S. M., and Top, E. M. (2011). Increased transfer of a multidrug resistance plasmid in *Escherichia coli* biofilms at the air-liquid interface. *Appl. Environ. Microbiol.* 77, 5079–5088. doi: 10.1128/AEM.00090-11

Kurono, N., Matsuda, A., Etchuya, R., Sobue, R., Sakaki, Y., Ito, M., et al. (2012). Genome-wide screening of *Escherichia coli* genes involved in execution and promotion of cell-to-cell transfer of non-conjugative plasmids: rodZ (yfgA) is essential for plasmid acceptance in recipient cells. *Biochem. Biophys. Res. Commun.* 421, 119–123. doi: 10.1016/j.bbrc.2012.03.127

Lang, A. S., Zhaxybayeva, O., and Beatty, J. T. (2012). Gene transfer agents: phage-like elements of genetic exchange. *Nat. Rev. Microbiol.* 10, 472–482. doi: 10.1038/nrmicro2802

Li, M., Stern, B., and Kamp, D. (1992). Ultrafast plasmid DNA preparation for rapid transformation. *Biotechniques* 13, 692–696.

Lorenz, M. G., and Wackernagel, W. (1994). Bacterial gene transfer by natural genetic transformation in the environment. *Microbiol. Rev.* 58, 563–602.

Maeda, S., Ito, M., Ando, T., Ishimoto, Y., Fujisawa, Y., Takahashi, H., et al. (2006). Horizontal transfer of nonconjugative plasmids in a colony biofilm of *Escherichia coli*. *FEMS Microbiol. Lett.* 255, 115–120. doi: 10.1111/j.1574-6968.2005.00072.x

Maeda, S., Kakihara, N., and Koishi, Y. (2003). Competency development of *Escherichia coli* in foodstuffs. *Microbes Environ.* 18, 100–103. doi: 10.1264/jsme2.18.100

Maeda, S., Sawamura, A., and Matsuda, A. (2004). Transformation of colonial *Escherichia coli* on solid media. *FEMS Microbiol. Lett.* 236, 61–64. doi: 10.1016/j.femsle.2004.05.023

Mandel, M., and Higa, A. (1970). Calcium-dependent bacteriophage DNA infection. *J. Mol. Biol.* 53, 159–162. doi: 10.1016/0022-2836(70)90051-3

Marshall, K. M., Bradshaw, M., and Johnson, E. A. (2010). Conjugative botulinum neurotoxin-encoding plasmids in *Clostridium botulinum*. *PLoS One* 5:e11087. doi: 10.1371/journal.pone.0011087

Matsuda, A., Kurono, N., Kawano, C., Shirota, K., Hirabayashi, A., Horino, M., et al. (2012). Genome-wide screen for *Escherichia coli* genes involved in repressing cell-to-cell transfer of non-conjugative plasmids. *Biochem. Biophys. Res. Commun.* 428, 445–450. doi: 10.1016/j.bbrc.2012.10.098

Matsumoto, A., Sekoguchi, A., Imai, J., Kondo, K., Shibata, Y., and Maeda, S. (2016a). Natural *Escherichia coli* strains undergo cell-to-cell plasmid transformation. *Biochem. Biophys. Res. Commun.* 481, 59–62. doi: 10.1016/j.bbrc.2016.11.018

Matsumoto, A., Sekoguchi, A., Murakami, Y., Imai, J., Kondo, K., Shibata, Y., et al. (2016b). "Competence development and horizontal plasmid transfer in natural *Escherichia coli* strain," in *Microbes in the Spotlight: Recent Progress in the Understanding of Beneficial and Harmful Microorganisms*, ed. M. A. Vilas (Florida, FL: Brown Walker Press), 468–473.

Ochman, H., and Selander, R. K. (1984). Standard reference strains of *Escherichia coli* from natural populations. *J. Bacteriol.* 157, 690–693.

Palchevskiy, V., and Finkel, S. E. (2006). *Escherichia coli* competence gene homologs are essential for competitive fitness and the use of DNA as a nutrient. *J. Bacteriol.* 188, 3902–3910. doi: 10.1128/JB.01974-05

Reusch, R. N., Hiske, T. W., and Sadoff, H. L. (1986). Poly-β-hydroxybutyrate membrane structure and its relationship to genetic transformability in *Escherichia coli*. *J. Bacteriol.* 168, 553–562. doi: 10.1128/jb.168.2.553-562.1986

Reusch, R. N., and Sadoff, H. L. (1988). Putative structure and functions of a poly-β-hydroxybutyrate/calcium polyphosphate channel in bacterial plasma membranes. *Proc. Natl. Acad. Sci. U.S.A.* 85, 4176–4180. doi: 10.1073/pnas.85.12.4176

Rodríguez-Beltrán, J., Rodríguez-Rojas, A., Yubero, E., and Blázquez, J. (2013). The animal food supplement sepiolite promotes a direct horizontal transfer of antibiotic resistance plasmids between bacterial species. *Antimicrob. Agents Chemother.* 57, 2651–2653. doi: 10.1128/AAC.02363-12

Rohrer, S., Holsten, L., Weiss, E., Banghezal, M., Fischer, W., and Haas, R. (2012). Multiple pathways of plasmid DNA transfer in *Helicobacter pylori*. *PLoS One* 7:e45623. doi: 10.1371/journal.pone.0045623

Sambrook, J., Fritsch, E. F., and Maniatis, T. (1989). *Molecular Cloning: A Laboratory Manual*, 2nd Edn. New York, NY: Cold Spring Harbor Laboratories.

Sambrook, J., and Russell, D. R. (2006). Transformation of *E. coli* by electroporation. *Cold Spring Harb. Protoc.* 21, doi: 10.1101/pdb.prot3933

Seitz, P., and Blokesch, M. (2013). Cues and regulatory pathways involved in natural competence and transformation in pathogenic and environmental Gram-negative bacteria. *FEMS Microbiol. Rev.* 37, 336–363. doi: 10.1111/j.1574-6976.2012.00353.x

Sekirov, I., Russell, S. L., Antunes, L. C., and Finlay, B. B. (2010). Gut microbiota in health and disease. *Physiol. Rev.* 90, 859–904. doi: 10.1152/physrev.00045.2009

Shibata, Y., Matsumoto, A., Horino, M., Hirabayashi, A., Shirota, K., Kawano, C., et al. (2014a). Genome-wide screen for *Escherichia coli* genes involved in repressing cell-to-cell transfer of a nonconjugative pSC101-derived plasmid. *Am. J. Life Sci.* 2, 345–350. doi: 10.11648/j.ajls.20140206.13

Shibata, Y., Ugumori, C., Takahashi, A., Sekoguchi, A., and Maeda, S. (2014b). Survey of lysogenic phages in the 72 strains of *Escherichia coli* collection of reference (ECOR) and identification of a phage derived from the ECOR52 strain. *Am. J. BioSci.* 2, 32–37. doi: 10.11648/j.ajbio.20140202.12

Sinha, S., Cameron, A. D. S., and Redfield, R. J. (2009). Sxy Induces a CRP-S Regulon in *Escherichia coli*. *J. Bacteriol.* 191, 5180–5195. doi: 10.1128/JB.00476-09

Sinha, S., and Redfield, R. J. (2012). Natural DNA Uptake by *Escherichia coli*. *PLoS One* 7:e35620. doi: 10.1371/journal.pone.0035620

Sobue, R., Kurono, N., Etchuya, R., and Maeda, S. (2011). Identification of a novel DNA element that promotes cell-to-cell transformation in *Escherichia coli*. *FEBS Lett.* 585, 2223–2228. doi: 10.1016/j.febslet.2011.05.040

Sugiura, C., Miyaue, S., Shibata, Y., Matsumoto, A., and Maeda, S. (2017). Bacteriophage P1vir-induced cell-to-cell plasmid transformation in *Escherichia coli*. *AIMS Microbiol.* 3, 784–797. doi: 10.3934/microbiol.2017.4.784

Sun, D. (2016). Two different routes for double-stranded DNA transfer in natural and artificial transformation of *Escherichia coli*. *Biochem. Biophys. Res. Commun.* 471, 213–218. doi: 10.1016/j.bbrc.2016.01.137

Sun, D., Wang, B., Zhu, L., Chen, M., and Zhan, L. (2013). Block and boost DNA transfer: opposite roles of OmpA in natural and artificial transformation of *Escherichia coli*. *PLoS One* 8:e59019. doi: 10.1371/journal.pone.0059019

Sun, D., Zhang, X., Wang, L., Prudhomme, M., Xie, Z., Martin, B., et al. (2009). Transforming DNA uptake gene orthologs do not mediate spontaneous plasmid transformation in *Escherichia coli*. *J. Bacteriol.* 191, 713–719. doi: 10.1128/JB.01130-08

Sun, D., Zhang, Y., Mei, Y., Jiang, H., Xie, Z., and Liu, H. (2006). *Escherichia coli* is naturally transformable in a novel transformation system. *FEMS Microbiol. Lett.* 265, 249–255. doi: 10.1111/j.1574-6968.2006.00503.x

Takahashi, R., Valeika, S. R., and Glass, K. W. (1992). A simple method of plasmid transformation of *E. coli* by rapid freezing. *Biotechniques* 13, 711–715.

Takeshita, S., Sato, M., Toba, M., Masahashi, W., and Hashimoto-Gotoh, T. (1987). High-copy-number and low-copy-number plasmid vectors for lacZα-complementation and chloramphenicol- or kanamycin-resistance selection. *Gene* 61, 63–74. doi: 10.1016/0378-1119(87)90365-9

Tenaillon, O., Skurnik, D., Picard, B., and Denamur, E. (2010). The population genetics of commensal *Escherichia coli*. *Nat. Rev. Microbiol.* 8, 207–217. doi: 10.1038/nrmicro2298

Thomas, C. M., and Nielsen, K. M. (2005). Mechanisms of, and barriers to, horizontal gene transfer between bacteria. *Nat. Rev. Microbiol.* 3, 711–721. doi: 10.1038/nrmicro1234

Tsen, S. D., Fang, S. S., Chen, M. J., Chien, J. Y., Lee, C. C., and Tsen, D. H. (2002). Natural plasmid transformation in *Escherichia coli*. *J. Biomed. Sci.* 9, 246–252. doi: 10.1159/000059425

von Wintersdorff, C. J., Penders, J., van Niekerk, J. M., Mills, N. D., Majumder, S., van Alphen, L. B., et al. (2016). Dissemination of antimicrobial resistance in microbial ecosystems through horizontal gene transfer. *Front. Microbiol.* 7, 173. doi: 10.3389/fmicb.2016.00173

Whitchurch, C. B., Tolker-Nielsen, T., Ragas, P. C., and Mattick, J. S. (2002). Extracellular DNA required for bacterial biofilm formation. *Science* 295, 1487. doi: 10.1126/science.295.5559.1487

Woegerbauer, M., Jenni, B., Thalhammer, F., Graninger, W., and Burgmann, M. (2002). Natural genetic transformation of clinical isolates of *Escherichia coli* in urine and water. *Appl. Environ. Microbiol.* 68, 440–443. doi: 10.1128/AEM.68.1.440-443.2002

Yoshida, N. (2007). Discovery and application of the Yoshida effect: nano-sized acicular materials enable penetration of bacterial cells by sliding friction force. *Recent Pat. Biotechnol.* 1, 194–201. doi: 10.2174/187220807782330147

Zenz, K. I., Neve, H., Geis, A., and Heller, K. J. (1998). *Bacillus subtilis* develops competence for uptake of plasmid DNA when growing in milk products. *Syst. Appl. Microbiol.* 21, 28–32. doi: 10.1016/S0723-2020(98)80005-2

Zhang, Y., Shi, C., Yu, J., Ren, J., and Sun, D. (2012). RpoS regulates a novel type of plasmid DNA transfer in *Escherichia coli*. *PLoS One* 7:e33514. doi: 10.1371/journal.pone.0033514

Zoetendal, E. G., Collier, C. T., Koike, S., Mackie, R. I., and Gaskins, H. R. (2004). Molecular ecological analysis of the gastrointestinal microbiota. *J. Nutr.* 134, 465–472. doi: 10.1093/jn/134.2.465

Conflict of Interest Statement: The authors declare that the research was conducted in the absence of any commercial or financial relationships that could be construed as a potential conflict of interest.

frontiers in Microbiology

ORIGINAL RESEARCH
published: 23 October 2018
doi: 10.3389/fmicb.2018.02489

Evidence of Illegitimate Recombination Between Two *Pasteurellaceae* Plasmids Resulting in a Novel Multi-Resistance Replicon, pM3362MDR, in *Actinobacillus pleuropneumoniae*

*Yinghui Li[1,2†], Giarlã Cunha da Silva[3†], Yanwen Li[1], Ciro C. Rossi[3], Roberto Fernandez Crespo[1], Susanna M. Williamson[4], Paul R. Langford[1], Denise Mara Soares Bazzolli[3] and Janine T. Bossé[1]**

[1] Section of Paediatrics, Department of Medicine, Imperial College London, London, United Kingdom, [2] Shenzhen Center for Disease Control and Prevention, Shenzhen, China, [3] Laboratório de Genética Molecular de Bactérias, Departamento de Microbiologia, Instituto de Biotecnologia Aplicada à Agropecuária, Universidade Federal de Viçosa, Viçosa, Brazil, [4] Animal and Plant Health Agency, Addlestone, United Kingdom

OPEN ACCESS

Edited by:
Katy Jeannot,
Laboratoire Chrono-Environnement, France

Reviewed by:
Christopher Morton Thomas, University of Birmingham, United Kingdom
Bruno Gonzalez-Zorn, Complutense University of Madrid, Spain

***Correspondence:**
Janine T. Bossé
j.bosse@imperial.ac.uk

[†] These authors have contributed equally to this work

Specialty section:
This article was submitted to Antimicrobials, Resistance and Chemotherapy, a section of the journal Frontiers in Microbiology

Received: 27 June 2018
Accepted: 28 September 2018
Published: 23 October 2018

Citation:
Li Y, da Silva GC, Li Y, Rossi CC, Fernandez Crespo R, Williamson SM, Langford PR, Bazzolli DMS and Bossé JT (2018) Evidence of Illegitimate Recombination Between Two Pasteurellaceae Plasmids Resulting in a Novel Multi-Resistance Replicon, pM3362MDR, in Actinobacillus pleuropneumoniae. Front. Microbiol. 9:2489. doi: 10.3389/fmicb.2018.02489

Evidence of plasmids carrying the tetracycline resistance gene, *tet*(B), was found in the previously reported whole genome sequences of 14 United Kingdom, and 4 Brazilian, isolates of *Actinobacillus pleuropneumoniae.* Isolation and sequencing of selected plasmids, combined with comparative sequence analysis, indicated that the four Brazilian isolates all harbor plasmids that are nearly identical to pB1001, a plasmid previously found in *Pasteurella multocida* isolates from Spain. Of the United Kingdom isolates, 13/14 harbor plasmids that are (almost) identical to pTetHS016 from *Haemophilus parasuis*. The remaining United Kingdom isolate, MIDG3362, harbors a 12666 bp plasmid that shares extensive regions of similarity with pOV from *P. multocida* (which carries bla_{ROB-1}, *sul2*, and *strAB* genes), as well as with pTetHS016. The newly identified multi-resistance plasmid, pM3362MDR, appears to have arisen through illegitimate recombination of pTetHS016 into the stop codon of the truncated *strB* gene in a pOV-like plasmid. All of the *tet*(B)-carrying plasmids studied were capable of replicating in *Escherichia coli*, and predicted origins of replication were identified. A putative origin of transfer (*oriT*) sequence with similar secondary structure and a *nic*-site almost identical to that of RP4 was also identified in these plasmids, however, attempts to mobilize them from an RP4-encoding *E. coli* donor strain were not successful, indicating that specific conjugation machinery may be required.

Keywords: plasmids, antimicrobial resistance, tetracycline, respiratory tract, *Pasteurellaceae*

INTRODUCTION

Resistance to tetracycline is widespread amongst isolates of *Actinobacillus pleuropneumoniae* in many countries (Archambault et al., 2012; Vanni et al., 2012; Dayao et al., 2016; El Garch et al., 2016). Despite this, tetracyclines continue to be the most widely used antimicrobial for treatment of respiratory and other diseases in food-producing animals in the United Kingdom and other European countries (Borriello, 2013; Garcia-Migura et al., 2014; European Medicines Agency and European Surveillance of Veterinary Antimicrobial Consumption, 2017).

Identification of the genes responsible for tetracycline resistance, and an understanding of the mechanisms underlying the spread of these genes, will help inform decisions regarding continued use of this important antimicrobial agent.

Although more than thirty different tetracycline resistance genes have been reported in different bacterial species (Chopra and Roberts, 2001), relatively few have been found in *A. pleuropneumoniae*, with *tet*(B) being the most common (Blanco et al., 2006; Dayao et al., 2016; Bossé et al., 2017; Michael et al., 2018). We recently reported that the *tet*(B) gene was found in the chromosome of 37.5% of United Kingdom isolates for which whole genome sequences (wgs) were determined, either as part of a large integrative conjugative element (ICE*Apl1*), or as a transposon insertion in the *comM* gene (Bossé et al., 2017). A further 14.5% of the tested isolates had *tet*(B) genes that appeared to be associated with plasmid sequences (Bossé et al., 2017). Wgs for six Brazilian isolates also indicate the presence of *tet*(B) associated with plasmid sequences in four of these isolates (Pereira et al., 2015). As small plasmids often appear to be common amongst members of the *Pasteurellaceae* (Michael et al., 2018), the aim of this study was to identify the *tet*(B) plasmids present in these sequenced isolates of *A. pleuropneumoniae*.

MATERIALS AND METHODS

A. pleuropneumoniae Isolates and Plasmids

Information regarding the 14 United Kingdom and 4 Brazilian *A. pleuropneumoniae* isolates and their wgs data (**Table 1**) was compiled from details described previously (Pereira et al., 2015; Bossé et al., 2017). Data regarding the tetracycline resistance plasmids identified in this study are also shown (**Table 1**). Plasmid sequences were initially identified in the draft genome sequences using ResFinder (Zankari et al., 2012) to identify contigs containing the *tet*(B) gene. BLASTn was then used to identify sequences with the highest identity to each of these contigs. Where it appeared that a single contig matched a known plasmid, the ends of the contigs were analyzed to identify overlapping sequences that allowed closure into a circular plasmid. Where it appeared that the contigs carrying *tet*(B) represented only partial plasmids, sequences of the plasmids with highest identity were then used to search the wgs using BLASTn to identify other contigs carrying plasmid-related sequences.

Plasmids were extracted from the *A. pleuropneumoniae* isolates MV780, MIDG2567, MIDG2656, MIDG2658, MIDG3202, MIDG3233, and MIDG3362 using the Qiaprep Spin Miniprep kit (Qiagen) according to the manufacturer's protocol. The correct joining of contigs (i.e., ends of a single, or overlapping multiple contigs, as appropriate) was verified either by inverse PCR to amplify the region between the 5′ and 3′ ends of the *tet*(B) gene, or by amplification across the predicted contig junctions. The complete sequence of each extracted plasmid was confirmed using a primer walking strategy. Descriptions of all primers used in this study are shown in **Table 2**. The annotated sequences of plasmids p780, pM2567Tet, pM2656Tet, pM2658Tet, pM3202Tet, pM3233Tet, and pM3362MDR have been deposited in Genbank

TABLE 1 | *Actinobacillus pleuropneumoniae* isolates carrying *tet*(B) resistance plasmids.

Isolate ID	Serovar	Location[a]	Year	MIC (μg/ml Tet)	Accession (wgs)	Contig in wgs[b]	Plasmid size[c]	Plasmid name	Most similar to
MIDG2567	8	Thirsk	2003	4	ERS134321	21, 71	3386*	pM2567Tet	pTetHS016[d]
MIDG2650	8	Thirsk	2005	16	ERS134316	10	3366	pM2650Tet	pTetHS016
MIDG2656	2	Winchester	2005	16	ERS134610	2	3366*	pM2656Tet	pTetHS016
MIDG2658	8	Thirsk	2005	16	ERS134322	15, 24	3376*	pM2658Tet	pTetHS016
MIDG2661	8	Bury St Edmunds	2005	16	ERS134325	51	3366	pM2661Tet	pTetHS016
MIDG2666	8	Bury St Edmunds	2005	≥16	ERS134330	4	3349	pM2666Tet	pTetHS016
MIDG3202	8	Bury St Edmunds	2006	16	ERS134333	2	3366*	pM3202Tet	pTetHS016
MIDG3233	6	Bristol	2008	16	ERS134364	7, 20	3366*	pM3233Tet	pTetHS016
MIDG3234	8	Starcross	2008	16	ERS134625	2, 109	3366	pM3234Tet	pTetHS016
MIDG3362	12	Thirsk	2008	8	ERS134382	7, 40, 111, 126	12666*	pM3362MDR	pTetHS016 and pOV[e]
MIDG3379	8	Thirsk	2009	16	ERS134397	14, 124	3376	pM3379Tet	pTetHS016
MIDG3380	8	Thirsk	2009	16	ERS134636	50	3376	pM3380Tet	pTetHS016
MIDG3382	8	Thirsk	2009	8	ERS134400	15	3366	pM3382Tet	pTetHS016
MIDG3394	7	Thirsk	2010	8	ERS155334	16	3366	pM3394Tet	pTetHS016
MV780	8	Brazil	2009	≥16	JSVV00000000	44, 47, 53	5128*	p780	pB1001[f]
MV460	8	Brazil	2007	≥16	JSVG00000000	48, 51, 54	5128	p460	pB1001
MV1022	8	Brazil	2011	≥16	JSVF00000000	45, 47, 51	5128	p1022	pB1001
MV5651	8	Brazil	2006	≥16	JSVY00000000	42, 45, 51	5128	p5651	pB1001

[a] *Other than the four Brazilian isolates (Pereira et al., 2015), specific locations are for previously described United Kingdom isolates (Bossé et al., 2017).* [b] *Contig number(s) in draft wgs containing plasmid sequences.* [c] *Sizes of isolated plasmids confirmed by sequencing are indicated (*), otherwise sizes were predicted bioinformatically.* [d] *pTetHS016 (accession KC818265) is a 3366 bp plasmid from a United Kingdom Haemophilus parasuis isolate (Luan et al., 2013).* [e] *pOV (accession NC_019381) is a 13,551 bp plasmid from Pasteurella multocida.* [f] *pB1001 (accession EU252517) is a 5128 bp plasmid from P. multocida in Spain.*

TABLE 2 | Primers used in this study.

Primer name	Sequence	Target/purpose
tetB_for	CGCATTGGTAATTACGTTATTCGATG	Amplification of an 1101 bp internal fragment of *tet*(B)
tetB_rev	GCTAAACCAATAATCCAAATCCAGC	
tetB_5′_out	CGTAATTACCAATGCGATCTTTGTC	Inverse PCR amplification and/or sequencing of the region between the ends of the *tet*(B) gene
tetB_3′_out	GTTAACCCCTCAAGCTCATGG	
rep_5′_out	TTGCCATAAGACTAGAGATTTCCTG	Sequencing out from 5′ end of *rep* in p780 (multiple priming sites in other plasmids)
rep_3′_out	TTTAAGAGGGGAATATGGCAACAC	Sequencing out from 3′ end of *rep* in plasmids other than p780 where multiple priming sites are present
3362_node40_out	TTGCCATAAGACTAGAGATTTCCTG	Confirmation of correct joining of contigs and sequencing of the pM3362MDR plasmid
3362_node111_out	AGCCCAAAAAGAGCCGATAGG	
3362_node126_out	TTAATGTTCAGCAGAGGGGAGG	
3362_rep_5′_out	TAGAACTCTCATTTCATCAAGCG	
3362_ISApl_5′_out	TCGTTGCACTTGGTTTGACAATTC	
3362_ISApl_3′_out	TGCCCTGTGCGAGTAAAATC	
780_rep_int_for	GGTTTTAGAGCCATCCATAACGG	Sequencing out from 3′ end of *rep* in p780
780_node44_out	GCCATTTTTACCTTCCTAATCTTCAG	Confirmation of correct joining of contigs and sequencing of the p780 plasmid

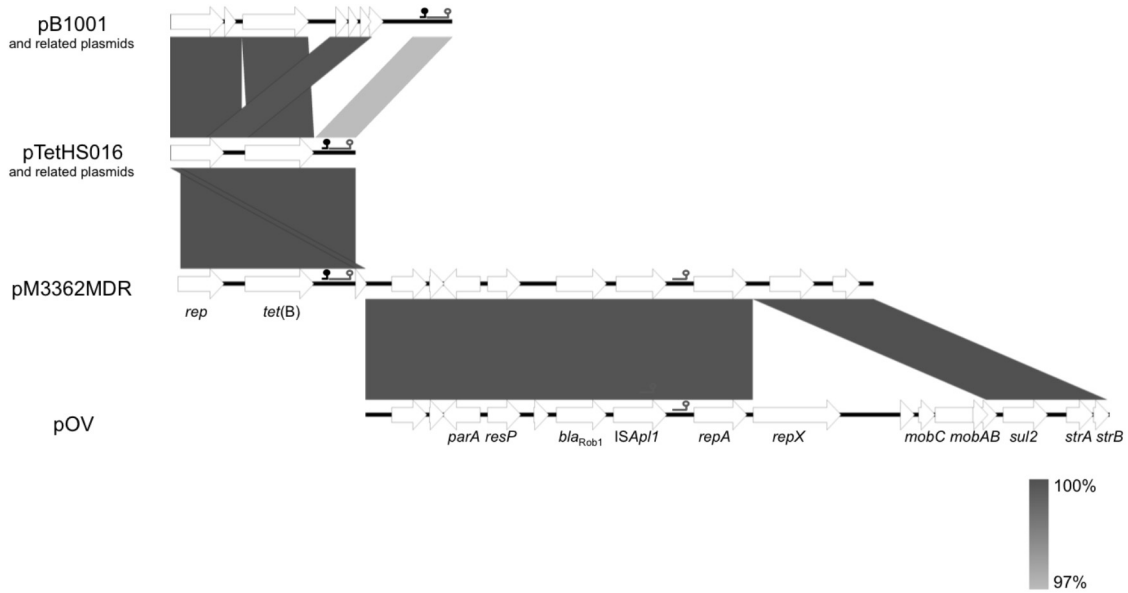

FIGURE 1 | Schematic representation of the structure and organization of genes in different *Pasteurellaceae tet*(B) and multi-resistance plasmids. pB1001 from *Pasteurella multocida* and related plasmids from *Actinobacillus pleuropneumoniae* isolates (see **Table 1**); pTetHS016 from *Haemophilus parasuis* and related plasmids from *A. pleuropneumoniae* isolates (see **Table 1**); pM3362MDR from *A. pleuropneumoniae* isolate MIDG3362; pOV from *P. multocida*. Open reading frames are shown as arrows, with the arrowhead indicating the direction of transcription. Genes with known/predicted function are labeled [*rep*, *repA*, *repX*: plasmid replication; *tet*(B): tetracycline resistance; *parA*: plasmid partitioning; *resP*: predicted resolvase; bla_{Rob-1}: β-lactam resistance; IS*Apl1*: transposase; *mobAB*, *mobC*: plasmid mobilization; *sul2*: sulfonamide resistance; *strA*, *strB*: streptomycin resistance]. The predicted origin of replication (*oriV*) is indicated by the symbol (●) and the origin of transfer (*oriT*) by the symbol (●) for each of the plasmids shown - note that pM3362MDR contains two different *oriV* sequences. Gray blocks between sequences indicate >97% nucleotide sequence identity according to the scale shown.

under the accession numbers MH457196 to MH457202, respectively.

Electroporation of Plasmids Into *Escherichia coli* MFD*pir*

Plasmids p780, pM2656Tet, and pM3362MDR were electroporated into the *E. coli* conjugal donor strain, MFD*pir* (Ferrieres et al., 2010). Transformants were selected on Brain Heart Infusion (BHI) agar supplemented with 0.3 mM diaminopimelic acid, containing 5 μg/ml tetracycline. The presence of plasmid in tetracycline resistant transformants was confirmed by PCR amplification using the *tetB*_for/*tetB*_rev primers (**Table 2**) prior to plasmid extraction, as above. Stability of the cloned plasmids in *E. coli* was assessed and compared to the endogenous plasmids in *A. pleuropneumoniae* as previously described (Moleres et al., 2015), with minor modifications. Briefly, following initial plating on selective agar, bacteria

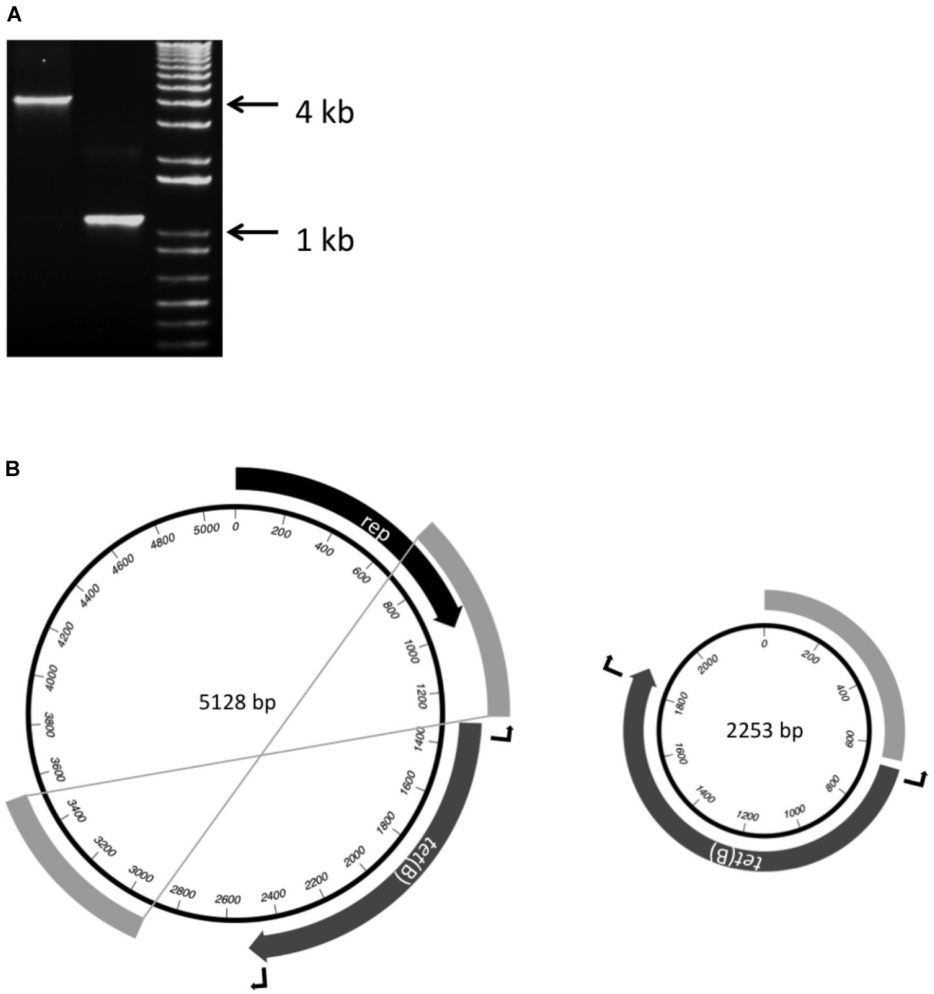

FIGURE 2 | Detection of two different sized amplicons **(A)** produced by inverse-PCR from the ends of the *tet*(B) gene using DNA extracted from the *A. pleuropneumoniae* isolate MV780. **(B)** Schematic representation of p780 (5128 bp) and a smaller plasmid (2253 bp) formed by recombination between the direct repeat sequences (shown as unlabelled gray bands) flanking the *tet*(B) gene, as indicated by the crossed lines joining the ends of the repeat sequences in p780. The locations of the outward-facing primers at the ends of the *tet*(B) gene are indicated by the bent arrows, and lengths of sequence between the primers in the respective plasmids correspond to the correspond to the 4 and 1.1 kb amplicons detected in **(A)**.

were cultured in 10 ml non-selective broth, which was serially passaged (1:100 dilution) eight times. Following the fourth and eighth passage, the stability of the plasmids was assessed by comparing the number of resistant cfu/ml on selective agar, to total cfu/ml on non-selective agar.

Conjugal Transfer Experiments

In order to investigate mobilization from the *E. coli* MFD*pir* clones containing plasmids p780, pM2656Tet, and pM3362MDR, we used the same plasmid-free, tetracycline susceptible clinical *A. pleuropneumoniae* isolates as previously used to demonstrate conjugal transfer of ICE*Apl*1 and ICE*Apl*2 (Bossé et al., 2016; Li et al., 2018), namely MIDG3376 (serovar 6), MIDG2465 (serovar 7), MIDG3217 (serovar 8), and MIDG3347 (serovar 12). Matings were performed as previously described (Bossé et al., 2009), with selection on BHI-NAD containing 2.5 μg/ml tetracycline. The conjugation experiments were performed twice on independent occasions, with MIDG2331Δ*ureC::nadV* [carrying *tet*(B) in ICE*Apl1*] as a positive control donor (Bossé et al., 2016).

RESULTS AND DISCUSSION

In each of the four Brazilian isolates, a 1206 bp *tet*(B) gene was on a 1611 bp contig that shares 100% identity with the *rep* and *tet*(B) sequences of pB1001 (**Figure 1**), a 5128 bp plasmid from *Pasteurella multocida* (San Millan et al., 2009). The remaining sequences of this plasmid were found on two further contigs (644 and 2231 or 2233 bp) in each isolate, with the 644 bp contig (containing the last 329 bp of *rep*) matching sequences both upstream and downstream of *tet*(B) in pB1001. When inverse PCR was used to determine the length of the sequence flanking the *tet*(B) gene, two products (circa 4 and 1.1 kb, respectively;

FIGURE 3 | Schematic representation of the site of insertion of the pTetHS016 plasmid sequence into a pOV-like plasmid during formation of pM3326MDR. The stop codon (TAG) of the *strB* gene in pOV is followed by an asterisk (*) indicating the end of the coding sequence. The insertion site of pTetHS016 into a pOV-like plasmid is indicated by a downward triangle. The TA dinucleotide present in the stop codon of *strB*, and that in the *rep* gene of pTetHS016, at which point the plasmids recombine, is shown in bold and underlined in each of the sequences shown. During recombination, the 5′ end of the pTetHS016 *rep* gene is displaced, forming the majority of the 210 bp ORF found downstream of the *oriV* in pM3362MDR. An alternate 5′ end for the *rep* gene in pM3362MDR is supplied from within the 3′ end of the disrupted *strB* gene (shown in blue text), whereas the stop codon of the 210 bp ORF in pM3362MDR is derived from sequence following the end of the *strB* gene (sequence shown in pink text). The majority of the *rep* gene in pM3362MDR is identical to that in pTetHS016 (sequence shown in red italic text).

Figure 2A) were amplified, which when sequenced, indicated that the smaller amplicon was produced by deletion of 2875 bp mediated by recombination between the direct repeat sequences flanking *tet*(B) (**Figure 2B**). This type of instability has been reported in other plasmids (Dianov et al., 1991; Oliveira et al., 2010). It is unclear whether the smaller plasmid, lacking the full-length *rep* gene, is capable of stable replication.

In eight United Kingdom isolates, a single contig was found to contain the entire sequence of a plasmid almost identical to pTetHS016 (**Figure 1**; accession KC818265), a 3366 bp plasmid from a United Kingdom *Haemophilus parasuis* isolate (Luan et al., 2013), encoding a 1257 bp *tet*(B) gene along with a 978 bp *rep* gene. In each case, direct repeat sequences at either end of the contig were detected that allowed closure into circular plasmids of similar sizes (**Table 1**). A further five isolates had sequences similar to pTetHS016 divided over two contigs (**Table 1**). Inverse PCR produced similar sized amplicons (circa 2.2 kb) for sequences flanking the *tet*(B) gene in isolates with the pTetHS016-like sequences found on one or two contigs (**Figure 1**). Complete sequencing of pM2567Tet, pM2658Tet, pM3202Tet, and pM3233Tet confirmed the predicted sizes, with slight differences between plasmids seen in the intergenic regions.

Comparison of pB1001 and pTetHS016 (**Figure 1**) revealed that they share 95% identity over the majority of the smaller plasmid sequence, indicating that they likely evolved from the same origin. Differences around the 5′ and 3′ ends of *tet*(B) account for the variation in length of this gene between the plasmids, with a 110 bp deletion in the pB1001-type replicons resulting in a start codon 16 residues into the protein encoded by the larger genes, and a single base deletion at the 3′ end resulting in an alternate stop codon. The *tet*(B) gene from the larger pB1001-type plasmids (as well as 350 bp downstream, not present in the smaller pTetHS016-type), shows 100% identity with chromosomal and plasmid sequences from various species including *E. coli*, *Salmonella enterica*, and *Shigella dysenteriae* (e.g., accession numbers CP025254, CP022069, and CP026778), indicating a likely enterobacterial source, as has been shown for other resistance genes in *Pasteurellaceae* plasmids (Michael et al., 2018).

In the genome of one United Kingdom isolate, MIDG3362, a 1257 bp *tet*(B) gene was identified by ResFinder on a 6496 bp contig, 3051 bp of which shares 100% identity with pTetHS016, and the remaining 3455 bp is 99% identical to sequences encoding *repA*, *sul2*, and *strA* found in pOV (accession NC_019381), a 13,551 bp plasmid from from *P. multocida*, and a related set of small multi-resistance plasmids from "*Actinobacillus porcitonsillarum*" (Matter et al., 2008) ranging in size from 8751 to 13,425 bp (accession numbers AJ830711, AM748705, AJ830712, and AM748706). These plasmids all further carry the β-lactamase gene, $bla_{\mathrm{Rob-1}}$. ResFinder results for MIDG3362 identified a 4820 bp contig carrying $bla_{\mathrm{Rob-1}}$, of which 4485 bp is 99% identical to sequences in pOV, and the remaining 336 bp is 100% identical with sequences in pTetHS016, with a 20 bp overlap, allowing the joining to

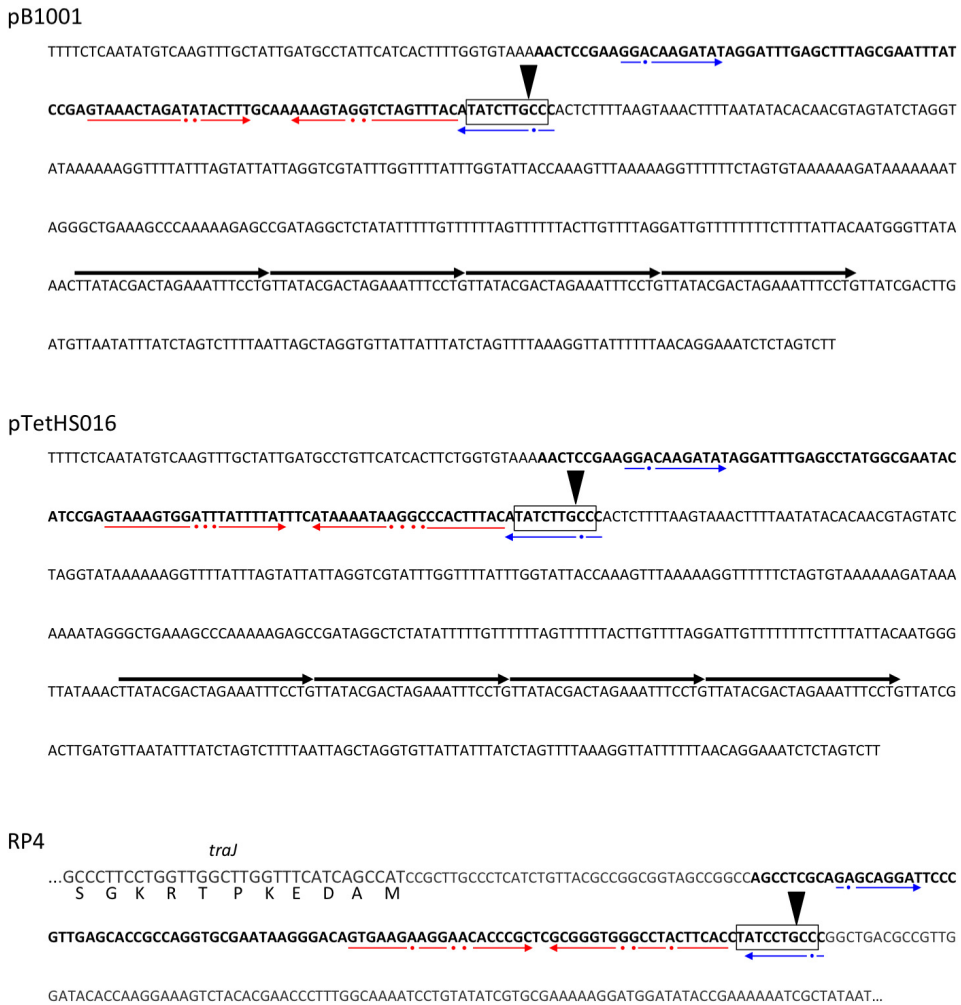

FIGURE 4 | Nucleotide sequences from plasmids pB1001, pTetHS016, and RP4 indicating the respective origin of transfer (*oriT*) regions in bold text, with the *nic* recognition site boxed and the site of cleavage indicated by a downward triangle. The major imperfect inverted repeat sequences in each are underlined with red arrows (broken, with dots indicating non-conserved bases), and the sequences of a second imperfect inverted repeat underlined with blue arrows (broken, with dots indicating non-conserved bases). In pB1001 (and related *A. pleuropneumoniae* plasmids – see **Table 1**), the *oriT* is located immediately upstream of the predicted origin of replication (*oriV*), an AT-rich region containing four iterons (direct repeats of the sequence TTATACGACTAGAAATTTCCTG; indicated by the four contiguous arrows above the text) involved in binding of the Rep protein. In RP4, the *oriT* is located immediately upstream of the *traJ* gene sequence (for which only the 5′ end is shown encoded on the complement strand, with bases of the coding sequence in larger font, and with the respective amino acids shown below each codon). In RP4, the sequence downstream of the *oriT* does not contain the *oriV*, but rather leads to the divergently transcribed *traK* gene, following 225 bp of intergenic sequence.

pTetHS016 sequences on the *tet*(B) carrying contig. A further 1375 bp sharing 100% identity with sequences from pOV was found distributed over two additional contigs in the MIDG3362 genome. Overlapping sequences were identified between the ends of these two contigs, and those of the *tet*(B)- and the $bla_{\mathrm{Rob-1}}$-carrying contigs, allowing closure of a complete circular plasmid which was confirmed by PCR amplification and sequencing of products spanning the junctions. This 12666 bp plasmid, pM3362MDR, contains an almost complete copy of the pTetHS016 sequence (**Figure 1**). The pTetHS016 plasmid appears to have integrated seamlessly into the stop codon of the truncated *strB* gene in plasmid pOV by a single cross-over event at a TA dinucleotide (**Figure 3**), resulting in disruption of the 978 bp *rep* gene, such that the 5′ end of the gene is part of a 210 bp orf found downstream, whilst the majority of the *rep* gene is present as an 843 bp orf upstream of *tet*(B), having acquired an alternate start codon from within the 3′ end of the *strB* gene of pOV. There are no apparent homologous sequences in the *rep* and *strB* genes, thus integration appears to have been through illegitimate recombination. A 4255 bp segment of pOV, spanning from *repX* through the *mobCAB* genes, is not present in pM3362MDR, where only a 199 bp remnant of the *mobA* gene is present between *repA* and *sul2*. Deletion of this segment may explain why attempts to mobilize pM3362MDR from a conjugal donor strain into plasmid-free isolates of *A. pleuropneumoniae* were unsuccessful (see below).

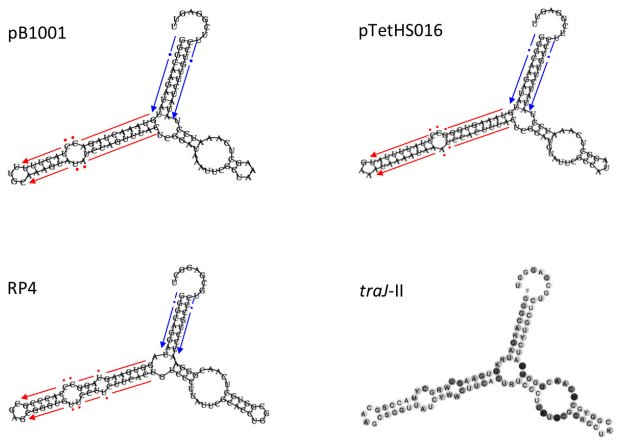

FIGURE 5 | Schematic representation of the secondary structures of the *oriT* regions of plasmids pB1001, pTetHS016, and RP4, compared to the consensus structure of the non-coding RNA *traJ*-II found upstream of the *traJ* gene in various conjugative plasmids and chromosomal sequences (Rfam family RF01760). The red and blue arrows (broken, with dots indicating non-conserved bases) flanking the hairpins in the different *oriT* sequences correspond to the respective imperfect inverted repeat sequences shown in **Figure 4**.

Replicons which have evolved to be stably maintained in *Pasteurellaceae* frequently contain resistance genes that appear to have been acquired from enterobacterial plasmids (Ares-Arroyo et al., 2018; Michael et al., 2018). This is likely due to the fact that most *Pasteurellaceae* plasmids are capable of stable replication in *E. coli*, whereas the converse is rarely true, suggesting some differences in the origin (*oriV*) and/or proteins required for replication (Michael et al., 2018). In *Pasteurellaceae* species, many plasmids are ColE1-type replicons (related to, but distinct from those found in *Enterobacteriaceae*), which tend to carry the *mobCAB* mobilization genes, with the origin of transfer (*oriT*) as well as the *oriV* found upstream of *mobC* (Ares-Arroyo et al., 2018). Replication of ColE1-type plasmids relies on host factors; whereas plasmids carrying their own *rep* genes have cognate *oriV* sequences, typically AT-rich regions containing direct repeats (iterons) which specifically bind the Rep protein (Rajewska et al., 2012; Lilly and Camps, 2015; Wegrzyn et al., 2016). Both Rep-encoding and ColE1-type replicons have been described in *Pasteurellaceae* species, and some plasmids carry more than one *oriV*; for example, the pOV plasmid has both a ColE1 origin, and a RepA-specific *oriV* (discussed below).

The three different plasmids in this study, which were confirmed to stably replicate in both *A. pleuropneumoniae* and *E. coli* over eight passages in the absence of selection, have an AT-rich (74%) region of 438–458 bp containing four contiguous direct repeats (iterons) of the 22 bp sequence TTATACGACTAGAAATTTCCTG (shown for pB1001 and pTetHS016 in **Figure 4**). Although there is sequence variation between the AT-rich regions of the different plasmids, the iterons are identical, supporting that these are sites for binding the Rep protein encoded by all of these plasmids. In the smaller pB1001- and pTetHS016-type plasmids, the predicted replication origin immediately precedes the 978 bp *rep* gene, whereas in pM3362MDR, it is upstream of the 210 bp orf containing the 5′ end of the *rep* gene, as discussed above. It is unclear if the truncated 843 bp *rep* gene in pM3362MDR is functional, as there is a second predicted *oriV* located upstream of the *repA* gene derived from the pOV-like replicon, which may be responsible for replication of this plasmid (**Figure 1**). This 292 bp region has an AT-content of 69%, and contains four contiguous direct repeats of the 22 bp sequence TTAAAACCCTACAGATTTACGG, which is likely the iteron specific for binding of the RepA protein. In support of this, an identical *oriV* was previously described in other plasmids encoding the same Rep protein (Matter et al., 2008).

Small mobilizable plasmids normally carry *mob* gene(s) encoding a relaxase (or multi-component relaxosome), which makes a single strand cut at the *nic* site of the *oriT* sequence, commonly found upstream (O'Brien et al., 2015). However, some mobilizable plasmids have been found that carry only a minimum *oriT*, requiring the relaxase to be supplied *in trans* (O'Brien et al., 2015). Relaxase proteins are specific for their cognate *oriT* sequences, and have been classified into six major families (i.e., MOB families C, F, H, P, V, and Q), which can be further divided into subfamilies (Garcillán-Barcia et al., 2009; Zrimec and Lapanje, 2018). Although the plasmids in this study do not encode known *mob* genes, they do all contain a 100–105 bp sequence (**Figures 4**, **5**) located immediately upstream of the common *oriV*, containing regions of dyad symmetry that are characteristic of *oriT* sequences (Ziegelin et al., 1989; Pansegrau et al., 1990; O'Brien et al., 2015). These sequences are predicted to form secondary structures similar to the bioinformatically predicated sRNA *traJ*-II (*traJ*-II; Rfam family RF01760; **Figure 5**), found in the 5′ UTR of the *traJ* gene in various plasmid and chromosomal sequences (Weinberg et al., 2010). Indeed, the predicted *traJ*-II sequence in conjugative plasmid RK2/RP4 (accession number K00832.1) corresponds to that previously described as the *oriT* of this plasmid (Ziegelin et al., 1989; Pansegrau et al., 1990). Recently, a plasmid classification method was developed based on analysis of conserved structures in non-coding regions, which were shown to be highly conserved and discriminative for predicting the MOB family, even in the absence of encoded relaxases (Zrimec and Lapanje, 2018). Results obtained using this tool support our prediction that the *oriT* sequences identified in the plasmids in this study, like that of RP4, correspond to the MOBP family. However, as the largest family, MOBP includes numerous relaxases, some of which require accessory proteins for specific binding of their cognate *oriT* prior to cleavage of the *nic* site (Pansegrau and Lanka, 1991; Parker et al., 2005; Garcillán-Barcia et al., 2009; Zrimec and Lapanje, 2018).

In addition to having similar secondary structure, the *oriT* sequences of the plasmids in this study have predicted *nic* sites that share a high degree of identity with that of RP4, differing only at one base, however, the sequences of the major inverted repeat (found immediately upstream of the *nic* site) differ markedly (**Figure 4**). The right arm of this repeat region has been shown

to provide specificity of the RP4 relaxosome via binding of the TraJ protein (Ziegelin et al., 1989; Pansegrau et al., 1990). We confirmed the inability of RP4-dependent conjugative transfer machinery, encoded by *E. coli* conjugal MFD*pir* (Ferrieres et al., 2010), to transfer representatives (pM2656Tet, pM3362MDR, and p780) of each of the three types of resistance plasmid in this study. Having been electroporated into MFD*pir*, the plasmids were shown to be capable of replication in this *E. coli* strain, as confirmed by PCR amplification of the encoded *tet*(B) gene from transformants, however, no transconjugants were obtained using any of the four plasmid-free *A. pleuropneumoniae* recipient strains. The control experiment demonstrated that these strains were successfully used as recipients for conjugal transfer of the tetracycline resistance integrative conjugative element, ICE*Apl1*, with conjugation frequencies of 10^{-4}–10^{-5}, both in this and the previous study (Bossé et al., 2016). It is possible that mobilization of the plasmids described in this study, homologs of which have been identified in different *Pasteurellaceae* species (suggesting horizontal transfer between them), requires specific conjugal transfer machinery that has yet to be identified. Various integrative and conjugative elements (ICEs) belonging to either the ICE*Hin1056* family (Mohd-Zain et al., 2004; Bossé et al., 2016), the SXT/R391 family (Li et al., 2018; Xu et al., 2018), or a set related ICEs including ICE*Pmu1* and ICE*Mh1* (Michael et al., 2012; Eidam et al., 2015), are present in different *Pasteurellaceae* species, but none have sequences similar to the predicted plasmid *oriT*s (or their major inverted repeats), suggesting the ICE-encoded relaxases would not likely be capable of mobilizing these plasmids.

In summary, we have identified and characterized three related tetracycline resistance plasmids circulating in isolates of *A. pleuropneumoniae* in the United Kingdom and Brazil. Two are almost identical to plasmids pTetHS016 and pB1001, found in other members of the *Pasteurellaceae* (i.e., *H. parasuis* and *P. multocida*, respectively), that carry only the *tet*(B) and *rep* genes. The third, pM3362MDR, is a novel multi-resistance plasmid, carrying $bla_{\mathrm{Rob-1}}$, *sul2*, and *strA* in addition to *tet*(B), and appears to have been derived from insertion of the pTetHS016 plasmid into pOV (from *P. multocida*), or a related plasmid. Co-existence of multiple plasmids in the same isolate has previously been reported for *P. multocida* and *A. pleuropneumoniae* (San Millan et al., 2009; Bossé et al., 2015), providing the opportunity for either homologous or illegitimate recombination. The presence of (nearly) identical plasmids in multiple *Pasteurellaceae* suggests horizontal transfer between these different species, which can share the same niche in the respiratory tract of pigs. Although a putative MOBP-related *oriT* was identified in all plasmids, we were unable to demonstrate mobilization using an *E. coli* donor strain expressing conjugation machinery specific for RP4-type plasmids. It is possible that these plasmids could be mobilized by cognate conjugation machinery, perhaps *Pasteurellaceae*-specific, which remains to be identified.

AUTHOR CONTRIBUTIONS

JB, PL, SW, GS, and DB conceived the study. SW provided UK clinical isolates. YHL, GS, JB, YWL, and CR produced the data. JB, YHL, GS, and RF analyzed the data. JB and YHL wrote the paper.

FUNDING

This work was supported by Fundação de Amparo à Pesquisa do Estado de Minas Gerais – FAPEMIG (APQ-02732-15); Conselho Nacional de Desenvolvimento Científico e Tecnológico – CNPq; Coordenação de Aperfeiçoamento de Pessoal de Nível Superior – CAPES/PROEX, and the Biotechnology and Biological Sciences Research Council (BB/K021109/1, BB/G018553/1, and BB/M023052/1). JB was also funded by CONFAP – the United Kingdom Academies Fellowship (FAPEMIG – APQ-00689-16). YHL was funded by San-Ming Project of Medicine in Shenzhen (No. SZSM201811071).

ACKNOWLEDGMENTS

We wish to thank Chris Teale from the APHA for his advice and input.

REFERENCES

Archambault, M., Harel, J., Gouré, J., Tremblay, Y. D. N., and Jacques, M. (2012). Antimicrobial susceptibilities and resistance genes of Canadian isolates of *Actinobacillus pleuropneumoniae*. *Microb. Drug Resist.* 18, 198–206. doi: 10.1089/mdr.2011.0150

Ares-Arroyo, M., Bernabe-Balas, C., Santos-López, A., Baquero, M. R., Prasad, K. N., Cid, D., et al. (2018). PCR-based analysis of ColE1 plasmids in clinical isolates and metagenomic samples reveals their importance as gene capture platforms. *Front. Microbiol.* 9:177. doi: 10.3389/fmicb.2018.00469

Blanco, M., Gutiérrez-Martín, C. B., Rodríguez-Ferri, E. F., Roberts, M. C., and Navas, J. (2006). Distribution of tetracycline resistance genes in *Actinobacillus pleuropneumoniae* isolates from Spain. *Antimicrob. Agents Chemother.* 50, 702–708. doi: 10.1128/AAC.50.2.702-708.2006

Borriello, S. P. (2013). *UK Veterinary Antibiotic Resistance and Sales Surveillance 2013*. Available at: www.vmd.defra.gov.uk/pdf/varss.pdf

Bossé, J. T., Durham, A. L., Rycroft, A. N., Kroll, J. S., and Langford, P. R. (2009). New plasmid tools for genetic analysis of *Actinobacillus pleuropneumoniae* and other Pasteurellaceae. *Appl. Environ. Microbiol.* 75, 6124–6131. doi: 10.1128/AEM.00809-09

Bossé, J. T., Li, Y., Fernandez Crespo, R., Chaudhuri, R. R., Rogers, J., Holden, M. T. G., et al. (2016). ICE*Apl1*, an integrative conjugative element related to ICEHin1056, identified in the pig pathogen *Actinobacillus pleuropneumoniae*. *Front. Microbiol.* 7:810. doi: 10.3389/fmicb.2016.00810

Bossé, J. T., Li, Y., Rogers, J., Fernandez Crespo, R., Li, Y., Chaudhuri, R. R., et al. (2017). Whole genome sequencing for surveillance of antimicrobial resistance in *Actinobacillus pleuropneumoniae*. *Front. Microbiol.* 8:311. doi: 10.3389/fmicb.2017.00311

Bossé, J. T., Li, Y., Walker, S., Atherton, T., Fernandez Crespo, R., Williamson, S. M., et al. (2015). Identification of *dfrA14* in two distinct plasmids conferring trimethoprim resistance in *Actinobacillus pleuropneumoniae*. *J. Antimicrob. Chemother.* 70, 2217–2222. doi: 10.1093/jac/dkv121

Chopra, I., and Roberts, M. (2001). Tetracycline antibiotics: mode of action, applications, molecular biology, and epidemiology of bacterial resistance. *Microbiol. Mol. Biol. Rev.* 65, 232–260. doi: 10.1128/MMBR.65.2.232-260.2001

Dayao, D., Gibson, J. S., Blackall, P. J., and Turni, C. (2016). Antimicrobial resistance genes in *Actinobacillus pleuropneumoniae*, *Haemophilus parasuis* and *Pasteurella multocida* isolated from Australian pigs. *Aust. Vet. J.* 94, 227–231. doi: 10.1111/avj.12458

Dianov, G. L., Kuzminov, A. V., Mazin, A. V., and Salganik, R. I. (1991). Molecular mechanisms of deletion formation in *Escherichia coli* plasmids - I. Deletion formation mediated by long direct repeats. *Mol. Gen. Genet.* 228, 153–159. doi: 10.1007/BF00282460

Eidam, C., Poehlein, A., Leimbach, A., Michael, G. B., Kadlec, K., Liesegang, H., et al. (2015). Analysis and comparative genomics of ICE*Mh1*, a novel integrative and conjugative element (ICE) of *Mannheimia haemolytica*. *J. Antimicrob. Chemother.* 70, 93–97. doi: 10.1093/jac/dku361

El Garch, F., de Jong, A., Simjee, S., Moyaert, H., Klein, U., Ludwig, C., et al. (2016). Monitoring of antimicrobial susceptibility of respiratory tract pathogens isolated from diseased cattle and pigs across Europe, 2009-2012: VetPath results. *Vet. Microbiol.* 194, 11–22. doi: 10.1016/j.vetmic.2016.04.009

European Medicines Agency and European Surveillance of Veterinary Antimicrobial Consumption (2017). *Sales of Veterinary Antimicrobial Agents in 30 European Countries in 2015*. London: EMA.

Ferrieres, L., Hemery, G., Nham, T., Guerout, A. M., Mazel, D., Beloin, C., et al. (2010). Silent mischief: bacteriophage Mu insertions contaminate products of *Escherichia coli* random mutagenesis performed using suicidal transposon delivery plasmids mobilized by broad-host-range RP4 conjugative machinery. *J. Bacteriol.* 192, 6418–6427. doi: 10.1128/JB.00621-10

Garcia-Migura, L., Hendriksen, R. S., Fraile, L., and Aarestrup, F. M. (2014). Antimicrobial resistance of zoonotic and commensal bacteria in Europe: the missing link between consumption and resistance in veterinary medicine. *Vet. Microbiol.* 170, 1–9. doi: 10.1016/j.vetmic.2014.01.013

Garcillán-Barcia, M. P., Francia, M. V., and la Cruz de, F. (2009). The diversity of conjugative relaxases and its application in plasmid classification. *FEMS Microbiol. Rev.* 33, 657–687.

Li, Y., Li, Y., Fernandez Crespo, R., Leanse, L. G., Langford, P. R., and Bossé, J. T. (2018). Characterization of the *Actinobacillus pleuropneumoniae* SXT-related integrative and conjugative element ICEApl2 and analysis of the encoded FloR protein: hydrophobic residues in transmembrane domains contribute dynamically to florfenicol and chloramphenicol efflux. *J. Antimicrob. Chemother.* 73, 57–65. doi: 10.1093/jac/dkx342

Lilly, J., and Camps, M. (2015). Mechanisms of theta plasmid replication. *Microbiol. Spectr.* 3:LAS-0029-2014. doi: 10.1128/microbiolspec.PLAS-0029-2014

Luan, S.-L., Chaudhuri, R. R., Peters, S. E., Mayho, M., Weinert, L. A., Crowther, S. A., et al. (2013). Generation of a Tn5 transposon library in *Haemophilus parasuis* and analysis by transposon-directed insertion-site sequencing (TraDIS). *Vet. Microbiol.* 166, 558–566. doi: 10.1016/j.vetmic.2013.07.008

Matter, D., Rossano, A., Sieber, S., and Perreten, V. (2008). Small multidrug resistance plasmids in *Actinobacillus porcitonsillarum*. *Plasmid* 59, 144–152. doi: 10.1016/j.plasmid.2007.11.003

Michael, G. B., Bossé, J. T., and Schwarz, S. (2018). Antimicrobial resistance in *Pasteurellaceae* of veterinary origin. *Microbiol. Spectr.* 6:ARBA-0022-2017. doi: 10.1128/microbiolspec.ARBA-0022-2017

Michael, G. B., Kadlec, K., Sweeney, M. T., Brzuszkiewicz, E., Liesegang, H., Daniel, R., et al. (2012). ICE*Pmu1*, an integrative conjugative element (ICE) of *Pasteurella multocida*: structure and transfer. *J. Antimicrob. Chemother.* 67, 91–100. doi: 10.1093/jac/dkr411

Mohd-Zain, Z., Turner, S. L., Cerdeño-Tárraga, A. M., Lilley, A. K., Inzana, T. J., Duncan, A. J., et al. (2004). Transferable antibiotic resistance elements in *Haemophilus influenzae* share a common evolutionary origin with a diverse family of syntenic genomic islands. *J. Bacteriol.* 186, 8114–8122. doi: 10.1128/JB.186.23.8114-8122.2004

Moleres, J., Santos-López, A., Lázaro, I., Labairu, J., Prat, C., Ardanuy, C., et al. (2015). Novel bla_{ROB-1}-bearing plasmid conferring resistance to β-Lactams in *Haemophilus parasuis* isolates from healthy weaning pigs. *Appl. Environ. Microbiol.* 81, 3255–3267. doi: 10.1128/AEM.03865-14

O'Brien, F. G., Yui Eto, K., Murphy, R. J. T., Fairhurst, H. M., Coombs, G. W., Grubb, W. B., et al. (2015). Origin-of-transfer sequences facilitate mobilisation of non-conjugative antimicrobial-resistance plasmids in *Staphylococcus aureus*. *Nucleic Acids Res.* 43, 7971–7983. doi: 10.1093/nar/gkv755

Oliveira, P. H., Prather, K. J., Prazeres, D. M. F., and Monteiro, G. A. (2010). Analysis of DNA repeats in bacterial plasmids reveals the potential for recurrent instability events. *Appl. Microbiol. Biotechnol.* 87, 2157–2167. doi: 10.1007/s00253-010-2671-7

Pansegrau, W., Balzer, D., Kruft, V., Lurz, R., and Lanka, E. (1990). In vitro assembly of relaxosomes at the transfer origin of plasmid RP4. *Proc. Natl. Acad. Sci. U.S.A.* 87, 6555–6559.

Pansegrau, W., and Lanka, E. (1991). Common sequence motifs in DNA relaxases and nick regions from a variety of DNA transfer systems. *Nucleic Acids Res.* 19, 3455–3455. doi: 10.1093/nar/19.12.3455

Parker, C., Becker, E., Zhang, X., Jandle, S., and Meyer, R. (2005). Elements in the co-evolution of relaxases and their origins of transfer. *Plasmid* 53, 113–118. doi: 10.1016/j.plasmid.2004.12.007

Pereira, M. F., Rossi, C. C., de Carvalho, F. M., de Almeida, L. G. P., Souza, R. C., de Vasconcelos, A. T. R., et al. (2015). Draft genome sequences of six *Actinobacillus pleuropneumoniae* serotype 8 Brazilian clinical isolates: insight into new applications. *Genome Announc.* 3:e01585-14. doi: 10.1128/genomeA.01585-14

Rajewska, M., Wegrzyn, K., and Konieczny, I. (2012). AT-rich region and repeated sequences – the essential elements of replication origins of bacterial replicons. *FEMS Microbiol. Rev.* 36, 408–434. doi: 10.1111/j.1574-6976.2011.00300.x

San Millan, A., Escudero, J. A., Gutierrez, B., Hidalgo, L., Garcia, N., Llagostera, M., et al. (2009). Multiresistance in *Pasteurella multocida* is mediated by coexistence of small plasmids. *Antimicrob. Agents Chemother.* 53, 3399–3404. doi: 10.1128/AAC.01522-08

Vanni, M., Merenda, M., Barigazzi, G., Garbarino, C., Luppi, A., Tognetti, R., et al. (2012). Antimicrobial resistance of *Actinobacillus pleuropneumoniae* isolated from swine. *Vet. Microbiol.* 156, 172–177. doi: 10.1016/j.vetmic.2011.10.022

Wegrzyn, K. E., Gross, M., Uciechowska, U., and Konieczny, I. (2016). Replisome assembly at bacterial chromosomes and iteron plasmids. *Front. Mol. Biosci.* 3:39. doi: 10.3389/fmolb.2016.00039

Weinberg, Z., Wang, J. X., Bogue, J., Yang, J., Corbino, K., Moy, R. H., et al. (2010). Comparative genomics reveals 104 candidate structured RNAs from bacteria, archaea, and their metagenomes. *Genome Biol.* 11:R31. doi: 10.1186/gb-2010-11-3-r31

Xu, J., Jia, H., Cui, G., Tong, H., Wei, J., Shao, D., et al. (2018). ICE*Apl*Chn1, a novel SXT/R391 integrative conjugative element (ICE), carrying multiple antibiotic resistance genes in *Actinobacillus pleuropneumoniae*. *Vet. Microbiol.* 220, 18–23. doi: 10.1016/j.vetmic.2018.05.002

Zankari, E., Hasman, H., Cosentino, S., Vestergaard, M., Rasmussen, S., Lund, O., et al. (2012). Identification of acquired antimicrobial resistance genes. *J. Antimicrob. Chemother.* 67, 2640–2644. doi: 10.1093/jac/dks261

Ziegelin, G., Fürste, J. P., and Lanka, E. (1989). TraJ protein of plasmid RP4 binds to a 19-base pair invert sequence repetition within the transfer origin. *J. Biol. Chem.* 264, 11989–11994.

Zrimec, J., and Lapanje, A. (2018). DNA structure at the plasmid origin-of-transfer indicates its potential transfer range. *Sci. Rep.* 8:1820. doi: 10.1038/s41598-018-20157-y

Conflict of Interest Statement: The authors declare that the research was conducted in the absence of any commercial or financial relationships that could be construed as a potential conflict of interest.

frontiers in Microbiology

ORIGINAL RESEARCH
published: 30 October 2018
doi: 10.3389/fmicb.2018.02579

The Role of IS*CR1*-Borne P_{OUT} Promoters in the Expression of Antibiotic Resistance Genes

Claire Lallement, Cécile Pasternak, Marie-Cécile Ploy and Thomas Jové**

INSERM, CHU Limoges, RESINFIT, U1092, University of Limoges, Limoges, France

The IS*CR1* (Insertion sequence Common Region) element is the most widespread member of the IS*CR* family, and is frequently present within γ-proteobacteria that occur in clinical settings. IS*CR1* is always associated with the 3′Conserved Segment (3′CS) of class 1 integrons. IS*CR1* contains outward-oriented promoters P_{OUT}, that may contribute to the expression of downstream genes. In IS*CR1*, there are two P_{OUT} promoters named P_{CR1-1} and P_{CR1-2}. We performed an *in silico* analysis of all publically available IS*CR1* sequences and identified numerous downstream genes that mainly encode antibiotic resistance genes and that are oriented in the same direction as the P_{OUT} promoters. Here, we showed that both P_{CR1-1} and P_{CR1-2} significantly increase the expression of the downstream genes $bla_{CTX-M-9}$ and *dfrA19*. Our data highlight the role of IS*CR1* in the expression of antibiotic resistance genes, which may explain why IS*CR1* is so frequent in clinical settings.

Keywords: antibiotic resistance, promoters, IS*CR1*, expression, insertion sequence element

OPEN ACCESS

Edited by:
Katy Jeannot, UMR6249 Chrono Environnement, France

Reviewed by:
Apostolos Liakopoulos, Leiden University, Netherlands
Jozsef Soki, University of Szeged, Hungary

****Correspondence:***
Marie-Cécile Ploy
marie-cecile.ploy@unilim.fr
Thomas Jové
thomas.jove@unilim.fr

Specialty section:
This article was submitted to Antimicrobials, Resistance and Chemotherapy, a section of the journal Frontiers in Microbiology

Received: *10 July 2018*
Accepted: *09 October 2018*
Published: *30 October 2018*

Citation:
Lallement C, Pasternak C, Ploy M-C and Jové T (2018) The Role of ISCR1-Borne P_{OUT} Promoters in the Expression of Antibiotic Resistance Genes. Front. Microbiol. 9:2579. doi: 10.3389/fmicb.2018.02579

INTRODUCTION

Antimicrobial resistance is often mediated by the dissemination of antibiotic resistance genes (ARG) that are carried by mobile genetic elements (MGEs) including plasmids, insertion sequences (IS), transposons (Tn) and integron gene cassettes (Partridge, 2011) which are harbored by bacteria across all phyla and environments (Aminov, 2011). In addition, some MGEs may carry promoters that ensure or increase expression of downstream ARG. Several IS including IS*1999*, IS*Ecp1*, IS*Kpn23* (reviewed in Vandecraen et al., 2017) display a complete outwardly oriented functional promoter usually referred as P_{OUT} that enhances expression of downstream ARGs. Other IS like IS*1* or IS*257* only contain the −35 element that generates a hybrid functional promoter when associated with a downstream putative −10 element (Goussard et al., 1991; Simpson et al., 2000). Most often, these IS-borne promoters allow sufficient expression of ARGs to confer the antibiotic resistance phenotype. IS from the IS*CR* family are related to the IS*91* family and display a *rcr* gene encoding a putative RCR transposase belonging to the ubiquitous HUH endonuclease superfamily (Chandler et al., 2013). HUH transposases of the IS*91* family catalyze the transposition of their cognate IS by the rolling-circle replication of the element from one boundary, named *ori*IS, to the other referred to as the *ter*IS (Tavakoli et al., 2000; del Pilar Garcillán-Barcia et al., 2001; Yassine et al., 2015). However, so far, there is no experimental evidence for transposition of any of the IS*CR* elements. Four out of the fifteen members of the IS*CR* family are commonly found in γ-proteobacteria, namely IS*CR1*, IS*CR2*, IS*CR3* and IS*CR5*, and IS*CR1* predominates in strains isolated in clinical settings (Toleman et al., 2006). IS*CR1* was first identified as a conserved region disrupting the 3′ conserved segment (3′CS) of class 1 integrons

(**Figure 1A**; Stokes et al., 1993). The region downstream of IS*CR1* (*ori*IS side) is variable and often associated with ARG (Arduino et al., 2002; Toleman et al., 2006; Rodríguez-Martínez et al., 2007; Wachino et al., 2011). Previous studies identified the presence of two putative promoters located on the *ori*IS side of the IS*CR1*, namely P_{CR1-1} and P_{CR1-2}, suggesting that IS*CR1* could impact the expression of downstream genes (**Figure 1B**; Mammeri et al., 2005; Rodriguez-Martinez et al., 2006). To assess the potential function of these promoters in the expression of downstream genes, we first performed an extensive *in silico* analysis of all IS*CR1* sequences publically available (GenBank®) to determine the diversity of putative downstream ARGs. Here, we show experimentally by means of a reporter gene assay that IS*CR1* directly contributes to the expression of different ARGs via these two P_{OUT} promoters.

MATERIALS AND METHODS

Bacterial Strains and Plasmids

Bacterial strains and plasmids are listed in (**Supplementary Table S1**). Bacterial strains were grown in Lysogeny Broth (LB) broth at 37°C. Media were supplemented with kanamycin (25 μg/mL) when required.

Plasmid Constructions

We used the reporter plasmid pSU38Δtot*lacZ* (Jové et al., 2010) and three derived plasmids in which IS*CR1* and/or regions adjacent to IS*CR1* were inserted in transcriptional fusion with the reporter gene *lacZ*. Fragments of IS*CR1* and/or regions adjacent to IS*CR1* were amplified from two *Salmonella enterica* subsp. *enterica* strains carrying IS*CR1* followed by either $bla_{CTX-M-9}$, or *dfrA19* genes (Espéli et al., 2001) as they belong to the most prevalent antibiotic resistance gene families found in the variable region downstream IS*CR1*. Primers (Sigma-Aldrich®) used for cloning are listed in **Supplementary Table S2**. For each construction, amplifications were performed using the Phusion® Polymerase (Thermo Fisher Scientific). PCR products were loaded and visualized by means of a 0.8% agarose gel, extracted and purified with the Wizard® SV Gel and PCR Clean-Up System (Promega, Madison, WI, United States). PCR products were cloned into the EcoRI and BamHI unique restriction sites of pSU38Δtot*lacZ*. Transformants were selected on LB medium supplemented with kanamycin. Recombinant plasmids were verified by PCR with primers targeting the insert and by sequencing.

β-Galactosidase Assays

β-galactosidase assays were performed in the *E. coli* MG1656 strain (**Supplementary Table S1**; Espéli et al., 2001) as previously described (Miller, 1993) for nine independent assays for each construct.

Minimum Inhibitory Concentration (MIC) Determination

Minimum inhibitory concentrations were performed by the microdilution method in Mueller-Hinton broth in three independent experiments as recommended by the French Antibiogram committee guidelines[1].

Statistical Analysis

Statistical analyses were performed using the Mann-Whitney test with two paired groups.

GenBank® IS*CR1* Element Sequence Analysis

The amino acid sequence of the RCR1 transposase encoded by IS*CR1* (accession number CAJ84008) was blasted with BLASTp (NCBI). The matching sequences were filtered to retain RCR1 peptide sequences with an amino acid identity level (equal or) higher than 98%. Corresponding nucleotide sequences in which the *ori*IS region was partial or truncated were discarded. The remaining nucleotide sequences were sorted out in 93 groups according to the nature of the first gene adjacent to IS*CR1*: non-annotated nucleotide sequences with identified open reading frame (ORF) longer than 150 bp were included into the analysis. To define a novel gene group, we used a cut-off of 95% amino acid identity of the encoded protein, except for antimicrobial resistance genes (ARGs) for which a single amino-acid variation was used as threshold for inclusion into a group. Finally, one nucleotide sequence representing each gene group was submitted to blastN to identify previously non-annotated nucleotide sequences (only 100% identical sequences were kept). This data extraction was performed on 2017-01-19.

Quantification of $bla_{CTX-M-9}$ and *dfrA19* Transcripts

Total RNA was extracted with the NucleoSpin® RNA Extraction Kit (Macherey-Nagel Inc.). Contaminating DNA was removed from RNA samples by using the Turbo DNA-free Kit (Ambion). cDNAs were synthesized from 1 μg of DNase-treated total RNA by using PrimeScript™ RT Reagent kit (TaKaRa Clontech). cDNA was quantified by PerfeCTa® SYBR® Green FastMix® Kit (Quanta BioSciences™) with adequate oligonucleotides (**Supplementary Table S2**). Three independent experiments were performed, each in triplicate. Relative expressions of the $bla_{CTX-M-9}$ (Primers 16 and 17) and *dfrA19* (Primers 18 and 19) genes were estimated by normalizing transcript copy number to those of the housekeeping gene *rpoB* (Primer 20 and 21). The impact of IS*CR1 ori*IS has been calculated as ratio between the relative expression of each gene in presence and in absence of the IS*CR1 ori*IS.

RESULTS AND DISCUSSION

Diversity of the IS*CR1* Downstream Genes

In this study, 1127 distinct sequences containing the IS*CR1* element extracted from GenBank® were analyzed *in silico*. The

[1]http://www.sfm-microbiologie.org/UserFiles/files/casfm/CASFMV1_0_MARS_2017.pdf

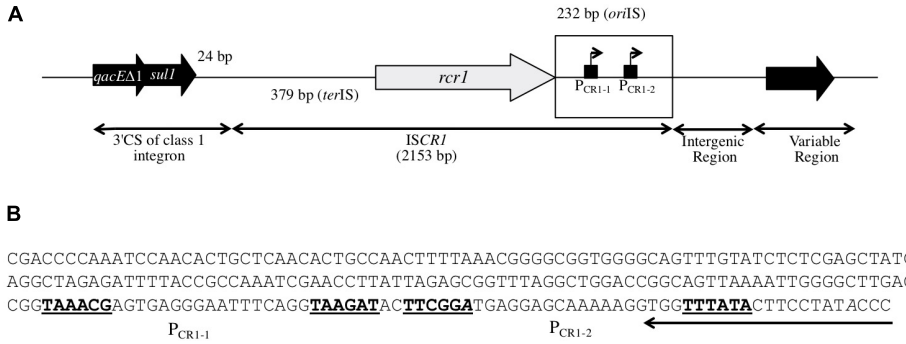

FIGURE 1 | Structure of IS*CR1*. **(A)** Schematic representation of the IS*CR1* element in its genetic context. IS*CR1* is inserted 24 bp downstream of the *sul1* gene (sulfonamide resistance gene) found in the class 1 integrons 3′ Conserved Segment (3′CS). IS*CR1* is flanked by an *ori*IS-(232 bp) and a *ter*IS-containing region (379 bp). It includes a *rcr1* transposase gene, the P*rcr1* promoter for *rcr1* and two putative outward P_{CR1-1} and P_{CR1-2} promoters. A variable region is located downstream IS*CR1*, separated by an intergenic region. The *ori*IS-containing region is boxed. **(B)** Nucleotide sequence of the 232 bp *ori*IS-containing region of IS*CR1*. The *ori*IS sequence that delimitates IS*CR1* is highlighted. The –35 and –10 elements of the putative P_{CR1-1} and P_{CR1-2} promoters are written in bold. Their corresponding transcriptional start sites as previously mapped are indicated in italics.

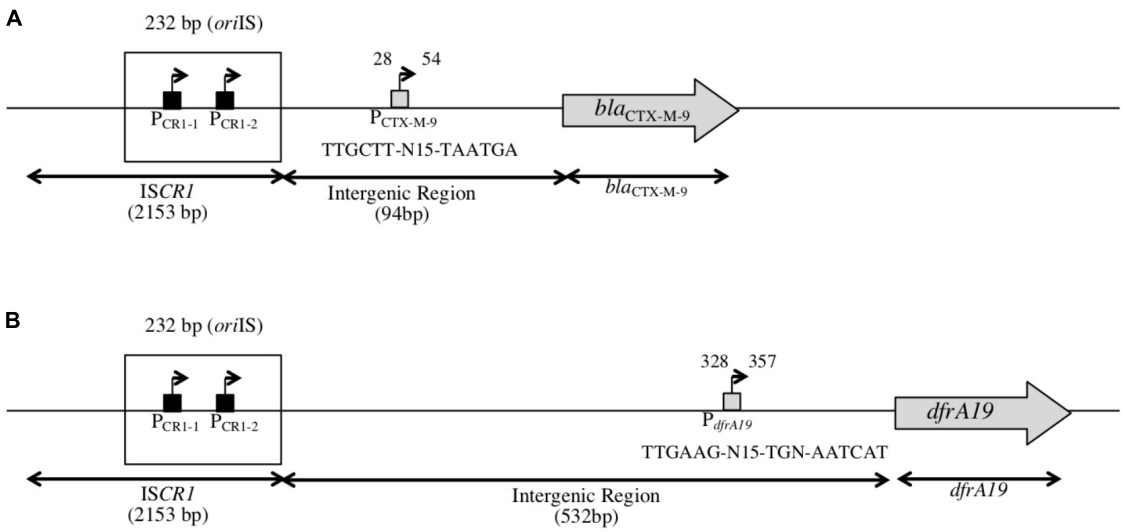

FIGURE 2 | Structure of the genetic context of $bla_{CTX-M-9}$ and *dfrA19* genes downstream of IS*CR1*. **(A)** Schematic representation of the genetic context of $bla_{CTX-M-9}$ as found in our *in silico* analysis, located 94 bp away from IS*CR1* (accession number: AF174129). $P_{CTX-M-9}$ indicates a putative promoter for $bla_{CTX-M-9}$ located in the intergenic region, 28 bp away from IS*CR1*. **(B)** Schematic representation of the genetic context of *dfrA19* as found in our *in silico* analysis, located 532 bp away from IS*CR1* (accession number: AM234698). *dfrA19* indicates a putative promoter for *dfrA19* located in the intergenic region, 328 bp away from IS*CR1*.

majority of these sequences was recovered from γ-proteobacteria (99.9%) while others were found to be present in uncultured bacteria ($n = 4$) (**Supplementary Table S3**). All IS*CR1* sequences in this study were associated with the 3′ CS region of class 1 integrons (left-hand side, **Figure 1**). In contrast, the downstream region of IS*CR1* was identified to be very variable (right-hand side, **Figure 1**). Interestingly, a large percentage of the analyzed IS*CR1* elements ($n = 946$, 84%) carried an adjacent gene oriented in the same direction as the *rcr1* encoding transposase gene (top strand). This suggests that these genes might be expressed from the IS*CR1* P_{OUT} promoters (**Figure 1**). The functions of these top strand genes adjacent to IS*CR1* fell into three categories (**Supplementary Table S4**). The most represented genes ($n = 429$) encoded truncated insertion sequence transposases, most often IS*Ec28* ($n = 418$), more rarely IS*Ec29*, IS*Aba125* or IS*Ecp1* (**Supplementary Table S4**). The second most important group ($n = 379$) was identified as known or putative ARGs encoding resistance to five families of antibiotics: trimethoprim ($n = 125$), β-lactams (including extended-spectrum β-lactamase, ESBL, genes) ($n = 121$), quinolones ($n = 113$), chloramphenicol ($n = 12$), and aminoglycosides ($n = 8$). For each antibiotic family, different genes or alleles were identified, that may lead to different resistance phenotypes (**Supplementary Table S4**). The last group ($n = 138$) includes genes involved in other cellular process or genes of unknown function (**Supplementary Table S4**).

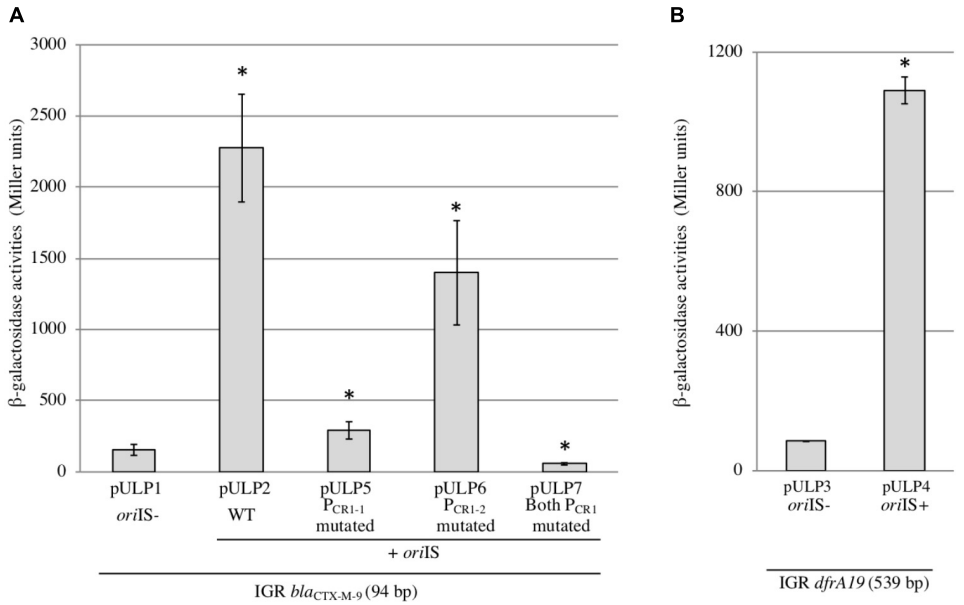

FIGURE 3 | Activities and characterization of the IS*CR1* P_{OUT} promoters. β-galactosidase activities were measured from *lacZ*-transcriptional fusions with the intergenic region (IGR) cloned either in absence (*ori*IS–) or in presence (*ori*IS+) of the 232 bp long IS*CR1 ori*IS region. The genes tested were $bla_{CTX-M-9}$ **(A)** and *dfrA19* **(B)**. Derivatives in which one or both P_{CR1} promoters were mutated were also tested for $bla_{CTX-M-9}$ **(A)**. Constructions are described in (**Supplementary Table S1**). The results are the average of at least three independent experiments. *$p < 0.001$.

IS*CR1* Contributes to the Downstream Expression of ARGs via Its P_{OUT} Promoters

To investigate the impact of P_{OUT} promoters on the expression of downstream genes, we focused on the two following ARGs: $bla_{CTX-M-9}$ (conferring an Extended-Spectrum Beta-Lactamase resistance phenotype) (accession number: AM234698) and *dfrA19* (resistance to trimethoprim) (accession number: AF174129), which were the ARG sequences most frequently found in our *in silico* analysis. Their coding sequences are located 94 and 532 bp away from the *ori*IS, respectively (**Figure 2**); this distance is thereafter referred as to the intergenic region or IGR. We cloned each IGR in front of the promoter-less *lacZ* gene in absence or in presence of the IS*CR1 ori*IS region (that contains the P_{OUT} promoters) and compared the resulting β-galactosidase activities. When the *lacZ* coding sequence was preceded by each IGR alone, the level of β-galactosidase activity ranged from 84 MU (Miller Units) to 155 MU for *dfrA19*, and $bla_{CTX-M-9}$, respectively (**Figure 3A**, pULP1 and **Figure 3B**, pULP3). These results indicate the presence of a functional promoter in each IGR. Accordingly, a conserved σ^{70} promoter sequence was identified in the IGR of $bla_{CTX-M-9}$ (TTGCTT-N_{15}-TAATGA) and *dfrA19* (TTGAAG-N_{15}-TGN-AATCAT), which could account for the observed β-galactosidase expression (**Figure 2**). However, when both the *ori*IS and the IGR were present, the β-galactosidase activity was enhanced by 13- and 15-fold for *dfrA19* and $bla_{CTX-M-9}$, respectively (**Figure 3A**, pULP2 and **Figure 3B**, pULP4). These results indicate that the IS*CR1 ori*IS region significantly increases the expression level of downstream genes and confirm that IS*CR1* harbors a functional P_{OUT} promoter. We thus showed that both IS*CR1 ori*IS and IGR are involved in gene expression of *dfrA19* and $bla_{CTX-M-9}$. However, as we observed in our *in silico* analysis (**Supplementary Table S4**), the sequence and length of the IGR vary from 0 to 1211 bp. Further analysis with other IS*CR1* elements with different downstream genes are needed to elucidate to which extent the sequence of the IGR contribute to downstream gene expression.

To determine whether the positive effect of the IS*CR1 ori*IS on the expression of the downstream gene relies on the two P_{OUT} promoters, P_{CR1-1} (TAAACG-N_{17}-TAAGAT) and P_{CR1-2} (TTCGGA-N_{18}-TTTATA), we constructed derivatives of pULP2 (*ori*IS-$IGR_{CTX-M-9}$-*lacZ*) in which the putative −10 element, of either P_{CR1-1} or P_{CR1-2} or both promoters was mutated. Mutation of P_{CR1-1} (pULP5) or P_{CR1-2} (pULP6) reduced by 85 and 40%, respectively, the overall β-galactosidase activity compared to the pULP2 wild-type construction (**Figure 2A**). Concomitant mutations of both P_{CR1-1} and P_{CR1-2} dropped the expression to the basal level detected in absence of *ori*IS (**Figure 3A**, pULP7 versus pULP1). These results indicated that both P_{CR1-1} and P_{CR1-2} are functional and, together, are responsible for the contribution of IS*CR1* to the expression of downstream top strand genes. Consistently, several earlier reports mapped transcriptional START sites in the *ori*IS that are compatible with the P_{CR1-1} and P_{CR1-2} (Mammeri et al., 2005; Rodriguez-Martinez et al., 2006). P_{CR1-1} also appears to be stronger than P_{CR1-2} in agreement with its higher conservation degree of its −10 hexamer, with respect to the σ70 consensus sequence (four bases out of six versus three for P_{CR1-2}). These

tandem promoters display a synergistic effect but the exact underlying mechanisms remain to be elucidated.

The IS*CR1 ori*IS Is Required to Confer the $bla_{CTX-M-9}$-Mediated Resistance

To assess whether the increased level of gene expression due to the IS*CR1 ori*IS region has a phenotypic impact, we measured the level of resistance conferred by *dfrA19* and $bla_{CTX-M-9}$ genes in absence or in presence of the *ori*IS region in *Escherichia coli*. For this purpose, each gene was cloned in pSU38Δtot*lacZ* (**Supplementary Table S1**) with its own IGR preceded or not by the *ori*IS region. Subsequently, we determined the MIC of the respective clones in presence of the corresponding antibiotic (cefotaxime or trimethoprim) (see below). The *Escherichia coli* MG1655*lac*- strain harboring the empty plasmid (pSU38Δtot*lacZ*) was susceptible to both cefotaxime (MIC $<$ 0.5 μg/mL) and trimethoprim (MIC $<$ 4 μg/mL). When MG1655*lac*- is transformed with a pSU38Δtot*lacZ* derivative that harbors the $bla_{CTX-M-9}$ coding sequence alone (pULP13) or preceded by its own IGR (pULP12), the MIC for cefotaxime was also $<$0.5 μg/mL. The MIC for cefotaxime significantly increased in pULP11 which contains both IGR and *ori*IS region (MIC $>$ 512 μg/mL). These findings demonstrated that the IS*CR1 ori*IS region is required for $bla_{CTX-M-9}$ to confer a cefotaxime resistant phenotype, most likely mediated by the activity of P_{CR1-1} and P_{CR1-2}. We performed quantification of transcripts and showed that the $bla_{CTX-M-9}$ transcript number increased by 99-fold (98.82 ± 8.29) in presence of IGR. These results correlate with MIC findings.

In contrast, when preceded by its IGR, the level of trimethoprim resistance conferred by *dfrA19* was similar in absence or in presence of the *ori*IS region (pULP08 MIC = $>$ 2048 μg/mL, pULP09 MIC = $>$ 2048 μg/mL), while the *dfrA19* coding sequence alone did not confer any resistance (pULP10, MIC $<$ 4 μg/mL). Susceptibility to higher concentrations of trimethoprim could not be determined since they excess its solubility in DMSO. The *dfrA19* resistance gene confers a higher level of resistance compared to other *dfrA* alleles, such as *dfrA10* for example (MIC: 500 μg/mL) (Parsons et al., 1991). We observed a similar resistance phenotype (trimethoprim MIC = $>$ 2048 μg/mL) in absence or in presence of the *ori*IS region. These results were surprising according to β-galactosidase results obtained with or without the IGR sequence (**Figure 3**). Quantification of transcripts of *dfrA19* confirmed that the IGR plays a role in the expression of the gene. Indeed, we obtained a 20-fold change of transcript number (20.03 ± 4.1, *dfrA19*) in presence of IGR. Such dissociation between the resistance phenotype and the level of gene expression has been previously described (Barraud and Ploy, 2015). Furthermore, this might also be explained by the nature of the enzyme encoded by *dfr* genes. Indeed, DFR enzymes are insensitive toward trimethoprim, so neither a high concentration of antibiotic nor the quantity of DFR enzymes will affect the level of resistance. Little is known about the *dfrA19* gene and noticeably, it seems to only occur associated with IS*CR1* element.

CONCLUSION

Our data highlight the functionality of the two P_{OUT} promoters carried by the IS*CR1* element. The fact that those two functional P_{OUT} promoters contribute to the expression of various downstream genes, including ARG may explain why IS*CR1* is so frequent in clinical settings. Indeed, IS*CR1* gives an advantage to the bacteria for antimicrobial resistance expression and one can hypothesize that antibiotic selective pressure has promoted the selection of IS*CR1*-carrying bacteria.

AUTHOR CONTRIBUTIONS

M-CP and TJ conceived the study. TJ coordinated the study. CL, TJ, and CP performed the experiments. All authors analyzed the data and wrote the manuscript.

FUNDING

CL gratefully acknowledges the Ministère de l'Enseignement Supérieur, de la Recherche et de l'Innovation (MESRI), and the Fonds Européen de Développement Régional (FEDER) for her doctoral training grant. The funders had no role in study design, data collection and interpretation, or the decision to submit the work for publication.

ACKNOWLEDGMENTS

We thank Amy Gassama for providing us with the *S. enterica* subsp. *enterica* serovar Keurmassar strain and Manon Mellier for her assistance. We also thank Elena Buelow for critical reading of the manuscript.

SUPPLEMENTARY MATERIAL

The Supplementary Material for this article can be found online at: https://www.frontiersin.org/articles/10.3389/fmicb.2018.02579/full#supplementary-material

REFERENCES

Aminov, R. I. (2011). Horizontal gene exchange in environmental microbiota. *Front. Microbiol.* 2:158. doi: 10.3389/fmicb.2011.00158

Arduino, S. M., Roy, P. H., Jacoby, G. A., Orman, B. E., Pineiro, S. A., and Centron, D. (2002). $bla_{CTX-M-2}$ is located in an unusual class 1 integron (In35) which includes Orf513. *Antimicrob. Agents Chemother.* 46, 2303–2306. doi: 10.1128/AAC.46.7.2303-2306.2002

Barraud, O., and Ploy, M.-C. (2015). Diversity of class 1 integron gene cassette rearrangements selected under antibiotic pressure. *J. Bacteriol.* 197, 2171–2178. doi: 10.1128/JB.02455-14

Chandler, M., de la Cruz, F., Dyda, F., Hickman, A. B., Moncalian, G., and Ton-Hoang, B. (2013). Breaking and joining single-stranded DNA: the HUH endonuclease superfamily. *Nat. Rev. Microbiol.* 11, 525–538. doi: 10.1038/nrmicro3067

del Pilar Garcillán-Barcia, M., Bernales, I., Mendiola, M. V., and de la Cruz, F. (2001). Single-stranded DNA intermediates in IS*91* rolling-circle transposition. *Mol. Microbiol.* 39, 494–501. doi: 10.1046/j.1365-2958.2001.02261.x

Espéli, O., Moulin, L., and Boccard, F. (2001). Transcription attenuation associated with bacterial repetitive extragenic BIME elements. *J. Mol. Biol.* 314, 375–386. doi: 10.1006/jmbi.2001.5150

Garnier, F., Raked, N., Gassama, A., Denis, F., and Ploy, M.-C. (2006). Genetic environment of quinolone resistance gene *qnrB2* in a complex *sul1*-type integron in the newly described *Salmonella enterica* serovar Keurmassar. *Antimicrob. Agents Chemother.* 50, 3200–3202. doi: 10.1128/AAC.00293-06

Goussard, S., Sougakoff, W., Mabilat, C., Bauernfeind, A., and Courvalin, P. (1991). An IS*1*-like element is responsible for high-level synthesis of extended-spectrum β-lactamase TEM-6 in enterobacteriaceae. *Microbiology* 137, 2681–2687.

Jové, T., Da, Re, S., Denis, F., Mazel, D., and Ploy, M.-C. (2010). Inverse correlation between promoter strength and excision activity in class 1 integrons. *PLoS Genet.* 6:e1000793. doi: 10.1371/journal.pgen.1000793

Mammeri, H., Loo, M. V. D., Poirel, L., Martinez-Martinez, L., and Nordmann, P. (2005). Emergence of plasmid-mediated quinolone resistance in *Escherichia coli* in Europe. *Antimicrob. Agents Chemother.* 49, 71–76. doi: 10.1128/AAC.49.1.71-76.2005

Miller, J. H. (1993). *A Short Course In Bacterial Genetics: A Laboratory Manual And Handbook For Escherichia coli And Related Bacteria*. Cold Spring Harbor, NY: Cold Spring Harbor Laboratory Press.

Parsons, Y., Hall, R. M., and Stokes, H. W. (1991). A new trimethoprim resistance gene, dhfrX, in the In7 integron of plasmid pDGO100. *Antimicrob. Agents Chemother.* 35, 2436–2439. doi: 10.1128/AAC.35.11.2436

Partridge, S. R. (2011). Analysis of antibiotic resistance regions in gram-negative bacteria. *FEMS Microbiol. Rev.* 35, 820–855. doi: 10.1111/j.1574-6976.2011.00277.x

Rodriguez-Martinez, J.-M., Poirel, L., Canton, R., and Nordmann, P. (2006). Common region CR1 for expression of antibiotic resistance genes. *Antimicrob. Agents Chemother.* 50, 2544–2546. doi: 10.1128/AAC.00609-05

Rodríguez-Martínez, J. M., Velasco, C., García, I., Cano, M. E., Martínez-Martínez, L., and Pascual, A. (2007). Characterisation of integrons containing the plasmid-mediated quinolone resistance gene *qnrA1* in *Klebsiella pneumoniae*. *Int. J. Antimicrob. Agents* 29, 705–709. doi: 10.1016/j.ijantimicag.2007.02.003

Simpson, A. E., Skurray, R. A., and Firth, N. (2000). An IS257-derived hybrid promoter directs transcription of a tetA(K) tetracycline resistance gene in the *Staphylococcus aureus* chromosomal mecregion. *J. Bacteriol.* 182, 3345–3352. doi: 10.1128/JB.182.12.3345-3352.2000

Stokes, H. W., Tomaras, C., Parsons, Y., and Hall, R. M. (1993). The partial 3"-conserved segment duplications in the integrons In6 from pSa and In7 from pDGO100 have a common origin. *Plasmid* 30, 39–50. doi: 10.1006/plas.1993.1032

Tavakoli, N., Comanducci, A., Dodd, H. M., Lett, M.-C., Albiger, B., and Bennett, P. (2000). IS*1294*, a DNA element that transposes by RC transposition. *Plasmid* 44, 66–84. doi: 10.1006/plas.1999.1460

Toleman, M. A., Bennett, P. M., and Walsh, T. R. (2006). IS*CR* elements: novel gene-capturing systems of the 21st century? *Microbiol. Mol. Biol. Rev.* 70, 296–316. doi: 10.1128/MMBR.00048-05

Vandecraen, J., Chandler, M., Aertsen, A., and Van Houdt, R. (2017). The impact of insertion sequences on bacterial genome plasticity and adaptability. *Crit. Rev. Microbiol.* 43, 709–730. doi: 10.1080/1040841X.2017.1303661

Wachino, J.-I., Yoshida, H., Yamane, K., Suzuki, S., Matsui, M., Yamagishi, T., et al. (2011). SMB-1, a novel subclass B3 metallo- -lactamase, associated with ISCR1 and a class 1 integron, from a carbapenem-resistant *Serratia marcescens* clinical isolate. *Antimicrob. Agents Chemother.* 55, 5143–5149. doi: 10.1128/AAC.05045-11

Yassine, H., Bientz, L., Cros, J., Goret, J., Bebear, C., Quentin, C., et al. (2015). Experimental evidence for IS*1294b*-mediated transposition of the blaCMY-2 cephalosporinase gene in enterobacteriaceae. *J. Antimicrob. Chemother.* 70, 697–700. doi: 10.1093/jac/dku472

Conflict of Interest Statement: The authors declare that the research was conducted in the absence of any commercial or financial relationships that could be construed as a potential conflict of interest.

frontiers in Microbiology

ORIGINAL RESEARCH
published: 19 November 2018
doi: 10.3389/fmicb.2018.02664

Conjugative Transfer of a Novel Staphylococcal Plasmid Encoding the Biocide Resistance Gene, *qacA*

*Patrick T. LaBreck[1], Gregory K. Rice[2,3], Adrian C. Paskey[1,2], Emad M. Elassal[4,5], Regina Z. Cer[2,3], Natasha N. Law[4,5,6], Carey D. Schlett[4,5], Jason W. Bennett[7,8], Eugene V. Millar[4,5], Michael W. Ellis[9], Theron Hamilton[2], Kimberly A. Bishop-Lilly[2] and D. Scott Merrell[1,8]**

[1] Department of Microbiology and Immunology, Uniformed Services University of the Health Sciences, Bethesda, MD, United States, [2] Naval Medical Research Center, Biological Defense Research Directorate, Fort Detrick, MD, United States, [3] Leidos, Reston, VA, United States, [4] Henry M. Jackson Foundation for the Advancement of Military Medicine, Rockville, MD, United States, [5] Infectious Diseases Clinical Research Program, Department of Preventive Medicine and Biostatistics, Uniformed Services University of the Health Sciences, Bethesda, MD, United States, [6] Martin Army Community Hospital, Fort Benning, GA, United States, [7] Walter Reed Army Institute of Research, Silver Spring, MD, United States, [8] Department of Medicine, Uniformed Services University of the Health Sciences, Bethesda, MD, United States, [9] University of Toledo College of Medicine and Life Sciences, Toledo, OH, United States

OPEN ACCESS

Edited by:
Katy Jeannot, UMR6249 Chrono Environnement, France

Reviewed by:
Edgardo Sepulveda, Centro de Investigación Científica y de Educación Superior de Ensenada (CICESE), Mexico
Yajun Song, Beijing Institute of Microbiology and Epidemiology, China

***Correspondence:**
D. Scott Merrell
douglas.merrell@usuhs.edu

Specialty section:
This article was submitted to Antimicrobials, Resistance and Chemotherapy, a section of the journal Frontiers in Microbiology

Received: *13 August 2018*
Accepted: *18 October 2018*
Published: *19 November 2018*

Citation:
LaBreck PT, Rice GK, Paskey AC, Elassal EM, Cer RZ, Law NN, Schlett CD, Bennett JW, Millar EV, Ellis MW, Hamilton T, Bishop-Lilly KA and Merrell DS (2018) Conjugative Transfer of a Novel Staphylococcal Plasmid Encoding the Biocide Resistance Gene, qacA. Front. Microbiol. 9:2664. doi: 10.3389/fmicb.2018.02664

Staphylococcus aureus is the leading cause of skin and soft tissue infections (SSTI). Some *S. aureus* strains harbor plasmids that carry genes that affect resistance to biocides. Among these genes, *qacA* encodes the QacA Multidrug Efflux Pump that imparts decreased susceptibility to chlorhexidine, a biocide used ubiquitously in healthcare facilities. Furthermore, chlorhexidine has been considered as a *S. aureus* decolonization strategy in community settings. We previously conducted a chlorhexidine-based SSTI prevention trial among Ft. Benning Army trainees. Analysis of a clinical isolate (C02) from that trial identified a novel *qacA*-positive plasmid, pC02. Prior characterization of *qacA*-containing plasmids is limited and conjugative transfer of those plasmids has not been demonstrated. Given the implications of increased biocide resistance, herein we characterized pC02. *In silico* analysis identified genes typically associated with conjugative plasmids. Moreover, pC02 was efficiently transferred to numerous *S. aureus* strains and to *Staphylococcus epidermidis*. We screened additional *qacA*-positive *S. aureus* clinical isolates and pC02 was present in 27% of those strains; other unique *qacA*-harboring plasmids were also identified. Ten strains were subjected to whole genome sequencing. Sequence analysis combined with plasmid screening studies suggest that *qacA*-containing strains are transmitted among military personnel at Ft. Benning and that strains carrying *qacA* are associated with SSTIs within this population. The identification of a novel mechanism of *qacA* conjugative transfer among Staphylococcal strains suggests a possible future increase in the prevalence of antiseptic tolerant bacterial strains, and an increase in the rate of infections in settings where these agents are commonly used.

Keywords: antiseptic, Chlorhexidine digluconate, *Staphylococcus aureus*, plasmid acquisition, conjugation

IMPORTANCE

QacA is known to decrease bacteria susceptibility to chlorhexidine. Given the profound implications of increased resistance to chlorhexidine, it is vital to understand the mechanisms that contribute to the spread of *qacA* among bacteria. Analysis of a clinical *S. aureus* isolate revealed the first direct evidence of horizontal transfer of *qacA* across strains; transfer was mediated via a conjugative plasmid, pC02. In addition to transfer of *qacA* to multiple *S. aureus* strains, the plasmid was also conjugated to other members of the Staphylococcus genus. The *S. aureus* strain that harbors the *qacA*-positive conjugative plasmid was associated with a SSTI cluster among military trainees. The identification of *qacA* on a conjugative plasmid within a clinically successful strain stresses the importance of continued surveillance for *qacA* in *S. aureus* clinical isolates and underscores current efforts for increased antiseptic stewardship.

INTRODUCTION

Community-Associated Methicillin-resistant *Staphylococcus aureus* (CA-MRSA) infections are a significant issue in the United States, and it is estimated that they are responsible for 65% of all MRSA infections (Dukic et al., 2013). In contrast to Healthcare-Associated MRSA (HA-MRSA), which typically only infects individuals with comorbidities, CA-MRSA is a common cause of skin and soft tissue infections (SSTI) in healthy populations. While overall CA-MRSA rates are climbing, certain populations are disproportionately affected, including groups that live in confined settings, such as inmates and military trainees (Aiello et al., 2006; Beauparlant, 2016; Boivin et al., 2016).

Asymptomatic colonization with *S. aureus* is common; ∼30% of healthy individuals harbor *S. aureus* in the nares and as many as 20% of these individuals are persistently colonized (Kluytmans et al., 1997; Wertheim et al., 2005). Colonization of multiple body sites is known to occur (Albrecht et al., 2015; Singh et al., 2016), and colonization is a clear risk factor for *S. aureus* infection (Albrecht et al., 2015). Given these possibilities, decolonization of *S. aureus* has been employed as a disease prevention strategy (Buehlmann et al., 2008; Coates et al., 2009). Indeed, antimicrobials such as mupirocin and/or chlorhexidine can be administered to high-risk patients as a means to decolonize these individual and to decrease the potential for subsequent infections; several studies have shown decolonization with these agents as a successful means of reducing HA-MRSA infections (Buehlmann et al., 2008; Septimus and Schweizer, 2016). These successful colonization interventions within the hospital setting have prompted calls for a similar approach for the prevention of CA-MRSA (Fritz et al., 2011; Ellis et al., 2014; Karanika et al., 2016; Tidwell et al., 2016).

Two interventional trials among military trainees previously evaluated the effectiveness of chlorhexidine against SSTI (Morrison et al., 2013; Ellis et al., 2014). The trial among Army trainees at Fort Benning, Georgia specifically examined the effectiveness of a once-weekly use of chlorhexidine-based body wash (HibiClens) (Ellis et al., 2014). Trainees in groups randomized to use chlorhexidine received a bottle of 4% chlorhexidine soap to use for their extra weekly shower. Participants were monitored for SSTI, and those with purulent SSTI had abscess and nasal swabs taken. The swabs were used for bacterial culture and isolates of *S. aureus* were collected.

Given the concern that exposure to any antimicrobial can select for resistant isolates, each of the isolates was subsequently screened for increased chlorhexidine resistance as defined by the positive detection of *qacA/B* by real-time PCR; these genes encode for the QacA/B efflux pumps that are associated with decreased susceptibility to chlorhexidine. Of 615 isolates, 1.6% were shown to be *qacA/B*-positive (Schlett et al., 2014). This prevalence of *qacA/B* positive isolates is comparable to previous prevalence reports within North America (Longtin et al., 2011; Fritz et al., 2012; Popovich et al., 2014). However, the prevalence of *qacA/B* strains varies greatly and rates in North America are considerably lower than in Europe and Asia (Mayer et al., 2001; Noguchi et al., 2005; Ghasemzadeh-Moghaddam et al., 2014). The high rates of *qacA/B* presence in those areas of the world lead to concerns about the implication of bacteria with decreased susceptibility to biocides like chlorhexidine. Furthermore, while true "resistance" to chlorhexidine has yet to be observed, it is possible that the presence of *qacA* may provide a fitness advantage *in-vivo* to sub-optimal concentrations of chlorhexidine (Madden and Sifri, 2018).

Various studies have sought to understand the ability of individual Qac efflux pumps to mediate decreased susceptibility to antiseptics. For example, the QacA efflux pump has been shown to confer protection against quaternary ammonium compounds and to divalent organic cations like chlorhexidine. Conversely, while QacB is highly similar to QacA and is also part of the same major facilitator superfamily (MFS), QacB appears to offer little/no protection to divalent organic cations (Paulsen et al., 1996). The other Qac efflux pumps (QacC-QacJ and QacZ) are part of the Small Multidrug Transporter (SMR) family and each have various effects on antiseptic resistance (Furi et al., 2013; Wassenaar et al., 2015). The genes encoding the Qac efflux pumps are located on plasmids, which impacts possible mechanisms of spread of these genes across strains. For example, *qacC,* which is also known as *smr*, was previously found to be carried on conjugative plasmids as well as on small rolling circle plasmids (Littlejohn et al., 1991; Morton et al., 1993; Berg et al., 1998). Furthermore, transduction has been shown to facilitate transfer of plasmid-born *qacB* across strains. Conversely, *qacA* has only been found on large non-conjugative multidrug resistance plasmids; these plasmids lack the transfer, or *tra* genes, that are required for conjugative transfer (Tennent et al., 1989; McCarthy and Lindsay, 2012). As a result, horizontal transfer of *qacA* has not previously been documented (Nakaminami et al., 2007). Thus, it is not clear how or whether *qacA* is able to be horizontally spread across *S. aureus* strains, and if so, whether such spread could contribute to the prevalence of this factor in the *S. aureus* population.

Among the *qacA/B* positive strains obtained from the SSTI prevention trial (Ellis et al., 2014), we previously characterized a single clinical isolate, 2014.C02 (C02), obtained from a case of

SSTI in the chlorhexidine study group (Johnson et al., 2015). C02 showed a significant decrease in susceptibility to chlorhexidine and whole genome sequencing (WGS) revealed a novel 61.5 kb plasmid (pC02) that harbored *qacA*. Intriguingly, this plasmid showed limited homology to the prototypical *qacA*-positive plasmid (pSK1) that is found among *S. aureus* strains (Jensen et al., 2010). Sequence analysis of pC02 identified genes for resistance to cadmium, antiseptics, β-lactams and erythromycin (Johnson et al., 2015). Furthermore, the annotation of pC02 revealed potential conjugation genes. Given that horizontal transfer of *qacA* has not previously been demonstrated, we explored the ability of *qacA* to be mobilized across *S. aureus* strains. Herein we report the first evidence of conjugative transfer of *qacA* and show that this transfer can also occur to other members of the Staphylococcus genus; conjugal transfer was sufficient to mediate decreased susceptibility to chlorhexidine in the recipient strains. Detailed characterization of additional *qacA*/B clinical isolates that were identified in the study revealed several strains that harbored pC02, presenting the intriguing possibility that natural horizontal transfer of pC02 and concomitant reduced susceptibility to chlorhexidine may facilitate strain survival in this population.

MATERIALS AND METHODS

Bacterial Strains, Plasmids, and Growth Conditions

All the bacterial strains and plasmids used in this study are listed in **Table 1**. Strains were cultured in BBL™ Muller Hinton II (Cation-Adjusted) Broth (MHB) or Trypic Soy Broth (TSB) (Becton Dickinson, Franklin Lakes, NJ). For solid media, broth was supplemented with 1.7% agar (Alfa Aesar, Waltham, MA). Where needed, strains were cured of their plasmid as described in Udo et al. (1997). Briefly, a culture was grown overnight shaking at 37°C and then diluted 1:500 in TSB. This culture was grown at 42°C for 48 h and dilutions were then plated on TSA and grown at 37°C to obtain single colonies. Plates containing isolated colonies were replica plated to MHA and MHA supplemented with 20 μg/mL of cadmium chloride and then grown at 37°C. Cadmium sensitive colonies were double purified and screened with the pC02 PCR screen described below to test for the presence of the large plasmid(s). Large plasmid cured strains were made resistant to rifampin and novobiocin as previously described by selecting mutant strains that were resistant to rifampin (Sigma-Aldrich, St Louis, MO) followed by subsequent passage in increasing concentrations of novobiocin (Sigma) (Udo et al., 1997).

PFGE, Real-Time PCR, Antibiotic Susceptibility Testing

The strains isolated from Ft. Benning were globally characterized to define pulse field type, gene presence and antibiotic resistance patterns as previously described (Schlett et al., 2014).

Sequencing

DNA extraction for Pacbio sequencing was performed from overnight liquid cultures using phenol-chloroform extraction with the Easy-DNA kit (Invitrogen, Waltham, MA). The DNA samples were sent to the University of Maryland Institute for Genome Sciences and sequenced with Pacbio RSII (Pacific Biosciences, Menlo Park, CA).

DNA extraction for Illumina sequencing was performed from overnight liquid cultures using the Wizard Kit (Promega, Madison, WI) and libraries were produced using the Nextera XT DNA Library Preparation Kit (Illumina, Inc., San Diego, CA) according to the manufacturer's instructions. Libraries were multiplexed and sequenced using an Illumina MiSeq 600-cycle kit and 2 × 300 base pair read lengths. Sequence read quality was analyzed with FastQC (Andrews, 2016) and low-quality bases were trimmed with Sickle (Joshi and Fass, 2011). Illumina and Pacbio sequence reads were assembled using SPAdes (Bankevich et al., 2012) and plasmidSPAdes (Antipov et al., 2016). The resulting contig sequences were compared to each other, to published reference genomes, and to PCR, Sanger sequencing, and agarose gel electrophoresis results of restriction enzyme digested and non-digested DNA in order to correctly assign contigs as chromosomal or plasmid as well as to look for assembly artifacts.

In order to determine the closest published reference for single nucleotide variation (SNV) analysis, the longest contig from each assembly was aligned against the National Center for Biotechnology Information (NCBI) nucleotide database using BLAST (Altschul et al., 1990). Based on these results, *S. aureus* USA300 strain TCH1516 (NCBI accession number CP000730) was selected as the reference. SNV data were analyzed using methods previously described (Millar et al., 2017). Briefly, the Bacterial and Archaeal Genome Analyzer (Williams, 2016) a wrapper for proven third-party bioinformatics tools, was used. Sequence reads were mapped to the reference using BWA (Li and Durbin, 2009), and variant calls and filtering were performed with GATK (McKenna et al., 2010). Genomic regions that contained insertions/deletions (indels), potential chromosomal rearrangements, and sequence repeats known to increase the likelihood of false-positive variant calls were excluded from the SNV set. A multiple sequence alignment (MSA) was created from nucleotide substitutions, small deletions called by GATK, and putative large deletions detected in the BWA sequence alignments where no reads mapped. A maximum likelihood tree was constructed from the nucleic acid MSA using PhyML (version 3.2) (Guindon et al., 2010) tree search with the GTR substitution model. Areas in the MSA containing structural variants (indels) were masked in the PHYLIP representation of the MSA as undetermined nucleotides and excluded from consideration in phylogenetic tree construction. A full list of indels and SNVs are available as **Supplemental Tables 1**, **2**, respectively.

Gene content comparisons among strains were conducted using RAST for gene annotation and visualization (Aziz et al., 2008; Overbeek et al., 2014; Brettin et al., 2015).

Chlorhexidine Susceptibility Testing

The minimum inhibitory concentration (MIC) of chlorhexidine for each strain was tested as previously described (Johnson et al., 2015). Briefly, ∼1.5 × 10^5 colony forming units (CFU)

TABLE 1 | Bacterial strains used in the study.

Strain name[a]	Lab strain designation	Description[b]	Battalion and Company	Platoon[c]	Collection Date	Study Group[d]	Accession number of whole genome	MLST[e]	Antibiotic Susceptibility[f]	Real-time PCR Results[g]	References
S.aureus 2014.C01 (C01)	DSM1417	CI	A 2-58	4	12-Jul-11	CHG	CP012119.2	ST8	Ery^R,Lvx^R,Oxa^R,Sxt^S, Cli^S	*femA, mecA, pvl*	(Johnson et al., 2015)
S. aureus 2014.C02 (C02)	DSM1418	CI	A 2-58	4	21-Sep-11	CHG	CP012120.2	ST8	Ery^R,Lvx^R,Oxa^R,Sxt^S, Cli^S	*qacA, femA, mecA, pvl*	(Johnson et al., 2015)
S. aureus 1626.N	DSM1487	N	A 2-54	2	11-Mar-11	S	Not Sequenced	ST8	Ery^R,Lvx^S,Oxa^R,Sxt^S, Cli^S	*qacA, femA, mecA, mupA, pvl*	This study
S. aureus 2148.N	DSM1488	N	B 1-19	4	13-Oct-11	ES	CP016856.2	ST72	Ery^S,Lvx^S,Oxa^S,Sxt^S, Cli^S	*femA, pvl*	This study
S. aureus 5107.N	DSM1489	N	F 3-330	4	26-Jul-10	S	Not Sequenced	?	Ery^R,Lvx^S,Oxa^R,Sxt^S, Cli^S	*femA, mecA, pvl*	This study
S. aureus 5116.N	DSM1490	N	A 1-50	1	26-Jul-10	ES	Not Sequenced	ST8	Ery^R,Lvx^S,Oxa^R,Sxt^S, Cli^S	*femA, mecA*	This study
S. aureus 5118.N	DSM1491	N	E 3-330	2	26-Jul-10	S	CP016855.2	ST8	Ery^R,Lvx^S,Oxa^R,Sxt^S, Cli^S	*qacA, femA, mecA*	This study
S. aureus 3011.C01	DSM1493	CI	B 1-50	-	17-Mar-11	ES	Not Sequenced	ST8	Ery^R,Lvx^R,Oxa^R,Sxt^S, Cli^S	*femA, mecA, pvl*	this study
S. aureus 3020.C01	DSM1494	CI	A 2-58	-	19-Jul-11	CHG	CP025495.1	ST8	Ery^R,Lvx^R,Oxa^R,Sxt^S, Cli^S	*qacA, femA, mecA, pvl*	This study
S. aureus 1971.C01	DSM1495	CI	C 2-54	3	8-Sep-11	S	CP016858.2	ST8	Ery^R,Lvx^R,Oxa^R,Sxt^S, Cli^S	*qacA, femA, mecA, mupA, pvl*	This study
S. aureus 1624.C01	DSM1496	CI	A 2-54	2	11-Mar-11	S	Not Sequenced	ST8	Ery^R,Lvx^S,Oxa^R,Sxt^S, Cli^S	*qacA, femA, mecA, mupA, pvl*	This study
S. aureus 1626.C01	DSM1497	CI	A 2-54	2	11-Mar-11	S	MCID00000000.2	ST8	Ery^R,Lvx^S,Oxa^R,Sxt^S, Cli^S	*qacA, femA, mecA, mupA, pvl*	This study
S. aureus 1625.C01	DSM1498	CI	E 2-19	3	11-Mar-11	CHG	CP016863.2	ST8	Ery^R,Lvx^S,Oxa^R,Sxt^S, Cli^S	*femA, mecA, pvl*	this study
S. aureus 2148.C01	DSM1499	CI	B 1-19	4	11-Oct-11	ES	CP017094.2	ST8	Ery^R,Lvx^S,Oxa^S,Sxt^S, Cli^S	*qacA, femA, pvl*	This study
S. aureus 1534.C01	DSM1500	CI	B 2-58	1	29-Oct-10	CHG	Not Sequenced	ST8	Ery^R,Lvx^R,Oxa^R,Sxt^S, Cli^S	*femA, mecA, pvl*	This study
S. aureus 2075.N02	DSM1501	N	B 2-58	4	19-Sep-11	CHG	Not Sequenced	ST8	Ery^R,Lvx^S,Oxa^S,Sxt^S, Cli^S	*qacA, femA, pvl*	This study
S. aureus 2116.N02	DSM1502	N	B 2-58	4	28-Sep-11	CHG	Not Sequenced	ST8	Ery^R,Lvx^S,Oxa^S,Sxt^S, Cli^S	*qacA, femA, pvl*	This study
S. aureus 1960.N02	DSM1503	N	C 2-19	1	1-Sep-11	CHG	Not Sequenced	ST72	Ery^S,Lvx^S,Oxa^S,Sxt^S, Cli^R	*femA*	This study

(Continued)

TABLE 1 | Continued

Strain name[a]	Lab strain designation	Description[b]	Battalion and Company	Platoon[c]	Collection Date	Study Group[d]	Accession number of whole genome	MLST[e]	Antibiotic Susceptibility[f]	Real-time PCR Results[g]	References
S. aureus 1969.N	DSM1504	N	A 2-58	4	7-Sep-11	CHG	CP016861.2	ST8	Ery^R,Lvx^R,Oxa^R,Sxt^S, Cli^S	*qacA, femA, mecA, pvl*	This study
S. aureus C02-RN	DSM1553	Large plasmid-cured strain *S.aureus* C02, Cadmium sensitive, Rifampin and Novobiocin resistant							Ery^S, Cad^S, Rif^R, Nov^R	NT	This study
S. aureus 42-RN	DSM1573	*S. aureus* RN4220, Cadmium sensitive, Rifampin and Novobiocin resistant							Ery^S, Cad^S, Rif^R, Nov^R	NT	This study
S. aureus 25-RN	DSM1575	Large plasmid-cured 1625.C01, Cadmium sensitive, Rifampin and Novobiocin resistant							Ery^S, Cad^S, Rif^R, Nov^R	NT	This study
S. capitis RN	DSM1581	Erythromycin sensitive, Rifampin and Novobiocin resistant							Ery^S, Cad^R, Rif^R, Nov^R	NT	This study
S. epidermidis RP62A-RN	DSM1582	Cadmium sensitive, Rifampin and Novobiocin resistant							Ery^S, Cad^R, Rif^R, Nov^R	NT	(Gill et al., 2005)
E. faecalis OG1-RF	DSM1580	Erythromycin sensitive, Rifampin and Fusidic acid resistant							Ery^S, Cad^R, Rif^R, Fus^R	NT	(Dunny et al., 1978)
S. aureus C02-RN TC	DSM1671	Transconjugant obtained from 2014.C02 to C02-RN mating							Cad^R, Rif^R, Nov^R	NT	This study
S. aureus C02-RN TC2	DSM1672	Transconjugant obtained from 1969.N to C02-RN mating							Cad^R, Rif^R, Nov^R	NT	This study
S. aureus 42-RN TC	DSM1673	Transconjugant obtained from 2014.C02 to 42-RN mating							Cad^R, Rif^R, Nov^R	NT	This study
S. capitis RN TC	DSM1674	Transconjugant obtained from 2014.C02 to *S. capitis* RN mating							Ery^R, Rif^R, Nov^R	NT	This study

[a] *RN indicates rifampin novobiocin resistant lab generated strain. RF indicates rifampin and fusidic acid resistant lab generated strain.*

[b] *CI, Clinical Isolate; N, Nasal colonizing Isolate.*

[c] *–, no data available.*

[d] *CHG, Chlorhexidine. S, Standard. ES, Enhanced Standard. Standard indicates a preventative medical briefing and access to an SSTI clinic. Enhanced standard indicates the standard intervention, an additional shower each week and enhanced SSTI education and surveillance. Chlorhexidine indicates receipt of a bottle of 4% chlorhexidine soap to use for the extra weekly shower in addition to the interventions received in the enhanced standard group.*

[e] *MLST, Multilocus Sequence Type; ?, Novel sequence type.*

[f] *R, resistant; S, susceptible; Ery, erythromycin; Lvx, levofloxacin; Oxa, Oxacillin; Sxt, Sulfamethoxazole/Trimethoprim; Cli, Clindamycin; Cad, Cadmium; Rif, Rifampicin; Novo, Novobiocin; Fus, Fusidic acid. All clinical isolates were susceptible to linezolid, doxycycline, rifampin, vancomycin, gentamicin, and ceftaroline.*

[g] *genes shown to be present in strains by real-time PCR. NT, not tested.*

were inoculated into MHB containing increasing concentrations of purified (≥99.5%) chlorhexidine (Sigma). The cultures were grown at 37°C degrees overnight, shaking at 220 rpm. The MIC was determined by visual analysis of the culture's turbidity. Graphs were generated with Prism Software (GraphPad Software Inc., La Jolla, CA) with three independent replicates.

DNA Extraction, pC02 Plasmid Screening, MLST Sequencing

S. aureus strains were grown overnight in MHB and 1.5 mL of each sample was centrifuged to pellet the cells. Cell pellets were treated with 0.1 mg of lysostaphin for 30–45 min at 37°C and plasmid DNA was purified using the QIAprep Spin Miniprep Kit (Qiagen, Germantown, MD). Chromosomal DNA was purified using the Wizard Genomic DNA Purification Kit (Promega) after lysostaphin treatment of cells for 30–45 min.

The primer sequences used to PCR amplify the backbone of pC02 are listed in **Supplemental Table 3**. Initially, primers were designed to be evenly spaced around the pC02 plasmid but the original primer set that annealed in the 40,000 kb region yielded multiple products. Thus, these primers were redesigned, shifted upstream and became primer-pair 7. The PCRs were performed in 25 μL reactions containing nuclease-free water, plasmid DNA, GoTaq Green Master Mix (Promega), and 0.3 μM each of the forward and reverse primers (Integrated DNA Technologies, Coralville, IA). PCR cycling conditions were as follows: incubation at 95°C for 180 s, 28 cycles of 95°C for 30 s, 53°C for 30 s and 72°C for 160 s followed by a final extension of 72°C for 5 min. The reaction amplicons were separated and visualized on 1% agarose gels.

For strains that were not subjected to WGS, the *qacA/B* gene was amplified and a portion was sequenced as previously described (Johnson et al., 2015). Utilized primers are listed in **Supplemental Table 3**. The plasmid map image (**Figure 1**) was generated with AngularPlasmid http://angularplasmid.vixis.com (AngularPlasmid, 2015).

MLST was performed as previously described (Enright et al., 2000). The trimmed sequences of *arc*, *aroE*, *glpF*, *gmk*, *pta*, *tpi*, *yqi*, were submitted to the MLST website: http://saureus.mlst.net/ (Imperial College in London, United Kingdom) for typing.

Conjugative Transfer

Filter-mating experiments were completed similar to a previous description (Forbes and Schaberg, 1983). Briefly, for *S. aureus*, recipient and donor cells were grown overnight in MHB and then subcultured 1:50 in MHB the next day. The cells were grown to an OD_{600} of 0.3–0.4 and 0.25 mL of both the recipient and donor cultures were then added to 2.5 mL of prewarmed MHB. The cells were then collected on a 0.45 μm filter and placed cell-side down on prewarmed Muller Hinton II (Cation-Adjusted) Agar (MHA). The mating mixtures were incubated overnight at 37°C and the following morning, filters were removed from the agar and vortexed vigorously for 1 min in 1.5 mL of PBS to release the cells from the filter. 10 μL of the cell suspension was taken to determine the recipient CFU and the remaining cells were plated onto selective media. Recipient CFU were enumerated on MHA supplemented with 5 μg/mL of novobiocin sodium salt (Sigma) and 10 μg/mL of rifampicin (Sigma). The transconjugants were identified after 48–72 h of growth on MHA supplemented with 5 μg/mL novobiocin, 10 μg/mL of rifampicin and 20 μg/mL of cadmium chloride. For experiments where *Staphylococcus epidermidis* was the recipient, numbers of recipient cells were determined by plating on TSA supplemented with 5 μg/mL novobiocin sodium salt and 10 μg/mL rifampicin and transconjugants were enumerated after 48 h of growth on TSA supplemented with 5 μg/mL of novobiocin sodium salt, 10 μg/mL of rifampicin and 10 μg/mL of erythromycin. For conjugation experiments where *Enterococcus faecalis* was the recipient, MHB/MHA were substituted with TSB/Trypic Soy Agar (TSA), respectively, in order to obtain similar growth between *S. aureus* and *E. faecalis*. Numbers of recipient cells were determined by plating on TSA supplemented with 10 μg/mL fusidic acid sodium salt (Sigma) and 10 μg/mL rifampicin. The transconjugants were identified after 48 h of growth on TSA supplemented with 10 μg/mL of fusidic acid sodium salt, 10 μg/mL of rifampicin and 10 μg/mL of erythromycin (Sigma). In all cases, the conjugation frequency was determined by dividing the number of transconjugants by the number of recipient cells. The reported frequencies are the average of at least three independent experiments. To confirm that transconjugants actually contained the pC02 plasmid, a subset of the isolates were restreaked onto their appropriate selective media, and then screened by colony PCR using primer-pair 7 of the pC02 screen.

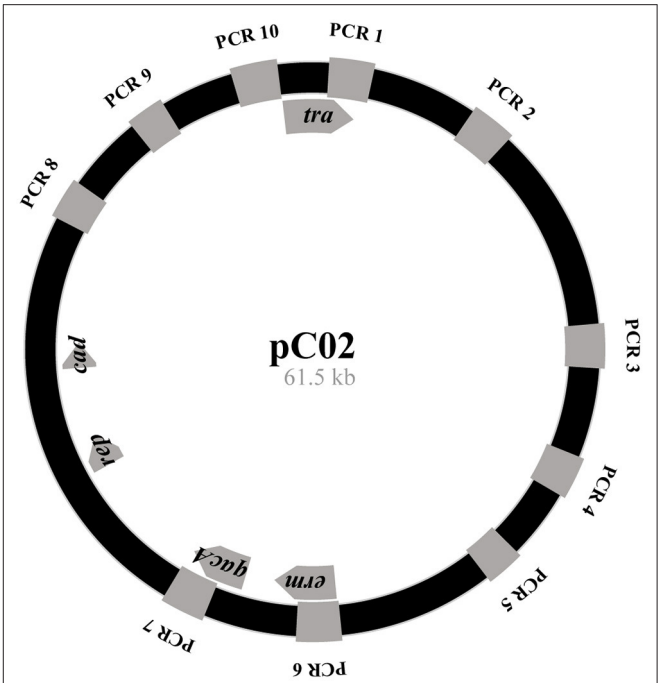

FIGURE 1 | Simplified pC02 plasmid map. Regions amplified during the pC02 PCR screen are indicated by gray boxes along the plasmid backbone. Genes of interest are labeled in the gray arrows: *cad* (cadmium resistance loci), *tra* (putative conjugation gene) *erm* (erythromycin resistance loci), *qacA* (*qacA/R* loci) *rep* (replication A). Image drawn to scale.

Transduction Control Assays

The possibility of movement of pC02 by phage was tested in several possible ways. First, the filter-mating protocol was conducted with the following modifications: 0.22 μm filter-sterilized supernatants (0.250 mL) from the C02 donor were mixed with 0.250 mL of the C02-RN recipient cells in 2.5 mL of MHB. This mixture was incubated at 30°C for 90 min, and then cells were collected on a 0.45 μm filter. Following collection on the 0.45 μm filter, the assay proceeded as described for the other filter-mating experiments.

Secondly, the necessity of cell-to-cell contact for conjugation was tested using a modified filter-mating assay. Briefly, C02 and C02-RN were grown to an OD_{600} of 0.3 to 0.4. 0.25 mL of both the C02-RN recipient and C02 donor cultures were individually added to separate culture flasks containing 2.5 mL of prewarmed MHB. The donor and recipient cells were individually collected on separate 0.45 μm filters. The recipient cell filter was placed cell-side-down on MHA and the donor cell filter was placed on top of the recipient filter with the cells adjacent to the back of the recipient filter. At the end of the mating assay, both of the filters were removed and vortexed together in 1.5 mL of PBS and processed as described above. Finally, to examine the possibility of any endogenous phage release, donor cells were also pretreated with mitomycin C (Sigma) to induce any possible phage. Overnight cultures of C02 were diluted 1:100 in 10 mL of TSB and grown at 37°C to an OD_{600} of 0.6–0.8. 1.0–2.5 μg/mL of mitomycin C was then added to the cultures and induction was allowed to proceed at 30°C for 6–8 h before cultures were placed at 4°C for 16 h. Afterwards, the cultures were filter sterilized through a 0.45 μm filter and then serial diluted in phage buffer (Novick, 1963). Resident phage were titrated by serial dilution with RN4220 on TSA plates with TSB soft agar (0.5%). No plaques were ever obtained.

RESULTS

Initial Characterization of *qacA/B*-Positive Isolates

A previous molecular epidemiologic study used WGS to identify a clonal HA-MRSA outbreak strain that contained a *qacA*-positive plasmid that may have given the strain a fitness advantage within the hospital environment (Senn et al., 2016). However, there is a lack of genomic information available for CA-MRSA strains that carry *qacA*. To characterize both colonizing and clinically relevant *qacA*-positive *S. aureus* strains, we initially examined 11 *qacA*/B positive strains and 8 *qacA*/B-negative control strains (**Tables 1**, **2**) that were all obtained from a chlorhexidine-based SSTI prevention trial (Ellis et al., 2014; Schlett et al., 2014); the previously characterized C01 (*qacA*-) and C02 (*qacA*+) strains (Johnson et al., 2015) were included for comparison (**Table 1**). These *S. aureus* strains were collected from all three study groups (chlorhexidine, standard and enhanced standard-see **Table 1** footnote d) from July 2010 through October 2011. All of the strains were USA300 with the exception of one Methicillin-Sensitive *Staphylococcus aureus* (MSSA) strain (2148.N), which had a pulse field-type that was indistinguishable. A majority of the strains were from two MLST lineages (ST8, ST72) and one strain (5107.N) had a previously uncharacterized sequence type due to a novel *aroE* allele. Antibiotic susceptibility testing revealed erythromycin resistance was common in the strains, occurring in 16/18 (88%) strains. Additionally, one strain (1960.N02) was also resistant to clindamycin. All tested strains were susceptible to sulfamethoxazole. Moreover, *mupA*, which is required for high-level resistance to mupirocin, was identified in four strains that contained *qacA/B*.

To specifically examine the *qacA/B*-positive strains for the presence of pC02, we developed a PCR based screen. A total of 10 primer-pairs were designed to span the entire pC02 sequence (**Figure 1**). Of these, the primers in primer-pair 7 annealed to *qacA/B* and to the pC02 backbone. Additionally, an internal *qacA/B* primer pair was also included in the screen. A total of 3/11 *qacA/B*-positive strains, including the C02 control, yielded positive PCR amplicons for all 10 primer-pairs within the pC02 screen, suggesting that these strains carry pC02 or a pC02-like plasmid (**Table 2**). In addition to the pC02-like amplicon pattern, among *qacA/B*-positive strains we also identified two additional amplicon patterns; 4/11 strains amplified with primer pairs 6, 8 and the internal *qacA/B* primers while 4/11 amplified with primer pairs 6, 7, 8 and the internal *qacA/B* primers. Among the *qacA*-negative strains, two major patterns were observed; five strains showed a pattern that was indistinguishable from the C01 isolate (amplicons with primer pairs 6 and 8, termed pC01-like) and two strains yielded no amplification products.

Given the functional data that indicate differences in the ability of QacA and QacB to mediate reduced susceptibility to chlorhexidine (Paulsen et al., 1996), we sequenced the *qacA/B* amplicon to distinguish *qacA* and *qacB*. Of the seven identified single nucleotide variants (SNVs) that discriminate *qacA* from *qacB*, a single SNV at residue 323 is responsible for an amino acid substitution that confers the substrate specificity for the efflux pumps (Paulsen et al., 1996). Sequencing analysis from the amplicon produced from the internal *qacA/B* primers (**Supplemental Table 3**) revealed that all of the strains encoded the *qacA* sequence at this key residue (data not shown). *En masse*, the data from this screen suggested that several different *qacA*-containing plasmid types were present in this study population and that pC02 or a pC02-like plasmid was present in clinical isolates that were obtained from multiple individuals.

Chlorhexidine Susceptibility Testing

Given that the presence of *qacA* has been shown in some, but not all, cases to be associated with decreased susceptibility to chlorhexidine (Johnson et al., 2013; McDanel et al., 2013) and given that our sequencing results indicated that all of the *qac*-positive strains carried *qacA*, we next sought to determine whether these strains showed decreased susceptibility to chlorhexidine. Broth dilution assays using pure chlorhexidine revealed a 3–4 fold decrease in susceptibility to chlorhexidine in all strains that harbored *qacA* (**Table 2**). When the MIC values were plotted based on plasmid type (**Table 2**), all strains carrying *qacA* displayed a statistically significant decrease in susceptibility to chlorhexidine as compared to strains lacking *qacA* (**Figure 2**). Furthermore, the plasmid-pattern group

TABLE 2 | pC02-based PCR screen.

Strains[a]	Study Arm[b]	1[c]	2	3	4	5	6	7	8	9	10	*qacA*	Average CHG MIC μg/mL[d]	Median CHG MIC μg/ml of plasmid-pattern group[e]
REFERENCE STRAINS														
2014.C01*	CHG	–	–	–	–	–	+	–	+	–	–	–	**0.33**	
2014.C02*	CHG	+	+	+	+	+	+	+	+	+	+	+	**0.90**	
STRAINS FROM SSTI PREVENTION TRIAL														
1960.N02$	CHG	–	–	–	–	–	–	–	–	–	–	–	**0.20**	**0.22 (0.20–0.23)**
2148.N$*	ES	–	–	–	–	–	–	–	–	–	–	–	**0.23**	
1534.C01	CHG	–	–	–	–	–	+	–	+	–	–	–	**0.30**	
1625.C01	CHG	–	–	–	–	–	+	–	+	–	–	–	**0.30**	
3011.C01	ES	–	–	–	–	–	+	–	+	–	–	–	**0.20**	**0.30 (0.20–0.33)**
5107.N	S	–	–	–	–	–	+	–	+	–	–	–	**0.27**	
5116.N	ES	–	–	–	–	–	+	–	+	–	–	–	**0.33**	
1624.C01	S	–	–	–	–	–	+	–	+	–	–	+	**1.03**	
1626.C01*	S	–	–	–	–	–	+	–	+	–	–	+	**1.07**	**1.05 (0.63–1.07)**
1626.N*	S	–	–	–	–	–	+	–	+	–	–	+	**1.07**	
1971.C01	S	–	–	–	–	–	+	–	+	–	–	+	**0.63**	
1969.N	CHG	+	+	+	+	+	+	+	+	+	+	+	**1.00**	**1.0 (0.90–1.03)**
3020.C01	CHG	+	+	+	+	+	+	+	+	+	+	+	**1.03**	
2075.N02$	CHG	–	–	–	–	–	+	+	+	–	–	+	**1.30**	
2116.N02$	CHG	–	–	–	–	–	+	+	+	–	–	+	**1.30**	**1.3 (1.10–1.37)**
2148.C01$*	ES	–	–	–	–	–	+	+	+	–	–	+	**1.37**	
5118.N	S	–	–	–	–	–	+	+	+	–	–	+	**1.10**	

[a] *$, MSSA isolate. *multiple isolates were obtained from the same patient/numbers in the strain name indicate individual patient designations.*

[b] *CHG, chlorhexidine; ES, enhanced standard; S, standard.*

[c] *Number 1–10 indicate the primer sets used for the pC02 screen, qacA is an independent PCR for qacA/B. +, PCR amplification. - no PCR amplification.*

[d] *CHG, chlorhexidine; MIC, minimum inhibitory concentration.*

[e] *Group range and median.*

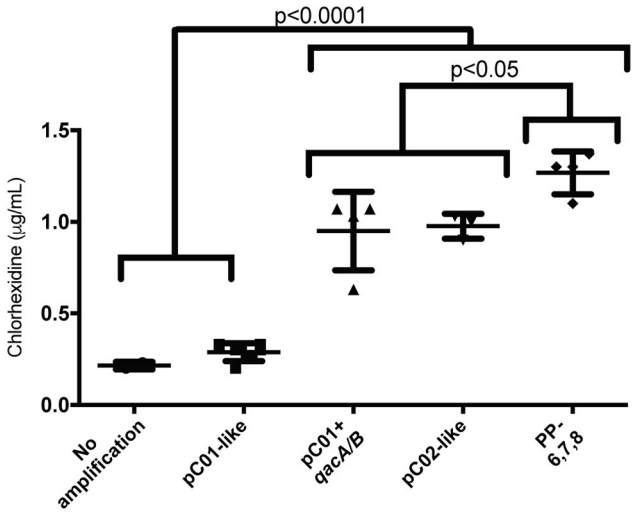

FIGURE 2 | Chlorhexidine MIC for each plasmid-pattern group. The MIC of chlorhexidine for each strain was determined by broth dilution. All strains were grouped according to the results of the pC02 PCR screen as follows: No amplification, strains that didn't amplify at all with the pC02 primer set; pC01-like, strains that had an amplification pattern that matched the control 2014.C01 isolate (amplification with 6 and 8); pC01+*qacA/B*, strains that had an amplification pattern that matched 2014.C01 but also amplified with the *qacA/B* primer set; pC02-like, strains that had an amplification pattern that matched the control 2014.C02 strain; and PP-6,7,8, strains that showed amplification with primer sets 6, 7, 8, and *qacA/B*. Graphed values represent means from three independent replicates for each strain. Error bars represent the standard deviation of the group mean. Statistically significant differences are indicated as determined by a one-way Anova with correction for multiple comparisons using Tukey's multiple comparison method.

(positive for primer-pair 6,7,8) displayed significantly higher resistance to chlorhexidine than all other strains that contained *qacA* (**Figure 2**). Taken together, these results indicate that *S. aureus* strains that carry *qacA* show a decreased susceptibility to chlorhexidine.

Whole Genome Sequencing of Selected Clinical Isolates

While MLST and PFGE profiles can provide fast preliminary information concerning strain relatedness, these techniques do not accurately determine strain clonality or provide detailed genomic information regarding the chromosome or mobile genetic elements, such as plasmids, which often carry resistance determinants and virulence genes (McCarthy and Lindsay, 2012). To further characterize the obtained *S. aureus* strains, eight strains were selected for WGS: two *qacA* negative strains, and two strains from every *qacA* positive plasmid-pattern group (**Table 2**). In addition, C01 and C02, which were both previously sequenced using PacBio technology (Johnson et al., 2015), were included for resequencing using MiSeq. To improve the accuracy of the assembled genomes, each strain was ultimately sequenced using both MiSeq and PacBio technologies. The average (min-max) read depth obtained with the MiSeq was 110 (range 67–167), whereas for the PacBio data the average (min-max) read depth was 17 (range 11–24). Analysis of the co-assembled Illumina short read and PacBio long read sequencing data revealed that each of the strains sequenced in this study had a similarly-sized chromosome, ranging in size from ∼2.7 to 2.9 million base pairs. Additionally, each strain carried at least one, and in many cases, several plasmids of varying sizes. The various replicons and their sizes are presented in **Table 3**.

Overall, the 10 chromosomes sequenced in this study were found to be very similar to one another and to the reference strain USA300_TCH1516 (Highlander et al., 2007). However, a few interesting differences were observed. For example, gross inspection of chromosomal sequence alignments indicated three main areas of significant sequence variation with respect to the reference: a region in and around the gene encoding the replication initiation protein; a nearby region encoding a cassette chromosome recombinase A, a Zn-dependent hydroxyacylglutathione hydrolase/polysulfide binding protein, and some hypothetical proteins; and perhaps most significantly, a roughly 13 kilobase (kb) super-antigen encoding pathogenicity island (PAI; **Supplemental Figure 1**). This PAI, which is found in *S. aureus* USA300_TCH1516, was found to be absent in three of the 10 strains sequenced in this study. In strain USA300_TCH1516 and in seven of the strains described herein, this PAI encodes 17 genes, including genes for superantigen enterotoxin SEK, superantigen enterotoxin SEL, and secreted protein Ear. To verify that the apparent lack of this PAI in strains C02, 3020.C01, and 1969.N was not due to a missassembly, we performed BLAST against chromosomal and plasmid contigs as well as mapping of raw reads to the PAI sequence; in all cases the absence of the PAI was verified.

To examine relatedness of the strains, single nucleotide variation (SNV)-based phylogenies were constructed. Applying the GATK standard "hard" filter, and after filtering variants that occur in regions of genome repeats and putative chromosomal rearrangements, a total of 785 SNVs were identified (**Supplemental Table 2**). One of the nasal carriage isolates, 2148.N, was an outlier from the remainder of the strains and was subsequently removed from the phylogenetic tree that is presented in **Figure 3**; the original tree is presented in **Supplemental Figure 2**. Of note, the other two sequenced nasal carriage isolates clustered in a single clade with several SSTI isolates. Additionally of note, C02 and 3020.C01 were essentially clonal with the nasal carriage isolate 1969.N, perhaps reflecting the origin of these three isolates from the same battalion and company within the span of 2 months (**Table 1**). These three strains were also the only three sequenced strains in this study that were found to lack a PAI. Between C02 and 3020.C01, only six SNVs were identified, five of which were located in coding regions. Of those five, three were synonymous SNVs. Between 3020.C01 and 1969.N, eleven SNVs were identified, nine of which were in coding regions; of those nine, seven were synonymous. Between 1969.N and C02, seven SNVs were identified, six of which were located in coding regions; of those six, two were synonymous. **Table 4** represents the SNVs by position (with respect to the coordinates of the reference genome *S. aureus* USA300_TCH1516; NC_010079.1) for each of the three isolates that were found to be clonal. The bulk of the SNVs

TABLE 3 | Summary of *S. aureus* replicons.

Strain (NCBI bioproject)	Chromosome Size (bp)	Plasmid Size (bp)	Plasmid Accession Number	*qacA* (Y/N)
S. aureus strain C01 (PRJNA287576)	2,917,985	pC01a 3,269	CP025490.1	N
		pC01b 27,043	CP012118.2	N
S. aureus strain C02 (PRJNA287791)	2,864,345	pC02a 3,269	CP025489.1	N
		pC02 61,539	CP012121.2	Y
S. aureus strain 1625.C01 (PRJNA321054)	2,877,915	p1625.C01 27,067	CP016862.2	N
S. aureus strain 1626.C01 (PRJNA321114)	2,871,639*	p1626.C01a 3,269	CM009343.1	N
		p1626.C01b 27,209	CM009344.1	N
		p1626.C01c 43,994	CM009345.1	Y
S. aureus strain 1969.N (PRJNA321120)	2,864,344	p1969.Na 3,269	CP025487.1	N
		p1969.Nb 61,505	CP016860.2	Y
S. aureus strain 1971.C01 (PRJNA321116)	2,873,208	p1971.C01a 3,269	CP025486.1	N
		p1971.C01b 21,841	CP016859.2	Y
		p1971.C01c 37,941	CP016857.2	N
S. aureus strain 2148.C01 (PRJNA321118)	2,856,605	p2148.C01a 3,266	CP025488.1	N
		p2148.C01b 32,660	CP017095.2	Y
S. aureus strain 2148.N (PRJNA321119)	2,748,803	p2148.N 3,459	CP025481.1	N
S. aureus strain 3020.C01 (PRJNA321117)	2,865,166	p3020.C01a 3,269	CP025496.1	N
		p3020.C01b 61,505	CP025497.1	Y
S. aureus strain 5118.N (PRJNA321122)	2,873,063	p5118.Na 3,269	CP025482.1	N
		p5118.Nb 53,799	CP016854.2	Y

**Scaffolded assembly in multiple contigs.*

were identified in a gene encoding an enoyl-ACP reductase. Of note, all of the SNVs in this gene were found to be synonymous substitutions. We hypothesize that that this may be due to the essential nature of the product of this gene, which is used to complete the fatty acid chain elongation cycle and is necessary for a properly functioning cell membrane (Chaudhuri et al., 2009). Specifically, it catalyzes the stereospecific reduction of a double bond between the C2 and C3 positions of the growing fatty acid chain (Priyadarshi et al., 2010).

Consistent with the very similar chromosomal sequences for C02, 3020.C01, and 1969.N, these three strains also had similar plasmid profiles, each having one roughly 3 kb plasmid and one roughly 61 kb plasmid; all three strains were *qac*A-positive by PCR (**Table 2**). Comparison of the WGS data for all of the strains in this study, showed roughly three categories of plasmid (**Table 3**) (1) an ∼3 kb plasmid, which was identified in nine of ten strains and found to have 65–100% nucleotide identity among the ten strains; (2) an ∼27–32 kb plasmid, which was identified in four of ten strains and found to have 69–99% nucleotide identity; and (3) an ∼61kb plasmid, which was identified in three of ten strains and found to have 99.78–99.94% nucleotide identity. Among the various plasmid size categories, the 3 kb plasmids were all cryptic plasmids with the exception of p2148.N, which harbored a predicted cadmium transporter. The 3kb plasmids all contained Rep_1 rolling circle replication initiation proteins (Kwong et al., 2017). Conversely, the large plasmids all carried theta replicating RepA_N domain replication initiation proteins. In addition to a RepA_N protein, p1626.C01c and p1971.C01c also harbored a Rep_2 and Rep_1 rolling circle replication initiation protein, respectively. The multiple replication proteins suggest a recent plasmid integration event with a small rolling circle replicating plasmid. The 27 kb plasmids were nearly identical and contained genes for macrolide, β-lactams and cadmium resistance. In addition to the resistance genes carried on the 27 kb plasmids, the 32 kb plasmid (p2148.C01b) harbored a 6.5 kb region containing *qacA* and an IS5/IS1182 family transposase. The 61kb pC02-like plasmids carried *qacA* and resistance genes for cadmium, macrolides and β-lactams. When the plasmids were grouped and analyzed based on *qacA* status and not size, we found that the plasmids that carried *qacA* ranged in size from 21 to 61 kb. As a whole, the large plasmids contained numerous insertion elements, including IS6, IS257, and IS5 transposases. Moreover, enzymes required for DNA mobilization, including invertases and resolvases, were found throughout the large plasmids. Indeed, examination of the plasmid population as a whole, suggested modularity in the staphylococcal plasmids where some segments were highly conserved between the various plasmid groups. Additionally, putative metabolic genes were identified in several plasmids, for example, p5118.Nb harbored two enzymes predicted to play a role in the ribulose monophosphate pathway for formaldehyde detoxification (Orita et al., 2006). *En masse*, these findings highlight the constant genetic flux that occurs between these extrachromosomal genetic molecules. Overall the

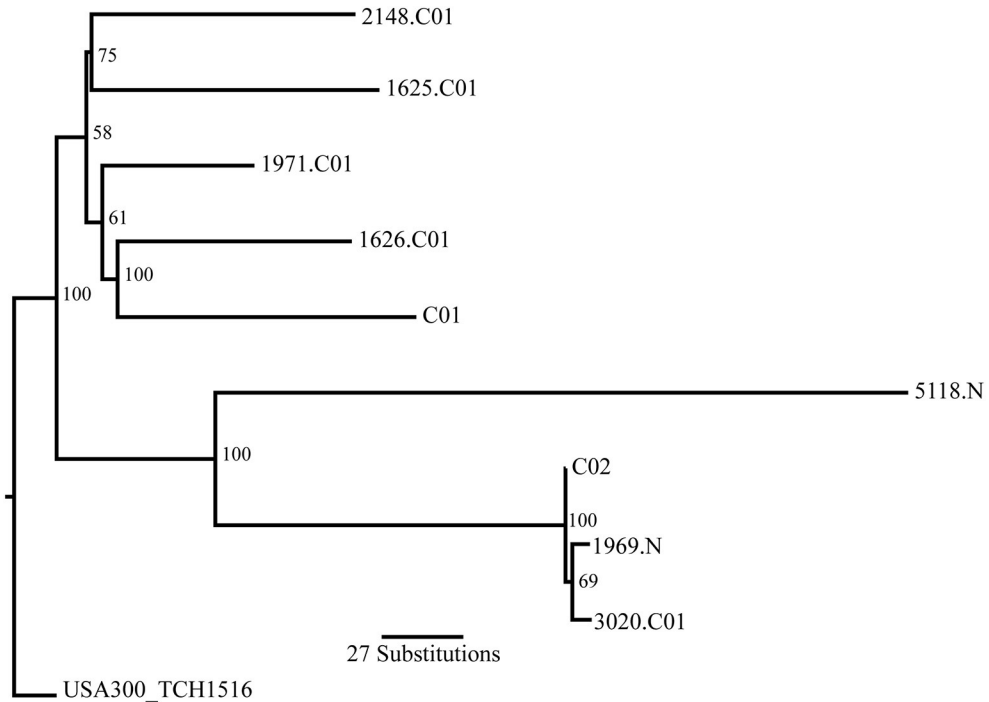

FIGURE 3 | Dendrogram of MRSA isolates that were subjected to whole genome sequencing and analysis in this study. A multiple sequence alignment (MSA) was created from nucleotide substitutions. A maximum likelihood tree was constructed with *S. aureus* USA300_TCH1516 as the root from the nucleic acid MSA using PhyML (version 3.2) tree search with the GTR substitution model and 1000 bootstrap replicates. Bootstrap values are shown at the base of the individual nodes.

genetic diversity seen across these plasmids likely contributes to the ability of Staphylococcus to adapt to a wide variety of environments and stresses.

Conjugative Transfer of the *qacA*-Positive Plasmid pC02

Previous sequence analysis of the *qacA*-containing pC02 plasmid identified a putative type IV secretion system (Johnson et al., 2015). To further investigate the pC02 components, the resequenced plasmid was re-annotated with the Rapid Annotation using Subsystem Technology (RAST) service (Aziz et al., 2008; Overbeek et al., 2014; Brettin et al., 2015). RAST revealed a putative TraG protein, which is commonly associated with conjugative plasmids (Firth et al., 1993; Morton et al., 1993). Although the exact function of TraG has yet to be identified in Gram-positive bacteria, it is believed to function as a coupling protein for the relaxase enzyme and the membrane bound secretion system (Cabezón et al., 1997). Additionally, RAST identified a putative conjugal ATPase, TraE, which is also known as VirB4. TraE helps supply the energy necessary for conjugative transfer (Walldén et al., 2012). The presence of two genes commonly associated with conjugation systems and the significance of possible conjugal transfer of *qacA*-containing plasmids in *S. aureus* led us to explore the conjugation potential of pC02. We questioned whether pC02 could be mobilized by conjugation from the parental C02 strain to a pC02 plasmid-cured derivative that was resistant to rifampin and novobiocin (C02-RN). Filter-mating assays with C02 (donor) and C02-RN (recipient) followed by selection of transconjugants on rifampin, novobiocin and cadmium (pC02 contains a cadmium resistance gene), revealed an average frequency of conjugation of 7.51×10^{-9} (**Table 5**). Moreover, the other *S. aureus* strains that harbored pC02 (3020.C01 and 1969.N) were able to transfer their plasmid to C02-RN at a similar frequency (**Table 5**). Transfer required cell-to-cell contact as transconjugants were never identified when the donor and recipient cells were separated by a filter.

To examine the host range of pC02 conjugation, five additional recipient strains were tested: two *S. aureus* strains, two *S. epidermidis* strains and one *Enterococcus faecalis* strain. For the additional *S. aureus* strains, we chose the common lab strain RN4220 as well as a *qacA* minus strain from our collection (1625.C01). These two *S. aureus* strains both yielded transconjugates at a similar frequency to that seen with C02-RN. The *S. epidermidis* strains included a lab passaged strain (DSM1581) as well as strain RP62a, which is a recent clinical isolate (Gill et al., 2005). Again, transfer of pC02 to the lab strain occurred at a similar frequency to that seen with C02-RN. However, transfer to the clinical isolate was a very rare event; only a single transconjugant was ever detected for the *S. epidermidis* RP62a assays. Cross genera conjugation via mating with *E. faecalis* OG1-RF (Dunny et al., 1978) was not detected (**Table 5**). This conjugal transfer of pC02 was unique as the other *qacA*-positive plasmids found in strains 1626.N, 5118.N, and

TABLE 4 | Identified SNVs in strains that harbored pC02.

Position[a]	Gene product	C02	3020.C01	1969.N
494641	Hypothetical protein			Non-synonymous SNV
704843	–		SNV (noncoding)	
1014474	Enoyl-ACP reductase	Synonymous SNV	Synonymous SNV	
1014480		Synonymous SNV	Synonymous SNV	
1014681		Ambiguous basecall	Synonymous SNV	
1014693		Ambiguous basecall	Synonymous SNV	
1014699			Synonymous SNV	
1014708			Synonymous SNV	
1466112	Thymidylate synthase		Non-synonymous SNV	Non-synonymous SNV
1466151			Non-synonymous SNV	Non-synonymous SNV
1567680	Minor structural protein			Non-synonymous SNV
2650114	Lantibiotic ABC transporter ATP-binding protein	Synonymous SNV		Synonymous SNV
2850131	-			SNV (noncoding)

[a] *Single nucleotide variations (SNVs) by position (coordinates with respect to the reference genome for methicillin-resistant MRSA USA300_TCH1516; NC_010079.1) for each of the three isolates that were found to be clonal.*

TABLE 5 | Conjugative transfer of pC02.

			Conjugation Frequency	
Donor	**Recipient**	**Conjugation**	**Average[a]**	**Standard Dev[b]**
C02	C02-RN	Yes	7.51E-09	6.58E-09
3020.C01	C02-RN	Yes	9.59E-09	5.39E-09
1969.N	C02-RN	Yes	1.42E-08	8.79E-09
C02	42-RN	Yes	8.20E-09	9.15E-09
3020.C01	42-RN	Yes	3.25E-09	3.98E-09
1969.N	42-RN	Yes	1.87E-09	5.83E-10
C02	1625-RN	Yes	1.29E-08	7.19E-09
3020.C01	1625-RN	Yes	3.95E-08	2.95E-08
1969.N	1625-RN	Yes	2.46E-09	1.91E-09
C02	*S. capitis* RN	Yes	6.82E-09	3.65E-09
C02	*S. epidermidis* RP62A-RN	Yes	7.25E-11	1.77E-10
C02	*E. faecalis* OG1-RF	Not observed	ND in 2.29E10	NA
1626.N	C02-RN	Not observed	ND in 1.26E10	NA
5118.N	C02-RN	Not observed	ND in 1.14E10	NA
1971.C01	C02-RN	Not observed	ND in 1.10E10	NA

[a] *ND, not detected in indicated number of examined recipient CFU.*
[b] *NA, not applicable.*

1971.C01 were unable to be mobilized by conjugation; the lack of mobilization is likely no surprise given the absence of identifiable putative transfer genes on any of these other plasmids.

To ensure that pC02 was being mobilized by conjugation and not by phage-mediated transduction, supernatants collected from donor strains were mixed with recipient cells and the appearance of transductants was assessed; supernatants from overnight and log phase donor cultures were examined. No transductants were ever identified, suggesting that pC02 mobilization does occur via conjugation. Furthermore, to check for endogenous phage within C02, mitomycin C induction at various concentrations produced no visible plaques at a limit of detection of 100 plaque forming units.

Given that *qacA* containing strains showed decreased susceptibility to chlorhexidine (**Figure 2**) and that pC02 was able to mobilize *qacA* to multiple recipient strains, we next asked whether conjugal transfer of pC02 was sufficient to affect chlorhexidine susceptibility of the recipient strains; we tested individual transconjugants from various matings for their susceptibility to chlorhexidine. Indeed, we found that all tested *S. aureus* pC02-containing transconjugants displayed an observable decrease in their susceptibility to chlorhexidine as

compared to their respective parental strains (**Figure 4A**). This decrease in susceptibility was not only seen with the *S. aureus* transconjugants, but was also seen with *S. epidermidis*; the pC02-containing strain showed a 3-fold increase in chlorhexidine resistance as compared to the parental *S. epidermidis* strain (**Figure 4B**). Thus, transfer of pC02 and *qacA* was sufficient to impart decreased susceptibility to chlorhexidine in a susceptible strain background. *En masse*, our conjugation results show the first demonstration of conjugative transfer of *qacA* across *S. aureus* strains and to other Staphylococcal species; the downstream result of mobilization of *qacA* for the recipient cells was a decrease in susceptibility to chlorhexidine.

DISCUSSION

The dissemination of *qacA* among bacteria presents a potential risk to the efficacy of the highly employed chlorhexidine antiseptic. Mobile genetic elements are known for their ability to disseminate resistance elements quickly between bacteria. While *qacA* has been found in some *S. aureus* strains, it has previously only been found to exist on non-conjugative plasmids that are not easily horizontally disseminated to other strains. Our prior characterization of a clinical isolate that showed decreased susceptibility to chlorhexidine revealed a novel *qacA*-containing plasmid (pC02) that encoded possible conjugation genes (Johnson et al., 2015). Herein, we identified additional strains from Ft. Benning that carry pC02, showed that those strains represent an infectious clonal *qacA*-positive lineage and demonstrated the successful conjugal transfer of *qacA*-positive pC02 to multiple strains of *S. aureus* and to *S. epidermidis*.

The clonal nature of the pC02-containing strains C02, 1969.N and 3020.C01 was confirmed by WGS, which revealed very few SNVs among the three strains (**Table 4**). Of note, all three of these strains were isolated from different soldiers who were part of the same company (∼200 soldiers). While two of the soldiers were part of the same platoon (a subgroup of a company comprised of ∼50 soldiers), platoon data was not available for one individual (**Table 1**). Of these strains, 3020.C01 was isolated ∼2 months before the other two strains. Moreover, while C02 and 3020.C01 were isolated from purulent abscesses, 1969.N was a nasal isolate. Thus, at a minimum pC02-containing strains can colonize or infect and can be spread among individuals in close contact. There are likely numerous opportunities for transmission of these strains, given that trainees train and live in the same physical environment for the 14-week training duration. It is worth noting that all three strains were isolated from individuals in groups randomized to receive chlorhexidine. Given that pC02 contains *qacA,* these strains may have been given a fitness advantage in the presence of routine (i.e., weekly) exposure to chlorhexidine. Similarly, an outbreak strain of ST228 MRSA was previously shown to harbor *qacA* in nearly all of the clinical isolates obtained from a tertiary care hospital in Switzerland (Senn et al., 2016); in the hospital environment, microbial exposure to chlorhexidine would likely be a constant, selective pressure. In a recent study, *S. epidermidis* isolates were collected from industrial cleanrooms and startlingly revealed to carry *qacA/B* at a high rate; 98.3% (56/57) of the isolates carried *qacA/B* (Ribič et al., 2017). This extreme example suggests that in environments where there is a constant exposure to chlorhexidine or other quaternary compounds, there is a strong selective pressure for Staphylococcal species to acquire and maintain *qacA/B*. While the specific advantage of CA-MRSA strains that contain *qacA* may be debatable, the increased usage of chlorhexidine in households and the increased incidence of CA-MRSA in hospital settings could provide the selection needed for rapid dispersal of *qacA* to various *Staphylococcal* species. Indeed, the demonstrated conjugal transfer of pC02 (**Table 5**) may represent one mechanism by which the prevalence of *qacA* may continue to increase.

It is worth noting that in addition to pC02 containing strains, we also identified and sequenced a variety of large (>21 kb) non-conjugative *qacA* positive plasmids. Furthermore, we showed that the presence of *qacA* on any of those plasmids was associated with a decreased susceptibility to chlorhexidine (**Table 2** and **Figure 2**). Unexpectedly, one of the *qacA*-positive plasmid groups (PCR positive for region 6,7,8) showed a significantly higher MIC than the other *qacA*-positive plasmid groups. WGS sequence analysis of the two strains chosen for sequencing from that plasmid group did not reveal mutations in *qacA* or *qacR*, the latter of which encodes for the *qacA* transcriptional regulator, QacR. Thus, the increase in resistance to chlorhexidine displayed by these strains may be attributed to a higher copy number of these particular *qacA*-harboring plasmids or to additional differences that are particular to these strain backgrounds. In support of the importance of the strain background, we note that even though transconjugants that obtained pC02 showed decreased susceptibility to chlorhexidine (**Figures 4A,B**), the level of resistance was never as high as that seen in the original pC02 containing strains (**Table 2** and **Figure 2**). Thus, additional strain specific components likely contribute to the overall level of chlorhexidine resistance imparted by the presence of *qacA*.

Compared to previously sequenced plasmids, the *qacA*-positive plasmids in our study showed overall sequence homology levels that ranged from 32 to 80%. Areas that showed homology to other plasmids typically had nearly 100% nucleotide identity while other areas showed virtually no conservation. This finding further supports the previously demonstrated modularity of Staphylococcal plasmids (McCarthy and Lindsay, 2012). Indeed, the high level of recombination and genetic exchange that is seen between Staphylococcal plasmids may assist in the selection of dominant clonal Staphylococcal strains that can then be responsible for outbreaks within hospitals and communities (DeLeo et al., 2010). The high levels of recombination seen between Staphylococcal plasmids in tandem with the constant exchange of genetic material via transduction, conjugation, and mobilization of non-conjugative plasmids highlights the overall genetic promiscuity of Staphylococcal plasmids (Deghorain and Van Melderen, 2012; McCarthy and Lindsay, 2012; O'Brien et al., 2015). While the role of the components carried on these modular plasmids is rather poorly characterized, presumably genes must impart some form of selection in various environmental niches. To this end, we note that within our population, *qacA* was often carried on plasmids

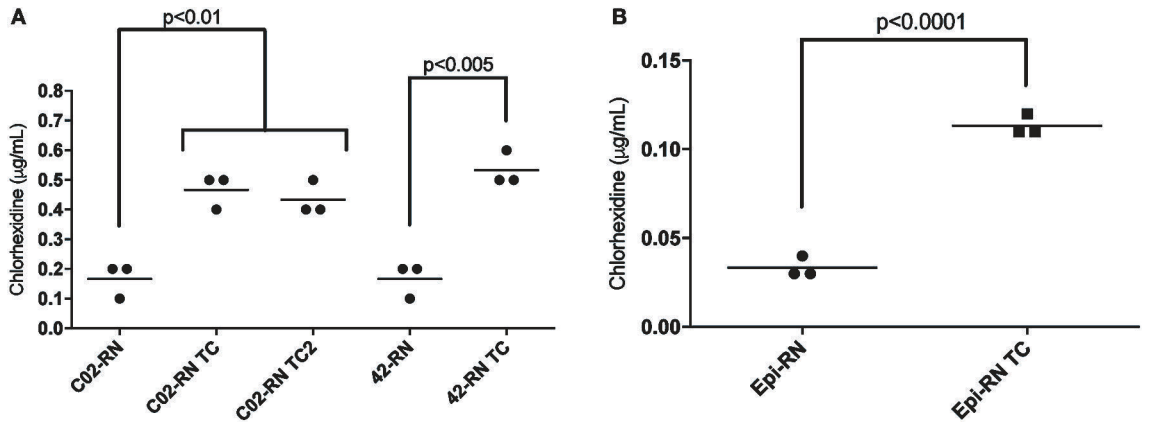

FIGURE 4 | Chlorhexidine MIC for transconjugant strains. The MIC to chlorhexidine for each indicated strain was determined by broth dilution. **(A)** C02-RN TC is a transconjugant obtained from mating C02 with C02-RN. C02-RN TC2 is a transconjugant obtained from mating 1969.N with C02-RN. 42-RN TC is a transconjugant obtained from mating C02 with 42-RN. 42-RN and C02-RN are pC02-free recipient cells. **(B)** Epi-RN TC is a transconjugant obtained from mating C02 with *S. capitis* RN. Epi-RN is pC02-free recipient *S. capitis* RN. Graphed values represent three independent replicates for each strain and the bar indicates the mean. Statistically significant differences are indicated as determined by a Student's *t* test; a correction for multiple comparisons using the Holm-Sidak's method was applied for C02-RN, C02-RN TC and C02-RN TC2.

that contained additional resistance determinants; this has also been observed in previous studies (Jensen et al., 2010; McCarthy and Lindsay, 2012). The importance of this finding lies in the fact that any selective pressure that selects for the presence of a single gene will also co-select for the stability of the other resistance genes found on large plasmids or other shared mobile elements (Carter et al., 2017). Thus, in hospitals and other environments where antiseptics are used liberally, residual chlorhexidine could drive an increase in multidrug resistant strains of Staphylococcus (Bjorland et al., 2005; Madden and Sifri, 2018). Importantly, the implication of chlorhexidine-driven co-selection is not only applicable to Staphylococcus; *qacA* has recently been identified in *Enterococcus faecalis*, *E. faecium*, *Acinetobacter baumannii*, and *Klebsiella pneumoniae* strains (Bischoff et al., 2012; Guo et al., 2015; Rizzotti et al., 2016; Liu et al., 2017).

While conjugative transfer of biocide resistance genes, such as *qacC,* has been previously shown (Lyon et al., 1987), prior to the work described herein, *qacA* had yet to be definitively identified on a conjugative element. Despite this, we do note one previous report that may indicate that *qacA* may have resided on a conjugative plasmid (pSAJ1) that was isolated in the 1980's from Japan (Yamamoto et al., 1988). The characterization of pSAJ1 that was conducted at that time showed restriction sites on the suspected antiseptic resistance gene that are very similar to the *qacA* sequence. Moreover, the authors showed that pSAJ1 is responsible for an antiseptic resistance profile that is similar to strains that carry *qacA*. While pSAJ1 was not sequenced and it is not clear if the plasmid did in fact carry *qacA*, the presence of *qacA* on a conjugative plasmid that was circulating in Asia in the 1980's could partially explain the very high prevalence of *qacA/B* found in current Staphylococcal strains from Asia (Wang et al., 2008a,b; Shamsudin et al., 2012; Cho et al., 2018). Currently, the rates of *qacA* positivity among community acquired *S. aureus* strains in the United States is fairly low: 0-1.6% (Fritz et al., 2012; Popovich et al., 2014; Schlett et al., 2014). However, given our herein described discovery of a *qacA*-containing plasmid that can be conjugated across *S. aureus* strains and even to some strains of *S. epidermidis*, one has to wonder if we are on the verge of observing a dramatic increase in the prevalence of *qacA* containing strains? Indeed, when one combines the ability of bacterial strains to move resistance components with the selective pressure imposed by indiscriminate use of antiseptics, it becomes almost too easy to envision a not so distant future where antiseptic resistance becomes a critical conversation. Clearly, continued surveillance and increased antiseptic stewardship are warranted for the continued clinical success of even antiseptics.

AUTHOR CONTRIBUTIONS

PL, TH, KB-L, and DM conceived and designed the study. AP, and PL performed the sequencing and PL, GR, RC, and KB-L performed the bioinformatic analyses. CS, JB, EM, ME and NL designed and executed the original chlorhexidine intervention trial. PL, AP and EE processed and characterized the bacterial clinical isolates.

FUNDING

These studies were supported by a U.S. Department of Defense Program project grant (HT9404-12-1-0019) and a Uniformed Services University Student Grant (T0734265).

ACKNOWLEDGMENTS

We would like to thank Dr. Cara Olsen for her help with statistical analyses and Dr. Kristi Frank for *S. epidermidis* RP62A and *E. faecalis* OG1-RF strains. The contents of this publication are the sole responsibility of the author(s) and do not necessarily

reflect the views, opinions, or policies of Uniformed Services University, Henry M. Jackson Foundation for the Advancement of Military Medicine, the Department of Defense, the Navy, nor the U.S. Government. DSM and KBL are employees of the U.S. Government and JB and TH are military service members. This work was prepared as part of their official duties. Title 17 U.S.C. 105 provides that 'Copyright protection under this title is not available for any work of the United States Government.' Title 17 U.S.C. 101 defines a U.S. Government work as a work prepared by a military service member or employee of the U.S. Government as part of a person's official duties.

SUPPLEMENTARY MATERIAL

The Supplementary Material for this article can be found online at: https://www.frontiersin.org/articles/10.3389/fmicb.2018.02664/full#supplementary-material

REFERENCES

Aiello, A. E., Lowy, F. D., Wright, L. N., and Larson, E. L. (2006). Meticillin-resistant *Staphylococcus aureus* among US prisoners and military personnel: review and recommendations for future studies. *Lancet Infect. Dis.* 6, 335–341. doi: 10.1016/S1473-3099(06)70491-1

Albrecht, V. S., Limbago, B. M., Moran, G. J., Krishnadasan, A., Gorwitz, R. J., McDougal, L. K., et al. (2015). *Staphylococcus aureus* colonization and strain type at various body sites among patients with a closed abscess and uninfected controls at US emergency departments. *J. Clin. Microbiol.* 53, 01371–01315. doi: 10.1128/JCM.01371-15

Altschul, S. F., Gish, W., Miller, W., Myers, E. W., and Lipman, D. J. (1990). Basic local alignment search tool. *J. Mol. Biol.* 215, 403–410. doi: 10.1016/S0022-2836(05)80360-2

Andrews, S. (2016). *FastQC. Babraham Bioinformatics.* Available online at: https://www.bioinformatics.babraham.ac.uk/projects/fastqc/ (Accessed November 2, 2016).

AngularPlasmid (2015). *AngularPlasmid. Vixis*. Available online at: http://angularplasmid.vixis.com/about.php (Accessed March 10, 2018).

Antipov, D., Hartwick, N., Shen, M., Raiko, M., Lapidus, A., and Pevzner, P. (2016). plasmidSPAdes: assembling plasmids from whole genome sequencing data. *Bioinformatics* 32, 3380–3387. doi: 10.1093/bioinformatics/btw493

Aziz, R. K., Bartels, D., Best, A. A., DeJongh, M., Disz, T., Edwards, R. A., et al. (2008). The RAST Server: rapid annotations using subsystems technology. *BMC Genomics* 9:75. doi: 10.1186/1471-2164-9-75

Bankevich, A., Nurk, S., Antipov, D., Gurevich, A. A., Dvorkin, M., Kulikov, A. S., et al. (2012). SPAdes: a new genome assembly algorithm and its applications to single-cell sequencing. *J. Comput. Biol.* 19, 455–477. doi: 10.1089/cmb.2012.0021

Beauparlant, M. (2016). A metapopulation model for the spread of MRSA in correctional facilities. *Infect. Dis. Model.* 1, 11–27. doi: 10.1016/j.idm.2016.06.001

Berg, T., Firth, N., Apisiridej, S., Hettiaratchi, A., Leelaporn, A., and Skurray, R. A. (1998). Complete nucleotide sequence of pSK41: evolution of staphylococcal conjugative multiresistance plasmids. *J. Bacteriol.* 180, 4350–4359.

Bischoff, M., Bauer, J., Preikschat, P., Schwaiger, K., Mölle, G., and Hölzel, C. (2012). First detection of the antiseptic resistance gene *qacA/B* in *Enterococcus faecalis*. *Microb. Drug Resist.* 18, 7–12. doi: 10.1089/mdr.2011.0092

Bjorland, J., Steinum, T., Kvitle, B., Waage, S., Sunde, M., and Heir, E. (2005). Widespread distribution of disinfectant resistance genes among staphylococci of bovine and caprine origin in Norway. *J. Clin. Microbiol.* 43, 4363–4368. doi: 10.1128/JCM.43.9.4363-4368.2005

Boivin, M., Cowan, D., Packnett, E., and Garvin, N. (2016). *AMSARA 2016 Annual Report*. Available online at: http://www.amsara.amedd.army.mil/AMSARAAR.aspx (Accessed March, 2018).

Brettin, T., Davis, J. J., Disz, T., Edwards, R. A., Gerdes, S., Olsen, G. J., et al. (2015). RASTtk: a modular and extensible implementation of the RAST algorithm for building custom annotation pipelines and annotating batches of genomes. *Sci. Rep.* 5:8365. doi: 10.1038/srep08365

Buehlmann, M., Frei, R., Fenner, L., Dangel, M., Fluckiger, U., and Widmer, A. (2008). Highly effective regimen for decolonization of methicillin-resistant *Staphylococcus aureus* carriers. *Infect. Control Hosp. Epidemiol.* 29, 510–516. doi: 10.1086/588201

Cabezón, E., Sastre, J. I., and De La Cruz, F. (1997). Genetic evidence of a coupling role for the TraG protein family in bacterial conjugation. *Mol. General Genet.* 254, 400–406. doi: 10.1007/s004380050432

Carter, G. P., Schultz, M. B., Baines, S. L., da Silva, A. G., Heffernan, H., Tiong, A., et al. (2017). Topical antibiotic use co-selects for the carriage of mobile genetic elements conferring resistance to unrelated antimicrobials in *Staphylococcus aureus*. *Antimicrob. Agents Chemother.* 62:e02000-17. doi: 10.1128/AAC.02000-17

Chaudhuri, R. R., Allen, A. G., Owen, P. J., Shalom, G., Stone, K., Harrison, M., et al. (2009). Comprehensive identification of essential *Staphylococcus aureus* genes using Transposon-Mediated Differential Hybridisation (TMDH). *BMC Genomics* 10:291. doi: 10.1186/1471-2164-10-291

Cho, O. H., Park, K. H., Song, J. Y., Hong, J. M., Kim, T., Hong, S. I., et al. (2018). Prevalence and microbiological characteristics of *qacA/B*-positive methicillin-resistant *Staphylococcus aureus* isolates in a surgical intensive care unit. *Microb. Drug Resist.* 24, 283–289. doi: 10.1089/mdr.2017.0072

Coates, T., Bax, R., and Coates, A. (2009). Nasal decolonization of *Staphylococcus aureus* with mupirocin: strengths, weaknesses and future prospects. *J. Antimicrob. Chemother.* 64, 9–15. doi: 10.1093/jac/dkp159

Deghorain, M., and Van Melderen, L. (2012). The Staphylococci phages family: an overview. *Viruses* 4, 3316–3335. doi: 10.3390/v4123316

DeLeo, F. R., Otto, M., Kreiswirth, B. N., and Chambers, H. F. (2010). Community-associated meticillin-resistant *Staphylococcus aureus*. *Lancet* 375, 1557–1568. doi: 10.1016/S0140-6736(09)61999-1

Dukic, V. M., Lauderdale, D. S., Wilder, J., Daum, R. S., and David, M. Z. (2013). Epidemics of community-associated methicillin-resistant *Staphylococcus aureus* in the United States: a meta-analysis. *PLoS ONE* 8:e52722. doi: 10.1371/journal.pone.0052722

Dunny, G. M., Brown, B. L., and Clewell, D. B. (1978). Induced cell aggregation and mating in *Streptococcus faecalis*: evidence for a bacterial sex pheromone. *Proc. Natl. Acad. Sci. USA.* 75, 3479–3483. doi: 10.1073/pnas.75.7.3479

Ellis, M. W., Schlett, C. D., Millar, E. V., Wilkins, K. J., Crawford, K. B., Morrison-Rodriguez, S. M., et al. (2014). Hygiene strategies to prevent methicillin-resistant *Staphylococcus aureus* skin and soft tissue infections: a cluster-randomized controlled trial among high-risk military trainees. *Clin. Infect. Dis.* 58, 1540–1548. doi: 10.1093/cid/ciu166

Enright, M. C., Day, N. P., Davies, C. E., Peacock, S. J., and Spratt, B. G. (2000). Multilocus sequence typing for characterization of methicillin-resistant and methicillin-susceptible clones of *Staphylococcus aureus*. *J. Clin. Microbiol.* 38, 1008–1015.

Firth, N., Ridgway, K. P., Byrne, M. E., Fink, P. D., Johnson, L., Paulsen, I. T., et al. (1993). Analysis of a transfer region from the staphylococcal conjugative plasmid pSK41. *Gene* 136, 13–25. doi: 10.1016/0378-1119(93)90442-6

Forbes, B. A., and Schaberg, D. R. (1983). Transfer of resistance plasmids from *Staphylococcus epidermidis* to *Staphylococcus aureus*: evidence for conjugative exchange of resistance. *J. Bacteriol.* 153, 627–634.

Fritz, S. A., Camins, B. C., Eisenstein, K. A., Fritz, J. M., Epplin, E. K., Burnham, C.-A., et al. (2011). Effectiveness of measures to eradicate *Staphylococcus aureus* carriage in patients with community-associated skin and soft tissue infections: a randomized trial. *Infect. Control Hosp. Epidemiol.* 32, 872–880. doi: 10.1086/661285

Fritz, S. A., Hogan, P. G., Camins, B. C., Ainsworth, A. J., Patrick, C., Martin, M. S., et al. (2012). *Staphylococcus aureus* mupirocin and chlorhexidine resistance

in patients with community-onset skin and soft tissue infections. *Antimicrob. Agents Chemother.* 57, 559–568. doi: 10.1128/AAC.01633-12

Furi, L., Ciusa, M. L., Knight, D., Di Lorenzo, V., Tocci, N., Cirasola, D., et al. (2013). Evaluation of reduced susceptibility to quaternary ammonium compounds and bisbiguanides in clinical isolates and laboratory-generated mutants of *Staphylococcus aureus*. *Antimicrob. Agents Chemother.* 57, 3488–3497. doi: 10.1128/AAC.00498-13

Ghasemzadeh-Moghaddam, H., van Belkum, A., Hamat, R. A., van Wamel, W., and Neela, V. (2014). Methicillin-susceptible and-resistant *Staphylococcus aureus* with high-level antiseptic and low-level mupirocin resistance in Malaysia. *Microb. Drug Resist.* 20, 472–477. doi: 10.1089/mdr.2013.0222

Gill, S. R., Fouts, D. E., Archer, G. L., Mongodin, E. F., DeBoy, R. T., Ravel, J., et al. (2005). Insights on evolution of virulence and resistance from the complete genome analysis of an early methicillin-resistant *Staphylococcus aureus* strain and a biofilm-producing methicillin-resistant *Staphylococcus epidermidis* strain. *J. Bacteriol.* 187, 2426–2438. doi: 10.1128/JB.187.7.2426-2438.2005

Guindon, S., Dufayard, J. F., Lefort, V., Anisimova, M., Hordijk, W., and Gascuel, O. (2010). New algorithms and methods to estimate maximum-likelihood phylogenies: assessing the performance of PhyML 3.0. *Syst. Biol.* 59, 307–321. doi: 10.1093/sysbio/syq010

Guo, W., Shan, K., Xu, B., and Li, J. (2015). Determining the resistance of carbapenem-resistant *Klebsiella pneumoniae* to common disinfectants and elucidating the underlying resistance mechanisms. *Pathog. Glob. Health* 109, 184–192. doi: 10.1179/2047773215Y.0000000022

Highlander, S. K., Hultén, K. G., Qin, X., Jiang, H., Yerrapragada, S., Mason, E. O., et al. (2007). Subtle genetic changes enhance virulence of methicillin resistant and sensitive *Staphylococcus aureus*. *BMC Microbiol.* 7:99. doi: 10.1186/1471-2180-7-99

Jensen, S. O., Apisiridej, S., Kwong, S. M., Yang, Y. H., Skurray, R. A., and Firth, N. (2010). Analysis of the prototypical *Staphylococcus aureus* multiresistance plasmid pSK1. *Plasmid* 64, 135–142. doi: 10.1016/j.plasmid.2010.06.001

Johnson, J. G., Saye, E. J., Jimenez-Truque, N., Soper, N., Thomsen, I., Talbot, T. R., et al. (2013). Frequency of disinfectant resistance genes in pediatric strains of methicillin-resistant *Staphylococcus aureus*. *Infect. Control Hosp. Epidemiol.* 34, 1326–1327. doi: 10.1086/673983

Johnson, R. C., Schlett, C. D., Crawford, K., Lanier, J. B., Merrell, D. S., and Ellis, M. W. (2015). Recurrent methicillin-resistant *Staphylococcus aureus* cutaneous abscesses and selection of reduced chlorhexidine susceptibility during chlorhexidine use. *J. Clin. Microbiol.* 53, 3677–3682. doi: 10.1128/JCM.01771-15

Joshi, N. A., and Fass, J. N. (2011). *A Sliding-Window, Adaptive, Quality-Based Trimming Tool for FastQ files (Version 1.33) [Software]*. Available online at: https://github.com/najoshi/sickle.

Karanika, S., Kinamon, T., Grigoras, C., and Mylonakis, E. (2016). Colonization with methicillin-resistant *Staphylococcus aureus* and risk for infection among asymptomatic athletes: a systematic review and metaanalysis. *Clin. Infect. Dis.* 63, 195–204. doi: 10.1093/cid/ciw240

Kluytmans, J., van Belkum, A., and Verbrugh, H. (1997). Nasal carriage of *Staphylococcus aureus*: epidemiology, underlying mechanisms, and associated risks. *Clin. Microbiol. Rev.* 10, 505–520. doi: 10.1128/CMR.10.3.505

Kwong, S. M., Ramsay, J. P., Jensen, S. O., and Firth, N. (2017). Replication of staphylococcal resistance plasmids. *Front. Microbiol.* 8:2279. doi: 10.3389/fmicb.2017.02279

Li, H., and Durbin, R. (2009). Fast and accurate short read alignment with Burrows–Wheeler transform. *Bioinformatics* 25, 1754–1760. doi: 10.1093/bioinformatics/btp324

Littlejohn, T. G., DiBerardino, D., Messerotti, L. J., Spiers, S. J., and Skurray, R. A. (1991). Structure and evolution of a family of genes encoding antiseptic and disinfectant resistance in *Staphylococcus aureus*. *Gene* 101, 59–66. doi: 10.1016/0378-1119(91)90224-Y

Liu, W. J., Fu, L., Huang, M., Zhang, J. P., Wu, Y., Zhou, Y. S., et al. (2017). Frequency of antiseptic resistance genes and reduced susceptibility to biocides in carbapenem-resistant *Acinetobacter baumannii*. *J. Med. Microbiol.* 66, 13–17. doi: 10.1099/jmm.0.000403

Longtin, J., Seah, C., Siebert, K., McGeer, A., Simor, A., Longtin, Y., et al. (2011). Distribution of antiseptic resistance genes *qacA*, *qacB*, and *smr* in methicillin-resistant *Staphylococcus aureus* isolated in Toronto, Canada, from 2005 to 2009. *Antimicrob. Agents Chemother.* 55, 2999–3001. doi: 10.1128/AAC.01707-10

Lyon, B. R., Gillespie, M. T., Byrne, M. E., May, J. W., and Skurray, R. A. (1987). Plasmid-mediated resistance to gentamicin in *Staphylococcus aureus*: the involvement of a transposon. *J. Med. Microbiol.* 23:101. doi: 10.1099/00222615-23-2-101

Madden, G. R., and Sifri, C. D. (2018). Antimicrobial resistance to agents used for *Staphylococcus aureus* decolonization: is there a reason for concern? *Curr. Infect. Dis. Rep.* 20, 26. doi: 10.1007/s11908-018-0630-0

Mayer, S., Boos, M., Beyer, A., Fluit, A. C., and Schmitz, F.-J. (2001). Distribution of the antiseptic resistance genes *qacA*, *qacB* and *qacC* in 497 methicillin-resistant and-susceptible European isolates of *Staphylococcus aureus*. *J. Antimicrob. Chemother.* 47, 896–897. doi: 10.1093/jac/47.6.896

McCarthy, A. J., and Lindsay, J. A. (2012). The distribution of plasmids that carry virulence and resistance genes in *Staphylococcus aureus* is lineage associated. *BMC Microbiol.* 12:104. doi: 10.1186/1471-2180-12-104

McDanel, J. S., Murphy, C. R., Diekema, D. J., Quan, V., Kim, D. S., Peterson, E. M., et al. (2013). Chlorhexidine and mupirocin susceptibilities of methicillin-resistant *Staphylococcus aureus* from colonized nursing home residents. *Antimicrob. Agents Chemother.* 57, 552–558. doi: 10.1128/AAC.01623-12

McKenna, A., Hanna, M., Banks, E., Sivachenko, A., Cibulskis, K., Kernytsky, A., et al. (2010). The genome analysis toolkit: a mapreduce framework for analyzing next-generation DNA sequencing data. *Genome Res.* 20, 1297–1303. doi: 10.1101/gr.107524.110

Millar, E. V., Rice, G. K., Elassal, E. M., Schlett, C. D., Bennett, J. W., Redden, C. L., et al. (2017). Genomic characterization of USA300 methicillin-resistant *Staphylococcus aureus* (MRSA) to evaluate intraclass transmission and recurrence of skin and soft tissue infection (SSTI) among high-risk military trainees. *Clin. Infect. Dis.* 65, 461–468. doi: 10.1093/cid/cix327

Morrison, S. M., Blaesing, C. R., Millar, E. V., Chukwuma, U., Schlett, C. D., Wilkins, K. J., et al. (2013). Evaluation of methicillin-resistant *Staphylococcus aureus* skin and soft-tissue infection prevention strategies at a military training center. *Infect. Control Hosp. Epidemiol.* 34, 841–843. doi: 10.1086/671278

Morton, T., Eaton, D., Johnston, J., and Archer, G. (1993). DNA sequence and units of transcription of the conjugative transfer gene complex (trs) of *Staphylococcus aureus* plasmid pGO1. *J. Bacteriol.* 175, 4436–4447. doi: 10.1128/jb.175.14.4436-4447.1993

Nakaminami, H., Noguchi, N., Nishijima, S., Kurokawa, I., So, H., and Sasatsu, M. (2007). Transduction of the plasmid encoding antiseptic resistance gene *qacB* in *Staphylococcus aureus*. *Biol. Pharmaceut. Bull.* 30, 1412–1415. doi: 10.1248/bpb.30.1412

Noguchi, N., Suwa, J., Narui, K., Sasatsu, M., Ito, T., Hiramatsu, K., et al. (2005). Susceptibilities to antiseptic agents and distribution of antiseptic-resistance genes *qacA/B* and *smr* of methicillin-resistant *Staphylococcus aureus* isolated in Asia during 1998 and 1999. *J. Med. Microbiol.* 54, 557–565. doi: 10.1099/jmm.0.45902-0

Novick, R. (1963). Analysis by transduction of mutations affecting penicillinase formation in *Staphylococcus aureus*. *Microbiology* 33, 121–136.

O'Brien, F. G., Yui Eto, K., Murphy, R. J., Fairhurst, H. M., Coombs, G. W., Grubb, W. B., et al. (2015). Origin-of-transfer sequences facilitate mobilisation of non-conjugative antimicrobial-resistance plasmids in *Staphylococcus aureus*. *Nucleic Acids Res.* 43, 7971–7983. doi: 10.1093/nar/gkv755

Orita, I., Sato, T., Yurimoto, H., Kato, N., Atomi, H., Imanaka, T., et al. (2006). The ribulose monophosphate pathway substitutes for the missing pentose phosphate pathway in the archaeon *Thermococcus kodakaraensis*. *J. Bacteriol.* 188, 4698–4704. doi: 10.1128/JB.00492-06

Overbeek, R., Olson, R., Pusch, G. D., Olsen, G. J., Davis, J. J., Disz, T., et al. (2014). The SEED and the Rapid Annotation of microbial genomes using Subsystems Technology (RAST). *Nucleic Acids Res.* 42(Database issue), D206–D214. doi: 10.1093/nar/gkt1226

Paulsen, I. T., Brown, M. H., Littlejohn, T. G., Mitchell, B. A., and Skurray, R. A. (1996). Multidrug resistance proteins QacA and QacB from *Staphylococcus aureus*: membrane topology and identification of residues involved in substrate specificity. *Proc. Natl. Acad. Sci. U.S.A.* 93, 3630–3635. doi: 10.1073/pnas.93.8.3630

Popovich, K. J., Aroutcheva, A., Hota, B., Beavis, K. G., Hayden, M. K., and Weinstein, R. A. (2014). Anatomic sites of colonization with community-associated methicillin-resistant *Staphylococcus aureus*. *Infect. Control Hosp. Epidemiol.* 35, 1192–1194. doi: 10.1086/677627

Priyadarshi, A., Kim, E. E., and Hwang, K. Y. (2010). Structural insights into *Staphylococcus aureus* enoyl-ACP reductase (FabI), in complex with NADP and triclosan. *Proteins Struct. Funct. Bioinform.* 78, 480–486. doi: 10.1002/prot.22581

Ribič, U., Klančnik, A., and Jeršek, B. (2017). Characterization of *Staphylococcus epidermidis* strains isolated from industrial cleanrooms under regular routine disinfection. *J. Appl. Microbiol.* 122, 1186–1196. doi: 10.1111/jam.13424

Rizzotti, L., Rossi, F., and Torriani, S. (2016). Biocide and antibiotic resistance of *Enterococcus faecalis* and *Enterococcus faecium* isolated from the swine meat chain. *Food Microbiol.* 60, 160–164. doi: 10.1016/j.fm.2016.07.009

Schlett, C. D., Millar, E. V., Crawford, K. B., Cui, T. Y., Lanier, J. B., Tribble, D. R., et al. (2014). Prevalence of chlorhexidine-resistant methicillin-resistant *Staphylococcus aureus* following prolonged exposure. *Antimicrob. Agents Chemother.* 58, 4404–4410. doi: 10.1128/AAC.02419-14

Senn, L., Clerc, O., Zanetti, G., Basset, P., Prod'hom, G., Gordon, N. C., et al. (2016). The stealthy superbug: the role of asymptomatic enteric carriage in maintaining a long-term hospital outbreak of ST228 methicillin-resistant *Staphylococcus aureus*. *MBio* 7, e02039–e02015. doi: 10.1128/mBio.02039-15

Septimus, E. J., and Schweizer, M. L. (2016). Decolonization in prevention of health care-associated infections. *Clin. Microbiol. Rev.* 29, 201–222. doi: 10.1128/CMR.00049-15

Shamsudin, M., Alreshidi, M., Hamat, R., Alshrari, A., Atshan, S., and Neela, V. (2012). High prevalence of *qacA/B* carriage among clinical isolates of meticillin-resistant *Staphylococcus aureus* in Malaysia. *J. Hosp. Infect.* 81, 206–208. doi: 10.1016/j.jhin.2012.04.015

Singh, J., Johnson, R. C., Schlett, C. D., Elassal, E. M., Crawford, K. B., Mor, D., et al. (2016). Multi-body-site microbiome and culture profiling of military trainees suffering from skin and soft tissue infections at Fort Benning, Georgia. *mSphere* 1, e00232–e00216. doi: 10.1128/mSphere.00232-16

Tennent, J. M., Lyon, B. R., Midgley, M., Jones, G., Purewal, A. S., and Skurray, R. A. (1989). Physical and biochemical characterization of the *qacA* gene encoding antiseptic and disinfectant resistance in *Staphylococcus aureus*. *J. Gen. Microbiol.* 135, 1–10.

Tidwell, J., Kirk, L., Luttrell, T., and Pike, C. A. (2016). CA-MRSA decolonization strategies: do they reduce recurrence rate? *J. Wound Ostomy Continence Nurs.* 43, 577–582. doi: 10.1097/WON.0000000000000277

Udo, E. E., Jacob, L., and Mokadas, E. (1997). Conjugative transfer of high-level mupirocin resistance from *Staphylococcus haemolyticus* to other staphylococci. *Antimicrob. Agents Chemother.* 41, 693–695. doi: 10.1128/AAC.41.3.693

Walldén, K., Williams, R., Yan, J., Lian, P. W., Wang, L., Thalassinos, K., et al. (2012). Structure of the VirB4 ATPase, alone and bound to the core complex of a type IV secretion system. *Proc. Natl. Acad. Sci. U.S.A.* 109, 11348–11353. doi: 10.1073/pnas.1201428109

Wang, C., Cai, P., Zhan, Q., Mi, Z., Huang, Z., and Chen, G. (2008a). Distribution of antiseptic-resistance genes *qacA/B* in clinical isolates of meticillin-resistant *Staphylococcus aureus* in China. *J. Hosp. Infect.* 69, 393–394. doi: 10.1016/j.jhin.2008.05.009

Wang, J.-T., Sheng, W.-H., Wang, J.-L., Chen, D., Chen, M.-L., Chen, Y.-C., et al. (2008b). Longitudinal analysis of chlorhexidine susceptibilities of nosocomial methicillin-resistant *Staphylococcus aureus* isolates at a teaching hospital in Taiwan. *J. Antimicrob. Chemother.* 62, 514–517. doi: 10.1093/jac/dkn208

Wassenaar, T. M., Ussery, D., Nielsen, L. N., and Ingmer, H. (2015). Review and phylogenetic analysis of *qac* genes that reduce susceptibility to quaternary ammonium compounds in Staphylococcus species. *Eur. J. Microbiol. Immunol.* 5, 44–61. doi: 10.1556/EuJMI-D-14-00038

Wertheim, H. F., Melles, D. C., Vos, M. C., van Leeuwen, W., van Belkum, A., Verbrugh, H. A., et al. (2005). The role of nasal carriage in *Staphylococcus aureus* infections. *Lancet Infect. Dis.* 5, 751–762. doi: 10.1016/S1473-3099(05)70295-4

Williams, D. (2016). *Bacterial and Archaeal Genome Analyser [Online]. GitHub.* Available online at: https://github.com/daveuu/baga. (Accessed November 2, 2016).

Yamamoto, T., Tamura, Y., and Yokota, T. (1988). Antiseptic and antibiotic resistance plasmid in *Staphylococcus aureus* that possesses ability to confer chlorhexidine and acrinol resistance. *Antimicrob. Agents Chemother.* 32, 932–935. doi: 10.1128/AAC.32.6.932

Conflict of Interest Statement: The authors declare that the research was conducted in the absence of any commercial or financial relationships that could be construed as a potential conflict of interest.

frontiers in Microbiology

ORIGINAL RESEARCH
published: 19 November 2018
doi: 10.3389/fmicb.2018.02702

Distribution of Transferable Antibiotic Resistance Genes in Laboratory-Reared Edible Mealworms (*Tenebrio molitor* L.)

*Andrea Osimani[1], Vesna Milanović[1], Federica Cardinali[1], Cristiana Garofalo[1], Francesca Clementi[1], Sara Ruschioni[1], Paola Riolo[1], Nunzio Isidoro[1], Nino Loreto[1], Roberta Galarini[2], Simone Moretti[2], Annalisa Petruzzelli[3], Eleonora Micci[3], Franco Tonucci[3] and Lucia Aquilanti[1]**

[1] *Dipartimento di Scienze Agrarie, Alimentari ed Ambientali, Università Politecnica delle Marche, Ancona, Italy,* [2] *Istituto Zooprofilattico Sperimentale dell'Umbria e delle Marche, Perugia, Italy,* [3] *Istituto Zooprofilattico Sperimentale dell'Umbria e delle Marche, Centro di Riferimento Regionale Autocontrollo, Pesaro, Italy*

OPEN ACCESS

Edited by:
Katy Jeannot, UMR6249 Chrono Environnement, France

Reviewed by:
Jorge Contreras-Garduño, Universidad Nacional Autónoma de México, Mexico
Karol Fijałkowski, West Pomeranian University of Technology, Poland

***Correspondence:**
Lucia Aquilanti
l.aquilanti@univpm.it

Specialty section:
This article was submitted to Antimicrobials, Resistance and Chemotherapy, a section of the journal Frontiers in Microbiology

Received: *23 June 2018*
Accepted: *23 October 2018*
Published: *19 November 2018*

Citation:
Osimani A, Milanović V, Cardinali F, Garofalo C, Clementi F, Ruschioni S, Riolo P, Isidoro N, Loreto N, Galarini R, Moretti S, Petruzzelli A, Micci E, Tonucci F and Aquilanti L (2018) Distribution of Transferable Antibiotic Resistance Genes in Laboratory-Reared Edible Mealworms (Tenebrio molitor L.). Front. Microbiol. 9:2702. doi: 10.3389/fmicb.2018.02702

In the present study, the distribution of antibiotic resistance genes in laboratory-reared fresh mealworm larvae (*Tenebrio molitor* L.), their feeding substrates (carrots and wheatmeal), and frass was assessed. Microbial counts on selective media added with antibiotics highlighted the presence of lactic acid bacteria resistant to ampicillin and vancomycin and, more specifically, enterococci resistant to the latter antibiotic. Moreover, staphylococci resistant to gentamicin, erythromycin, tetracycline, and vancomycin were detected. Enterobacteriaceae resistant to ampicillin and gentamicin were also found, together with Pseudomonadaceae resistant to gentamicin. Some of the genes coding for resistance to macrolide-lincosamide-streptogramin B (MLS_B) [*erm*(A), *erm*(C)], vancomycin [*vanA*, *vanB*], tetracycline [*tet*(O)], and β-lactams [*mecA* and *blaZ*] were absent in all of the samples. For the feeding substrates, organic wheatmeal was positive for *tet*(S) and *tet*(K), whereas no AR genes were detected in organic carrots. The genes *tet*(M), *tet*(K), and *tet*(S) were detected in both mealworms and frass, whereas gene *aac-aph,* coding for resistance to amynoglicosides was exclusively detected in frass. No residues for any of the 64 antibiotics belonging to 10 different drug classes were found in either the organic wheatmeal or carrots. Based on the overall results, the contribution of feed to the occurrence of antibiotic resistance (AR) genes and/or antibiotic-resistant microorganisms in mealworm larvae was hypothesized together with vertical transmission via insect egg smearing.

Keywords: novel foods, edible insects, metagenomic DNA analysis, nested-PCR, insect resistome

INTRODUCTION

"*Them insects eats up every blessed green thing that do grow, and us farmers starves. Well, eat them, and grow fat*" (Vincent M. Holt). In 1885, Vincent M. Holt published a small brochure, titled "*Why not eat insects?*" in which he explained his theory of "entomophagy," referring to the human practice of eating insects. The pamphlet, which was reprinted in 1995, ended with some interesting recipes for insect-based menus (Holt, 1995). At present, the eccentric nature of the above-mentioned text

should be considered more closely. Insects are widely consumed in Asia, Africa, and South America, where they constitute part of the traditional diets of at least 2 billion people. By contrast, in Europe, they are rarely consumed and are often associated with low prestige and poor countries (van Huis et al., 2013; Verbeke, 2015). Nevertheless, insects can provide an alternative source of high-quality protein and nutritionally valuable substances (e.g., good lipids, micronutrients, B-group vitamins, and fibers) that are exploitable by the food industry (Schlüter et al., 2016).

As reported by van Huis (2016), in a few European countries, such as Belgium, the Netherlands, Austria, and France, the production and consumption of processed edible insects is tolerated in some ways, whereas in Switzerland, it is allowed. In these countries, the rearing of insects for both human and animal consumption is mainly carried out by small private enterprises, but the edible insect sector is rapidly growing; thus, the need for specific food laws to regulate insect rearing and processing is increasingly urgent (van Huis, 2016).

Recently, the European Union issued Regulation (EU) No 2015/2283 of the European Parliament and the Council of 25 November 2015 on novel foods that will go into effect 1 January 2018, introducing a simplified and centralized procedure for introducing edible insects into the EU market. As novel foods, the safety of edible insects must be assessed before they can be considered safe, since insects can be a source of toxic substances and pathogenic microorganisms. As reported by Schlüter et al. (2016), there is still a lack of knowledge regarding the risks associated with the use of insects in the production of foods and food ingredients.

Regarding the microbiological risks, several studies have already been focused on the microbiota of edible insects through conventional microbiological analyses and advanced DNA-based techniques (Simpanya et al., 2000; Banjo et al., 2006; Klunder et al., 2012; Stoops et al., 2016; Garofalo et al., 2017; Osimani et al., 2017a; Vandeweyer et al., 2017). The results of these studies highlighted the presence of potential human pathogens, suggesting the need for a deeper investigation of the correlation between the microbiota and insect rearing conditions.

In addition to opportunistic human pathogens, even bacteria harboring transferable antibiotic resistance (AR) genes pose a serious threat to human health. The emergence and spread of transferable AR is a global public health problem that requires action across all government sectors and society. As reported by the World Health Organization (WHO), new AR mechanisms are constantly emerging and spreading globally, threatening our ability to treat common infectious diseases, which results in prolonged illness, disability, and death (World Health Organization, 2014). To date, many investigations have been focused on AR in bacteria found in humans, animals, and foods. AR genes are now considered emerging environmental contaminants due to their ability to be transferred to the environment from both humans and foods of vegetable (Thanner et al., 2016) and animal origin (He et al., 2016). Cox (2015) has recently suggested that the routine use of antibiotics in food-producing animals selects for antibiotic-resistant microorganisms that compromise human health, bringing us closer to a "post-antibiotic era" with multidrug-resistant "super-bugs."

Insects can undoubtedly represent a source of antibiotic-resistant bacteria (Zurek and Ghosha, 2014). However, currently available data on the occurrence of antibiotic resistance in edible insects are very limited, with only a few published studies (Milanović et al., 2016; Osimani et al., 2017b,c; Vandeweyer et al., 2019) that deal with the distribution of selected AR genes in various edible insects. To the authors' knowledge, no investigations have been carried out to date to specifically correlate the occurrence of transferable AR genes in edible insects with their rearing conditions. Moreover, no studies have been carried out to determine the loads and dynamics of antibiotic resistance in specific microbial groups in edible insects.

Given this information, the distribution of AR genes in laboratory-reared fresh mealworm larvae (*Tenebrio molitor* L.), their feeding substrates (wheatmeal plus carrots as a water supplement), and frass (excrement from larvae mixed with substrate residues) was assessed. To this end, antibiotic-resistant microorganisms were enumerated onto selective growth media with antimicrobials. Moreover, the prevalence of 12 selected genes coding for resistance to antibiotics conventionally used in clinical practice such as MLS_B [*erm*(A), *erm*(B), *erm*(C)], vancomycin [*vanA*, *vanB*], tetracyclines [*tet*(M), *tet*(O), *tet*(S), *tet*(K)], β-lactams [*mecA*, *blaZ*] and amynoglicosides [*aac()-Ie aph(2″)-Ia*] (abbreviated as *aac-aph*) was determined using optimized PCR and nested PCR assays. The target genes were chosen among those that are most frequently detected in both human pathogens and commensal food-borne bacteria (Devirgiliis et al., 2011; Aarts and Margolles, 2015), which are widely recognized as potential reservoirs for these AR genes (Rolain, 2013). In parallel, the presence of 64 antibiotics that belong to 10 different drug families (amphenicols, beta-lactams, diamino-pyrimidine, lincosamides, macrolides, pleuromutilins, quinolones, rifamycins, sulfonamides, and tetracyclines) was assessed in the feed substrates.

MATERIALS AND METHODS

Insect Rearing Conditions

Mealworm larvae were purchased from a local pet store (Moby Dick, Jesi, Italy). They were grown in plastic boxes (21 x 30 x 6 cm) placed in a climate-controlled chamber at 28°C, 60% relative humidity (RH), and a 24-h dark photoperiod until the pupal stage was reached. Before use, the plastic boxes used for rearing were sanitized with a 3% active chlorine solution to avoid unwanted contamination. Organic wheatmeal, obtained from a local mill factory (Molino Agostini s.r.l, Osimo, Italy), and organic carrots (washed and peeled using sterile scalpels) were supplied as feed and water sources, respectively as suggested by Broekhovenv et al. (2015), Cortes Ortiz et al. (2016) and Dreassi et al. (2017) for the improvement of the insect growth. Pupae were sexed based on their morphology (Bhattacharya et al., 1970). Groups of 100 pupae, each including 50 females and 50 males, were placed in different plastic boxes containing fresh organic wheatmeal and carrots to allow adults to lay eggs. The second generation of larvae was grown under the same

conditions as those described above. Three different batches of second-generation mealworms were reared in parallel. **Figure 1** reports the rearing steps and the collected samples; the latter are described below. No antibiotics were used for the treatment of insects during rearing.

Sampling

One batch of organic wheatmeal was aseptically sampled (∼1 kg) prior to its use as feed for mealworms; aliquots of washed and peeled organic carrots (∼100 g) used as a water supplement were also sampled under sterile conditions and pooled in one single sample. Carrots were not subjected to microbial counting because only the cores of the completely intact roots that were collected under sterile conditions have been administered to mealworms, thus assuring the absence of any microbial contamination.

Last instar larvae were individually collected from the three batches of second-generation mealworms and pooled together. Analogously, aliquots of frass were sampled from the three plastic boxes after collection of second-generation last instar larvae and pooled together for further analyses. The pooling of the samples was performed in order to reduce the effect of biological variation. All samples were collected into sterile plastic bags with sterile instruments.

Bacterial Enumeration

Ten grams of each pooled sample was homogenized in 90 mL of sterile peptone water (0.1% bacteriological peptone) at 260 rpm for 3 min using a Stomacher apparatus (400 Circulator, International PBI, Milan, Italy). Serial dilutions were prepared aseptically in peptone water, and 100 μL or 1-mL aliquots of each dilution were plated in duplicate onto agar plates for the enumeration of aerobic mesophilic bacteria, lactic acid bacteria (LAB), staphylococci (coagulase negative and positive), Pseudomonadaceae, enterococci and Enterobacteriaceae. For the enumeration of spore-forming bacteria, homogenates (10^{-1} dilution) of each sample were heat-shocked for 15 min at 80°C to inactivate the vegetative cells, then immediately cooled on ice, serially diluted in sterile peptone water and spread onto Plate Count Agar (PCA) (Milanović et al., 2017). The media, spreading method and the growth conditions are reported in **Table 1.**

For the viable counts of antibiotic-resistant bacteria that were present in the analyzed samples, the media listed in **Table 1** were supplemented with concentrations of ampicillin, gentamicin, erythromycin, tetracycline and vancomycin based on the breakpoint values defined by the European Committee on Antimicrobial Susceptibility Testing (EUCAST, 2017) for each group of analyzed bacteria (**Table 1**). The results of bacterial enumeration were expressed as the mean ± standard deviation of the log of colony-forming units (cfu) per gram of sample.

Detection of Antibiotic Residues in Organic Wheatmeal and Carrots

The analysis of the 64 antibiotics listed in **Table 2**, which belong to ten drug families (amphenicols, beta-lactams, diamino-pyrimidines, lincosamides, macrolides, pleuromutilins, quinolones, rifamycins, sulfonamides and tetracyclines), was carried out in wheatmeal and pooled carrots as described by Moretti et al. (2016) with some modifications regarding the sample preparation protocol of the wheatmeal. Briefly, 2 g of organic wheatmeal was sequentially extracted using acetonitrile/water 50/50 (v/v), acetonitrile containing formic acid at 0.1%, and an aqueous solution of 0.1 M Na_2EDTA. An aliquot was collected from each extract and placed into a tube. After evaporation, the extract was redissolved in ammonium acetate buffer prior to injection. For testing, a Thermo Ultimate 3,000 Ultra High-Performance Liquid Chromatography system coupled with a high-resolution Q-Exactive mass spectrometer (Thermo Scientific, San Jose, CA, USA) operating in positive electrospray ionization mode was used. Chromatographic separation was performed with a Poroshell 120 EC-C18 column (100 × 3.0 mm, 2.7 μm) using gradient elution (mobile phases: methanol and water containing 0.1% of formic acid). The acquisition mode was fully scanned with some analytes in t-SIM to overcome the strong matrix effects in wheatmeal. The results were expressed as μg of antibiotic per kg of food matrix (μgkg^{-1} or ppb) with detection limits equal to 100 and 10 μgkg^{-1} (cefacetrile: 33 μgkg^{-1}) for wheatmeal and carrots, respectively.

Reference Strains

Twelve antibiotic-resistant bacterial strains, each carrying one AR gene of interest, were used as positive controls in the PCR and nested PCR reactions (**Table 3**). *Enterococcus faecalis* JH2-2 (Jacob and Hobbs, 1974), free of AR genes under study, was used as a negative control.

DNA Extraction

The DNA from the 12 reference strains and the negative control strain *E. faecalis* JH2-2 was extracted as described by Hynes et al. (1992), with some modifications as reported by Osimani et al. (2015). The metagenomic DNA from organic wheatmeal, pooled samples of peeled organic carrots, second-generation mealworm larvae, and frass was extracted using the PowerFood Microbial DNA Isolation Kit (Mo Bio Laboratories, Carlsbad, United States) as previously described by Milanović et al. (2016). The organic wheatmeal and the carrots were subjected to DNA extraction prior to their use as a feed and a water supplement. The DNA extracts were assessed for quantity and purity by optical readings at 260, 280, and 234 nm using a UV-Vis Shimadzu UV-1800 spectrophotometer (Shimadzu, Kyoto, Japan).

PCR and Nested PCR Amplification of AR Genes

DNA extracts obtained from wheatmeal and each pooled sample (carrots, mealworms, and frass) were amplified in PCR assays targeting *erm*(A), *erm*(B), *erm*(C), *tet*(M), *tet*(O), *tet*(S), *tet*(K), *vanA*, *vanB, blaZ*, *mecA*, and *aac-aph* genes. The specific mechanisms of resistance for these genes are reported in **Table 3**. The samples that were negative following the first round of PCR were further subjected to nested PCR. Amplification conditions and primers used for PCR and nested PCR were previously described by Garofalo et al. (2007) and Milanović et al. (2016) and are reported in **Tables S1, S2**.

Two microliters of DNA extract (containing ∼10 ng of microbial DNA) or PCR product was amplified by PCR or

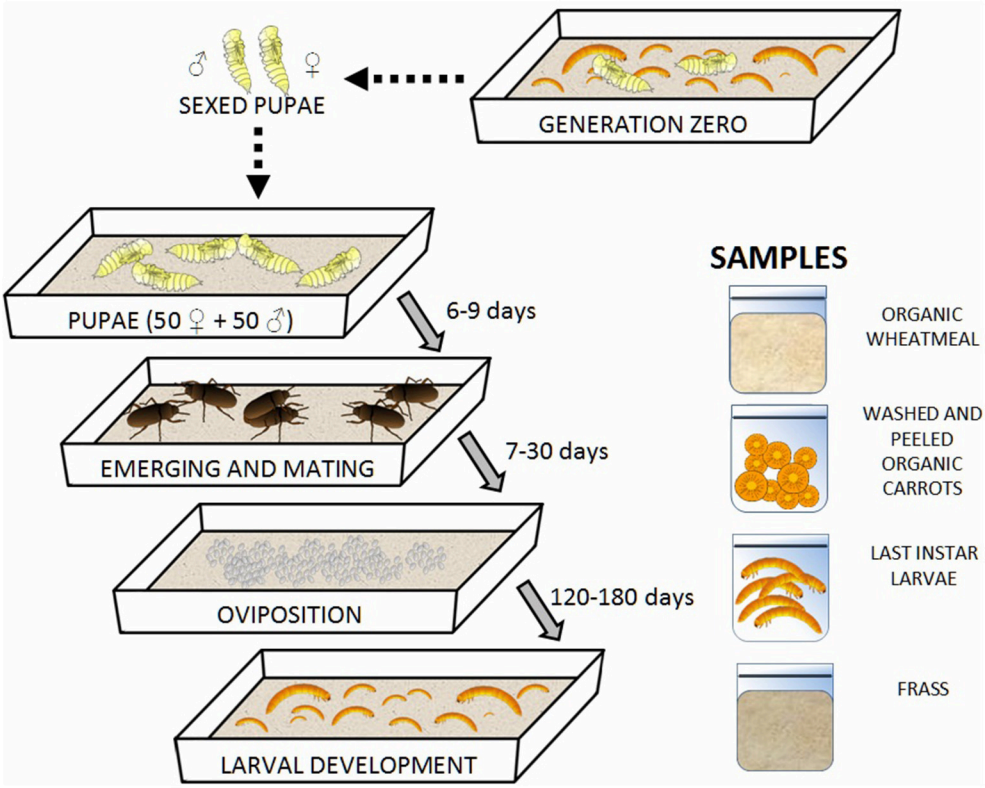

FIGURE 1 | Rearing steps of mealworms and collected samples.

nested PCR, respectively, in a total volume of 25 μL under the same conditions reported by Osimani et al. (2017b). Briefly, the reaction mixture contained the following: 1X buffer, 50 pmol of each primer, 0.2 mM of dNTPs (2.5 mM for the amplification of *erm* genes in both assays), and 0.75 U of Taq polymerase. Positive (**Table 3**) and negative (*E. faecalis* JH2-2) controls were used in each PCR assay. PCR mixture supplemented with water instead of DNA was used as a blank. All amplifications were carried out in a MyCycler thermal cycler (Bio-Rad Laboratories, Hercules, United States). Five microliters of each PCR product was analyzed by electrophoresis through a 1.5% (w/v) agarose gel (Conda pronadisa, Spain) in 0.5X TBE (45 mM Tris-borate, 1 mM EDTA) containing 0.5 $\mu g mL^{-1}$ ethidium bromide at 75 V for 45 min. A 100-bp DNA Ladder (SibEnzyme Ltd., Academtown, Russia) was used as a molecular weight standard. A Complete Photo XT101 system (Explera, Jesi, Italy) was used to visualize gels under UV light. For each tested AR gene, randomly selected PCR products were sequenced by Genewiz (Hope End, Takeley, United Kingdom) to verify the annealing of oligos to the proper target sequences.

Statistical Analysis

Microbial count data were subjected to one-way analysis of variance (ANOVA) carried out using JMP statistical software version 11.0.0 (SAS Institute Inc., NC, United States). Differences were considered significant at $P < 0.05$.

RESULTS AND DISCUSSION

In this study, a PCR-based metagenomic approach has been applied to investigate the distribution of 12 selected AR genes in a laboratory scale *T. molitor* rearing cycle. The novelty of this approach relies on the possibility of evaluating the occurrence of AR under controlled rearing conditions without any selective pressure exerted by antibiotics. Such an approach also allowed to exclude any possible interference of insect manipulation and/or processing on the occurrence of transferable AR genes and antibiotic-resistant microorganisms in edible insects, thus constituting an advancement on the knowledge in respect with the available literature on the same topic (Milanović et al., 2016; Osimani et al., 2017b,c; Vandeweyer et al., 2019).

Among edible insects, *T. molitor* undoubtedly represents a very promising food source being very rich in protein and fat and easy to breed (Gasco et al., 2016; Zhao et al., 2016; Osimani et al., 2017a). It is also a good source of polyunsaturated fatty acids whose consumption is considered a potential means of improving health (Mozzon et al., 2002; Haddad et al., 2012; Pacetti et al., 2013). Therefore, its potential use in the food industry can rapidly increase (Stoops et al., 2017).

The results of the viable counts of aerobic mesophilic bacteria, spore-forming bacteria, lactic acid bacteria, enterococci, staphylococci, Enterobacteriaceae and Pseudomonadaceae assessed in this study are reported in **Table 1**. To the authors'

TABLE 1 | Culture media, incubation conditions and results of bacterial counts in wheatmeal used as feed, fresh mealworm larvae and frass of the three pooled rearing batches.

Growth medium	Presumptive microorganism	Growth conditions	Plating method	Reference	Organic wheatmeal	Mealworm larvae	Frass
					log cfu g^{-1}		
PCA	Aerobic mesophilic bacteria	30°C;48 h	Pour	(American Public Health Association, 1976)	1.5 ± 0.08^{c}	9.3 ± 0.04^{a}	7.8 ± 0.01^{b}
	Spore forming bacteria				$<1^{c}$	2.3 ± 0.03^{b}	4.1 ± 0.02^{a}
MRS	Lactic acid bacteria	30°C;48–72 h	Pour	(De Man et al., 1960)	1.9 ± 0.08^{c}	8.3 ± 0.01^{a}	5.8 ± 0.01^{b}
MRS + ampicillin (8 mg L^{-1})*	Ampicillin resistant lactic acid bacteria				$<1^{c}$	2.2 ± 0.04^{a}	1.7 ± 0.05^{b}
MRS + vancomycin (8 mg L^{-1}) *	Vancomycin resistant lactic acid bacteria				1.3 ± 0.03^{c}	7.1 ± 0.01^{a}	3.9 ± 0.01^{b}
ESA	Enterococci	37°C;24–48 h	Spread	(Slanetz and Bartley, 1957)	1.6 ± 0.07^{c}	7.9 ± 0.01^{a}	6.7 ± 0.03^{b}
ESA + ampicillin (8 mg L^{-1}) *	Ampicillin resistant enterococci				$<1^{a}$	$<1^{a}$	$<1^{a}$
ESA + gentamicin (128 mg L^{-1}) *	HLAR enterococci				$<1^{a}$	$<1^{a}$	$<1^{a}$
ESA + vancomycin (4 mg L^{-1}) *	Vancomycin resistant enterococci				$<1^{c}$	5.7 ± 0.03^{a}	2.6 ± 0.01^{b}
MSA	Staphylococci	37°C;24–48 h	Spread	(Chapman, 1945; Bannerman, 2003)	$<1^{b}$	5.8 ± 0.01^{a}	5.4 ± 0.01^{a}
MSA + gentamicin (1 mg L^{-1}) *	Gentamicin resistant staphylococci				$<1^{b}$	5.7 ± 0.01^{a}	5.3 ± 0.01^{a}
MSA + erythromycin (2 mg L^{-1}) *	Erythromycin resistant staphylococci				$<1^{c}$	4.9 ± 0.04^{a}	2.8 ± 0.10^{b}
MSA + tetracycline (2 mg L^{-1})*	Tetracycline resistant staphylococci				$<1^{c}$	5.2 ± 0.01^{a}	4.6 ± 0.01^{b}
MSA + vancomycin (2 mg L^{-1}) *	Vancomycin resistant coagulase positive staphylococci				$<1^{b}$	4.1 ± 0.04^{a}	4.3 ± 0.01^{a}
MSA + vancomycin (4 mg L^{-1}) *	Vancomycin resistant coagulase negative staphylococci				$<1^{c}$	3.8 ± 0.01^{b}	4.3 ± 0.09^{a}
VRBGA	Enterobacteriaceae	37°C;24 h	Pour	(American Public Health Association, 1976)	$<1^{c}$	7.5 ± 0.01^{a}	5.8 ± 0.01^{b}
VRBGA + ampicillin (8 mg L^{-1}) *	Ampicillin resistant Enterobacteriaceae				$<1^{c}$	6.1 ± 0.01^{a}	5.0 ± 0.01^{b}
VRBGA + gentamicin (4 mg L^{-1}) *	Gentamicin resistant Enterobacteriaceae				$<1^{c}$	2.5 ± 0.01^{a}	1.2 ± 0.20^{b}
PAB	Pseudomonadaceae	30°C;24–48 h	Spread	(Geftic et al., 1979)	1.0 ± 0.00^{b}	6.7 ± 0.03^{a}	6.1 ± 0.02^{a}
PAB + gentamicin (4 mg L^{-1}) *	Gentamicin resistant Pseudomonadaceae				$<1^{c}$	5.7 ± 0.03^{a}	3.2 ± 0.01^{b}

*PCA, Plate Count Agar; MRS, de Man Rogosa Sharpe agar; ESA, Enterococcus Selective Agar, MSA, Mannitol Salt Agar; VRBGA, Violet Red Bile Glucose Agar; PAB, Pseudomonas Agar Base; HLAR, High-Level Aminoglycoside Resistance *the breakpoint values defined by European Committee on Antimicrobial Susceptibility Testing (EUCAST, 2017)*
Results of bacterial counts are expressed as mean values ± standard deviation of three independent experiments (one for each batch)
Means followed by different letters are significantly different ($P < 0.05$).

knowledge, this is the very first study on the enumeration of antibiotic resistant microorganisms in edible insects as revealed by viable plate counting.

As a general trend, viable counts of aerobic mesophilic bacteria in wheatmeal were in the range of those reported by Alfonzo et al. (2017) for whole-meal semolinas collected from different Italian regions, which ranged between < 1 and 4.0 ± 0.3 log cfu g^{-1}. Even in the pooled samples of mealworm larvae and frass, the load of this microbial group was similar to that found in the same matrices by Vandeweyer et al. (2017) and Wynants et al. (2017), respectively, with the latter reporting viable counts between 8.8 and 11.4 log cfu g^{-1}.

For spore-forming bacteria, viable counts in the feed were again similar to those reported by Valerio et al. (2012) in semolina, with loads ranging between < 1 and 2 log cfu g^{-1}. This bacterial group is commonly found in cereals and cereal-based matrices. It is noteworthy that spore-forming bacterial species can represent the causative agents of food-borne intoxication because of their toxin-forming ability. Regarding mealworms, these microbial group counts were again in the ranges reported

TABLE 2 | List of the 64 antibiotics determined in wheatmeal and carrots used as feed.

#	Antibiotic	#	Antibiotic
1	Thiamphenicol	33	Erithromycin A
2	Florfenicol	34	Spiramycin I
3	Florfenicol Amine	35	Neospiramycin
4	Cephapirin	36	Tylosin A
5	Desacetylcephapirin	37	Tilmicosin
6	Ceftiofur	38	Tulathromycin
7	Cefalexin	39	Tulathromycin marker
8	Cefquinome	40	Tildipirosin
9	Cefazolin	41	Tylvalosin (acetyl-isovaleryltyrosine)
10	Cefoperazone	42	3-O-Acetyltylosin
11	Cefalonium	43	Gamithromycin
12	Cefacetrile	44	Tiamulin
13	Penicillin G	45	Valnemulin
14	Amoxicillin	46	Rifaximin
15	Ampicillin	47	Sulfanilamide
16	Cloxacillin	48	Sulfamethazine
17	Dicloxacillin	49	Sulfapyridine
18	Oxacillin	50	Sulfadiazine
19	Nafcillin	51	Sulfadimethoxine
20	Penicillin V	52	Sulfamonomethoxine
21	Difloxacin	53	Sulfaquinoxaline
22	Flumequine	54	Sulfathiazole
23	Oxolinic Acid	55	Sulfaguanidinae
24	Ciprofloxacin	56	Sulfamerazine
25	Enrofloxacin	57	Sulfamethoxazole
26	Danofloxacin	58	Chlortetracycline
27	Marbofloxacin	59	Epichlorotetracycline
28	Sarafloxacin	60	Oxitetracyclin
29	Nalidixic Acid	61	Epioxitetracyclin
30	Norfloxacin	62	Doxycycline
31	Trimethoprim	63	Tetracyclin
32	Lincomycin	64	Epitetracycline

TABLE 3 | Bacterial reference strains used in this study.

AR gene	Gene function	Strains positive for AR genes
erm(A)	rRNA methylase gene	*Staphylococcus aureus* M.P. [a]
erm(B)	rRNA methylase gene	*Enterococcus hirae* Api 2.16 [a]
erm(C)	rRNA methylase gene	*Staphylococcus* spp. SE12 [b]
vanA	Peptidoglycan precursors encoding gene	*Enterococcus faecium* PF3U [b]
vanB	Peptidoglycan precursors encoding gene	*Enterococcus faecalis* ATCC 51299 [c]
tet(M)	Ribosomal protection RP gene	*Lactobacillus casei/paracasei* ILC2279 [b]
tet(O)	Ribosomal protection RP gene	*Streptococcus pyogenes* 7008 [a]
tet(S)	Ribosomal protection RP gene	*Enterococcus italicus* 1102 [b]
tet(K)	Efflux gene	*Staphylococcus aureus* COL. [a]
mecA	β-lactamase encoding gene	*Staphylococcus aureus* 27R [b]
blaZ	β-lactamase encoding gene	*Staphylococcus aureus* ATCC 2921 [c]
aac-aph	Aminoglycoside acetyltransferase encoding gene	*Enterococcus faecium* M48 [a]

[a] *Collection of Dipartimento di Scienze della Vita e dell'Ambiente (DiSVA), Università Politecnica delle Marche, Italy.*
[b] *Collection of Dipartimento di Scienze Agrarie, Alimentari ed Ambientali (D3A), Università Politecnica delle Marche, Italy.*
[c] *ATCC, American Type Culture Collection.*

by different authors for the same insect species (Klunder et al., 2012; Stoops et al., 2016, 2017; Vandeweyer et al., 2017).

LAB counts in wheatmeal were similar to those recorded in whole-meal semolinas by Alfonzo et al. (2017), ranging between < 1 and 3.5 ± 0.4 log cfu g^{-1}. It is known that LAB contamination is very common in cereal grains where their occurrence can be both endophytic or environmental (Alfonzo et al., 2013). In fresh larvae, LAB showed an average load of 8.3 log cfu g^{-1} that was in the range of the values reported by both Stoops et al. (2016) and Vandeweyer et al. (2017) for larvae of the same species, where these microorganisms had an average value of about 7 log cfu g^{-1}.

Regarding the LAB counts, notably higher mean values were seen in the mealworm larvae with respect to wheatmeal or frass. Different pictures emerged when considering the loads of ampicillin- and vancomycin-resistant LAB. Indeed, in all of the samples analyzed, the viable counts of LAB on MRS with ampicillin were significantly lower than those on the same medium with no antibiotics. In more detail, in organic wheatmeal, no LAB resistant to ampicillin were detected ($<$ 1 log cfu g^{-1}), whereas in larvae and frass, the counts of ampicillin-resistant LAB were 6 and 4 orders of magnitude lower, respectively. As reviewed by Clementi and Aquilanti (2011), ampicillin resistance is poorly documented in LAB; however, resistant strains in this microbial group have occasionally been isolated from foods of animal origin, including *Lactobacillus plantarum* from raw meat (Aquilanti et al., 2007) or *Enterococcus* spp. from milk and cheese (Riboldi et al., 2009). Interestingly, members of the genus *Enterococcus* have already been found in the microbiota of edible insects and in both dried and fresh mealworms (Garofalo et al., 2017; Vandeweyer et al., 2017; Wynants et al., 2017).

Regarding the LAB counts on MRS with vancomycin, bacterial loads in wheatmeal were on the same order of magnitude as those assessed on MRS without antibiotic (about 2 log cfu g^{-1}); in contrast, the loads of vancomycin-resistant LAB in mealworm larvae and frass were one and two orders of magnitude lower, respectively. Among LAB, foodborne leuconostocs, pediococci and most lactobacilli species are known to be intrinsically resistant to vancomycin, whereas the majority of lactococci and enterococci are susceptible to this antibiotic (Clementi and Aquilanti, 2011).

As far as enterococci are concerned, neither ampicillin-resistant nor high-level aminoglycoside-resistant (HLAR) enterococci were enumerated in the analyzed samples (loads $<$ 1 log cfu g^{-1}), despite the high counts of this microbial group on Enterococcus Selective Agar (ESA) medium. Conversely, vancomycin-resistant enterococci were identified in both mealworm larvae and frass, with average viable counts of 5.7

and 2.6 log cfu g^{-1}, respectively. Antibiotic-resistant enterococci have a great clinical importance due to the contribution of these microorganisms to nosocomial infection risk. To date, several reports described the occurrence of foodborne enterococci that are highly resistant to vancomycin (Riboldi et al., 2009), thus supporting the need to deepen our knowledge about the distribution of these microorganisms in novel foods.

When the counts of staphylococci are considered, there were no viable colonies from wheatmeal on Mannitol Salt Agar (MSA) medium. In contrast, larvae and frass showed comparable counts at about 5–6 log cfu g^{-1}. To the authors' knowledge, there is a scarcity of available information on staphylococci counts in edible insects. Very recently, Wynants et al. (2017) found viable coagulase-positive staphylococci below 2 log cfu g^{-1} in fresh larvae of *Alphitobius diaperinus* intended for human consumption. A few years before, Oliveira et al. (2014) isolated pathogenic strains of *Staphylococcus aureus* in several live insects (ants, cockroaches, flies, wasps, gnats, moths and butterflies) from Brazilian hospitals.

In the present study, staphylococci resistant to all assayed antibiotics were enumerated in all of the analyzed samples except wheatmeal. As a general trend, mean counts between 2.8 and 5.7 cfu g^{-1} were observed, with erythromycin-resistant staphylococci in frass having the lowest mean counts and gentamicin-resistant staphylococci in larvae having the highest. As reported by Haaber et al. (2017), staphylococci, including pathogenic *S. aureus*, can readily adapt to changing environments and can acquire AR genes through different mechanisms. Although the method by which transfer occurs *in vivo* is still unclear, transduction and conjugation are considered the most prevalent mechanisms. Although antibiotic-resistant staphylococci have already been isolated from a number of animal-based foods (Chajecka-Wierzchowska et al., 2015; Fijałkowski et al., 2016), no reports on the occurrence of AR in staphylococci from edible insects are yet available.

Concerning Enterobacteriaceae in wheatmeal, no growth was seen on both Violet Red Bile Glucose Agar (VRBGA) and VRBGA with ampicillin or gentamicin. As a general trend, higher counts were seen in larvae with respect to frass, irrespective of the growth medium used. For the loads of Enterobacteriaceae on VRBGA, our results are in accordance with those of Vandeweyer et al. (2017) and Wynants et al. (2017) analyses of fresh industrially reared *T. molitor* larvae.

Finally, regarding Pseudomonadaceae, in wheatmeal plated on Pseudomonas Agar Base (PAB), mean counts of 1 log cfu g^{-1} were detected. These microorganisms, and particularly members of the genus *Pseudomonas*, are known to exert plant-promoting activity in the wheat rhizosphere (Godino et al., 2016), thus explaining their presence in wheatmeal used as feed. Higher mean values were seen in both larvae and frass at about 6 log cfu g^{-1} in respect with wheatmeal. Concerning viable counts on PAB with gentamicin, wheatmeal had mean counts below 1 log cfu g^{-1}, whereas larvae and frass had significantly higher mean values at 5.7 and 3.2 log cfu g^{-1}, respectively. Notoriously, *Pseudomonas* includes both spoilage species and opportunistic pathogens (e.g., *Pseudomonas aeruginosa*), which have previously been detected in insects such as cockroaches, grasshoppers and lygaeid bugs (Grabowski and Klein, 2017).

In the present study, the DNA extracted directly from the pooled samples of fresh mealworm larvae, feed substrates (wheatmeal and pooled carrots), and frass collected from a laboratory-scale production chain of *T. molitor* was analyzed by using a PCR-based approach. In more detail, samples negative after first round of amplification reactions were further subjected to nested PCR with an internal primer set, which was specifically conceived to hybridize to secondary internal targets within the main amplified regions. This allows for more sensitive detection of the targeted genes, ranging from 10^0 [*tet*(M), *erm*(C), *vanA*, *blaZ*] to 10^3 [*erm*(A)] copies per sample, depending on the gene (Garofalo et al., 2007). In accordance with the results obtained in previous studies (Milanović et al., 2016; Osimani et al., 2017b,c), the enhanced sensitivity of nested PCR allowed for increased detection of most of the target AR genes.

Regarding fresh larvae, *erm*(A), *erm*(C), *vanA*, *vanB*, *tet*(O), *mecA*, *blaZ*, and *aac-aph* were absent in all of the samples.

In contrast, mealworms carried the tetracycline resistance genes *tet*(M), *tet*(K), and *tet*(S) and the MLS_B resistance gene *erm*(B) (**Table 4**).

Due to their wide-ranging spectrum of activity, tetracyclines represent one of the most widely used classes of antibiotics in clinics. In Gram-negative bacteria, tetracycline resistance mechanisms involve efflux pump systems that are encoded by different tetracycline resistance genes (Hwang et al., 2017). As reported by the ECDC, EFSA, and EMA, significant positive associations were observed between tetracycline AR in human cases of salmonellosis and campylobacteriosis and in tetracycline consumption in animals in Europe, with a possible role in co-selection through the genetic linkage of resistance genes (ECDC/EFSA/, 2015).

There is still a lack of knowledge regarding AR associated with edible insects. Very recently, Osimani et al. (2017b,c) found a high distribution of *tet*(M), *tet*(K), and *tet*(S) in ready-to-eat grasshoppers and mealworms purchased from both European and non-European producers. Moreover, high detection frequencies of the same tetracycline resistance genes have previously been reported by Milanović et al. (2016) in commercially available dried mealworms. In a few investigations, tetracycline-resistant isolates were collected from various insect-based matrices. In more detail, Usui et al. (2015) isolated tet^R *Escherichia coli* strains from both flies and feces of livestock from different farms, suggesting a role for these insects in spreading transferable resistance among the different farms under investigation. A few years before, Larson et al. (2008) found that insects associated with stored feed could be vectors of tetracycline-resistant enterococci.

Macrolides are one of the most important antibiotics used in the clinical treatment of various illnesses, including community-acquired pneumonia, infections caused by *Shigella* and *Salmonella,* and sexually transmitted diseases. Bacterial resistance to this class of antibiotics is determined by an erythromycin ribosomal methyltransferase gene (Fyfe et al., 2016). Regarding resistance to macrolides, the results obtained

TABLE 4 | Results of PCR and nested PCR amplification of AR genes in samples of carrots and wheatmeal used as feed, and fresh mealworm larvae and frass of the three pooled rearing batches.

Sample	Assay	Antibiotic resistance gene											
		erm(A)	*erm*(B)	*erm*(C)	*vanA*	*vanB*	*tet*(M)	*tet*(O)	*tet*(S)	*tet*(K)	*mecA*	*blaZ*	*aac-aph*
Organic carrots	PCR	−	−	−	−	−	−	−	−	−	−	−	−
	n-PCR	−	−	−	−	−	−	−	−	−	−	−	−
Organic wheatmeal	PCR	−	−	−	−	−	−	−	−	−	−	−	−
	n-PCR	−	−	−	−	−	−	−	+	+	−	−	−
Mealworm larvae	PCR	−	−	−	−	−	−	−	+	−	−	−	−
	n-PCR	−	+	−	−	−	+	−	n.d.	+	−	−	−
Frass	PCR	−	−	−	−	−	−	−	+	−	−	−	−
	n-PCR	−	+	−	−	−	+	−	n.d.	+	−	−	+

PCR, positive after PCR; n-PCR: positive after nested PCR; n.d. not determined.

in the present study agree with those reported by Milanović et al. (2016) and Osimani et al. (2017b) for ready-to-eat insects. Furthermore, Osimani et al. (2017c) recently found resistance to erythromycin in samples of dried edible mealworms ready for consumption that are produced in both European and non-European countries. In more detail, Osimani et al. (2017c) found a very high occurrence of *erm*(B)-positive samples in mealworms produced in France. To the authors' knowledge, no other studies on erythromycin resistance in insects are presently available in the scientific literature.

In frass *tet*(M), *tet*(K), *tet*(S), and *aac-aph* were detected (**Table 4**). Aminoglycosides are normally used as broad-spectrum antibiotics against aerobic Gram-negative bacteria. Resistance to this class of antibiotics, which includes streptomycin, neomycin, kanamycin, gentamicin, and tobramycin, can be exerted via N-acetylation, O-nucleotidylation, and/or O-phosphorylation inactivation and efflux pumps (Sheikhalizadeh et al., 2017). In 2008, Larson et al. first isolated strains of *Enterococcus gallinarum* from maize weevil (*Sitophilus zeamais* Motschulsky) and the warehouse beetle (*Trogoderma variabile* Ballion) that were resistant to streptomycin and neomycin, while more recently, Osimani et al. (2017b,c) detected resistance genes to this class of antibiotics in commercially available ready-to-eat grasshoppers and mealworms.

Although in the present study no vancomycin resistance genes were detected, it is worth noting that Osimani et al. (2017c) have recently found *vanA*- and *vanB*-positive samples in ready-to-eat mealworms collected from European producers located in France and Belgium. These findings are particularly important since the increasing emergence of vancomycin-resistant *Enterococcus faecium* strains has recently been reported by the EFSA/ECDC (2016).

Insect frass is a minimally investigated rearing waste, especially in terms of the occurrence of transferable AR. As recently reported by He et al. (2016), rearing wastes can result in environmental contamination by AR genes, leading to potential risks to food safety and human health. This hypothesis was also supported by other studies, which demonstrated that the levels of genes conferring resistances to tetracyclines and MLS_B remained high in animal wastes during composting, lagoon storage, anaerobic digestion, and wetland construction (Wang et al., 2012; Brooks et al., 2014; Huang et al., 2014; Tao et al., 2014).

The results of the quantitative assessment of antibiotic residues in organic wheatmeal and carrots are reported in **Table 2**. The choice to analyze these substrates was driven by the results of a meta-analysis revealing that even organic produce, including vegetables, can effectively be contaminated with pesticides and antibiotic residues, with the latter potentially exerting a selective pressure on the resident microbiota (Smith-Spangler et al., 2012). None of the screened antibiotics were found in the two feed substrates, considering the limits of detection of 100 and 10 μgkg^{-1} (cefacetrile: 33 μgkg^{-1}) for wheatmeal and carrots, respectively.

Regarding the screened AR genes, organic wheatmeal was found to carry both *tet*(S) and *tet*(K) (**Table 4**), whereas no AR genes were detected in organic carrots. Although the microorganisms contaminating the organic wheatmeal used as feed presumably were not subjected to selective pressure by antibiotics, Lin and Kussel (2016) reported that the occurrence of AR is highly dependent on the antibiotic exposure dynamics. The same authors demonstrated that the physiological memory of microbial cells can strongly modulate the emergence of resistance (Lin and Kussel, 2016). In a relatively recent study, Fernández-Fuentes et al. (2012) detected multi-resistant microbial strains in organic foods, including strains of *Chryseobacterium* sp. resistant to erythromycin, *Enterobacter* resistant to amoxicillin and cefuroxime, *E. casseliflavus* resistant to amoxicillin and erythromycin, *Enterococcus faecium* resistant to amoxicillin and erythromycin, and *Pantoea agglomerans* resistant to cefuroxime.

CONCLUSIONS

As a general trend, lower bacterial counts were ascertained in wheatmeal compared to the larvae and frass. On the one hand, this might suggest that the microorganisms originating from wheatmeal colonize and multiply in the gut of larvae. On the other hand, the vertical transmission of microorganisms could have contributed to both the composition and quantity of

microorganisms in the larvae and frass (Engel and Moran, 2013; Itoh et al., 2014; Shapira, 2016).

Moreover, the occurrence of *tet*(S) and *tet*(K) in organic wheatmeal, larvae and frass suggests the effective role of feed in the occurrence of AR genes and/or antibiotic resistant microorganisms in larvae, under no selective pressure exerted by antibiotics. In addition, the fact that larvae and frass were found to carry AR genes that were not detectable in organic wheatmeal seems to confirm that AR genes or antibiotic-resistant microorganisms (e.g., symbionts) can be transferred vertically via insect egg smearing.

AR in bacteria associated with food animals represents a risk to human health. In light of the use of edible insects as a new source of protein, the evaluation of AR within the production chain of this novel food constitutes a step forward in risk assessment.

The results overall collected by analyzing fresh larvae reared in a laboratory facility under no selective pressure exerted by antibiotics (either used as growth promoters or emergency treatment or even occurring as residues in feed) suggest that edible insects can be natural carrier of AR.

AUTHOR CONTRIBUTIONS

VM, FeC, and CG carried out microbiological and molecular analyses. SR, PR, NI, and NL reared the edible insects under study. RG, SM, AP, EM, and FT carried out chemical analyses on insects and substrates. AO, LA, and FrC conceived the research, critically analyzed the results and wrote the manuscript.

ACKNOWLEDGMENTS

This study was financially supported by the Università Politecnica delle Marche, Ancona, Italy, by the project Edible insects: new frontiers in food-FOODIN.

We wish to thank Dr. Rico Marabini for his valuable support with the molecular analyses.

SUPPLEMENTARY MATERIAL

The Supplementary Material for this article can be found online at: https://www.frontiersin.org/articles/10.3389/fmicb.2018.02702/full#supplementary-material

REFERENCES

Aarts, H., and Margolles, A. (2015). Antibiotic resistance genes in food and gut (non-pathogenic) bacteria. Bad Genes in good bugs. *Front. Microbiol.* 5:754. doi: 10.3389/fmicb.2014.00754

Alfonzo, A., Miceli, C., Nasca, A., Franciosi, E., Ventimiglia, G., Di Gerlando, R., et al. (2017). Monitoring of wheat lactic acid bacteria from the field until the first step of dough fermentation. *Food Microbiol.* 62, 256–269. doi: 10.1016/j.fm.2016.10.014

Alfonzo, A., Ventimiglia, G., Corona, O., Di Gerlando, R., Gaglio, R., Francesca, N., et al. (2013). Diversity and technological potential of lactic acid bacteria of wheat flours. *Food Microbiol.* 36, 343–354. doi: 10.1016/j.fm.2013.07.003

American Public Health Association (1976). *Compendium of Methods for the Microbiological Examination of Foods*. Washington, DC: APHA Inc.

Aquilanti, L., Garofalo, C., Osimani, A., Silvestri, G., Vignaroli, C., and Clementi, F. (2007). Isolation and molecular characterization of antibiotic-resistant lactic acid bacteria from poultry and swine meat products. *J. Food Prot.* 70, 557–565. doi: 10.4315/0362-028X-70.3.557

Banjo, A. D., Lawal, O. A., and Adeyemi, A. J. (2006). The microbial fauna associated with the larvae of *Oryctes monocerus*. *J. Appl. Sci. Res.* 2, 837–843.

Bannerman, T. L. (2003). "*Staphylococcus*, *Micrococcus*, and other catalase-positive cocci that grow aerobically," in *Manual of Clinical Microbiology, 8th Edn*. Vol. 1. eds P. R. Murray, E. J. Baron, J. H. Jorgensen, M. A. Pfaller, and R. H. Yolken (Washington, DC: American Society for Microbiology), 384–404.

Bhattacharya, A. K., Ameel, J. J., and Waldbauer, G. P. (1970). A method for sexing living pupal and adult yellow mealworms. *Ann. Entomol. Soc. Am.* 63, 1783–1783. doi: 10.1093/aesa/63.6.1783

Broekhovenv,V. S., Oonincx, D. G., Huis, V. A., and Loon, V. J. J. A. (2015). Growth performance and feed conversion efficiency of three edible mealworm species (*Coleoptera: Tenebrionidae*) on diets composed of organic by-products. *J. Insect Physiol.* 73, 1–10. doi: 10.1016/j.jinsphys.2014.12.005

Brooks, J. P., Adeli, A., and McLaughlin, M. R. (2014). Microbial ecology, bacterial pathogens, and antibiotic resistant genes in swine manure wastewater as influenced by three swine management systems. *Water Res.* 57, 96–103. doi: 10.1016/j.watres.2014.03.017

Chajecka-Wierzchowska, W., Zadernowska, A., Nalepa, B., Sierpinska, M., and Łaniewska-Trokenheim, L. (2015). Coagulase-negative staphylococci (CoNS) isolated from ready-to-eat food of animal origin - Phenotypic and genotypic antibiotic resistance. *Food Microbiol.* 46, 222–226. doi: 10.1016/j.fm.2014.08.001

Chapman, G. H. (1945). The significance of sodium chloride in studies of staphylococci. *J. Bacteriol.* 50, 201–203.

Clementi, F., and Aquilanti, L. (2011).Recent investigations and updated criteria for the assessment of antibiotic resistance in food lactic acid bacteria. *Anaerobe* 17, 394–398. doi: 10.1016/j.anaerobe.2011.03.021

Cortes Ortiz, J. A., Ruiz, A. T., Morales-Ramos, J. A., Thomas, M., Rojas, M. G., Tomberlin, J. K., et al. (2016). "Insect mass production technologies," in *Insects as Sustainable Food Ingredients*, eds A. T. Dossey, J. A. Morales-Ramos, and M. G. Rojas (San Diego, CA: Academic Press), 153–201. doi: 10.1016/B978-0-12-802856-8.00006-5

Cox, L. A. (2015). "Antimicrobial Resistance and Food Safety," in *Food Microbial Safety and Animal Antibiotics, Methods and Techniques* eds Chen C-Y., Yan X, and Jackson C. R. (Oxford: Academic Press; Elsevier), 303–323.

De Man, J. C., Rogosa, M., and Sharpe, M. E. (1960). A medium for the cultivation of lactobacilli. *J. Appl. Bacteriol.* 23, 130–135. doi: 10.1111/j.1365-2672.1960.tb00188.x

Devirgiliis, C., Barile, S., and Perozzi, G. (2011). Antibiotic resistance determinants in the interplay between food and gut microbiota. *Genes Nutr.* 6, 275–284. doi: 10.1007/s12263-011-0226-x

Dreassi, E., Cito, A., Zanfini, A., Materozzi, L., Botta, M., and Francardi, V. (2017). Dietary fatty acids influence the growth and fatty acid composition of the yellow mealworm Tenebrio molitor (*Coleoptera: Tenebrionidae*). *Lipids* 52, 285–294. doi: 10.1007/s11745-016-4220-3

ECDC/EFSA/ (2015). (European Centre for Disease Prevention and Control), EFSA (European Food Safety Authority) and (European Medicines Agency). ECDC/EFSA/ first joint report on the integrated analysis of the consumption of antimicrobial agents and occurrence of antimicrobial resistance in bacteria from humans and food-producing animals. Stockholm/Parma/London: ECDC/EFSA/, (2015). *EFSA J.* 13:4006. doi: 10.2903/j.efsa.2015.4006

EFSA/ECDC (2016). (European Food Safety Authority), ECDC (European Centre for Disease Prevention and Control), The European Union summary report on antimicrobial resistance in zoonotic and indicator bacteria from humans, animals and food in 2014. *EFSA J.* 14:4380. doi: 10.2903/j.efsa.2016.4380

Engel, P., and Moran, N. A. (2013). The gut microbiota of insects – diversity in structure and function. *FEMS Microbiol. Rev.* 37, 699–735. doi: 10.1111/1574-6976.12025

EUCAST (The European Committee on Antimicrobial Susceptibility Testing) (2017). *Breakpoint Tables for Interpretation of MICs and Zone Diameters*. version 7.1, 2017. Available online at: http://www.eucast.org

Fernández-Fuentes, M. A., Ortega Morente, E., Abriouel, H., Pérez Pulido, R., and Gálvez, A. (2012). Isolation and identification of bacteria from organic foods: sensitivity to biocides and antibiotics. *Food Control* 26, 73–78. doi: 10.1016/j.foodcont.2012.01.017

Fijałkowski, K., Peitler, D., and Karakulska, J. (2016). Staphylococci isolated from ready-to-eatmeat – identification, antibiotic resistance and toxin gene profile. *Int. J. Food Microbiol.* 238, 113–120. doi: 10.1016/j.ijfoodmicro.2016.09.001

Fyfe,. C., Grossman, T. H., Kerstein, K., and Sutcliffe, J. (2016). Resistance to macrolide antibiotics in public health pathogens. *Cold Spring Harb. Perspect. Med.* 6:a025395. doi: 10.1101/cshperspect.a025395

Garofalo, C., Osimani, A., Milanović, V., Taccari, M.,Cardinali, F., Aquilanti, L., et al. (2017). The microbiota of marketed processed edible insects as revealed by high-throughput sequencing. *Food Microbiol.* 62, 15–22. doi: 10.1016/j.fm.2016.09.012

Garofalo, C., Vignaroli, C., Zandri, G., Aquilanti, L., Bordoni, D., Osimani, A., et al. (2007). Direct detection of antibiotic resistance genes in specimens of chicken and pork meat. *Int. J. Food Microbiol.* 113, 75–83. doi: 10.1016/j.ijfoodmicro.2006.07.015

Gasco, L., Henry, M., Piccolo, G., Marono, S., Gai, F., Renna, M., et al. (2016). *Tenebrio molitor* meal in diets for European sea bass (*Dicentrarchus labrax* L.) juveniles: growth performance, whole body composition and *in vivo* apparent digestibility. *Anim. Feed Sci. Tech.* 220, 34–45. doi: 10.1016/j.anifeedsci.2016.07.003

Geftic, S. G., Heymann, H., and Adair, F. W. (1979). Fourteen year survival of *Pseudomonas cepacia* in a salts solution preserved with benzalkonium chloride. *Appl. Environ. Microbiol.* 37, 505–510.

Godino, A., Prìncipe, A., and Fischer, S. (2016). A ptsP deficiency in PGPR *Pseudomonas fluorescens* SF39a affects bacteriocin production and bacterial fitness in the wheat rhizosphere. *Res. Microbiol.* 167, 178–189. doi: 10.1016/j.resmic.2015.12.003

Grabowski, N. T., and Klein, G. (2017). Bacteria encountered in raw insect, spider, scorpion, and centipede taxa including edible species, and their significance from the food hygiene point of view. *Trends Food Sci. Tech.* 63, 80–90. doi: 10.1016/j.tifs.2017.01.007

Haaber, J., Penadés, J. R., and Ingmer, H. (2017). Transfer of antibiotic resistance in *Staphylococcus aureus*. *Trends Microbiol.* 25, 893–905. doi: 10.1016/j.tim.2017.05.011

Haddad, I., Mozzon, M., and Frega, N. G. (2012). Trends in fatty acids positional distribution in human colostrum, transitional, and mature milk. *Eur. Food Res. Technol.* 235, 325–332. doi: 10.1007/s00217-012-1759-y

He, L.-Y., Ying, G.-G., Liu, Y.-S., Su, H.-C., Chen, J., Liu, S.-S., et al. (2016). Discharge of swine wastes risks water quality and food safety: antibiotics and antibiotic resistance genes from swine sources to the receiving environments. *Environ. Int.* 92–93, 210–219. doi: 10.1016/j.envint.2016.03.023

Holt, V. M. (1995). "Why not eat insects?" in *Text Reset From the Original 1885 edition,* ed D. H. Meeuws (Oxford: Thornton's), 67.

Huang, X., Liu, C., Li, K., Su, J., Zhu, G., and Liu, L. (2014). Performance of vertical up-flow constructed wetlands on swine wastewater containing tetracyclines and tet genes. *Water Res.*. 70, 109–117. doi: 10.1016/j.watres.2014.11.048

Hwang, D., Kim, S. M., and Kim, H. J. (2017). Modelling of tetracycline resistance gene transfer by commensal Escherichia coli food isolates that survived in gastric fluid conditions. *Int. J. Antimicrob. Agents* 49, 81–87. doi: 10.1016/j.ijantimicag.2016.10.009

Hynes, W. L., Ferretti, J. J., Gilmore, M. S., and Segarra, R. A. (1992). PCR amplification of streptococcal DNA using crude cell lysates. *FEMS Microbiol. Lett.* 73, 139–142. doi: 10.1111/j.1574-6968.1992.tb05303.x

Itoh, H., Aita, M., Nagayama, A., Meng, X.-Y., Kamagata, Y., Navarro, R., et al. (2014). Evidence of environmental and vertical transmission of *Burkholderia symbionts* in the oriental chinch bug, *Cavelerius saccharivorus* (*Heteroptera: Blissidae*). *Appl. Environ. Microbiol.* 80, 5974–5983. doi: 10.1128/AEM.01087-14

Jacob, A. E., and Hobbs, S. J. (1974). Conjugal transfer of plasmidborne multiple antibiotic resistance in *Streptococcus faecalis* var. *zymogenes. J. Bacteriol.* 117, 360–372.

Klunder, H. C., Wolkers-Rooijackers, J., Korpela, J. M., and Nout, M. J. R. (2012). Microbiological aspects of processing and storage of edible insects. *Food Control* 26, 628–631. doi: 10.1016/j.foodcont.2012.02.013

Larson, Z., Subramanyam, B., Zurek, L., and Herrman, T. (2008). Diversity and antibiotic resistance of enterococci associated with stored-product insects collected from feed mills. *J. Stored Prod. Res.* 44, 198–203. doi: 10.1016/j.jspr.2007.08.007

Lin, W.-H., and Kussel, E. (2016). Complex interplay of physiology and selection in the emergence of antibiotic resistance. *Curr. Biol.* 26, 1486–1493. doi: 10.1016/j.cub.2016.04.015

Milanović, V., Osimani, A., Pasquini, M., Aquilanti, L., Garofalo, C., Taccari, M., et al. (2016). Getting insight into the prevalence of antibiotic resistance genes in specimens of marketed edible insects. *Int. J. Food Microbiol.* 227, 22–28. doi: 10.1016/j.ijfoodmicro.2016.03.018

Milanović, V., Osimani, A., Taccari, M., Garofalo, C., Butta, A., Clementi, F., et al. (2017). Insight into the bacterial diversity of fermentation woad dye vats as revealed by PCR-DGGE and pyrosequencing. *J. Ind. Microbiol. Biotechnol.* 44, 997–1004 doi: 10.1007/s10295-017-1921-4

Moretti, S., Cruciani, G., Romanelli, S., Rossi, R., Saluti, G., and Galarini, R. (2016). Multiclass method for the determination of 62 antibiotics in milk. *J. Mass Spectrom.* 51, 792–804. doi: 10.1002/jms.3834

Mozzon, M., Frega, N. G., Fronte, B., and Tocchini, M. (2002). Effect of dietary fish oil supplements on levels of n-3 polyunsaturated fatty acids, trans acids and conjugated linoleic acid in ewe milk. *Food Technol. Biotech.* 40, 213–219.

Oliveira, P. S., Souza, S. G., Campos, G. B., da Silva, D. C., Sousa, D. S., Araújo S. P. et al. (2014). Isolation, pathogenicity and disinfection of *Staphylococcus aureus* carried by insects in two public hospitals of Vitória da Conquista, Bahia, Brazil. *Braz. J. Infect. Dis.* 18, 129–136. doi: 10.1016/j.bjid.2013.06.008

Osimani, A., Cardinali, F., Aquilanti, L., Garofalo, C., Roncolini, A., Milanović, V., et al. (2017c). Occurrence of transferable antibiotic resistances in commercialized ready-to-eat mealworms (*Tenebrio molitor L.*). *Int. J. Food Microbiol.* 263, 38–46. doi: 10.1016/j.ijfoodmicro.2017.10.009

Osimani, A., Garofalo, C., Aquilanti, L., Milanović, V., Cardinali, F., Taccari, M., et al. (2017b). Transferable antibiotic resistances in marketed edible grasshoppers (*Locusta migratoria migratorioides*). *J. Food Sci.* 82, 1184–1192. doi: 10.1111/1750-3841.13700

Osimani, A., Garofalo, C., Aquilanti, L., Milanović, V., and Clementi, F. (2015). Unpasteurised commercial boza as a source of microbial diversity. *Int. J. Food Microbiol.* 194, 62–70. doi: 10.1016/j.ijfoodmicro.2014.11.011

Osimani, A., Garofalo, C., Milanović, V., Taccari, M., Cardinali, F., Aquilanti, L., et al. (2017a). Insight into the proximate composition and microbial diversity of edible insects marketed in the European Union. *Eur. Food Res. Technol.* 243, 1157–1171. doi: 10.1007/s00217-016-2828-4

Pacetti, D., Mozzon, M., Lucci, P., and Frega, N. G. (2013). Bioactive fish fatty acids: health effects and their use as functional food ingredients. *Curr. Nutr. Food Sci.* 9, 283–297. doi: 10.2174/15734013113096660015

Riboldi, G. B., Frazzon, J., Alves d'Azevedo, P., and Frazzon, A. P. (2009). Antimicrobial resistance profile of *Enterococcus* spp. isolated from food in southern Brazil. *Braz. J. Microbiol.* 40, 125–128. doi: 10.1590/S1517-838220090001000021

Rolain, J. M. (2013). Food and human gut as reservoirs of transferable antibiotic resistance encoding genes. *Front. Microbiol.* 4:173. doi: 10.3389/fmicb.2013.00173

Schlüter, O., Rumpold, B., Holzhauser, T., Roth, A., Vogel, R. F., Quasigroch, W., et al. (2016). Safety aspects of the production of foods and food ingredients from insects. *Mol. Nutr. Food Res.* 61, 1–14. doi: 10.1002/mnfr.201600520

Shapira, M. (2016). Gut microbiotas and host evolution: scaling up symbiosis. *Trends Ecol. Evol.* 31, 539–549. doi: 10.1016/j.tree.2016.03.006

Sheikhalizadeh, V., Hasani, A., Ahangarzadeh Rezaee, M., Rahmati-Yamchi, M., Hasani, A., Ghotaslou, R., et al. (2017). Comprehensive study to investigate the role of various aminoglycoside resistance mechanisms in clinical isolates of *Acinetobacter baumannii*. *J. Infect. Chemother.* 23, 74–79. doi: 10.1016/j.jiac.2016.09.012

Simpanya, M. F., Allotey, J., and Mpuchane, S. (2000). A mycological investigation of phane, and edible caterpillar of an emperor moth, *Imbrasia belina*. *J. Food Prot.* 63 , 137–140. doi: 10.4315/0362-028X-63.1.137

Slanetz, L. W., and Bartley, C. H. (1957). Numbers of enterococci in water, sewage, and feces determined by the membrane filter technique with an improved medium. *J. Bacteriol.* 74, 591–595.

Smith-Spangler, C., Brandeau, M. L., Hunter, G. E., Bavinger, J. C., Pearson, M., Eschbach, P. J., et al. (2012). Are organic foods safer or healthier than conventional alternatives?: a systematic review. *Ann. Intern. Med.* 157, 348–366. doi: 10.7326/0003-4819-157-5-201209040-00007

Stoops, J., Crauwels, S., Waud, M., Claes, J., Lievens, B., and Van Campenhout, L. (2016). Microbial community assessment of mealworm larvae (*Tenebrio molitor*) and grasshoppers (*Locusta migratoria migratorioides*) sold for human consumption. *Food Microbiol.* 53, 122–127. doi: 10.1016/j.fm.2015.09.010

Stoops, J., Vandeweyer, D., Crauwels, S., Verrethb, C., Boeckxd, H., Van Der Borght, M., et al. (2017). Minced meat-like products from mealworm larvae (*Tenebrio molitor* and *Alphitobius diaperinus*): microbial dynamics during production and storage. *Inn. Food Sci. Emerg. Tech.* 41, 1–9. doi: 10.1016/j.ifset.2017.02.001

Tao, C. W., Hsu, B. M., Ji, W. T., Hsu, T. K., Kao, P. M., Hsu, C. P., et al. (2014). Evaluation of five antibiotic resistance genes in wastewater treatment systems of swine farms by real-time PCR. *Sci. Total Environ.* 496, 116–121. doi: 10.1016/j.scitotenv.2014.07.024

Thanner, S., Drissner, D., and Walshc, F. (2016). Antimicrobial resistance in AGRICULTURE. *MBio* 7:e02227–e02215. doi: 10.1128/mBio.02227-15

Usui, M., Shirakawa, T., Fukuda, A., and Tamura, Y. (2015). The role of flies in disseminating plasmids with antimicrobial-resistance genes between farms. *Microb. Drug Resist.* 21, 562–569. doi: 10.1089/mdr.2015.0033

Valerio, F., De Bellis, P., Di Biase, M., Lonigro, S. L., Giussani, B., Visconti, A., et al. (2012). Diversity of spore-forming bacteria and identification of *Bacillus amyloliquefaciens* as a species frequently associated with the ropy spoilage of bread. *Int. J. Food Microbiol.* 156, 278–285. doi: 10.1016/j.ijfoodmicro.2012.04.005

van Huis, A. (2016). Edible insects are the future? *Proc. Nutr. Soc.* 75, 294–305. doi: 10.1017/S0029665116000069

van Huis, A., Van Itterbeeck, J., Klunder, H., Mertens, E., Halloran, A., and Vantomme, P. (2013). *Edible Insects: Future Prospects for Food and Feed Security.* Food and Agriculture Organization of the United Nations, Rome. FAO Forestry Paper, FAO, 187.

Vandeweyer, D., Crauwels, S., Lievens, B., and Van Campenhout, L. (2017). Metagenetic analysis of the bacterial communities of edible insects from diverse production cycles at industrial rearing companies. *Int. J. Food Microbiol.* 261, 11–18. doi: 10.1016/j.ijfoodmicro.2017.08.018

Vandeweyer, D., Milanović, V., Garofalo, C., Osimani, A., Clementi, F., Van Campenhout, L., et al. (2019). Real-time PCR detection and quantification of selected transferable antibiotic resistance genes in fresh edible insects from Belgium and the Netherlands. *Int. J. Food Microbiol.* 290, 288–295. doi: 10.1016/j.ijfoodmicro.2018.10.027

Verbeke, W. (2015). Profiling consumers who are ready to adopt insects as a meat substitute in a Western society. *Food Qual. Prefer.* 39, 147–155. doi: 10.1016/j.foodqual.2014.07.008

Wang, L., Oda, Y., Grewal, S., Morrison, M., Michel, F. C., and Yu, Z. (2012). Persistence of resistance to erythromycin and tetracycline in swine manure during simulated composting and lagoon treatments. *Microb. Ecol.* 63, 32–40. doi: 10.1007/s,00248-011-9921-9

World Health Organization (2014). *Antimicrobial Resistance: Global Report on Surveillance.* World Health Organization (ISBN: 9241564741).

Wynants, E., Crauwels, S., Lievens, B., Luca, S., Claes, J., Borremans, A., et al. (2017). Effect of post-harvest starvation and rinsing on the microbial numbers and the bacterial community composition of mealworm larvae (*Tenebrio molitor*). *Inn. Food Sci. Emerg. Technol.* 42, 8–15. doi: 10.1016/j.ifset.2017.06.004

Zhao, X., Vázquez-Gutiérrez, J. L., Johansson, D. P., Landberg, R., and Langton, M. (2016). Yellow mealworm protein for food purposes - extraction and functional properties. *PLoS ONE* 11:e0147791. doi: 10.1371/journal.pone.0147791

Zurek, L., and Ghosha, A. (2014). Insects represent a link between food animal farms and the urban environment for antibiotic resistance traits. *Appl. Environ. Microbiol.* 80, 3562–3567. doi: 10.1128/AEM.00600-14

Conflict of Interest Statement: The authors declare that the research was conducted in the absence of any commercial or financial relationships that could be construed as a potential conflict of interest.

frontiers in Microbiology

ORIGINAL RESEARCH
published: 04 December 2018
doi: 10.3389/fmicb.2018.02989

Clonal Spread of *Escherichia coli* ST93 Carrying *mcr-1*-Harboring IncN1-IncHI2/ST3 Plasmid Among Companion Animals, China

Jing Wang†, Xin-Yi Huang†, Ying-Bi Xia, Ze-Wen Guo, Zhen-Bao Ma, Meng-Ying Yi, Lu-Chao Lv, Pei-Lan Lu, Jie-Cong Yan, Jia-Wei Huang, Zhen-Ling Zeng and Jian-Hua Liu**

College of Veterinary Medicine, Key Laboratory of Zoonosis of Ministry of Agricultural and Rural Affairs, South China Agricultural University, Guangzhou, China

OPEN ACCESS

Edited by:
Dongchang Sun, Zhejiang University of Technology, China

Reviewed by:
Guo-bao TIAN, Sun Yat-sen University, China
Yongfei Hu, China Agricultural University, China
Nora Lía Padola, National University of Central Buenos Aires, Argentina
Yonghong Xiao, Zhejiang University, China

***Correspondence:**
Zhen-Ling Zeng
zlzeng@scau.edu.cn
Jian-Hua Liu
jhliu@scau.edu.cn

† These authors have contributed equally to this work

Specialty section:
This article was submitted to Antimicrobials, Resistance and Chemotherapy, a section of the journal Frontiers in Microbiology

Received: *27 June 2018*
Accepted: *19 November 2018*
Published: *04 December 2018*

Citation:
Wang J, Huang X-Y, Xia Y-B, Guo Z-W, Ma Z-B, Yi M-Y, Lv L-C, Lu P-L, Yan J-C, Huang J-W, Zeng Z-L and Liu J-H (2018) Clonal Spread of Escherichia coli ST93 Carrying mcr-1-Harboring IncN1-IncHI2/ST3 Plasmid Among Companion Animals, China. Front. Microbiol. 9:2989. doi: 10.3389/fmicb.2018.02989

The purpose of this study was to investigate the occurrence of plasmid-mediated colistin resistance gene *mcr-1* in Enterobacteriaceae isolates from companion animals in Guangzhou, China. Enterobacteriaceae isolated from 180 samples collected from cats and dogs were screened for *mcr-1* by PCR and sequencing. MCR-1-producing isolates were further characterized by multilocus sequence typing and pulsed-field gel electrophoresis (PFGE). Plasmid characterization was performed by conjugation, replicon typing, S1-PFGE, and Southern blot hybridization. Plasmid pHN6DS2 as a representative IncN1-IncHI2/ST3 plasmid from ST93 *E. coli* was fully sequenced. pHN6DS2-like plasmids were screened by PCR-mapping and sequencing. The *mcr-1* gene was detected in 6.25% (8/128) *Escherichia coli* isolates, of which, five belonged to *E. coli* ST93 and had identical PFGE patterns, resistance profiles and resistance genes. *mcr-1* genes were located on ∼244.4 kb plasmids ($n = 6$), ∼70 kb plasmids, and ∼60 kb plasmids, respectively. Among them, five *mcr-1*-carrying plasmids were successfully transferred to recipient by conjugation experiments, and were classified as IncN1-IncHI2/ST3 (∼244.4 kb, $n = 4$, all obtained from *E. coli* ST93), and IncI2 (∼70 kb, $n = 1$), respectively. Plasmid pHN6DS2 contained a typical IncHI2-type backbone, with IncN1 segment (Δ*repA*-Iterons I-*gshB*-ΔIS*1294*) inserted into the multiresistance region, and was similar to other *mcr-1*-carrying IncHI2/ST3 plasmids from Enterobacteriaceae isolates of various origins in China. The remaining five *mcr-1*-bearing plasmids with sizes of ∼244.4 kb were identified to be pHN6DS2-like plasmids. In conclusion, clonal spread of ST93 *E. coli* isolates was occurred in companion animals in Guangzhou, China.

Keywords: colistin resistance, companion animals, *Escherichia coli*, *mcr-1*, plasmids

INTRODUCTION

Colistin has been a last-resort treatment option in human medicine for infections caused by multi-resistant Gram-negative bacteria (Kaye et al., 2016). Resistance to colistin had only been involved with chromosomal mutations until the identification of plasmid-mediated colistin resistance gene *mcr-1* from a porcine *Escherichia coli* isolate in China in 2015 (Liu et al., 2016). The emergence and dissemination of *mcr-1* is a significant global concern and poses a serious threat to clinical treatment. Since the discovery of *mcr-1*, it has been increasingly reported in Enterobacteriaceae

from humans, animals, food products, and the environment worldwide, particularly in China (Jeannot et al., 2017; Wang et al., 2018). To date, *mcr-1* has been identified on various plasmid types, with IncI2, IncHI2, and IncX4 being the major carriers, and IS*Apl1* is involved in *mcr-1* mobilization between DNA molecules (e.g., plasmid, chromosome) (Matamoros et al., 2017; Li et al., 2018; Wang et al., 2018). Previous studies have demonstrated high *mcr-1* prevalence in *E. coli* isolates from food-producing animals (pigs and chickens) and meat (pork and chicken meat) in China (Liu et al., 2016, 2017; Wu et al., 2018). However, *mcr-1* has been rarely reported in companion animals, though 8.7% Enterobacteriaceae isolates were identified to carry *mcr-1* among companion animals in Beijing, China, meanwhile, *mcr-1*-positive *E. coli* isolates may transfer between companion animals and close contactors in a pet store in Guangzhou, China (Sun et al., 2016; Zhang et al., 2016; Lei et al., 2017). Thus, in this study, we investigated the prevalence and characterization of *mcr-1* in Enterobacteriaceae isolates from companion animals in Guangzhou, China, to provide insights into the spread of *mcr-1* in companion animals.

MATERIALS AND METHODS

Sample Collection and *mcr-1* Detection

During July to August 2016, 180 samples were collected from cats and dogs at four animal hospitals located in four districts in Guangzhou, China, including 68 feces samples from healthy animals, 112 samples (feces, urine, eye secretion, ear exudates, nasal secretion, and skin) from diseased animals (**Table 1**). Samples were incubated in LB broth for 16∼24 h and then inoculated on the MacConkey agar. One isolate per sample was selected and identified by MALDI-TOF mass spectrometry or 16S rRNA sequencing (**Supplementary Table S1**). In all isolates, *mcr-1* was detected by PCR and sequencing (**Supplementary Table S1**).

Molecular Typing

The genetic diversity of *mcr-1*-positive *E. coli* isolates was characterized by multilocus sequence typing (MLST)[1]. Five *mcr-1*-carrying ST93 *E. coli* isolates in this study and the *mcr-1*-positive ST93 *E. coli* strain PET01, that was previously obtained from a cat in Guangzhou, China (Zhang et al., 2016) were further analyzed by pulsed-field gel electrophoresis (PFGE) (Gautom, 1997).

Conjugation/Transformation Experiments and Plasmid Characterization

Conjugation experiments were carried out using streptomycin-resistant *E. coli* C600 as the recipient strain as previously described (Chen et al., 2007). Transconjugants were selected using 2 mg/L colistin and 3,000 mg/L streptomycin. Transfer frequencies were calculated as the number of transconjugants per recipient, experiments were performed in triplicate. Transformation was conducted by heat-shock and electroporation using *E. coli* strain DH5α as the recipient strain, and selected by 2 mg/L colistin. The presence of *mcr-1* in the transconjugants was confirmed by PCR and sequencing. Transconjugants with a single *mcr-1*-carrying plasmid, verified by S1-PFGE (Barton et al., 1995) and Southern blot hybridization, were selected for further study. The location of *mcr-1* in the original isolates which failed to obtain transconjugants/transformants was determined by S1-PFGE and Southern blot hybridization. All the transconjugants were characterized by PCR-based replicon typing and IncI2 and IncX4 plasmids were screened according to previously described protocols (Carattoli et al., 2005; Johnson et al., 2012; Lv et al., 2013). IncHI2 plasmids were further characterized by plasmid double locus sequence typing (García-Fernández and Carattoli, 2010). The genetic structure of *mcr-1* was determined by PCR mapping and sequencing in five transconjugants and three original isolates without transconjugants/transformants (**Supplementary Table S2**).

Antimicrobial Susceptibility Testing

The original *mcr-1*-positive *E. coli* isolates, the recipient strain C600, and transconjugants were tested for their susceptibility to ampicillin, cefotaxime, imipenem, gentamycin, amikacin, tetracycline, chloramphenicol, florfenicol, ciprofloxacin, sulfamethoxazole/trimethoprim, colistin, and fosfomycin by the agar dilution method or the broth microdilution method (limited to colistin). Antimicrobial susceptibility tests were performed and interpreted according to M100, 28th edition of the CLSI (Wayne, PA, United States) (Clinical Laboratory Standards Institute [CLSI], 2018). Colistin ($>$ 2 mg/L), and florfenicol ($>$ 16 mg/L) were interpreted according to the clinical breakpoints or epidemiological cutoff values of EUCAST.[2] The *E. coli* strain ATCC 25922 was used for quality control. The mutations within *gyrA* and *parC* were detected in ciprofloxacin-resistant *mcr-1*-positive *E. coli* isolates (**Supplementary Table S1**). Other resistance genes, including bla_{CTX-M}, *floR*, *rmtB*, *oqxAB*, and *fosA3* were screened in original *mcr-1*-positive isolates and their transconjugants using the primers listed in **Supplementary Table S1**.

Plasmid Sequencing

Plasmid pHN6DS2, as a representative IncN1-IncHI2/ST3 plasmid from ST93 *E. coli* isolate, was selected to extract from the transconjugant using QIAGEN® Plasmid Midi Kit (Qiagen, Hilden, Germany) and sequenced by Illumina Miseq technology (Illumina, San Diego, CA, United States). Sequence reads were assembled into contigs with SOAPdenovo version 2.04. Nine contigs of pHN6DS2 were assembled into the complete plasmid sequence with PCR amplification and Sanger sequencing (**Supplementary Table S3**) using related *mcr-1*-carrying plasmids as references by BLAST[3]. Analysis and annotation of plasmid pHN6DS2 were performed using the RAST server (Aziz et al.,

[1]http://enterobase.warwick.ac.uk/species/index/ecoli

[2]https://mic.eucast.org/Eucast2/

[3]http://blast.ncbi.nlm.nih.gov/Blast.cgi

TABLE 1 | Source and origin of Enterobacteriaceae isolates obtained from companion animals in Guangzhou, China.

Sampling Location	Sampling time	Specimen source	No. of samples	Sick or healthy	Specimen type (no. of samples)	No. of isolates		
						E. coli	*K.pneumoniae*	*E. cloacae*
Animal hospital 1	Aug 5th–12th	cat	2	S	Feces (1) Urine (1)	1		
		dog	28	S	Feces (14) Urine (14)	14	8	2
		All	30			15		
Animal hospital 2	July 10th–17th	cat	15	H	Feces (3)	2		
	July 26th–Aug 3rd			S	Feces (10), urine (1), eye secretion (1)	10		1
		dog	36	H	Feces (30)	25	4	
				S	Feces (3), urine (3)	4		
		All	51			41		
Animal hospital 3	July 12th–19th	cat	12	H	Feces (5)	5		
	July 21st–30th			S	Feces (4), urine (1), eye secretion (1), ear exudates (1)	2		
		dog	43	H	Feces (15)	11		1
				S	Feces (15), urine (1), nasal secretion (8), ear exudates (3), skin (1)	16	5	
		All	55			34		
Animal hospital 4	Aug 13th–20th	cat	6	H	Feces (4)	4		
				S	Feces (2)	1		
		dog	38	H	Feces (11)	9	1	
				S	Feces (27)	24	3	
		All	44			38		
Total			180			128	21	4

H, healthy companion animals for vaccination; S, sick companion animals diagnosed by veterinarians, including sick animals with hematuresis, urethritis, pneumonia, diarrhea, cough, bone fracture, patellar dislocation, tumor, hysterectomy, otitis externa, canine distemper, sarcoptic acariasis, cystitis, hepatitis, hydrocephalus, and some unknown diseases. Samples were consecutively taken from all animals admitting the four hospitals during sampling time.

2008), ISfinder[4], ResFinder[5], RAC[6], BLAST[7], and the Gene Construction Kit 4.5 (Textco BioSoftware, Inc., Raleigh, NC, United States). The remaining transconjugants or original isolates containing ∼244.4 kb *mcr-1*-bearing plasmid were examined for pHN6DS2-like plasmids by PCR and sequencing (**Supplementary Table S4**).

Nucleotide Sequence Accession Number

The nucleotide sequences of plasmid pHN6DS2 has been deposited in the GenBank database under the accession number MH459020.

RESULTS AND DISCUSSION

Identification of *mcr-1* and Antimicrobial Susceptibility

A total of 128 *E. coli*, 21 *Klebsiella pneumoniae*, and 4 *Enterobacter cloacae* isolates were obtained from 180 samples of companion animals origin (**Table 1**). Among them, *mcr-1* was present in eight (6.25%) *E. coli* isolates, two from healthy animals and six from diseased animals (**Table 2**). The isolates from diseased animals (6/72, 8.33%) showed higher *mcr-1* prevalence than those from healthy animals (2/56, 3.57%; $P > 0.05$). However, we did not identify *mcr-1* in *K. pneumoniae* or *E. cloacae* isolates. Although *mcr-1* prevalence in companion animals was greatly lower than that among food-producing animals in China (Liu et al., 2017; Wu et al., 2018), it was similar to the previously described *mcr-1* detection in companion animals in Beijing, China (Lei et al., 2017).

As shown in **Table 1**, all *mcr-1*-positive strains exhibited minimal inhibitory concentration (MIC) of 4 mg/L to colistin, and showed resistance to ampicillin, tetracycline, sulfamethoxazole/trimethoprim, and fosfomycin, but susceptibility to amikacin and imipenem; seven displayed resistance to gentamycin, chloramphenicol and florfenicol. The *mcr-1*-positive isolates also harbored other resistance genes, including bla_{CTX-M} ($n = 8$), *fosA3* ($n = 8$), *floR* ($n = 7$), and *oqxAB* ($n = 2$) (**Table 2**). In addition, seven *mcr-1*-bearing isolates exhibited resistance to ciprofloxacin with mutations in *gyrA* (S83L and D87Y) and *parC* (S57T and/or S80I) (**Table 2**).

Since colistin is not applied to companion animals in China, pet food containing chicken meat might be one source of *mcr-1*

[4]https://www-is.biotoul.fr//

[5]https://cge.cbs.dtu.dk//services/ResFinder/

[6]https://galileoamr.arcbio.com/mara/

[7]http://blast.ncbi.nlm.nih.gov/Blast.cgi

TABLE 2 | Characteristics of *mcr-1*-carrying *E. coli* isolates.

Strain	Origin (Physical condition)	Sampling location and time	MLST (ST)	Other resistance genes	Colistin MIC (mg/L)	mutations		Other resistance patterns	Genetic structure of *mcr-1*	Location of *mcr-1* (plasmid)
						gyrA	*parC*			
GZ6DS2*	dog-1, urine (hematuresis)	Hospital 2, July 2016	93	$bla_{CTX-M-64}$/ $bla_{CTX-M-14}$/*floR*/*fosA3*	4	S83L D87Y	S57T S80I	AMP/CTX/GEN/TET/ CHL/FFC/SXT/ FOS/CIP	IS*Apl1*-*mcr-1*-pap2	∼244.4 kb IncN1-IncHI2/ST3
GZ6DS9*	dog-2, nasal secretion (pneumonia)	Hospital 3, July 2016	93	$bla_{CTX-M-64}$/ $bla_{CTX-M-14}$/*floR*/*fosA3*	4	S83L D87Y	S57T S80I	AMP/CTX/GEN/TET/ CHL/FFC/SXT/ FOS/CIP	IS*Apl1*-*mcr-1*-pap2	∼244.4 kb IncN1-IncHI2/ST3
GZ6CS9	cat-1, feces (diarrhea)	Hospital 2, July 2016	93	$bla_{CTX-M-64}$/ $bla_{CTX-M-14}$/*floR*/*fosA3*	4	S83L D87Y	S57T S80I	AMP/CTX/GEN/TET/ CHL/FFC/SXT/ FOS/CIP	IS*Apl1*-*mcr-1*-pap2	∼244.4 kb
GZ6DH17*	dog-3, feces (H)	Hospital 3, July 2016	93	$bla_{CTX-M-64}$/ $bla_{CTX-M-14}$/*floR*/*fosA3*	4	S83L D87Y	S57T S80I	AMP/CTX/GEN/TET/ CHL/FFC/SXT/ FOS/CIP	IS*Apl1*-*mcr-1*-pap2	∼244.4 kb IncN1-IncHI2/ST3
GZ6DH18*	dog-4, feces (H)	Hospital 3, July 2016	93	$bla_{CTX-M-64}$/ $bla_{CTX-M-14/floR}$/fosA3	4	S83L D87Y	S57T S80I	AMP/CTX/GEN/TET/ CHL/FFC/SXT/ FOS/CIP	ISApl1-mcr-1-pap2	∼244.4 kb IncN1-IncHI2/ST3
GZ6DS4*	dog-5, feces (cough, diarrhea)	Hospital 2, July 2016	1011	$bla_{CTX-M-64}$/floR/ fosA3/oqxAB	4	S83L D87Y	S80I	AMP/CTX/GEN/TET/ CHL/FFC/SXT/FOS/CIP	mcr-1-pap2	∼70 kb IncI2
GZ6DS68	dog-6, feces (S)	Hospital 4, Aug 2016	3285	$bla_{CTX-M-55}$/fosA3	4	S83L D87Y	S80I	AMP/CTX/TET/SXT/ FOS/CIP	mcr-1-pap2	∼60 kb
GZ6DS69	dog-7, feces (S)	Hospital 4, Aug 2016	NEW	$bla_{CTX-M-14}$/ $bla_{CTX-M-15}$/floR/ fosA3/oqxAB	4			AMP/CTX/GEN/TET/ CHL/FFC/SXT/FOS	ISApl1-mcr-1-pap2	∼244.4 kb

AMP, ampicillin; CTX, cefotaxime; GEN, gentamycin; TET, tetracycline; CHL, chloramphenicol; FFC, florfenicol; SXT, sulfamethoxazole/trimethoprim; FOS, fosfomycin; CIP, ciprofloxacin. All isolates were susceptible to amikacin and imipenem. Asterisk indicates isolates from which the mcr-1 gene can be transferred to recipients by conjugation experiments. H, healthy; S, sick, specific disease was not recorded or unknown. The isolate was identified as New ST with alleles adk10, fumC27, gyrB4, icd10, mdh8, purA1, and recA2, respectively. The most related ST is ST7507 with alleles adk10, fumC27, gyrB4, icd10, mdh8, purA8, and recA2, respectively. Resistance genes and resistance phenotypes transferred to the recipient by conjugation experiments are underlined.

(Lei et al., 2017). Close contact to food-producing animals in local hog and poultry markets, as well as to humans, might also be the potential origins. Furthermore, the widely use of cephalosporins, aminoglycosides, and fluoroquinolones in companion animal medicine (data not shown) could allow for the co-selection of isolates harboring *mcr-1*, as well as bla_{CTX-M} and *fosA3*, conferring resistance to crucial clinical antibiotics.

Molecular Typing

Eight *mcr-1*-positive *E. coli* isolates were assigned to ST93 ($n = 5$), ST1011, ST3285, and a new ST, respectively (**Table 2**). ST93 has been sporadically described as avian and human extra-intestinal pathogenic or diarrhoeagenic *E. coli* in humans, animals, and food products worldwide (Chen et al., 2014; Maluta et al., 2014; Vogt et al., 2014), and particularly it has been previously detected as *mcr-1* carriers from a pig in Laos (Olaitan et al., 2015, 2016), from a cat in Guangzhou, China (Zhang et al., 2016), and from a patient in Finland (Gröndahl-Yli-Hannuksela et al., 2018). The five *mcr-1*-carrying ST93 *E. coli* isolates were obtained from both intestinal and extraintestinal sites from two animal hospitals located within a distance of 7 km. They showed indistinguishable PFGE patterns which differed from previously described *mcr-1*-harboring ST93 *E. coli* isolate PET01 from a cat in Guangzhou (Zhang et al., 2016; **Figure 1**), indicating that clonal spread of *mcr-1*-harboring *E. coli* had occurred among companion animals within two hospitals in Guangzhou. The observation that they had identical antimicrobial susceptibility profiles, resistance genes, and mutations within *gyrA* and *parC* may further support this hypothesis (**Table 2**). However, small numbers of samples were collected from four animal hospitals in this study, thus limiting this hypothesis. The prevalence and dissemination mechanisms of *mcr-1* in companion animals in Guangzhou should be further investigated by using large scale samples from more animal hospitals. Though rare, it is possible for these two hospitals to exchange animal patients. The possibility of acquisition of *mcr-1*-harboring ST93 *E. coli* from a common ancestor could not be ruled out. Although horizontal transfer mediated by mobile elements such as insertion sequence and plasmids has been the major reason for *mcr-1* worldwide dissemination, clonal spread of *mcr-1*-harboring strains, such as *E. coli* ST93 in the present study, *Salmonella* Typhimurium ST34 in pigs (Li et al., 2016; Yi et al., 2017) might be another reason accounting for *mcr-1* transmission. Most importantly, the potential of *mcr-1* transmission mediated by MCR-1-producing clones from companion animals to humans through close contact should not be underestimated, which might have already occurred in China by *E. coli* ST354 and ST101 clones (Zhang et al., 2016; Lei et al., 2017).

Characterization of *mcr-1*-Carrying Plasmids

Five strains successfully transferred *mcr-1* to *E. coli* C600 at frequencies of 10^{-2} to 10^{-4} transconjugants/recipient (**Supplementary Table S5**), and the remaining three strains failed to transfer *mcr-1* to *E. coli* C600 or DH5α by conjugation or transformation. S1-PFGE and Southern hybridization indicated

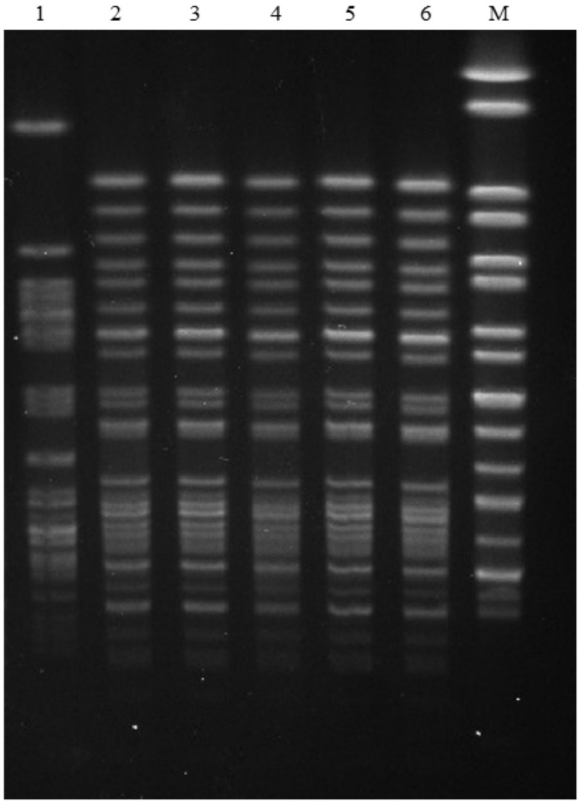

FIGURE 1 | PFGE patterns of five *mcr-1*-carrying *E. coli* ST93 strains in this study and the *mcr-1*- carrying *E. coli* ST93 strain PET01 that was isolated from a cat in a pet shop from Guangzhou (Zhang et al., 2016). Lanes: (1) PET01; (2) GZ6DS2; (3) GZ6DS9; (4) GZ6CS9; (5) GZ6DH17; (6) GZ6DH18; (9) GZ6DS69; (10) GZ6DS68; M *Salmonella enterica* serovar Braenderup H9812 Marker.

that *mcr-1* was located on ∼244.4 kb plasmids ($n = 6$), ∼60 kb plasmids ($n = 1$), or ∼70 kb plasmid ($n = 1$) (**Table 2**). Additionally, five *mcr-1*-harboring transconjugants with single plasmid were classified as IncN1-IncHI2/ST3 (∼244.4 kb, $n = 4$) which were all obtained from ST93 *E. coli* isolates, and IncI2 (∼70 kb, $n = 1$) (**Table 2** and **Supplementary Figure S1**), which agree with previous observation that IncHI2 and IncI2 plasmids have been the major vectors for *mcr-1* global dissemination (Matamoros et al., 2017; Wang et al., 2018). Furthermore, the transconjugants showed elevated MICs for colistin (1∼2 mg/L; 8-16-fold) compared with the recipient *E. coli* C600. In addition, co-transfer of resistance to ampicillin, cefotaxime, gentamycin, chloramphenicol, florfenciol, sulfamethoxazole/trimethoprim, and fosfomycin was observed in four transconjugants with IncN1-IncHI2/ST3 plasmid from ST93 *E. coli* isolates, resistance genes $bla_{CTX-M-14}$, *floR* and *fosA3* were also co-transferred with *mcr-1* (**Table 2**). The co-transfer of $bla_{CTX-M-64}$ with *mcr-1* on an IncI2 plasmid in the remaining transconjugant caused resistance to ampicillin and cefotaxime (**Table 2**). The presence of other resistance genes co-located on the same plasmid allows for the selection of *mcr-1* under pressure posed by other agents, thus facilitating *mcr-1* transmission.

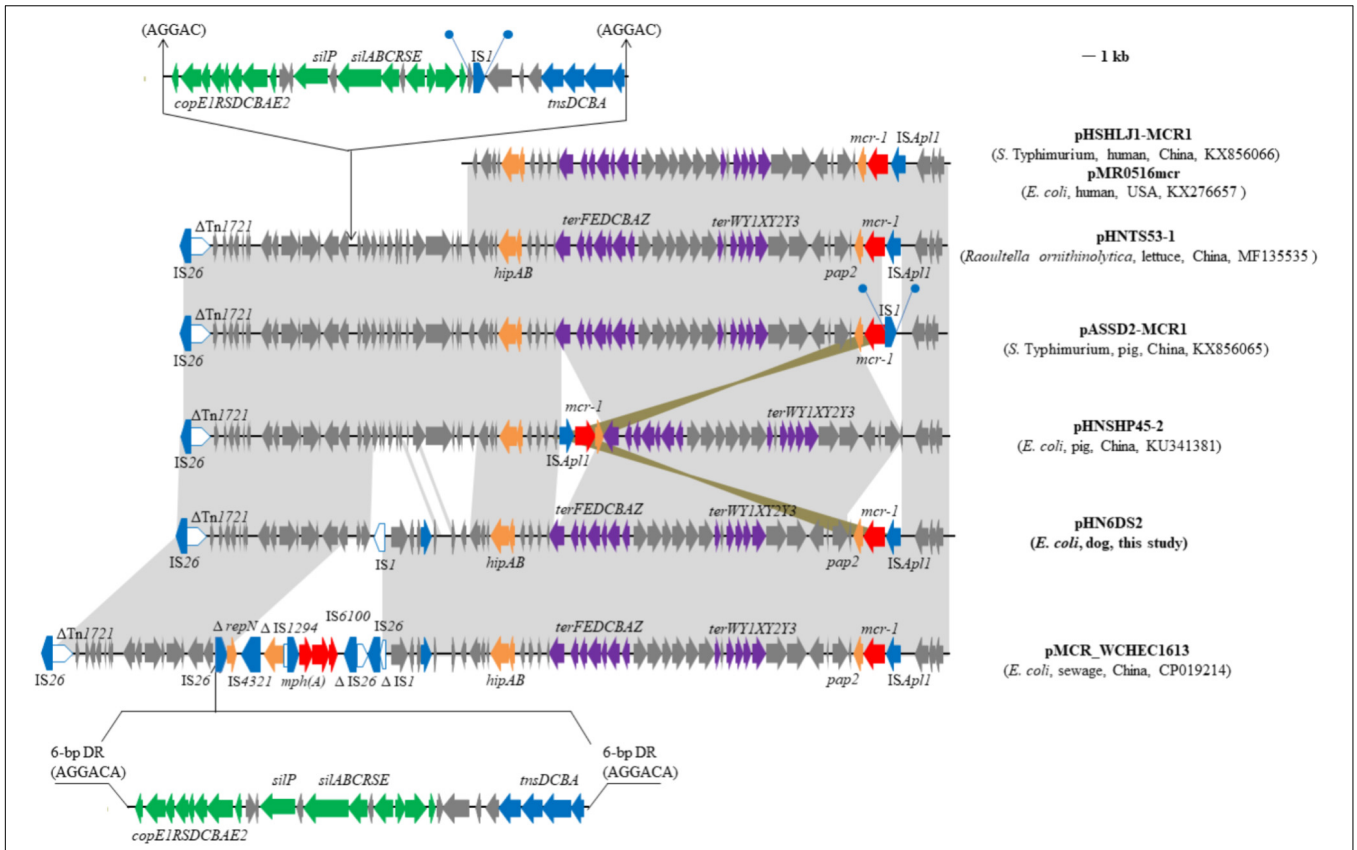

FIGURE 2 | Genetic organization of the partial sequence containing *mcr-1* of plasmid pHN6DS2, and structural comparison with other *mcr-1*-carrying plasmids. Arrows indicate the positions of the genes and the direction. Regions with > 99% homology are shaded in gray or azure. Δ indicates a truncated gene or mobile element. Direct repeats are indicated by arrows and blue circles. Tall bars represent the 38 bp inverted repeat (IR) of transposons. The backbone is indicated by dotted lines.

It has been hypothesized that *mcr-1* is initially captured and mobilized by the composite transposon Tn*6330* (IS*Apl1-mcr-1-pap2*-IS*Apl1*), followed by the loss of IS*Apl1* over time, leading to the formation of *mcr-1* in diverse genetic structures, with the structure *mcr-1-pap2* being dominant, followed by the structure IS*Apl1-mcr-1-pap2* (Snesrud et al., 2018; Wang et al., 2018). The genetic structure of *mcr-1* in our study was determined by PCR mapping. We did not observe the complete Tn*6330*, but the presence of IS*Apl1* upstream was common, identified in six transconjugants or original isolates with ∼244.4 kb *mcr-1*-carrying plasmids, the structure *mcr-1-pap2* was also identified (n = 2) (**Table 2**). Our results further support that mobile elements (IS*Apl1*, IncHI2, and IncI2 plasmids) play an important role in the mobilization and dissemination of *mcr-1* in *E. coli* from different sources.

Plasmid Sequencing and Comparative Analysis

Plasmid pHN6DS2 had a size of 253, 783 bp, and was organized similarly to other IncHI2 plasmids, containing regions for functions of replication, multiresistance, conjugal transfer, maintenance, and stability (**Supplementary Figure S2**).

Interestingly, a fragment with the least size of 37, 258-bp including the module. IS*Apl1-mcr-1-pap2* and a set of tellurite resistance determinants (*ter*YXWZABCDEF) in plasmid pHN6DS2 from canine *E. coli* was similar to several other IncHI2/ST3 plasmids found in Enterobacteriaceae isolates from various sources in China, such as plasmids pHNTS53-1 (*Raoultella ornithinolytica*, lettuce, MF135535), pHSHLJ1-MCR1 (*S.* Typhimurium, human, KX856066), pMCR_WCHEC1613 (*E. coli*, environment, CP019214) (Zhao et al., 2017), and pASSD2-MCR1 (*S.* Typhimurium, pig, KX856065) (**Figure 2**). However, IS*Apl1* was absent and IS*1* was inserted upstream of *mcr-1* flanked by 9-bp direct repeats (DRs) in plasmid pASSD2-MCR1 (**Figure 2**). Furthermore, the fragment was also identical to the corresponding region of the IncHI2-IncF recombinant plasmid pMR0516mcr obtained from clinical *E. coli* isolate in the United States (McGann et al., 2016; **Figure 2**). However, the module IS*Apl1-mcr-1-pap2* was inserted into the backbone of plasmid pHNSHP45-2 (Zhi et al., 2016) with different location and orientation (**Figure 2**).

Furthermore, the multiresistance region (MRR) of pHN6DS2 contained numerous resistance genes, such as *aphA1*, *tetM*, *sul3*, *aadA1*, *cmlA1*, *aadA2*, *floR*, $bla_{CTX-M-14}$, and *fosA3*, and complete or truncated insertion sequences and transposons (e.g.,

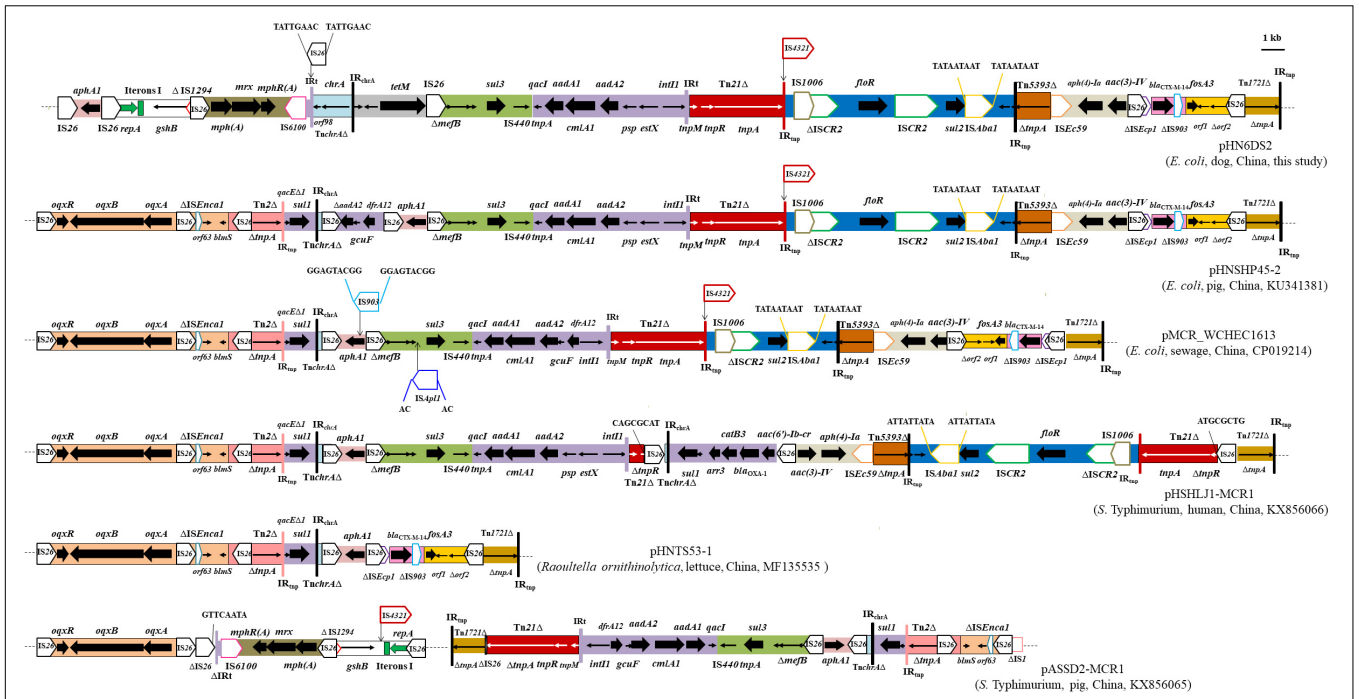

FIGURE 3 | Genetic organization of the multiresistance region of plasmid pHN6DS2, and structural comparison with other *mcr-1*-carrying plasmids. The extents and directions of antibiotic resistance (thick arrows) and other genes are indicated. Δ indicates a truncated gene or mobile element. ISs are shown as boxes labeled with their name. Labeled vertical arrows with IS boxes indicate the insertion sites of IS elements. Direct repeats are indicated by arrows and sequence. Tall bars represent the 38 bp inverted repeat (IR) of transposons. The backbone is indicated by dotted lines.

TABLE 3 | Characteristics of pHN6DS2-like plasmids in this study.

Isolates	HP1-IS*26*-*aphA1*	IS*26*-*repN*	*aphA1*-IS*26*-*repN*	*gshB*-IS*1294*-IS*26*-*mphA*	*fosA3*-IS*26*-Tn*1721*	Tn*1721*-HP2	IS*Apl1*-*mcr-1*-*pap2* insertion site at plasmid
GZ6DS9-2C*	P	P	P	N	P	P	Like pHN6DS2
GZ6DH17-3C*	P	P	N	N	P	P	Like pHN6DS2
GZ6DH18-1C*	P	P	N	N	P	P	Like pHN6DS2
GZ6CS9	P	P	P	N	P	P	Like pHN6DS2
GZ6DS69	N	P	N	P	P	P	Like pHN6DS2

Asterisk indicates transconjugants; HP: hypothetical protein, located in IncHI2 plasmid backbone. P, positive; N, negative.

IS*26*, Tn*21*, IS*4321*, IS*1006*, ISCR2, IS*Aba1*, Tn*5393*, IS*Ec59*, IS*Ecp1*, IS*903*, and Tn*1721*) (**Figure 3**). As a multi-replicon plasmid, pHN6DS2 harbored an approximately 3-kb IncN1 segment (Δ*repA*-Iterons I-*gshB*-ΔIS*1294*), containing IncN replication initiation gene *repA* truncated by IS*26*, five tandem 37-bp repeats within iterons region, *gshB* encoding glutathione synthetase, and 114 bp of the *ori*IS end of IS*1294* (**Figure 3**). The similar structure was also observed in plasmid pASSD2-MCR1 with the exception of IS*4321* insertion (**Figure 3**). The macrolide phosphotransferase region harboring several *mph* genes was located downstream of the IncN segment, and was followed by IS*6100*, 123-bp of Tn*402*, incomplete Tn*21*-like transposon Tn*chrA*, and a 2, 067-bp segment containing tetracycline resistance gene *tetM* (**Figure 3**). IS*26* was inserted in inverted repeat at the *tni* end of Tn*402*, named IRt, flanked by 8-bp DRs (**Figure 3**).

The MRR of pHN6DS2 was similar to that of pHNSHP45-2, but differed by acquisition of the ∼10.5-kb *oqxAB* resistance module (Tn*6010*-ΔIS*Enca1*-*orf63*-*blmS*-ΔTn*2*-IS*26*-ΔTn*2*) and an ∼4.3-kb segment harboring the | *qacE*Δ*1*| *sul1*| Δ*aadA2*| *gcuF*| *dfrA12*| cassette array which was interrupted by partial Tn*chrA* and IS*26*, and by loss of the IncN segment, *mph* region, and *tetM* region (**Figure 3**). Similarly, MRRs of *mcr-1*-carrying plasmids pMCR_WCHEC1613, pHSHLJ1-MCR1, pHNTS53-1, and pASSD2-MCR1 were related to those of pHN6DS2 and pHNSHP45-2, differed by insertions, deletions, or rearrangement of various regions harboring antimicrobial resistance genes such as *oqxAB*, *sul3*, *floR*, $bla_{CTX-M-14}$, and *fosA3*, and mobile element such as Tn*21*, ISCR2, IS*4321* (**Figure 3**). Notably, IS*26*, via transposition and homologous recombination, seems to play an important role in the

formation of distinct but also related MRRs. The remaining three transconjugants carrying IncN1-IncHI2/ST3 plasmids and two original isolates with ∼244.4 kb *mcr-1*-bearing plasmids were also examined for pHN6DS2-like plasmids. All five transconjugants or original isolates harbored pHN6DS2-like plasmids with identical insertion of the module IS*Apl1-mcr-1-pap2* but variable MRRs (**Table 3**).

These data suggested that similar *mcr-1*-carrying IncHI2/ST3 plasmids, after acquiring, losing or reorganizing various regions, could spread among Enterobacteriaceae species in livestock, humans, vegetables, and the environment, particularly in different regions in China. The presence of pHN6DS2-like plasmids further supported this hypothesis and highlighted the potential of pHN6DS2-like plasmid to become an efficient vehicle for *mcr-1* dissemination between distinct organisms or regions.

CONCLUSION

In conclusion, the spread of *mcr-1* in companion animals in the present study might be mainly attributed to clonal dissemination of *E. coli* ST93 isolates within two hospitals, associated with IncN1-IncHI2/ST3 plasmids. Although the origin of *mcr-1* in companion animals is unclear, it is possible for *mcr-1*-positive clones or plasmids to transfer from companion animals to humans through close contact, thus the dissemination of *mcr-1* among companion animals needs continued vigilance.

ETHICS STATEMENT

This study was carried out in accordance with the recommendation of ethical guidelines of South China Agricultural University. Individual written informed consent for the use of samples was obtained from all the animal owners.

AUTHOR CONTRIBUTIONS

J-HL, Z-LZ, and JW conceived the study. X-YH, Y-BX, JW, Z-WG, Z-BM, M-YY, L-CL, P-LL, J-CY, and J-WH carried out the experiments. JW, X-YH, and Y-BX analyzed the data. JW wrote the manuscript. J-HL and Z-LZ revised the manuscript. All authors read and approved the final manuscript.

FUNDING

This work was supported in part by the grants from National Natural Science Foundation of China (NSFC) (31625026 and 31830099), National Key Basic Research Program of China (No. 2013CB127200), and the National Training Program of Innovation and Entrepreneurship for Undergraduates (No. 201710564202).

ACKNOWLEDGMENTS

We thank Jia Long, Yang He, Jun-Jie Weng, and Zhuo-Wen Lu for assistance in sample collection from companion animals. We also thank Guo-Bao Tian for providing ST93 *E. coli* strain PET01.

SUPPLEMENTARY MATERIAL

The Supplementary Material for this article can be found online at: https://www.frontiersin.org/articles/10.3389/fmicb.2018.02989/full#supplementary-material

REFERENCES

Aziz, R. K., Bartels, D., Best, A. A., DeJongh, M., Disz, T., Edwards, R. A., et al. (2008). The RAST server: rapid annotations using subsystems technology. *BMC Genomics* 9:75. doi: 10.1186/1471-2164-9-75

Barton, B. M., Harding, G. P., and Zuccarelli, A. J. (1995). A general method for detecting and sizing large plasmids. *Anal. Biochem.* 226, 235–240. doi: 10.1006/abio.1995.1220

Carattoli, A., Bertini, A., Villa, L., Falbo, V., Hopkins, K. L., and Threlfall, E. J. (2005). Identification of plasmids by PCR-based replicon typing. *J. Microbiol. Methods* 63, 219–228. doi: 10.1016/j.mimet.2005.03.018

Chen, L., Chen, Z. L., Liu, J. H., Zeng, Z. L., Ma, J. Y., and Jiang, H. X. (2007). Emergence of RmtB methylase-producing *Escherichia coli* and *Enterobacter cloacae* isolates from pigs in China. *J. Antimicrob. Chemother.* 59, 880–885. doi: 10.1093/jac/dkm065

Chen, Y., Chen, X., Zheng, S., Yu, F., Kong, H., Yang, Q., et al. (2014). Serotypes, genotypes and antimicrobial resistance patterns of human diarrhoeagenic *Escherichia coli* isolates circulating in southeastern China. *Clin. Microbiol. Infect.* 20, 52–58. doi: 10.1111/1469-0691.12188

Clinical Laboratory Standards Institute [CLSI] (2018). *Performance Standards for Antimicrobial Susceptibility Testing [S]. CLSI Supplement M100*, 28th Edn. Wayne, PA: Clinical and Laboratory Standards Institute.

García-Fernández, A., and Carattoli, A. (2010). Plasmid double locus sequence typing for IncHI2 plasmids, a subtyping scheme for the characterization of IncHI2 plasmids carrying extended-spectrum beta-lactamase and quinolone resistance genes. *J. Antimicrob. Chemother.* 65, 1155–1161. doi: 10.1093/jac/dkq101

Gautom, R. K. (1997). Rapid pulsed-field gel electrophoresis protocol for typing of *Escherichia coli* O157:H7 and other gram-negative organisms in 1 day. *J. Clin. Microbiol.* 35, 2977–2980.

Gröndahl-Yli-Hannuksela, K., Lönnqvist, E., Kallonen, T., Lindholm, L., Jalava, J., Rantakokko-Jalava, K., et al. (2018). The first human report of mobile colistin resistance gene, mcr-1, in Finland. *APMIS* 126, 413–417. doi: 10.1111/apm.12834

Jeannot, K., Bolard, A., and Plésiat, P. (2017). Resistance to polymyxins in Gram-negative organisms. *Int. J. Antimicrob. Agents* 49, 526–535. doi: 10.1016/j.ijantimicag.2016.11.029

Johnson, T. J., Bielak, E. M., Fortini, D., Hansen, L. H., Hasman, H., Debroy, C., et al. (2012). Expansion of the IncX plasmid family for improved identification and typing of novel plasmids in drug-resistant *Enterobacteriaceae*. *Plasmid* 68, 43–50. doi: 10.1016/j.plasmid.2012.03.001

Kaye, K. S., Pogue, J. M., Tran, T. B., Nation, R. L., and Li, J. (2016). Agents of last resort: polymyxin resistance. *Infect. Dis. Clin. North. Am.* 30, 391–414. doi: 10.1016/j.idc.2016.02.005

Lei, L., Wang, Y., Schwarz, S., Walsh, T. R., Ou, Y., Wu, Y., et al. (2017). mcr-1 in *Enterobacteriaceae* from companion animals, Beijing, China, 2012-2016. *Emerg. Infect. Dis.* 23, 710–711. doi: 10.3201/eid2304.161732

Li, R., Yu, H., Xie, M., Chen, K., Dong, N., Lin, D., et al. (2018). Genetic basis of chromosomally-encoded mcr-1 gene. *Int. J. Antimicrob. Agents* 51, 578–585. doi: 10.1016/j.ijantimicag.2017.11.015

Li, X. P., Fang, L. X., Song, J. Q., Xia, J., Huo, W., Fang, J. T., et al. (2016). Clonal spread of mcr-1 in PMQR-carrying ST34 *Salmonella* isolates from animals in China. *Sci. Rep.* 6:38511. doi: 10.1038/srep38511

Liu, B. T., Song, F. J., Zou, M., Zhang, Q. D., and Shan, H. (2017). High incidence of *Escherichia coli* strains coharboring mcr-1 and blaNDM from chickens. *Antimicrob. Agents Chemother.* 61:e02347-16. doi: 10.1128/AAC/02347-16

Liu, Y. Y., Wang, Y., Walsh, T. R., Yi, L. X., Zhang, R., Spencer, J., et al. (2016). Emergence of plasmid-mediated colistin resistance mechanism MCR-1 in animals and human beings in China: a microbiological and molecular biological study. *Lancet Infect. Dis.* 16, 161–168. doi: 10.1016/S1473-3099(15)00424-7

Lv, L., Partridge, S. R., He, L., Zeng, Z., He, D., Ye, J., et al. (2013). Genetic characterization of IncI2 plasmids carrying blaCTX-M-55 spreading in both pets and food animals in China. *Antimicrob. Agents Chemother.* 57, 2824–2827. doi: 10.1128/AAC.02155-12

Maluta, R. P., Logue, C. M., Casas, M. R., Meng, T., Guastalli, E. A., and Rojas, T. C. (2014). Overlapped sequence types (STs) and serogroups of avian pathogenic (APEC) and human extra-intestinal pathogenic (ExPEC) *Escherichia coli* isolated in Brail. *PLoS One* 9:e105016. doi: 10.1371/journal.pone.0105016

Matamoros, S., van Hattem, J. M., Arcilla, M. S., Willemse, N., Melles, D. C., Penders, J., et al. (2017). Global phylogenetic analysis of *Escherichia coli* and plasmids carrying the mcr-1 gene indicates bacterial diversity but plasmid restriction. *Sci. Rep.* 7:15364. doi: 10.1038/s41598-017-15539-7

McGann, P., Snesrud, E., Maybank, R., Corey, B., Ong, A. C., Clifford, R., et al. (2016). *Escherichia coli* harboring mcr-1 and blaCTX-M on a novel IncF plasmid: first report of mcr-1 in the United States. *Antimicrob. Agents Chemother.* 60, 4420–4421. doi: 10.1128/AAC.01103-16

Olaitan, A. O., Chabou, S., Okdah, L., Morand, S., and Rolain, J. M. (2016). Dissemination of the mcr-1 colistin resistance gene. *Lancet Infect. Dis.* 16:147. doi: 10.1016/S1473-3099(15)00540-X

Olaitan, A. O., Thongmalayvong, B., Akkhavong, K., Somphavong, S., Paboriboune, P., Khounsy, S., et al. (2015). Clonal transmission of a colistin-resistant *Escherichia coli* from a domesticated pig to a human in Laos. *J. Antimicrob. Chemother.* 70, 3402–3404. doi: 10.1093/jac/dkv252

Snesrud, E., McGann, P., and Chandler, M. (2018). The birth and demise of the ISApl1-mcr-1-ISApl1 composite transposon: the vehicle for transferable colistin resitance. *mBio* 9:e02381-17. doi: 10.1128/mBio.02381-17

Sun, J., Yang, R. S., Zhang, Q., Feng, Y., Fang, L. X., Xia, J., et al. (2016). Co-transfer of blaNDM-5 and mcr-1 by an IncX3-X4 hybrid plasmid in *Escherichia coli*. *Nat. Microbiol.* 1:16176. doi: 10.1038/nmicrobiol.2016.176

Vogt, D., Overesch, G., Endimiani, A., Collaud, A., Thomann, A., and Perreten, V. (2014). Occurrence and genetic characteristics of third-generation cephalosporin-resistant *Escherichia coli* in Swiss retail meat. *Microb. Drug. Resist.* 20, 485–494. doi: 10.1089/mdr.2013.0210

Wang, R., van Dorp, L., Shaw, L. P., Bradley, P., Wang, Q., Wang, X., et al. (2018). The global distribution and spread of the mobilized colistin resistance gene mcr-1. *Nat. Commun.* 9:1179. doi: 10.1038/s41467-018-03205-z

Wu, R., Yi, L. X., Yu, L. F., Wang, J., Liu, Y., Chen, X., et al. (2018). Fitness advantage of mcr-1-bearing IncI2 and IncX4 plasmids in vitro. *Front. Microbiol.* 9:331. doi: 10.3389/fmicb.2018.00331

Yi, L., Wang, J., Gao, Y., Liu, Y., Doi, Y., Wu, R., et al. (2017). mcr-1-harboring *Salmonella enterica* Serovar Typhimurium sequence type 34 in pigs. *China Emerg. Infect. Dis.* 23, 291–295. doi: 10.3201/eid2302.161543

Zhang, X. F., Doi, Y., Huang, X., Li, H. Y., Zhong, L. L., Zeng, K. J., et al. (2016). Possible transmission of mcr-1-harboring *Escherichia coli* between companion animals and human. *Emerg. Infect. Dis.* 22, 1679–1681. doi: 10.3201/eid2209.160464

Zhao, F., Feng, Y., Lü, X., McNally, A., and Zong, Z. (2017). Remarkable diversity of *Escherichia coli* carrying mcr-1 from hospital sewage with the identification of two new mcr-1 variants. *Front. Microbiol.* 8:2094. doi: 10.3389/fmicb.2017.02094

Zhi, C., Lv, L., Yu, L. F., Doi, Y., and Liu, J. H. (2016). Dissemination of the mcr-1 colistin resistance gene. *Lancet Infect. Dis.* 16, 292–293. doi: 10.1016/S1473-3099(16)00067-0

Conflict of Interest Statement: The authors declare that the research was conducted in the absence of any commercial or financial relationships that could be construed as a potential conflict of interest.

frontiers in Microbiology

ORIGINAL RESEARCH
published: 08 January 2019
doi: 10.3389/fmicb.2018.03212

Multidrug Resistant Uropathogenic *Escherichia coli* ST405 With a Novel, Composite IS*26* Transposon in a Unique Chromosomal Location

Piklu Roy Chowdhury[1,2*†], *Jessica McKinnon*[1†], *Michael Liu*[1] *and Steven P. Djordjevic*[1*]

[1] *The ithree Institute, University of Technology Sydney, Ultimo, NSW, Australia,* [2] *NSW Department of Primary Industries, Elizabeth Macarthur Agricultural Institute, Macarthur, NSW, Australia*

OPEN ACCESS

Edited by:
Yonghong Xiao, Zhejiang University, China

Reviewed by:
Leila Vali, Kuwait University, Kuwait
Angelica Reyes-Jara, Universidad de Chile, Chile

***Correspondence:**
Piklu Roy Chowdhury
piklu.bhattacharya@uts.edu.au
Steven P. Djordjevic
steven.djordjevic@uts.edu.au

† These authors have contributed equally to this work

Specialty section:
This article was submitted to Antimicrobials, Resistance and Chemotherapy, a section of the journal Frontiers in Microbiology

Received: *05 September 2018*
Accepted: *11 December 2018*
Published: *08 January 2019*

Citation:
Roy Chowdhury P, McKinnon J, Liu M and Djordjevic SP (2019) Multidrug Resistant Uropathogenic Escherichia coli ST405 With a Novel, Composite IS26 Transposon in a Unique Chromosomal Location. Front. Microbiol. 9:3212. doi: 10.3389/fmicb.2018.03212

Escherichia coli ST405 is an emerging urosepsis pathogen, noted for carriage of bla_{CTX-M}, bla_{NDM}, and a repertoire of virulence genes comparable with O25b:H4-ST131. Extraintestinal and multidrug resistant *E. coli* ST405 are poorly studied in Australia. Here we determined the genome sequence of a uropathogenic, multiple drug resistant *E. coli* ST405 (strain 2009-27) from the mid-stream urine of a hospital patient in Sydney, Australia, using a combination of Illumina and SMRT sequencing. The genome of strain 2009-27 assembled into two unitigs; a chromosome comprising 5,287,472 bp and an IncB/O plasmid, pSDJ2009-27, of 89,176 bp. *In silico* and phenotypic analyses showed that strain 2009-27 is a serotype O102:H6, phylogroup D ST405 resistant to ampicillin, azithromycin, kanamycin, streptomycin, trimethoprim, and sulphafurazole. The genes encoding resistance to these antibiotics reside within a novel, mobile IS*26*-flanked transposon, identified here as Tn*6242*, in the chromosomal gene *yjdA*. Tn*6242* comprises four modules that each carries resistance genes flanked by IS*26,* including a class 1 integron with *dfrA17* and *aadA5* gene cassettes, a variant of Tn*6029*, and *mphA*. We exploited unique genetic signatures located within Tn*6242* to identify strains of ST405 from Danish patients that also carry the transposon in the same chromosomal location. The acquisition of Tn*6242* into *yjdA* in ST405 is significant because it (i) is vertically inheritable; (ii) represents a reservoir of resistance genes that can transpose onto resident/circulating plasmids; and (iii) is a site for the capture of further IS*26*-associated resistance gene cargo.

Keywords: IS*26*, compound transposon, class 1 integrons, antibiotic resistance, *Escherichia coli* ST405

INTRODUCTION

Escherichia coli are commensals of vertebrate species but pathovars have evolved that cause both intestinal (intestinal pathogenic *E. coli*; IPEC) and extraintestinal infections in humans and in food producing and companion animals. Extraintestinal pathogenic *Escherichia coli* (ExPEC) have a fecal origin but have acquired the ability to colonize urinary tract epithelium causing

cystitis, pyelonephritis and sepsis and are a leading cause of meningitis and wound infections (Johnson et al., 2003; Smith et al., 2007). ExPEC are among the most frequently isolated Gram negative pathogens (Poolman and Wacker, 2016) and are increasingly resistant to broader classes of antimicrobials.

IS*26* plays a key role in the capture and spread of genes encoding resistance to different classes of antimicrobials, including drugs of last resort (Harmer et al., 2014; Chen et al., 2015; Matsumura et al., 2015; Riccobono et al., 2015; Roy Chowdhury et al., 2015; Zhang et al., 2015; Zong et al., 2015; Zurfluh et al., 2015; Agyekum et al., 2016; Harmer and Hall, 2016; Beyrouthy et al., 2017; Liu et al., 2017). It can form independently mobile compound transposons containing tandem arrays of antimicrobial resistance genes (Cain and Hall, 2012a; Venturini et al., 2013; Reid et al., 2015; Roy Chowdhury et al., 2015), often in association with class 1 integrons and diverse transposons, creating complex resistance gene loci (CRL). IS*26* can also delete and invert DNA, often modifying the conserved regions (5′- CS and 3′-CS) of class 1 integrons that are a target of polymerase chain reaction (PCR) assays used to detect them and the resistance gene cargo they carry (Dawes et al., 2010; Roy Chowdhury et al., 2011, 2015; Venturini et al., 2013; Reid et al., 2017). These events often create novel signatures that can be exploited to track the CRL they reside in (Dawes et al., 2010; Roy Chowdhury et al., 2015). Notably, IS*26* promotes: (i) the formation of cointegrate plasmids from separate replicons that carry virulence and resistance genes (Mangat et al., 2017); (ii) plasmid fitness by deleting regions of DNA that incur a fitness cost to the host (Porse et al., 2016); and (iii) the co-assembly and mobilization of resistance genes efficiently in a *recA*$^{-}$ background by preferentially integrating in regions of genomes with a pre-existing copy of IS*26* (Harmer and Hall, 2016).

Extended-spectrum beta-lactamase (ESBL)-producing, multiple drug resistant ST405-D is an emerging ExPEC pathogen (Matsumura et al., 2012; Brolund et al., 2014; Gurnee et al., 2015). A phylogenetic study of the ST405 clonal lineage, and an analysis of mobile genetic elements that play an important role in the capture and spread of antimicrobial resistance in this lineage, has not been undertaken. It is not known if ST405 is a globally dispersed emerging clone or if disease is caused by sporadic episodes by genetically divergent ST405 strains.

As part of a larger study of multiple drug resistant uropathogenic *E. coli* (UPEC) from Sydney hospitals, two strains were shown to carry a unique genetic signature in a class 1 integron created by the insertion of an IS*26* in the 3′-CS. We characterized their genome sequences using both short- and long-read genome sequencing technologies and determined both to be ST405, phylogroup D with serotype O102:H6 (ST405-D-O102:H6). These events create opportunities for the further accumulation of antimicrobial resistance genes and are being targeted for sequence analysis to better understand how multiple drug resistance is emerging in Australia. Our analyses show that the strains carried a novel IS*26*-flanked composite transposon encoding resistance to multiple antibiotics in a unique chromosomal locus. Two ST405 genomes from Denmark with near identical structures were identified by interrogating *E. coli* genomes in the RefSeq database for molecular signatures unique to Tn*6242*.

MATERIALS AND METHODS

Strains, Isolation, and Culture Conditions

The *Escherichia coli* strains 2009-27 and 2009-30 were recovered one day apart from mid-stream urine of a patient being treated at the Sydney Adventist Hospital (SAN) in 2009. VITEK-2 species identification and phenotypic resistance profiling of the strains was performed at the SAN, testing for susceptibility to ampicillin, cephalexin, ciprofloxacin, gentamicin, nitrofurantoin, and trimethoprim using established microbiological protocols. At UTS, the strains were additionally tested using the calibrated dichotomous sensitivity (CDS) method (Bell et al., 2016) against 15 antibiotics (ampicillin 25 μg, azithromycin 15 μg, cefotaxime 5 μg, cefoxitin 30 μg, chloramphenicol 30 μg, ciprofloxacin 5 μg, co-trimoxazole 25 μg, gentamicin 10 μg, imipenem 10 μg, nalidixic acid 30 μg, nitrofurantoin 200 μg, streptomycin 25 μg, sulphafurazole 300 μg, tetracycline 10 μg, and trimethoprim 5 μg) and using *Escherichia coli* ACM 5185 as a reference control.

DNA Purification

For PCR and Illumina sequencing, genomic DNA was extracted from 2 ml overnight cultures growing in Lysogeny Broth (LB) broth supplemented with 50 μg/ml ampicillin using an ISOLATE-II Genomic DNA kit (Bioline, Australia). Fosmid DNA and extrachromosomal DNA (IS*26* mediated DNA-loops) were extracted using the ISOLATE-II plasmid mini kit from 1.5 ml of LB culture supplemented with appropriate antibiotics. For Single Molecule Real Time (SMRT) sequencing genomic DNA from 1.8 ml of an overnight culture was isolated using a moBio genomic DNA kit (Qiagen, Germany).

Fosmid Library Construction, Screening and PCR Conditions

A fosmid library of strain 2009-27 was constructed using the CopyControl Fosmid Library Production Kit (Epicenter) with pCC2-Fos as the vector, following the kit protocol. The library was propagated in *recA*- EPI300 chemically competent *E. coli* cells supplied by Epicenter. Five hundred individual colonies were screened for the presence of *intI1* gene using (HS915 and HS916) primers listed in **Supplementary Table S1**. The single fosmid clone used in the inverse PCR/loop out assay was selected on the basis of end sequences of the *intI1* positive fosmid clones and targeted PCR cartography experiments using primers listed in **Supplementary Table S1**.

Polymerase chain reaction consisted of 10 μl of MyTaq red (Bioline) Master Mix, 0.5 μM of each primer and 0.2 μM of template DNA in DNAse-RNAse free water (final volume 20 μl). Cycling conditions comprised of: initial denaturation step at 94°C for 2 min 30 s, 30 cycles of denaturation (94°C for 30 s) annealing (60°C for 30 s) and extension (72°C for 5 min),

with a final extension cycle of 72°C for 10 min. Annealing temperatures and extension step were varied depending on the melting temperatures of the primers and expected amplicon sizes. **Supplementary Table S1** lists the primers used. **Supplementary Figure S1** depicts the inverse PCR strategy used to identify circular elements comprising IS*26*-associated regions of the resistance locus.

Amplicon and Whole Genome Sequencing

Amplicons of interest were purified using a Promega Wizard® SV PCR and Gel Clean Up kit following the manufacturer's recommendations and sequenced using Sanger technology at the Australian Genome Research Facility, University of Queensland, in Brisbane. The genomes of strains 2009-27 and 2009-30 were initially sequenced at the ithree institute at UTS using a bench top Illumina MiSeq® sequencer and MiSeq V3 chemistry. The sequencing library was prepared following published protocols (Darling et al., 2014b). The 400 nt long paired end reads were assembled using an A5-MiSeq (ngopt_a5pipeline_linux-x64_20130919*)*.

DNA from strain 2009-27 was also sequenced using a PacBio RSII instrument at the Ramaciotti Centre for Genomics, UNSW, Sydney. Sequencing reads were assembled with HGAP and Quiver. The plasmid sequence was closed using Circlator (Hunt et al., 2015) and polished with Illumina MiSeq raw read sequences using PILON (Walker et al., 2014). Whole genome sequences of strain 2009-30 (Illumina) and strain 2009-27 (PacBio) are deposited in GenBank under accession numbers NXEQ00000000 and NXER00000000.

Preliminary genome annotations were generated using an online version of RAST (Overbeek et al., 2014) using FigFAM release 70. Putative virulence and antimicrobial resistance genes were identified using stand-alone BLASTn analyses and an in-house database, prior to manual verification using NCBI-ORF finder. Legitimate ORFs showed > 95% sequence similarity (E-value 0.001) across 100% of the query sequence. Sequences of interest were characterized using iterative BLASTn and BLASTp searches (Altschul et al., 1997).

Bioinformatics

Phylosift (Darling et al., 2014a) was used to infer phylogenetic relationships among ST405 strains 2009-27 and 2009-30 and 328 assembled *E. coli* ST405 genomes in Enterobase[1] as of June 29, 2017. A subset of 24 ST405 genomes that clustered together using marker gene phylogeny based PhyloSift analysis were subjected to core-genome alignment based phylogeny analysis using Parsnp (Treangen et al., 2014)[2] and selecting the -c (all genomes) and -x recombination filter flags. The assembled genome of biosample SAMEA4559509 (sample ERS1458688) was downloaded from Enterobase and used as a reference. Comparative, whole genome analyses were performed using Mauve (Darling et al., 2010). A SNP based phylogenetic tree of plasmid backbone sequences extracted from the longest locally collinear block derived from a progressiveMauve alignment was constructed using algorithms in FastTree_accu[3] and visualized using FigTree version 1.4.0.[4]

Multilocus sequence typing was performed *in silico* (eMLST) using the PubMLST database[5] and the Achtman *E. coli* MLST scheme[6] (Jolley and Maiden, 2010). Average nucleotide identity (ANI) was calculated using the ANI calculator portal at.[7] SMRT sequences from strain 2009-27 were used or all comparative genomic analyses.

RESULTS

Genomic Analysis of Strains 2009-27 and 2009-30

Illumina sequences of strains 2009-27 and 2009-30 assembled into 243 scaffolds (N50 = 89298; 47 × median coverage) and 191 scaffolds (N50 = 91427; 45 × median coverage), respectively. SMRT sequences of strain 2009-27 (N50 = 20303) assembled into two unitigs; a chromosome comprising 5,287,472bp and a plasmid (pSDJ2009-27) of 89,176 bp. *In silico* analyses showed that strains 2009-27 and 2009-30 were ST405, serotype O102:H6 and phylogroup D (ST405-D-O102:H6). Both strains were phenotypically resistant to ampicillin, azithromycin, streptomycin, trimethoprim and sulphafurazole. ANI analysis of the two genomes indicated that strains 2009-27 and 2009-30 are indistinguishable from one another (99.9% mean identity and 100% median identity).

Plasmid Analysis

pSDJ2009-27 typed as IncB/O/K/Z in plasmidFinder. The *repA* gene, encoding replication initiator protein, in pSDJ2009-27 was identical to *repA* in pR3521 (GU256641), a self-transmissible multi-drug resistant IncB/O plasmid encoding bla_{ACC-4}, bla_{SCO-1}, and bla_{TEM-1} from a patient in Greece (Papagiannitsis et al., 2011). No antimicrobial resistance genes were found on pSDJ2009-27 but it contained IncI1 plasmid-related *tra*-genes essential for conjugative transfer. Notably, the sequence of *repA* was also identical to *repA* in pO26-Vir (FJ386569.1) and showed ≥ 99% similarity to *repA* sequences in plasmids pR3521 (GU256641), pEC3I (KU932021), pHUSEC411-like (HG428756), and pHUSEC41-1 (HE603110) associated with IPEC. BLAST analysis showed that pSDJ2009-27 shared ≥ 99% identity over 89% of the query sequence with pO26-Vir (FJ386569.1) from Shiga-toxin producing O26:H11 strain H30 (Fratamico et al., 2011) (**Supplementary Figure S2**). A progressiveMauve alignment (**Supplementary Figure S3**) of the plasmid sequences with near identical *repA* genes revealed a ∼60 kb conserved fragment of high sequence similarity. Phylogenetic analysis of the aligned regions of these plasmids (**Supplementary Figure S4**) confirmed that pO26-Vir was the

[1]http://enterobase.warwick.ac.uk/

[2]https://github.com/marbl/Parsnp

[3]http://darlinglab.org/blog/2015/03/23/not-so-fast-fasttree.html

[4]http://tree.bio.ed.ac.uk/software/figtree/

[5]http://pubmlst.org/

[6]http://mlst.warwick.ac.uk/mlst/

[7]http://enve-omics.ce.gatech.edu/ani/index

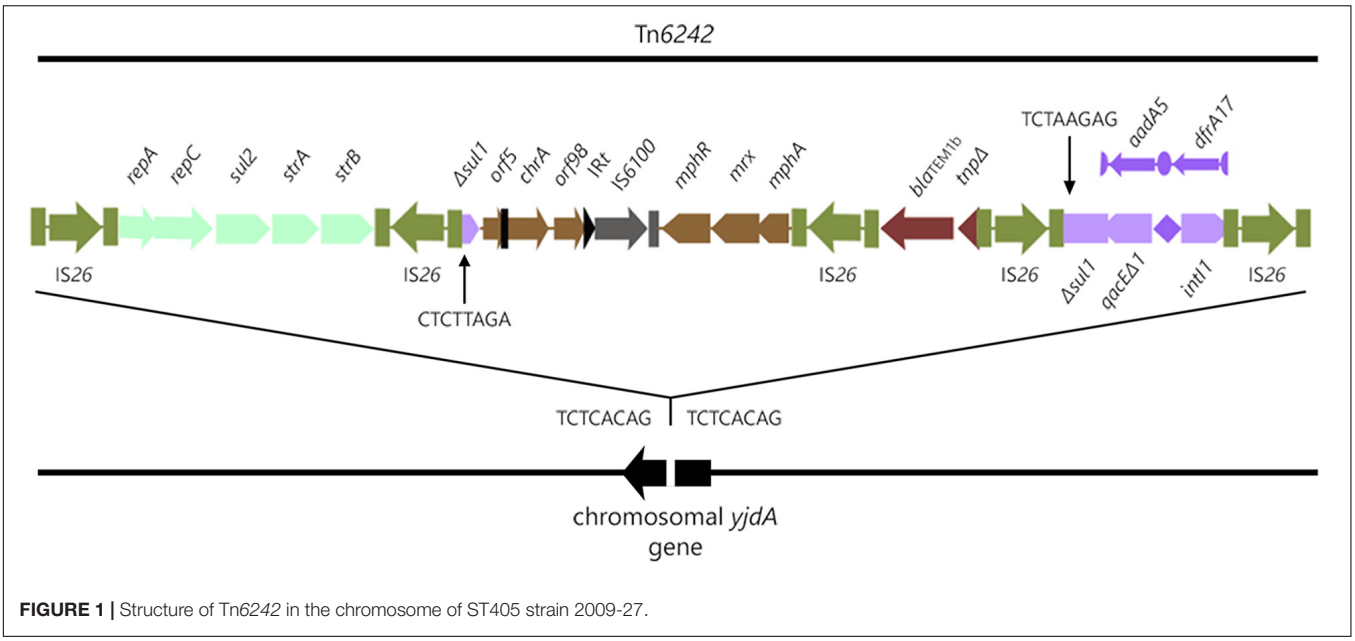

FIGURE 1 | Structure of Tn*6242* in the chromosome of ST405 strain 2009-27.

TABLE 1 | Resistance genes in ST405 genomes.

Resistance genes	2009-27	blood-09-0464	blood-9-0292	blood-90543	blood-90544	eo1776
tet(B)(AF326777)	x	100	100	100	100	100
tet(A)(AJ517790)	x	100	100	100	100	x
sul2 (GQ421466)*	99.63	100	100	100	100	x
sul2 (HQ840942)*	100	99.63	99.63	99.63	99.63	x
strA (AF321551)*	100	100	100	100	100	100
strB (M963920)*	99.88	99.88	99.88	x	x	x
bla_{TEM-1A}* (HM749966)	99.65	x	x	99.77	99.65	x
bla_{OXA-1} (J02967)	x	100	100	100	100	100
$bla_{CTX-M-88}$ (FJ873739)	x	99.89	99.89	99.89	99.89	99.89
aac(6′)*Ib-cr* (DQ303918)	x	100	100	100	100	100
aacA4 (KM278199)	x	99.64	99.64	99.64	99.64	99.64
dfrA17 (FJ460238)*	100	100	100	100	100	100
aadA5 (AF137361)*	100	100	100	100	100	100
sul1 (CP002151)*	100Δ	100	100	100	100	100
mph(A) (D16251)*	100	100	100	100	100	x

Numbers indicate the percentage identity across 100% of the input query sequence. An asterisk (*) indicates the resistance genes present within the boundaries of Tn6242. Δ indicates partial deletion at one end of the gene due to breaks in the scaffolds of the genome sequence.

most closely related plasmid and originated from a recent common ancestor. A comparative bi-directional peptide BLAST analysis of all ORFs identified by RAST within the 60 kb fragment in pSDJ2009-27 with those on pO26-Vir, pEC3I, pHUSEC411-like, and pHUSEC41-1 indicated that they contain genes for IncI plasmid maintenance, stability and transfer (**Supplementary Table S2**). pO26-Vir is a large (168-kb) mosaic plasmid that carries putative EHEC virulence genes *toxB*, *katP*, *ehxA*, and *espP*. Notably, ∼45-kb of pO26-Vir containing these genes is absent in pSDJ2009-27 (**Supplementary Figure S4** and **Supplementary Table S3**). We have recently described pO26-CRL (Venturini et al., 2010) (represented as the inner green circle in **Supplementary Figure S2**) from an O26:H- EHEC isolated from a patient with hemorrhagic colitis and pO26-CRL-125 (Venturini et al., 2013), that were also similar to pO26-Vir (**Supplementary Figure S2**).

Characterisation of the CRL in Strain 2009-27

The class 1 integron in strains 2009–27 and 2009–30 is flanked by direct copies of IS*26*, one of which was located 209 nucleotides downstream from the start site of the *sul1* gene in the 3′-CS, rendering *sul1* inactive. The variable region of the integron carried *dfrA17* and *aadA5* genes encoding resistance to trimethoprim and streptomycin. A PCR developed previously to identify novel IS*26*-mediated genetic signatures within the 3′-CS of class 1 integrons using a primer in *attI1* (L1 primer) in the 5′-CS and a primer in IS*26 tnpA* (JL-D2) (Dawes et al., 2010;

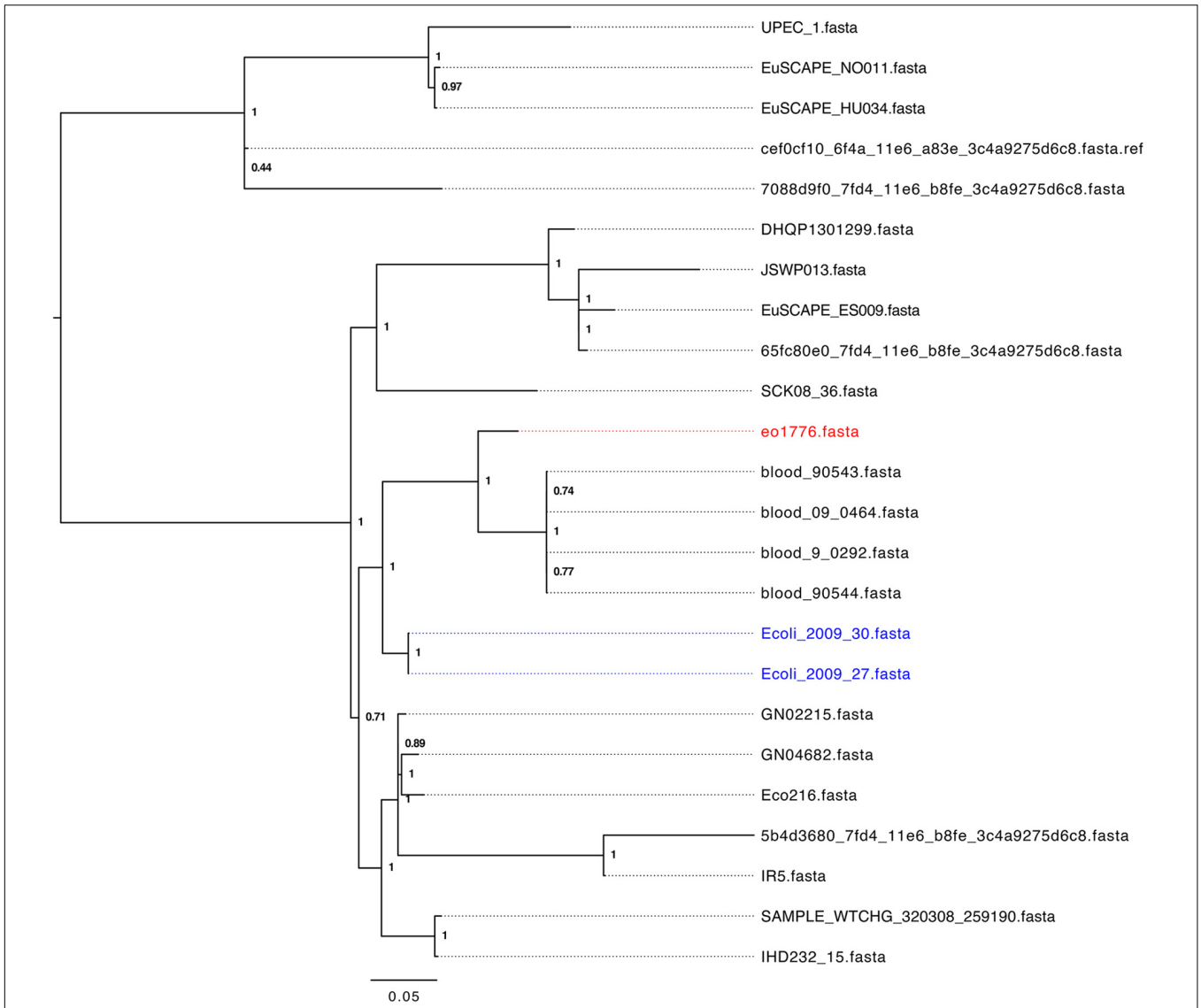

FIGURE 2 | Parsnp tree analysis of E. coli ST405 genomes phylogenetically related to strain 2009-27.

Roy Chowdhury et al., 2015) generated a unique amplicon of 2425-bp and this was exploited to track this unique genetic locus.

Analysis of the SMRT sequences from strain 2009–27 indicated it had a chromosomally located CRL, 19,774-bp [nucleotides 1732675 to 1752448, unitig_0 (NXER00000000)] in length. The CRL is flanked by direct copies of IS*26* and located within *yjdA* in the chromosome, a site not known for insertion of laterally acquired DNA (**Figure 1**). An eight nucleotide direct duplication (TCTCACAG) was identified (**Figure 1**) flanking the CRL indicating that IS*26* was responsible for its movement. The IS*26*-flanked transposon is registered as Tn*6242* in the transposon database.[8]

The structure of the CRL is modular, comprising five copies of IS*26* that flank modules 1–4 containing combinations of different antimicrobial resistance genes. Module 1 comprises *repA-repC-sul2-strA-strB* genes bounded by two inwardly orientated IS*26* elements, a structure that forms part of the Tn*6029* family of transposons (Dawes et al., 2010; Yau et al., 2010; Cain and Hall, 2012b; Roy Chowdhury et al., 2015). Module 2 is 6924-bp and comprises Δ*sul1*, Δ*orf5* interrupted by the inverted repeat of Tn*501* (IR_{Tn501}), *chrA*, *orf98*, the IR*t* inverted repeat typical of clinical class 1 integrons, IS*6100,* and the macrolide resistance operon *mphR-mrx-mphA*. The sequence between Δ*sul1* and the macrolide resistance operon is frequently reported in association with class 1 integrons on different *E. coli* plasmids from geographically distant sources (GenBank accession numbers LT632321.1; FQ482074.1; EU935739.1). Beyond the macrolide resistance operon is a third 1402-bp Tn*2*-derived IS*26* flanked module (module 3) comprising bla_{TEM-1b} and a ΔTn*2* transposase gene. bla_{TEM-1b}-associated Tn*2*-derivatives typically

[8]https://transposon.lstmed.ac.uk/tn-registry

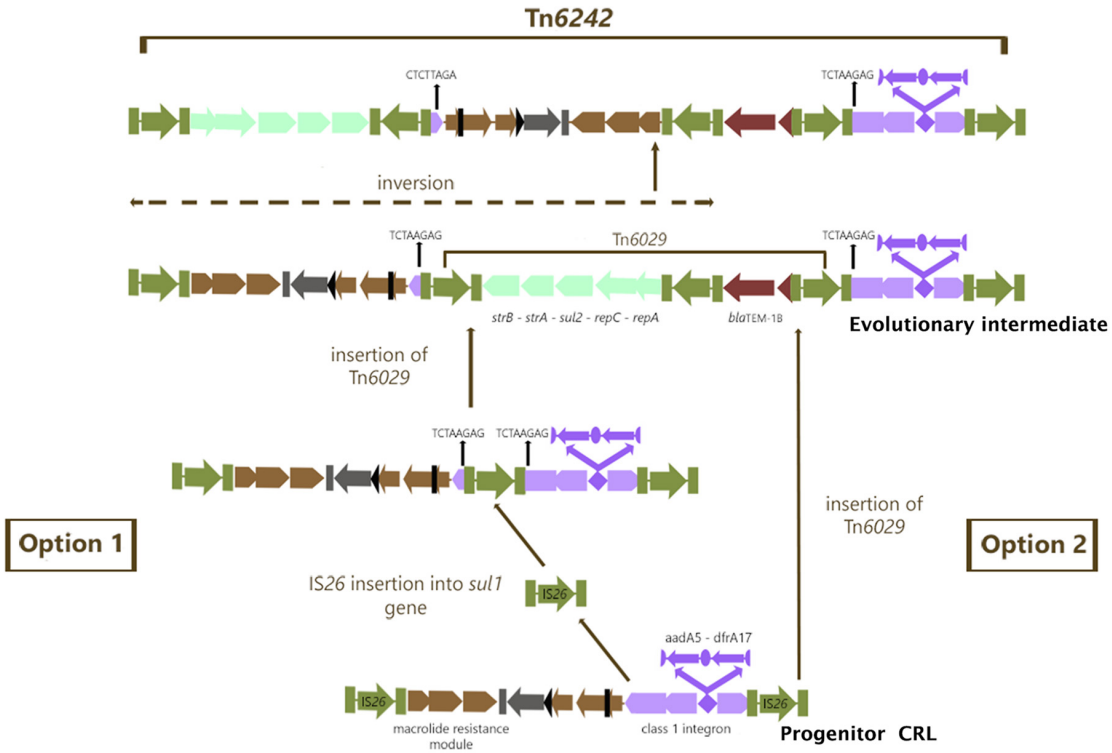

FIGURE 3 | Genealogy of Tn*6242*. Green color arrows bounded by green bars indicate IS*26*. The aqua colored group of arrows indicate module 1 consisting of the *repA-repc-sul2-strA-strB* genes, the light brown colored arrows indicate module 2 containing *orf5-chrA*-IS*6100-mphR-mrx-mphA* genes, the chocolate colored gene indicates module 3 with the bla_{TEM1b} gene and the violet colored arrows indicate the class 1 integron associated Δ*intI1-dfrA17-aadA5-qacE*Δ*1-sul1*Δ genes described as module 4. For more details of the genes and their orders please refer to **Figure 1**.

form part of the Tn*6029* family of transposons (Roy Chowdhury et al., 2015), although this 1402-bp fragment is unique (see later). A class 1 integron with a truncated copy of *intI1* comprises module 4 in the CRL (**Figure 1**). Δ*intI1* comprises 657 nucleotides and the deletion event presumably was associated with insertion of IS*26*. The recombination functional of Δ*intI1* is non-functional in strains 2009-27 and 2009-30 and the integron is not expected to integrate or exchange gene cassettes. The P_C promoter remains intact, however, and is expected to induce the expression of *aadA5* and *dfrA17* resistance genes, an observation consistent with phenotypic resistance to trimethoprim and streptomycin.

Prevalence of Tn*6242*

A 24.1-kb DNA fragment comprising 19.8-kb of the CRL and about 5 kb flanking both ends of *yjdA* gene was used to interrogate the GenBank RefSeq database. Two *E. coli* genomes (accession numbers NZ_KE701406.1 and NZ_KE699379.1) showed ≥ 99% sequence identity across 100% of the input query sequence (**Supplementary Figure S5**). NZ_KE701406.1 and NZ_KE699379.1 were ST405-D-O102:H6 and were from urine and blood of unrelated Danish patients, respectively. Each strain carried the four resistance gene modules of Tn*6242*, including the class 1 integron and associated cassette array, on one supercontig. Barring small deletions that may be products of assembly errors, these sequences were indistinguishable (**Supplementary Figure S5**).

Comparative Phylogenomics of ST405 Strains

To identify a cohort of ST405 strains related to strains 2009-27 and 2009-30 we initially performed a marker gene based phylogeny analysis of 328 assembled *E. coli*-ST405 genomes from Enterobase (26th July, 2017) using Phylosift (Darling et al., 2014a). Strains 2009-27 and 2009-30 clustered with 24 ST405 strains (**Supplementary Figure S6**) from human infections from unrelated geographic locations. Core genome alignment based phylogeny analysis of these 24 ST405 strains (**Figure 2**) identified e01776 to be the closest relative of 2009-27 (1414 SNP differences) while four strains, from patients in the United States with blood infections, showed between 1662 and 1665 SNP differences. Fifteen of the 24 strains (**Supplementary Table S4**) had an identical class 1 integron and the remaining nine had *intI1* interrupted by IS*26*. The insertion site of IS*26* in *intI1* occurred at two separate locations both of which were different to Δ*intI1* in Tn*6242* (**Supplementary Table S4**).

A BLASTn search (≥ 95% identity over 100% of the query sequence) of antimicrobial resistance and virulence genes in the genome of 2009-27 against an in-house database of resistance genes identified $bla_{CTX-M88}$ and bla_{OXA-1} in the five ST405

genomes that clustered with 2009-27 (**Table 1**). Several of the five *E. coli* ST405 genomes carry all the resistance genes characteristic of Tn*6242* (*dfrA17*, *aadA5*, *sul1*, *mph(A)*, *sul2*, *strA*, and *strB*) on the same scaffold. **Supplementary Table S5** depicts an alignment of the 19.7-kb region spanning Tn*6242* with the seven closely related *E. coli* ST405 genomes identified here. The four blood-borne *E. coli* ST405 strains had a copy of the class 1 integron with a Δ*intI1* variant, as well as the IS*6100*-associated macrolide resistance module that abuts the 3′-CS with *orf5*, *chrA*, and *orf98* genes on the same scaffold. Strain eo1776 did not carry the macrolide resistance module. Notably, all five strains contained an intact copy of *yjdA* and had a variable repertoire of virulence genes (**Supplementary Table S6**). Comparative plasmid profiling of the five closely related genomes with strain 2009-27 suggested that *E. coli* ST405 strains 09-90543 and 09-90544 also had an IncB/O/K/Z plasmid replicon in addition to IncFII and pCol replicons, while blood isolates 09-0464 and blood 09-0292 carried IncFII and pCol replicons. Strain eo1776 was unusual in that it only carried an IncFII replicon. These data suggest that the class 1 integron may be associated with IncFII plasmids in this collection.

Evolution of Tn*6242*

In module 4 of Tn*6242* the sulfonamide resistance gene *sul1* is interrupted by a fragment of DNA encoding $bla_{\mathrm{TEM-1B}}$ and the macrolide resistance operon in module 1 is flanked by oppositely facing copies of IS*26*. The reverse complement of the last eight bases of the *sul1* gene (TCTAAGAG) flanks one arm of module 2 while the complimentary sequence CTCTTAGA flanks the other end (**Figure 1**) of module 3. These observations, coupled with the fact that the orientation of module 2 and 3 is inverted in relation what is often seen in typical clinical class 1 integrons, suggest that modules 2 and 3 have undergone an IS*26*-mediated inversion, an event that can occur in regions of DNA flanked by oppositely facing copies of IS*26* (Roy Chowdhury et al., 2015). To explain the genealogy of Tn*6242* (**Figure 3**), a hypothetical progenitor of 10,698 bp, comprising an inverted copy of modules 2 and 3 that abuts the 3′-CS of the class 1 integron with *sul1* intact, was assembled *in-silico*. We also removed a copy of IS*26* that presumably inserted into the 3′-end of *sul1* in the progenitor. A BLASTn analysis was undertaken to determine if our hypothetical progenitor has been described previously. The analysis identified matches (100%) to integrons in plasmids 'p' from strain NCTC 13441 (LT632321.1), pETN48 from *E. coli* ST405-O102 (FQ482074.1), pEK499 (EU935739.1) from ST131-O25:H4, and pEC958 from *E. coli* ST131-O25b:H4 (HG941719.1) from Australia. From the progenitor sequence there are several features of Tn*6242* that indicate it may have formed in one of two ways. Option 1 in **Figure 3** depicts a copy of IS*26* inserting into *sul1*, generating a target site 8-bp duplication (TCTAAGAG), followed by the insertion of a Tn*6029*-family transposon (Harmer and Hall, 2015, 2016). In option 2 (**Figure 3**), a Tn*6029*-family transposon, rather than IS*26,* inserted in the *sul1* generating the same 8-bp target site duplication. The resulting structure, identified as the evolutionary intermediate in **Figure 3**, positions 209 nucleotides at the 3′-end of *sul1* gene away from the rest of the *sul1* gene. Tn*6029*- and Tn*6026*-family transposons are widely dispersed within *Salmonella enterica* and *E. coli* populations in Australia and are known to be associated with plasmid-encoded, mercury resistance transposons (Dawes et al., 2010; Venturini et al., 2013). Strain 2009-27 does not contain a mercury resistance transposon, indicating that the formation and mobilization of the CRL was driven by IS*26*. In the evolutionary intermediate, two inwardly facing copies of IS*26* flank *repA-repC-sul2-strA-strB* and the *mphR-mrx-mphA* module beyond with the intervening sequence (option 2, **Figure 3**), enabling us to trace an IS*26*-mediated inversion event, generating the structure seen in Tn*6242*.

Generation of Laterally Mobile Translocatable Units From Tn*6242*

It is conceivable that Tn*6242* can generate multiple translocatable units (TUs), each mobilizing a different combination of resistance gene module flanked by direct copies of IS*26*. To investigate this, we cloned the CRL into a pCC2Fos fosmid vector and propagated the fosmid in a *recA*- background (*E. coli* strain EP1300). An inverse PCR strategy (**Supplementary Figure S1**) was used to examine the ability of the module containing the macrolide resistance gene cluster and the integron-containing module to be rescued as a translocatable unit (TU). Sanger sequencing of inverse PCR amplicons that span across the IS*26* junctions indicated that all three TUs were generated (**Supplementary Figure S7**). Therefore, pSDJ2009-27 could act as a vector for Tn*6242* and generate different combinations of laterally mobile resistance gene modules flanked by direct copies of IS*26* from Tn*6242*.

DISCUSSION

Genome sequence analyses of ST405-D-O102:H6 strains 2009-27 and 2009-30 from the urine of the same patient that were resistant to ampicillin, azithromycin, streptomycin, trimethoprim, and sulphafurazole is presented here. In these Sydney strains, we describe the structure of a novel IS*26*-derived and laterally mobile compound transposon, identified here as Tn*6242*. Tn*6242* comprises a class 1 integron, a variant of Tn*6029,* and an *mphA* operon and these are sufficient to encode resistance to a panel of antibiotics described above. Notably, Tn*6242* is located within a unique chromosomal location in *yjdA*. We predict a series of genetic events that led to the formation of Tn*6242* and showed how the genetic signatures formed during its evolution were exploited to identify two MDR strains of ST405 from Denmark that carry minor variants of Tn*6242* in *yjdA*.

Our data suggest that this lineage of MDR ST405-D-O102:H6 may be globally disseminated. Analyses of phylogenetically related ST405 genomes in Enterobase indicate that they carry CRL with similar genetic cargo but were not associated with *yjdA*. Since most IS*26*-associated resistance regions are plasmid-encoded, the evolutionary events that created Tn*6242* in *yjdA* are likely to be recent. It will be important to monitor IS*26*-flanked CRL that associate with *yjdA* as it may represent a novel and emerging hotspot for the insertion of other IS*26*-flanked elements in the chromosome of clinically important *Enterobacteriaceae*.

The *repA-repC-sul2-strA-strB* module in Tn*6242* is flanked by two inwardly facing IS*26* elements and shares 99% sequence identity with structures found in pSRC26 (GQ150541), pSRC27-H (HQ840942.1) (Cain and Hall, 2012a), pO26-CRL (GQ259888.1), pO26-CRL-125 (KC340960.1), and pO111-CRL-115 (KC340959.1) (Venturini et al., 2013), all reported in Australia. However, the Tn*2* transposon in the $bla_{\mathrm{TEM-1b}}$ module is 1402-bp, and is much smaller than Tn*2* variants in Tn*6029* (1916-bp), Tn*6029B* (1831-bp), or Tn*6029C* (1820-bp) (Roy Chowdhury et al., 2015). BLAST analysis confirmed that the 1402-bp variant is novel suggesting that the deletion likely arose as a consequence of the inversion event described above. Notably, sequences that aligned with ≥ 99.9% identity to the input query were plasmids from Australia that carry derivatives of Tn*6029B*. Collectively, our data suggests that Tn*6242* may be a locally derived IS*26*-flanked transposon.

Finally, the backbone of a resident IncB/O/K/Z plasmid (pSDJ2009-27) showed ≥ 99% sequence identity with pO26Vir from an O26:H11 Shigatoxigenic *E. coli* and pO26-CRL from an enterohemorrhagic *E. coli* O26: H^- strain. STEC O26:H11/H- has been associated with Shiga toxin production and foodborne illness and are the second most frequent cause of EHEC-associated food-borne illness globally (Lajhar et al., 2017). pO26-Vir and pSDJ2009-27 carry a type IV pilus biosynthesis locus (*pil*) comprising *pilL - pilV* that may be important for biofilm formation (Srimanote et al., 2002). ExPEC have a fecal origin and plasmids circulating in IPEC may adapt to play important roles in ExPEC virulence. To our knowledge, such an observation has not been reported and this is the first time an IPEC virulence plasmid has been identified in uropathogenic *E. coli*.

ETHICS STATEMENT

This study does not require any ethics approval. The isolates in the study came from a larger collection of *E. coli* isolates set aside by the hospital microbiology laboratory for our research. They were collected in accordance with Hospital policy as part of routine microbiology of hospital patients. We received de-identified isolates so patient identity is not known. There was no requirement for ethics approval on de-identified samples when they collected.

AUTHOR CONTRIBUTIONS

PRC and SD conceptualized and designed the study, and co-wrote the manuscript. PRC and JM analyzed the data. JM also assisted in the generation of the first draft of the manuscript. ML was involved in the generation of short and long read sequencing of the genomes.

FUNDING

This project was funded by the Australian Centre for Genomic Epidemiological Microbiology (Ausgem), a strategic partnership between the NSW-Department of Primary Industries and the ithree Institute at the University of Technology Sydney. JM is the recipient of the Australian Postgraduate Research Award. The PacBio RSII sequencer used in this study was secured under ARC project LE150100031.

ACKNOWLEDGMENTS

We wish to acknowledge Natalie Miller and Nola Hitchik at the SAN Pathology Laboratories for supplying strains 2009-27 and 2009-30 and associated metadata. We wish to thank Max Cummins for assistance with the standalone BLASTn analysis presented in the phylogenomics section of this manuscript. PacBio sequencing was undertaken at the Ramaciotti Centre for Genomics at the University of New South Wales.

SUPPLEMENTARY MATERIAL

The Supplementary Material for this article can be found online at: https://www.frontiersin.org/articles/10.3389/fmicb.2018.03212/full#supplementary-material

FIGURE S1 | Inverse PCR strategy used to identify IS*26*-associated mobile elements.

FIGURE S2 | Alignment of regions of pO26-vir, pSDJ2009-27 and pO26_CRL which share ≥ 99% sequence identity over specific regions. Plasmid pO26-vir, represented in the outermost circle has color coded open reading frames indicating position of specific gene/ gene clusters. The maroon circle indicates regions present in pSDJ2009-27 and the green innermost green circle indicate pO26_CRL.

FIGURE S3 | Progressive Mauve alignments of pSDJ2009-27 and plasmids with identical *repA* genes. The ∼ 60-kb region of homology is highlighted with a red box.

FIGURE S4 | SNP tree of plasmids related to pSDJ2009-27.

FIGURE S5 | Alignment of Tn*6242* and flanking sequences with NZ_KE701406.1 and NZ_KE699379.1.

FIGURE S6 | Phylosift analysis of ST405 strains in Enterobase. Sydney ST405 strains included in this study are highlighted in red. No geographic location data was available for 12 strains.

FIGURE S7 | Structure of Tn*6242* with red arrows adobe specific modules which were experimentally proven to loops out under stress, with sanger sequencing of inverse PCR amplicons. Primers on top of the red arrows indicate the primers used in the PCR cartography experiment to select the *intI1* positive fosmid clone for the looping out experiment.

TABLE S1 | Primers and PCR conditions used in this work.

TABLE S2 | Comparative peptide BLAST analysis of the ORFs predicted from the sequence of pSDJ2009-27 by RAST and other closely related plasmids.

TABLE S3 | RAST annotation of SDJ2009-27.

TABLE S4 | Relative abundance of resistance genes in ST405.

TABLE S5 | BLASTn alignment of Tn*6242* in ST405 genomes.

TABLE S6 | Stand-alone BLASTn analysis of virulence genes in ST405. "1" indicates presence and "0" indicates absence of an identical copy of the gene in the respective genome.

REFERENCES

Agyekum, A., Fajardo-Lubian, A., Ai, X., Ginn, A. N., Zong, Z., Guo, X., et al. (2016). Predictability of phenotype in relation to common beta-lactam resistance mechanisms in *Escherichia coli* and *Klebsiella pneumoniae*. *J. Clin. Microbiol.* 54, 1243–1250. doi: 10.1128/JCM.02153-15

Altschul, S. F., Madden, T. L., Schaffer, A. A., Zhang, J., Zhang, Z., Miller, W., et al. (1997). Gapped BLAST and PSI-BLAST: a new generation of protein database search programs. *Nucleic Acids Res.* 25, 3389–3402. doi: 10.1093/nar/25.17.3389

Bell, S. M., Pham, J. N., Rafferty, D. L., and Allerton, J. K. (2016). *Antibiotic Susceptibility Testing by the CDS Method*. Kogarah: cdstest.net.

Beyrouthy, R., Robin, F., Lessene, A., Lacombat, I., Dortet, L., Naas, T., et al. (2017). MCR-1 and OXA-48 in vivo acquisition in KPC-producing *Escherichia coli* after colistin treatment. *Antimicrob. Agents Chemother.* 61:e2540-16. doi: 10.1128/AAC.02540-16

Brolund, A., Edquist, P. J., Makitalo, B., Olsson-Liljequist, B., Soderblom, T., Wisell, K. T., et al. (2014). Epidemiology of extended-spectrum beta-lactamase-producing *Escherichia coli* in Sweden 2007-2011. *Clin. Microbiol. Infect.* 20, O344–O352. doi: 10.1111/1469-0691.12413

Cain, A. K., and Hall, R. M. (2012a). Evolution of a multiple antibiotic resistance region in IncHI1 plasmids: reshaping resistance regions in situ. *J. Antimicrob. Chemother.* 67, 2848–2853. doi: 10.1093/jac/dks317

Cain, A. K., and Hall, R. M. (2012b). Evolution of IncHI2 plasmids via acquisition of transposons carrying antibiotic resistance determinants. *J. Antimicrob. Chemother.* 67, 1121–1127. doi: 10.1093/jac/dks004

Chen, C. M., Yu, W. L., Huang, M., Liu, J. J., Chen, I. C., Chen, H. F., et al. (2015). Characterization of IS26-composite transposons and multidrug resistance in conjugative plasmids from *Enterobacter cloacae*. *Microbiol. Immunol.* 59, 516–525. doi: 10.1111/1348-0421.12289

Darling, A. E., Jospin, G., Lowe, E., Matsen, F. A. T., Bik, H. M., and Eisen, J. A. (2014a). PhyloSift: phylogenetic analysis of genomes and metagenomes. *PeerJ* 2:e243. doi: 10.7717/peerj.243

Darling, A. E., Worden, P., Chapman, T. A., Roy Chowdhury, P., Charles, I. G., and Djordjevic, S. P. (2014b). The genome of *Clostridium difficile* 5.3. *Gut Pathog.* 6:4. doi: 10.1186/1757-4749-6-4

Darling, A. E., Mau, B., and Perna, N. T. (2010). progressiveMauve: multiple genome alignment with gene gain, loss and rearrangement. *PLoS One* 5:e11147. doi: 10.1371/journal.pone.0011147

Dawes, F. E., Kuzevski, A., Bettelheim, K. A., Hornitzky, M. A., Djordjevic, S. P., and Walker, M. J. (2010). Distribution of class 1 integrons with IS26-mediated deletions in their 3′-conserved segments in *Escherichia coli* of human and animal origin. *PLoS One* 5:e12754. doi: 10.1371/journal.pone.0012754

Fratamico, P. M., Yan, X., Caprioli, A., Esposito, G., Needleman, D. S., Pepe, T., et al. (2011). The complete DNA sequence and analysis of the virulence plasmid and of five additional plasmids carried by Shiga toxin-producing *Escherichia coli* O26:H11 strain H30. *Int. J. Med. Microbiol.* 301, 192–203. doi: 10.1016/j.ijmm.2010.09.002

Gurnee, E. A., Ndao, I. M., Johnson, J. R., Johnston, B. D., Gonzalez, M. D., Burnham, C. A., et al. (2015). Gut colonization of healthy children and their mothers with pathogenic ciprofloxacin-resistant *Escherichia coli*. *J. Infect. Dis.* 212, 1862–1868. doi: 10.1093/infdis/jiv278

Harmer, C. J., and Hall, R. M. (2015). IS26-mediated precise excision of the IS26-aphA1a translocatable unit. *mBio* 6:e1866-15. doi: 10.1128/mBio.01866-15

Harmer, C. J., and Hall, R. M. (2016). IS26-mediated formation of transposons carrying antibiotic resistance genes. *mSphere* 1:e38-16. doi: 10.1128/mSphere.00038-16

Harmer, C. J., Moran, R. A., and Hall, R. M. (2014). Movement of IS26-associated antibiotic resistance genes occurs via a translocatable unit that includes a single IS26 and preferentially inserts adjacent to another IS26. *mBio* 5:e01801-14. doi: 10.1128/mBio.01801-14

Hunt, M., Silva, N. D., Otto, T. D., Parkhill, J., Keane, J. A., and Harris, S. R. (2015). Circlator: automated circularization of genome assemblies using long sequencing reads. *Genome Biol.* 16:294. doi: 10.1186/s13059-015-0849-0

Johnson, J. R., Gajewski, A., Lesse, A. J., and Russo, T. A. (2003). Extraintestinal pathogenic *Escherichia coli* as a cause of invasive nonurinary infections. *J. Clin. Microbiol.* 41, 5798–5802. doi: 10.1128/JCM.41.12.5798-5802.2003

Jolley, K. A., and Maiden, M. C. (2010). BIGSdb: scalable analysis of bacterial genome variation at the population level. *BMC Bioinformatics* 11:595. doi: 10.1186/1471-2105-11-595

Lajhar, S. A., Brownlie, J., and Barlow, R. (2017). Survival capabilities of *Escherichia coli* O26 isolated from cattle and clinical sources in Australia to disinfectants, acids and antimicrobials. *BMC Microbiol.* 17:47. doi: 10.1186/s12866-017-0963-0

Liu, B. T., Song, F. J., Zou, M., Hao, Z. H., and Shan, H. (2017). Emergence of colistin resistance gene mcr-1 in *Cronobacter sakazakii* producing NDM-9 and in *Escherichia coli* from the same animal. *Antimicrob. Agents Chemother.* 61:e1444-16. doi: 10.1128/AAC.01444-16

Mangat, C. S., Bekal, S., Irwin, R. J., and Mulvey, M. R. (2017). A novel hybrid plasmid carrying multiple antimicrobial resistance and virulence genes in *Salmonella enterica* Serovar Dublin. *Antimicrob. Agents Chemother.* 61:e2601-16. doi: 10.1128/AAC.02601-16

Matsumura, Y., Yamamoto, M., Nagao, M., Hotta, G., Matsushima, A., Ito, Y., et al. (2012). Emergence and spread of B2-ST131-O25b, B2-ST131-O16 and D-ST405 clonal groups among extended-spectrum-beta-lactamase-producing *Escherichia coli* in Japan. *J. Antimicrob. Chemother.* 67, 2612–2620. doi: 10.1093/jac/dks278

Matsumura, Y., Yamamoto, M., Nagao, M., Tanaka, M., Takakura, S., and Ichiyama, S. (2015). Detection of *Escherichia coli* sequence type 131 clonal group among extended-spectrum beta-lactamase-producing *E. coli* using VITEK MS Plus matrix-assisted laser desorption ionization-time of flight mass spectrometry. *J. Microbiol. Methods* 119, 7–9. doi: 10.1016/j.mimet.2015.09.016

Overbeek, R., Olson, R., Pusch, G. D., Olsen, G. J., Davis, J. J., Disz, T., et al. (2014). The SEED and the rapid annotation of microbial genomes using Subsystems Technology (RAST). *Nucleic Acids Res.* 42, D206–D214. doi: 10.1093/nar/gkt1226

Papagiannitsis, C. C., Tzouvelekis, L. S., Kotsakis, S. D., Tzelepi, E., and Miriagou, V. (2011). Sequence of pR3521, an IncB plasmid from *Escherichia coli* encoding ACC-4, SCO-1, and TEM-1 beta-lactamases. *Antimicrob. Agents Chemother.* 55, 376–381. doi: 10.1128/AAC.00875-10

Poolman, J. T., and Wacker, M. (2016). Extraintestinal pathogenic *Escherichia coli*, a common human pathogen: challenges for vaccine development and progress in the field. *J. Infect. Dis.* 213, 6–13. doi: 10.1093/infdis/jiv429

Porse, A., Schonning, K., Munck, C., and Sommer, M. O. (2016). Survival and evolution of a large multidrug resistance plasmid in new clinical bacterial hosts. *Mol. Biol. Evol.* 33, 2860–2873. doi: 10.1093/molbev/msw163

Reid, C. J., Roy Chowdhury, P., and Djordjevic, S. P. (2015). Tn6026 and Tn6029 are found in complex resistance regions mobilised by diverse plasmids and chromosomal islands in multiple antibiotic resistant *Enterobacteriaceae*. *Plasmid* 80, 127–137. doi: 10.1016/j.plasmid.2015.04.005

Reid, C. J., Wyrsch, E. R., Roy Chowdhury, P., Zingali, T., Liu, M., Darling, A. E., et al. (2017). Porcine commensal *Escherichia coli*: a reservoir for class 1 integrons associated with IS26. *Microb. Genom.* 3:e000143. doi: 10.1099/mgen.0.000143

Riccobono, E., Di Pilato, V., Di Maggio, T., Revollo, C., Bartoloni, A., Pallecchi, L., et al. (2015). Characterization of IncI1 sequence type 71 epidemic plasmid lineage responsible for the recent dissemination of CTX-M-65 extended-spectrum beta-lactamase in the Bolivian Chaco region. *Antimicrob. Agents Chemother.* 59, 5340–5347. doi: 10.1128/AAC.00589-15

Roy Chowdhury, P., Charles, I. G., and Djordjevic, S. P. (2015). A role for Tn6029 in the evolution of the complex antibiotic resistance gene loci in genomic island 3 in enteroaggregative hemorrhagic *Escherichia coli* O104:H4. *PLoS One* 10:e0115781. doi: 10.1371/journal.pone.0115781

Roy Chowdhury, P., Ingold, A., Vanegas, N., Martinez, E., Merlino, J., Merkier, A. K., et al. (2011). Dissemination of multiple drug resistance genes by class 1 integrons in *Klebsiella pneumoniae* isolates from four countries: a comparative study. *Antimicrob. Agents Chemother.* 55, 3140–3149. doi: 10.1128/AAC.01529-10

Smith, J. L., Fratamico, P. M., and Gunther, N. W. (2007). Extraintestinal pathogenic *Escherichia coli*. *Foodborne Pathog. Dis.* 4, 134–163. doi: 10.1089/fpd.2007.0087

Srimanote, P., Paton, A. W., and Paton, J. C. (2002). Characterization of a novel type IV pilus locus encoded on the large plasmid of locus of enterocyte effacement-negative Shiga-toxigenic *Escherichia coli* strains that are virulent for humans. *Infect. Immunol.* 70, 3094–3100. doi: 10.1128/IAI.70.6.3094-3100.2002

Treangen, T. J., Ondov, B. D., Koren, S., and Phillippy, A. M. (2014). The Harvest suite for rapid core-genome alignment and visualization of thousands of intraspecific microbial genomes. *Genome Biol.* 15:524. doi: 10.1186/s13059-014-0524-x

Venturini, C., Beatson, S. A., Djordjevic, S. P., and Walker, M. J. (2010). Multiple antibiotic resistance gene recruitment onto the enterohemorrhagic *Escherichia coli* virulence plasmid. *FASEB J.* 24, 1160–1166. doi: 10.1096/fj.09-144972

Venturini, C., Hassan, K. A., Roy Chowdhury, P., Paulsen, I. T., Walker, M. J., and Djordjevic, S. P. (2013). Sequences of two related multiple antibiotic resistance virulence plasmids sharing a unique IS26-related molecular signature isolated from different *Escherichia coli* pathotypes from different hosts. *PLoS One* 8:e78862. doi: 10.1371/journal.pone.0078862

Walker, B. J., Abeel, T., Shea, T., Priest, M., Abouelliel, A., Sakthikumar, S., et al. (2014). Pilon: an integrated tool for comprehensive microbial variant detection and genome assembly improvement. *PLoS One* 9:e112963. doi: 10.1371/journal.pone.0112963

Yau, S., Liu, X., Djordjevic, S. P., and Hall, R. M. (2010). RSF1010-like plasmids in Australian *Salmonella enterica* serovar Typhimurium and origin of their sul2-strA-strB antibiotic resistance gene cluster. *Microb. Drug Resist.* 16, 249–252. doi: 10.1089/mdr.2010.0033

Zhang, R., Sun, B., Wang, Y., Lei, L., Schwarz, S., and Wu, C. (2015). Characterization of a cfr-carrying plasmid from porcine *Escherichia coli* that closely resembles plasmid pEA3 from the plant pathogen *Erwinia amylovora*. *Antimicrob. Agents Chemother.* 60, 658–661. doi: 10.1128/AAC.02114-15

Zong, Z., Ginn, A. N., Dobiasova, H., Iredell, J. R., and Partridge, S. R. (2015). Different IncI1 plasmids from *Escherichia coli* carry ISEcp1-blaCTX-M-15 associated with different Tn2-derived elements. *Plasmid* 80, 118–126. doi: 10.1016/j.plasmid.2015.04.007

Zurfluh, K., Poirel, L., Nordmann, P., Klumpp, J., and Stephan, R. (2015). First detection of *Klebsiella variicola* producing OXA-181 carbapenemase in fresh vegetable imported from Asia to Switzerland. *Antimicrob. Resist. Infect. Control* 4:38. doi: 10.1186/s13756-015-0080-5

Conflict of Interest Statement: The authors declare that the research was conducted in the absence of any commercial or financial relationships that could be construed as a potential conflict of interest.

frontiers in Microbiology

ORIGINAL RESEARCH
published: 14 January 2019
doi: 10.3389/fmicb.2018.03318

Sequencing and Genomic Diversity Analysis of IncHI5 Plasmids

Quanhui Liang[1,2†], Xiaoyuan Jiang[3†], Lingfei Hu[3], Zhe Yin[3], Bo Gao[3], Yuee Zhao[3], Wenhui Yang[3], Huiying Yang[3], Yigang Tong[3], Weixuan Li[2], Lingxiao Jiang[1] and Dongsheng Zhou[3*]*

[1] Department of Laboratory Medicine, Zhujiang Hospital, Southern Medical University, Guangzhou, China, [2] Department of Clinical Laboratory, The First People's Hospital of Foshan, Foshan, China, [3] State Key Laboratory of Pathogen and Biosecurity, Beijing Institute of Microbiology and Epidemiology, Beijing, China

IncHI plasmids could be divided into five different subgroups IncHI1–5. In this study, the complete nucleotide sequences of seven bla_{IMP}- or bla_{VIM}-carrying IncHI5 plasmids from *Klebsiella pneumoniae*, *K. quasipneumoniae,* and *K. variicola* were determined and compared in detail with all the other four available sequenced IncHI5 plasmids. These plasmids carried conserved IncHI5 backbones composed of *repHI5B* and a *repFIB*-like gene (replication), *parABC* (partition), and *tra1* (conjugal transfer). Integration of a number of accessory modules, through horizontal gene transfer, at various sites of IncHI5 backbones resulted in various deletions of surrounding backbone regions and thus considerable diversification of IncHI5 backbones. Among the accessory modules were three kinds of resistance accessory modules, namely Tn*10* and two antibiotic resistance islands designated ARI-A and ARI-B. These two islands, inserted at two different fixed sites (one island was at one site and the other was at a different site) of IncHI5 backbones, were derived from the prototype Tn*3*-family transposons Tn*1696* and Tn*6535*, respectively, and could be further discriminated as various intact transposons and transposon-like structures. The ARI-A or ARI-B islands from different IncHI5 plasmids carried distinct profiles of antimicrobial resistance markers and associated mobile elements, and complex events of transposition and homologous recombination accounted for assembly of these islands. The carbapenemase genes bla_{IMP-4}, bla_{IMP-38} and bla_{VIM-1} were identified within various class 1 integrons from ARI-A or ARI-B of the seven plasmids sequenced in this study. Data presented here would provide a deeper insight into diversification and evolution history of IncHI5 plasmids.

Keywords: IncHI5 plasmids, IMP, VIM, mobile elements, multidrug resistance

OPEN ACCESS

Edited by:
Katy Jeannot, UMR 6249 Chrono Environnement, France

Reviewed by:
Antonio Juárez, University of Barcelona, Spain
Christopher Morton Thomas, University of Birmingham, United Kingdom

***Correspondence:**
Lingxiao Jiang
jiang-lingxiao@163.com
Dongsheng Zhou
dongshengzhou1977@gmail.com

† These authors have contributed equally to this work

Specialty section:
This article was submitted to Antimicrobials, Resistance and Chemotherapy, a section of the journal Frontiers in Microbiology

Received: *20 August 2018*
Accepted: *20 December 2018*
Published: *14 January 2019*

Citation:
Liang Q, Jiang X, Hu L, Yin Z, Gao B, Zhao Y, Yang W, Yang H, Tong Y, Li W, Jiang L and Zhou D (2019) Sequencing and Genomic Diversity Analysis of IncHI5 Plasmids. Front. Microbiol. 9:3318. doi: 10.3389/fmicb.2018.03318

INTRODUCTION

Plasmids of the H incompatibility (IncH) group show two types of surface exclusion and incompatibility interactions, namely IncHI and IncHII (Taylor and Grant, 1977). The IncHI group can be further divided into five subgroups IncHI1 to IncHI5 based on their nucleotide sequence homology (Liang et al., 2017), but the incompatibility interactions between these subgroups are still unclear because no one has actually done real incompatibility tests. IncHI plasmids, often

>200 kb in size, have a wide host range including Enterobacteriaceae species and several other Gram-negative organisms (Maher and Taylor, 1993). IncHI1–5 have different replication gene profiles, namely *repHI1A*+*repHI1B*+*repFIA*-like, *repHI2A*+*repHI2C*, *repHI3B*+*repFIB*-like, *repHI4A*+*repHI4B*, and *repHI5B*+*repFIB*-like, respectively (Liang et al., 2017). IncHI plasmids generally possess two conjugal transfer regions *tra1* and *tra2*, and the ability of conjugative transfer is thermosensitive and the transfer efficiency is optimal between 22 and 30°C, but inhibited at 37°C (Sherburne et al., 2000). IncHI plasmids are important vectors of genes encoding for resistance not only to heavy metals (such as mercuric ions, copper, silver ions, tellurite, arsenate, and arsenite) but to antibiotics (such as β-lactams including carbapenems, quinolones, aminoglycosides, tetracyclines, amphenicols, and fosfomycin) (Cain and Hall, 2012).

Currently only four fully sequenced IncHI5 plasmids are available (last accessed June 28th, 2017), including pKOX_R1 (Accession No. CP003684) (Huang et al., 2013), pKpNDM1 (Accession No. JX515588) (Li et al., 2014), pKP04VIM (Accession No. KU318421), and pYNKP001-dfrA (Accession No. KY270853) (Liang et al., 2017). This study presents the complete nucleotide sequences of six bla_{IMP}-carrying IncHI5 plasmids and a bla_{VIM}-carrying one, and further comprehensive genomic comparison of all the 11 available sequenced IncHI5 plasmids enable to gain a deeper insight into genomic variation and evolution of IncHI5 plasmids.

MATERIALS AND METHODS

Bacterial Strains

Klebsiella quasipneumoniae A708 and *K. pneumoniae* A324 were isolated in 2014 from the blood specimens of two different patients from a teaching hospital in Guangzhou City, China. *K. pneumoniae* 13190 and 12208, and *K. variicola* 13450 were recovered in 2013 from the sputum, sputum and blood specimens of three different patients from a teaching hospital in Hangzhou City, China, respectively. *K. pneumoniae* 11219 was isolated in 2013 from a sputum specimen of a patient from a teaching hospital in Hefei City, China. *K. pneumoniae* 19051 was recovered in 2011 from a urine specimen of a patient from a public hospital in Ningbo, China.

Phenotypic Assays

Activity of Ambler class A/B/D carbapenemases in bacterial cell extracts was determined by a modified CarbaNP test (Wei et al., 2016). Bacterial antimicrobial susceptibility was tested by BioMérieux VITEK 2 and interpreted as per the 2017 CLSI guidelines (CLSI, 2017).

Conjugal Transfer

Conjugal transfer experiments were carried out with the rifampin-resistant *Escherichia coli* EC600 used as a recipient and the bla_{IMP}-positive A324 isolate as a donor. Three milliliters of overnight cultures of each of donor and recipient bacteria were mixed together, harvested and resuspended in 80 μL of Brain Heart Infusion (BHI) broth (BD Biosciences). The mixture was spotted on a 1 cm^2 hydrophilic nylon membrane filter with a 0.45 μm pore size (Millipore) that was placed on BHI agar (BD Biosciences) plate and then incubated for mating at 22°C for 24 h. Bacteria were washed from filter membrane and spotted on Muller-Hinton (MH) agar (BD Biosciences) plates containing 2500 μg/mL rifampin together with 4 μg/mL meropenem for selecting an *E. coli* transconjugant carrying bla_{IMP} (pA324-IMP).

Electroporation

To prepare competent cells for electroporation, 200 mL of overnight culture of *E. coli* TOP10 in Super Optimal Broth (SOB) at an optical density (OD_{600}) of 0.4 to 0.6 was washed three times with electroporation buffer (0.5 M mannitol and 10% glycerol) and concentrated into a final volume of 2 mL. One microgram of DNA were mixed with 100 μL of competent cells for electroporation at 25 μF, 200 Ω and 2.5 Kv. The resulting cells were suspended in 500 μL of SOB and an appropriate aliquot was spotted on SOB agar plates containing 4 μg/mL meropenem for selecting of an electroporant carrying bla_{IMP} (pA324-IMP).

Sequencing and Sequence Assembly

Genomic DNA was isolated from each of the A708, 13190, 11219, 12208, 13450, and 19051 isolates using a Qiagen blood & cell culture DNA maxi kit. Genome sequencing was performed with a sheared DNA library with average size of 15 kb (ranged from 10 to 20 kb) on a PacBio RSII sequencer (Pacific Biosciences, Menlo Park, CA, United States), as well as a paired-end library with an average insert size of 400 bp (ranged from 150 to 600 bp) on a HiSeq sequencer (Illumina, San Diego, CA, United States). The paired-end short Illumina reads were used to correct the long PacBio reads utilizing *proovread* (Hackl et al., 2014), and then the corrected PacBio reads were assembled *de novo* utilizing *SMARTdenovo*[1].

Plasmid DNA was isolated from the A324-IMP-TOP10 electroporant using a Large Construct Kit (Qiagen, Germany) and then sequenced from a mate-pair library with average insert size of 5 kb (ranged from 2 to 10 kb) using a MiSeq sequencer (Illumina, San Diego, CA, United States). Quality control, removing adapters and low quality reads, were performed using *Trimmomatic* 0.36 (Bolger et al., 2014). The filtered clean reads were then assembled using *Newbler* 2.6 (Nederbragt, 2014), followed by extraction of the consensus sequence with *CLC Genomics Workbench* 3.0 (Qiagen Bioinformatics). *Gapfiller* V1.11 (Boetzer and Pirovano, 2012) was used for gap closure.

Sequence Annotation and Comparison

Open reading frames and pseudogenes were predicted using *RAST* 2.0 (Brettin et al., 2015) combined with *BLASTP/BLASTN* searches (Boratyn et al., 2013) against the *UniProtKB/Swiss-Prot* database (Boutet et al., 2016) and the *RefSeq* database (O'Leary et al., 2016). Annotation of resistance genes, mobile elements, and other features was carried out using the online databases including *CARD* (Jia et al., 2017), *ResFinder* (Zankari et al., 2012),

[1]https://github.com/ruanjue/smartdenovo

TABLE 1 | Major features of IncHI5 plasmids analyzed.

Plasmid	Accession number	Host bacterium	Total length (bp)	Total number of ORFs	Mean G+C content (%)	Length of Backbone (bp)	Mean G+C content Of backbone (%)	Accessory modules			
								Resistance			Non-resistance
								ARI-A (Tn*1696*-derived)	ARI-B (Tn*6535*-derived)	Other	
pA324-IMP	MF344566	*K. pneumoniae* A324	271,153	296	46.6	215,443	44.7	Tn*6382*	Tn*6381*	–	IS*903*, IS*Kpn8*, an IS*4*-related region, Tn*1722*, IS*5*, and IS*Kpn37*
pKpNDM1	JX515588	*Raoultella planticola* KpNDM1	277,682	314	46.9	201,856	44.7	Tn*6401*	Tn*6381*	Tn*10*	IS*Ec33*, an IS*4*-related region, and IS*5*
pKP04VIM	KU318421	*K. pneumoniae* KP04	274,659	305	46.8	212,954	44.6	Tn*6400*	+	–	IS*Ec33*, IS*Kpn28*, IS*Kox3*, IS*Kpn37*, an IS*4*-related region, and Tn*6344*
p13190-VIM	MF344563	*K. pneumoniae* 13190	288,771	322	47.3	214,781	44.7	Tn*6384*	+	–	IS*Ec33*, IS*Kpn28*, IS*Kpn37*, an IS*4*-related region, and Tn*6344*
p12208-IMP	MF344562	*K. pneumoniae* 12208	323,333	351	46.8	214,525	44.7	Tn*6383*[#]	+[#]	–	IS*903*, IS*Ec33*, IS*Ec33*:IS*10L*, IS*10L*, IS*Kpn28*, IS*Kpn21*:IS*Kpn38*, Tn*6344*, and IS*Kpn37*
p11219-IMP	MF344561	*K. pneumoniae* 11219	319,852	344	47	199,392	44.2	+[#]	+[#]	–	IS*903*, IS*Ec33*, IS*Kpn8*–IS*Kpn28*, and IS*Kpn21*
pKOX_R1	CP003684	*K. michiganensis* E718	353,865	384	47.5	214,073	44.7	+[#]	+[#]	–	IS*903*, IS*102*, IS*Ec33*, IS*Kox3*, Tn*6344*, IS*Kpn21*, and IS*Kpn28*
p13450-IMP	MF344564	*K. variicola* 13450	344,478	379	47.4	212,597	44.7	+[#]	+[#]	–	IS*903*, IS*Ec33*, IS*Kpn37*, Tn*6344*, IS*Kpn21*, and IS*Kpn28*
p19051-IMP	MF344565	*K. pneumoniae* 19051	316,843	349	48.3	172,621	45.7	+[#]	+[#]	–	IS*903*, IS*Ec33*, IS*10L*, IS*Kpn37*, Tn*6344*, IS*Kpn21*, and IS*Kpn28*
pYNKP001-dfrA	KY270853	*R. ornithinolytica* YNKP001	234,154	274	46.2	190,173	44.6	Tn*6338*	–	–	IS*Kpn28*, IS*Kpn21*, and Tn*6344*
pA708-IMP	MF344567	*K. quasipneumoniae* A708	238,703	261	47.2	171,575	44.3	+	–	–	IS*903B*, IS*Kpn28*, IS*Kox1*, and Tn*6344*

Plasmids pKOX_R1 (Huang et al., 2013), pKpNDM1 (Li et al., 2014) and pKP04VIM were derived from GenBank, while pYNKP001-dfrA (Liang et al., 2017) and all the other seven plasmids (this study) were fully sequenced in our laboratory. A genomic comparison of all these 11 plasmids was interpreted in the main text. +: presence ARI-A or ARI-B, but identified as a transposon-like structure derived from Tn1696 or Tn6535, respectively; –: absence. [#]: a translocation event occurred between ARI-A and ARI-B in the relevant plasmid (see ***Supplementary Figure S4*** *for detail).*

ISfinder (Siguier et al., 2006), *INTEGRALL* (Moura et al., 2009), and *Tn Number Registry* (Roberts et al., 2008). Multiple and pairwise sequence comparisons were performed using *MUSCLE* 3.8.31 (Edgar, 2004) and *BLASTN*, respectively. Gene organization diagrams were drawn in *Inkscape* 0.48.1[2].

Phylogenetic Analysis

The backbone regions of indicative plasmids were aligned using *MUMmer* 3.0 (Kurtz et al., 2004). Inference of homologous recombination was performed using *ClonalFrameML* (Didelot and Wilson, 2015) to remove recombination-associated single-nucleotide polymorphisms (SNPs). A maximum-likelihood tree was constructed from recombination-free SNPs using *MEGA7* (Kumar et al., 2016) with a bootstrap iteration of 1000.

Nucleotide Sequence Accession Numbers

The complete nucleotide sequences of plasmids p11219-IMP, p12208-IMP, p13190-VIM, p13450-IMP, p19051-IMP, pA324-IMP, and pA708-IMP, and those of the A708, 12208, 13450, 11219, 13190, and 19051 chromosomes were submitted to GenBank under Accession Nos. MF344561 to MF344567, CP030171 to CP030174, CP026017, and CP022023, respectively.

RESULTS AND DISCUSSION

Overview of Sequenced IncHI5 Plasmids

The seven plasmids sequenced in the present work varied in size from about 238 kb to nearly 345 kb with variation in the number of predicted ORFs from 261 to 379 (**Table 1** and **Supplementary Figure S1**). All these plasmids belonged to the IncHI5 group, because each contained a conserved IncHI5 backbone especially including the IncHI5-type replication gene *repHI5B* and an additional *repFIB*-like gene (Liang et al., 2017). **Table 1** also lists the features of the previously four sequenced IncHI5 plasmids. Further comparative genomics of all these 11 plasmids revealed that the IncHI5 backbones were interrupted by various accessory modules (defined as acquired DNA regions associated and bordered with mobile elements) inserted at different sites. In addition, while pKOX_R1 (Huang et al., 2013), the first sequenced IncHI5 plasmid, was used previously as the IncHI5 reference (Liang et al., 2017), the newly sequenced pA324-IMP seemed a more appropriate reference in this analysis because it contained the most complete IncHI5 backbone (**Supplementary Figure S2**).

This large collection of IncHI5 plasmids allowed us to accurately distinguish backbone and accessory modules. This has allowed us to gain a deeper understanding of the evolution and diversification of IncHI5 plasmids.

General Comparison of Backbone Sequences

Pairwise sequence comparison using *BLASTN* showed that these 11 plasmids had >99% nucleotide identity across >73% of their backbone sequences (**Supplementary Table S1**). The major IncHI5 backbone genes or gene loci (including *repHI5B* together with its iterons and *repFIB*-like for replication, *parABC* for partition, and *tra1* for conjugal transfer) were conserved among all these 11 plasmids. Two conjugal transfer regions *tra1* and *tra2* were found in IncHI5 plasmids, but some of these plasmids lost *tra2*, which would impair their self-transferability (**Supplementary Table S3**). A total of 574 core SNPs (among them 115 were recombination-free) were identified from the backbone regions of these 11 plasmids. A maximum likelihood phylogenetic tree was constructed using these 115 recombination-free SNPs, and accordingly these 11 plasmids could be assigned into three clades I, II, and III (**Figure 1**).

Classification of Accessory Modules

These 11 plasmids harbored different profiles of accessory modules (**Table 1**) and different collections of resistance genes (**Supplementary Table S2**). The accessory modules were further divided into resistance (containing resistance genes) and non-resistance (containing no resistance genes) ones (**Table 1**). The resistance accessory modules included Tn*10* (an IS*10*-composite transposon carrying class B tetracycline-resistance genes) and two antibiotic resistance islands designated ARI-A and ARI-B. The presence and modular organization of ARI-A and ARI-B islands in the seven newly sequence plasmids and pYNKP001-dfrA (Liang et al., 2017) were validated by a set of PCR amplifications (see **Figures 3**, **4** for location of PCR primers and expected amplicons) that targeted various key jointing fragments of these islands and their surrounding backbone regions, using the genomic DNA of each corresponding wild-type isolate as template. The non-resistance accessory modules were composed of 12 different insertion sequences (ISs), four distinct IS-related regions, and two cryptic transposons Tn*6344* (**Supplementary Figure S3**) and Tn*1722*.

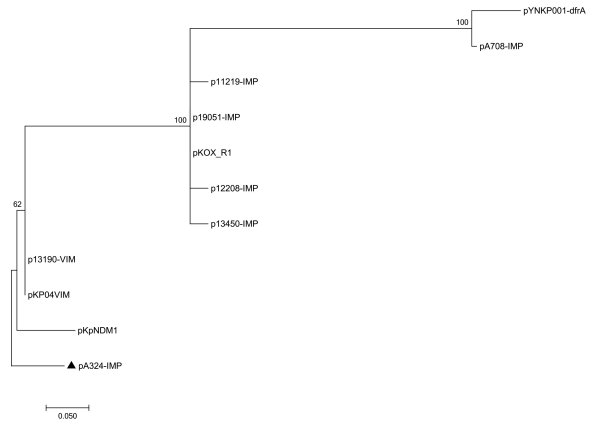

FIGURE 1 | Maximum-likelihood tree. The degree of support (percentage) for each cluster of associated taxa, as determined by bootstrap analysis, is shown next to each branch. The bar corresponds to the scale of sequence divergence. The triangle indicates IncHI5 reference plasmid pA324-IMP.

[2]https://inkscape.org/en/

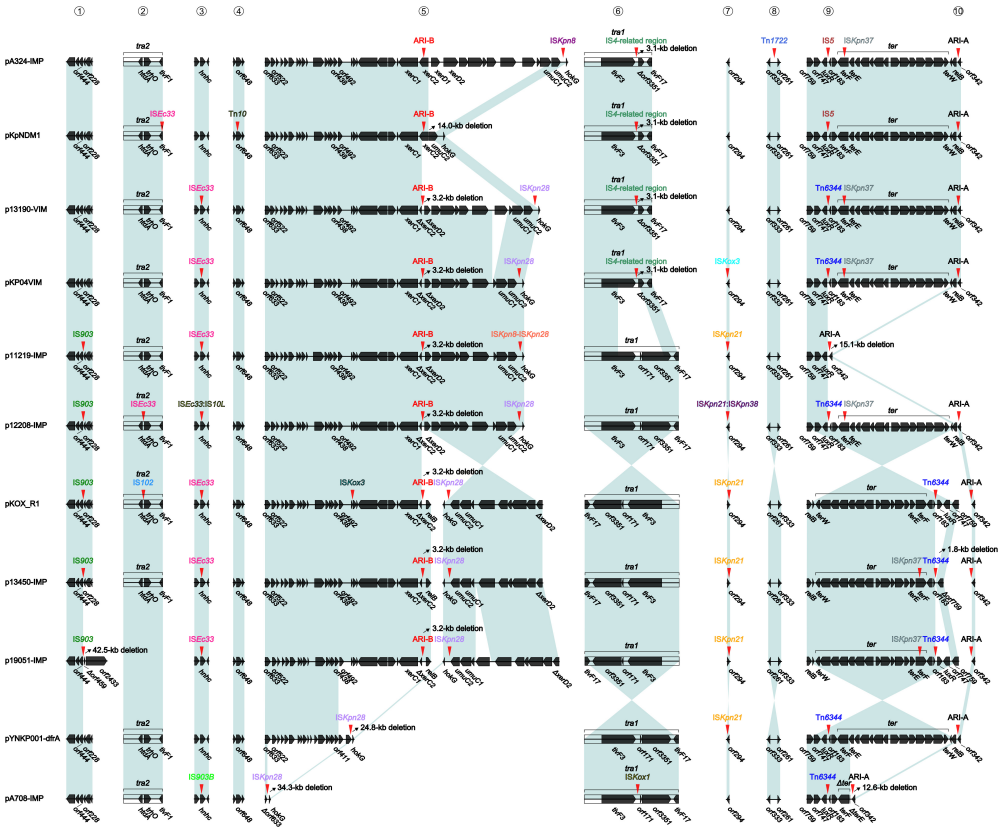

FIGURE 2 | Sites of insertion of accessory modules. Genes are denoted by arrows. Genes, mobile elements and other features are colored based on function classification. Shading denotes regions of homology (>95% nucleotide identity).

Massive Gene Acquisition and Loss in IncHI5 Plasmids

At least 10 major events of gene acquisition/loss accounted for modular diversity of these 11 plasmids across their genomes (**Figure 2**). First, IS*903* was inserted at a site upstream of *orf444* in five plasmids, additionally resulting in a 42.5-kb deletion (containing the whole *tra2* region) in p19051-IMP. Second, IS*Ec33*, IS*Ec33* and IS*102* were inserted at different sites within the *tra2* regions of pKpNDM1, p12208-IMP and pKOX_R1, respectively. Third, IS*903B* in pA708-IMP, IS*Ec33* in six plasmids, and IS*Ec33*:IS*10L* in p12208-IMP were inserted within *hnhc* (HNH endonuclease), splitting it into two separate parts Δ*hnhc*-5′ and Δ*hnhc*-3′. Fourth, in pKpNDM1, Tn*10* was inserted at a site within *orf648*, splitting it into two separate parts Δ*orf648*-5′ and Δ*orf648*-3′. Fifth, compared to the backbone region from *orf633* to *hokG* in pA324-IMP as a prototype structure, various insertions occurred in all the other plasmids: (i) insertion of IS*Kpn28* upstream of *hokG* resulted in deletion of a 34.3-kb region in pA708-IMP and that of a 24.8-kb region in pYNKP001-dfrA, respectively; however, upstream-of-*hokG* insertion of IS*Kpn8* in pA324-IMP, that of IS*Kpn28* in six plasmids, and that of IS*Kpn8*–IS*Kpn28* in p11219-IMP did not cause deletions; and (ii) insertion of ARI-B at a site within *xerC2* occurred in the following nine plasmids, which led to a 3.2-kb deletion in seven plasmids, a 14.0-kb deletion in pKpNDM1, and no deletion in pA324-IMP. Sixth, six plasmids had complete *tra1* regions; by contrast, four additional plasmids had undergone insertion of an IS*4*-related region at a site downstream of *tivF3* (resulting in a 3.1-kb deletion), and IS*kox1* was inserted at a site between *tivF3* and *orf171* in pA708-IMP (no further deletion occurred). All the above insertions and/or deletions within *tra1* and *tra2* might impair self-transferability of corresponding plasmids. Seventh, IS*Kpn21* in five plasmids, IS*Kox3* in pKP04VIM, and IS*Kpn21*:IS*Kpn38* in p12208-IMP were inserted at a site downstream of *orf294*. Eighth, Tn*1722* was inserted at a site between *orf333* and *orf261* in pA324-IMP. Ninth, IS*5* or Tn*6344* was inserted at a site between *luxR* and *orf183* in all the night plasmids except for p11219-IMP and p13450-IMP, and additionally the Tn*6344* insertion resulted in a 1.8-kb deletion in p13450-IMP. Tenth, the ARI-A islands were inserted at a site downstream of *orf342* in all the 11 plasmids, which resulted in the 12.6-kb deletion (covering *terE*-5′ and *terABCDZW*) in pA708-IMP and the 15.1-kb deletion (covering the complete *ter* gene cluster) in p11219-IMP; additionally, IS*Kpn37* was inserted at a site within *terF* in six plasmids. The above insertions would impair tellurium resistance gene expression.

In conclusion, massive gene acquisition and loss were found in IncHI5 plasmids: a wealth of accessory modules were integrated

FIGURE 3 | Organization of ARI-A islands and comparison to related regions. Genes are denoted by arrows. Genes, mobile elements and other features are colored based on their functional classification. Shading denotes regions of homology (nucleotide identity > 95%). Numbers in brackets indicate nucleotide positions within corresponding plasmids. The accession numbers of Tn*1696* (Partridge et al., 2001), Tn*125* (Poirel et al., 2012), Tn*6292* (Wei et al., 2016), Tn*1548* (Galimand et al., 2005), Tn*6347*, Tn*5563* (Yeo et al., 1998), Tn*5053* (Kholodii et al., 1993), IS*26*–bla_{SFO-1}–IS*26* unit (Sun et al., 2016), Tn*5393c* (L'Abée-Lund and Sørum, 2000), *aacC2–tmrB* region (Partridge et al., 2012), and Tn*1722* (Allmeier et al., 1992) for reference are U12338, JN872328, KU886034, AF550415, CP000447, U88088, L40585, KX710093, AF262622, JX101693, and X61367, respectively. Arrowheads indicated location of PCR primers and expected amplicons.

at various sites of IncHI5 backbones, which resulted in various deletions of surrounding backbone regions and thus considerable diversification of IncHI5 backbones.

Tn*1696*-Related ARI-A Islands

The ARI-A islands (**Figure 3**) were found in all the 11 plasmids analyzed and identified as Tn*1696* derivatives. Tn*1696*, a unit transposon belonging to the Tn*21* subgroup of Tn*3* family, was generated from insertion of a class 1 integron In4 into the resolution (*res*) site of a primary backbone structure: IRL (inverted repeat left)–*tnpA* (transposase)–*tnpR* (resolvase)–*res*–*mer* (mercury resistance locus)–IRR (inverted repeat right) (Partridge et al., 2001).

Being similar to Tn*1696*, the ARI-A islands from six plasmids had paired terminal 38-bp IRL/IRR and were further bracketed by 5-bp direct repeats (DRs; target site duplication signals for transposition), and thus they were identified as unit transposons designated Tn*6338*, Tn*6401*, Tn*6400*, Tn*6384*, Tn*6382,* and Tn*6383*, respectively. The remaining five ARI-A islands carried only IRLs (interrupted by IS*5075* that was a hunter of terminal IRL/IRR of Tn*21* subgroup transposons (Partridge and Hall, 2003)) but did not harbor IRRs (due to truncation at 3′-terminal regions of these islands), and thus they were identified as transposon-like structures rather than intact transposons.

In conclusion, the ARI-A islands was inserted at a site downstream of *orf342* in all 11 plasmids, and further discriminated as six intact transposons (among them Tn*6384*, Tn*6382,* and Tn*6383* were novel) and five transposon-like structures. These 11 islands were derived from Tn*1696* but differed from it mainly by insertion of distinct integrons or integron-related regions instead of In4 in Tn*1696*. These integrons could be divided into concise integrons each containing a single gene cassette (GC) array, and complex integrons each harboring one or more variable regions (VRs) in addition to the GC array. These GCs and VRs commonly carried antibiotic resistance genes.

Tn*6535*-Related ARI-B Islands

The ARI-B islands (**Figure 4**) as found in nine plasmids were identified as the derivatives of a prototype arsenic-resistance (*ars*) unit transposon Tn*6535*. As observed in the chromosome (Accession No. CP009706) of *Hafnia alvei* FB1 (Tan et al., 2014), Tn*6535* was assembled from integration of an *ars* region with a Tn*3*-family core transposition module *tnpA*–*res*–*tnpR*.

The ARI-B island from pA324-IMP or pKpNDM1 was identified as an unit transposon designated Tn*6381*, with presence of paired terminal 38-bp IRL/IRR and 5-bp DRs. Tn*6381* differed from Tn*6535* by insertion of a Tn*3*-family unit transposon Tn*6399b* at a site within *arsB*. Tn*6399a* (it was previously designated Tn*6901* because it was 6901 bp in length) was found in plasmid Rts1 from *Proteus vulgaris* (Murata et al., 2002) and carried several alcohol-metabolism genes (Chen et al., 2013), while interruption of *tnpA* by IS*1618* insertion turned Tn*6399a* into Tn*6399b*. Compared to Tn*6535* and Tn*6381*, all the other ARI-B islands contained only IRLs but not IRRs and identified as transposon-like structures. Various types of insertion events occurred within these ARI-B islands, leading to truncation of prototype regions as found in Tn*6535* and Tn*6381* as well as integration of foreign resistance markers and associated mobile elements.

ARI-B_{pKOX_R1} contained at least 10 resistance loci, including IS*26*–*fosA3*–IS*26* unit, IS*26*–bla_{SHV-12}–IS*26* unit, a 3-kb Tn*6029* remnant, ΔTn*6292*, In797, ΔTn*1548*, ΔTn*6535*, a truncated IS*26*–*catA2*–IS*26* unit, a residual *aacC2*–*tmrB* region, and a *mer* region (Liang et al., 2017). The resistance markers from ARI-$B_{p13450-IMP}$ and ARI-$B_{p19051-IMP}$ differed from pKOX_R1 by replacement of In797 with In823 and In792, respectively; moreover, Tn*6339* (containing bla_{TEM-1B} and $bla_{CTX-M-3}$) was

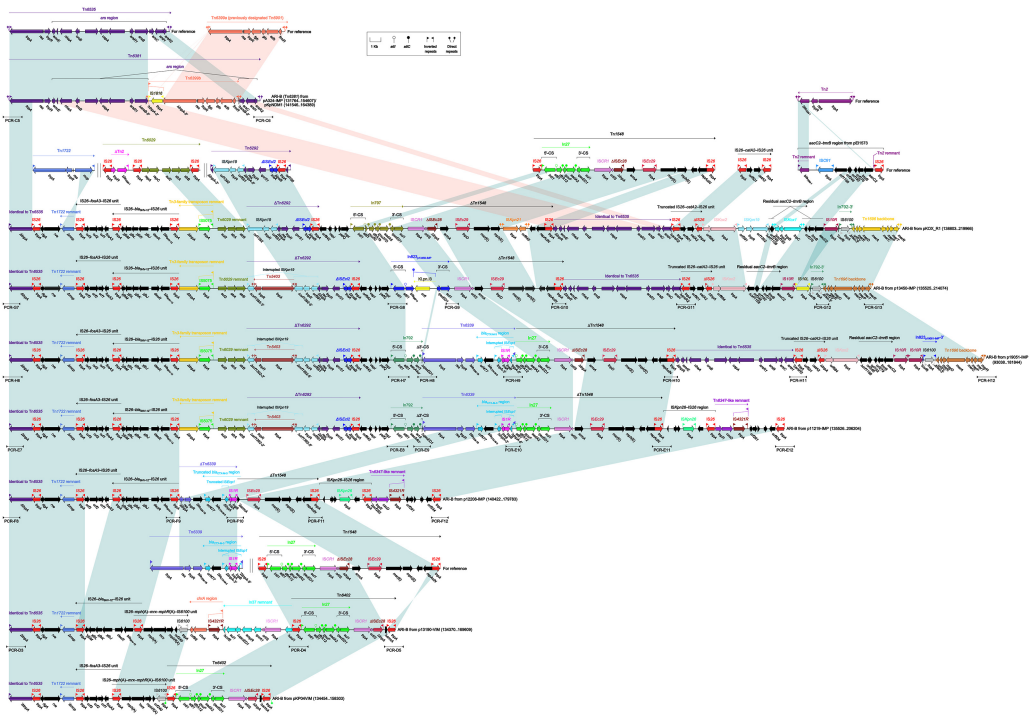

FIGURE 4 | Organization of ARI-B islands and comparison to related regions. Genes are denoted by arrows. Genes, mobile elements and other features are colored based on their functional classification. Shading denotes regions of homology (nucleotide identity > 95%). Numbers in brackets indicate nucleotide positions within corresponding plasmids. The accession numbers of Tn*6535* (Tan et al., 2014), Tn*6399a* (Murata et al., 2002), Tn*1722* (Allmeier et al., 1992), Tn*6029* (Cain et al., 2010), Tn*6292* (Wei et al., 2016), Tn*1548* (Galimand et al., 2005), IS*26*–*catA2*–IS*26* unit (Xiang et al., 2015), Tn*2* (Bailey et al., 2011), *aacC2*–*tmrB* region (Partridge et al., 2012), and Tn*6339* (Liang et al., 2017) for reference are CP009706, AP004237, X61367, HQ840942, KU886034, AF550415, KY270851, HM749967, JX101693, and CP003684, respectively. Arrowheads indicated location of PCR primers and expected amplicons.

inserted at a site between In*792* and ΔTn*1548* in p19051-IMP. The resistance markers from ARI-$B_{p11219\text{-}IMP}$ were composed of IS*26*–*fosA3*–IS*26*, IS*26*–$bla_{SHV\text{-}12}$–IS*26*, a Tn*6029* remnant, ΔTn*6292*, In*792*, Tn*6339*, and ΔTn*1548*. Similarly, IS*26*–*fosA3*–IS*26*, IS*26*–$bla_{SHV\text{-}12}$–IS*26*, ΔTn*6339*, and ΔTn*1548* were present in ARI-$B_{p12208\text{-}IMP}$. The resistance markers from ARI-$B_{p13190\text{-}VIM}$ consisted of IS*26*–$bla_{SHV\text{-}12}$–IS*26*, IS*26*–*mph(A)*–*mrx*–*mphR(A)*–IS*6100*, *chrA* region, a In*37* remnant

TABLE 2 | Antimicrobial drug susceptibility profiles.

Antibiotics	MIC (mg/L)/antimicrobial susceptibility				
	A324	A324-IMP-EC600	A324-IMP-TOP10	EC600	TOP10
Ampicillin	≥32/R	≥32/R	≥32/R	16/I	4/S
Ampicillin/sulbactam	≥32/R	≥32/R	≥32/R	8/S	4/S
Cefazolin	≥64/R	≥64/R	≥64/R	≤4/S	≤4/S
Ceftazidime	≥64/R	≥64/R	≥64/R	≤1/S	≤1/S
Ceftriaxone	≥64/R	≥64/R	≥64/R	≤1/S	≤1/S
Cefepime	≥64/R	≥64/R	≥64/R	≤1/S	≤1/S
Aztreonam	≥64/R	≥64/R	≥64/R	≤1/S	≤1/S
Imipenem	4/R	4/R	4/R	≤1/S	≤1/S
Meropenem	≥16/R	≥16/R	≥16/R	≤0.25/S	≤0.25/S
Amikacin	≤2/S	≤2/S	≤2/S	≤2/S	≤2/S
Tobramycin	8/I	4/S	8/I	≤1/S	≤1/S
Ciprofloxacin	≤0.25/S	≤0.25/S	≤0.25/S	≤0.25/S	≤0.25/S
Levofloxacin	≤0.25/S	0.5/S	≤0.25/S	0.5/S	≤0.25/S
Trimethoprim/sulfamethoxazole	≤20/S	≤20/S	≤20/S	≤20/S	≤20/S

S, sensitive; R, resistant; I, intermediately resistant.

and Tn*6402,* while those from ARI-$B_{pKP04VIM}$ were composed of IS*26*–*fosA3*–IS*26*, IS*26*–*mph(A)*–*mrx*–*mphR(A)*–IS*6100* and Tn*6402*. Tn*6402* was an IS*26*-composite transposon (delimited by 4-bp DRs at both ends) derived from Tn*1548*. Tn*6402* differed from Tn*1548* by deletion of *arsB*-3′–IS*Ec29*–*msr(E)*–*mph(E)*–*repAciN* and inversion of the 3′-end copy of IS*26*.

In conclusion, the ARI-B islands, integrated at a site within *xerC2* in nine plasmids, could be further identified as Tn*6381* and eight transposon-like structures. These nine ARI-B islands were derived from Tn*6535* but differed from it by insertion of various collections of mobile elements and associated resistance genes into the original Tn*6381* backbone.

All the transposon-like structures of ARI-A or ARI-B could not be annotated as intact transposons because they lacked paired terminal inverted repeats, and complex transposition and homologous recombination events accounted for assembly and diversification of these transposons and transposon-like structures. The ARI-A or ARI-B islands from different IncHI5 plasmids carried distinct profiles of resistance markers and associated mobile elements, promoting accumulation and spread of antimicrobial resistance among bacterial species.

Translocation of Large Regions Across ARI-A and ARI-B

Compared to the intact transposons Tn*6338*, Tn*6401*, Tn*6400*, Tn*6384*, Tn*6382,* and Tn*6383* (corresponding to ARI-A), and Tn*6381* (corresponding to ARI-B), two kinds of translocation events across ARI-A and ARI-B occurred in each of the following five plasmids (**Supplementary Figure S4**): (i) exchange of the ΔTn*1548*–to–IS*26* region (finally observed in ARI-B) and the ΔTn*1548*–to–Tn*6535* region (finally observed in ARI-A) in each of p12208-IMP and p11219-IMP; and (ii) movement of the Δ*orf6*–*mer* region from ARI-A to ARI-B in each of pKOX_R1, p13450-IMP, and p19051-IMP. These two kinds of translocation might be mediated by the common regions ΔTn*1548* and IS*6100*, respectively.

Carbapenemase Genes and Related Integrons

As for the seven plasmids sequenced in this study, the carbapenemase genes bla_{IMP-4}, bla_{IMP-38}, and bla_{VIM-1} were identified within $In823_{p11219-IMP/p12208-IMP/p19051-IMP}$, or $In1377_{pA708-IMP}$, $In1376_{pA324-IMP}$, and $In916_{p13190-VIM}$ respectively, from the ARI-A islands, while a bla_{IMP-4} gene was found within $In823_{p13450-IMP}$ from the ARI-B island. Of all the integrons identified in these seven plasmids, In1376 and In1377 were novel.

Transferability and Antimicrobial Susceptibility

As a representative IncHI5 plasmid, pA324-IMP could be transferred from the A324 isolate into *E. coli* EC600 and TOP10 through conjugation and electroporation, respectively, generating the A324-IMP-EC600 transconjugant and the A324-IMP-TOP10 electroporant, respectively. This was consistent with the presence of two complete sets of *tra1* and *tra2* genes in pA324-IMP, making it self-transferable. All the above three strains had class B carbapenemase activity (data not shown), and were resistant to all the cephalosporins and carbapenems tested (**Table 2**), which were resulted from production of IMP or VIM enzymes in these strains.

AUTHOR CONTRIBUTIONS

DZ and LJ conceived the study and designed experimental procedures. QL, XJ, LH, ZY, and WY performed the experiments. QL, XJ, BG, YZ, and HY analyzed the data. QL, XJ, YT, and WL contributed reagents and materials. DZ, QL, XJ, and LJ wrote the manuscript.

FUNDING

This work was supported by the National Key R&D Program (2017YFC1200800) of China.

SUPPLEMENTARY MATERIAL

The Supplementary Material for this article can be found online at: https://www.frontiersin.org/articles/10.3389/fmicb.2018.03318/full#supplementary-material

FIGURE S1 | Schematic maps of sequenced plasmids. Genes are denoted by arrows, and the backbone and accessory module regions are highlighted in black and color, respectively. The innermost circle presents GC-skew [(G−C)/(G+C)], with a window size of 500 bp and a step size of 20 bp. The next-to-innermost circle presents GC content. The accession numbers of pYNKP001-dfrA (Liang et al., 2017), pKP04VIM, pKpNDM1 (Li et al., 2014), and pKOX_R1 (Huang et al., 2013) for reference are KY270853, KU318421, JX515588, and CP003684, respectively.

FIGURE S2 | Linear comparison of plasmid genome sequences. Genes are denoted by arrows. Genes, mobile elements and other features are colored based on function classification. Shading denotes regions of homology (>95% nucleotide identity). The accession numbers of pYNKP001-dfrA (Liang et al., 2017), pKP04VIM, pKpNDM1 (Li et al., 2014), and pKOX_R1 (Huang et al., 2013) for reference are KY270853, KU318421, JX515588, and CP003684, respectively.

FIGURE S3 | Organization of Tn*6344* and comparison to related region. Genes are denoted by arrows. Genes, mobile elements and other features are colored based on their functional classification. Shading denotes regions of homology (nucleotide identity > 95%).

FIGURE S4 | Translocation between ARI-A and ARI-B islands. Genes are denoted by arrows. Genes, mobile elements and other features are colored based on their functional classification. Arrowheads indicated location of PCR primers and expected amplicons.

TABLE S1 | (a) Pairwise comparison of IncHI5 sequences using BLASTN. **(b)** Pairwise comparison of plamid backbone sequences using BLASTN.

TABLE S2 | Drug resistance genes in sequenced IncHI5 plasmids.

TABLE S3 | Conjugation transfer features of IncHI5 plasmids analyzed.

REFERENCES

Allmeier, H., Cresnar, B., Greck, M., and Schmitt, R. (1992). Complete nucleotide sequence of Tn 1721 : gene organization and a novel gene product with features of a chemotaxis protein. *Gene* 111, 11–20. doi: 10.1016/0378-1119(92)90597-I

Bailey, J. K., Pinyon, J. L., Anantham, S., and Hall, R. M. (2011). Distribution of the blaTEM gene and blaTEM-containing transposons in commensal *Escherichia coli*. *J. Antimicrob. Chemother.* 66, 745–751. doi: 10.1093/jac/dkq529

Boetzer, M., and Pirovano, W. (2012). Toward almost closed genomes with GapFiller. *Genome Biol.* 13:R56. doi: 10.1186/gb-2012-13-6-r56

Bolger, A. M., Lohse, M., and Usadel, B. (2014). Trimmomatic: a flexible trimmer for Illumina sequence data. *Bioinformatics* 30, 2114–2120. doi: 10.1093/bioinformatics/btu170

Boratyn, G. M., Camacho, C., Cooper, P. S., Coulouris, G., Fong, A., Ma, N., et al. (2013). BLAST: a more efficient report with usability improvements. *Nucleic Acids Res.* 41, W29–W33. doi: 10.1093/nar/gkt282

Boutet, E., Lieberherr, D., Tognolli, M., Schneider, M., Bansal, P., Bridge, A. J., et al. (2016). UniProtKB/Swiss-Prot, the manually annotated section of the UniProt KnowledgeBase: how to use the entry view. *Methods Mol. Biol.* 1374, 23–54. doi: 10.1007/978-1-4939-3167-5_2

Brettin, T., Davis, J. J., Disz, T., Edwards, R. A., Gerdes, S., Olsen, G. J., et al. (2015). RASTtk: a modular and extensible implementation of the RAST algorithm for building custom annotation pipelines and annotating batches of genomes. *Sci. Rep.* 5:8365. doi: 10.1038/srep08365

Cain, A. K., and Hall, R. M. (2012). Evolution of IncHI2 plasmids via acquisition of transposons carrying antibiotic resistance determinants. *J. Antimicrob. Chemother.* 67, 1121–1127. doi: 10.1093/jac/dks004

Cain, A. K., Liu, X., Djordjevic, S. P., and Hall, R. M. (2010). Transposons related to Tn1696 in IncHI2 plasmids in multiply antibiotic resistant *Salmonella enterica* serovar Typhimurium from Australian animals. *Microb. Drug Resist.* 16, 197–202. doi: 10.1089/mdr.2010.0042

Chen, L., Chavda, K. D., Fraimow, H. S., Mediavilla, J. R., Melano, R. G., Jacobs, M. R., et al. (2013). Complete nucleotide sequences of blaKPC-4- and blaKPC-5-harboring IncN and IncX plasmids from *Klebsiella pneumoniae* strains isolated in New Jersey. *Antimicrob. Agents Chemother.* 57, 269–276. doi: 10.1128/AAC.01648-12

CLSI (2017). *Performance Standards for Antimicrobial Susceptibility Testing: Twenty-Seventh Informational Supplement M100-S27*. Wayne, PA: CLSI.

Didelot, X., and Wilson, D. J. (2015). ClonalFrameML: efficient inference of recombination in whole bacterial genomes. *PLoS Comput. Biol.* 11:e1004041. doi: 10.1371/journal.pcbi.1004041

Edgar, R. C. (2004). MUSCLE: multiple sequence alignment with high accuracy and high throughput. *Nucleic Acids Res.* 32, 1792–1797. doi: 10.1093/nar/gkh340

Galimand, M., Sabtcheva, S., Courvalin, P., and Lambert, T. (2005). Worldwide disseminated armA aminoglycoside resistance methylase gene is borne by composite transposon Tn1548. *Antimicrob. Agents Chemother.* 49, 2949–2953. doi: 10.1128/AAC.49.7.2949-2953.2005

Hackl, T., Hedrich, R., Schultz, J., and Forster, F. (2014). proovread: large-scale high-accuracy PacBio correction through iterative short read consensus. *Bioinformatics* 30, 3004–3011. doi: 10.1093/bioinformatics/btu392

Huang, T. W., Wang, J. T., Lauderdale, T. L., Liao, T. L., Lai, J. F., Tan, M. C., et al. (2013). Complete sequences of two plasmids in a blaNDM-1-positive *Klebsiella oxytoca* isolate from Taiwan. *Antimicrob. Agents Chemother.* 57, 4072–4076. doi: 10.1128/AAC.02266-12

Jia, B., Raphenya, A. R., Alcock, B., Waglechner, N., Guo, P., Tsang, K. K., et al. (2017). CARD 2017: expansion and model-centric curation of the comprehensive antibiotic resistance database. *Nucleic Acids Res.* 45, D566–D573. doi: 10.1093/nar/gkw1004

Kholodii, G. Y., Yurieva, O. V., Lomovskaya, O. L., Gorlenko, Z., Mindlin, S. Z., and Nikiforov, V. G. (1993). Tn5053, a mercury resistance transposon with integron's ends. *J. Mol. Biol.* 230, 1103–1107. doi: 10.1006/jmbi.1993.1228

Kumar, S., Stecher, G., and Tamura, K. (2016). MEGA7: molecular evolutionary genetics analysis version 7.0 for bigger datasets. *Mol. Biol. Evol.* 33, 1870–1874. doi: 10.1093/molbev/msw054

Kurtz, S., Phillippy, A., Delcher, A. L., Smoot, M., Shumway, M., Antonescu, C., et al. (2004). Versatile and open software for comparing large genomes. *Genome Biol.* 5:R12. doi: 10.1186/gb-2004-5-2-r12

L'Abée-Lund, T. M., and Sørum, H. (2000). Functional Tn5393-like transposon in the R plasmid pRAS2 from the fish pathogen *Aeromonas salmonicida* subspecies salmonicida isolated in Norway. *Appl. Environ. Microbiol.* 66, 5533–5535. doi: 10.1128/AEM.66.12.5533-5535.2000

Li, J., Lan, R., Xiong, Y., Ye, C., Yuan, M., Liu, X., et al. (2014). Sequential isolation in a patient of *Raoultella planticola* and *Escherichia coli* bearing a novel ISCR1 element carrying blaNDM-1. *PLoS One* 9:e89893. doi: 10.1371/journal.pone.0089893

Liang, Q., Yin, Z., Zhao, Y., Liang, L., Feng, J., Zhan, Z., et al. (2017). Sequencing and comparative genomics analysis of the IncHI2 plasmids pT5282-mphA and p112298-catA and the IncHI5 plasmid pYNKP001-dfrA. *Int. J. Antimicrob. Agents* 49, 709–718. doi: 10.1016/j.ijantimicag.2017.01.021

Maher, D., and Taylor, D. E. (1993). Host range and transfer efficiency of incompatibility group HI plasmids. *Can. J. Microbiol.* 39, 581–587. doi: 10.1139/m93-084

Moura, A., Soares, M., Pereira, C., Leitao, N., Henriques, I., and Correia, A. (2009). INTEGRALL: a database and search engine for integrons, integrases and gene cassettes. *Bioinformatics* 25, 1096–1098. doi: 10.1093/bioinformatics/btp105

Murata, T., Ohnishi, M., Ara, T., Kaneko, J., Han, C. G., Li, Y. F., et al. (2002). Complete nucleotide sequence of plasmid Rts1: implications for evolution of large plasmid genomes. *J. Bacteriol.* 184, 3194–3202. doi: 10.1128/JB.184.12.3194-3202.2002

Nederbragt, A. J. (2014). On the middle ground between open source and commercial software - the case of the Newbler program. *Genome Biol.* 15:113. doi: 10.1186/gb4173

O'Leary, N. A., Wright, M. W., Brister, J. R., Ciufo, S., Haddad, D., McVeigh, R., et al. (2016). Reference sequence (RefSeq) database at NCBI: current status, taxonomic expansion, and functional annotation. *Nucleic Acids Res.* 44, D733–D745. doi: 10.1093/nar/gkv1189

Partridge, S. R., Brown, H., Stokes, H., and Hall, R. (2001). Transposons Tn1696 and Tn21 and their integrons In4 and In2 have independent origins. *Antimicrob. Agents Chemother.* 45, 1263–1270. doi: 10.1128/AAC.45.4.1263-1270.2001

Partridge, S. R., Ginn, A. N., Paulsen, I. T., and Iredell, J. R. (2012). pEl1573 Carrying blaIMP-4, from Sydney, Australia, is closely related to other IncL/M plasmids. *Antimicrob. Agents Chemother.* 56, 6029–6032. doi: 10.1128/AAC.01189-12

Partridge, S. R., and Hall, R. M. (2003). The IS1111 family members IS4321 and IS5075 have subterminal inverted repeats and target the terminal inverted repeats of Tn21 family transposons. *J. Bacteriol.* 185, 6371–6384. doi: 10.1128/JB.185.21.6371-6384.2003

Poirel, L., Bonnin, R. A., Boulanger, A., Schrenzel, J., Kaase, M., and Nordmann, P. (2012). Tn125-related acquisition of blaNDM-like genes in *Acinetobacter baumannii*. *Antimicrob. Agents Chemother.* 56, 1087–1089. doi: 10.1128/AAC.05620-11

Roberts, A. P., Chandler, M., Courvalin, P., Guedon, G., Mullany, P., Pembroke, T., et al. (2008). Revised nomenclature for transposable genetic elements. *Plasmid* 60, 167–173. doi: 10.1016/j.plasmid.2008.08.001

Sherburne, C. K., Lawley, T. D., Gilmour, M. W., Blattner, F. R., Burland, V., Grotbeck, E., et al. (2000). The complete DNA sequence and analysis of R27, a large IncHI plasmid from *Salmonella typhi* that is temperature sensitive for transfer. *Nucleic Acids Res.* 28, 2177–2186. doi: 10.1093/nar/28.10.2177

Siguier, P., Perochon, J., Lestrade, L., Mahillon, J., and Chandler, M. (2006). ISfinder: the reference centre for bacterial insertion sequences. *Nucleic Acids Res.* 34, D32–D36. doi: 10.1093/nar/gkj014

Sun, F., Zhou, D., Sun, Q., Luo, W., Tong, Y., Zhang, D., et al. (2016). Genetic characterization of two fully sequenced multi-drug resistant plasmids pP10164-2 and pP10164-3 from *Leclercia adecarboxylata*. *Sci. Rep.* 6:33982. doi: 10.1038/srep33982

Tan, J. Y., Yin, W. F., and Chan, K. G. (2014). Gene clusters of *Hafnia alvei* strain FB1 important in survival and pathogenesis: a draft genome perspective. *Gut Pathog.* 6:29. doi: 10.1186/1757-4749-6-29

Taylor, D. E., and Grant, R. B. (1977). Incompatibility and surface exclusion properties of H1 and H2 plasmids. *J. Bacteriol.* 131, 174–178.

Wei, F., Zhou, D., Qian, W., Luo, W., Zhang, D., Qiang, S., et al. (2016). Dissemination of IMP-4-encoding pIMP-HZ1-related plasmids among *Klebsiella pneumoniae* and Pseudomonas aeruginosa in a Chinese teaching hospital. *Sci. Rep.* 6:33419. doi: 10.1038/srep33419

Xiang, D. R., Li, J. J., Sheng, Z. K., Yu, H. Y., Deng, M., Bi, S., et al. (2015). Complete sequence of a novel IncR-F33:A-:B- plasmid pKP1034 harboring fosA3, blaKPC-2, blaCTX-M-65, blaSHV-12, and rmtB from an epidemic *Klebsiella pneumoniae* sequence Type 11 strain in China. *Antimicrob. Agents Chemother.* 60, 1343–1348. doi: 10.1128/AAC.01488-15

Yeo, C. C., Tham, J. M., Kwong, S. M., Yiin, S., and Poh, C. L. (1998). Tn5563, a transposon encoding putative mercuric ion transport proteins located on plasmid pRA2 of *Pseudomonas alcaligenes*. *FEMS Microbiol. Lett.* 165, 253–260. doi: 10.1111/j.1574-6968.1998.tb13154.x

Zankari, E., Hasman, H., Cosentino, S., Vestergaard, M., Rasmussen, S., Lund, O., et al. (2012). Identification of acquired antimicrobial resistance genes. *J. Antimicrob. Chemother.* 67, 2640–2644. doi: 10.1093/jac/dks261

Conflict of Interest Statement: The authors declare that the research was conducted in the absence of any commercial or financial relationships that could be construed as a potential conflict of interest.

frontiers in Microbiology

ORIGINAL RESEARCH
published: 15 January 2019
doi: 10.3389/fmicb.2018.03168

IS26-Flanked Composite Transposon Tn6539 Carrying the *tet*(M) Gene in IncHI2-Type Conjugative Plasmids From *Escherichia coli* Isolated From Ducks in China

Ya-wei Sun[1,2†], *Ying-ying Liu*[1†], *Hua Wu*[1†], *Ling-fei Wang*[1], *Jian-hua Liu*[1], *Li Yuan*[1], *Yu-shan Pan*[1], *Dan-dan He*[1] and *Gong-zheng Hu*[1*]

[1] Department of Pharmacology and Toxicology, College of Animal Husbandry and Veterinary Science, Henan Agricultural University, Zhengzhou, China, [2] Department of Animal Science, Henan Institute of Science and Technology, Xinxiang, China

OPEN ACCESS

Edited by:
Charles W. Knapp,
University of Strathclyde,
United Kingdom

Reviewed by:
Michael P. Ryan,
University of Limerick, Ireland
Rolf Dieter Joerger,
University of Delaware, United States

***Correspondence:**
Gong-zheng Hu
yaolilab@163.com

[†]These authors have contributed equally to this work

Specialty section:
This article was submitted to Antimicrobials, Resistance and Chemotherapy, a section of the journal Frontiers in Microbiology

Received: 25 June 2018
Accepted: 07 December 2018
Published: 15 January 2019

Citation:
Sun Y, Liu Y, Wu H, Wang L, Liu J, Yuan L, Pan Y, He D and Hu G (2019) IS26-Flanked Composite Transposon Tn6539 Carrying the tet(M) Gene in IncHI2-Type Conjugative Plasmids From Escherichia coli Isolated From Ducks in China. Front. Microbiol. 9:3168. doi: 10.3389/fmicb.2018.03168

Tet(M)-type proteins confer resistance to tetracycline and related antibiotics by interacting with the ribosome. Genes encoding Tet(M) have been found in a range of bacteria, including *Escherichia coli*. In the current study, conjugation experiments were performed between seven different tetracycline-resistant, azide-susceptible *E. coli* strains isolated from ducks and tetracycline-sensitive, azide-resistant *E.coli* J53. Transconjugants were obtained from two of the strains at a frequency of 1.2×10^{-8}. PCR, southern blotting and sequencing demonstrated that *tet*(M) in the transconjugants was located on a ∼50 kb IncHI2-type plasmid and was part of a composite transposon, designated Tn6539. This transposon is flanked by two IS26 elements in opposite orientation and contains the Tn3Δ*tnpA*+Δ*orf13-lp-tet*(M)+gamma delta+*tnpX*+Δ*tnpR* sequences. The Δ*orf13-lp-tet*(M) sequence was a highly conserved genetic fragment in *E. coli* harboring *tet*(M) and mainly located in the composite transposons flanked by IS6-family elements. In summary, Tn6539 is a new composite transposon capable of horizontal transfer of *tet*(M) among *E. coli* isolates.

Keywords: composite transposonTn6539, *tet*(M) gene, IS26 element, IncHI2-type plasmid, *Escherichia coli* isolates

INTRODUCTION

Resistance to tetracycline and related antibiotics can be conferred by efflux pumps, enzymatic inactivation and ribosomal protection proteins such as the ones encoded by *tet*(M). Tet(M) confers a wider spectrum of resistance to tetracyclines than efflux proteins except for Tet(B) and has the widest host range of any tetracycline resistance gene (Chopra and Roberts, 2001; Roberts and Schwarz, 2016). Currently, *tet*(M) has been found in more than 60 genera (http://faculty.washington.edu/marilynr/), likely because of the association of *tet*(M) with integrative and conjugative transposons, which facilitate horizontal transfer. For example, tet(M) was found to be associated with Tn916/Tn1545-like conjugative transposons in *Enterococcus* spp. (Cauwerts et al., 2007). Additionally, *tet*(M) was also found in Tn5801-like conjugative transposons in *Staphylococcus aureus* and Tn5397-like transposons in *Clostridium difficile* and *Enterococcus faecium* (Agersø et al., 2006; Vries et al., 2009). A *tet*(M) homolog was not found in clinical isolates of *Escherichia coli* until 2004 (Bryan et al., 2004), but has been described since then in isolates from

different sources (Jones et al., 2006; Tuckman et al., 2007; Jurado-Rabadán et al., 2014; Gilrane et al., 2017). The *E. coli* isolates carrying *tet*(M) not only conferred resistance to oxytetracycline, tetracycline and doxycycline, but also to minocycline (Jones et al., 2006; Hu et al., 2013). At the same time, Tet(M) protein has the potential to acquire mutation leading to increased MICs of tigecycline (Linkevicius et al., 2015). Therefore, the spread of *tet*(M) has made tetracycline treatment for *E. coli* infections a clinical dilemma. However, which mobile genetic elements facilitate horizontal transfer of *tet*(M) among *E. coli* isolates is still poorly understood. To the best of our knowledge, only one report has described a mobile element containing *tet*(M) flanked by IS26 and ISVs1 in human (Jones et al., 2006).

Our previous study revealed that *tet*(M) plays a role in doxycycline resistance of *E. coli* isolated from ducks in China (Hu et al., 2013). In the current study, seven of the previously isolated doxycycline-resistant strains were used in conjugation experiments and in two cases, transfer of *tet*(M) was apparently mediated by a plasmid that harbored a new composite transposon, designated Tn6539. The structure of this transposon was elucidated by PCR, cloning, and sequencing experiments.

MATERIALS AND METHODS

Bacterial Strains

Seven full-length *tet*(M)-positive *E. coli* isolates CY4, E5, W4, LF6, Y8, CY14, and 5Y (**Table 1**) containing part of *orf13*, the promoter regions of *tet*(M), the Tet(M) leader peptide gene, and intact *tet*(M) were previously isolated from ducks (Hu et al., 2013). *E. coli* J53 and *E. coli* DH5a were used as the recipient strain in mating experiment and the host strain in cloning experiments, respectively.

Conjugation Experiments

Seven *E. coli* isolates harboring full-length *tet*(M) were used for filter mating experiments with sodium azide-resistant *E. coli* J53 as a recipient as previously described (Devirgiliis et al., 2009). Briefly, overnight cultures of tetracycline-resistant, sodium azide-susceptible donor (*E. coli* isolate) and tetracycline-susceptible, sodium azide-resistant recipient (*E. coli* J53), grown in Luria-Bertani (LB) broth, were seeded at a 1:50 dilution in separate flasks of fresh LB broth. Following growth to log phase ($OD_{600}\approx0.6$) with shaking at the speed of 250 rpm at 37°C, 0.5 ml each of the donor and the recipient cultures were mixed and filtered through a 0.22-μm-pore-size membrane (Millipore Corp.) placed on prewarmed on MacConkey agar plates. After 24 h of incubation at 37°C, the cells were detached from filters in 5 ml of 1× phosphate-buffered saline (pH7.4), and serial dilutions were plated on MacConkey agar plates containing 16 mg/L doxycycline and 100 mg/L sodium azide. Controls (unmixed donors and recipient cells) were treated in the same manner. Transconjugant colonies were recovered following incubation at 37°C for 24 to 72 h. Furthermore, amplification of the sequences of *tet*(A), *tet*(B), *tet*(C), and *tet*(M) in the transconjugants were performed using the primer sets in **Table 2**. Template DNA was prepared as follows. Amounts of 1.5 ml of transconjugant culture were pelleted, and cells were boiled in 200 μl of H_2O for 15 min. After centrifugation, the supernatants were kept at −20°C. PCR was performed in a total volume of 50 μl, which contained 3 μl of supernatant, 50 pmol of each primer, 25 μl of PrimeSTAR® Max DNA Polymerase (TakaRa Biotechnology Co. Ltd, Japan). After an initial denaturation step of 3 min at 95°C, amplification was performed over 30 cycles, each one consisting of 30 s at 95°C, 30 s min at hybridization temperature [55°C for *tet*(A) and *tet*(C), 58°C for *tet*(B), and 52°C for *tet*(M)], and 1 min at 72°C, with a final extension step of 10 min at 72°C. The amplicons were sequenced using their corresponding primer set at commercial company (Shanghai Sangon Biological Engineering Technology and Services Co. Ltd, China). The sequences comparisons were performed using the BLASTtool available online at the National Center for Biotechnology Information of the National Library of Medicine (http://www.ncbi.nlm.nih.gov/blast/). Transconjugants carrying *tet*(M), but not *tet*(A), *tet*(B), or *tet*(C) were selected for further analysis.

Antimicrobial Susceptibility Testing

The susceptibility of *tet*(M)-positive transconjugants, their corresponding donors, and *E. coli* J53 to different antibiotics (**Table 3**) was determined by broth microdilution assays (Clinical Laboratory Standards Institute, 2014). Minimum inhibitory concentrations were determined on three independent occasions. *E. coli* ATCC 25922 was used for quality control in all susceptibility tests.

Plasmid Analysis

The incompatibility (Inc) groups of plasmids from transconjugants and their corresponding donors were determined by PCR-based replicon typing (Carattoli et al., 2005). Plasmids from the transconjugants and their corresponding donors (W4 and 5Y) were extracted using the QIAGEN Plasmid Midi Kit (Hilden, Germany) and subjected to electrophoresis on a 0.7% agarose gel. Plasmid size was estimated by comparison with reference plasmid DNAs of *E. coli* V517. The purified plasmids from W4 and 5Y were transferred to a nylon membrane (Roche Molecular Systems, Basel, Switzerland) and Southern blotting was carried out using a digoxigenin-labeled *tet*(M) PCR fragment [406 base pairs (bp), **Table 2**] as a probe.

Sequence Determinations

The *tet*(M)-positive conjugative plasmid pTW4 was digested with *Eco*RI and the fragments were ligated into the *Eco*RI-digested pBluescriptIISK(+). The recombined plasmids were electroporated into *E. coli* DH5α and white colonies were selected on LB/X-gal/IPTG agar supplemented with ampicillin (100 mg/L) and oxytetracycline (128 mg/L). The presence of *tet*(M) in transformants was confirmed by PCR using the primer set tetM-F and tetM-R (**Table 2**). The plasmid inserts were sequenced using M13 universal sequencing primers. The nucleotide and deduced protein sequences were analyzed with EditSeq and Megalign software (DNAstar, Madison, WI, USA). Sequence similarity and conserved domain searches were carried out using the BLASTtool available online at the National Center for Biotechnology Information of the

TABLE 1 | Bacterial strains used in this study.

Strain	Source/location	Multilocus sequence type	Phylogenetic grouping based on multiplex PCR	Genetic sequence /move genetic element carrying *tet*(M)	GenBank accession number
CY4	Dead duck/ Henan province	ST48	A	ΔIS26-Δ*orf13-lp-tet*(M)	KJ772289
5Y	Dead duck/ Henan province	ST156	B1	Tn6539-like	MF422120
E5	Dead duck/ Guangdong province	ST3839	D	ΔIS26-Δ*orf13-lp-tet*(M)	KJ772289
W4	Dead duck/ Fujian province	ST162	B1	Tn6539	KJ772290
LF6	Dead duck/ Fujian province	ST224	A	Δ*orf13-lp-tet*(M)	JF830611
Y8	Dead duck/ Zhejiang province	ST163	B1	Δ*orf13-lp-tet*(M)	JF830611
CY14	Dead duck/ Zhejiang province	ST224	B1	Δ*orf13-lp-tet*(M)	JF830611

TABLE 2 | Primers used in this study.

Primer	Sequence (5′-3′)	Start point(bp)[a]	Amplicon size (bp)	Use and notes	Reference sequence accession no[b]
tet(A) F	GCTACATCCTGCTTGCCTTG	797–816	210	Sequence of *tet*(A)	NC 015599
tet(A) R	CATAGATCGCCGTGAAGAGG	987–1006			
tet(B) F	TTGGTTAGGGGCAAGTTTTG	396–415	695	Sequence of *tet*(B)	MF969100
tet(B) R	GTAATGGGCCAATAACACCG	1035–1054			
tet(C) F	CTTGAGAGCCTTCAACCCAG	579–598	418	Sequence of *tet*(C)	NG 048181
tet(C) R	ATGGTCGTCATCTACCTGCC	977–996			
F1	GGTCATCAACACGGATAAAGC	2163–2183	1761	Sequence between *IS26* and *tet*(M)	KJ772290
F2	ATGTCCTGGCGTGTCTATGAT	3903–3923			
F4	AGAAATCCCTGCTCGGTGTAT	5426–5446	987	Sequence between *tet*(M) and *tnpX*	KJ772290
F5	GATGTTACTGGCTTGGTTTGA	6392–6412			
F6	CTTCATTTCCTATCGGTATCT	6242–6262	1887	Sequence between *tnpX* and *tnpR*	X60200
F7	AAGGTGTATCCATTCGGTTTA	8108–8128			
F8	CAACAACTCCTTTTGCCATT	7967–7986	1004	Sequence between Δ*tnpR* and reversed *IS26*	LO017738
F9	GAAGCAAATAGTCGGTGGTG	8951–8970			
F10	GCCCTATCCTACAGCGACAG	3073–3092	2500	Sequence between Δ*orf13* and *tet*(M)	KJ772290
F11	ATCCGACTATTTGGACGACG	5553–5572			
tetM-F	GTGGACAAAGGTACAACGAG	3795–3814	406	Sequence in *tet*(M)	KJ772290
tetM-R	CGGTAAAGTTCGTCACACAC	4181–4200			

[a] *Numbering is the sequence of KJ772290.*
[b] *GenBank accession numbers (www.ncbi.nlm.nih.gov).*

National Library of Medicine (http://www.ncbi.nlm.nih.gov/blast/).

PCR Mapping Analysis

Based on the sequence of the obtained inserted fragment between *hp* and partial *tnpX* (6,544 bp, the left sequence of KJ772290 in **Figure 2**) and the complete sequence of Tn1000 (accession number X60200), the primer set F6 and F7 (**Table 2**) was designed to amplify the sequence between *tnpX* and the truncated *tnpR*. The amplicon was ligated to the 3′-terminus of the inserted fragment. The sequence between partial *tnpR* sequence (Δ*tnpR*) and right-terminal IS26 element was amplified using the primer set F8 and F9 designed according to the corresponding sequence of plasmid PRC557 (accession no. LO017738).

To monitor whether similar genetic organization exists in the six remaining *E. coli* isolates, PCR mapping was performed using the primer set F6 and F7, F8 and F9, and the primer sets designed using the software Primer Primer 5.0 (PREMIER Biosoft, American) on the obtained sequence in the plasmid pTW4 (accession no. KJ772290). The primer sets are shown in **Table 2**, **Figure 2**. All PCR amplicons were sequenced using their corresponding primer set at commercial company (Shanghai

TABLE 3 | Characteristics of strains used in conjugation experiments.

Strains	MICs (unit: mg/L)									*tet* genes detected	Plasmid replicon types detected
	OXY	TET	DOX	AMK	NEO	CF	CTX	FLO	ENR		
J53	1	1	0.5	1	4	0.25	0.125	2	<0.25	ND	ND
W4	>512	512	128	>512	512	64	8	256	128	*tet*(A), *tet*(B), *tet* (C) *tet*(M)	HI2, FIB, Y, P, and A/C
TW4	256	128	16	>512	512	0.5	<0.5	64	1	*tet*(M)	HI2
5Y	>512	512	64	512	512	128	<0.5	256	128	*tet*(A), *tet*(B), *tet*(C) *tet*(M)	HI2, P, and A/C
T5Y	128	128	32	512	512	0.5	<0.5	64	0.5	*tet*(M)	HI2

OXY, oxytetracycline; TET, tetracycline; DOX, doxycycline; AMK, amikacin; NEO, neomycin; CF ceftiofur; CTX, cefotaxime; FLO, florfenicol; ENR, enrofloxacin; TW4 and T5Y is the tet(M)-positive transconjugant of E. coli isolate W4 and 5Y, respectively. ND, not tested.

Sangon Biological Engineering Technology & Services Co. Ltd, China), and the results were compared to sequences in the GenBank database using the BLAST tool.

Molecular Typing and Phylogenetic Analysis

The seven *E. coli* isolates were typed by multilocus sequence typing (MLST) (http://mlst.warwick.ac.uk/mlst/) as previously described (http://www.shigatox.net/mlst) (Clermont et al., 2015). Briefly, seven housekeeping genes (*aspC*, *clpX*, *fadD*, *icdA*, *lysP*, *mdh*, and *uidA*) were amplified and sequenced. The corresponding sequence types (STs) were matched using the electronic database on the *E. coli* MLST website. Additionally, the phylogenetic groups of the seven isolates were determined based on PCR detection of the *chuA* and *yiaA* genes and DNA fragment TSPE4.C2 (Clermont et al., 2000).

Nucleotide Sequencing and Submission of *tet*(M) Sequences

The nucleotide sequences containing full-length *tet*(M) were deposited in GenBank (accession numbers KJ772290, KJ772289, and MF422120).

RESULTS

Transfer of *tet*(M) and Multidrug Resistance

Two *tet*(M)-positive transconjugants (TW4 and T5Y) were obtained from donors W4 and 5Y at a frequency of 1.2×10^{-8}. As shown in **Table 3**, W4, 5Y, TW4, and T5Y exhibited resistance to tetracycline, oxytetracycline, and doxycycline. The minimum inhibitory concentrations of TW4 and T5Y to the above-mentioned drugs were 8- to 256-fold higher than those of the recipient strain *E. coli* J53. TW4 and T5Y also exhibited resistance to amikacin, neomycin, and florfenicol, suggesting that the corresponding resistance markers were co-transferred into the recipient strain. In addition, the transconjugants carrying *tet*(A) and *tet*(C) were also found on the selection plates.

Molecular Characteristics of Conjugative Plasmids

W4 and 5Y carried more than three plasmids (**Figure 1**). The sizes of the plasmids ranged from approximately 3.2 to more than 54.2 kb. Notably, TW4 and T5Y each carried only one plasmid (designated pTW4 and p5Y, respectively) of approximately 50 kb. Southern hybridization with the digoxigenin-labeled *tet*(M) PCR fragment indicated that isolates W4 and 5Y yielded one distinct signal located on this plasmid. PCR-based inc replicon typing showed that pTW4 and p5Y belonged to the HI2 type. The other plasmids in W4 and 5Y were positive for the HI2, FIB, Y, P, and A/C and the P, and A/C type, respectively.

Genetic Organization of *tet*(M) in Conjugative Plasmid and Sequence Analysis

The analysis of recombinant plasmids carrying *Eco*RI fragments from the conjugative plasmid pTW4 demonstrated that *tet*(M) was located on a fragment of approximately 6.5 kbp between *hp* and truncated *tnpX* (pTW4 plasmid in **Figure 2**). Sequence analysis indicated that a truncated orf13, the *tet*(M) leader peptide gene and *tet*(M) are located between bp 2989 and 5609 (numbering nucleotide position starts from the first base, G, in the sequence of KJ772290.). Sequence comparisons showed that the Δ*orf13-lp-tet*(M) exhibited ≥99% sequence identity to the corresponding sequences present in the GenBank database. Among them, the Δ*orf13-lp-tet*(M) exhibited 100% sequence identity to the corresponding sequence in the chromosome of *Straphylococcus rostri* (accession no. FN550102), *Streptococcus* spp. (CP008813 and CP003859), *E. faecalis* DENG (CP004081), and *E. coli* (CP021844).

At the left end of the *tet*(M)-containing *Eco*RI fragment, codons 1–1,067 were indistinguishable from those found in plasmid pM160133 (CP022165) and plasmid pSCE516-1 (KX023262) from *E. coli* isolates from a New York patient and chickens in China. These isolates contained two ORFs in the same orientation as *tet*(M) encoding a hypothetical protein and putative protein X. Additionally, codons 2522–5609 showed 100% sequence identity to the corresponding sequences in the chromosome of *E. coli* (CP021840 and CP021844), which contain an ORF in the transcription orientation of *tet*(M) in addition to

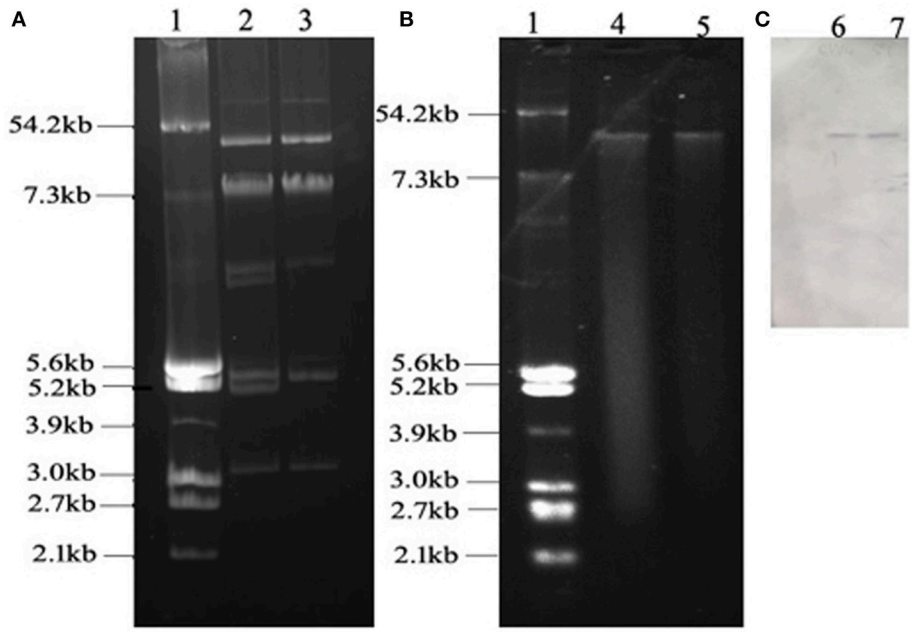

FIGURE 1 | (A) Agarose electrophoresis of plasmids from *E. coli* strains W4 and 5Y. **(B)** Agarose electrophoresis of plasmids from transconjugant *E. coli* TW4 and T5Y. **(C)** Southern blot of plasmids from W4 and 5Y and labeled *tet*(M) fragment. Lane 1, reference plasmid DNAs of *E. coli* V517; lane 2, plasmids from W4; lane 3, plasmids from 5Y; lane 4, plasmid from TW4; lane 5, plasmid from T5Y; lane 6, southern blot, plasmids from W4; lane 7, southern blot, plasmids from 5Y.

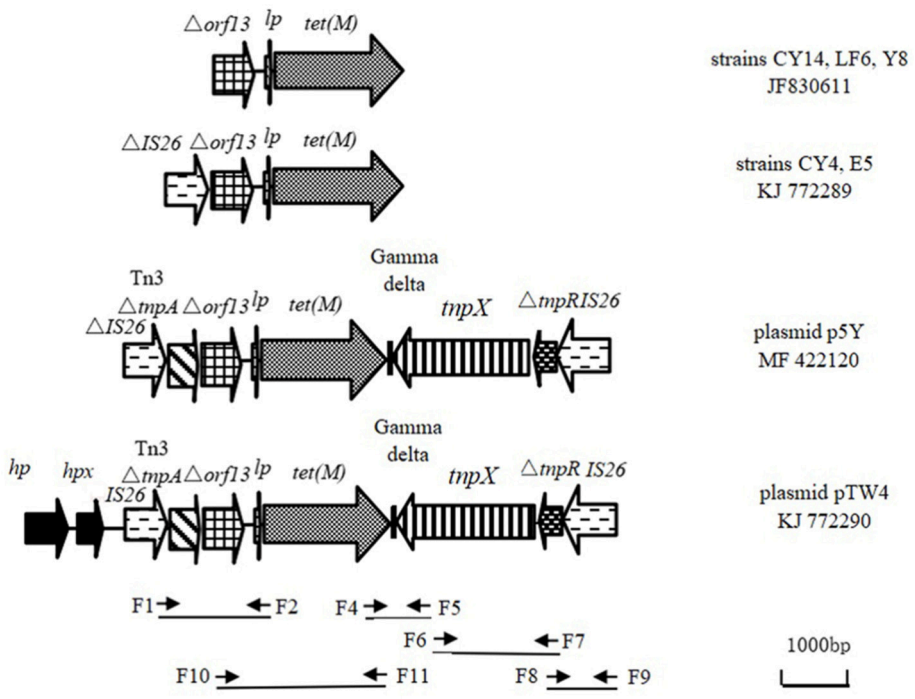

FIGURE 2 | Location of *tet*(M) in clinical isolates of *E. coli* and graphical representation of primer pairs along the tested genetic structure KJ772290 (*hp*), gene encoding hypothetical protein; *hpx*, gene encoding putative protein X; *lp*, gene encoding Tet(M) leader peptide; fragment between A and B position in the sequence KJ772290 was obtained by cloning experiments. Arrows represent the orientation of each primer and relative positions of the primers along the tested linear sequence.

the Δ*orf13-lp-tet*(M). This ORF located in the left of Δ*orf13-lp-tet*(M) in the plasmid pTW4 was indistinguishable from the corresponding sequence of the 3′-terminal of the gene encoding Tn3-family transposase (TnpA) found in plasmid pM160133 (CP022165). Notably, an intact IS26 element including 14-bp perfect terminal inverted repeats and IS26 transposase was found between the gene encoding putative protein X and truncated Tn3 *tnpA*.

At the right end of the *tet*(M)-containing *Eco*RI fragment (basepairs 2522 to 65544), Δ*orf13-lp-tet*(M)+gamma delta +incomplete *tnpX* were present in pTW4 and these sequences were 99% identical to the corresponding sequence in plasmids p41-3 (LC318054) and p15 (LC317981) from *E. coli* isolates from beef cattle in Japan. Obviously, the downstream of Δ*orf13-lp-tet*(M) is a Tn1000 element. To determine whether a complete Tn1000 was present, we designed a forward primer for the obtained *tnpX* sequence and reverse primers for different positions along the sequence of Tn1000 (X60200). A fragment, 1,887 bp in size, between *tnpX* and Δ*tnpR* was obtained using primer set F6 and F7 (**Table 2**). Alignment of Δ*orf13-lp-tet*(M) to part of the sequence of Tn1000 suggests that an unknown mobile genetic element is present upstream of Δ*tnpR*. IS26 elements typically exist in genomic DNA by forming regions containing antibiotic resistance genes flanked by two IS26 elements in the same or opposite orientations (Naas et al., 2001; Harmer and Hall, 2016). Since an intact IS26 element was detected in the *tet*(M)-containing EcoRI fragment, we further extended the sequence at its 3′-terminal end and obtained a fragment of 1,004 bp using primer set F8 and F9 (**Table 2**). Therefore, pTW4 contains IS26+Tn3Δ*tnpA*+Δ*orf13-lp-tet*(M)+gamma delta+*tnpX*+Δ*tnpR*+ reverse IS26 (**Figure 2**). The presence of two intact IS26 elements suggests that the genetic organization carrying *tet*(M) is a previously unknown composite transposon which has now been registered as Tn6539 in the Transposon Nomenclature Database from UCL Eastman (http://transposon.lstmed.ac.uk/tn-registry).

Genetic Sequences Carrying *tet*(M) in Six Remaining Strains of *E. coli* and Homology Analysis

The genetic sequences carrying *tet*(M) in the tested strains are shown in **Figure 2**. Four sequences from seven *E. coli* isolates carry the genetic fragment of Δ*orf13-lp-tet*(M). Among them, genomic DNAs from CY14, LF6, and Y8 only carry Δ*orf13-lp-tet*(M) which showed 99.1% nucleotide sequence identity to our previously obtained the sequence carrying *tet*(M) [JF83061]. A truncated IS26 element was located upstream of Δ*orf13* in the genomic DNA from CY4 and E5 (KJ772289). Additionally, the conjugative plasmid p5Y harbors a highly similar composite transposon to that in pTW4.

The similarities of Tn6539 in plasmid pTW4 with the sequences from *E. coli* deposited in GenBank are shown in **Figure 3**. The Δ*orf13-lp-tet*(M) fragment is located upstream or at the 3′-terminal end of part or the complete gene encoding Tn3-family transposase in the genomic DNA from the six *E. coli* isolates. The genomic DNAs from five of the six isolates carry intact IS6–family element(s). Among them, the chromosomal DNA from *E. coli* EC974 (CP021844) harbors a composite transposon consisting of *orf13-lp-tet*(M) and two IS15DIV elements belonging to the IS6-family in opposite orientations at its boundaries. Additionally, an Inc HI2–type plasmid pM160133 (CP022165) also carries a composite transposon with a similar genetic origination to that in the chromosome of *E. coli* EC974. The length of the genetic fragment flanked by two IS15DIVs elements was 22,182 bp and carried the resistance genes *aadA2*, *dfrA12*, and *floR* in addition to *tet*(M).

Genetic Relatedness and Phylogenetic Analysis of Seven *E. coli* Isolates

MLST analysis showed that the seven tested isolates had six different sequence types. W4, 5Y, CY4, E5, and Y8 belong to ST162, ST156, ST48, ST3839, and ST163, respectively. CY14 and LF6 belong to ST224. Notably, E5 belongs to a new MLST profile (ST3839). Phylogenetic analysis showed that the seven strains belonged to group A (CY4 and LF6), group B1 (W4, 5Y, Y8, and CY14), and group D (E5) which is commonly considered as including pathogenic bacteria (Clermont et al., 2000).

DISCUSSION

In this study, *tet*(M) was found in IncHI2-type conjugative plasmids from *E. coli* isolates W4 and 5Y. Although *tet*(M)-like genes are most commonly found in bacterial chromosome (Agersø et al., 2006; Vries et al., 2009), they also exist in conjugative plasmids from *Campylobacter jejuni* (Taylor et al., 1987), *Neisseria meningitidis*, *Kingella denitrificans*, *Eikenella corrodens* (Knapp et al., 1988), *Clostridium perfringens* (Yras and Rood, 1996), and *E. coli* (CP022165). Therefore, conjugative plasmids are an important vehicle facilitating the horizontal transfer of *tet*(M)-like genes between and across genera. IncHI2 plasmids play an important role in the acquisition and dissemination of antibiotic resistance genes among Gram-negative bacteria (Cain and Hall, 2012) and have been found to carry numerous classes of resistance genes including those conferring resistance to β-lactams (bla_{SHV}, bla_{CTX-M}, bla_{CMY}, bla_{OXA}, bla_{TEM}, and *NDM-1*), quinolones [*oqxAB*, *qnrA*, *qnrS*, *qnrB*, and *aac(6′)-Ib-cr*], aminoglycosides (*armA*, *aadA*, *aacA4*, *strA*, and *strB*), amphenicols (*catA1* and *floR*), trimethoprin (*dhfr1*), sulfonamides (*sul1* and *sul2*), fosfomycin (*fosA3*), and colistin (*mcr-1*) (Chen et al., 2016; Fang et al., 2016; Hadjadj et al., 2017). Additionally, these multidrug-resistant IncHI2-type plasmids are broadly distributed among different bacteria including *E. coli*, *Salmonella* spp., *Shigella flexnei*, *Klebesiella* spp., and *Enterobacter cloacae* (Liu et al., 2015; Kieffer et al., 2017). Thus, the IncHI2-type conjugative plasmids carrying *tet*(M) found in this study may spread between and across genera in the future, threatening tetracycline treatment in clinical practice.

IS26, a member of the IS6 insertion sequence family, contributes to the dissemination of antibiotic resistance genes in Gram-negative bacteria mainly by forming composite transposons. Most composite transposons contain a center region harboring resistance genes and two IS26 elements in

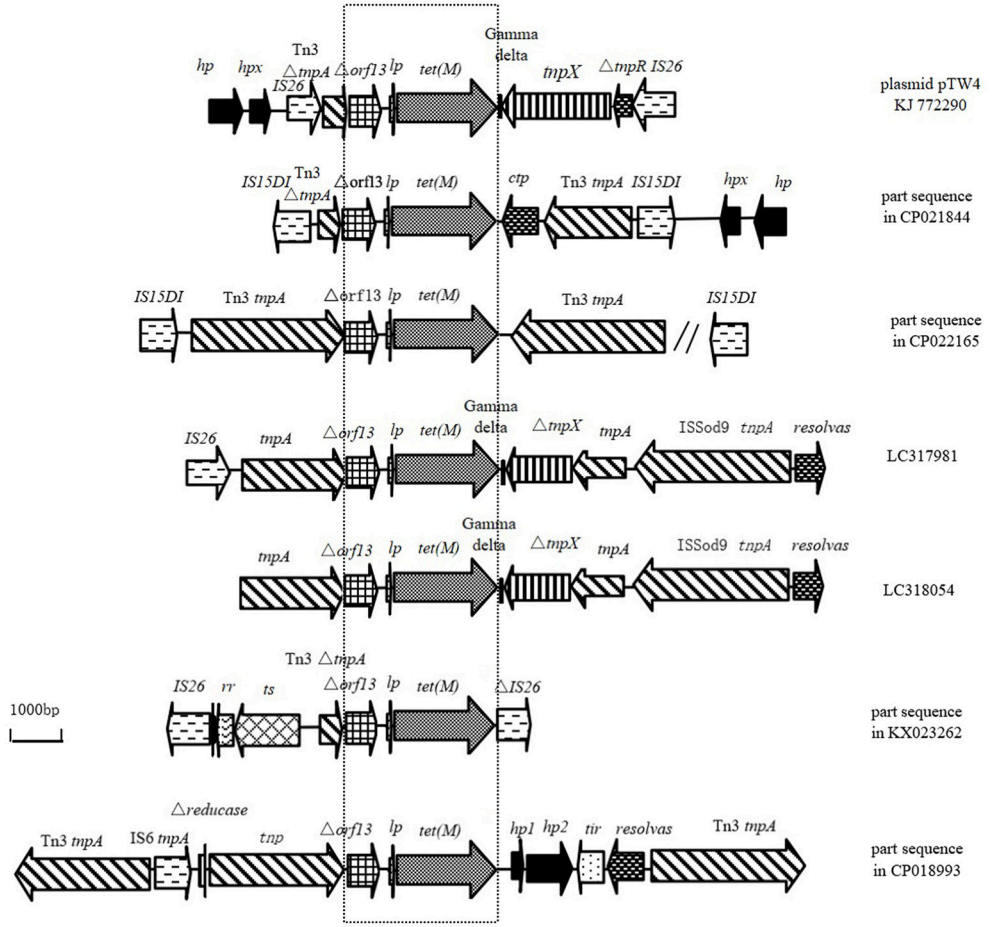

FIGURE 3 | Structural features surrounding the sequence of Δ*orf13* +*lp*+*tet*(M) in KJ772290 compared to other sequences deposited in GenBank. (Similar regions are indicated by dotted lines; *hp*, gene encoding hypothetical protein; *hpx*, gene encoding putative protein X; *lp*, gene encoding TetM leader peptide; *ctp*, gene encoding conjugative transfer protein; symbol "//" the sequence of 13,102 bp between Tn3 tnpA and IS15D1; *rr*, gene encoding RadR regulator; ts, gene encoding chromate transporter).

the same or opposite orientations at its bounders (Harmer and Hall, 2016). In Gram-negative bacteria, composition transposons are usually found with IS26 elements at their borders, but not flanked by 8-bp target site duplication (TSD), a hall marker of IS26 integration (Curiao et al., 2011; Zienkiewicz et al., 2013). Therefore, researchers considered that the composite transposons were formed by homologous recombination rather than a transposition. In 2014, a new model for IS26-mediated mobilization of resistance genes has been proposed by Harmer et al. (2014), whereby an IS26 element together with resistance gene(s), called a translocatable units (TU), is considered as a new family mobile genetic element. TU released from the genetic sequences can recognized another IS26 as target and is incorporated immediately adjacent to it in the same orientation. This results in IS26 element arraying in tandem and the formation of composite transposons. The frequency of cointegrate formation mediated by TU was 60-fold higher than that mediated by a single IS26, which indicated that an intact IS26 element in genetic sequences owns a stronger ability to recruit another IS26-mediated resistance genes. Furthermore, it was confirmed that TU integration could occur by Tnp (transposase in IS26 element)-catalyzed reaction or RecA-dependent homologous recombination. However, Tnp-catalyzed reaction was 100-fold more efficient than RecA-dependent homologous recombination (Harmer and Hall, 2015). In addition, He et al. (2015) analyzed the distinct patterns of sequences flanking 70 IS26 copies in eight genomes from Carbapenemase-producing *Enterobacteriaceae* and found that IS26 promoted rearrangement of resistance plasmids by both inter- and intramolecular replicative transposition (He et al., 2015). In the current study, Tn6539 was found to be a composite transposon containing Δ*orf13-lp-tet*(M) and two IS26 elements in opposite orientations at its borders. This type of composite transposon was first found in a multidrug-resistant plasmid from an *E. coli* MG-1 and named Tn2000. The center region flanked by two IS26 elements in Tn2000 is a class 1 integrin, In*53*, carrying nine functional resistance gene cassettes (Naas et al., 2001). Structures of composite transposons similar to that

of Tn6539 were found in plasmids from *E. coli* isolates from different sources (Literacka et al., 2009; Smet et al., 2010; Yang et al., 2014), but the molecular mechanism of their movement among Gram-negative bacteria remains unknown and requires further analysis.

CONCLUSION

We described the organization of a novel composite transposon Tn6539 in an IncHI2-type conjugative plasmid from two *E. coli* isolates with different genetic backgrounds. The transposon carries *tet*(M) and two intact IS26 elements in opposite orientations at its bounders.

AUTHOR CONTRIBUTIONS

GH and LY conceived and designed the experiments. YS, YL, HW, and LW performed the experiments. JL, YP, and YS analyzed the data. DH and HW contributed reagents materials analysis tools. YS and GH wrote the paper.

ACKNOWLEDGMENTS

This work was supported in part by the National Key Research and Development Program of China (2016YFD05101304) and National Natural Science Foundation of China-Henan Talent Training Joint fund (U1504327).

REFERENCES

Agersø, Y., Pedersen, A. G., and Aarestrup, F. M. (2006). Identification of Tn5397-like and Tn916-like transposons and diversity of the tetracycline resistance gene *tet*(M) in enterococci from humans, pigs and poultry. *J. Antimicrob. Chemother.* 57, 832–839. doi: 10.1093/jac/dkl069

Bryan, A., Shapir, N., and Sadowsky, M. J. (2004). Frequency and distribution of tetracycline resistance genes in genetically diverse, nonselected, and nonclinical *Escherichia coli* strains isolated from diverse human and animal sources. *Appl. Environ. Microbiol.* 70, 2503–2507. doi: 10.1128/AEM.70.4.2503-2507.2004

Cain, A. K., and Hall, R. M. (2012). Evolution of IncHI2 plasmids via acquisition of transposons carrying antibiotic resistance determinants. *J. Antimicrob. Chemother.* 67, 1121–1127. doi: 10.1093/jac/dks004

Carattoli, A., Bertini, A., Villa, L., Falbo, V., Hopkins, K. L., and Threlfall, E. J. (2005). Identification of plasmids by PCR-based replicon typing. *J. Microbiol. Methods* 63, 219–228. doi: 10.1016/j.mimet.2005.03.018

Cauwerts, K., Decostere, K., Graef, E. M. D., Haesebrouck, F., and Pasmans, F. (2007). High prevalence of tetracycline resistance in *Enterococcus* isolates from broilers carrying the *erm*(B) gene. *Avian Dis.* 36, 395–399. doi: 10.1080/03079450701589167

Chen, W. Y., Fang, T. Z., Zhou, X. J., Zhang, D. F., Shi, X. M., and Shi, C. L. (2016). IncHI2 Plasmids are predominant in antibiotic-resistant *Salmonella* isolates. *Front. Microbiol.* 7:1566. doi: 10.3389/fmicb.2016.01566

Chopra, I., and Roberts, M. Y. (2001). Tetracycline antibiotics: mode of action, applications, molecular biology, and epidemiology of bacterial resistance. *Microbiol. Mol. Bio Rev.* 65, 232–260. doi: 10.1128/MMBR.65.2.232-260.2001

Clermont, O., Bonacorsi, S., and Bingen, E. (2000). Rapid and simple determination of the *Escherichia coli* phylogenetic group. *Appl. Environ. Microbiol.* 66, 4555–4558. doi: 10.1128/AEM.66.10.4555-4558.2000

Clermont, O., Gordon, D., and Denamur, E. (2015). Guide to the various phylogenetic classification schemes for *Escherichia coli* and the correspondence among schemes. *Microbiolgy* 161, 980–988. doi: 10.1099/mic.0.000063

Clinical and Laboratory Standards Institute (2014). *Performance Standards for Antimicrobial Susceptibility Testing: Twenty-Fourth Informational Supplement M100-S24*. Wayne, PA: CLSI.

Curiao, T., Cantón, R., Garcillán-Barcia, M. P., Cruz, F., Baquero, F., and Coque, T. M. (2011). Association of composite IS26-*sul3* elements with highly transmissible inci1 plasmids in extended-spectrum-β-lactamase-producing *Escherichia coli* clones from humans. *Antimicrob Agents Chemother.* 55, 2451–2457. doi: 10.1128/AAC.01448-10

Devirgiliis, C., Coppola, D., Barile, S., Colonna, B., and Perozzi, G. (2009). Characterization of the Tn916 conjugative transposon in a food-borne strain of *Lactobacillus paracase*. *Appl. Environ. Microbiol.* 75, 3866–3871. doi: 10.1128/AEM.00589-09

Fang, L. X., Li, X. P., Li, L., Li, S. M., Liao, X. P., Sun, J., et al. (2016). Co-spread of metal and antibiotic resistance within ST3-IncHI2 plasmids from *E. coli* isolates of food-producing animals. *Sci. Rep.* 6:25312. doi: 10.1038/srep25312

Gilrane, V. L., Lobo, S., Huang, W. H., Zhuge, J., Yin, C. H., Chen, D., et al. (2017). Complete genome sequence of a colistin-resistant *Escherichia coli* strain harboring mcr-1 on an IncHI2 plasmid in the United States. *Genome Announcements* 5, e01095–e01017. doi: 10.1128/genomeA.01095-17

Hadjadj, L., Riziki, T., Zhu, Y., Li, J., Diene, S. M., and Rolain, J. M. (2017). Study of *mcr-1* gene-mediated colistin resistance in Enterobacteriaceae isolated from humans and animals in different countries. *Gene* 8:394. doi: 10.3390/genes8120394

Harmer, C. J., and Hall, R. M. (2015). IS26-mediated precise excision of the IS26-aphA1a translocatable unit. *MBIO* 6, e01866–e01815. doi: 10.1128/mBio.01866-15

Harmer, C. J., and Hall, R. M. (2016). IS26-mediated formation of transposons carrying antibiotic resistance genes. *mSphere* 1, e00038–e00016. doi: 10.1128/mSphere.00038-16

Harmer, C. J., Moran, R. A., and Hall, R. M. (2014). Movement of IS26-associated antibiotic resistance genes occurs via a translocatable unit that includes a single IS26 and preferentially inserts adjacent to another IS26. *MBIO* 5, e0180–e0114. doi: 10.1128/mBio.01801-14

He, S., Hickman, A. B., Varani, A. M., Siguier, P., Chandler, M., Dekker, J. P., et al. (2015). Insertion sequence IS26 reorganizes plasmids in clinically isolated multidrug-resistant bacteria by replicative transposition. *MBIO* 6:e00762. doi: 10.1128/mBio.00762-15

Hu, G. Z., Pan, Y. S., Wu, H., Hu, H., Xu, R., Yuan, L., et al. (2013). Prevalence of tetracycline resistance genes and identification of *tet*(M) in clinical isolates of *Escherichia coli* from sick ducks in China. *J. Med. Microbiol.* 62, 851–858. doi: 10.1099/jmm.0.051896-0

Jones, C. H., Tuckman, M., Murphy, E., and Bradford, P. A. (2006). Identification and sequence of a *tet*(M) tetracycline resistance determinant homologue in clinical isolates of *Escherichia coli*. *J. Bacteriol.* 188, 7151–7164. doi: 10.1128/JB.00705-06

Jurado-Rabadán, S., Fuente, R., Ruiz-Santa-Quiteria, J. A., Orden, J. A., de Vries, L. E., and Agersø, Y. (2014). Detection and linkage to mobile genetic elements of tetracycline resistance gene *tet*(M) in *Escherichia coli* isolates from pigs. *BMC Vet. Res.* 10:155. doi: 10.1186/1746-6148-10-155

Kieffer, N., Aires-de-Sousa, M., Nordmann, P., and Poirel, L. (2017). High rate of MCR-1–producing *Escherichia coli* and *Klebsiella pneumoniae* among pigs, Portugal. *Emerg Infect. Dis.* 23, 2023–2029. doi: 10.3201/eid2312.170883

Knapp, J. S., Johnson, S. R., Zemilman, J. M., Roberts, M. C., and Morse, S. A. (1988). High-level tetracycline resistance resulting from TetM in strains of *Neisseria* spp., *Kingella denitrificans*, and *Eikenella corrodens*. *Antimicrob. Agents Chemother.* 32, 765–767. doi: 10.1128/AAC.32.5.765

Linkevicius, M., Sandegren, L., and Andersson, D. I. (2015). Potential of tetracycline resistance proteins to evolve tigecycline resistance. *Antimicrob. Agents Chemother.* 60, 789–796. doi: 10.1128/AAC.02465-15

Literacka, E., Bedenic, B., Baraniak, A., Fiett, J., Tonkic, M., Jajic-Bencic, I., et al. (2009). $bla_{\mathrm{CTX-M}}$ genes in *Escherichia coli* strains from Croatian Hospitals are located in new ($bla_{\mathrm{CTX-M-3a}}$) and widely spread ($bla_{\mathrm{CTX-M-3a}}$ and $bla_{\mathrm{CTX-M-15}}$) genetic structures. *Antimicrob Agents Chemother.* 53, 1630–1635. doi: 10.1128/AAC.01431-08

Liu, G. L., Qin, S. S., Xu, H., Xu, L. J., Zhao, D., Liu, X. C., et al. (2015). New Delhi metallo-β-lactamase 1(NDM-1), the dominant carbapenemase detected

in carbapenem-resistant *Enterobacter cloacae* from Henan province, China. *PLoS ONE* 10:e0135044. doi: 10.1371/journal.pone.0135044

Naas, T., Mikami, Y., Imai, T., Poirel, L., and Nordmann, P. (2001). Characterization of In53, a class 1 plasmid- and composite transposon-located integron of *Escherichia coli w*hich carries an unusual array of gene cassettes. *J. Bacteriol*. 1, 235–249. doi: 10.1128/JB.183.1.235-249.2001

Roberts, M. C., and Schwarz, S. (2016). Tetracycline and phenicol resistance genes and mechanisms: importance for agriculture, the environment, and humans. *J. Environ. Qual*. 45, 576–592. doi: 10.2134/jeq2015.04.0207

Smet, A., Nieuwerburgh, F. V., Vandekerckhove, T. T. M., Martel, A., Deforce, D., Butaye, P., et al. (2010). Complete nucleotide sequence of CTX-M-15-plasmids from clinical *Escherichia coli* isolates: insertional events of transposons and insertion sequences. *PLOS ONE* 5:e11202. doi: 10.1371/journal.pone.0011202

Taylor, D. E., Hiratsuka, K., Ray, H., and Manavathu, E. K. (1987). Characterization and expression of a cloned tetracycline resistance determinant from *Campylobacter jejuni* plasmid pUA466. *J. Bacteriol.* 169, 2984–2989. doi: 10.1128/jb.169.7.2984-2989.1987

Tuckman, M., Petersen, P. J., Howe, A. Y. M., Orlowski, M., Mullen, S., Chan, K., et al. (2007). Occurrence of tetracycline resistance genes among *Escherichia coli* isolates from the phase 3 clinical trials for tigecycline. *Antimicrob Agents Chemother*. 51, 3205–3211. doi: 10.1128/AAC.00625-07

Vries, L. E., Christensen, H., Skov, R. L., Aarestrup, F. M., and Agersø, Y. (2009). Diversity of the tetracycline resistance gene *tet*(M) and identification of Tn916-and Tn5801-like (Tn6014) transposons in *Staphylococcus aureus* from humans and animals. *J. Antimicrob. Chemother*. 64, 490–500. doi: 10.1093/jac/dkp214

Yang, X. Y., Liu, W. L., Liu, Y. Y., Wang, J., Lv, L. C., Chen, X. J., et al. (2014). F33: A-: B-, IncHI2/ST3, and IncI1/ST71 plasmids drive the dissemination of *fosA3* and $bla_{CTX--M-55/-14/-65}$ in *Escherichia coli* from chickens in China. *Front. Microbiol.* 5:688. doi: 10.3389/fmicb.2014.00688

Yras, D. L., and Rood, J. I. (1996). Genetic organization and distribution of tetracycline resistance determinants in *Clostridium perfringens*. *Antimicrob. Agents Chemother*. 40, 2500–2504. doi: 10.1128/AAC.40.11.2500

Zienkiewicz, M., Kern-Zdanowicz, I., Carattoli, A., Gniadkowski, M., and Cegłowski, P. (2013). Tandem multiplication of the IS26-flanked amplicon with the bla_{SHV-5} gene within plasmid p1658/97. *FEMS Microb. Lett*. 341, 27–36. doi: 10.1111/1574-6968.12084

Conflict of Interest Statement: The authors declare that the research was conducted in the absence of any commercial or financial relationships that could be construed as a potential conflict of interest.

frontiers in Microbiology

ORIGINAL RESEARCH
published: 22 January 2019
doi: 10.3389/fmicb.2019.00015

The IS*Apl1*$_2$ Dimer Circular Intermediate Participates in *mcr-1* Transposition

Yu-Zhang He[1,2†], Xing-Ping Li[1,2†], Yuan-Yuan Miao[1,2], Jun Lin[3], Ruan-Yang Sun[1,2], Xiao-Pei Wang[1,2], Ya-Ya Guo[1,2], Xiao-Ping Liao[1,2], Ya-Hong Liu[1,2], Youjun Feng[1,4,5,6] and Jian Sun[1,2]**

[1] National Risk Assessment Laboratory for Antimicrobial Resistance of Animal Original Bacteria, South China Agricultural University, Guangzhou, China, [2] Guangdong Provincial Key Laboratory of Veterinary Pharmaceutics Development and Safety Evaluation, South China Agricultural University, Guangzhou, China, [3] Department of Animal Science, The University of Tennessee, Knoxville, Knoxville, TN, United States, [4] Department of Medical Microbiology and Parasitology, Zhejiang University School of Medicine, Hangzhou, China, [5] Department of General Intensive Care Unit of the Second Affiliated Hospital, Zhejiang University School of Medicine, Hangzhou, China, [6] College of Animal Sciences, Zhejiang University, Hangzhou, China

OPEN ACCESS

Edited by:
Yonghong Xiao,
Zhejiang University, China

Reviewed by:
Beiwen Zheng,
Zhejiang University, China
Zuowei Wu,
Iowa State University, United States

***Correspondence:**
Youjun Feng
fengyj@zju.edu.cn
Jian Sun
jiansun@scau.edu.cn

[†] These authors have contributed equally to this work

Specialty section:
This article was submitted to Antimicrobials, Resistance and Chemotherapy, a section of the journal Frontiers in Microbiology

Received: 24 August 2018
Accepted: 08 January 2019
Published: 22 January 2019

Citation:
He Y-Z, Li X-P, Miao Y-Y, Lin J, Sun R-Y, Wang X-P, Guo Y-Y, Liao X-P, Liu Y-H, Feng Y and Sun J (2019) The ISApl1$_2$ Dimer Circular Intermediate Participates in mcr-1 Transposition. Front. Microbiol. 10:15. doi: 10.3389/fmicb.2019.00015

Objectives: The mobile colistin resistance gene *mcr-1* is a serious threat to global human and animal health. The composite transposon Tn*6330* and its circular intermediate were proposed to be involved in the spread of *mcr-1* but their roles remain poorly understood.

Methods: To further explore the intermediates during the transposition of Tn*6330*, we engineered *Escherichia coli* strains that carry an intact Tn*6330* transposon or its deletion derivatives. PCR assays were performed to detect IR-IR junctions and possible circular intermediates. We carried out transposition experiments to calculate transposition frequency. The transposition sites were characterized by whole genome sequence and ISMapper-based analyses.

Results: The presence of an intact Tn*6330* was demonstrated to be essential for the successful transposition of *mcr-1*, although both Tn*6330* and Tn*6330*-ΔIR could form circular intermediates. The insertion sequence junction structure was observed in all constructed plasmids but the IS*Apl1* dimer was only formed in one construct containing an intact Tn*6330*. The average frequency of *mcr-1* transposition in an *E. coli* strain possessing an intact Tn*6330* was $\sim 10^{-6}$ per transformed cell. We identified 27 integration sites for the Tn*6330* transposition event. All the transposition sites were flanked by 2 bp target duplications and preferentially occurred in AT-rich regions.

Conclusion: These results indicate that *mcr-1* transposition relies on the presence of an intact Tn*6330*. In addition, formation of the tandem repeat IS*Apl1*$_2$ could represent a crucial intermediate. Taken together, the current investigations provide mechanistic insights in the transposition of *mcr-1*.

Keywords: transposition mechanism, *mcr-1*, circular intermediate, IS*Apl1*, colistin resistance

INTRODUCTION

Polymyxins are cationic antimicrobial cyclic polypeptides that have been reintroduced as a final clinical option for carbapenem-resistant bacteria (Li et al., 2006; Poirel et al., 2017a). The mobilized colistin resistance *mcr-1* gene encodes a phosphoethanolamine (PEA) lipid A transferase that catalyzes PEA addition to the 4′-phosphate of lipid A glucosamine moieties (Gao et al., 2016; Feng, 2018; Wei et al., 2018; Xu et al., 2018). This modification confers bacterial resistance to polymyxin (Liu et al., 2016). Since its discovery, *mcr-1* has been detected in over 50 countries and its reservoirs include humans, animals, and foods and associated environments (Sun et al., 2017b; Shen et al., 2018). The coexistence of MCR-1 and extended-spectrum beta-lactamases (ESBL) or carbapenemases poses a challenge to public health safety and clinical therapies (Sun et al., 2018).

The *mcr-1*-bearing plasmids are diverse although the *mcr-1* gene is often accompanied by a highly active 1,070 bp IS*Apl1* element (Sun et al., 2017a; Wang et al., 2018). IS*Apl1* belongs to the IS*30* family containing a 307-amino-acid-long DDE-type transposase surrounded by imperfect terminal inverted repeat sequences (21/27 nucleotide identity) (Tegetmeyer et al., 2008). In general, the *mcr-1-pap2* cassette lacks a flanking IS*Apl1*, possesses one IS*Apl1* immediately upstream or is flanked by two IS*Apl1* elements. The IS*Apl1-mcr-1-pap2*-IS*Apl1* transposable cassette was named Tn*6330* (Li et al., 2017).

The *mcr-1* gene was most likely mobilized by IS*Apl1* mediated composite transposon (Tn*6330*) (Snesrud et al., 2016, 2018). To demonstrate the function of the composite transposon Tn*6330*, Poirel et al. (2017b) constructed Tn*6330.2* in which the *mcr-1* gene was inactivated with a $bla_{\mathrm{TEM-1}}$ insertion, and characterized Tn*6330* participating in the mobilization of *mcr-1* gene. A circular intermediate comprised of IS*Apl1-mcr-1-pap2* was identified as essential for *mcr-1* mobilization and was generated from the downstream IS*Apl1* (Li et al., 2017). However, a circular intermediate does not necessarily require the complete IS*Apl1*. A circular intermediate originating from a truncated IS*Apl1* immediately downstream of *mcr-1* could also be detected (Zhao et al., 2017). Therefore, the circular intermediate for *mcr-1* mobilization is unclear.

Insertion sequence (IS) dimers can be detected by the presence of an inverted repeat (IR) junction, a full copy IS adjacent to a truncated IS or a circular IS (Olasz et al., 1993; Kiss and Olasz, 1999). For example, this has found experimentally by the detection of IR-IR junctions formed by site specific dimerization in tandem IS*30* elements (Kiss and Olasz, 1999). However, it is not known whether an IS*Apl1* dimer is formed during Tn*6330* transposition. To address this issue, we engineered a collection of plasmids bearing Tn*6330* and its derivatives and demonstrated that transposition of *mcr-1* relied on intact Tn*6330* for efficient integration into the *Escherichia coli* genome. Additionally, we found a tandem IS*Apl1* repeat IS*Apl1*$_2$*-mcr-1-pap2* that could represent a crucial intermediate during Tn*6330* transposition.

MATERIALS AND METHODS

Strains

Escherichia coli MG1655 (wild-type) and *E. coli* MG1655 (*recA*::Km) strains were used as host strains in the transposition experiments (**Table 1**; Gerdes et al., 2003). *E. coli* strain BW25141 strain contained the *pir* gene possessing an R6K replication origin (Datsenko and Wanner, 2000) and was used as a host to construct suicide plasmids bearing Tn*6330* and derivatives (**Table 1**). The *E. coli* swine strain CBJ3C was used as a template to amplify Tn6330 (**Table 1**). The Tn*6330* upstream IS*Apl1* (5′-TTTCCAA-3′) and downstream IS*Apl1* (5′-CTTCCAA-3′) differed by only one bp (underlined) (**Figure 1**).

Plasmid Construction

Tn*6330*, Tn*6330*-ΔIR, Tn*6330*-ΔIS*Apl1*(DO) (downstream) and Tn*6330*-ΔIS*Apl1*(UP) (upstream) were cloned into suicide plasmid pSV03 (Rakowski and Filutowicz, 2013) and were named pJS01, pJS02, pJS03, and pJS04, respectively (**Table 1**, **Figure 1A**, and **Supplementary Figure S1**). Primers used for plasmid constructions are listed in **Table 2**.

In pJS01, the structure of IS*Apl1-mcr-1-pap2*-IS*Apl1* and flanking sequences were amplified by PCR using primers TUtestF-BglII and TUtestR-XhoI with *E. coli* CBJ3C template DNA. Primers R6K-BglII and R6K-XhoI were used to amplify the backbone of pSV03, which includes the conditional replication origin R6K and chloramphenicol resistance gene (CmR). A ligation was performed giving rise to recombinant plasmid pJS01. The plasmid was transformed into *E. coli* BW25141 and selected on Luria-Bertani (LB) agar plates supplemented with 25 μg/ml chloramphenicol (Cm). The integrity of both IS*Apl1* elements and *mcr-1* was confirmed by PCR and sequence analysis.

The plasmid pJS02 was used to amplify a partial *mcr-1*, *pap2*, and IS*Apl1*-ΔIRR (IR right) fragment using primers P1 and IR-F. It was constructed using a fragment containing Cm^R that was amplified using primers CmR-F that lacked the 27 bp IRR and SacR containing a *SacI* site. The amplicons were connected by overlapping PCR resulting in a DNA fragment of the downstream IS*Apl1* lacking the 27 bp IRR that was bounded by *PstI* and *SacI* restriction enzyme sites. The sequence containing a fragment of the upstream IS*Apl1* without a 27bp IRL (IR left) containing *PstI* and *SacI* restriction sites at the ends was obtained in the same manner using primers Sac-F, CmR-R, IR-R and P2. The amplified fragments were digested with *PstI* and *SacI* and joined using T4 ligase. Plasmid pJS02 was confirmed as described above for pJS01.

Plasmids pJS03 and pJS04 were derived using primers UP-TR, UP-TF and DO-F and DO-R to amplify DNA fragments lacking the downstream copy of IS*Apl1* or upstream copy of IS*Apl1*, respectively. After self-ligation, the plasmids were screened and confirmed as for pJS01 above.

The Detection of Circular Intermediate and IR-IR Junction

All constructed plasmids carrying Tn*6330* or its derivatives were tested for the ability of IS*Apl1-mcr-1* to generate circular forms using reverse PCR with primers CTItestU and CTItestD

TABLE 1 | Strains and plasmids used in this study.

Strain	Description	Reference
E. coli MG1655 (wild-type)	K-12 strain F$^-$ λ$^-$ *ilvG rfb-50 rph-1*	Gerdes et al., 2003
E. coli MG1655 (*recA*::Km)	K-12 strain F$^-$ λ$^-$ *ilvG rfb-50 rph-1 recA*	Gerdes et al., 2003
E. coli BW25141	F-, Δ*araDB567*, Δ*lacZ*$_{4787}$(::*rrnB3*), Δ*phoBR580*, λ-, *galU95*, Δ*uidA3*::*pir*+, *recA1*, *endA9*(del-*ins*)::FRT, *rph-1*, Δ*rhaDB568*, *hsdR514*	
E. coli CBJ3C	Clinical isolate carrying Tn*6330*	
pSV03	Cm^R, replication origin from *E. coli* plasmid R6K; requires the R6K initiator protein *pir* for replication	This study
pKD4	Lambda red recombinase system template plasmid	
pKD46	Lambda red recombinase system template plasmid	
pJS01	Suicide plasmid (R6K replication origin) contains IS*Apl1-mcr-1-pap2*-IS*Apl1*	This study
pJS02	Suicide plasmid (R6K replication origin) contains Tn*6330* (IS*Apl1-mcr-1-pap2*-IS*Apl1*) without upstream IRL and downstream IRR	This study
pJS03	Suicide plasmid (R6K replication origin) contains IS*Apl1-mcr-1-pap2*	This study
pJS04	Suicide plasmid (R6K replication origin) contains *mcr-1-pap2*- IS*Apl1*	This study

that targeted *mcr-1* and *pap2*, respectively. To identify IR-IR junctions, PCR and Sanger sequencing were performed using primers MIS-F and MIS-R which were directed outward from IS*Apl1* (**Table 2**).

Transposition Assays

Transposition assays were performed as previously described (Bontron et al., 2016). In brief, suicide plasmids pJS01, pJS02, pJS03, and pJS04 were electroporated into *E. coli* MG1655 (wild-type) and *E. coli* MG1655 (*recA*::Km) using a Biorad MicroPulser (Hercules, CA, United States) and the protocol supplied by the manufacturer. The bacteria were suspended in 1ml LB and incubated for 1 h at 37°C with agitation and serially diluted onto LB-agar containing 2 μg/ml colistin to select for transposition events. The presence of the full-length transposon Tn*6330* was confirmed using PCR with primers in **Supplementary Table S1**. The transposition frequencies were calculated by dividing the number of transposition events by the number of transformed cells in triplicate (Milewska et al., 2015).

Mapping of Transposon Insertion Sites

Transposon insertion sites in *E. coli* MG1655 (*recA*::Km) were identified from random genomic DNA samples of each confirmed transposant prepared from overnight cultures using the TIANamp Bacteria DNA Kit (Tiangen, Dalian, China). The DNA of all the transposants was then mixed together into a single pool and a 300-bp library was constructed for Illumina paired-end sequencing (Illumina, San Diego, CA, United States). Illumina sequences were assembled *de novo* using SOAP software (Luo et al., 2012). The contigs carrying *mcr-1* and IS*Apl1* fragments were concatenated through the ISmapper analysis (Hawkey et al., 2015). Then the gaps were closed using PCR mapping and Sanger sequencing as shown in **Figure 2**. The primers targeted in the sequences of chromosome and *mcr-1-pap2* was designed in different insert regions (**Supplementary Table S1** and **Table 1**) to determine transposition sites.

To characterize the genetic context of Tn*6330* in clinical strains, the sequences carrying Tn*6330* in GenBank were collected. For each transposition event, the relative frequencies of each A and T, and G and C of the region extending from 50 nucleotides upstream to 50 nucleotides downstream from the insert target were calculated and plotted on a line graph (Tang et al., 2017). The pictures of the relative frequencies of the bases at each position were generated with the Pictogram program[1].

RESULTS

Transposition of the Composite Transposon

We identified the transposition abilities of the Tn*6330* derivatives by cloning into suicide plasmids that were then electroporated into strain BW25141 (*pir*$^+$). These suicide plasmids were transformed into two *E. coli* recipient strains MG1655 (wild-type) and MG1655 *(recA*::Km). Survival was contingent upon transposition of the selectable markers into the host genome. The transposition frequencies of pJS01 into both *E. coli* strains occurred at 2.7×10^{-6} per transformed cell. PCR and Sanger sequencing results showed that the downstream (5′-CTTCCAA-3′) and upstream (5′-TTTCCAA-3′) of IS*Apl1* in Tn*6330* in the insertion sites were different, indicating complex transposition events (data not shown). In contrast, all other constructs failed to generate cell survival in the presence of colistin (2 μg/ml). This indicated that Tn*6330*-ΔIR, Tn*6330*-ΔIS*Apl1*(DO), and Tn*6330*-ΔIS*Apl1*(up) could not transpose successfully.

Interestingly, we found evidence for the formation of circular intermediates containing the IS*Apl1-mcr-1-pap2* structure (CM-S) from plasmids harboring Tn*6330* and Tn*6330*-ΔIR. However, if the upstream or downstream IS*Apl1* was removed, no circular form could be detected (**Figures 1B,D** and **Table 3**).

All these transposition events generated IR-IR junctions were separated by 2 bp spacers (**Figures 1C,E**, **3**). This would be possible through the formation of IS*Apl1* dimers (pJS01, **Figure 1C**), a truncated IS*Apl1* next to a truncated IS*Apl1* (pJS02) or a circularized IS*Apl1* that was possible with all constructs (Kiss and Olasz, 1999).

[1]http://genes.mit.edu/pictogram.html

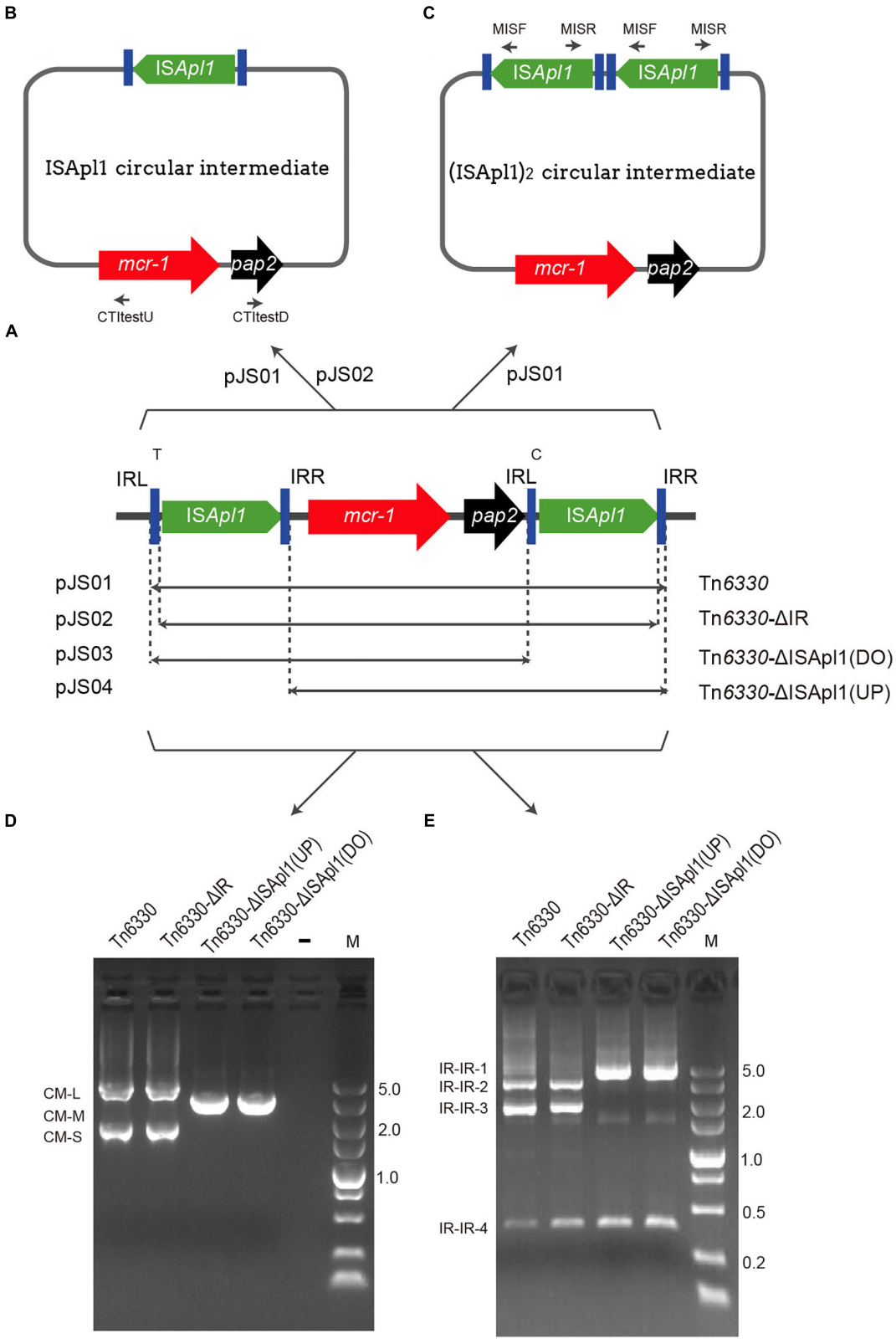

FIGURE 1 | Schematic representation of *mcr*-bearing transposons and verification of the presence of an IS*Apl1*- mediated circular intermediate. **(A)** Structures of Tn*6330* derivatives and plasmid hosts. **(B)** A circular intermediate and **(C)** An IS*Apl1* dimer circular intermediate. **(D,E)** Agarose gel electrophoresis of PCR products

(Continued)

FIGURE 1 | Continued
generated from screening assays using *Escherichia coli* strains containing the indicated Tn constructs. **(D)** Reverse PCR assay using primers CTI test U and CTI test D to identify IS*Apl1-mcr-1-pap2* intermediates. CM-L (circular form) represents the remnants of the *pap2*, IS*Apl1* backbone of the suicide plasmid, IS*Apl1* and part of *mcr-1*. **(E)** PCR products generated using primers MISF and MISR to screen for the presence of IR-IR junctions.

TABLE 2 | Primers used for plasmid construction.

Primer	Sequence (5′ → 3′)[a]	Reference
TUtestF-BglII	TACGCAGATCTACTACTGTGGCTAAGCCTCAAC	This study
TUtestR-XhoI	TACGCCTCGAGACGGAGAGTAACAACACGATGC	This study
R6K-BglII	TACGCAGATCTCCATGTCAGCCGTTAAGTGT	This study
R6K-XhoI	TACGCCTCGAGGTTGATCGGCACGTAAGAGG	This study
R6K-BamHI	TACGCGGATCCGTTGATCGGCACGTAAGAGG	This study
R6K-EcoRI	TACGCGAATTCCCATGTCAGCCGTTAAGTGT	This study
P1	GGCTGCAGACGCACAGCA	This study
IR-F	TTTTTTGAAGTAAACTTCATAAGGTGTTTTCCAACC	This study
CmR-F	ACCTTATGAAGTTTACTTCAAAAAAAGACTAAAAGAGAAGGGAGT	This study
Sac-R	CCAAGCGAGCTCGATATCAA	This study
Sac-F	TTGATATCGAGCTCGCTTGG	This study
CmR-R	ATTATATTCTAGTTGATGAGTACTTCTTTTTCTCTTTAAGTTGAGGCTTAGCC	This study
IR-R	AAAAAGAAGTACTCATCAACTAGAATATAATTTTGTTTCCACAC	This study
P2	ATTGCTGTGCGTCTGCAGCCA	This study
UP-TF	AGACTAAAAGAGAAGGGAGTG	This study
UP-TR	CGATTAAACTTGTTCACCCTTC	This study
DO-F	CTCTCAAGTGTATATTCAGTATGGG	This study
DO-R	CTCTTTAAGTTGAGGCTTAGCC	This study
CTItestU	CGATGATAACAGCGTGGTGATC	This study
CTItestD	TTGCCGATGCTTGATAGTATGC	This study
MIS-F	CAATCAGTGGAGCGAAGTTG	This study
MIS-R	CTGTTTTGTGCGTTCGTTGC	This study

[a] *Restriction sites are underlined.*

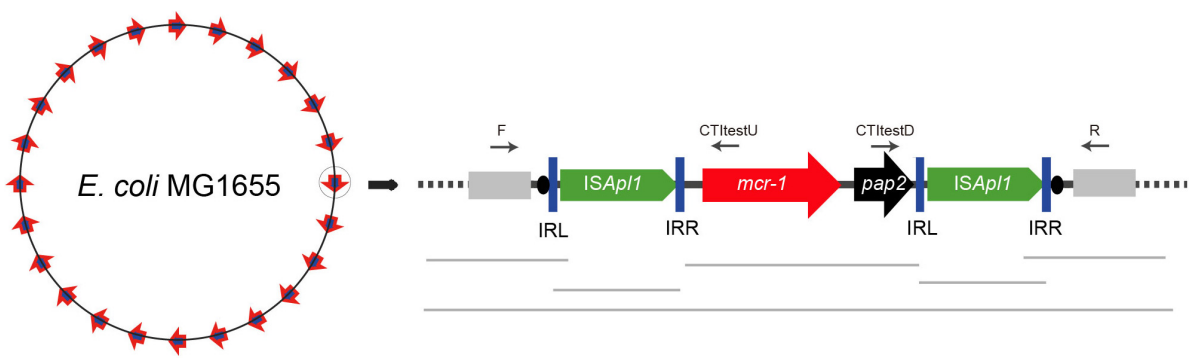

FIGURE 2 | Schematic for determination of the transposition site by WGS and PCR. Sequences of *E. coli* MG1655 are shown as rectangles in light gray. The inverted repeats (IRL and IRR) are represented as blue vertical bars and DRs as black ovals.

TABLE 3 | Transposition frequencies of suicide plasmids bearing *mcr-1* genes.

Plasmid	Transposase	Reverse PCR	IR-IR junction	Transposition frequency (wild type)[a]	Transposition frequency (recA::Km)
pJS01	+	+	+	2.78×10^{-6}	2.71×10^{-6}
pJS02	−	+	+	−	−
pJS03	+	−	+	−	−
pJS04	+	−	+	−	−

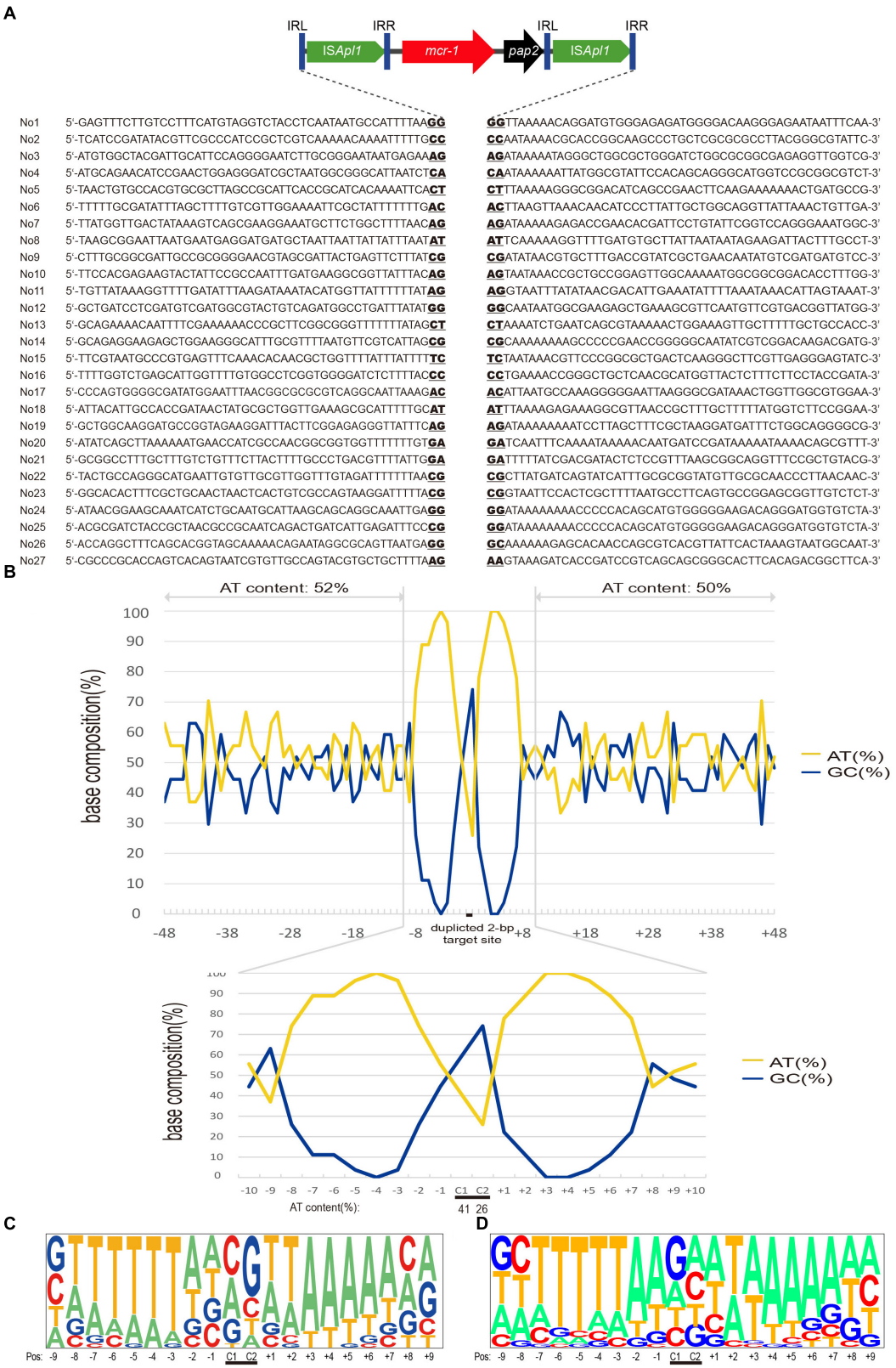

FIGURE 3 | Target site analyses of Tn*6330* transposons. **(A)** Molecular characterization of 27 transposition events of Tn*6330* transposons in *E. coli* MG1655 (*recA*::Km). The duplicated 2-bp target site is underlined in the context of the surrounding 48 nucleotides upstream and downstream of the target sites. **(B)** Statistical

(Continued)

FIGURE 3 | Continued
analyses of the 27 transposition sites. The percentage of AT and GC at each position from 48 nucleotides upstream to 48 nucleotides downstream of the target site are shown. The 2-bp duplicated target site (c1 and c2) are indicated by black bars. The AT and GC percentages of regions spanning positions –48 to –3 and positions +3 to +48 and that of the region spanning positions –2 to 2 are indicated in the upper and lower graphs, respectively. Relative nucleotide frequencies at each target site deduced from the **(C)** 27 experimental transposition events shown in **(A)** and **(D)** from 26 Tn*6330* transposons in clinical isolates obtained from GenBank (**Supplementary Table S2**).

Target Site Specificity

Whole genome sequence (WGS) and ISMapper-based analyses revealed 27 integration sites. The Illumina reads have been deposited in GenBank under accession no. SRR8365224. The insert locations of the *mcr-1* gene were further confirmed by PCR and Sanger sequencing. The majority of these events (24/27) generated 2-bp duplications and occurred in AT-rich regions with a high preference for insertion between T and A. The mean AT content extending in each direction from the 2-bp target sites (–50 to –2 bp and +2 to +50 bp) were 52 and 50%, respectively (**Figure 3**). In addition, the AT content increased nearer the target site and was 100% at positions –4, +3 and +4 and 74 to 96% at positions –7, –6, –5, –2, +1, +2, +5, +6 and +7. At the duplicated target site positions (c1 and c2) the AT content was lower (26 to 41%) (**Figure 3B**).

Distribution of Tn*6330*-Like Transposons in Enterobacteriaceae

To further characterize the transposon events in clinical strains, we collected sequences harboring the Tn*6330*-like structures from GenBank in isolates from more than ten regions including China, Hong Kong, Taiwan, Japan, Malaysia, Thailand, United States, Italy, Germany, Switzerland, Argentina, and Canada (**Supplementary Table S2**). We found that 47 sequences had 2-bp target directed repeats, a characteristic signature of transposition events of Tn*6330*-like transposons. The AT preferences of Tn*6330* insertions were similar to that *in vitro* mobilization assays presented above (**Figure 3D**).

DISCUSSION

In this study we demonstrated the functionality of Tn*6330* transposition from plasmids where cell survival was dependent on transposition of the *mcr-1* selective marker. The intact Tn*6330* in plasmid pJS01 transposed efficiently into the *E. coli* chromosome. Transposition occurs *via* a highly reactive intermediate such as IS*30*$_2$ and provides a molecular model for IS*30*-like transposition. This also relied on a circular intermediate carrying an active IR-IR junction (Olasz et al., 1993; Kiss and Olasz, 1999). The IS*Apl1* element in Tn*6330* belongs to the IS*30* family so we examined the role of IS*Apl1*$_2$ carrying joined IRs in IS*Apl1*- mediated transposon. Previous studies provided evidence that the reverse PCR amplicon IS*Apl1-mcr-1-pap2* acted as a circular intermediate (Li et al., 2017; Zhao et al., 2017). However, this could not distinguish between that structure and (IS*Apl1*)$_2$-*mcr-1-pap2*. All four of our plasmid constructs generated IR-IR junctions.

The genuine IS*30*-like circular intermediate of Tn*6330* composed of (IS*Apl1*)$_2$-*mcr-1-pap2* was only formed from pJS01 (**Figure 1C**). This was dependent upon the IS*Apl1* IR-IR junction and the production of the transposase for successful transposition into the *E. coli* chromosome (Kiss and Olasz, 1999). Plasmids pJS02, pJS03 and pJS04 could not form the IS*Apl1*$_2$-*mcr-1-pap2* circular intermediates and failed to transpose. This would also explain that *mcr-1* in the absence of flanked copies of IS*Apl1* or just one copy of IS*Apl1* originated from an ancestral Tn*6330* (Snesrud et al., 2018). The transposition of *mcr-1* relied on an intact Tn*6330*.

Transposition frequencies of suicide plasmids carrying Tn*6330* were high at rates of 10^{-6} per transformed cell both in wild type and *recA* mutant MG1655 strain. The relatively high Tn*6330* transposition frequency together with frequent insertion into transmissible plasmid targets might explain why the *mcr-1* gene is globally prevalent. Tn*6330* has been found in *E. coli*, *Salmonella enterica*, *Klebsiella pneumoniae*, *Citrobacter freundii*, and *Citrobacter braakii* (**Supplementary Table S2**). The composite transposon Tn*6330* might lose one or both copies of IS*Apl1* through illegitimate recombination giving rise to different types of genetic contexts such as IS*Apl1-mcr-1-pap2*, *mcr-1-pap2*, ΔTn*6330* and others (Snesrud et al., 2016). Loss of IS*Apl1* seems to be conducive to *mcr-1* maintenance increasing the stability of this gene in the host genome or plasmids and raising the risk of *mcr-1* dissemination.

The target site of Tn*6330* was AT rich in the 6 bp surrounding the duplicated target site. In *E. coli* clinical isolates, the same features were present both in plasmids and chromosomal regions consistent with previous works (Snesrud et al., 2016, 2018; Poirel et al., 2017b). Both the experimental transposants and *E. coli* clinical isolates showed a high frequency of T on the upstream and A on the downstream sides of the Tn*6330* target site. These findings contrast with previous descriptions that indicated target site duplication always carried a C or a G or both suggesting a relatively even distribution of A, T, G and C.

Though Poirel et al. (2017b) have demonstrated the mobility of the *mcr-1* gene by transposition, some differences exist in our study: (1) we found the suicide plasmids harboring *mcr-1* could successfully transpose into the bacterial chromosome using the colistin resistant phenotype during the process of transposition. We found no visible toxic effects to the presence of MCR-1. Toxic effects of MCR-1 that limited colonization of *mcr-1* in regular bacterial cells might be caused by high plasmid copy number (Yang et al., 2017). (2) We characterized 27 transposon sites using WGS and ISMapper. Compared with previous digestion and inverse PCR strategies, the ISMapper

method might be more convenient and efficient (Poirel et al., 2017b). (3) The regions of the downstream IS*Apl1* (CTTCCAA) were different from the upstream IS*Apl1* (TTTCCAA) in all the transposants; the same as initial Tn*6330* in pJS01. This result suggested that the transposition events were not from the IS*Apl1-mcr-1-pap2* circular form. This was further evidence for an IS*Apl1* dimer-mediated composite transposon (Snesrud et al., 2018). In addition, our study for the first time indicates that an IS*Apl1* dimer plays a crucial role as a genuine circular intermediate. This contrasts with previous studies indicating that the IS*Apl1-mcr-1-pap2* circular form results in the transposition of *mcr-1* (Li et al., 2017; Zhao et al., 2017). A reverse PCR amplicon does not completely characterize a circular intermediate since it cannot identify the IS-IS junction.

In summary, our results further verified that the transposition of *mcr-1* is only mediated by an intact Tn*6330* but not the amplicon identified by reverse PCR, the IS*Apl1-mcr-1-pap2* circular form. In addition, the IS*Apl1* dimer IS*Apl1*$_2$*-mcr-1-pap2* represents a crucial intermediate in *mcr-1* transmission. Future studies will focus on the regulatory mechanisms of Tn*6330* transposition in the search for a viable path to block the spread of the colistin resistance gene *mcr-1*.

AUTHOR CONTRIBUTIONS

JS designed this project. Y-ZH, Y-YM, X-PW, and Y-YG performed the experiments. Y-ZH, X-PLi, YF, and JS analyzed the data. X-PLi and R-YS made the figures. X-PLi wrote this manuscript. JL, X-PLiao, YF, and JS edited and revised the manuscript. Y-HL coordinated the whole project.

FUNDING

This work was supported by the National Key R&D Program of China (2016YFD0501300), the Program of Changjiang Scholars and Innovative Research Team in University of Ministry of Education of China (IRT13063), and Pearl River S&T Nova Program of Guangzhou (Grant No. 201610010036).

SUPPLEMENTARY MATERIAL

The Supplementary Material for this article can be found online at: https://www.frontiersin.org/articles/10.3389/fmicb.2019.00015/full#supplementary-material

REFERENCES

Bontron, S., Nordmann, P., and Poirel, L. (2016). Transposition of Tn*125* encoding the NDM-1 carbapenemase in *Acinetobacter baumannii*. *Antimicrob. Agents Chemother.* 60, 7245–7251. doi: 10.1128/AAC.01755-16

Datsenko, K. A., and Wanner, B. L. (2000). One-step inactivation of chromosomal genes in *Escherichia coli* K-12 using PCR products. *Proc. Natl. Acad. Sci. U.S.A.* 97, 6640–6645. doi: 10.1073/pnas.120163297

Feng, Y. (2018). Transferability of MCR-1/2 polymyxin resistance: complex dissemination and genetic mechanism. *ACS Infect. Dis.* 4, 291–300. doi: 10.1021/acsinfecdis.7b00201

Gao, R., Hu, Y., Li, Z., Sun, J., Wang, Q., Lin, J., et al. (2016). Dissemination and mechanism for the MCR-1 colistin resistance. *PLoS Pathog.* 12:e1005957. doi: 10.1371/journal.ppat.1005957

Gerdes, S. Y., Scholle, M. D., Campbell, J. W., Balázsi, G., Ravasz, E., Daugherty, M. D., et al. (2003). Experimental determination and system level analysis of essential genes in *Escherichia coli* MG1655. *J. Bacteriol.* 185, 5673–5684. doi: 10.1128/jb.185.19.5673-5684.2003

Hawkey, J., Hamidian, M., Wick, R. R., Edwards, D. J., Billman-Jacobe, H., Hall, R. M., et al. (2015). ISMapper: identifying transposase insertion sites in bacterial genomes from short read sequence data. *BMC Genomics* 16:667. doi: 10.1186/s12864-015-1860-2

Kiss, J., and Olasz, F. (1999). Formation and transposition of the covalently closed IS*30* circle: the relation between tandem dimers and monomeric circles. *Mol. Microbiol.* 34, 37–52. doi: 10.1046/j.1365-2958.1999.01567.x

Li, J., Nation, R. L., Turnidge, J. D., Milne, R. W., Coulthard, K., Rayner, C. R., et al. (2006). Colistin: the re-emerging antibiotic for multidrug-resistant gram-negative bacterial infections. *Lancet Infect. Dis.* 6, 589–601. doi: 10.1016/S1473-3099(06)70580-1

Li, R., Xie, M., Zhang, J., Yang, Z., Liu, L., Liu, X., et al. (2017). Genetic characterization of *mcr-1*-bearing plasmids to depict molecular mechanisms underlying dissemination of the colistin resistance determinant. *J. Antimicrob. Chemother.* 72, 393–401. doi: 10.1093/jac/dkw411

Liu, Y. Y., Wang, Y., Walsh, T. R., Yi, L. X., Zhang, R., Spencer, J., et al. (2016). Emergence of plasmid-mediated colistin resistance mechanism MCR-1 in animals and human beings in China: a microbiological and molecular biological study. *Lancet Infect. Dis.* 16, 161–168. doi: 10.1016/S1473-3099(15)00424-7

Luo, R., Liu, B., Xie, Y., Li, Z., Huang, W., Yuan, J., et al. (2012). SOAPdenovo2: an empirically improved memory-efficient short-read de novo assembler. *Gigascience* 1:18. doi: 10.1186/2047-217X-1-18

Milewska, K., Wegrzyn, G., and Szalewska-Palasz, A. (2015). Transformation of *Shewanella baltica* with ColE1-like and P1 plasmids and their maintenance during bacterial growth in cultures. *Plasmid* 81, 42–49. doi: 10.1016/j.plasmid.2015.07.001

Olasz, F., Stalder, R., and Arber, W. (1993). Formation of the tandem repeat (IS30)2 and its role in IS30-mediated transpositional DNA rearrangements. *Mol. Gen. Genet.* 239, 177–187.

Poirel, L., Jayol, A., and Nordmann, P. (2017a). Polymyxins: antibacterial activity, susceptibility testing, and resistance mechanisms encoded by plasmids or chromosomes. *Clin. Microbiol. Rev.* 30, 557–596. doi: 10.1128/CMR.00064-16

Poirel, L., Kieffer, N., and Nordmann, P. (2017b). In-vitro study of ISApl1-mediated mobilization of the colistin resistance gene mcr-1. *Antimicrob. Agents Chemother.* 61:e00127-17. doi: 10.1128/AAC.00127-17

Rakowski, S. A., and Filutowicz, M. (2013). Plasmid R6K replication control. *Plasmid* 69, 231–242. doi: 10.1016/j.plasmid.2013.02.003

Shen, Y., Zhou, H., Xu, J., Wang, Y., Zhang, Q., Walsh, T. R., et al. (2018). Anthropogenic and environmental factors associated with high incidence of mcr-1 carriage in humans across China. *Nat. Microbiol.* 3, 1054–1062. doi: 10.1038/s41564-018-0205-8

Snesrud, E., He, S., Chandler, M., Dekker, J. P., Hickman, A. B., McGann, P., et al. (2016). A model for transposition of the colistin resistance gene *mcr-1* by IS*Apl1*. *Antimicrob. Agents Chemother.* 60, 6973–6976. doi: 10.1128/AAC.01457-16

Snesrud, E., McGann, P., and Chandler, M. (2018). The birth and demise of the IS*Apl1-mcr-1*-IS*Apl1* composite transposon: the vehicle for transferable colistin resistance. *MBio* 9:e02381-17. doi: 10.1128/mBio.02381-17

Sun, J., Fang, L. X., Wu, Z., Deng, H., Yang, R. S., Li, X. P., et al. (2017a). Genetic analysis of the IncX4 plasmids: Implications for a unique pattern in the *mcr-1* acquisition. *Sci. Rep.* 7:424. doi: 10.1038/s41598-017-00095-x

Sun, J., Zeng, X., Li, X. P., Liao, X. P., Liu, Y. H., and Lin, J. (2017b). Plasmid-mediated colistin resistance in animals: current status and future directions. *Anim. Health Res. Rev.* 18, 136–152. doi: 10.1017/S1466252317000111

Sun, J., Zhang, H., Liu, Y. H., and Feng, Y. (2018). Towards understanding MCR-like colistin resistance. *Trends Microbiol.* 26, 794–808. doi: 10.1016/j.tim.2018.02.006

Tang, Y., Li, G., Liang, W., Shen, P., Zhang, Y., and Jiang, X. (2017). Translocation of carbapenemase gene *bla*KPC-2 both internal and external to transposons occurs via novel structures of Tn*1721* and exhibits distinct movement patterns. *Antimicrob. Agents Chemother.* 61:e01151-17. doi: 10.1128/AAC.01151-17

Tegetmeyer, H. E., Jones, S. C., Langford, P. R., and Baltes, N. (2008). IS*Apl1*, a novel insertion element of *Actinobacillus pleuropneumoniae*, prevents ApxIV-based serological detection of serotype 7 strain AP76. *Vet. Microbiol.* 128, 342–353. doi: 10.1016/j.vetmic.2007.10.025

Wang, R., van Dorp, L., Shaw, L. P., Bradley, P., Wang, Q., Wang, X., et al. (2018). The global distribution and spread of the mobilized colistin resistance gene *mcr-1*. *Nat. Commun.* 9:1179. doi: 10.1038/s41467-018-03205-z

Wei, W., Srinivas, S., Lin, J., Tang, Z., Wang, S., Ullah, S., et al. (2018). Defining ICR-Mo, an intrinsic colistin resistance determinant from *Moraxella osloensis*. *PLoS Genet.* 14:e1007389. doi: 10.1371/journal.pgen.1007389

Xu, Y., Wei, W., Lei, S., Lin, J., Srinivas, S., and Feng, Y. (2018). An evolutionarily conserved mechanism for intrinsic and transferable polymyxin resistance. *MBio* 9:e02317-17. doi: 10.1128/mBio.02317-17

Yang, Q., Li, M., Spiller, O. B., Andrey, D. O., Hinchliffe, P., Li, H., et al. (2017). Balancing mcr-1 expression and bacterial survival is a delicate equilibrium between essential cellular defence mechanisms. *Nat. Commun.* 8:2054. doi: 10.1038/s41467-017-02149-0

Zhao, F., Feng, Y., Lu, X., McNally, A., and Zong, Z. (2017). Remarkable diversity of *Escherichia coli* carrying *mcr-1* from hospital sewage with the identification of two new *mcr-1* variants. *Front. Microbiol.* 8:2094. doi: 10.3389/fmicb.2017.02094

Conflict of Interest Statement: The authors declare that the research was conducted in the absence of any commercial or financial relationships that could be construed as a potential conflict of interest.

The reviewer BZ declared a shared affiliation, with no collaboration, with one of the authors, YF to the handling Editor at the time of review.

frontiers in Microbiology

ORIGINAL RESEARCH
published: 29 January 2019
doi: 10.3389/fmicb.2019.00048

Replicon-Based Typing of IncI-Complex Plasmids, and Comparative Genomics Analysis of IncIγ/K1 Plasmids

Defu Zhang[1,2,3,4†], Yuzong Zhao[1,2,3,4†], Jiao Feng[4], Lingfei Hu[4], Xiaoyuan Jiang[4], Zhe Zhan[4], Huiying Yang[4], Wenhui Yang[4], Bo Gao[4], Jinglin Wang[4], Jianrong Li[1,2,3], Zhe Yin[4] and Dongsheng Zhou[4*]*

[1] National and Local Joint Engineering Research Center of Storage, Processing and Safety Control Technology for Fresh Agricultural and Aquatic Products, Bohai University, Jinzhou, China, [2] Fresh Food Storage and Processing Technology Research Institute of Liaoning Provincial Universities, Bohai University, Jinzhou, China, [3] College of Food Science and Project Engineering, Bohai University, Jinzhou, China, [4] State Key Laboratory of Pathogen and Biosecurity, Beijing Institute of Microbiology and Epidemiology, Beijing, China

OPEN ACCESS

Edited by:
Charles W. Knapp,
University of Strathclyde,
United Kingdom

Reviewed by:
Jian-Hua Liu,
South China Agricultural University,
China
Liang Li,
Los Angeles Biomedical Research Institute, United States

***Correspondence:**
Zhe Yin
jerry9yin@163.com
Dongsheng Zhou
dongshengzhou1977@gmail.com

[†] These authors have contributed equally to this work

Specialty section:
This article was submitted to Antimicrobials, Resistance and Chemotherapy, a section of the journal Frontiers in Microbiology

Received: 28 September 2018
Accepted: 14 January 2019
Published: 29 January 2019

Citation:
Zhang D, Zhao Y, Feng J, Hu L, Jiang X, Zhan Z, Yang H, Yang W, Gao B, Wang J, Li J, Yin Z and Zhou D (2019) Replicon-Based Typing of IncI-Complex Plasmids, and Comparative Genomics Analysis of IncIγ/K1 Plasmids. Front. Microbiol. 10:48. doi: 10.3389/fmicb.2019.00048

IncI-complex plasmids can be divided into seven subgroups IncI1, IncI2, IncIγ, IncB/O, IncK1, IncK2, and IncZ. In this study, a replicon-based scheme was proposed for typing IncI-complex plasmids into four separately clustering subgroups IncI2, IncI1/B/O, IncIγ/K1 and IncK2/Z, the last three of which were combined from IncI1 and IncB/O, IncIγ and IncK1, and IncK2 and IncZ, respectively. Four IncIγ/K1 plasmids p205880-NR2, p14E509-CTXM, p11011-CTXM and p61806-CTXM were fully sequenced and compared with IncIγ/K1 reference pCT, IncI2 reference R721, IncI1/B/O reference R64 and IncK2/Z reference pO26-CRL-125. These plasmids shared conserved gene organization in the replication and conjugal transfer regions, but displaying considerable sequence diversity among different subgroups. Remarkable modular differences were observed in the maintenance and transfer leading regions. p205880-NR2 contained no resistance genes or accessory modules, while the other seven plasmids acquired one or more accessory modules, which harbored mobile elements [including unit transposons, insertion sequence (IS)-based transposition units and individual IS elements] and associated resistance markers (especially including those involved in resistance to β-lactams, aminoglycosides, tetracyclins, phenicols, streptomycins, trimethoprims, sulphonamides, tunicamycins and erythromycins). Data presented here provided a deeper insight into diversification and evolution of IncI-complex plasmids.

Keywords: IncI-complex plasmids, IncIγ/K1, CTX-M, multi-drug resistance, plasmids

INTRODUCTION

Plasmids of the I incompatibility complex (IncI-complex) produce I-type pili. Based on morphological and serological similarities of their pili, IncI-complex plasmids can be divided into at least seven subgroups, namely IncI1 (= IncIα or Com1), IncI2 (= IncIδ), IncIγ, IncB/O, IncK1, IncK2, and IncZ (Tschäpe and Tietze, 2010; Papagiannitsis et al., 2011; Rozwandowicz et al., 2017). IncI-complex plasmids are low copy-number, narrow-host-range, conjugative plasmids, varying in size from 50 to 250 kb. The backbone of an IncI-complex plasmid can be divided

into regions of replication, maintenance, transfer leading and conjugal transfer (Sampei et al., 2010). Two protein genes (*repZ* and *repY*), one regulatory RNA gene (*inc*) and four functional DNA sequences (*CIS*, *oriV*, *ter*, and iterons) in the replication region are essential for plasmid replication and copy number control (Sampei et al., 2010). The partitioning genes *parA* and *parB* in the maintenance region are responsible for active partition of replicated DNA into daughter cells during cell division. Two gene clusters *tra* and *pil* in the conjugal transfer region encoded the thick rigid pilus as the primary pili implicated in conjugation transfer, and the thin flexible pilus increasing conjugation rate in liquid medium, respectively (Bradley, 1984). A multiple inversion system named shufflon mediates rearrangement of PilV protein by a plasmid-encoded site-specific recombinase Rci (Komano et al., 1987). This recombination event selects one of seven different *pilV* genes, which is responsible for the determination of recipient specificity (Komano et al., 1994).

The purpose of this study is to provide a deeper insight into genomic diversity and evolution of IncI-complex plasmids. First, a replicon-based scheme was established to divide IncI-complex plasmids into four subgroups IncI2, IncI1/B/O, IncIγ/K1, and IncK2/Z. Then, four IncIγ/K1 plasmids p14E509-CTXM, p11011-CTXM, p61806-CTXM, and p205880-NR2 were fully sequenced and compared to the reference plasmids pCT (accession number FN868832) (Cottell et al., 2011), R721 (accession number AP002527), R64 (accession number AP005147) (Sampei et al., 2010), and pO26-CRL-125 (accession number KC340959) (Venturini et al., 2013) of the above four subgroups.

MATERIALS AND METHODS

Bacterial Isolates

Escherichia coli 14E509 was isolated in 2014 from a urine specimen of an infant with pneumonia in a public hospital in Henan City, China. *E. coli* 11011 was isolated in 2014 from a bile specimen of an elderly patient with bile duct calculus in a public hospital in Ningbo City, China. *E. coli* 61806 was isolated in 2015 from a whole blood specimen of an elderly patient with septic shock in a teaching hospital in Henan City, China. *Klebsiella pneumoniae* 205880 was isolated in 2012 from a sputum specimen of an elderly patient with pneumonia in a teaching hospital in Chongqing City, China.

Genomic DNA Sequencing and Sequence Assemble

Genomic DNA was isolated from each isolate using a Qiagen Blood & Cell Culture DNA Maxi Kit (Qiagen, Hilden, Germany). The genomic DNA of strain 61806 was sequenced from a mate-pair libraries with average insert size of 5 kb (ranged from 2 to 10 kb) using a MiSeq sequencer (Illumina, CA, United States). Quality control, removing adapters and low quality reads, were performed using *Trimmomatic* 0.36 (Bolger et al., 2014). The filtered clean reads were then assembled using *Newbler* 2.6 (Nederbragt, 2014), followed by extraction of the consensus sequence with *CLC Genomics Workbench* 3.0 (Qiagen Bioinformatics). Gaps between contigs were filled using a combination of PCR and Sanger sequencing using an ABI 3730 Sequencer (LifeTechnologies, CA, United States), and *Gapfiller* V1.11 (Boetzer and Pirovano, 2012) was used for gap closure.

For all the other three isolates (14E509, 11011 and 205880), genome sequencing was performed with a sheared DNA library with average size of 15 kb (ranged from 10 to 20 kb) on a PacBio RSII sequencer (Pacific Biosciences, CA, United States), as well as a paired-end library with an average insert size of 400 bp (ranged from 150 to 600 kb) on a HiSeq sequencer (Illumina, CA, United States). The paired-end short Illumina reads were used to correct the long PacBio reads utilizing *proovread* (Hackl et al., 2014), and then the corrected PacBio reads were assembled *de novo* utilizing *SMARTdenovo* (available from https://github.com/ruanjue/smartdenovo).

Sequence Annotation and Genome Comparison

Open reading frames and pseudogenes were predicted using *RAST* 2.0 (Brettin et al., 2015) combined with *BLASTP/BLASTN* (Boratyn et al., 2013) searches against the *UniProtKB/Swiss-Prot* database (Boutet et al., 2016) and the *RefSeq* database (O'Leary et al., 2016). Annotation of resistance genes, mobile elements, and other features was carried out using the online databases including *CARD* (Jia et al., 2017), *ResFinder* (Zankari et al., 2012), *ISfinder* (Siguier et al., 2006), *INTEGRALL* (Moura et al., 2009), and *Tn Number Registry* (Roberts et al., 2008). Multiple and pairwise sequence comparisons were performed using *MUSCLE* 3.8.31 (Edgar, 2004) and *BLASTN*, respectively. Gene organization diagrams were drawn in *Inkscape* 0.48.1[1].

Phylogenetic Analysis

The nucleotide sequences of *repZ* coding regions of indicative plasmids were aligned using *MUSCLE* 3.8.31 (Edgar, 2004). Unrooted neighbor-joining trees were generated from aligned *repZ* sequences using *MEGA7* (Kumar et al., 2016), and evolutionary distances were estimated using maximum composite likelihood method, with a bootstrap iteration of 1000.

Plasmid Conjugal Transfer

Plasmid conjugal transfer experiments were carried out with the rifampin-resistant *E. coli* EC600 or the sodium azide-resistant *E. coli* J53 being used as a recipient and each of the 14E509, 11011 and 61806 isolates as a donor. Three milliliters of overnight cultures of each of donor and recipient bacteria were mixed together, harvested and resuspended in 80 μl of Brain Heart Infusion (BHI) broth (BD Biosciences, NJ, United States). The mixture was spotted on a 1 cm^2 hydrophilic nylon membrane filter with a 0.45 μm pore size (Millipore, MA, United States) that was placed on BHI agar (BD Biosciences, NJ, United States) plate and then incubated for mating at 37°C for 12 to 18 h. Bacteria were washed from filter membrane and spotted on

[1]https://inkscape.org/en/

Muller–Hinton (MH) agar (BD Biosciences, NJ, United States) plates containing 1000 μg/ml rifampin or 200 μg/ml sodium azide together with 200 μg/ml ampicillin for selecting an *E. coli* transconjugant that carrying bla_{CTX-M}.

Double-Disk Synergy Test

To detect ESBL activity, the double-disk synergy test was performed as recommended by the National Committee for Clinical and Laboratory Standards Institute (CLSI) guideline (CLSI, 2015). Briefly, the bacterial strains tested were spread onto MH agar plates and four disks containing cefotaxime (30 μg), ceftazidime (30 μg), cefotaxime (30 μg) plus clavulanic acid (10 μg), and ceftazidime (30 μg) plus clavulanic acid (10 μg) were applied to each agar plate. The agar plates were incubated overnight at 37°C, and the production of ESBL was inferred when the zone of either cephalosporin was ≥5 mm larger than those without clavulanic acid.

Bacterial Antimicrobial Susceptibility Test

Bacterial antimicrobial susceptibility was tested by BioMérieux VITEK 2 and interpreted as per the Clinical and Laboratory Standards Institute (CLSI) guidelines (CLSI, 2015).

Nucleotide Sequence Accession Numbers

The complete sequence of plasmids p14E509-CTXM, p11011-CTXM, p205880-NR2, and p61806-CTXM were submitted to GenBank under accession numbers MG764547, MF344575, MF344577, and MF344576, respectively.

RESULTS AND DISCUSSION

Replicon-Based Typing of IncI-Complex Plasmids

To better understand the evolutionary relationship of IncI-complex plasmids, a phylogenetic tree (**Figure 1**) was constructed from the nucleotide sequences of *repZ* (replication initiation) coding regions of 66 representative (arbitrarily selected) sequenced IncI-complex plasmids (**Supplementary Table S1**). These 66 plasmids could be divided into four separately clustering subgroups, namely IncI2, IncI1/B/O, IncIγ/K1, and IncK2/Z, the last three of which were combined from IncI1 and IncB/O, IncIγ and IncK1, and IncK2 and IncZ, respectively. As shown by pairwise comparison of *repZ* sequences, plasmids within each of these four subgroups shared >95% nucleotide identity, by contrast <95% sequence identity was observed between different subgroups (**Supplementary Table S2**).

Putative iterons (RepZ-binding sites) were found to be located 176 to 301 bp downstream of *repZ* for all these 66 plasmids analyzed (**Supplementary Table S1**). Plasmids within each of these four subgroups shared a conserved iteron motif (**Figure 1**) and an identical iteron copy number (**Supplementary Table S1**). Iteron motifs from different subgroups dramatically differed from one another except for IncIγ/K1 and IncI1/B/O (these two had very similar iteron motifs). IncK2/Z plasmids had two copy numbers of iteron, while plasmids of all the other subgroups had three copy numbers.

Plasmid compatibility among original seven subgroups of IncI-complex had been partially validated experimentally (Praszkier et al., 1991; Rozwandowicz et al., 2017). IncIγ reference plasmid R621a was compatible with IncI1 plasmids (Bird and Pittard, 1982), and IncK2 plasmids was compatible with IncK1 reference plasmid pCT and IncB/O reference plasmid pR3521 (Rozwandowicz et al., 2017). IncZ plasmids were compatible with IncK1, IncIγ and IncI1 plasmids (Praszkier and Pittard, 2005). Plasmid compatibility among the four IncI-complex subgroups IncIγ/K1, IncI1/B/O, IncK2/Z, and IncI2 needed to be elucidated.

Overview of Sequenced IncIγ/K1 Plasmids

The four IncIγ/K1 plasmids p14E509-CTXM, p11011-CTXM, p61806-CTXM, and p205880-NR2 sequenced in the present work varied in size from about 83 kb to nearly 132 kb with variation in corresponding number of predicted ORFs (**Table 1**). The former three plasmids integrated various accessory modules (defined as acquired DNA regions associated with or bordered by mobile elements), which harbored resistance genes and metabolic gene clusters, and associated unit transposons, insertion sequence (IS)-based transposition units and individual IS elements. By contrast, p205880-NR2 contained no resistance genes or accessory modules (**Table 1** and **Supplementary Figure S1**), thereby representing a prototype IncIγ/K1 plasmid.

These four IncIγ/K1 plasmids, together with pCT (IncIγ/K1 reference), R721 (IncI2 reference), R64 (IncI1/B/O reference) and pO26-CRL-125 (IncK2/Z reference), were included in a genomic comparison. Considerable modular and sequence diversity were found among the backbones of these eight plasmids (**Supplementary Table S3** and **Figure 2**). IncIγ/K1 plasmids p61806-CTXM and pCT shared >99% nucleotide identity across >81% of their backbone sequences. IncIγ/K1 plasmids p14E509-CTXM, p11011-CTXM and p205880-NR2, and IncI1/B/O plasmid R64 shared >99% nucleotide identity across >74% of their backbone sequences. pCT and IncK2/Z plasmid pO26-CRL-125 shared >95% nucleotide identity over >70% of their backbone sequences. The backbone of IncI2 plasmid R721 displayed very low level (<3% BLAST coverage and >82% nucleotide identity) of sequence identity to the other seven plasmids.

Each of these eight plasmids had its unique backbone genes or gene loci, especially including those in the maintenance regions. All these plasmids shared the backbone genes or gene loci *inc-repY-repZ-CIS-oriV*-ter (plasmid replication), *parA* (maintenance), and *nicA*, *rlx*, *rci*, *pil* and *tra* (conjugal transfer) and also the conserved gene organization in the replication and conjugal transfer regions, but with remarkable nucleotide and amino acid diversity among different subgroups.

Notably, p61806-CTXM and pCT had IncIγ/K1-type conjugal transfer regions, while p14E509-CTXM, p11011-CTXM and p205880-NR2 had IncI1/B/O-type conjugal transfer regions

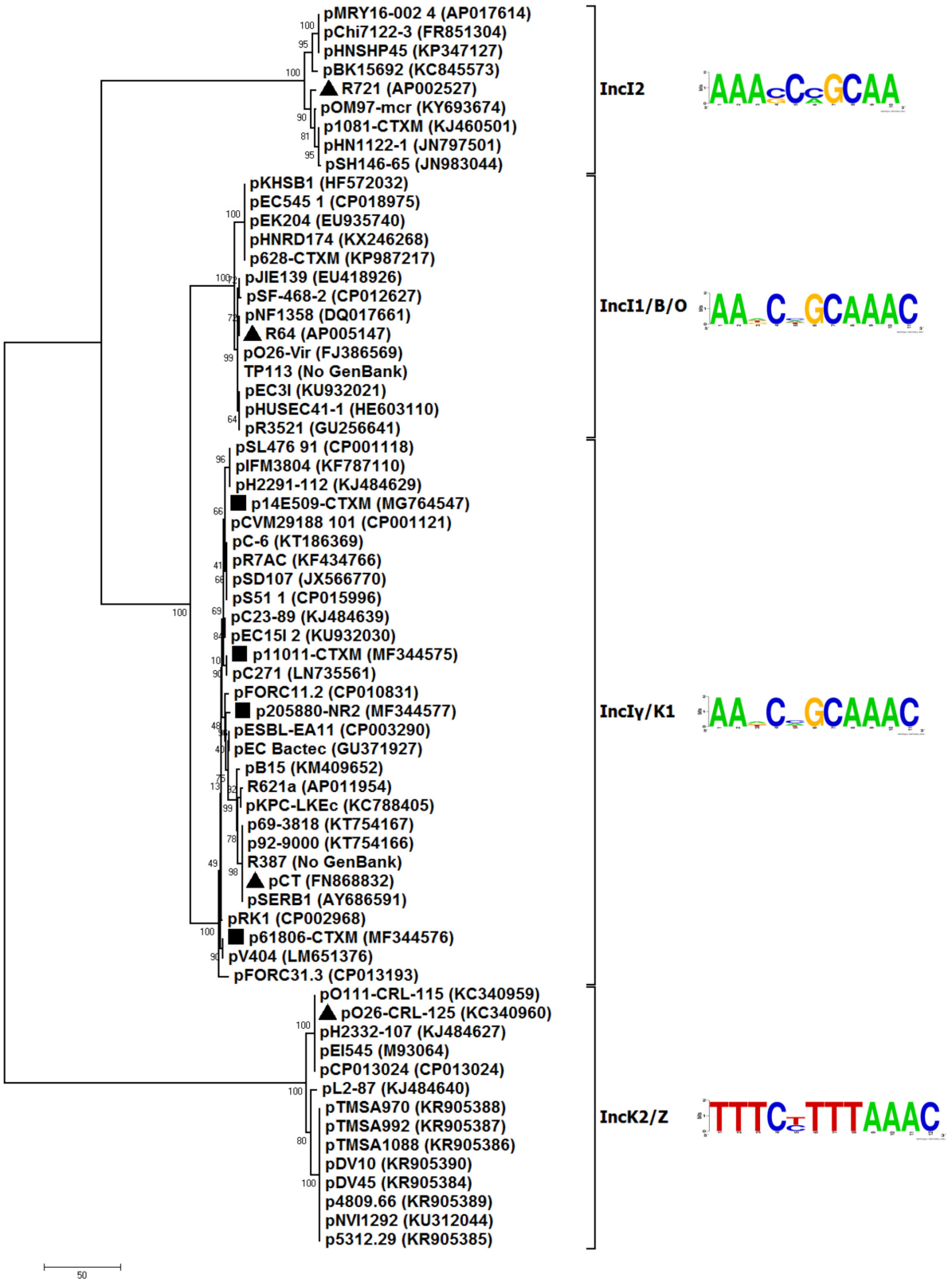

FIGURE 1 | Neighbor-joining phylogenetic tree. The degree of support (percentage) for each cluster of associated taxa, as determined by bootstrap analysis, is shown next to each branch. The bar corresponds to the scale of sequence divergence. Triangles indicate reference plasmids for IncIγ/K1, IncI2, IncI1/B/O, and IncK2/Z subgroups, while squares denote four plasmids sequences in this study.

TABLE 1 | Major features of plasmids analyzed.

Category	IncI1/B/O plasmid	IncIγ/K1 plasmids					IncK2/Z plasmid	IncI2 plasmid
	R64[@]	p205880-NR2[$]	p14E509-CTXM[$]	p11011-CTXM[$]	p61806-CTXM[$]	pCT[@]	pO26-CRL-125[@]	R721[@]
Total length (bp)	120,826	82,822	112,544	131,779	104,270	93,629	124,908	75,582
Total number of ORFs	142	100	128	159	138	119	141	109
Mean G+C content, %	49.6%	50.3%	50.1%	50.9%	52.5%	52.7%	53.3%	42.6%
Length of backbone sequence (bp)	103,582	82,822	99,279	97,310	94,485	83,915	96,005	60,062
Accessory modules	IS*2*:Tn*5393l* region[#]	Not found	$bla_{CTX-M-14}$-containing region[#]	$bla_{CTX-M-65}$-containing region[#]	$bla_{CTX-M-14}$-containing region[#], and Δ*IS26*	$bla_{CTX-M-14}$-containing region[#], IS*Kox3*, IS*Cro1*, and IS*Sso4*	Tn*6414*-ΔTn*1721* region[#]	Tn*7*[#], and IS*150*
	Do not carrying bla_{CTX-M} genes			Carrying $bla_{CTX-M-14or65}$ genes			Do not carrying bla_{CTX-M} genes	

[$], *sequenced in this study;* [@], *reference plasmids derived from GenBank;* [#], *carrying resistance genes. The sequence of each plasmid was divided into one or more accessory modules (defined as acquired DNA regions associated with or bordered by mobile elements) and the remaining backbone regions.*

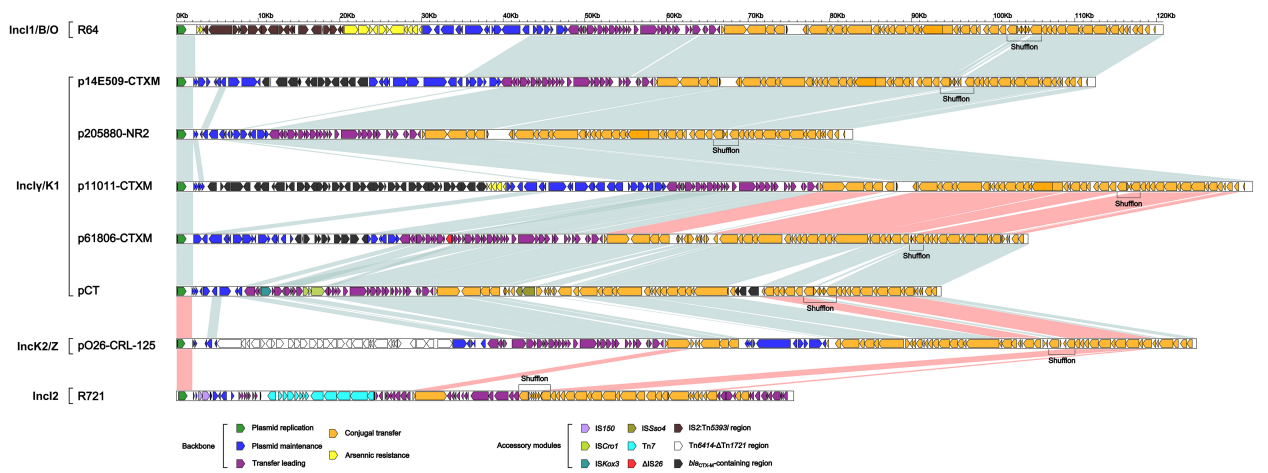

FIGURE 2 | Linear comparison of sequenced plasmids. Genes are denoted by arrows and colored based on gene function classification. Shading regions denote regions of homology (light blue: >95% nucleotide identity; light red: very low nucleotide identity with conserved gene functions).

as observed in R64. It was speculated that homologous recombination-mediated horizontal transfer of conjugal transfer regions occurred between IncIγ/K1 and IncI1/B/O.

Accessory Modules

p14E509-CTXM, p11011-CTXM, p61806-CTXM, pCT, R721, R64 and pO26-CRL-125 carried different profiles of accessory modules (**Table 1**). R721 harbored two separate accessory modules, namely Tn*7* (see reference Zhan et al., 2018 for gene organization) and IS*150*. R64 contained a single 17.2 kb accessory module, designated the IS*2*:Tn*5393l* region, which was generated from insertion of Tn*5393l* [a novel derivative of prototype Tn*5393c* (Cain and Hall, 2011)] into IS*2* (**Supplementary Figure S2**). pO26-CRL-125 contained a 28.9 kb Tn*6414*-ΔTn*1721* region (as its sole accessory module) with a Tn*6414*-$oriV_{IncP-1\alpha}$-ΔTn*1721* structure (**Supplementary Figure S3**). Tn*6414* was a novel derivative of Tn*21*, which was resulted from insertion of In2 into a backbone structure carrying the core transposition module *tnpAR-res-tnpM* together with the *mer* locus. Tn*6414* differed from Tn*21* by insertion of In13 instead of In2. In13 is atypical due to integration of two overlapping transposons Tn*6029* and Tn*4325* downstream of the *dfrA5* single-gene cassette.

IncI-complex plasmids carry a wide range of resistance genes (**Supplementary Table S4**), among which extended-spectrum β-lactamase (ESBL) genes are often identified. Indeed, each of the four IncIγ/K1 plasmids p14E509-CTXM, pCT, p61806-CTXM, and p11011-CTXM carried a bla_{CTX-M}-containing

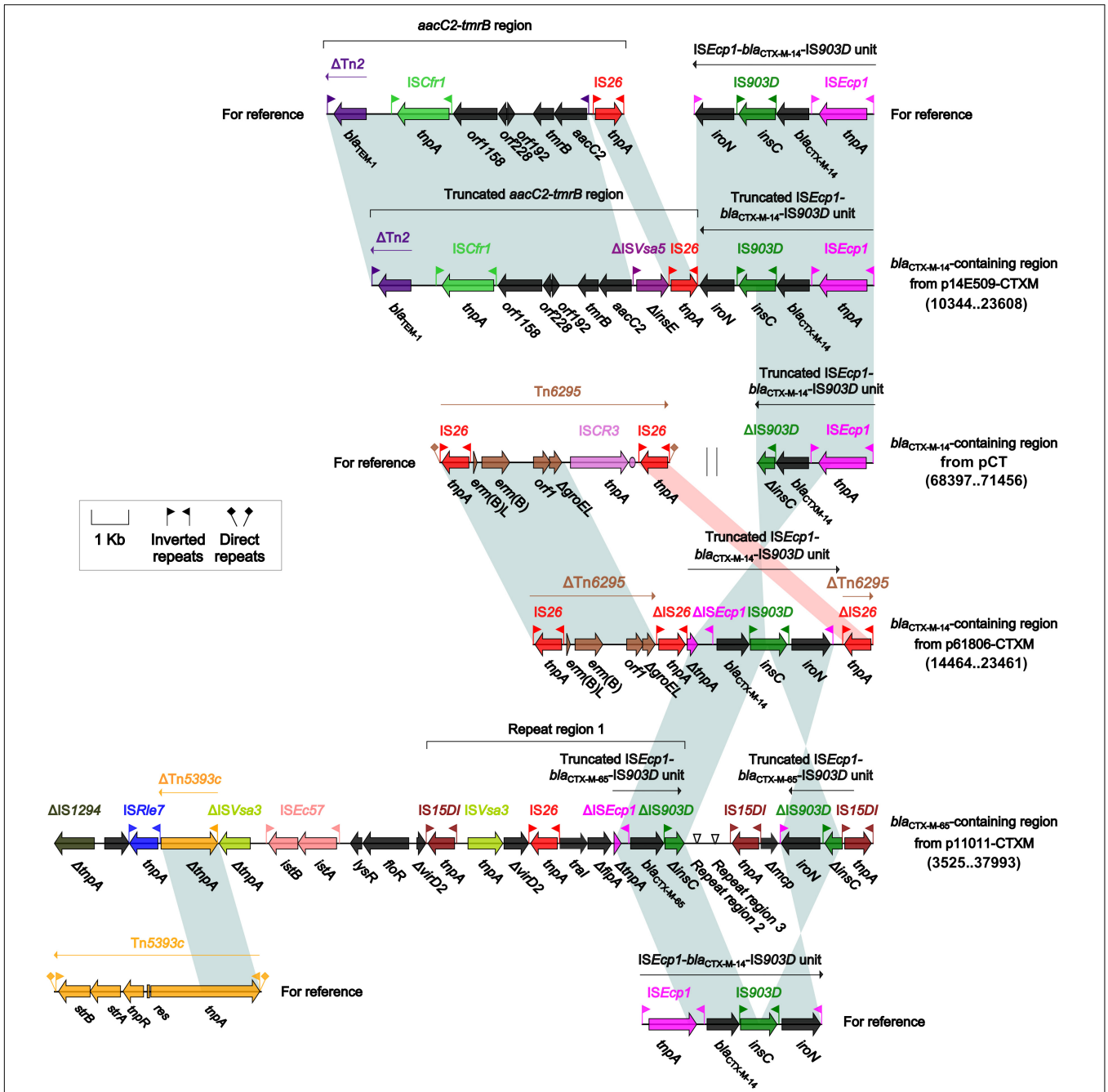

FIGURE 3 | bla_{CTX-M}-containing regions. Genes are denoted by arrows. Genes, mobile elements and other features are colored based on function classification. Shading denotes regions of homology (>95% nucleotide identity). Numbers in brackets indicate nucleotide positions within corresponding plasmids. The accession numbers of the *aacC2–tmrB* region, the *ISEcp1–bla*$_{CTX-M-14}$–IS*903D* unit, Tn*6295* and Tn*5393c* for reference are JX101693, KP987215, KX646543, and AF262622, respectively.

region (**Figure 3**); besides, individual IS elements were found as additional accessory modules: IS*Kox3*, IS*Cro1*, and IS*Sso4* in pCT, and ΔIS*26* in p61806-CTXM. In these four bla_{CTX-M}-containing regions, different truncated versions of prototype IS*Ecp1-bla*$_{CTX-M-14\text{ or }65}$-IS*903D* unit were connected with additional resistance regions: truncated *aacC2-tmrB* region in p14E509-CTXM, ΔTn*6295* in p61806-CTXM, and the other three copies of truncated IS*Ecp1-bla*$_{CTX-M-14\text{ or }65}$-IS*903D* unit in p11011-CTXM. Complex homologous recombination, which was probably mediated by the common region IS*15DI*, would be involved in assembly of these repeated bla_{CTX-M}-containing regions. Connection of bla_{CTX-M}-containing regions with additional resistance regions led to MDR of p14E509-CTXM and p11011-CTXM.

Transferability and Antimicrobial Susceptibility

The bla_{CTX-M}-carrying plasmids p14E509-CTXM, p11011-CTXM and p61806-CTXM could be transferred from the wild-type isolates into *E. coli* J53 or EC600 through conjugation, generating three transconjugants 14E509-CTXM-J53, 11011-CTXM-EC600 and 61806-CTXM-EC600, respectively. All these three transconjugants had the ESBL activity (data not shown) and, as expected, were resistant to ampicillin, piperacillin, cefazolin, cefuroxime and ceftazidime but remained susceptible to ampicillin/sulbactam, piperacillin/tazobactam, imipenem and meropenem (**Supplementary Table S5**).

ETHICS STATEMENT

The use of human specimens and all related experimental protocols were approved by the Committee on Human Research of the Henan Provincial People's Hospital, Ningbo Medical Treatment Center Lihuili Hospital, the First Affiliated Hospital of Henan University, and the First Affiliated Hospital of Chongqing Medical University, and carried out in accordance with the approved guidelines. The research involving biohazards and all related procedures were approved by the Biosafety Committee of the Beijing Institute of Microbiology and Epidemiology.

AUTHOR CONTRIBUTIONS

DsZ and ZY conceived the study and designed experimental procedures. DfZ, YZ, JF, LH, and XJ performed the experiments. ZZ, HY, WY, BG, JW, and JL analyzed the data. ZZ, YZ, and JF contributed reagents and materials. DsZ, ZY, DfZ and YZ wrote this manuscript.

FUNDING

This work was supported by the National Key Program (2018ZX10733402) for Infectious Diseases of China and the National Key R&D Program of China (2018YFC1200100).

SUPPLEMENTARY MATERIAL

The Supplementary Material for this article can be found online at: https://www.frontiersin.org/articles/10.3389/fmicb.2019.00048/full#supplementary-material

FIGURE S1 | Plasmid schematic maps. Genes are denoted by arrows, and the backbone and accessory module regions are highlighted in black and gray, respectively. The innermost circle presents GC-skew [(G−C)/(G+C)], with a window size of 500 bp and a step size of 20 bp. The next-to-innermost circle presents GC content.

FIGURE S2 | The IS*2*:Tn*5393*/ region from R64. Genes are denoted by arrows. Genes, mobile elements and other features are colored based on function classification.

FIGURE S3 | The MDR region from pO26-CRL-125. Genes are denoted by arrows. Genes, mobile elements and other features are colored based on function classification. Shading denotes regions of homology (>95% nucleotide identity). Numbers in brackets indicate nucleotide position within pO26-CRL-125. The accession numbers of Tn*1721* and Tn*21* for reference are X61367 and AF071413, respectively.

REFERENCES

Bird, P. I., and Pittard, J. (1982). An unexpected incompatibility interaction between two plasmids belonging to the I compatibility complex. *Plasmid* 8, 211–214. doi: 10.1016/0147-619X(82)90059-2

Boetzer, M., and Pirovano, W. (2012). Toward almost closed genomes with GapFiller. *Genome Biol.* 13:R56. doi: 10.1186/gb-2012-13-6-r56

Bolger, A. M., Lohse, M., and Usadel, B. (2014). Trimmomatic: a flexible trimmer for Illumina sequence data. *Bioinformatics* 30, 2114–2120. doi: 10.1093/bioinformatics/btu170

Boratyn, G. M., Christiam, C., Cooper, P. S., George, C., Amelia, F., Ning, M., et al. (2013). BLAST: a more efficient report with usability improvements. *Nucleic Acids Res.* 41, 29–33. doi: 10.1093/nar/gkt282

Boutet, E., Lieberherr, D., Tognolli, M., Schneider, M., Bansal, P., Bridge, A. J., et al. (2016). UniProtKB/Swiss-Prot, the manually annotated section of the uniprot knowledgebase: how to use the entry view. *Methods Mol. Biol.* 1374, 23–54. doi: 10.1007/978-1-4939-3167-5_2

Bradley, D. E. (1984). Characteristics and function of thick and thin conjugative pili determined by transfer-derepressed plasmids of incompatibility groups I1, I2, I5, B, K and Z. *J. Gen. Microbiol.* 130, 1489–1502. doi: 10.1099/00221287-130-6-1489

Brettin, T., Davis, J. J., Disz, T., Edwards, R. A., Gerdes, S., Olsen, G. J., et al. (2015). RASTtk: a modular and extensible implementation of the RAST algorithm for building custom annotation pipelines and annotating batches of genomes. *Sci. Rep.* 5:8365. doi: 10.1038/srep08365

Cain, A. K., and Hall, R. M. (2011). Transposon Tn5393e carrying the aphA1-containing transposon Tn6023 upstream of strAB does not confer resistance to streptomycin. *Microb. Drug Resist.* 17, 389–394. doi: 10.1089/mdr.2011.0037

CLSI (2015). *Performance Standards for Antimicrobial Susceptibility Testing: Twenty-Fifth Informational Supplement M100-S25*. Wayne, PA: Clinical and Laboratory Standards Institute.

Cottell, J. L., Webber, M. A., Coldham, N. G., Taylor, D. L., Cerdeno-Tarraga, A. M., Hauser, H., et al. (2011). Complete sequence and molecular epidemiology of IncK epidemic plasmid encoding blaCTX-M-14. *Emerg. Infect. Dis.* 17, 645–652. doi: 10.3201/eid1704.101009

Edgar, R. C. (2004). MUSCLE: multiple sequence alignment with high accuracy and high throughput. *Nucleic Acids Res.* 32, 1792–1797. doi: 10.1093/nar/gkh340

Hackl, T., Hedrich, R., Schultz, J., and Forster, F. (2014). proovread: large-scale high-accuracy PacBio correction through iterative short read consensus. *Bioinformatics* 30, 3004–3011. doi: 10.1093/bioinformatics/btu392

Jia, B., Raphenya, A. R., Alcock, B., Waglechner, N., Guo, P., Tsang, K. K., et al. (2017). CARD 2017: expansion and model-centric curation of the comprehensive antibiotic resistance database. *Nucleic Acids Res.* 45, D566–D573. doi: 10.1093/nar/gkw1004

Komano, T., Kim, S. R., Yoshida, T., and Nisioka, T. (1994). DNA rearrangement of the shufflon determines recipient specificity in liquid mating of IncI1 plasmid R64. *J. Mol. Biol.* 243, 6–9. doi: 10.1006/jmbi.1994.1625

Komano, T., Kubo, A., and Nisioka, T. (1987). Shufflon: multi-inversion of four contiguous DNA segments of plasmid R64 creates seven different open reading frames. *Nucleic Acids Res.* 15, 1165–1172. doi: 10.1093/nar/15.3.1165

Kumar, S., Stecher, G., and Tamura, K. (2016). MEGA7: molecular evolutionary genetics analysis version 7.0 for bigger datasets. *Mol. Biol. Evol.* 33, 1870–1874. doi: 10.1093/molbev/msw054

Moura, A., Soares, M., Pereira, C., Leitão, N., Henriques, I., and Correia, A. (2009). INTEGRALL: a database and search engine for integrons, integrases and gene cassettes. *Bioinformatics* 25, 1096–1098. doi: 10.1093/bioinformatics/btp105

Nederbragt, A. J. (2014). On the middle ground between open source and commercial software - the case of the Newbler program. *Genome Biol.* 15:113. doi: 10.1186/gb4173

O'Leary, N. A., Wright, M. W., Rodney, B. J., Stacy, C., Diana, H., Rich, M. V., et al. (2016). Reference sequence (RefSeq) database at NCBI: current status, taxonomic expansion, and functional annotation. *Nucleic Acids Res.* 44, D733–D745. doi: 10.1093/nar/gkv1189

Papagiannitsis, C. C., Tzouvelekis, L. S., Kotsakis, S. D., Tzelepi, E., and Miriagou, V. (2011). Sequence of pR3521, an IncB plasmid from *Escherichia coli* encoding ACC-4, SCO-1, and TEM-1 β-Lactamases. *Antimicrob. Agents Chemother.* 55, 376–381. doi: 10.1128/AAC.00875-10

Praszkier, J., and Pittard, A. J. (2005). Control of replication in I-complex plasmids. *Plasmid* 53, 97–112. doi: 10.1016/j.plasmid.2004.12.005

Praszkier, J., Wei, T., Siemering, K., and Pittard, J. (1991). Comparative analysis of the replication regions of IncB, IncK, and IncZ plasmids. *J. Bacteriol.* 173, 2393–2397. doi: 10.1128/jb.173.7.2393-2397.1991

Roberts, A. P., Chandler, M., Courvalin, P., Guedon, G., Mullany, P., Pembroke, T., et al. (2008). Revised nomenclature for transposable genetic elements. *Plasmid* 60, 167–173. doi: 10.1016/j.plasmid.2008.08.001

Rozwandowicz, M., Brouwer, M. S. M., Zomer, A. L., Bossers, A., Harders, F., Mevius, D. J., et al. (2017). Plasmids of distinct IncK lineages show compatible phenotypes. *Antimicrob. Agents Chemother.* 61:e01954-16. doi: 10.1128/AAC.01954-16

Sampei, G., Furuya, N., Tachibana, K., Saitou, Y., Suzuki, T., Mizobuchi, K., et al. (2010). Complete genome sequence of the incompatibility group I1 plasmid R64. *Plasmid* 64, 92–103. doi: 10.1016/j.plasmid.2010.05.005

Siguier, P., Perochon, J., Lestrade, L., Mahillon, J., and Chandler, M. (2006). ISfinder: the reference centre for bacterial insertion sequences. *Nucleic Acids Res.* 34, 32–36. doi: 10.1093/nar/gkj014

Tschäpe, H., and Tietze, E. (2010). Characterization of conjugative plasmids belonging to a new incompatibility group (IncZ). *J. Basic Microbiol.* 23, 393–401.

Venturini, C., Hassan, K. A., Roy Chowdhury, P., Paulsen, I. T., Walker, M. J., and Djordjevic, S. P. (2013). Sequences of two related multiple antibiotic resistance virulence plasmids sharing a unique IS26-related molecular signature isolated from different *Escherichia coli* pathotypes from different hosts. *PLoS One* 8:e78862. doi: 10.1371/journal.pone.0078862

Zankari, E., Hasman, H., Cosentino, S., Vestergaard, M., Rasmussen, S., Lund, O., et al. (2012). Identification of acquired antimicrobial resistance genes. *J. Antimicrob. Chemother.* 67, 2640–2644. doi: 10.1093/jac/dks261

Zhan, Z., Hu, L., Jiang, X., Zeng, L., Feng, J., Wu, W., et al. (2018). Plasmid and chromosomal integration of four novel blaIMP-carrying transposons from *Pseudomonas aeruginosa*, *Klebsiella pneumoniae* and an *Enterobacter* sp. *J. Antimicrob. Chemother.* 73, 3005–3015. doi: 10.1093/jac/dky288

Conflict of Interest Statement: The authors declare that the research was conducted in the absence of any commercial or financial relationships that could be construed as a potential conflict of interest.

frontiers in Microbiology

ORIGINAL RESEARCH
published: 12 February 2019
doi: 10.3389/fmicb.2019.00211

Characterization of Clinically Relevant Strains of Extended-Spectrum β-Lactamase-Producing *Klebsiella pneumoniae* Occurring in Environmental Sources in a Rural Area of China by Using Whole-Genome Sequencing

Xiaohui Chi[1†], *Björn Berglund*[2,3†], *Huiyun Zou*[1], *Beiwen Zheng*[3], *Stefan Börjesson*[2,4], *Xiang Ji*[1], *Jakob Ottoson*[5], *Cecilia Stålsby Lundborg*[6], *Xuewen Li*[1*] and *Lennart E. Nilsson*[2]

[1] Department of Environment and Health, School of Public Health, Shandong University, Jinan, China, [2] Department of Clinical and Experimental Medicine, Linköping University, Linköping, Sweden, [3] State Key Laboratory for Diagnosis and Treatment of Infectious Disease, Collaborative Innovation Center for Diagnosis and Treatment of Infectious Diseases, The First Affiliated Hospital, College of Medicine, Zhejiang University, Hangzhou, China, [4] Department of Animal Health and Antimicrobial Strategies, National Veterinary Institute, Uppsala, Sweden, [5] Department of Risk and Benefit Assessment, National Food Agency, Uppsala, Sweden, [6] Department of Public Health Sciences, Global Health—Health Systems and Policy, Medicines, Focusing Antibiotics, Karolinska Institutet, Stockholm, Sweden

Klebsiella pneumoniae is a gram-negative, opportunistic pathogen, and a common cause of healthcare-associated infections such as pneumonia, septicemia, and urinary tract infection. The purpose of this study was to survey the occurrence of and characterize *K. pneumoniae* in different environmental sources in a rural area of Shandong province, China. Two hundred and thirty-one samples from different environmental sources in 12 villages were screened for extended-spectrum β-lactamase-(ESBL)-producing *K. pneumoniae*, and 14 (6%) samples were positive. All isolates were multidrug-resistant and a few of them belonged to clinically relevant strains which are known to cause hospital outbreaks worldwide. Serotypes, virulence genes, serum survival, and phagocytosis survival were analyzed and the results showed the presence of virulence factors associated with highly virulent clones and a high degree of phagocytosis survivability, indicating the potential virulence of these isolates. These results emphasize the need for further studies designed to elucidate the role of the environment in transmission and dissemination of ESBL-producing *K. pneumoniae* and the potential risk posed to human and environmental health.

Keywords: *Klebsiella pneumoniae*, extended-spectrum β-lactamase, environment, feces, water, multilocus sequence typing, pulsed-field gel electrophoresis, whole-genome sequencing

OPEN ACCESS

Edited by:
Charles W. Knapp, University of Strathclyde, United Kingdom

Reviewed by:
Miguel A. De la Cruz, Mexican Social Security Institute (IMSS), Mexico
Haijian Zhou, National Institute for Communicable Disease Control and Prevention (CDC), China

***Correspondence:**
Xuewen Li
lxw@sdu.edu.cn

[†]*These authors have contributed equally to this work*

Specialty section:
This article was submitted to Antimicrobials, Resistance and Chemotherapy, a section of the journal Frontiers in Microbiology

Received: *30 September 2018*
Accepted: *24 January 2019*
Published: *12 February 2019*

Citation:
Chi X, Berglund B, Zou H, Zheng B, Börjesson S, Ji X, Ottoson J, Stålsby Lundborg C, Li X and Nilsson LE (2019) Characterization of Clinically Relevant Strains of Extended-Spectrum β-Lactamase-Producing Klebsiella pneumoniae Occurring in Environmental Sources in a Rural Area of China by Using Whole-Genome Sequencing. Front. Microbiol. 10:211. doi: 10.3389/fmicb.2019.00211

INTRODUCTION

The increasing prevalence of antibiotic resistance among bacteria worldwide has become a major issue affecting the global public health (Grundmann, 2014). Extended-spectrum β-lactamases (ESBLs) are a group of enzymes that can hydrolyze penicillins, cephalosporins, and aztreonam, and is one of the main resistance determinants causing resistance to extended-spectrum β-lactam antibiotics in gram-negative bacteria. The main types of ESBLs are SHV, TEM, and CTX-M, the latter of which has become the main epidemic genotype worldwide.

Klebsiella pneumoniae is a gram-negative, opportunistic pathogen commonly associated with health-care associated infections (HAIs) such as pneumonia, septicemia, and urinary tract infections (Lee et al., 2012). *K. pneumoniae* has a high capacity to acquire mobile genetic elements such as plasmids containing antibiotic resistance genes (Burmolle et al., 2012). Because of the selection pressure exerted by a widespread use of antibiotics, strains of *K. pneumoniae* endemic at hospitals are often multidrug-resistant (Magiorakos et al., 2012), and treatment of HAIs caused by these strains are often difficult (Hou et al., 2015; Huang et al., 2015). Particularly problematic are strains of *K. pneumoniae* which are resistant to the last-resort antibiotics carbapenems (Little et al., 2014; Tijet et al., 2014; Cubero et al., 2016). For these reasons, monitoring of *K. pneumoniae* in the clinics is essential in the management of HAIs.

In recent years, the environment has been highlighted as an important factor in the dissemination of antibiotic-resistant bacteria and antibiotic resistance genes (Machado and Bordalo, 2014). An important factor in facilitating the dissemination of antibiotic resistance is likely selection pressures exerted by antibiotic residues in waste from anthropogenic wastewater and discharge from animal production facilities. The impact and effect of environmental contamination of antibiotic-resistant bacteria on human and environmental health has not yet been fully elucidated. A first step to determining this is to survey, monitor, and characterize the clinically important bacteria with clinically relevant antibiotic resistance determinants occurring in the environment, however, data on the occurrence and characteristics of ESBL-producing *K. pneumoniae* in environmental sources is scarce. Additionally, the few studies performed usually focus on prevalence in a single environmental matrix such as a body of water or animal manure (Mollenkopf et al., 2013; Zhang et al., 2015), and whole-genome characterization of the isolates are lacking (Zadoks et al., 2011; Ben Said et al., 2015).

In the current study, we screened 231 environmental samples for ESBL-producing *K. pneumoniae* and performed whole-genome sequencing on the 14 positive isolates detected, in order to survey the occurrence of and characteristics of this bacterial pathogen in different environmental sources in a rural area of Shandong province, China.

MATERIALS AND METHODS

Sample Collection

Samples were collected in a rural area of Shandong Province, China, in July 2015 (**Figure 1**). Details of the sampling procedure have been described elsewhere (Sun et al., 2018). Pig manure, wild bird feces, vegetables (cucumber, beans, and chives), and environmental samples were collected with ESwab tubes (Copan, Brescia, Italy) from the study villages. Sample types included: pig manure ($n = 30$), wastewater ($n = 42$), soil ($n = 23$), vegetables ($n = 23$), outlet sediment ($n = 14$), drinking water ($n = 44$), river water ($n = 25$), river sediment ($n = 24$), and feces from

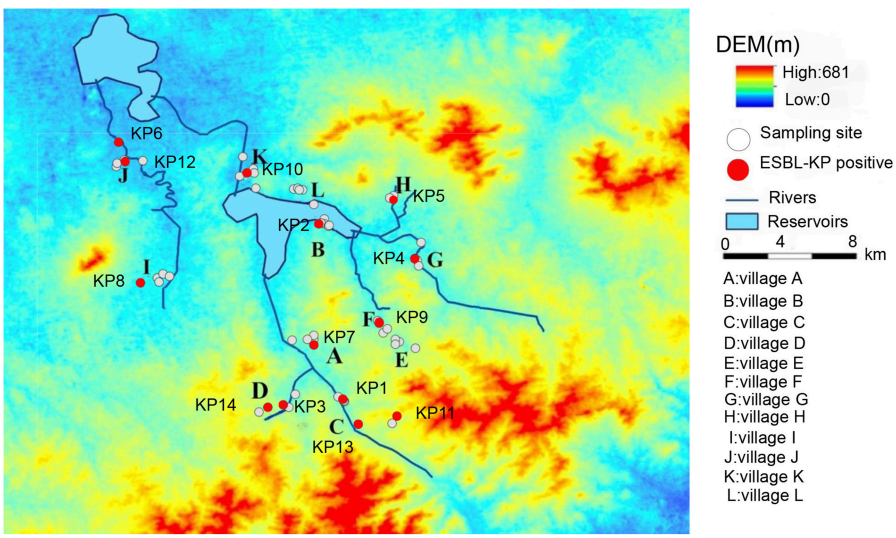

FIGURE 1 | Map showing village locations (A–L) and the surrounding area in a region of rural Shandong, China, where 231 environmental samples were collected for screening for ESBL-producing *K. pneumoniae*. White spots denote locations where samples were negative for ESBL-producing *K. pneumoniae* and red spots denote locations were samples were positive for ESBL-producing *K. pneumoniae*.

wild birds ($n = 6$). All samples were put in cool-boxes with ice-packs (4–8°C) upon collection and were transported for ∼6 h to Shandong Center for Disease Control and Prevention (Jinan). Upon arrival, all samples were put in long-term storage at −80°C until cultivation.

Cultivation of Samples and Screening for ESBL-Producing *K. pneumoniae*

Prior to cultivation, the samples were collected from the low temperature freezers and allowed to reach room temperature. All samples were screened for ESBL-producing *K. pneumoniae* by cultivation on ChromID ESBL agar (bioMérieux, Marcy l'Etoile, France). For water, soil, river sediment, and vegetable samples, a pre-enrichment step in 2–3 ml Brain Heart Infusion Broth (BD, Sparks, USA) was performed overnight before being applied on the screening plates. Each sample was cultivated unselectively on a sheep blood agar plate (Babio, Jinan, China) to verify the viability of bacteria in the sample. All samples were applied on agar plates by a primary streak using the brush in the ESwab and then sub-streaked using a sterile 1 μl plastic loop. The agar plates were incubated for 18–24 h at 37°C. After incubation, growth was recorded and suspected *K. pneumoniae* colonies were identified based on color and morphology, according to the manufacturer's instructions (bioMérieux), sub-cultured on CHROMagar Orientation agar (CHROMagar Company, Paris, France), and incubated overnight at 37°C. From the CHROMagar Orientation agar, suspected *K. pneumoniae* were transferred to storage tubes with glycerol and stored in −80°C until further analyses. After applying samples on the respective agar plates, the remaining fluid in the ESwab tubes were transferred to 2 ml tubes and mixed with 30% glycerol for long-term storage at −80°C.

Verification of ESBL-Producing *K. pneumoniae*

Species confirmation of presumptive *K. pneumoniae* isolates were performed with matrix-assisted laser desorption ionization time-of-flight mass spectrometry (MALDI-TOF-MS) by using a Shimadzu with saramis premium (Shimadzu Corporation, Kyoto, Japan). ESBL-production was verified by using the double disc diffusion method using cefotaxime, ceftazidime, each alone, and in combination with clavulanic acid according to the manufacturer's protocol (Oxoid, Basingstoke, UK). *Klebsiella pneumoniae* ATCC700603 was used as control strain.

Antibiotic Susceptibility Testing of ESBL-Producing *K. pneumoniae*

The confirmed ESBL-producing isolates were cultured on blood agar overnight at 37°C and were subsequently tested for susceptibility to 17 different antibiotics listed in **Table 1**. Antibiotic susceptibility was determined by evaluating minimal inhibitory concentrations (MICs) obtained with the agar dilution method by using the protocol recommended by the Clinical and Laboratory Standards institute (CLSI). Susceptibility was determined in accordance with the European Committee on Antimicrobial Susceptibility Testing, breakpoint tables for interpretation of MICs and zone diameters version 8.1, 2018 (http://www.eucast.org) for all antibiotics except tetracycline and nitrofurantoin, for which CLSI breakpoints version 2017 were used. Since clinical breakpoints of florfenicol are not available for Enterobacteriaceae at EUCAST or CLSI, a resistance breakpoint of >16 mg/L, based on the epidemiological cut-off values for the closely related *Escherichia coli* and *Salmonella* spp. available at EUCAST, was used. Isolates were considered to be multidrug-resistant if resistant to antibiotics from more than two different classes of antibiotics (Magiorakos et al., 2012).

Determination of Clonal Relatedness With Pulsed-Field Gel Electrophoresis

The clonal relatedness of the ESBL-positive *K. pneumoniae* isolates was determined via pulsed-field gel electrophoresis (PFGE) as previously described (Chen et al., 2017).Briefly, DNA plugs were digested using XbaI restriction enzyme (Takara Bio Inc., Kyoto, Japan) for 2 h. PFGE was undertaken on a CHEF-DR III (Bio-Rad, Hercules, CA, USA) using the following parameters: running time 18 h, temperature 14°C, field strength 6 V/cm^2, angles 120°, initial pulse time 2.2 s, final pulse time 63.8 s. Two isolates were considered related to each other if the homology of the digested patterns was more than or equal to 80%.

Serum Bactericidal and Phagocytosis Assays

Serum bactericidal and phagocytosis assays were modified from previously described protocols (O'Shaughnessy et al., 2012; Kobayashi et al., 2016). In short, blood was venesected from 10 healthy persons for the serum bactericidal assay and from three healthy persons for the phagocytosis assay. The participants had provided written informed consent prior to participation in the study. Blood was left to clot at 4°C for 8 h, and subsequently centrifuged at 4°C. Inactivated serum was acquired by incubation in a water bath at 56°C for 30 min. Serum bactericidal assays were performed by adding 20 μL of bacterial suspension (10^8 cfu/mL) to 180 μL of normal or inactivated serum, and incubating the mixture at 37°C for 1 h after which the mixture was quickly placed on ice. From the reaction mixture, 50 μL were diluted 100-fold in PBS and viable count was performed by plating 100 μL on Mueller-Hinton agar and inoculating for 18–24 h. Serum bactericidal assays for each isolate were performed in duplicates at three separate times, and the survival rates were calculated as the ratios between the viable counts in the normal and inactivated serum, based on the means of the replicates.

For the phagocytosis assays; neutrophils were purified from the freshly drawn blood, and enumerated in a Neubauer chamber. Neutrophils were cultured in 24-well plates for 30 min. The phagocytosis assay was performed by adding either 10^6 neutrophils or an equal volume of autoclaved water (for the control experiments) to a mixture of 200 μL of bacterial suspension (10^8 cfu/mL), 100 μL of inactivated serum, and 600 μL phosphate-buffered saline, with subsequent incubation

TABLE 1 | Antibiotic susceptibility profiles of ESBL-producing *K. pneumoniae* of isolates from river water (RW), rivers sediment (RS), pig manure (PM), soil (S), and vegetables (V).

Isolate	Source	MIC (mg/L)[a]																
		CL	AMC	TZP	CTX	CAZ	MEM	ETP	IPM	GEN	AMK	TE	TGC	CIP	SXT	FOF	F	FFC
KP1	RW	0.125	**16**	**32**	2	2	0.015	0.015	0.25	**32**	4	**128**	2	**16**	**>16**	**256**	**256**	**>32**
KP2	RW	0.06	**16**	**256**	**8**	0.5	0.03	0.06	0.125	**32**	8	**128**	2	**16**	**>16**	**256**	**512**	**>32**
KP3	RW	0.125	**16**	**128**	**8**	**16**	0.015	0.015	0.06	**32**	2	**128**	2	**0.5**	**>16**	**128**	**256**	4
KP4	RW	0.125	**32**	**256**	**32**	1	0.015	0.015	0.125	**128**	2	**64**	2	**8**	**8**	**>256**	**256**	**>32**
KP5	RW	0.125	**32**	**256**	**>32**	1	0.03	0.015	0.125	1	2	**128**	2	**1**	**8**	**>256**	**256**	8
KP6	RW	0.125	**32**	**256**	**>32**	1	0.015	0.03	0.125	**64**	4	**128**	4	**16**	**8**	**256**	**256**	**>32**
KP7	PM	0125	**16**	**256**	**8**	0.5	0.015	0.06	0.125	**32**	4	**128**	2	**16**	**>16**	**256**	**256**	**>32**
KP8	PM	0.125	**16**	4	**8**	1	0.015	0.015	0.125	**16**	2	**128**	1	**4**	**8**	**256**	**128**	**32**
KP9	S	0.125	**32**	**256**	**4**	1	0.015	0.03	0.125	**64**	4	**128**	2	**8**	**8**	**512**	**256**	**>32**
KP10	S	0.06	**32**	**256**	**>32**	1	0.015	0.05	0.125	**64**	2	**128**	4	**0.5**	**8**	**>256**	64	2
KP11	V	0.125	**16**	**256**	**8**	1	0.015	0.015	0.125	**16**	2	**128**	1	**1**	**>16**	**256**	64	**>32**
KP12	V	0.06	**32**	**256**	**>32**	1	0.03	0.03	0.125	**>128**	8	**128**	2	**4**	**8**	**>256**	**256**	**>32**
KP13	RS	0.125	**16**	**256**	**8**	0.5	0.015	0.06	0.125	**32**	4	**128**	0.5	**16**	**>16**	**256**	**128**	**>32**
KP14	WW	0.125	**16**	**256**	**8**	1	0.015	0.03	0.06	**32**	4	**128**	1	**16**	**>16**	**256**	**512**	**>32**

Resistance is indicated in bold and intermediate is indicated in underlined. [a]*MICs were determined by agar dilution methods for all antibiotics except for colistin, for which broth microdilution was used. Resistance is indicated in bold. CL, colistin; AMC, amoxicillin/clavulanate; TZP, piperacillin/tazobactam; CTX, cefotaxime; CAZ, ceftazidime; MEM, meropenem; GEN, gentamicin; AMK, amikacin; TE, tetracycline; TGC, tigecycline, CIP, ciprofloxacin; SXT, trimethoprim/sulfamethoxazole; FOF, fosfomycin; F, nitrofurantoin; FFC, florfenicol. Antimicrobial susceptibility profiles were determined using clinical breakpoints recommended by the EUCAST criteria (http://www.eucast.org/clinical_breakpoints/), except for tetracycline and nitrofurantion, for which the Clinical and Laboratory Standards Institute (CLSI, 2017) breakpoints were used, and florfenicol, for which a resistance breakpoint of >16 mg/L, based on the epidemiological cut-off values for the closely related Escherichia coli and Salmonella spp. available at EUCAST, was used.*

of the mixture at 37°C for 1 h, followed by termination of the reaction by adding 100 μL 0.1% Triton X-100 (Shanghai Aladdin Biochemical Technology, Shanghai, China) and placing on ice for 15 min. Bacteria were enumerated by viable count performed by plating 100 μL of the reaction mixture, diluted 1000-fold dilution in PBS, on Mueller-Hinton agar plates, and inoculating for 18–24 h. Phagocytosis assays for each isolate were performed in duplicates at two separate times, and the survival rates were calculated as the ratios between the viable counts in the phagocytosis assay and the controls, based on the means of the replicates.

Whole-Genome Sequencing of ESBL-Producing *K. pneumoniae*

DNA of all ESBL-positive isolates was extracted from pure cultures of *K. pneumoniae* using a Gentra Puregene Yeast/Bact. Kit (QIAGEN, Hilden, Germany). Whole-genome sequencing was performed on the extracted DNA by Novogene (Beijing, China) using the Illumina HiSeq sequencing platform. Raw sequences were assembled by using SPAdes 3.11 (Anton et al., 2012) (**Table S1**) and annotated via RAST. All draft genomes were deposited at NCBI (accession number: RCGE00000000-RCGR00000000). Occurrence of antibiotic resistance genes and multilocus sequence typing (MLST) was performed by querying the databases at the Center for Genomic Epidemiology (www.genomicepidemiology.org). Lipopolysaccharide-based serotyping (O-type) and capsule polysaccharide-based serotyping (K-type) were performed by using Kaptive Web (Wick et al., 2018). Presence of virulence genes were determined by using the Institut Pasteur MLST and whole genome MLST databases (http://bigsdb.pasteur.fr/klebsiella/klebsiella.html). In addition, the operons encoding type 1 fimbriae (*fimABCDEFGHIK*) and type 3 fimbriae (*mrkABCDFHIJ*) were evaluated, as were the gene sequences for the outer membrane porins (OMPs) OmpK35 and OmpK36. *ompK36* allele group was determined based on genetic polymorphisms between bp 500 and 1,000, as previously described (Du et al., 2018). The genetic environment surrounding the CTX-M-type ESBL-genes were annotated and investigated using Easyfig 2.2.3. All genomes in the study dataset were annotated using the Prokka prokaryotic (Seemann, 2014) annotation pipeline, and using Roary: the Pan Genome Pipeline (Page et al., 2015) to obtain a system of linked qualified single nucleotide polymorphisms (SNPs) identified by mapping raw reads to core genes development.

Statistical Analysis

Mann-Whitney tests were used to determine differences in MICs for cefoxitin and ceftazidime between isolates carrying genes encoding CTX-M ESBLs of different groups. Viable counts from the serum bactericidal and phagocytosis assays were compared with their respective controls and differences were determined using repeated measures ANOVA with Bonferroni multiple comparison tests performed *post-hoc*. All statistical tests were carried out using Prism 5 for Windows.

RESULTS

Screening for ESBL-Producing *K. pneumoniae*

A total of 14 (6%) isolates of ESBL-producing *K. pneumoniae* were isolated from 231 environmental samples. The positive rate of ESBL-producing *K. pneumoniae* isolates in different environmental matrices were: river water 24% (6/25), soil 9% (2/23), vegetables 9% (2/23), pig manure 7% (2/30), river sediment 4% (1/24), and wastewater 2% (1/42). No isolates were detected in the sewage outlet sediment, drinking water, or wild bird fecal samples.

Antibiotic Susceptibility Testing

The antibiotic susceptibility testing (**Table 1**) showed that all isolates were susceptible to amikacin, colistin and the carbapenems meropenem, imipenem, and ertapenem. Susceptibility to ceftazidime was high (86%). None of the isolates were susceptible to cefotaxime, amoxicillin-clavulanic acid, ciprofloxacin, trimethoprim-sulfamethoxazole, tetracycline, nitrofurantoin or fosfomycin. Susceptibility rates to gentamicin (7%), piperacillin-tazobactam (7%), and florfenicol (21%) were low. The isolates showed a low (29%) susceptibility rate to tigecycline. All isolates were multidrug-resistant (i.e., resistant to antibiotics of more than two classes of antibiotics).

Antibiotic Resistance Genes

Data on antibiotic resistance genes are presented in **Table 2**. All isolates carried CTX-M-type ESBL-genes. Seven isolates (50%) carried $bla_{\mathrm{CTX-M-3}}$, six isolates (43%) carried $bla_{\mathrm{CTX-M-14}}$, and only one isolate carried $bla_{\mathrm{CTX-M-104}}$. Additionally, the ESBL-gene $bla_{\mathrm{SHV-27}}$ was detected in two isolates. The genetic environment surrounding the CTX-M genes are shown in **Figure 2**. Two distinct genetic environments and three distinct genetic environments were determined among the isolates carrying $bla_{\mathrm{CTX-M-3}}$ and $bla_{\mathrm{CTX-M-14}}$, respectively.

All isolates carried *fosA*, *oqx-* *sul-*, *dfr-*, and *tet-* genes, encoding fosfomycin-, quinolone-, sulphonamide-, trimethoprim-, and tetracycline resistance, respectively. Aminoglycosides resistance genes were also common (93% of isolates), as were the florfenicol resistance gene *floR* (86% of isolates).

Serotyping and Virulence-Associated Genes

Serotyping was performed based on both lipopolysaccharide (O-serotype) and capsular polysaccharide (K-serotype) (**Table 3**). The O-serotypes were distributed as follows; O2 ($n = 5$), O1 ($n = 4$), O3 ($n = 2$), OL101 ($n = 1$), and OL103 ($n = 1$). One isolate (KP4) had poor match confidence against any known O-type (<90% coverage and two truncated/missing genes) and was determined to be non-typeable. The K-serotype-associated K loci among the isolates were diverse; two isolates had KL34, whereas KL3, KL18, KL23, KL28, KL31, KL38, KL49, KL57, KL106, KL107, and KL127 were found in one isolate each. One isolate (KP4) had poor match confidence against any known K-serotype and was determined to be non-typeable.

TABLE 2 | Antibiotic resistance genes and STs of ESBL-producing *K. pneumoniae* isolates from environmental samples.

Isolate	Source	Antibiotic resistance genes	MLST
KP1	RW	ARR-3, *strA*, *strB*, *aph(3′)*-Ia, *aadA16*, *aac(3)*-IId, *qnrS1*, *oqxA*, *oqxB*, *qnrB52*, *fosA*, *mph(A)*, *sul1*, *sul2*, *dfrA27*, *tet(A)*, *floR*, *aac(6′)*Ib-cr, bla_{TEM-1B}, bla_{SHV-27}, $bla_{CTX-M-14}$	ST967
KP2	RW	ARR-3, *strA*, *strB*, *aph(3′)*-Ia, *aadA16*, *aac(3)*-IId, *qnrS1*, *oqxA*, *oqxB*, *qnrB49*, *fosA*, *mph(A)*, *sul1*, *sul2*, *dfrA27*, *tet(A)*, *floR*, *aac(6′)*Ib-cr, $bla_{CTX-M-3}$, bla_{SHV-28}, bla_{TEM-1B}	ST15
KP3	RW	*fosA*, *qnrS1*, *oqxA*, *oqxB*, *aac(3)*-IId, *strA*, *strB*, *sul1*, *sul2*, *dfrA1*, *tet(A)*, bla_{TEM-1B}, $bla_{CTX-M-14}$, bla_{SHV-1}	ST101
KP4	RW	ARR-3, *strA*, *strB*, *aph(3′)*-Ia, *aadA16*, *aac(3)*-IId, *qnrS1*, *oqxA*, *oqxB*, *fosA*, *mph(A)*, *sul2*, *sul1*, *dfrA27*, *tet(A)*, *floR*, *aac(6′)*Ib-cr, $bla_{CTX-M-3}$, bla_{SHV-1}, bla_{TEM-1B}	ST3003
KP5	RW	*fosA*, *qnrS1*, *oqxA*, *oqxB*, *sul1*, *dfrA1*, *tet(A)*, bla_{SHV-11}, $bla_{CTX-M-14}$	ST659
KP6	RW	ARR-3, *strA*, *strB*, *aph(3′)-Ia*, *aadA16*, *aac(3)-IId*, *sul1*, *sul2*, *fosA*, *mph(A)*, *qnrS1*, *oqxB*, *oqxA*, *qnrB49*, *dfrA27*, *tet(A)*, *floR*, *aac(6′)*Ib-cr, bla_{SHV-1}, $bla_{CTX-M-14}$	ST314
KP7	PM	ARR-3, *strA*, *strB*, *aph(3′)*-Ia, *aadA16*, *aac(3)*-IId, *oqxA*, *oqxB*, *qnrS1*, *qnrB49*, *fosA*, *mph(A)*, *sul1*, *sul2*, *dfrA27*, *tet(A)*, *floR*, *aac(6′)*Ib-cr, $bla_{CTX-M-3}$, bla_{SHV-26}, bla_{TEM-1B}	ST1967
KP8	PM	ARR-3, *fosA*, *qnrS1*, *qnrB49*, *oqxA*, *oqxB*, *strA*, *strB*, *aph(3′)*-Ia, *aadA16*, *aac(3)*-IId, *mph(A)*, *sul1*, *sul2*, *dfrA27*, *tet(A)*, *floR*, *aac(6′)*Ib-cr, bla_{TEM-1B}, bla_{SHV-11}, $bla_{CTX-M-3}$	New
KP9	S	ARR-3, *strA*, *strB*, *aph(3′)*-Ia, *aadA16*, *aac(3)*-IId, *qnrS1*, *oqxA*, *oqxB*, *fosA*, *mph(A)*, *sul2*, *sul1*, *dfrA27*, *tet(A)*, *floR*, *aac(6′)*Ib-cr, $bla_{CTX-M-3}$, bla_{SHV-1}, bla_{TEM-1B}	ST999
KP10	S	*fosA*, *sul1*, *aac(3)*-IId, *oqxA*, *oqxB*, *qnrS1*, *dfrA1*, *tet(A)*, $bla_{CTX-M-14}$, bla_{SHV-82}	ST1738
KP11	V	ARR-3, *fosA*, *oqxA*, *oqxB*, *qnrB49*, *strA*, *strB*, *aph(3′)*-Ia, *aadA16*, *aac(3)*-IId, *mph(A)*, *sul1*, *sul2*, *dfrA27*, *tet(A)*, *floR*, *aac(6′)*Ib-cr, bla_{TEM-1B}, bla_{SHV-11}, $bla_{CTX-M-3}$	New
KP12	V	ARR-3, *fosA*, *oqxA*, *oqxB*, *strA*, *strB*, *aph(3′)*-Ia, *aadA16*, *aac(3)*-IId, *mph(A)*, *sul2*, *sul1*, *dfrA27*, *tet(A)*, *floR*, *aac(6′)*Ib-cr, $bla_{CTX-M-3}$, bla_{SHV-27}, bla_{TEM-1B}	ST661
KP13	RS	ARR-3, *fosA*, *oqxA*, *oqxB*, *aph(3′)*-Ia, *aadA16*, *mph(A)*, *sul1*, *dfrA27*, *tet(D)*, *floR*, *catA2*, *aac(6′)*Ib-cr, bla_{SHV-11}, $bla_{CTX-M-14}$	ST11
KP14	WW	ARR-3, *strB*, *aadA16*, *aadA2*, *aac(3)*-IId, *aph(3′)*-Ia, *qnrB6*, *oqxA*, *oqxB*, *fosA*, *erm(B)*, *sul1*, *sul2*, *dfrA27*, *tet(A)*, *tet(D)*, *floR*, *aac(6′)*Ib-cr, *cfr*, bla_{SHV-11}, bla_{TEM-1A}, $bla_{CTX-M-104}$	ST258

The samples were collected from river water (RW), pig manure (PM), soil (S), vegetable (V), river sediment (RS), and wastewater (WW).

Querying of virulence-associated genes and serotyping was performed *in silico* by using the whole-genome sequencing data (**Table 3**). All isolates carried the *fim* and *mrk* operons which encode type 1 and type 3 fimbriae, respectively. The *kfu* and the *kvg* operons were detected in four isolates and two isolates, respectively. Additionally, two isolates carried the operon encoding the yersiniabactin siderophore (*ybtSXQPA-irp2-irp1-ybtUTE-fyuA*) (**Table 3**). The genes encoding the OMPs OmpK35 and OmpK36 were also evaluated in all isolates. None of the isolates carried an *ompK35* with any mutations clearly affecting the protein function except isolate K13, which carried an *ompK35* with a nucleotide substitution (c202t) engendering a premature stop codon (Q68Stop) causing a 81% truncation of the protein (shortening it from 359 to 67 aa). Based on *ompK36* polymorphisms, the isolates could be divided in three different allele groups; group A ($n = 7$), group D ($n = 5$), and group C ($n = 2$).

Serum Bactericidal and Phagocytosis Assays

The survivability of the isolates in serum bactericidal and phagocytosis assays were evaluated as the differences in viable counts between the assay and control experiments (**Table 3**). For the serum bactericidal assay, 10 isolates (71%) had significantly lower survivability compared to the controls ($P < 0.05$); eight of these isolates had survival rates ranging from 30 to 74%. Two isolates (KP2 and KP10) had survival rates of 1 and 2%, respectively, which was significantly lower compared to the other isolates ($P < 0.01$). Four isolates (KP3, KP8, KP11, and KP12) did not differ significantly from the controls and had survival rates ranging from 68 to 122%. In the phagocytosis assay, only one isolate (KP11) had a significantly lower survival rate (55%) compared to the control ($P < 0.01$); the remaining isolates showed survival rates ranging from 67 to 108%.

Phylogenetic Analysis

A total of 13 different STs were found among the 14 ESBL-producing *K. pneumoniae* isolates in this study (**Table 2**), including ST11, ST15, ST101, ST258, ST659, ST661, ST967, ST999, ST11967, ST3003, and ST1738. Two isolates shared 100% nucleotide sequences (KP8, isolated from vegetables, and KP11, isolated from pig manure) in the MLST genes, but were of a previously undescribed type. These two isolates also presented high similarity in the PFGE-analysis (**Figure S1**). In addition, the results of the PFGE indicated a close genetic relationship between three other isolates, KP9 (from soil), KP13 (from river sediment), and KP14 (from wastewater). A phylogenetic tree based on SNPs was computed from 9,045 gene clusters obtained from the 14 isolates (**Figure 3**). The analysis revealed a close genetic relationship between isolates KP8 and KP11, among which no SNP-differences could be discerned. Isolates KP13 and KP14 also showed high genetic similarity.

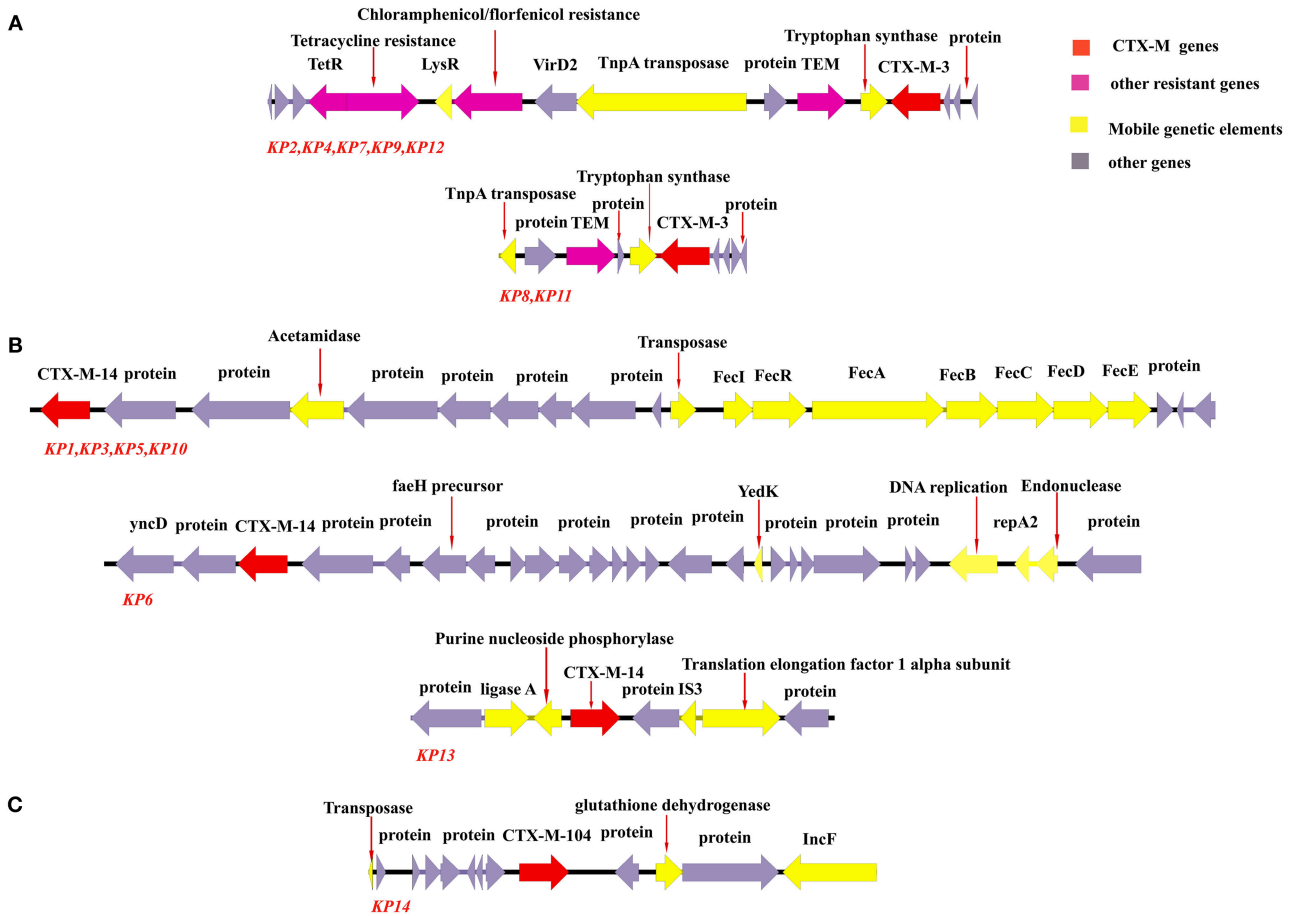

FIGURE 2 | Genetic environment of CTX-M genes among *K. pneumoniae* isolated from environmental sources. Arrows represent direction of transcription. Red open reading frames (ORFs) denote the CTX-M genes, purple ORFs denote other antibiotic resistance genes, yellow ORFs denote genes related to mobile genetic elements, and gray ORFs denote other genes or genes of unknown function. **(A)** The genetic environments of $bla_{CTX-M-3}$ were similar in isolates KP2, KP4, KP7, KP9, and KP12. The two isolates KP8 and KP11 also shared a similar genetic environment surrounding $bla_{CTX-M-3}$. **(B)** Isolates KP1, KP3, KP5, and KP10 all carried $bla_{CTX-M-14}$ and shared the same genetic environment surrounding the gene, whereas isolates KP6 and KP13 had unique genetic environments surrounding $bla_{CTX-M-14}$. **(C)** The genetic environment of $bla_{CTX-M-104}$ in the one isolate in the study which carried the gene.

DISCUSSION

In the current study, 231 environmental samples were collected from a rural farming area in Shandong province, China, and screened for ESBL-producing *K. pneumoniae*. The results showed that the positive rate among the samples was 6%. Among the different environmental sources sampled, the detection rate was highest in river water (24%), followed by soil (9%), vegetables (9%), pig manure (7%), river sediment (4%), and wastewater (2%). The prevalence in river water was higher than the prevalence in the wastewaters connected to pig discharge. This could reflect the comparatively lower prevalence in pig manure (7%). The river water on the other hand, was mainly influenced by anthropogenic discharge originating from the surrounding community and directly from inhabitants using the water. The higher prevalence in anthropogenically affected water compared to pig discharge wastewater may reflect that human rather than animal sources are more important for the environmental presence of ESBL-producing *K. pneumoniae* in the local area. In China, ESBL-producing *K. pneumoniae* has been reported in spring water adjacent to restaurants and hotels at a mountain resort close to Tai'an, Shandong province (Li et al., 2015) and in water from the Pearl River in Guangzhou (Ye et al., 2017). A fairly high prevalence rate of 36% was also reported in the Yangtze River in Chongqing (Chen et al., 2010). Overall, the findings in the different environmental sources in the study area indicate a need to clarify the role and importance of the environment in the potential for transmission and dissemination of ESBL-producing *K. pneumoniae* and subsequent risk for transmission.

All isolates were susceptible to colistin and carbapenems. The susceptible rate to ceftazidime was high (86%); only one isolate was resistant. Resistance to ceftazidime in *K. pneumoniae* has been shown to be engendered by loss of the OMP OmpK35 (Etsuko et al., 2016). The single resistant isolate in the current study (KP3) carried an *ompK35* with a nonsense mutation

TABLE 3 | Serotypes, virulence characteristics, and virulence-associated genes of ESBL-producing *K. pneumoniae* from environmental samples.

	KP1	KP2	KP3	KP4	KP5	KP6	KP7	KP8	KP9	KP10	KP11	KP12	KP13	KP14
MLST	ST967	ST15	ST101	ST3003	ST659	ST314	ST1967	New	ST999	ST1738	New	ST661	ST11	ST258
O serotype	O1	OL103	O1	N.D.	O2	O2	O2	O1	OL101	O3	O1	O2	O3	O2
K locus	KL18	KL49	KL106	N.D.	KL3	KL23	KL57	KL34	KL127	KL38	KL34	KL28	KL31	KL107
Serum survival	74%	2%	82%	34%	51%	30%	53%	111%	47%	1%	122%	68%	67%	39%
P value	<0.05	<0.001		<0.001	<0.001	<0.001	<0.001		<0.001	<0.001			<0.05	<0.01
Phagocytosis survival	74%	104%	94%	75%	75%	78%	81%	104%	67%	74%	55%	97%	108%	75%
P value											<0.01			
OmpK35	WT	WT	WT	WT	WT	WT	WT	WT	WT	WT	WT	WT	Q68Stop	WT
ompK36 allele group	C	D	C	A	D	D	N.D.	A	D	D	A	A	A	A
Type 1 fimbriae	+	+	+	+	+	+	+	+	+	+	+	+	+	+
Type 3 fimbriae	+	+	+	+	+	+	+	+	+	+	+	+	+	+
kfu	–	+	+	–	–	–	–	+	–	–	+	–	–	–
kvg	–	–	–	–	–	–	–	+	–	–	+	–	–	–
Yersiniabactin	–	–	+	–	–	–	–	–	–	+	–	–	–	–

P-values are indicated for tests comparing viable counts for serum bactericidal and phagocytosis assays to their respective controls. P > 0.05 are omitted for clarity. WT, wild type; N.D., non-determinable.

which translated into an OmpK35 truncated by 81%, likely rendering the protein nonfunctional. For the antibiotics cefotaxime, amoxicillin-clavulanic acid, piperacillin-tazobactam, ciprofloxacin, trimethoprim-sulfamethoxazole, tetracycline, fosfomycin, gentamicin, and nitrofurantoin, susceptible rates were low, between 0 and 7%. The high MIC-values to these antibiotics correlated to a correspondingly high carriage rate of antibiotic resistance genes. All isolates carried genes conferring resistance to trimethoprim, sulphonamides, quinolones, tetracycline, fosfomycin, and aminoglycosides. The susceptible rate to florfenicol was low (21%), and all of the non-susceptible isolates carried the florfenicol resistance gene *floR*. Additionally, MICs were high for tigecycline, and only a few isolates were susceptible (29%). Notably, all isolates collected in this study were multidrug-resistant.

CTX-M-genes were carried by all isolates in this study. The most prevalent was $bla_{\text{CTX-M-3}}$, a gene of the CTX-M-1-group, which was detected in seven isolates (50%), followed by $bla_{\text{CTX-M-14}}$, a gene of the CTX-M-9-group, which was detected in five isolates (43%). MICs of the tested cephalosporins ceftazidime and cefoxitin were not significantly different for isolates with CTX-M-1 group enzymes as compared to isolates with CTX-M-9 group enzymes. CTX-M-genes are the most common genes encoding ESBLs worldwide, and are prevalent among Enterobacteriaceae (Naseer and Sundsfjord, 2011; Bevan et al., 2017). Regarding the epidemiology of CTX-M-genes, most studies performed have focused on *E. coli*. Although there are regional differences pertaining to the distribution of specific CTX-M-genes, $bla_{\text{CTX-M-14}}$ and $bla_{\text{CTX-M-15}}$ are predominant in clinical isolates worldwide, which also holds true in China (Shin et al., 2011; An et al., 2012; Xia et al., 2014; Bevan et al., 2017). For *K. pneumoniae* in China, the predominance of certain CTX-M-types differ depending on study. For instance, one study on isolates collected from seven hospital in Beijing reported a predominance of CTX-M-14 (An et al., 2012), whereas another study from a single hospital in Beijing reported CTX-M-10 to be the most common (Li et al., 2012). Another study in a hospital in Guangdong reported CTX-M-9 to be the most common CTX-M-type (Du et al., 2014) The most common gene in the current study, $bla_{\text{CTX-M-3}}$, is rarely reported in China, although this is likely due to a larger volume of data being available on ESBLs among *E. coli* as compared to *K. pneumoniae*. For instance, a study on clinical isolates of *K. pneumoniae* from hospitals in Jilin, China, showed that 48% of CTM-X-producing isolates carried $bla_{\text{CTX-M-3}}$ (Li et al., 2014) and another study on *K. pneumoniae* isolates collected at a hospital in Henan, China, showed that $bla_{\text{CTX-M-3}}$ was carried by 38% of the CTX-M-producers, which was second in prevalence only by carriers of $bla_{\text{CTX-M-14}}$ (40%) (Guo et al., 2017).

Additionally, the genetic environments surrounding the CTX-M-genes were analyzed (**Figure 2**). $bla_{\text{CTX-M-3}}$ ($n = 7$) was located on two distinct genetic fragments among the isolates, whereas $bla_{\text{CTX-M-14}}$ ($n = 6$) was located on three distinct genetic fragments. These results show that several mobile genetic elements are likely responsible for the dissemination of CTX-M-genes in the local environment. Notably, five isolates (KP2, KP4, KP7, KP9, and KP12) sharing

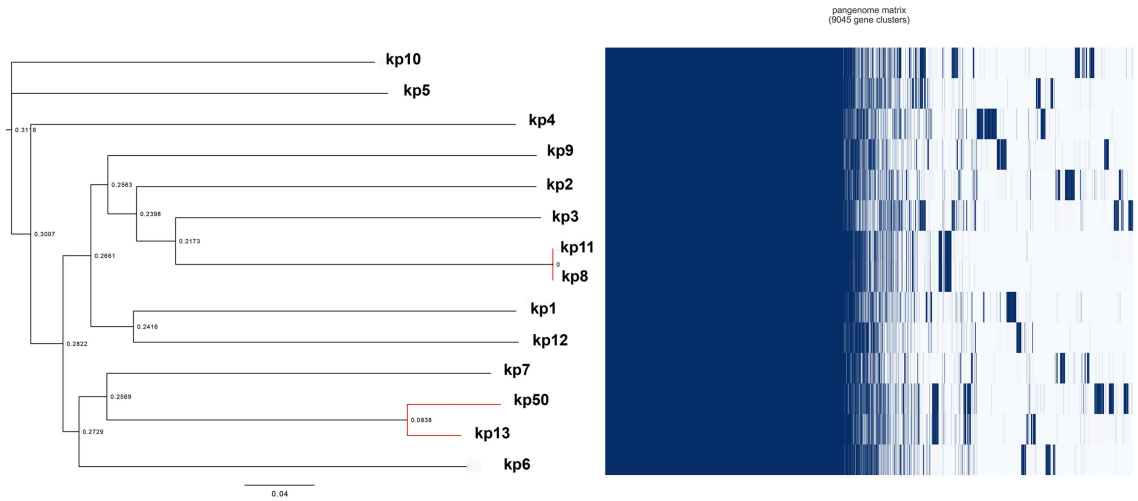

FIGURE 3 | Phylogeny of ESBL-producing *K. pneumoniae* isolated from environmental sources based on differences in SNPs. Red branches indicate isolates which were found related in the PFGE-analysis. The value represents the proportion of the scale of SNP differences.

the same genetic environment surrounding $bla_{CTX-M-3}$, also carried the florfenicol resistance gene *floR* on the same genetic element, indicating the potential of co-selection of ESBL-producing *K. pneumoniae* via florfenicol exposure. The high variety of ESBL-genes and other antibiotic resistance genes among *K. pneumoniae* isolated from environmental sources indicate the potential for transfer of these genes to other bacteria present in the same sources. Reversely, the *K. pneumoniae* isolates may potentially acquire additional antibiotic resistance determinants from environmentally occurring bacteria.

Isolates of *K. pneumoniae* expressing ESBLs have been linked to higher virulence compared to *K. pneumoniae* isolates lacking ESBLs. In one study, isolates collected from hospital-acquired bacteremia showed that ESBL-producing *K. pneumoniae* were significantly more resistant to serum killing compared to isolates lacking ESBLs (Lin et al., 2016). Another study on isolates from clinical specimens from hospitalized patients found that ESBL-producing *K. pneumoniae* to a higher degree carried both type 1 and type 3 fimbriae and were more capable of invasion of ileocecal and bladder epithelial cells (Sahly et al., 2008). ESBL-production has also been strongly linked to human isolates of *K. pneumoniae*, and it has further been indicated that community-acquired *K. pneumoniae* tend to carry fewer acquired antibiotic resistance genes (Holt et al., 2015). In general, the difference between clinical and environmental isolates of *K. pneumoniae* is not as well-studied.

In the current study, virulence among the environmental isolates of *K. pneumoniae* was evaluated based on serum bactericidal and phagocytosis assays, serotypes, and virulence-associated genes. Ten isolates had significantly lower survivability in serum compared to the controls ($P < 0.05$), two of which (KP2 and KP10) had considerably lower survival rates (1 and 2%, respectively) compared to the other isolates ($P < 0.01$); indicating a difference in degree of survivability in serum for the isolates in this study. Four isolates, KP3, KP8, KP11, and KP12, did not significantly differ in survivability compared to the controls, and had survival rates ranging from 68 to 122%, indicating that these were potentially serum-resistant. For the phagocytosis assay, only one isolate (KP11) had significantly lower survivability compared to the control, implying a high degree of phagocytosis resistance among the isolates. Notably, three isolates (KP3, KP8, and KP12) had high survival rates in both the serum bactericidal and phagocytosis assay, indicating the potential virulence of these isolates.

Serotyping was performed *in silico* by using the whole-genome sequencing data (**Table 3**). O-serotypes O1, O2, and O3 are the serotypes most commonly isolated from human hosts, and O1 in particular is the most common serotype associated with disease in humans (Rainer et al., 2016) Interestingly, these serotypes predominated among the environmental isolates collected in this study; five isolates were O2, four isolates were O1 and two isolates were O3. Among K-serotypes, K1 and K2 are associated to hypervirulence in *K. pneumoniae* (Rainer et al., 2016), however, none of the isolates in this study carried the KL1 or KL2 loci associated to either of these K-serotypes.

Virulence gene analysis revealed that all isolates carried the *fim* and *mrk* operons which encodes type 1 and type 3 fimbriae, virulence factors ubiquitous in *K. pneumoniae* (Wu et al., 2012; Paczosa and Mecsas, 2016). Both fimbriae mediate adhesion and biofilm formation. Type 1 fimbriae are expressed in the urinary bladder and have been shown to contribute to urinary tract infections (Struve et al., 2009; Paczosa and Mecsas, 2016). Type 3 fimbriae mediate biofilm formation and are involved in adhesion to medical devices, and may be an important factor for *K. pneumoniae* in biofilm-associated infections as well as gaining entry into the host and persistence in the clinical environment rather than facilitating infections in the host (Huang et al., 2009; Struve et al., 2009).

The OMP OmpK36 appears to play a role in *K. pneumoniae* for both antibiotic resistance and virulence, as deficiencies in the protein has been shown to lead to elevated MICs for some antibiotics (likely due to decreased membrane permeability) and lowered virulence (Paczosa and Mecsas, 2016). Genetic polymorphisms in *ompK36* can be used as a basis for classification into four different *ompK36* alleles, each of which is associated with altered protein function. Interestingly, isolates carrying a group C allele have been associated with STs, K-serotypes, and virulence genes associated with hypervirulent *K. pneumoniae* lineages, and have additionally been shown to display higher virulence in a mouse lethality model (Yan et al., 2015; Du et al., 2018). In the current study, two isolates (KP1 and KP3) were found to carry group C alleles of *ompK36*.

Four isolates carried the *kfu* operon, which encodes components of an ABC transport system which mediates uptake of ferric iron. Kfu is associated with hypervirulent strains of *K. pneumoniae*, and its expression has been shown to be important for virulence in mouse models (Luo et al., 2014; Paczosa and Mecsas, 2016). In the current study, two isolates (KP3 and KP10) containing the yersiniabactin virulence operon were found, and where from river water and soil, respectively. Yersiniabactin is a siderophore which helps *K. pneumoniae* survive during respiratory tract infections (Bachman et al., 2011), and has been shown to be strongly associated with infection in humans (Holt et al., 2015). Yersiniabactin is also overrepresented among hypervirulent strains (Paczosa and Mecsas, 2016). One of these isolates (KP3) also carried the *kfu* operon.

The genetic relationship of the isolates was analyzed using MLST, PFGE, and SNPs, and the isolates were found to exhibit a high diversity. For the 14 isolates, 13 different STs were determined (**Figure 2**, **Table 2**). The two isolates (KP8, KP11) which shared ST (i.e., identical sequence in MLST genes) belonged to a previously undescribed ST, and showed a close relation in the PFGE analysis. This was confirmed by the SNP-analysis, in which the two isolates had identical SNPs (**Figure 3**). These isolates also shared identical genetic environments surrounding $bla_{\mathrm{CTX-M-3}}$ (**Figure 2**). Other STs detected in this study included clinically relevant STs such as ST11, ST15, ST101, and ST258. ST11 and ST258, both members of clonal group (CG) 258, are the most common carbapenem-resistant *K. pneumoniae* isolated from clinical samples worldwide (Lee et al., 2016). ST258 is commonly reported to cause hospital outbreaks in North America, Latin America, and Europe (Ruiz-Garbajosa et al., 2013; Geraci et al., 2015; Gomez et al., 2016; Lee et al., 2016). ST11 is more commonly reported from hospital outbreaks in Asian countries, including China (Qi et al., 2011; Lee et al., 2016). Recently, a clone of carbapenem-resistant ST11 *K. pneumoniae* having acquired a hypervirulence-plasmid was reported to cause an outbreak at a hospital in Hangzhou, China (Gu et al., 2018). ST15 and ST101 are two other globally occurring strains of *K. pneumoniae* associated with hospital outbreaks. For example, ESBL-producing ST15 has been reported in hospital outbreaks in the Netherlands (Zhou et al., 2016) and Hungary (Damjanova et al., 2008), and carbapenem-resistant ST15 has been reported in outbreaks in Bulgaria (Markovska et al., 2015), Portugal (Vubil et al., 2017), Vietnam (Tada et al., 2017), and Nepal (Chung The et al., 2015). For ST101, hospital outbreaks of carbapenem-resistant *K. pneumoniae* have been reported in Algeria (Loucif et al., 2016) and Greece (Avgoulea et al., 2018). A study in Turkey (Can et al., 2018) on colistin-resistant *K. pneumoniae* isolated from patients found that colistin-resistant ST101 were prevalently carbapenem-resistant, and occurrence of ST101 in the patient was found to be a significant independent predictor of patient mortality. The ST101 isolate in the current study (KP3) had several factors associated with virulence and high-risk clones; it belonged to the commonly disease-associated O-serotype O1, carried a group C *ompK36* allele and carried the hypervirulence-associated *kfu* and yersiniabactin operons. Additionally, the isolate showed high survivability in the serum bactericidal and phagocytosis assays (82 and 94%, respectively) indicating that this is potentially a highly virulent clone.

In our study, the ST11, ST15, ST101, and ST258 isolates were detected in river sediment, river water, and wastewater. The presence of clinically relevant strains of *K. pneumoniae* in aquatic environments in association to human settlements indicates a potential for the environment as a transmission route of these strains. These isolates may have originated from human or animal guts colonized by the strains, and could have disseminated via feces and untreated wastewater. Although the data collected in this study is not sufficient to conclusively demonstrate transmission of *K. pneumoniae* strains between different environmental media, some interesting observations could nevertheless be made. For instance, KP8, isolated from pig manure, and KP11, isolated from vegetables, shared STs and were highly similar in the PFGE- and SNP-analysis, which may indicate the possibility of transmission from animals to humans via consumption of produce (**Figure S1**). The isolates were from the geographically separate villages C and I. Although of different STs, KP9, KP13, and KP14 also showed similar PFGE- and SNP-profiles, indicating that there may exist possible transmission routes between wastewater (KP14), river sediment (KP13), and soil (KP9). Bacteria in these environmental matrices could further potentially spread to humans, via for example surface and ground water, and irrigation of fields used for vegetable cultivation and finally consumption by humans. KP9, KP13, and KP14 were isolated from villages F, C, and D, respectively. Although villages C and D are located adjacent to each other, connected by a river, village F is separated from the aforementioned villages. Although the number of isolates in this study were too few to make a robust spatial analysis, the occurrence of genetically related isolates from different environmental matrices in geographically separate locations indicate the potential existence of a transmission mechanism.

CONCLUSION

There is a scarcity of studies investigating occurrence of *K. pneumoniae* in the environment and the role of environmental transmission routes for dissemination of the pathogen. We sampled different environmental sources in a rural region of Shandong province, China, and screened the samples for

ESBL-producing *K. pneumoniae*, and 6% of the samples were determined to be positive. All of the isolates were multidrug-resistant and several belonged to clinically relevant strains which are known to cause hospital outbreaks worldwide. Serotypes, virulence genes, serum survival, and phagocytosis survival were analyzed and showed the presence of virulence factors associated with highly virulent clones and a high degree of phagocytosis survivability, indicating the potential virulence of these isolates. The occurrence of ESBL-producing *K. pneumoniae* in the environment indicates inadequate treatment of domestic sewage and waste in the rural area. In addition, these results emphasize the need for further studies designed to elucidate the role of the environment in transmission and dissemination of ESBL-producing *K. pneumoniae* and the potential risk posed to human and environmental health.

ETHICS STATEMENT

Ethical permission was granted by the Research Ethics Committee of the First Affiliated Hospital, College of Medicine, Zhejiang University, reference number 2018#1031.

AUTHOR CONTRIBUTIONS

XL, LN, CSL, JO, SB, BZ and BB conceived of and designed the study. XC, HZ, XJ and XL performed the sampling. XC and XJ performed the experiments. XC, BB and HZ analyzed the data. XC completed the first draft of the manuscript. BB, BZ, SB, JO, CSL, XL and LN critically revised the manuscript. All co-authors approved of the final version of the manuscript.

FUNDING

This project was supported by the National Natural Science Foundation of China (41771499, 81361138021), the Fundamental Research Funds of Shandong University (2018JC102), the Swedish Research Council (D0879801) and the Swedish Research Council Formas (2016-00640).

ACKNOWLEDGMENTS

We would like to thank the participants, co-ordinators, and administrators for their support during the study. Thanks to the IMPACT Consortium for its efforts in this project.

SUPPLEMENTARY MATERIAL

The Supplementary Material for this article can be found online at: https://www.frontiersin.org/articles/10.3389/fmicb.2019.00211/full#supplementary-material

REFERENCES

An, S., Chen, J., Wang, Z., Wang, X., Yan, X., Li, J., et al. (2012). Predominant characteristics of CTX-M-producing *Klebsiella pneumoniae* isolates from patients with lower respiratory tract infection in multiple medical centers in China. *FEMS Microbiol. Lett.* 332, 137–145. doi: 10.1111/j.1574-6968.2012.02586.x

Anton, B., Sergey, N., Dmitry, A., Alexey, A., Gurevich, A., Dvorkin, M., et al. (2012). SPAdes: a new genome assembly algorithm and its applications to single-cell sequencing. *J. Comput. Biol.* 19, 455–477. doi: 10.1089/cmb.2012.0021

Avgoulea, K., Di Pilato, V., Zarkotou, O., Sennati, S., Politi, L., Cannatelli, A., et al. (2018). Characterization of extensively- or pandrug-resistant ST147 and ST101 OXA-48-producing *Klebsiella pneumoniae* isolates causing bloodstream infections in ICU patients. *Antimicrob Agents Chemother*. 62, AAC.02457–17. doi: 10.1128/AAC.02457-17

Bachman, M. A., Oyler, J. E., Burns, S. H., Caza, M., Lepine, F., Dozois, C. M., et al. (2011). *Klebsiella pneumoniae* yersiniabactin promotes respiratory tract infection through evasion of lipocalin 2. *Infect. Immun.* 79, 3309–3316. doi: 10.1128/IAI.05114-11

Ben Said, L., Jouini, A., Klibi, N., Dziri, R., Alonso, C. A., Boudabous, A., et al. (2015). Detection of extended-spectrum beta-lactamase (ESBL)-producing *Enterobacteriaceae* in vegetables, soil and water of the farm environment in Tunisia. *Int. J. Food Microbiol.* 203, 86–92. doi: 10.1016/j.ijfoodmicro.2015.02.023

Bevan, E. R., Jones, A. M., and Hawkey, P. M. (2017). Global epidemiology of CTX-M beta-lactamases: temporal and geographical shifts in genotype. *J Antimicrob Chemother*. 72, 2145–2155. doi: 10.1093/jac/dkx146

Burmolle, M., Norman, A., Sorensen, S. J., and Hansen, L. H. (2012). Sequencing of IncX-plasmids suggests ubiquity of mobile forms of a biofilm-promoting gene cassette recruited from Klebsiella pneumoniae. *PLoS ONE* 7:e41259. doi: 10.1371/journal.pone.0041259

Can, F., Menekse, S., Ispir, P., Atac, N., Albayrak, O., Demir, T., et al. (2018). Impact of the ST101 clone on fatality among patients with colistin-resistant *Klebsiella pneumoniae infection*. *J. Antimicrob. Chemother.* 73, 1235–41. doi: 10.1093/jac/dkx532

Chen, H., Shu, W., Chang, X., Chen, J., Guo, A. Y., and Tan, Y. (2010). The profile of antibiotics resistance and integrons of extended-spectrum beta-lactamase producing thermotolerant coliforms isolated from the Yangtze River basin in Chongqing. *Environ. Pollut.* 158, 2459–2464. doi: 10.1016/j.envpol.2010.03.023

Chen, K., Chan, E. W., Xie, M., Ye, L., Dong, N., and Chen, S. (2017). Widespread distribution of mcr-1-bearing bacteria in the ecosystem, 2015 to 2016. *Eurosurveillance* 22:17-00206. doi: 10.2807/1560-7917.ES.2017.22.39.17-00206

Chung The, H., Karkey, A., Pham Thanh, D., Boinett, C. J., Cain, A. K., Ellington, M., et al. (2015). A high-resolution genomic analysis of multidrug-resistant hospital outbreaks of *Klebsiella pneumoniae*. *EMBO Mol. Med.* 7, 227–239. doi: 10.15252/emmm.201404767

CLSI (2017). *M100 Performance Standards for Antimicrobial Susceptibility Testing, 27th Edn*. Wayne, PA: CLSI.

Cubero, M., Grau, I., Tubau, F., Pallares, R., Dominguez, M. A., Liñares, J., et al. (2016). Hypervirulent *Klebsiella pneumoniae* clones causing bacteraemia in adults in a teaching hospital in Barcelona, Spain (2007-2013). *Clin. Microbiol. Infect.* 22, 154–160. doi: 10.1016/j.cmi.2015.09.025

Damjanova, I., Toth, A., Paszti, J., Hajbel-Vekony, G., Jakab, M., Berta, J., et al. (2008). Expansion and countrywide dissemination of ST11, ST15 and ST147 ciprofloxacin-resistant CTX-M-15-type beta-lactamase-producing *Klebsiella pneumoniae* epidemic clones in Hungary in 2005–the new 'MRSAs'? *J. Antimicrob. Chemother.* 62, 978–985. doi: 10.1093/jac/dkn287

Du, F., Wei, D.D., Wan, L., Cao, X. W., Zhang, W., and Liu, Y. (2018). Evaluation of ompK36 allele groups on clinical characteristics and virulence features of *Klebsiella pneumoniae* from bacteremia. *J. Microbiol. Immunol. Infect.* doi: 10.1016/j.jmii.2018.08.018. [Epub ahead of print].

Du, J., Li, P., Liu, H., Lu, D., Liang, H., and Dou, Y. (2014). Phenotypic and molecular characterization of multidrug resistant *Klebsiella pneumoniae*

isolated from a university teaching hospital, China. *PLoS ONE* 9:e95181. doi: 10.1371/journal.pone.0095181

Etsuko, S., Seiji, K., and Hiroshi, N. (2016). *Klebsiella pneumoniae* major porins OmpK35 and OmpK36 allow more efficient diffusion of β-Lactams than their *Escherichia coli* homologs OmpF and OmpC. *J. Bacteriol.* 198, 3200–3208. doi: 10.1128/JB.00590-16

Geraci, D. M., Bonura, C., Giuffre, M., Saporito, L., Graziano, G., Aleo, A., et al. (2015). Is the monoclonal spread of the ST258, KPC-3-producing clone being replaced in southern Italy by the dissemination of multiple clones of carbapenem-nonsusceptible, KPC-3-producing *Klebsiella pneumoniae*? *Clin. Microbiol. Infect.* 21, e15–e17. doi: 10.1016/j.cmi.2014.08.022

Gomez, S. A., Rapoport, M., Piergrossi, N., Faccone, D., Pasteran, F., De Belder, D., et al. (2016). Performance of a PCR assay for the rapid identification of the *Klebsiella pneumoniae* ST258 epidemic clone in Latin American clinical isolates. *Infect. Genet. Evol.* 44, 145–146. doi: 10.1016/j.meegid.2016.06.018

Grundmann, H. (2014). Towards a global antibiotic resistance surveillance system: a primer for a roadmap. *Ups J. Med. Sci.* 119, 87–95. doi: 10.3109/03009734.2014.904458

Gu, D., Dong, N., Zheng, Z., Lin, D., Huang, M., Wang, L., et al. (2018). A fatal outbreak of ST11 carbapenem-resistant hypervirulent *Klebsiella pneumoniae* in a Chinese hospital: a molecular epidemiological study. *Lancet Infect. Dis.* 18, 37–46. doi: 10.1016/S1473-3099(17)30489-9

Guo, X., Cao, Z., Dai, Z., Li, Y., He, X., Hu, X., et al. (2017). Antimicrobial susceptibility and molecular epidemiology of multidrug-resistant *Klebsiella pneumoniae* in Central China. *Jpn. J. Infect. Dis.* 70, 229–234. doi: 10.7883/yoken.JJID.2016.049

Holt, K. E., Wertheim, H., Zadoks, R. N., Baker, S., Whitehouse, C. A., Dance, D., et al. (2015). Genomic analysis of diversity, population structure, virulence, and antimicrobial resistance in *Klebsiella pneumoniae*, an urgent threat to public health. *Proc. Natl. Acad. Sci.* 112, E3574–E3581. doi: 10.1073/pnas.1501049112

Hou, X. H., Song, X. Y., Ma, X. B., Zhang, S. Y., and Zhang, J. Q. (2015). Molecular characterization of multidrug-resistant Klebsiella pneumoniae isolates. *Braz. J. Microbiol.* 46, 759–768. doi: 10.1590/S1517-838246320140138

Huang, S. Y., Pan, K. Y., Liu, X. Q., Xie, X. Y., Dai, X. L., Chen, B. J., et al. (2015). Analysis of the drug-resistant characteristics of *Klebsiella pneumoniae* isolated from the respiratory tract and CTX-M ESBL genes. *Genet. Mol. Res.* 14, 12043–12048. doi: 10.4238/2015.October.5.17

Huang, Y. J., Liao, H. W., Wu, C. C., and Peng, H. L. (2009). MrkF is a component of type 3 fimbriae in *Klebsiella pneumoniae*. *Res. Microbiol.* 160, 71–79. doi: 10.1016/j.resmic.2008.10.009

Kobayashi, S. D., Porter, A. R., Dorward, D. W., Brinkworth, A. J., Chen, L., Kreiswirth, B. N., et al. (2016). Phagocytosis and killing of carbapenem-resistant ST258 *Klebsiella pneumoniae* by human neutrophils. *J. Infect. Dis.* 213, 1615–1622. doi: 10.1093/infdis/jiw001

Lee, C. R., Lee, J. H., Park, K. S., Kim, Y. B., Jeong, B. C., and Lee, S. H. (2016). Global dissemination of carbapenemase-producing *Klebsiella pneumoniae*: epidemiology, genetic context, treatment options, and detection methods. *Front. Microbiol.* 7:895. doi: 10.3389/fmicb.2016.00895

Lee, J. C., Lee, E. J., Lee, J. H., Jun, S. H., Choi, C. W., Kim, S. I., et al. (2012). *Klebsiella pneumoniae* secretes outer membrane vesicles that induce the innate immune response. *FEMS Microbiol. Lett.* 331, 17–24. doi: 10.1111/j.1574-6968.2012.02549.x

Li, B., Li, M., Qu, L., Wang, M., and Guo, J. (2014). Prevalence and characteristics of extended-spectrum beta-lactamase-producing *Klebsiella pneumoniae* isolated from pediatric inpatients with respiratory tract infections at a teaching hospital in China. *Scand. J. Infect. Dis.* 46, 200–203. doi: 10.3109/00365548.2013.859393

Li, B., Yi, Y., Wang, Q., Woo, P. C., Tan, L., Jing, H., et al. (2012). Analysis of drug resistance determinants in *Klebsiella pneumoniae* isolates from a tertiary-care hospital in Beijing, China. *PLoS ONE* 7:e42280. doi: 10.1371/journal.pone.0042280

Li, S., Zhu, Z. C., Wang, L., Zhou, Y. F., Tang, Y. J., and Miao, Z. M. (2015). Prevalence and characterization of extended-spectrum beta-lactamase-producing *Enterobacteriaceae* in spring waters. *Lett. Appl. Microbiol.* 61, 544–548. doi: 10.1111/lam.12489

Lin, H. A., Huang, Y. L., Yeh, K. M., Siu, L. K., Lin, J. C., and Chang, F. Y. (2016). Regulator of the mucoid phenotype A gene increases the virulent ability of extended-spectrum beta-lactamase-producing serotype non-K1/K2 *Klebsiella pneumonia*. *Sci. Direct* 49, 494–501. doi: 10.1016/j.jmii.2014.08.023

Little, M. L., Qin, X., Zerr, D. M., and Weissman, S. J. (2014). Molecular epidemiology of colonizing and disease-causing *Klebsiella pneumoniae* in paediatric patients. *J. Med. Microbiol.* 63, 610–616. doi: 10.1099/jmm.0.063354-0

Loucif, L., Kassah-Laouar, A., Saidi, M., Messala, A., Chelaghma, W., and Rolain, J. M. (2016). Outbreak of OXA-48-producing *Klebsiella pneumoniae* involving a sequence type 101 clone in Batna University hospital, algeria. *Antimicrob. Agents Chemother.* 60, 7494–7497. doi: 10.1128/AAC.00525-16

Luo, Y., Wang, Y., Ye, L., and Yang, J. (2014). Molecular epidemiology and virulence factors of pyogenic liver abscess causing *Klebsiella pneumoniae* in China. *Clin. Microbiol. Infect.* 20, O818–O824. doi: 10.1111/1469-0691.12664

Machado, A., and Bordalo, A. A. (2014). Prevalence of antibiotic resistance in bacteria isolated from drinking well water available in Guinea-Bissau (West Africa). *Ecotoxicol. Environ Saf.* 106, 188–194. doi: 10.1016/j.ecoenv.2014.04.037

Magiorakos, A. P., Srinivasan, A., Carey, R. B., Carmeli, Y., Falagas, M. E., Giske, C. G., et al. (2012). Multidrug-resistant, extensively drug-resistant and pandrug-resistant bacteria: an international expert proposal for interim standard definitions for acquired resistance. *Clin. Microbiol. Infect.* 18, 268–281. doi: 10.1111/j.1469-0691.2011.03570.x

Markovska, R., Stoeva, T., Schneider, I., Boyanova, L., Popova, V., Dacheva, D., et al. (2015). Clonal dissemination of multilocus sequence type ST15 KPC-2-producing *Klebsiella pneumoniae* in Bulgaria. *APMIS* 123, 887–894. doi: 10.1111/apm.12433

Mollenkopf, D. F., Mirecki, J. M., Daniels, J. B., Funk, J. A., Henry, S. C., Hansen, G. E.,et al. (2013). *Escherichia coli* and *Klebsiella pneumoniae* producing CTX-M cephalosporinase from swine finishing barns and their association with antimicrobial use. *Appl. Environ. Microbiol.* 79, 1052–1054. doi: 10.1128/AEM.03169-12

Naseer, U., and Sundsfjord, A. (2011). The CTX-M conundrum: dissemination of plasmids and *Escherichia coli* clones. *Microb. Drug Resist.* 17, 83–97. doi: 10.1089/mdr.2010.0132

O'Shaughnessy, C. M., Cunningham, A. F., and MacLennan, A. C. (2012). The stability of complement-mediated bactericidal activity in human serum against salmonella. *PLoS One*. 7:e49147. doi: 10.1371/journal.pone.0049147

Paczosa, M. K., and Mecsas, J. (2016). *Klebsiella pneumoniae*: going on the offense with a strong defense. *Microbiol. Mol. Biol. Rev.* 80, 629–661. doi: 10.1128/MMBR.00078-15

Page, A. J., Cummins, C. A., Hunt, M., Wong, V., K., Reuter, S., Holden, M. T., et al. (2015). Roary: rapid large-scale prokaryote pan genome analysis. *Bioinformatics* 31, 3691–3693. doi: 10.1093/bioinformatics/btv421

Qi, Y., Wei, Z., Ji, S., Du, X., Shen, P., and Yu, Y. (2011). ST11, the dominant clone of KPC-producing *Klebsiella pneumoniae* in China. *J. Antimicrob. Chemother.* 66, 307–312. doi: 10.1093/jac/dkq431

Rainer, F., Eva, H., Kelly Wyres, L., Matthew Ellington, J., Kowarik, M., Holt, K. E., et al. (2016). The diversity of *Klebsiella pneumoniae* surface polysaccharides. *Microb. Genomics* 2:e000073. doi: 10.1099/mgen.0.000073

Ruiz-Garbajosa, P., Curiao, T., Tato, M., Gijon, D., Pintado, V., Valverde, A., et al. (2013). Multiclonal dispersal of KPC genes following the emergence of non-ST258 KPC-producing *Klebsiella pneumoniae* clones in Madrid, Spain. *J. Antimicrob. Chemother.* 68, 2487–2492. doi: 10.1093/jac/dkt237

Sahly, H., Navon-Venezia, S., Roesler, L., Hay, A., Carmeli, Y., Podschun, R., et al. (2008). Extended-spectrum beta-lactamase production is associated with an increase in cell invasion and expression of fimbrial adhesins in *Klebsiella pneumoniae*. *Antimicrob. Agents Chemother.* 52, 3029–3034. doi: 10.1128/AAC.00010-08

Seemann, T. (2014). Prokka: rapid prokaryotic genome annotation. *Bioinformatics* 30, 2068–2069. doi: 10.1093/bioinformatics/btu153

Shin, J., Kim, D. H., and Ko, K. S. (2011). Comparison of CTX-M-14- and CTX-M-15-producing *Escherichia coli* and *Klebsiella pneumoniae* isolates from patients with bacteremia. *J. Infect.* 63, 39–47. doi: 10.1016/j.jinf.2011.05.003

Struve, C., Bojer, M., and Krogfelt, K. A. (2009). Identification of a conserved chromosomal region encoding *Klebsiella pneumoniae* type 1 and type 3 fimbriae and assessment of the role of fimbriae in pathogenicity. *Infect. Immun.* 77, 5016–5024. doi: 10.1128/IAI.00585-09

Sun, Q., Wang, Y., Li, X. W., and Zheng, B., W. (2018). Study protocol for One Health data collections, analyses and intervention of the Sino-Swedish integrated multisectoral partnership for antibiotic resistance

containment (IMPACT). *BMJ Open* 8:e017832. doi: 10.1136/bmjopen-2017-017832

Tada, T., Tsuchiya, M., Shimada, K., Nga, T. T. T., Thu, L. T., A., Phu, T. T., et al. (2017). Dissemination of Carbapenem-resistant Klebsiella pneumoniae clinical isolates with various combinations of Carbapenemases (KPC-2, NDM-1, NDM-4, and OXA-48) and 16S rRNA Methylases (RmtB and RmtC) in Vietnam. *BMC Infect. Dis.* 17:467. doi: 10.1186/s12879-017-2570-y

Tijet, N., Sheth, P. M., Lastovetska, O., Chung, C., Patel, S. N., and Melano, R. G. (2014). Molecular characterization of *Klebsiella pneumoniae* carbapenemase (KPC)-producing *Enterobacteriaceae* in Ontario, Canada, 2008-2011. *PLoS ONE* 9:e116421. doi: 10.1371/journal.pone.0116421

Vubil, D., Figueiredo, R., Reis, T., Canha, C., Boaventura, L., and DA Silva, G. J. (2017). Outbreak of KPC-3-producing ST15 and ST348 Klebsiella pneumoniae in a Portuguese hospital. *Epidemiol. Infect.* 145, 595–599. doi: 10.1017/S0950268816002442

Wick, R. R., Heinz, E., Holt, K. E., and Wyres, K. L. (2018). Kaptive web: user-friendly capsule and lipopolysaccharide serotype prediction for Klebsiella genomes. *J. Clin. Microbiol.* 56, e00197–e00118. doi: 10.1128/JCM.00197-18

Wu, C. C., Lin, C. T., Cheng, W. Y., Huang, C. J., Wang, Z. C., and Peng, H. L. (2012). Fur-dependent MrkHI regulation of type 3 fimbriae in *Klebsiella pneumoniae* CG43. *Microbiology* 158, 1045–1056. doi: 10.1099/mic.0.053801-0

Xia, S., Fan, X., Huang, Z., Xia, L., Xiao, M., Chen, R., et al. (2014). Dominance of CTX-M-type extended-spectrum beta-lactamase (ESBL)-producing *Escherichia coli* isolated from patients with community-onset and hospital-onset infection in China. *PLoS ONE* 9:e100707. doi: 10.1371/journal.pone.0100707

Yan, J. J., Wang, M. C., Zheng, P. X., Tsai, L. H., and Wu, J. J. (2015). Associations of the major international high-risk resistant clones and virulent clones with specific ompK36 allele groups in Klebsiella pneumoniae in Taiwan. *N. Microb. N. Infect.* 5, 1–4. doi: 10.1016/j.nmni.2015.01.002

Ye, Q., Wu, Q., Zhang, S., Zhang, J., Yang, G., Wang, H., et al. (2017). Antibiotic-resistant extended spectrum ss-lactamase- and plasmid-mediated AmpC-producing enterobacteriaceae isolated from retail food products and the pearl river in Guangzhou, China. *Front. Microbiol.* 8:96. doi: 10.3389/fmicb.2017.00096

Zadoks, R. N., Griffiths, H. M., Munoz, M. A., Ahlstrom, C., Bennett, G. J., Thomas, E., et al. (2011). Sources of Klebsiella and Raoultella species on dairy farms: be careful where you walk. *J. Dairy Sci.* 94, 1045–1051. doi: 10.3168/jds.2010-3603

Zhang, H., Zhou, Y., Guo, S., and Chang, W. (2015). Prevalence and characteristics of extended-spectrum beta-lactamase (ESBL)-producing *Enterobacteriaceae* isolated from rural well water in Taian, China, 2014. *Environ. Sci. Pollut. Res. Int.* 22, 11488–11492. doi: 10.1007/s11356-015-4387-9

Zhou, K., Lokate, M., Deurenberg, R. H., Tepper, M., Arends, J. P., Raangs, E. G. C., et al. (2016). Use of whole-genome sequencing to trace, control and characterize the regional expansion of extended-spectrum beta-lactamase producing ST15 *Klebsiella pneumoniae*. *Sci. Rep.* 6:20840. doi: 10.1038/srep20840

Conflict of Interest Statement: The authors declare that the research was conducted in the absence of any commercial or financial relationships that could be construed as a potential conflict of interest.

frontiers in Microbiology

ORIGINAL RESEARCH
published: 26 February 2019
doi: 10.3389/fmicb.2019.00213

Genetic Characterization of a *bla*$_{VIM-24}$-Carrying IncP-7β Plasmid p1160-VIM and a *bla*$_{VIM-4}$-Harboring Integrative and Conjugative Element Tn*6413* From Clinical *Pseudomonas aeruginosa*

Lijun Zeng[1,2†], *Zhe Zhan*[1,3†], *Lingfei Hu*[1], *Xiaoyuan Jiang*[1], *Yanjun Zhang*[3], *Jiao Feng*[1], *Bo Gao*[1], *Yuee Zhao*[1], *Wenhui Yang*[1], *Huiying Yang*[1], *Zhe Yin*[1*] and *Dongsheng Zhou*[1*]

[1] State Key Laboratory of Pathogen and Biosecurity, Beijing Institute of Microbiology and Epidemiology, Beijing, China, [2] Department of Clinical Laboratory, The 307th Hospital of the Chinese People's Liberation Army, Beijing, China, [3] Zhejiang Provincial Center for Disease Control and Prevention, Hangzhou, China

This study presents three novel integrons In1394, In1395, and In1443, three novel unit transposons Tn*6392*, Tn*6393*, and Tn*6403*, one novel conjugative element (ICE) Tn*6413*, and the first sequenced IncP-7 resistance plasmid p1160-VIM from clinical *Pseudomonas aeruginosa*. Detailed sequence comparison of p1160-VIM (carrying Tn*6392* and Tn*6393*) and Tn*6413* (carrying Tn*6403*) with related elements were performed. Tn*6392*, Tn*6393*, and Tn*6403* were generated from integration of In1394 (carrying *bla*$_{VIM-24}$), In1395 and In1443 (carrying *bla*$_{VIM-4}$) into prototype Tn*3*-family unit transposons Tn*5563*, Tn*1403*, and Tn*6346*, respectively. To the best of our knowledge, this is the first report of a *bla*$_{VIM-24}$-carrying *P. aeruginosa* isolate.

Keywords: IncP-7 plasmid, unit transposon, integrative and conjugative element, *bla*$_{VIM}$, *Pseudomonas aeruginosa*

OPEN ACCESS

Edited by:
Charles W. Knapp,
University of Strathclyde,
United Kingdom

Reviewed by:
Hong-Yu Ou,
Shanghai Jiao Tong University, China
Mariagrazia Perilli,
University of L'Aquila, Italy

****Correspondence:***
Zhe Yin
jerry9yin@163.com
Dongsheng Zhou
dongshengzhou1977@gmail.com

† These authors have contributed equally to this work

Specialty section:
This article was submitted to Antimicrobials, Resistance and Chemotherapy, a section of the journal Frontiers in Microbiology

Received: *11 September 2018*
Accepted: *24 January 2019*
Published: *26 February 2019*

Citation:
Zeng L, Zhan Z, Hu L, Jiang X, Zhang Y, Feng J, Gao B, Zhao Y, Yang W, Yang H, Yin Z and Zhou D (2019) Genetic Characterization of a bla$_{VIM-24}$-Carrying IncP-7β Plasmid p1160-VIM and a bla$_{VIM-4}$-Harboring Integrative and Conjugative Element Tn6413 From Clinical Pseudomonas aeruginosa. Front. Microbiol. 10:213. doi: 10.3389/fmicb.2019.00213

INTRODUCTION

Plasmids of thirteen incompatibility groups in *Pseudomonas* (IncP-1 to IncP-7 and IncP-9 to IncP-14) have been recognized, varying in genetic structure, size and host range. IncP-7 plasmids, with a narrow host range, are of particular interest in environmental biodegradative potentials. Most sequenced members of this group, such as pCAR1 (Maeda et al., 2003), pND6_1 (Li et al., 2004), pWW53 (Pickup and Williams, 1985), pDK1 (Kunz and Chapman, 1981), and pHE24 (**Supplementary Table S1**), belong to toluene catabolic or degradation plasmids (D-plasmids) rather than resistance plasmids (R-plasmids).

Integrative and conjugative elements (ICEs), also known as conjugative transposons, are typically found integrated into host bacterial chromosomes and encode integrase (Int), excisionase (Xis) and type IV secretion system responsible for integration, excision, interbacterial transfer, respectively. ICEs confer antibiotic resistance (such as Tn*916*) (Franke and Clewell, 1981), heavy

metal resistance (such as R391) (Peters et al., 1991), and carbon utilization (such as ICEclc) (Gaillard et al., 2006).

Verona integron-encoded metallo-β-lactamase (VIM) is one of the most predominant families among class B carbapenemases and can hydrolyze nearly all β-lactams including carbapenems, except aztreonam (Queenan and Bush, 2007). This study dealt with a detailed genetic characterization of a novel *bla*$_{VIM-24}$-carrying IncP-7β plasmid p1160-VIM and a novel *bla*$_{VIM-4}$-carrying ICE Tn*6413* recovered from two different clinical *P. aeruginosa* isolates.

MATERIALS AND METHODS

Bacterial Isolates

Pseudomonas aeruginosa 1160 was isolated in 2015 from a sputum specimen of an elderly patient in a teaching hospital in Hebei Province, China. *P. aeruginosa* 6762 was recovered in 2016 from a sputum specimen of an elderly patient in a public hospital in Lanzhou Province, China. Bacterial species was identified by 16S rRNA gene sequencing and PCR detection of *P. aeruginosa*-specific *oafA* gene (Choi et al., 2013).

Conjugal Transfer

Conjugal transfer experiments were carried out with rifampin-resistant *P. aeruginosa* PAO1 used as recipients and each of the *bla*$_{VIM}$-positive 1160 or 6762 isolate as donor. Three milliliters of overnight cultures of each of donor and recipient bacteria were mixed together, harvested and resuspended in 80 μl of Brain Heart Infusion (BHI) broth (BD Biosciences). The mixture was spotted on a 1 cm^2 hydrophilic nylon membrane filter with a 0.45 μm pore size (Millipore) that was placed on BHI agar (BD Biosciences) plate and then incubated for mating at 30°C for 12 to 18 h. Bacteria were washed from filter membrane and spread on Muller-Hinton (MH) agar (BD Biosciences) plates containing 1000 μg/ml rifampin together with 2 μg/ml meropenem for selecting an *P. aeruginosa* transconjugant carrying *bla*$_{VIM}$.

Sequencing and Annotation

The genomic DNA of strain 6762 or the plasmid DNA of strain 1160 was isolated using an UltraClean Microbial Kit or a Large Construct Kit (Qiagen, NW, Germany), respectively, and then sequenced from a mate-pair library with average insert size of 5 kb (ranged from 2 to 10 kb) using a MiSeq sequencer (Illumina, CA, United States). DNA contigs were assembled based on their contig coverages using Newbler 2.6 (Nederbragt, 2014). Open reading frames and pseudogenes were predicted using RAST 2.0 (Brettin et al., 2015) combined with BLASTP/BLASTN (Boratyn et al., 2013) searches against the UniProtKB/Swiss-Prot database (Boutet et al., 2016) and the RefSeq database (O'Leary et al., 2016). Annotation of resistance genes, mobile elements, and other features was carried out using the online databases including CARD (Liang et al., 2017), ResFinder (Zankari et al., 2012), ISfinder (Siguier et al., 2006), INTEGRALL (Moura et al., 2009), and the Tn Number Registry (Roberts et al., 2008). Multiple and pairwise sequence comparisons were performed using MUSCLE 3.8.31 (Edgar, 2004) and BLASTN, respectively. Gene organization diagrams were drawn in Inkscape 0.48.1[1].

Phylogenetic Analysis

The nucleotide sequences of *repA* coding regions of indicative plasmids were aligned using MUSCLE 3.8.31 (Edgar, 2004). The unrooted neighbor-joining trees were generated from the aligned *repA* sequences using MEGA7 (Kumar et al., 2016), and evolutionary distances were estimated using the maximum composite likelihood method, with a bootstrap iteration of 1000.

Phenotypic Assays

Activity of Ambler class A/B/D carbapenemases in bacterial cell extracts was determined by a modified CarbaNP test (Wei et al., 2016). Bacterial antimicrobial susceptibility was tested by BioMérieux VITEK 2 and interpreted as per the 2017 Clinical and Laboratory Standards Institute (CLSI) guidelines (Wayne, 2017).

Nucleotide Sequence Accession Numbers

The sequence of p1160-VIM and that of the 6762 chromosome were submitted to GenBank under accession numbers MF144194 and CP030075, respectively.

RESULTS AND DISCUSSION

Overview of Sequenced p1160-VIM and Tn*6413*

Two *bla*$_{VIM}$-positive *P. aeruginosa* isolates, designated 1160 and 6762, were subjected to high-throughput genome sequencing. The 1160 isolate harbored a *bla*$_{VIM-24}$-carrying plasmid p1160-VIM, which had a circular DNA sequence of 205.4 kb in length, with an average G+C content of 56.3%. p1160-VIM belonged to the IncP-7 group because it had a IncP-7 *repA* gene responsible for plasmid replication initiation.

A 114.1-kb *bla*$_{VIM-4}$-harboring ICE Tn*6413* was found to integrate into tRNA^{Gly} gene in the 6762 chromosome. The modular structure of each of p1160-VIM and Tn*6413* was divided into the backbone (responsible for replication, maintenance and conjugal transfer) and separate accessory modules (defined as acquired DNA regions associated with mobile elements) integrated at different sites of the backbone (**Supplementary Figures S1**, **S2** and **Table 1**).

p1160-VIM could be transferred from the 1160 isolate into *P. aeruginosa* PAO1 through conjugation, generating the transconjugant 1160-VIM-PAO1. The self-transmissible nature of p1160-VIM was consistent with the presence of complete conjugal transfer regions in this plasmid. Strains 1160 and 1160-VIM-PAO1 had class B carbapenemase activity, and they were resistant to cefuroxime, ceftazidime, ceftriaxone and cefepime (with minimal inhibitory concentration values ≥ 64), and imipenem and meropenem (with minimal inhibitory concentration values ≥ 4), which were resulted from production

[1]https://inkscape.org/en/

TABLE 1 | Major features of plasmids and ICEs analyzed.

Category	Plasmids			Chromosomally integrated ICEs			
	pCAR1	**pDK1**	**p1160-VIM**	**Tn*6413***	**Tn*6533***	**Tn*6534***	**Tn*6417***
Accession number	AB088420	AB434906	MF144194	CP030075	AP014651	KX196168	CP013993
Group	IncP-7α	IncP-7β	IncP-7β	Tn*6417*	Tn*6417*	Tn*6417*	Tn*6417*
Reference of the relevant group	Yes	Yes					Yes
Total length (bp)	199,035	128,921	205,426	114,067	109,026	118,715	108,186
Total number of ORFs	217	117	237	157	112	104	107
Mean G+C content, %	56.3	56	56.2	60.5	61.3	61.3	61.3
Length of the backbone (bp)	115,716	76,947	135,455	84,038	84,181	83,215	85,992
Accessory modules	Tn*4676*, IS*pa73*, a Tn*3*-family transposon remnant, IS*Pre3*, and IS*Pre4*	Tn*4662*, Tn*4663*, IS*1162*, and IS*pa81*	Tn*6392*$, Tn*6393*$, IS*pa75*, IS*pa79*, IS*pa80*, IS*pa81*, IS*pa83*, and IS*Pre2*	Tn*6403*$	Tn*6531*$	Tn*6530*$	Tn*6532*$
Host bacterium	*P. resinovorans* CA10	*P. putida* HS1	*P. aeruginosa* 1160	*P. aeruginosa* 6762	*P. aeruginosa* NCGM257	*P. aeruginosa* RI_IH-2	*P. aeruginosa* DHS01
Nucleotide positions in the chromosome	–	–	–	337873.. 451939	5233626.. 5342651	1..118715	5365108.. 5473293

p1160-VIM and Tn6413 were sequenced this work, and all the other elements analyzed were derived from GenBank. $, carrying resistance genes.

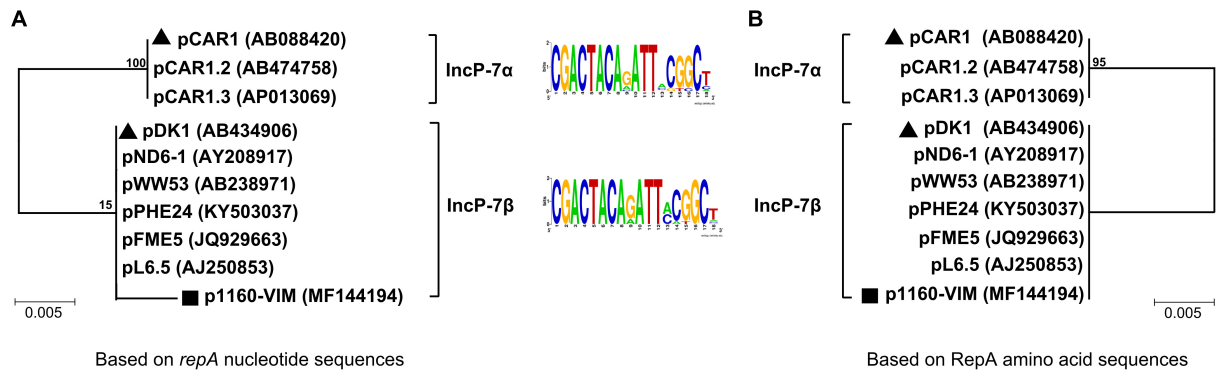

FIGURE 1 | Neighbor-joining phylogenetic trees of sequenced IncP-7 plasmids. Phylogenetic trees are constructed based on *repA* nucleotide **(A)** and amino acid sequences **(B)**, respectively. Degree of support (percentage) for each cluster of associated taxa, as determined by bootstrap analysis, is shown next to each branch. Triangles indicate IncP-7α and IncP-7β reference plasmids, while squares denote p1160-VIM sequenced in this work.

of VIM enzymes in these strains. Repeated conjugation attempts failed to transfer Tn*6413* from the 6762 isolate to PAO1.

Subgrouping of IncP-7 Plasmids Including p1160-VIM

A group of ten completely or partially sequenced plasmids (**Supplementary Table S1**; including p1160-VIM) with IncP-7 *repA* genes (≥ 95% nucleotide identity to that of p1160-VIM), were collected, and two phylogenetic trees (**Figure 1**) were constructed based on *repA* nucleotide and amino acid sequences, respectively. These ten plasmids could be divided into two separately clustering subgroups designated IncP-7α and IncP-7β. As shown by pairwise comparison of *repA* nucleotide sequences, plasmids within each of these two subgroups showed ≥ 99% nucleotide identity, while plasmids from these two different subgroups displayed ≤ 96% nucleotide identity (**Supplementary Table S2a**). Considerable genetic diversity was found between the *repA* genes of IncP-7α and IncP-7β, representing two separated lineages.

Predicted iterons (RepA-binding sites) were found within the *oriV* region downstream of *repA*, and plasmids from both subgroups shared a conserved iteron motif and an identical iteron copy number (**Figure 1** and **Supplementary Table S1**).

pCAR1 (Maeda et al., 2003) and pDK1 (Kunz and Chapman, 1981) were identified as IncP-7α and IncP-7β reference plasmids, respectively, because they were the first sequenced plasmids harboring complete conjugal transfer regions. In the phylogenetic

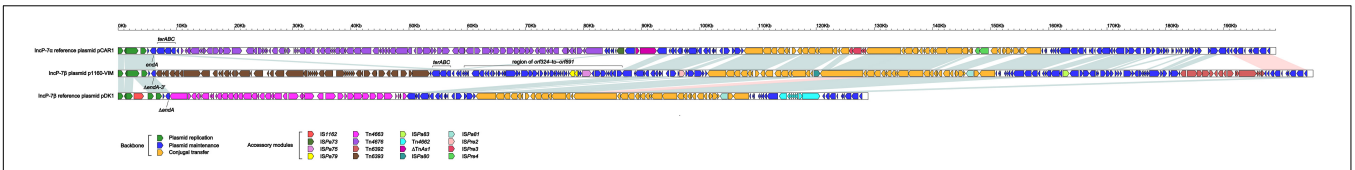

FIGURE 2 | Linear comparison of p1160-VIM with related plasmids. A linear comparison is carried out for complete DNA sequences of pCAR1 (accession number AB088420), p1160-VIM (this study), and pDK1 (accession number AB434906). Genes are denoted by arrows. Genes, mobile elements and other features are colored based on function classification. Blue shading denotes regions of homology (> 95% nucleotide identity), and pink shading denotes regions of homology (nucleotide identity between 90 and 95%).

TABLE 2 | Drug resistance genes in mobile elements sequenced this study.

Mobile element	Resistance marker	Resistance phenotype	Nucleotide position	Region located
p1160-VIM	*strAB*	Aminoglycoside resistance	8845..10484	Tn*6393*
	sul1	Sulphonamide resistance	18181..19020 40901..41740	
	qacED1	Quaternary ammonium compound resistance	19014..19361 41734..42081	
	folA	Trimethoprim resistance	19489..20022	
	qnrVC	Quinolone resistance	26051..26707	
	mph(E)	Macrolide resistance	34491..35375	
	msr(E)	Macrolide resistance	35431..36906	
	aadA1a	Streptomycin resistance	43627..44418	
	catB3q	Chloramphenicol resistance	46142..46774	
	ereA1c	Erythromycin resistance	46884..48104	
	aacA4	Aminoglycoside resistance	188445..188963 189993..190511	Tn*6392*
	bla$_{VIM-24}$	Carbapenem resistance	189102..189902	
	mer	Mercuric resistance	195914..197025	
Tn*6413*	*aadA2*	Streptomycin resistance	398558..399337	—
	qacED1	Quaternary ammonium compound resistance	399501..399848 411418..411765	
	sul1	Sulphonamide resistance	399842..400681 411759..412598	
	msr(E)	Macrolide resistance	402951..404426	
	mph(E)	Macrolide resistance	404482..405366	
	bla$_{VIM-4}$	Carbapenem resistance	409112..409996	
	aacA7	Aminoglycoside resistance	410090..410548	
	aacA4	Aminoglycoside resistance	410731..411249	
	mer	Mercuric resistance	414543..418060	

tree based on nucleotide sequences, p1160-VIM displayed a long branch, which resulted from presence of five single nucleotide polymorphisms (SNPs) in p1160-VIM, while all other plasmids had identical *repA* sequences (**Supplementary Figure S3**). Notably, these five SNPs did not lead to mutations of RepA amino acid sequences.

Comparison of p1160-VIM With pCAR1 and pDK1

pCAR1, pDK1 and p1160-VIM were included in a genomic comparison. These three plasmids had > 92% nucleotide identity across > 52% of their backbone sequences (**Supplementary Table S2b**), and their conserved backbone was composed of gene or gene loci responsible for replication initiation (*repA*), partitioning (*parABCW*), and conjugal transfer (*rlx*, *cpl*, *tivF3*, and *tivF6*). There were three major modular differences within their backbones (**Figure 2**): (i) a *terABC* region could be found in p1160-VIM and pCAR1 rather than pDK1; (ii) a 23.9-kb *orf324*–to–*orf891* region was found in only p1160-VIM; and (iii) the *endA* gene was intact in pCAR1 but was interrupted or truncated in p1160-VIM and pDK1. All these modular differences were resulted from integration of relevant accessory modules.

pCAR1, pDK1, and p1160-VIM carried totally different profiles of accessory modules (**Table 1**), which were composed of 10 distinct IS elements (IS*Pre2*, IS*Pre3*, IS*Pre4*, IS*1162*, IS*pa73*, IS*pa75*, IS*pa79*, IS*pa80*, IS*pa81*, and IS*pa83*), 5 different intact Tn*3*-family unit transposons (Tn*4676* from pCAR1, Tn*4662*, and Tn*4663* from pDK1, and Tn*6392* and Tn*6393* from p1160-VIM; a typical unit transposon encodes a transposase and a site-specific recombinase or resolvase as core transposition determinants, and also carries one or several accessory genes), and one Tn*3*-family transposon remnant. Only Tn*6392* and Tn*6393* of the above accessory modules (**Table 2**). Tn*4676* (**Supplementary Figure S4a**) carried core transposition genes (*tnpAC* and *tnpST*) genetically related to Tn*4651* (Maeda et al., 2003), and also

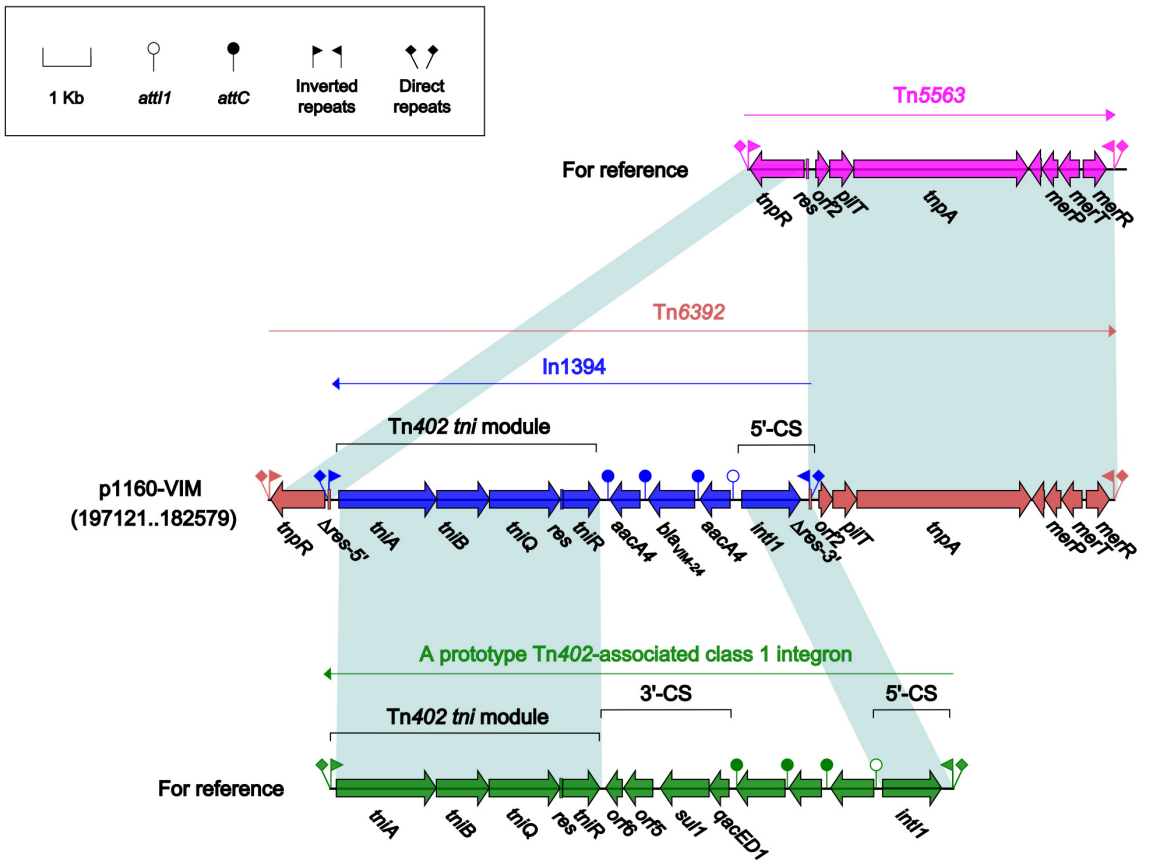

FIGURE 3 | Organization of Tn*6392* and comparison to related regions. Genes are denoted by arrows. Genes, mobile elements and other features are colored based on their functional classification. Shading denotes regions of homology (nucleotide identity > 95%). Numbers in brackets indicate nucleotide positions within corresponding plasmid sequences. Accession number of Tn*5563* for reference is U88088.

an *ant* (two-component anthranilate 1,2-dioxygenase) operon (Urata et al., 2004) interrupted by insertion of IS*Pre1* and a *car* (carbazole/dioxin degradation) operon (Nojiri et al., 2001). Tn*4662* encoded a RelBE toxin-antitoxin system involved in plasmid maintenance. Tn*4663* (**Supplementary Figure S4b**) was derived from Tn*4659* (Yano et al., 2007) and harbored a toluene-catabolic *xyl* gene cluster (Yano et al., 2010).

Comparison of Tn*6392* With Tn*5563*

Tn*6392* (**Figure 3**) from p1160-VIM was a novel derivative of Tn*5563*, which was originally characterized in *P. alcaligenes* and had the structure IRL (inverted repeat left)–*tnpR* (resolvase)–*res* (resolution site)–*orf2* (hypothetical protein)–*pliT* (*pilT* domain-containing protein)–*tnpA* (transposase)–*mer* (mercuric resistance gene locus)–IRR (inverted repeat right), bracketed by 5-bp or 7-bp direct repeats (DRs; target site duplication signals) at both ends (Yeo et al., 1998). Tn*6392* differed from Tn*5563* by insertion of a novel class 1 integron In1394 into *res*. The prototype Tn*402*-associated class 1 integron was typically organized as IRi (inverted repeat at the integrase end), 5'-CS [5'-conserved segment: *intI1* (integrase)-*attI1* (a specific recombination site)], GCA (gene cassette array), 3'-CS [3'-conserved segment: *qacED1*–*sul1*–*orf5*–*orf6*], a Tn*402 tni* module [*tniA* (transposase)–*tniB* (ATP-binding protein)–*tniQ* (transposition auxiliary protein)–*res*–*tniR* (serine resolvase)], and IRt (inverted repeat at the *tni* end) (Gillings et al., 2008). In1394, bracketed by 5 bp DRs at both ends, contained all the above core integron structures except 3'-CS. The GCA of In1394 consisted of a *bla*$_{VIM-24}$ gene and two copies of *aacA4*.

Comparison of Tn*6393* With Tn*1403*

Tn*6393* (**Figure 4**) was a novel derivative from Tn*1403* after insertion of a novel class 1 integron In1395 instead of In28 at the same position within *res*. Tn*1403* was initially identified in *P. aeruginosa* and displayed a backbone structure IRL–*tnpAR*–*res*–*sup*–*uspA*–*dksA*–*yjiK*–IRR, with integration of accessory modules In28 and Tn*5393c* into *res* and *dksA*, respectively (Stokes et al., 2007). In1395 belonged to complex class 1 integron, which was typically organized as IRi–5'-CS–VR1 (variable region 1)–3'-CS1 (the first copy of 3'-CS1: *qacED1*–*sul1*)–IS*CR1* (comment region)–VR2 (variable region 2)–3'-CS2 (a second 3'-CS: *qacED1*–*sul1*–*orf5*–*orf6*)–*tni*–IRt. In1395, bracketed by 5-bp DRs at both ends, was composed

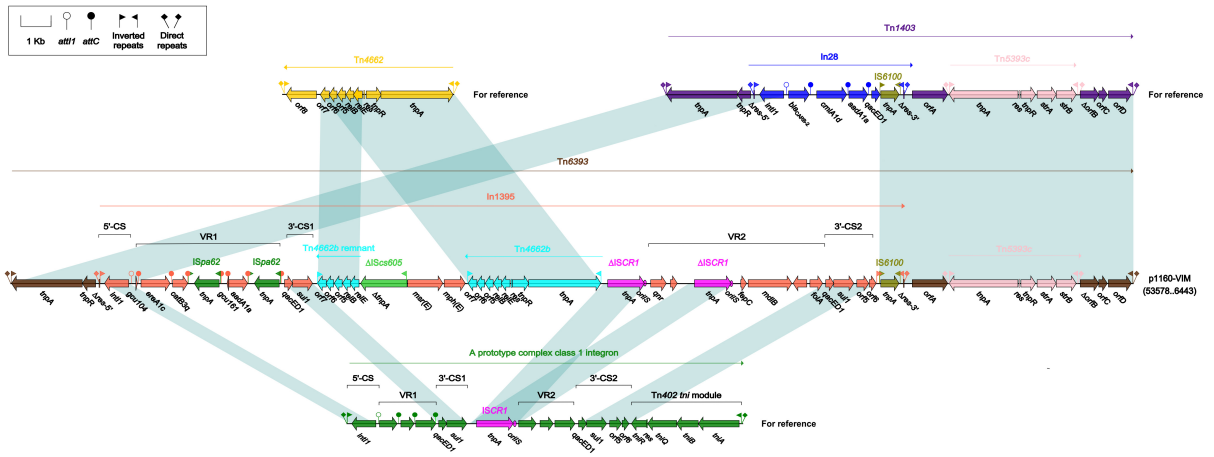

FIGURE 4 | Organization of Tn*6393* and comparison to related regions. Genes are denoted by arrows. Genes, mobile elements and other features are colored based on their functional classification. Shading denotes regions of homology (nucleotide identity > 95%). Numbers in brackets indicate nucleotide positions within corresponding plasmid sequences. Accession number of Tn*1403* for reference is AF313472.

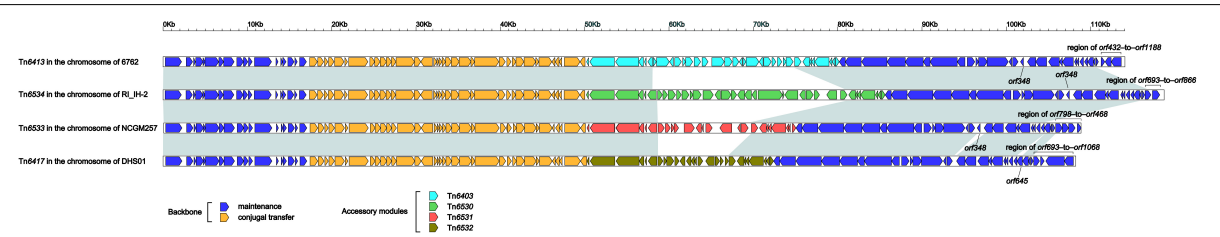

FIGURE 5 | Linear comparison of Tn*6413* with related ICEs. A linear comparison is carried out for DNA sequences of Tn*6413* (this study), Tn*6534* (accession number KX196168), Tn*6533* (accession number AP014651), and Tn*6417* (accession number CP013993). Genes are denoted by arrows. Genes, mobile elements and other features are colored based on function classification. Shading denotes regions of homology (> 95% nucleotide identity).

of IRi, 5'-CS, VR1 [GCA: *gcu104–aacA1–catB3q*:IS*pa62–gcu161–ereA1c*:IS*pa62*], 3'-CS1, IS*CR1* (further interrupted by ΔTn*4662b*–ΔIS*cs605*–*msr*(E)–*mph*(E)–Tn*4662b*), VR2 [containing *qnr*, ΔIS*CR1*, *folA* and other genes], 3'-CS2, IS*6100* (replacing *tni*) and IRt.

Comparison of Tn*6413* With Tn*6534*, Tn*6533*, and Tn*6417*

Tn*6413* (**Supplementary Figure S2**) was a novel ICE that could be divided into a single 30-kb accessory module Tn*6403* (**Figure 6**) and the remaining backbone regions. Tn*6413* belonged to a collection of 31 ICE or ICE-like sequences (**Supplementary Table S3**, including Tn*6417*, Tn*6534*, and Tn*6533*) with > 95% nucleotide identity across > 59% of Tn*6413* backbone. Tn*6417* was the first sequenced one and identified as the reference of these 31 Tn*6417*-family ICE sequences. A genomic comparison (**Figure 5**) was subjected to Tn*6413*, Tn*6534*, Tn*6533*, and Tn*6417* because they shared mostly highly similar backbones with 99% nucleotide identity and > 94% query coverage. These four Tn*6417*-family ICEs, which genetically differed from the two existing ICE families in *P. aeruginosa* (Kung et al., 2010) shared conserved DNA processing and conjugation genes. Three major modular differences were fund within the backbones of these four ICEs: (i) presence of *orf348* in only Tn*6417*; (ii) presence of *orf645* in only Tn*6417*; and iii) 3'-terminal regions (*orf432*–to–*orf1188*, *orf693*–to–*orf866*, *orf798*–to–*orf468*, and *orf693*–to–*orf1068* from Tn*6413*, Tn*6534*, Tn*6533* and Tn*6417*, respectively) differed from one another.

Each of these four Tn*6417*-family ICEs carried a single accessory module: Tn*6403*, Tn*6531*, Tn*6530*, and Tn*6532* (**Figure 6**) from Tn*6413*, Tn*6533*, Tn*6534*, and Tn*6417*, respectively; all these accessory modules were integrated at the same site of the ICE backbones and identified as Tn*6346* derivatives. The Tn*3*-family unit transposon Tn*6346*, originally found in heavy metal-tolerant *Achromobacter* spp., was a hybrid of the core transposition module *tnpAR–res* of Tn*5051* and the *mer* region of Tn*501* (Ng et al., 2009). Tn*6403*, Tn*6531*, Tn*6530*, and Tn*6532* differed from Tn*6346* by (i) interruption of original *tnpA*$_{Tn6346}$ due to insertion of IS*1071*, and (ii) insertion of four different class 1 integrons at the same position within the *urf2* gene of *mer*. Tn*6403*, Tn*6530* and Tn*6532*, rather than Tn*6531*, were bracketed by 5-bp DRs.

In127, In1328, In1155, and In159 found in Tn*6403*, Tn*6531*, Tn*6530*, and Tn*6532*, respectively, were intact integrons because all of them had paired terminal 25-bp repeats. Except

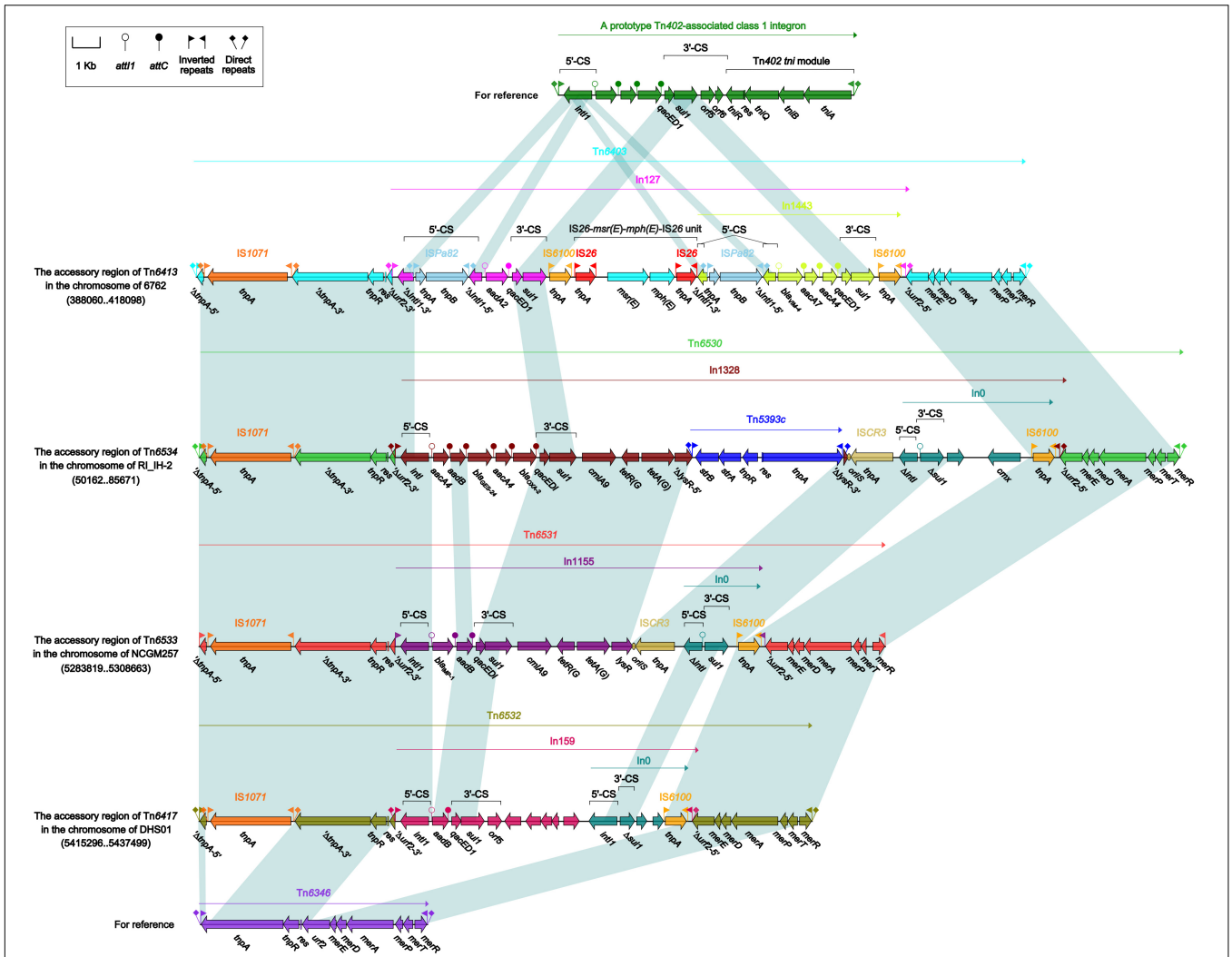

FIGURE 6 | Organization of Tn*6403* and comparison with related regions. Genes are denoted by arrows. Genes, mobile elements and other features are colored based on their functional classification. Shading denotes regions of homology (nucleotide identity > 95%). Numbers in brackets indicate nucleotide positions within corresponding chromosome sequences. Accession number of Tn*6346* for reference is EU696790.

In1155, all the other three were bracketed by 5-bp DRs. Notably, these integrons captured additional elements beside GCAs: IS*26*–*msr*(E)–*mph*(E)–IS*26* unit and a novel *bla*$_{VIM-4}$-carrying class 1 integron In1443, *cmlA9*–*tetRA*(G)–Tn*5393c*–IS*CR3* and *cmx*-carrying In0, *cmlA9*–*tetRA*(G)–IS*CR3* and empty In0, and empty In0 in In127, In1328, In1155, and In159, respectively. In1443 was organized as IRi–5'-CS (interrupted by insertion of IS*Pa82*)–GCA (*bla*$_{VIM-4}$–*aadA7*–*aadA4*)–Δ3'-CS–IS*6100* (replacing *tni*)–IRt.

CONCLUSION

IncP-7 R-plasmids are not commonly found in natural isolates, and p1160-VIM represents the first fully sequenced IncP-7 R-plasmid. Based on *repA* sequences, IncP-7 plasmids can be further divided into two separately clustering subgroups IncP-7α and IncP-7β. The two novel *bla*$_{VIM}$-carrying transposons Tn*6392* and Tn*6413*, which are integrated into the IncP-7β plasmid p1160-VIM and the *P. aeruginosa* chromosome, respectively, represent two different categories of transposons: Tn*3*-family unit transposon and Tn*6417*-family ICE. Tn*6392* and Tn*6413* contain novel class 1 integrons In1394 and In1443, which harbor the two GCAs *aacA4*–*bla*$_{VIM-24}$–*aacA4* and *bla*$_{VIM-4}$–*aadA7*–*aadA4,* respectively. The *bla*$_{VIM-24}$ gene was initially discovered from a *Klebsiella pneumoniae* isolate in Colombia in 2011 (Montealegre et al., 2011). This study presents the first report of a *bla*$_{VIM-24}$-carrying *P. aeruginosa* isolate and a *bla*$_{VIM}$-carrying IncP-7 plasmid. Both p1160-VIM and Tn*6413* are conjugative (self-transmissible) mobile elements, promoting horizontal transfer of resistance genes carried. Presence of IRi/IRt and a complete *tni* module would ensure In1394 self-transferable, while replacement of *tni* by IS*6100* would impair mobility of In1443. Class 1 integrons (e.g., In1394 and In1443)

could be integrated into a transposon (e.g., Tn*6392* and Tn*6413*) to restore or enhance their mobility.

ETHICS STATEMENT

The use of human specimens and all related experimental protocols were approved by the Committee on Human Research of the First Affiliated Hospital of Hebei North University and that of the General Hospital of Xinjiang Military Region, and carried out in accordance with the approved guidelines. The research involving biohazards and all related procedures were approved by the Biosafety Committee of the Beijing Institute of Microbiology and Epidemiology.

AUTHOR CONTRIBUTIONS

DZ and ZY conceived the study and designed experimental procedures. LZ, ZZ, LH, XJ, and YJZ performed the experiments. LZ, ZZ, YJZ, JF, BG, YEZ, and WY analyzed the data. LZ, ZZ, and HY contributed reagents and materials. DZ, ZY, LZ, and ZZ wrote this manuscript.

FUNDING

This work was supported by the National Key R&D Program (2018YFC1200100) of China.

SUPPLEMENTARY MATERIAL

The Supplementary Material for this article can be found online at: https://www.frontiersin.org/articles/10.3389/fmicb.2019.00213/full#supplementary-material

FIGURE S1 | Plasmid schematic maps. Three plasmids pCAR1, pDK1 and p1160-VIM are included. Genes are denoted by arrows, and the backbone and accessory module regions are highlighted in black and color, respectively. Innermost circle presents GC-skew [(G−C)/(G+C)], with a window size of 500 bp and a step size of 20 bp. Next-to-innermost circle presents GC content.

FIGURE S2 | ICE schematic maps. Four ICEs Tn*6413*, Tn*6534*, Tn*6533,* and Tn*6417* are included. Genes are denoted by arrows, and the backbone and accessory module regions are highlighted in black and color, respectively. Innermost circle presents GC-skew [(G−C)/(G+C)], with a window size of 500 bp and a step size of 20 bp. Next-to-innermost circle presents GC content.

FIGURE S3 | Alignment of *repA* nucleotide sequences. Red-labeled nucleotides indicate SNP sites. Sequence of IncP-7β reference plasmid pDK1 was bolded.

FIGURE S4 | Organization of Tn*4676* or Tn*4663* comparison with related regions. Genes are denoted by arrows. Genes, mobile elements and other features are colored based on their functional classification. Blue shading denotes regions of homology (nucleotide identity > 95%), and pink shading denotes regions of homology (average nucleotide identity 82%). Numbers in brackets indicate nucleotide positions within corresponding plasmid sequences. Accession number of Tn*4651* for reference is AJ344068.

TABLE S1 | Collection of *repA* and iteron sequences of IncP-7 plasmids.

TABLE S2 | Pairwise comparison of *repA* and backbone sequences.

TABLE S3 | List of the *Tn6417*-related sequences.

REFERENCES

Boratyn, G. M., Christiam, C., Cooper, P. S., George, C., Amelia, F., Ning, M., et al. (2013). Blast: a more efficient report with usability improvements. *Nucleic Acids Res.* 41, 29–33. doi: 10.1093/nar/gkt282

Boutet, E., Lieberherr, D., Tognolli, M., Schneider, M., Bansal, P., Bridge, A. J., et al. (2016). UniProtKB/Swiss-prot, the manually annotated section of the uniprot knowledgebase: how to use the entry view. *Methods Mol. Biol.* 1374, 23–54. doi: 10.1007/978-1-4939-3167-5_2

Brettin, T., Davis, J. J., Disz, T., Edwards, R. A., Gerdes, S., Olsen, G. J., et al. (2015). RASTtk: a modular and extensible implementation of the RAST algorithm for building custom annotation pipelines and annotating batches of genomes. *Sci. Rep.* 5:8365. doi: 10.1038/srep08365

Choi, H. J., Kim, M. H., Cho, M. S., Kim, B. K., Kim, J. Y., Kim, C., et al. (2013). Improved PCR for identification of *Pseudomonas aeruginosa*. *Appl. Microbiol. Biotechnol.* 97, 3643–3651. doi: 10.1007/s00253-013-4709-0

Edgar, R. C. (2004). MUSCLE: multiple sequence alignment with high accuracy and high throughput. *Nucleic Acids Res.* 32, 1792–1797. doi: 10.1093/nar/gkh340

Franke, A. E., and Clewell, D. B. (1981). Evidence for a chromosome-borne resistance transposon (Tn916) in *Streptococcus faecalis* that is capable of "conjugal" transfer in the absence of a conjugative plasmid. *J. Bacteriol.* 145:494.

Gaillard, M., Vallaeys, T., Vorholter, F. J., Minoia, M., Werlen, C., Sentchilo, V., et al. (2006). The clc element of *Pseudomonas* sp. strain B13, a genomic island with various catabolic properties. *J. Bacteriol.* 188, 1999–2013. doi: 10.1128/JB.188.5.1999-2013.2006

Gillings, M., Boucher, Y., Labbate, M., Holmes, A., Krishnan, S., Holley, M., et al. (2008). The evolution of class 1 integrons and the rise of antibiotic resistance. *J. Bacteriol.* 190, 5095–5100. doi: 10.1128/JB.00152-08

Kumar, S., Stecher, G., and Tamura, K. (2016). MEGA7: molecular evolutionary genetics analysis version 7.0 for bigger datasets. *Mol. Biol. Evol.* 33, 1870–1874. doi: 10.1093/molbev/msw054

Kung, V. L., Ozer, E. A., and Hauser, A. R. (2010). The accessory genome of *Pseudomonas aeruginosa*. *Microbiol. Mol. Biol. Rev.* 74, 621–641. doi: 10.1128/MMBR.00027-10

Kunz, D. A., and Chapman, P. J. (1981). Isolation and characterization of spontaneously occurring TOL plasmid mutants of *Pseudomonas putida* HS1. *J. Bacteriol.* 146, 952–964.

Li, W., Shi, J., Wang, X., Han, Y., Tong, W., Ma, L., et al. (2004). Complete nucleotide sequence and organization of the naphthalene catabolic plasmid pND6-1 from *Pseudomonas* sp. strain ND6. *Gene* 336, 231–240. doi: 10.1016/j.gene.2004.03.027

Liang, Q., Zhe, Y., Zhao, Y., Liang, L., Jiao, F., Zhe, Z., et al. (2017). Sequencing and comparative genomics analysis of the IncHI2 plasmids pT5282-mphA and p112298-catA and the IncHI5 plasmid pYNKP001-dfrA. *Int. J. Antimicrob. Agents* 49, 709–718. doi: 10.1016/j.ijantimicag.2017.01.021

Maeda, K., Nojiri, H., Shintani, M., Yoshida, T., Habe, H., and Omori, T. (2003). Complete nucleotide sequence of carbazole/dioxin-degrading plasmid pCAR1 in *Pseudomonas resinovorans* strain CA10 indicates its mosaicity and the presence of large catabolic transposon Tn4676. *J. Mol. Biol.* 326, 21–33. doi: 10.1016/s0022-2836(02)01400-6

Montealegre, M. C., Correa, A., Briceno, D. F., Rosas, N. C., De La Cadena, E., Ruiz, S. J., et al. (2011). Novel VIM metallo-beta-lactamase variant, VIM-24, from a *Klebsiella pneumoniae* isolate from Colombia. *Antimicrob. Agents Chemother.* 55, 2428–2430. doi: 10.1128/AAC.01208-10

Moura, A., Soares, M., Pereira, C., Leitão, N., Henriques, I., and Correia, A. (2009). INTEGRALL: a database and search engine for integrons, integrases and gene cassettes. *Bioinformatics* 25, 1096–1098. doi: 10.1093/bioinformatics/btp105

Nederbragt, A. J. (2014). On the middle ground between open source and commercial software - the case of the Newbler program. *Genome Biol.* 15:113. doi: 10.1186/gb4173

Ng, S. P., Davis, B., Palombo, E. A., and Bhave, M. (2009). A Tn5051-like mer-containing transposon identified in a heavy metal tolerant strain Achromobacter sp. AO22. *BMC Res. Notes* 2:38. doi: 10.1186/1756-0500-2-38

Nojiri, H., Sekiguchi, H., Maeda, K., Urata, M., Nakai, S. I., Yoshida, T., et al. (2001). Genetic characterization and evolutionary implications of a car gene cluster in the carbazole degrader Pseudomonas sp. Strain CA10. *J. Bacteriol.* 183, 3663–3679. doi: 10.1128/JB.183.12.3663-3679.2001

O'Leary, N. A., Wright, M. W., Rodney, B. J., Stacy, C., Diana, H., Rich, M. V., et al. (2016). Reference sequence (RefSeq) database at NCBI: current status, taxonomic expansion, and functional annotation. *Nucleic Acids Res.* 44:D733. doi: 10.1093/nar/gkv1189

Peters, S. E., Hobman, J. L., Strike, P., and Ritchie, D. A. (1991). Novel mercury resistance determinants carried by IncJ plasmids pMERPH and R391. *Mol. Gen. Genet.* 228, 294–299. doi: 10.1007/BF00282479

Pickup, R. W., and Williams, P. (1985). Evolutionary conservation ofgenescoding formeta pathway enzymeswithin TOL Plasmids pWWO andpWW53. *J. Bacteriol.* 164, 887–895.

Queenan, A. M., and Bush, K. (2007). Carbapenemases: the versatile -lactamases. *Clin. Microbiol. Rev.* 20, 440–458. doi: 10.1128/cmr.00001-07

Roberts, A. P., Chandler, M., Courvalin, P., Guedon, G., Mullany, P., Pembroke, T., et al. (2008). Revised nomenclature for transposable genetic elements. *Plasmid* 60, 167–173. doi: 10.1016/j.plasmid.2008.08.001

Siguier, P., Perochon, J., Lestrade, L., Mahillon, J., and Chandler, M. (2006). ISfinder: the reference centre for bacterial insertion sequences. *Nucleic Acids Res.* 34, 32–36. doi: 10.1093/nar/gkj014

Stokes, H. W., Elbourne, L. D., and Hall, R. M. (2007). Tn1403, a multiple-antibiotic resistance transposon made up of three distinct transposons. *Antimicrob. Agents Chemother.* 51, 1827–1829. doi: 10.1128/AAC.01279-06

Urata, M., Miyakoshi, M., Kai, S., Maeda, K., Habe, H., Omori, T., et al. (2004). Transcriptional regulation of the ant operon, encoding two-component anthranilate 1,2-dioxygenase, on the carbazole-degradative plasmid pCAR1 of *Pseudomonas resinovorans* strain CA10. *J. Bacteriol.* 186, 6815–6823. doi: 10.1128/JB.186.20.6815-6823.2004

Wayne, P. A. (2017). *Performance Standards for Antimicrobial Susceptibility Testing: Twenty-Seventh Informational Supplement M100-S27*. Wayne, PA: CLSI.

Wei, F., Zhou, D., Qian, W., Luo, W., Zhang, D., Qiang, S., et al. (2016). Dissemination of IMP-4-encoding pIMP-HZ1-related plasmids among *Klebsiella pneumoniae* and *Pseudomonas aeruginosa* in a Chinese teaching hospital. *Sci. Rep.* 6:33419. doi: 10.1038/srep33419

Yano, H., Garruto, C. E., Sota, M., Ohtsubo, Y., Nagata, Y., Zylstra, G. J., et al. (2007). Complete sequence determination combined with analysis of transposition/site-specific recombination events to explain genetic organization of IncP-7 TOL plasmid pWW53 and related mobile genetic elements. *J. Mol. Biol.* 369, 11–26. doi: 10.1016/j.jmb.2007.02.098

Yano, H., Miyakoshi, M., Ohshima, K., Tabata, M., Nagata, Y., Hattori, M., et al. (2010). Complete nucleotide sequence of TOL plasmid pDK1 provides evidence for evolutionary history of IncP-7 catabolic plasmids. *J. Bacteriol.* 192, 4337–4347. doi: 10.1128/JB.00359-10

Yeo, C. C., Tham, J. M., Kwong, S. M., Yiin, S., and Poh, C. L. (1998). Tn5563, a transposon encoding putative mercuric ion transport proteins located on plasmid pRA2 of *Pseudomonas alcaligenes*. *FEMS Microbiol. Lett.* 165, 253–260. doi: 10.1111/j.1574-6968.1998.tb13154.x

Zankari, E., Hasman, H., Cosentino, S., Vestergaard, M., Rasmussen, S., Lund, O., et al. (2012). Identification of acquired antimicrobial resistance genes. *J. Antimicrob. Chemother.* 67:2640. doi: 10.1093/jac/dks261

Conflict of Interest Statement: The authors declare that the research was conducted in the absence of any commercial or financial relationships that could be construed as a potential conflict of interest.

frontiers in Microbiology

ORIGINAL RESEARCH
published: 01 March 2019
doi: 10.3389/fmicb.2019.00194

Fate of Antibiotic Resistant *Pseudomonas putida* and Broad Host Range Plasmid in Natural Soil Microcosms

*Xiao-Ting Fan[1,2], Hu Li[1], Qing-Lin Chen[1], Yu-Sen Zhang[1,2], Jun Ye[1], Yong-Guan Zhu[1,2,3] and Jian-Qiang Su[1]**

[1] Key Laboratory of Urban Environment and Health, Institute of Urban Environment, Chinese Academy of Sciences, Xiamen, China, [2] University of Chinese Academy of Sciences, Beijing, China, [3] State Key Laboratory of Urban and Regional Ecology, Research Center for Eco-Environmental Sciences, Chinese Academy of Sciences, Beijing, China

Plasmid conjugation is one of the dominant mechanisms of horizontal gene transfer, playing a noticeable role in the rapid spread of antibiotic resistance genes (ARGs). Broad host range plasmids are known to transfer to diverse bacteria in extracted soil bacterial communities when evaluated by filter mating incubation. However, the persistence and dissemination of broad range plasmid in natural soil has not been well studied. In this study, *Pseudomonas putida* with a conjugative antibiotic resistance plasmid RP4 was inoculated into a soil microcosm, the fate and persistence of *P. putida* and RP4 were monitored by quantitative PCR. The concentrations of *P. putida* and RP4 both rapidly decreased within 15-day incubation. *P. putida* then decayed at a significantly lower rate during subsequent incubation, however, no further decay of RP4 was observed, resulting in an elevated RP4/*P. putida* ratio (up to 10) after 75-day incubation, which implied potential transfer of RP4 to soil microbiota. We further sorted RP4 recipient bacteria from the soil microcosms by fluorescence-activated cell sorting. Spread of RP4 increased during 75-day microcosm operation and was estimated at around 10^{-4} transconjugants per recipient at the end of incubation. Analysis of 16S rRNA gene sequences of transconjugants showed that host bacteria of RP4 were affiliated to more than 15 phyla, with increased diversity and shift in the composition of host bacteria. *Proteobacteria* was the most dominant phylum in the transconjugant pools. Transient transfer of RP4 to some host bacteria was observed. These results emphasize the prolonged persistence of *P. putida* and RP4 in natural soil microcosms, and highlight the potential risks of increased spread potential of plasmid and broader range of host bacteria in disseminating ARGs in soil.

Keywords: antibiotic resistance, horizontal gene transfer, conjugation, quantitative PCR, spread potential, flow cytometric sorting, phylogenetic analysis

OPEN ACCESS

Edited by:
Dongchang Sun, Zhejiang University of Technology, China

Reviewed by:
Peter Mullany, University College London, United Kingdom
Christopher Morton Thomas, University of Birmingham, United Kingdom
Barth F. Smets, Technical University of Denmark, Denmark

***Correspondence:**
Jian-Qiang Su
jqsu@iue.ac.cn

Specialty section:
This article was submitted to Antimicrobials, Resistance and Chemotherapy, a section of the journal Frontiers in Microbiology

Received: *30 September 2018*
Accepted: *23 January 2019*
Published: *01 March 2019*

Citation:
Fan X-T, Li H, Chen Q-L, Zhang Y-S, Ye J, Zhu Y-G and Su J-Q (2019) Fate of Antibiotic Resistant Pseudomonas putida and Broad Host Range Plasmid in Natural Soil Microcosms. Front. Microbiol. 10:194. doi: 10.3389/fmicb.2019.00194

INTRODUCTION

The global increased antimicrobial resistance level in human pathogens has posed significant threat to human health (UNEP, 2017). Other than clinical settings, antibiotic resistance genes (ARGs) have been frequently detected with elevated diversity and abundance in soil (Zhu et al., 2013). Bacteria could become antibiotic resistant via gene mutation, or horizontal gene transfer

(HGT) that would facilitate exchange of genetic information and contribute significantly to the evolution of bacteria (Boto, 2010; Soucy et al., 2015). HGT-mediated evolution would confer selective advantages to the host when facing environmental stress and thus promote the adaptation of bacteria under selective pressures (Daubin and Szollosi, 2016).

Plasmid conjugation is one of the most important mechanisms of HGT (Sorensen et al., 2005; Thomas and Nielsen, 2005), contributing to the wide spread of ARGs among environmental bacteria and human pathogens. Conjugative plasmids are often implicated in the rapid propagation and proliferation of ARGs (Dodd, 2012). These plasmids contain genes for the formation of pilus to transfer copies of themselves to other bacteria, enabling horizontal transfer of complete set of genes on the plasmid, including ARGs (Willetts and Wilkins, 1984; Willey et al., 2008). Furthermore, the transfer of diverse non-conjugative resistance plasmids can be facilitated by origin-of-transfer sequences of mobilizable plasmid (O'Brien et al., 2015). The massive use of antibiotics has resulted in high concentration of antibiotic residues in the environments, which may serve as a selection pressure that promote the dissemination of ARGs among environmental bacteria, including pathogenic species (Pruden et al., 2012; Guo et al., 2018). In addition, conjugative plasmids selected with antibiotics have been found to persist among bacterial populations or invade new strains even without antibiotics pressure (Dionisio et al., 2005).

The dissemination of ARGs caused by conjugation highly depends on the conjugation frequency and host range of plasmids. Broad host range plasmids are of high interest due to their transfer potency between phylogenetically distant hosts. Plasmid conjugation has been extensively studied in mating systems using typical pure strains as donors and recipients. Transconjugants can be quantified by colony counting on selective plates and the estimated transfer frequencies differs due to plasmids type, donor and recipient species, density ratio, mating time, and medium (Henschke and Schmidt, 1990; Modrie et al., 2010). However, culture-based screening of transconjugants can only partially determine the transfer frequency and identities of transconjugants in complex bacterial communities due to the limitation in culturing environmental bacteria (Elsas et al., 1989, 1990). Using fluorescent reporter genes to track plasmids made it possible to investigate the spread of resistance plasmids among environmental bacteria. To study the transfer of RP4 in activated sludge, the plasmid was marked with reporter gene *gfp* and detected by fluorescence microscopy, transfer frequencies were estimated in the range of 4×10^{-6} to 10^{-5} per recipient over a range of donor to recipient ratios (Geisenberger et al., 1999). Transconjugants obtained plasmids that marked with fluorescent genes can be sorted by fluorescence activated cell sorting (FACS) and identified by 16S rRNA gene sequencing (Musovic et al., 2006; Klumper et al., 2015).

Although these studies have expanded our understanding on plasmid conjugation, these mating experiments were generally conducted in relatively shorter mating period (4–72 h) (Sørensen et al., 2003; Wang et al., 2015b; Lin et al., 2016; Li et al., 2018) and optimized lab conditions that enabling sufficient cell-to-cell contact between donors and recipients (Musovic et al., 2010; Klumper et al., 2015, 2016; Li et al., 2018). Plasmid conjugation in soil could be affected by many factors including soil bacterial community composition, nutrients competition, and selective forces such as antibiotic and metal (Trevors et al., 1989; Elsas et al., 1990; Fox et al., 2008; Musovic et al., 2014; Klumper et al., 2016). However, current knowledge about plasmid conjugation in soil with complex bacterial communities is limited. The concentrations of donor bacteria and plasmid may significantly change after inoculation into soil, and the cell-to-cell contact between donors and recipients in soil is expected to decrease compared with filter mating systems, which could then affect plasmid conjugation in soil. In addition, retransfer of plasmid from transconjugants to the other bacterial populations may occur under extended incubation time.

To address these questions, soil microcosms were set up to investigate plasmid conjugation in soil. The aim of the study is to estimate the spread potential (SP) of plasmid and identify the phylogenetic affiliation of transconjugants in close to natural condition. *Pseudomonas putida* containing a broad host range plasmid tagged with green fluorescent protein (*gfp*) gene was used as donors and was inoculated into the soil microcosms. We tracked the abundance of both donor strains and plasmids in soil at intervals by qPCR. Transconjugants were collected with FACS and the 16S rRNA gene of transconjugants were amplified and sequenced.

MATERIALS AND METHODS

Donor Strain and Plasmid

Pseudomonas putida KT2442 was used as donor, which was chromosomally tagged with *dsRed* and *lacI*^{q} and harbored a broad host range IncP conjugative plasmid RP4 (Musovic et al., 2010). Plasmid RP4, containing resistance genes against ampicillin (Amp), kanamycin (Km), and tetracycline (Tc), was marked with *gfp* and a *lacI*^{q} repressible promoter upstream of *gfp* gene, *gfp* expression was inhibited in donor strains, but when the plasmid transfer to a recipient, *gfp* expression is possible (both the donor strain and plasmid were kindly provided by Professor Barth F. Smets, Technical University of Denmark). The donor strains were grown aerobically under 180 rpm at 37°C overnight in LB medium supplemented with 100 μg ml^{-1} Amp, 50 μg ml^{-1} Km and 20 μg ml^{-1} Tc. The bacterial cells were harvested by centrifugation at 8500 *g* for 15 min and the cell pellets were washed twice and re-suspended in 0.9% sterile saline solution, the concentration of resulting donor inoculants was measured by colony-forming unit (CFU) counting.

Soil Microcosms Set Up

Surface soil (sandy loam) was collected from a vegetable field in Xiamen, China, and was passed through a 2 mm sieve. Before inoculation, the original soil microbiota was extracted by Nycodenz density gradient separation (Burmolle et al., 2003; Eichorst et al., 2015) and the concentration of cells was 2.08×10^8 cells g^{-1} dry soil which was determined by flow cytometry (FlowSight Imaging Flow Cytometer, Amnis Millipore, United States) after SYTO 9 staining. Soil microcosms were

prepared in four replicate plastic pots by thoroughly mixing donor bacteria suspension into 500 g soil for each pot, providing a final donor strain density of 1.57×10^8 CFU g^{-1} dry soil. The microcosms were incubated for 75 days in a greenhouse at room temperature (28°C in the night and 35°C in the daytime on average) and were regularly irrigated twice daily to keep the water content at 60% field water capacity. Control soil without donor inoculation were prepared and incubated at the same condition. Soil samples were collected from each pot on day 0, 1, 2, 3, 4, 5, 10, 15, 20, 30, 60, and 75 and were partitioned into two sub-samples: one stored in 4°C for Nycodenz extraction of bacterial cells and one stored in −20°C for total DNA extraction.

DNA Extraction and qPCR

Soil DNA was extracted from 0.5 g of soil using FastDNA Spin kit for soil (MP Biomedical, Santa Ana, CA, United States). The concentrations of donor strain and plasmid were measured by quantification of *dsRed* and *gfp* genes, respectively. All quantifications were performed in triplicate using Roche 480 (Roche Molecular Systems Inc., Branchburg, NJ, United States). Real-Time PCR assays were performed in a total volume of 20 μl with 10 μl 2 × SYBR Premix ExTaq II (TaKaRa, Japan), 10 ng bovine serum albumin, 0.8 μl each primer (10 μM), 1 μl template DNA and 6.4 μl of nuclease-free PCR-grade water. The concentration of donor *P. putida* KT2442 in each sample was determined by quantifying a 702-bp region of *dsRed* gene using the primers dsRed-F (5′-ATATAGCATGCGGTCTTCCAAGAATGTTATCAA-3′) and dsRed-R (5′-CTCTCAAGCTTCCCGGGTTAAAGGAACAGAT GGTGGCG-3′) (Tolker-Nielsen et al., 2000). Quantitative amplifications were performed with the following thermal cycles: 95°C for 5 min, followed by 40 cycles of 95°C for 50s, 60°C for 50 s, 72°C for 50 s, and a final extension at 72°C for 10 min. The concentration of plasmid RP4 was measured by quantifying a 89-bp region of *gfp* gene using the primers gfp-F (5′-GAAGATGGAAGCGTTCAA-3′) and gfp-R (5′-AGGTAATGGTTGTCTGGTA-3′) (Hale et al., 2015) with a thermal cycles as follows: 95°C for 5 min, followed by 40 cycles of 95°C for 40 s, 58°C for 30 s, 72°C for 30 s, and a final extension at 72°C for 10 min. Copy numbers of 16S rRNA gene were quantified by qPCR as described previously (Zhu et al., 2017). Details for preparation of standard curves of these genes were provided in **Supplemental Method** (**Supplementary Figure S1**). Control soil without inoculation was systematically incubated, sampled and was subjected to DNA extraction and gene quantification in parallel.

Means and standard deviations of qPCR results were calculated with Microsoft Office Excel 2016. Gene copy numbers were normalized by the weight of the dry soil. Concentrations of donor KT2442 and plasmid RP4 in soil microcosms were converted to $\lg(C_t/C_0)$ (Tolker-Nielsen and Molin, 2000), where *Ct* corresponds the concentration at time *t*, C_0 corresponds the concentration at time 0 (Al-Jassim et al., 2017). The phrase "spread potential" was selected to indicate the diffusion and proliferation of plasmid RP4 in the soil microbiota during incubation period. SP is considered as the ratio of transconjugants to recipients and was roughly estimated using the formula:

$$SP_{qPCR} = (C_{gfp}/x - C_{dsRed})/(C_{16SrRNA}/4 - C_{dsRed})$$

SP_{qPCR} refers to the SP of RP4 estimated by qPCR, C is the concentration of gene determined by qPCR, presented as copies per gram dry soil. $C_{gfp}/x - C_{dsRed}$ presents the number of transconjugants per gram of dry soil with assumption that every donor strain maintains plasmid. IncP plasmids are typically 1–3 copies per cell, here x refers to the copies of RP4 per cell and 1 or 3 was used for calculation, thus the range of SP_{qPCR} could be estimated. The average number of 16S rRNA-encoding genes per bacterial cell is currently estimated at 4.1 on the basis of the Ribosomal RNA Database (Klappenbach et al., 2001; Chen et al., 2017). $C_{16SrRNA}/4$ presents the number of total bacteria per gram of dry soil.

Flow Cytometry Sorting of Transconjugants

Bacteria from collected soil samples were extracted by Nycodenz density gradient separation and were re-suspended in PBS. Soil (1.5 g) was homogenized in 5 ml 1× phosphate buffer saline (PBS) supplemented with 0.5% (v/v) Tween-20 in triplicates. The mixtures were shaken for 30 min by a vortex in room temperature then added to the top of Nycodenz (HistoDenz, Sigma, United States) solution at 1.31 g ml^{-1} (6 g HistoDenz was dissolved in 10 ml sterile ultra-pure water) carefully, followed by centrifugation at 8500 *g* for 15 min. The upper PBS and bacteria layers were carefully collected, fivefold diluted (v/v) in PBS and centrifuged at 8500 *g* for 20 min (Musovic et al., 2010). The upper solution was discarded, the resulting pellet was re-suspended and centrifuged again until the bacteria were concentrated to 1 ml suspension.

Bacterial cells including indigenous soil bacteria (no fluorescence), transconjugants (green fluorescence) and donor strains (red fluorescence) were scaled by FlowSight Imaging Flow Cytometer (Amnis Millipore, United States). Transconjugants were sorted using S3e Cell Sorter (Bio-Rad, United States). The flow cytometer was equipped by 488 and 561 nm two-laser systems. GFP fluorescent signal was excited by 488 nm laser and collected in bandpass Filter1 (525/30 nm). DsRed fluorescent was excited by 561 nm and checked in Filter2 (586/25 nm). *Escherichia coli* K12 was prepared as a fluorescence negative control. *E. coli* K12 harbored RP4::*gfp* was used as *gfp*-positive control. Donor strain *P. putida* KT2442 (RP4::*gfp*) was prepared as *dsRed*-positive and *gfp*-negative control. According to the fluorescent intensity of control bacteria, the events with high green fluorescence intensity and no red fluorescence intensity were gated, sorted and collected to a 5 ml BD Falcon collection tubes based on the signal of FSC, SSC, Filter1, and Filter 2. Then the enriched *gfp*-positive events were subjected to an additional sorting under the purity mode to ensure that all collected particles were *gfp* positive.

To test the accuracy of FACS, green fluorescence of sorted transconjugants were confirmed by confocal laser

scanning microscopy immediately. We also conducted a filter mating experiment using several pure bacterial strains as recipients. Mixtures of *Mangrovibacter yixingensis*, *Enterobacter tabaci*, *Enterobacillus tribolii*, *Pseudomonas aeruginosa* PAO1, *Burkholderia* sp., *Rhodococcus* sp., *Bacillus* sp., and *Staphylococcus* sp. with equal density were added to KT242/RP4 suspension at 1:1 cell ratio and filtered on 0.22 μm membrane filters (Millipore, United States). The filters with mating mixtures were placed on R2A agar and incubated at 37°C for 10 h. The mating cells were suspended in PBS for further flow cytometric sorting. Each green fluorescence-positive cell was sorted with single mode and collected in 100 μl PCR tubes. The plasmid marker gene *gfp* was amplified after whole genome amplification from 16 single transconjugants. GFP genes were 100% detected in each single cell and no donor strain or non-mating bacteria were sorted when verified by 16S rRNA gene amplification and sequencing.

The SP of RP4 estimated by flow cytometric sorting (SP_{FCM}) was roughly calculated using the formula:

$$SP_{FCM} = gfp \text{ positive cells} / (\text{total cells} - dsRed \text{ positive cells})$$

The plasmid-carrying donor strain was inoculated in the soil microcosms, which were incubated for 75 days. Plasmids transfer to recipients at different time and green fluorescent proteins in those transconjugant cells express with various levels. We only sorted out the events with higher fluorescent intensity to avoid the negative cells without RP4 being sorted.

Amplification and Analysis of 16S rRNA Gene of Transconjugants

Sorted cells of each sample were concentrated in 100 μl PCR tubes and were subjected to three thermal cycles including 15 s in 100°C water and 45 s on ice. The V4–V5 region of 16S rRNA gene was amplified using primer 515F (5′-GTGCCAGCMGCCGCGG-3′) and 907R (5′-CCGTCAATCMTTTRAGTTT-3′) (Zhou et al., 2011). Each 2 × 50 μl PCR reactions contained 25 μl ExTaq (TaKaRa, Japan), 1 μl BSA of 20 μg ml^{-1}, 1 μl each primer of 10 μM, 5 μl cell lysate as template and 17.5 μl nuclease-free PCR-grade water. The thermal program consisted of 95°C for 5 min, followed by 25 cycles of 95°C for 30 s, 58°C for 30 s, 72°C for 30 s, and a final extension at 72°C for 10 min. Non-template controls were included for detecting any contamination during PCR preparation (Chen et al., 2018). The amplicons were purified, quantified and sequenced on an Illumina Hiseq 2500 platform (Novogene, China) (Zhu et al., 2017). Raw pair-end reads were filtered to remove reads with low average quality scores and short reads (<300 nt). Sequences were processed with the Quantitative Insights Into Microbial Ecology (QIIME 1.9.1) pipeline (Caporaso et al., 2010; Edgar, 2010) as described previously (Zhu et al., 2017) for Operational Taxonomic Units (OTUs) clustering and taxonomic affiliation. Shannon index was generated to compare the level of bacterial diversity.

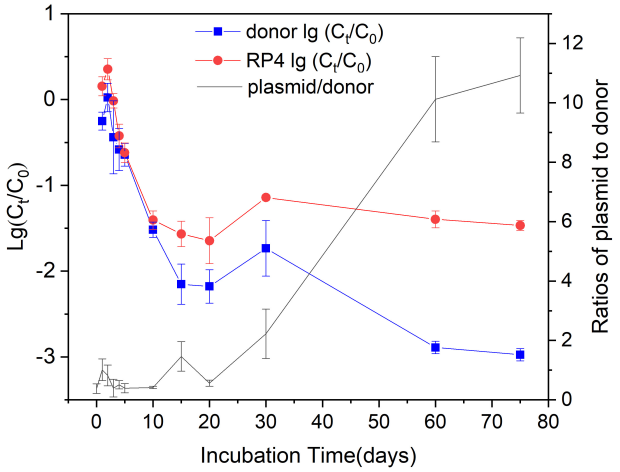

FIGURE 1 | The decay of the donor and plasmid during incubation. Log values of the ratios of donor (plasmid) concentration at time *t* to the initial concentration were shown on the left *Y*-axis. The donor and plasmid concentrations were represented by the copy numbers of *dsRed* and *gfp* gene, respectively. The right *Y*-axis showed the ratios of plasmid RP4 to donor. Error bars represent standard error (SE) of sampling replicates on each time point (n = 3 or 4).

Phylogenetic trees were constructed using MEGA 7 and iTOL[1] (Letunic and Bork, 2016).

To determine the potential pathogen species in the transconjugant pools, all the high-quality 16S rRNA gene sequences from each sample were blasted against a bacterial pathogen database with an E-value $< 1 \times 10^{-10}$ and a sequence identity >99%. The bacterial pathogen database including 557 pathogenic species was constructed in our previous study (Chen et al., 2016).

RESULTS

Fate of Donor Strain and Plasmid RP4

We quantified the marker genes *gfp* and *dsRed* to determine the concentrations of the plasmid RP4 and the donor strain KT2442, respectively. The fate of RP4 and KT2442 showed a similar decreased trend at the early stage of the microcosm operation, but differed at the late phase, resulting in a significantly increased RP4/KT2442 ratio during the incubation. The copy numbers of 16S rRNA gene in soil with KT2442/RP4 inoculation and control soil were at similar levels (3.3–4.9 × 10^9 copies g^{-1} dry soil), and they both remained relatively stable during the incubation.

Both the fate of KT2442 and RP4 showed biphasic behaviors during the 75-days incubation. KT2442 was inoculated into the soil at an initial concentration of about 10^8 CFU g^{-1} dry soil. They rapidly decreased 2.1 and 1.6 log to 10^6 copies g^{-1} dry soil within 15 days incubation, respectively (**Figure 1**). After 15-days of incubation, the fate of KT2442 and RP4 followed different trends. KT2442 decayed at a significantly lower rate during

[1]http://itol.embl.de/

subsequent incubation and persisted at a concentration around 10^5 copies g^{-1} dry soil on the 60th and 75th day. However, no further decay of RP4 was observed, the concentration of RP4 persisted at a level of 10^6 copies g^{-1} dry soil since the 10th day. Consequently, RP4/ KT2442 ratio significantly increased to around 10, indicating the occurrence of conjugation of RP4 to soil microbiota.

Spread Potential of Plasmid RP4

We estimated the SP based on qPCR and flow cytometric sorting data, respectively. Copy numbers of *gfp* were consistently lower than that of *dsRed* until the 60th day, so it was not possible to estimate the SP in early soil microcosm samples using data of qPCR. SP_{qPCR} in samples of 60th day and 75th day was calculated using the formula described before, the results were 4.65×10^{-4}–1.79×10^{-3} transconjugants per recipient (TC/R) and 3.63×10^{-4}–1.42×10^{-3} TC/R, respectively.

Soil microbiota extracted from collected samples during incubation was analyzed and sorted by fluorescence activated cell sorter (FACS), including the early samples. The sorting results showed that RP4 had transferred to soil microbiota in the early stage of incubation. SP_{FCM} of samples on the 5th day was 7.5×10^{-5} TC/R, while it increased to 2.5×10^{-4} TC/R on the 75th day. Only cells with strong green fluorescence signal were collected by flow cytometry, so the transconjugant numbers could be underestimated.

Phylogenetic Analysis of Transconjugant Pools

Transconjugants were sorted and subjected to taxonomic identification based on 16S rRNA gene sequences. The results indicated that transconjugants covered most of the major bacterial phyla, and the diversity of transconjugants differed at different time points. More than 300 transconjugant OTUs over 15 phyla were acquired from D5 samples. *Proteobacteria* was the most dominant phylum, contributing 85.7% of the transconjugant pools, followed by *Bacteroidetes* (3.17%), gram-positive *Firmicutes* (2.53%), and *Actinobacteria* (1.64%) (**Figure 2A**). The diversity of transconjugants significantly increased in D75 samples, in which three times more transconjugant OTUs were identified and affiliated to 20 phyla. Shannon index of D5 transconjugants was 2.38, while it was 4.41 of D75 transconjugant pools. *Proteobacteria*, *Bacteroidetes*, *Firmicutes*, and *Actinobacteria* were still the dominant phyla, contributing 95.6% of total transconjugants (**Figure 2A**). The relative abundance of *Actinobacteria* increased to 4.32% including 30 genera, while there were only 21 genera with lower abundance in D5 samples. The proportion of Gammaproteobacteria increased from 36.8 to 60.7% and Alphaproteobacteria decreased from 21.4 to 4.58%.

Nine of the top 20 genera of D75 were shared with D5 (**Figure 2B**), they were *Acinetobacter*, *Methylobacterium*, *Massilia*, *Klebsiella*, *Limnohabitans*, *Flavobacterium*, *Pseudomonas*, *Streptomyces*, and *Pelomonas*, among which 7 genera were affiliated to *Proteobacteria*. The relative abundance of shared top genera changed over time. *Acinetobacter* and *Massilia* occupied high proportions in both transconjugant pools. *Methylobacterium* was the second dominant genus of D5 transconjugants, with a relative proportion of 16.6%, while it decreased to 1.01% in D75. On the contrary, *Pseudomonas* was the most dominant genus of D75, contributed to 18.0% of transconjugant pool when excluding out the donor strain species *P. putida*. While it was 1.28% in D5. *Pseudomonas*, *Acinetobacter*, and *Staphylococcus* were detected with relative high frequency. Opportunistic pathogenic species such as *Acinetobacter baumannii*, *Aeromonas veronii*, *Enterobacter cloacae*, *Pseudomonas mendocina*, and *Staphylococcus aureus* were identified in the further sequence analysis (**Supplementary Table S1**). Transconjugant pools between D5 and D75 shared 63.7% genera (**Figure 2C**), indicating that plasmid transferred into most genera of the recipients at the early invasion stage. However, a total of 88 unique genera were detected in D75 samples, indicating significantly increased diversity of transconjugants. In addition, only 19 unique genera were detected in D5 samples, implying that these recipients may lose RP4 in subsequent incubation. Analysis of core OTUs of transconjugants accounting for 95% of the sequences indicated 127 OTUs in D75 and 66 OTUs of D5 (**Figure 2D**), among which, only 44 OTUs were shared between D5 and D75 samples.

Phylogenetic trees were constructed using the sequences of OTUs with relative abundance more than 0.01% in the transconjugant pools. The phylogenetic distance between donor strain *P. putida* and the transconjugants was shown, as well as the relative abundance of OTUs (**Figure 3**). RP4 transferred from *P. putida* to a broad range of recipients including phylogenetic distant group. However, the advantage of *Proteobacteria* was outstanding, with more than half of branches were identified to be *Proteobacteria*. Remarkably, much more branches identified to be *Pseudomonas* appeared in tree of D75, indicating the advantage of intra-genus transfer.

DISCUSSION

Human activities, including land application of manure, sewage sludge and wastewater, are providing direct routes for disseminating antibiotic resistant bacteria and genes to soil (Zhu et al., 2018). The spread of ARGs in soil is closely associated with HGT, however, studies on the HGT in soil are challenging due to the complexity of HGT process in soil (Williams-Nguyen et al., 2016). In this study, we use quantitative PCR and an established fluorescent bioreporter system to estimate the SP and delineate the taxonomic affiliation of recipient populations of a plasmid carrying multiple ARGs in soil. Occurrence of HGT need physical contact between donor and recipient populations, thus the population density of donor strain in soil is an important parameter for HGT (Martinez et al., 2015).

Using *P. putida* KT2442 harboring RP4 as a model strain, we thus investigated the dynamics of donor in a vegetable soil microcosm. We observed a biphasic decay behavior of both *P. putida* KT2442 and RP4. This biphasic decay had been well documented in *P. putida*, *E. coli* and pathogens (Brouwer et al., 2017; Mantilla-Calderon and Hong, 2017). The concentrations of

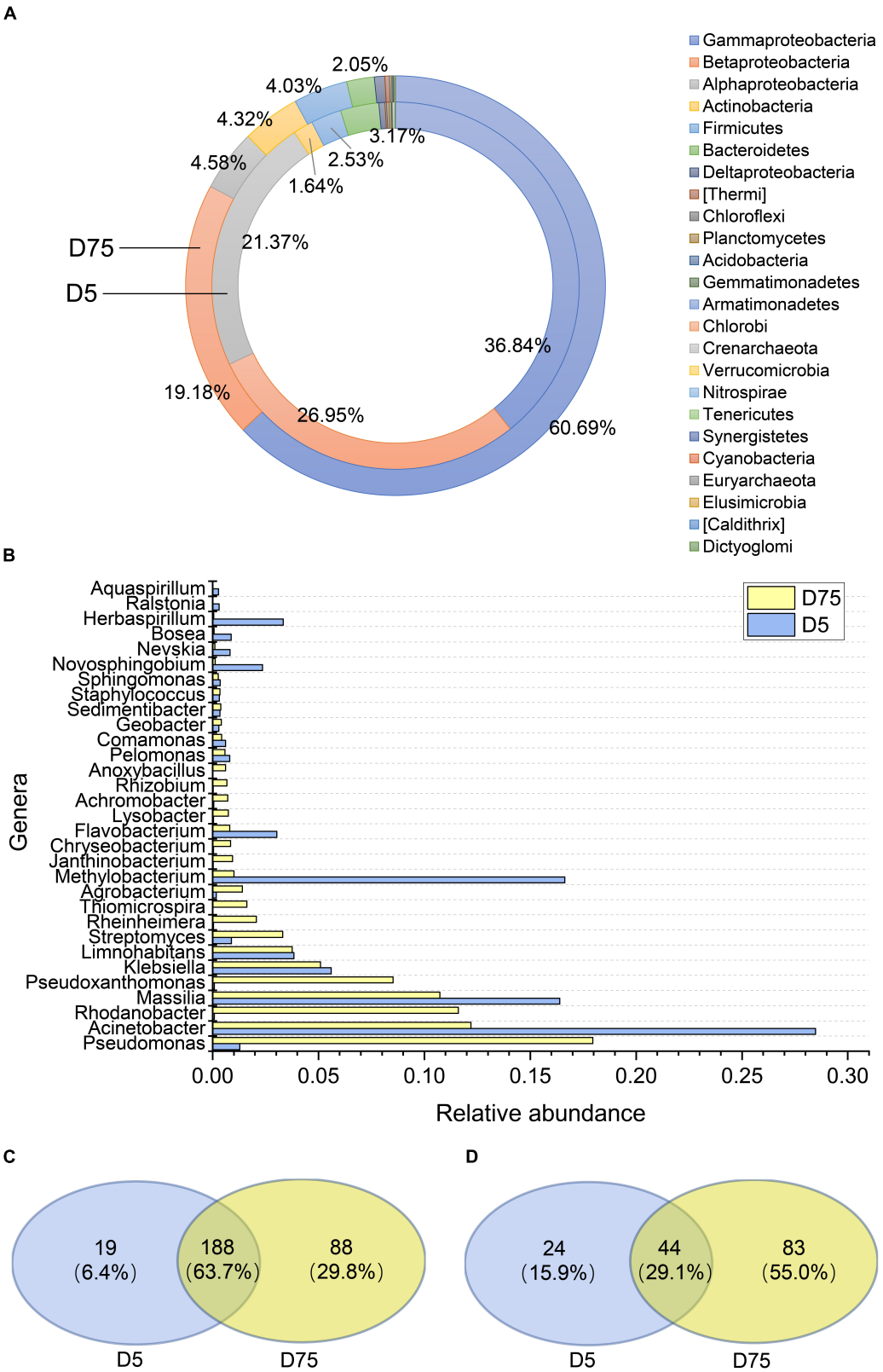

FIGURE 2 | Composition of sorted transconjugant pools on day 5 and day 75. **(A)** Phylum distribution. **(B)** The relative abundance of the top 20 genera on day 5 or day 75. **(C)** Venn diagram showing the number of shared and unique genera between D5 and D75. **(D)** Venn diagram showing the number of shared and unique core OTUs that contributed 95% sequences among D5 and D75 samples.

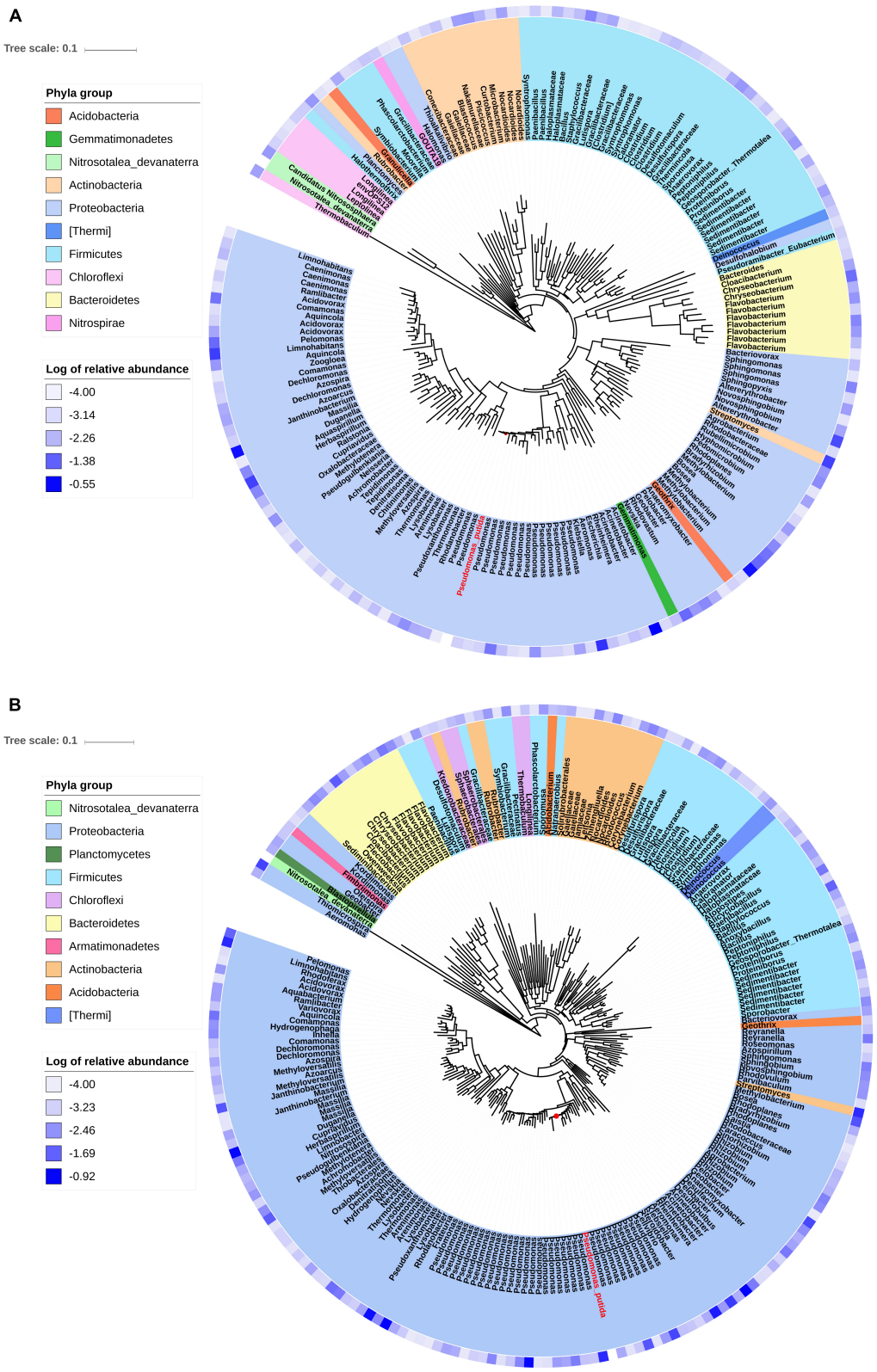

FIGURE 3 | Phylogenetic tree showing the identified OTUs that contributed more than 0.01% in the transconjugant pools. **(A)** Showing transconjugants on D5. **(B)** Showing transconjugants on D75. The 16S rRNA gene sequence of *Pseudomonas putida* (donor strain) was shown in red letters and *Nitrosotalea devanaterra* (distant relative species to most of the transconjugants) was imported as the reference. The blue gradient circle at the periphery of the tree represents log of relative abundance of the OTU in the transconjugant pools.

dsRed and *gfp* were average 1.3×10^8 and 4.3×10^7 copies g^{-1} dry soil after initial spiking event, and they slightly increased at first 2 days after inoculation, which might be due to the division of donor strains and was in accordance with previous studies (Elsas et al., 1989; Henschke and Schmidt, 1990). Concentration of *P. putida* KT2442 rapidly decreased but a significantly reduced decay rate was observed after 15 days, and the copy number of *dsRed* maintained at 10^5 copies g^{-1} dry soil at the late stage of incubation. *P. putida* is frequently detected in natural soil and this result suggested that *P. putida* KT2442 survived and established in soil for a relatively longer period, which may highly affect the persistence and proliferation of plasmid, as well as the transfer of plasmid (Turner et al., 1998).

Plasmid RP4 showed a similar decay at the early stage of incubation, however, no further decay was observed after 15 day. The copy numbers of *gfp* plateaued at average 10^6 copies g^{-1} dry soil during the following incubation period, resulting an escalated plasmid/donor ratio that peaked at 10 on day 60. The plasmid decay kinetics may mainly be affected by three factors, the lysis of host bacteria and subsequent release of plasmid, the stability of plasmid in host bacteria, and plasmid transfer between host and recipient populations. Previous reports have shown that IncP plasmid is stable in *Pseudomonas* (Shintani et al., 2006; Yano et al., 2007), thus cellular decay of *P. putida* KT2442 may drive the kinetic of RP4 at the early stage of incubation. Though the copies of RP4 decreased rapidly and were lower to the concentrations of KT2442 at the early stage, plasmid transfer potentially occurred during the period, which was confirmed by flow cytometric sorting and analysis of transconjugants. It was reported that transconjugants appeared immediately after introduction of *E. coli* C600(RP4) or *P. putida* BH(RP4) into soil microcosms (Inoue et al., 2009). The donor bacteria were added with a cell ratio at 1:1 to indigenous soil bacteria, which was a relative high level although this ratio had been reported in previous studies (Elsas et al., 1990; Kozdrój, 2008; Lin et al., 2016; Stalder and Top, 2016). We conducted the experiment with a cell ratio at 1:1 for two reasons. Firstly, a higher conjugation frequency was observed when the mating densities of donor and recipients were equal according to a early study (Qiu et al., 2012). Secondly, added bacteria would decay rapidly when inoculated into microcosms (Elsas et al., 1989; Inoue et al., 2009; Bonot and Merlin, 2010), a high initial concentration of donors may be conducive to maintaining the donor cells and the subsequent analysis of plasmid transfer in this long-term experiment. Further experiments should be conducted with a gradient of donor cells for better understanding the transfer of plasmid in soil.

An established fluorescent bioreporter approach was adopted to estimate the SP of RP4 in soil, which was 7.5×10^{-5} TC/R on day 5 and 2.5×10^{-4} TC/R on day 75. The SP significantly increased during incubation, the longer incubation period with donor in soil microcosms may partially contribute to the spread of plasmid in this study, which provide sufficient time for plasmid transfer between donors and recipients, or even between transconjugants and recipients. The composition of recipient bacterial community is another factor that could significantly affect the SP of plasmid (Lopatkin et al., 2016). For example, the transfer frequency that estimated via a 48-h filter mating experiment using the same donor strain and plasmid with sewage sludge microbiota ranged from 3 to 50 conjugation events per 100000 cells (Li et al., 2018). Other factors, including antibiotics (Subbiah et al., 2011), nanomaterials (Qiu et al., 2012), metals (Klumper et al., 2016), UV irradiation (Lin et al., 2016), or ionic liquid (Wang et al., 2015a) may also affect the plasmid transfer in soil. Further studies should be conducted to investigate the effect of multiple factors on plasmid transfer and persistence in soil. The overall conjugation dynamics were determined by conjugation efficiency and propagation of transconjugants (Lopatkin et al., 2016). Discriminating the contribution of these two processes is challenging in soil. Nevertheless, our results provided an overall estimation of the proportion of host bacteria of plasmid in soil microbiota, which is essential for evaluating the potential role of plasmid transfer in mediating the dissemination of ARGs in soil after long-term exposure to antibiotic resistant bacteria.

Phylogenetic analysis of sorted transconjugants indicated that RP4 disseminated to a broad range of hosts, which had been documented in previous reports, with *Proteobacteria* being the predominant phylum (Klumper et al., 2015, 2016; Li et al., 2018), followed by *Bacteroidetes*, *Firmicutes*, and *Actinobacteria*. Gammaproteobacteria, known as the dominant hosts for the broad host range plasmid (Suzuki et al., 2010; Norberg et al., 2011), occupied 41.75% of total transconjugants in day 75. The most dominant genera in transconjugant pool of D75 including *Pseudomonas*, *Acinetobacter*, and *Rhodanobacter* were all from this class. However, it was observed that the phylogenetic diversity increased during the incubation with 88 unique genera were detected in day 75, implying that the plasmid may transfer to a broader range of taxa upon extended exposure time in soil than we expected. As the concentrations of *P. putida* KT2442 and RP4 were at roughly the same level from day 15 to 30, the increased diversity of transconjugant pools could be attributed, at least in part, to the plasmid transfer between transconjugants and recipient populations. A significant shift of transconjugant pool composition was also observed, for examples, 11 of the top 20 genera in day 75 were different from those in day 5 samples (**Figure 3B**). *Rhodovastum* (0.15%)/*Sphingopyxis* (0.13%) (Alphaproteobacteria), and *Planctomyces* (0.17%, *Planctomycetes*) were detected on day 5, but were not recovered on day 75. These data indicated that RP4 transiently transferred to members of these genera but they lost the plasmid during the following incubation, probably due to the fitness cost of the plasmid or the plasmid cannot replicate in these recipients. Nevertheless, the existing of transient host bacteria could aid in the survival and persistence of plasmid (Yano et al., 2013) in soil, and consequently contribute to the dissemination of ARGs in soil.

AUTHOR CONTRIBUTIONS

J-QS and Y-GZ designed the experiments. X-TF and HL performed the microcosm experiments and qPCR. X-TF

performed the flow cytometric sorting. Q-LC, Y-SZ, and JY conducted the phylogenetic analysis. All authors contributed to data analysis. X-TF and J-QS wrote the manuscript with comments from all authors.

FUNDING

This study was financially supported by the National Key Research and Development Program from Ministry of Science and Technology (2016YFD0800205), National Natural Science Foundation of China (31722004), K.C. Wong Education Foundation and Youth Innovation Promotion Association, CAS.

ACKNOWLEDGMENTS

We thank Prof. Barth F. Smets (Technical University of Denmark) for kindly providing *P. putida* KT2442::*dsRed* and RP4::*gfp*, and Tian-Lei Qiu and Xu-Ming Wang from Beijing Academy of Agriculture and Forestry Sciences for support in cell sorting by flow cytometry.

SUPPLEMENTARY MATERIAL

The Supplementary Material for this article can be found online at: https://www.frontiersin.org/articles/10.3389/fmicb.2019.00194/full#supplementary-material

REFERENCES

Al-Jassim, N., Mantilla-Calderon, D., Wang, T., and Hong, P. Y. (2017). Inactivation and gene expression of a virulent wastewater *Escherichia coli* strain and the nonvirulent commensal *Escherichia coli* DSM1103 strain upon solar irradiation. *Environ. Sci. Technol.* 51, 3649–3659. doi: 10.1021/acs.est.6b05377

Bonot, S., and Merlin, C. (2010). Monitoring the dissemination of the broad-host-range plasmid pB10 in sediment microcosms by quantitative PCR. *Appl. Environ. Microbiol.* 76, 378–382. doi: 10.1128/AEM.01125-09

Boto, L. (2010). Horizontal gene transfer in evolution: facts and challenges. *Proc. Biol. Sci.* 277, 819–827. doi: 10.1098/rspb.2009.1679

Brouwer, A. F., Eisenberg, M. C., Remais, J. V., Collender, P. A., Meza, R., and Eisenberg, J. N. (2017). Modeling biphasic environmental decay of pathogens and implications for risk analysis. *Environ. Sci. Technol.* 51, 2186–2196. doi: 10.1021/acs.est.6b04030

Burmolle, M., Hansen, L. H., Oregaard, G., and Sorensen, S. J. (2003). Presence of N-acyl homoserine lactones in soil detected by a whole-cell biosensor and flow cytometry. *Microb. Ecol.* 45, 226–236. doi: 10.1007/s00248-002-2028-6

Caporaso, J. G., Kuczynski, J., Stombaugh, J., Bittinger, K., Bushman, F. D., Costello, E. K., et al. (2010). QIIME allows analysis of high-throughput community sequencing data. *Nat. Methods* 7:335. doi: 10.1038/nmeth.f.303

Chen, Q., An, X., Li, H., Su, J., Ma, Y., and Zhu, Y. G. (2016). Long-term field application of sewage sludge increases the abundance of antibiotic resistance genes in soil. *Environ. Int.* 9, 1–10. doi: 10.1016/j.envint.2016.03.026

Chen, Q.-L., Fan, X.-T., Zhu, D., An, X.-L., Su, J.-Q., and Cui, L. (2018). Effect of biochar amendment on the alleviation of antibiotic resistance in soil and phyllosphere of *Brassica chinensis* L. *Soil Biol. Biochem.* 119, 74–82. doi: 10.1016/j.soilbio.2018.01.015

Chen, Q. L., Li, H., Zhou, X. Y., Zhao, Y., Su, J. Q., Zhang, X., et al. (2017). An underappreciated hotspot of antibiotic resistance: the groundwater near the municipal solid waste landfill. *Sci. Total Environ.* 609, 966–973. doi: 10.1016/j.scitotenv.2017.07.164

Daubin, V., and Szollosi, G. J. (2016). Horizontal gene transfer and the history of life. *Cold Spring Harb. Perspect. Biol.* 8:a018036. doi: 10.1101/cshperspect.a018036

Dionisio, F., Conceicao, I. C., Marques, A. C., Fernandes, L., and Gordo, I. (2005). The evolution of a conjugative plasmid and its ability to increase bacterial fitness. *Biol. Lett.* 1, 250–252. doi: 10.1098/rsbl.2004.0275

Dodd, M. C. (2012). Potential impacts of disinfection processes on elimination and deactivation of antibiotic resistance genes during water and wastewater treatment. *J. Environ. Monit.* 14, 1754–1771. doi: 10.1039/c2em00006g

Edgar, R. C. (2010). Search and clustering orders of magnitude faster than BLAST. *Bioinformatics* 26, 2460–2461. doi: 10.1093/bioinformatics/btq461

Eichorst, S. A., Strasser, F., Woyke, T., Schintlmeister, A., Wagner, M., and Woebken, D. (2015). Advancements in the application of NanoSIMS and Raman microspectroscopy to investigate the activity of microbial cells in soils. *FEMS Microbiol. Ecol.* 91:fiv106. doi: 10.1093/femsec/fiv106

Elsas, J. D. V., Trevors, J. T., Overbeek, L. S. V., and Starodub, M. E. (1989). Survival of *Pseudomonas fluorescens* containing plasmids RP4 or pRK2501. *Can. J. Microbiol.* 35, 951–959. doi: 10.1139/m89-157

Elsas, J. D. V., Trevors, J. T., Starodub, M. E., and Overbeek, L. S. V. (1990). Transfer of plasmid RP4 between pseudomonads after introduction into soil; influence of spatial and temporal aspects of inoculation. *FEMS Microbiol. Lett.* 73, 1–11. doi: 10.1016/0378-1097(90)90718-6

Fox, R. E., Zhong, X., Krone, S. M., and Top, E. M. (2008). Spatial structure and nutrients promote invasion of IncP-1 plasmids in bacterial populations. *ISME J.* 2, 1024–1039. doi: 10.1038/ismej.2008.53

Geisenberger, O., Ammendola, A., Christensen, B. B., Molin, S., Schleifer, K.-H., and Eberl, L. (1999). Monitoring the conjugal transfer of plasmid RP4 in activated sludge and in situ identification of the transconjugants. *FEMS Microbiol. Lett.* 174, 9–17. doi: 10.1111/j.1574-6968.1999.tb13543.x

Guo, X., Yan, Z., Zhang, Y., Xu, W., Kong, D., Shan, Z., et al. (2018). Behavior of antibiotic resistance genes under extremely high-level antibiotic selection pressures in pharmaceutical wastewater treatment plants. *Sci. Total Environ.* 612, 119–128. doi: 10.1016/j.scitotenv.2017.08.229

Hale, L., Luth, M., and Crowley, D. (2015). Biochar characteristics relate to its utility as an alternative soil inoculum carrier to peat and vermiculite. *Soil Biol. Biochem.* 81, 228–235. doi: 10.1016/j.soilbio.2014.11.023

Henschke, R. B., and Schmidt, F. R. J. (1990). Plasmid mobilization from genetically engineered bacteria to members of the indigenous soil microflora in situ. *Curr. Microbiol.* 20, 105–110. doi: 10.1007/bf02092881

Inoue, D., Soda, S., Tsutsui, H., Yamazaki, Y., Murashige, K., Sei, K., et al. (2009). Occurrence and persistence of indigenous transconjugants carrying conjugative plasmids in soil. *J. Biosci. Bioeng.* 108, 231–234. doi: 10.1016/j.jbiosc.2009.03.014

Klappenbach, J. A., Saxman, P. R., Cole, J. R., and Schmidt, T. M. (2001). rrndb: the ribosomal RNA operon copy number database. *Nucleic Acids Res.* 29, 181–184. doi: 10.1093/nar/29.1.181

Klumper, U., Dechesne, A., Riber, L., Brandt, K. K., Gulay, A., Sorensen, S. J., et al. (2016). Metal stressors consistently modulate bacterial conjugal plasmid uptake potential in a phylogenetically conserved manner. *ISME J.* 11, 152–165. doi: 10.1038/ismej.2016.98

Klumper, U., Riber, L., Dechesne, A., Sannazzarro, A., Hansen, L. H., Sorensen, S. J., et al. (2015). Broad host range plasmids can invade an unexpectedly diverse fraction of a soil bacterial community. *ISME J.* 9, 934–945. doi: 10.1038/ismej.2014.191

Kozdrój, J. (2008). Survival, plasmid transfer and impact of *Pseudomonas fluorescens* introduced into soil. *J. Environ. Sci. Health A Environ. Sci. Eng. Toxicol.* 32, 1139–1157. doi: 10.1080/10934529709376601

Letunic, I., and Bork, P. (2016). Interactive tree of life (iTOL) v3: an online tool for the display and annotation of phylogenetic and other trees. *Nucleic Acids Res.* 44, W242–W245. doi: 10.1093/nar/gkw290

Li, L., Dechesne, A., He, Z., Madsen, J. S., Nesme, J., Sørensen, S. J., et al. (2018). Estimating the transfer range of plasmids encoding antimicrobial resistance in a wastewater treatment plant microbial community. *Environ. Sci. Technol. Lett.* 5, 260–265. doi: 10.1021/acs.estlett.8b00105

Lin, W., Li, S., Zhang, S., and Yu, X. (2016). Reduction in horizontal transfer of conjugative plasmid by UV irradiation and low-level chlorination. *Water Res.* 91, 331–338. doi: 10.1016/j.watres.2016.01.020

Lopatkin, A. J., Huang, S., Smith, R. P., Srimani, J. K., Sysoeva, T. A., Bewick, S., et al. (2016). Antibiotics as a selective driver for conjugation dynamics. *Nat. Microbiol.* 1:16044. doi: 10.1038/nmicrobiol.2016.44

Mantilla-Calderon, D., and Hong, P.-Y. (2017). Fate and persistence of a pathogenic NDM-1-positive *Escherichia coli* strain in anaerobic and aerobic sludge microcosms. *Appl. Environ. Microbiol.* 83:e00640-17. doi: 10.1128/aem.00640-17

Martinez, J. L., Coque, T. M., and Baquero, F. (2015). Prioritizing risks of antibiotic resistance genes in all metagenomes. *Nat. Rev. Microbiol.* 13:396. doi: 10.1038/nrmicro3399-c2

Modrie, P., Beuls, E., and Mahillon, J. (2010). Differential transfer dynamics of pAW63 plasmid among members of the *Bacillus cereus* group in food microcosms. *J. Appl. Microbiol.* 108, 888–897. doi: 10.1111/j.1365-2672.2009.04488.x

Musovic, S., Dechesne, A., Sorensen, J., and Smets, B. F. (2010). Novel assay to assess permissiveness of a soil microbial community toward receipt of mobile genetic elements. *Appl. Environ. Microbiol.* 76, 4813–4818. doi: 10.1128/AEM.02713-09

Musovic, S., Klumper, U., Dechesne, A., Magid, J., and Smets, B. F. (2014). Long-term manure exposure increases soil bacterial community potential for plasmid uptake. *Environ. Microbiol. Rep.* 6, 125–130. doi: 10.1111/1758-2229.12138

Musovic, S., Oregaard, G., Kroer, N., and Sorensen, S. J. (2006). Cultivation-independent examination of horizontal transfer and host range of an IncP-1 plasmid among gram-positive and gram-negative bacteria indigenous to the barley rhizosphere. *Appl. Environ. Microbiol.* 72, 6687–6692. doi: 10.1128/AEM.00013-06

Norberg, P., Bergstrom, M., Jethava, V., Dubhashi, D., and Hermansson, M. (2011). The IncP-1 plasmid backbone adapts to different host bacterial species and evolves through homologous recombination. *Nat. Commun.* 2:268. doi: 10.1038/ncomms1267

O'Brien, F. G., Yui Eto, K., Murphy, R. J., Fairhurst, H. M., Coombs, G. W., Grubb, W. B., et al. (2015). Origin-of-transfer sequences facilitate mobilisation of non-conjugative antimicrobial-resistance plasmids in *Staphylococcus aureus*. *Nucleic Acids Res.* 43, 7971–7983. doi: 10.1093/nar/gkv755

Pruden, A., Arabi, M., and Storteboom, H. N. (2012). Correlation between upstream human activities and riverine antibiotic resistance genes. *Environ. Sci. Technol.* 46, 11541–11549. doi: 10.1021/es302657r

Qiu, Z., Yu, Y., Chen, Z., Jin, M., Yang, D., Zhao, Z., et al. (2012). Nanoalumina promotes the horizontal transfer of multiresistance genes mediated by plasmids across genera. *Proc. Natl. Acad. Sci. U.S.A.* 109, 4944–4949. doi: 10.1073/pnas.1107254109

Shintani, M., Yano, H., Habe, H., Omori, T., Yamane, H., Tsuda, M., et al. (2006). Characterization of the replication, maintenance, and transfer features of the IncP-7 plasmid pCAR1, which carries genes involved in carbazole and dioxin degradation. *Appl. Environ. Microbiol.* 72, 3206–3216. doi: 10.1128/AEM.72.5.3206-3216.2006

Sorensen, S. J., Bailey, M., Hansen, L. H., Kroer, N., and Wuertz, S. (2005). Studying plasmid horizontal transfer in situ: a critical review. *Nat. Rev. Microbiol.* 3, 700–710. doi: 10.1038/nrmicro1232

Sørensen, S. J., Sørensen, A. H., Hansen, L. H., Oregaard, G., and Veal, D. (2003). Direct detection and quantification of horizontal gene transfer by using flow cytometry and gfp as a reporter gene. *Curr. Microbiol.* 47, 129–133. doi: 10.1007/s00284-002-3978-0

Soucy, S. M., Huang, J., and Gogarten, J. P. (2015). Horizontal gene transfer: building the web of life. *Nat. Rev. Genet.* 16, 472–482. doi: 10.1038/nrg3962

Stalder, T., and Top, E. (2016). Plasmid transfer in biofilms: a perspective on limitations and opportunities. *NPJ Biofilms Microb.* 2:16022. doi: 10.1038/npjbiofilms.2016.22

Subbiah, M., Top, E. M., Shah, D. H., and Call, D. R. (2011). Selection pressure required for long-term persistence of blaCMY-2-positive IncA/C plasmids. *Appl. Environ. Microbiol.* 77, 4486–4493. doi: 10.1128/AEM.02788-10

Suzuki, H., Yano, H., Brown, C. J., and Top, E. M. (2010). Predicting plasmid promiscuity based on genomic signature. *J. Bacteriol.* 192, 6045–6055. doi: 10.1128/JB.00277-10

Thomas, C. M., and Nielsen, K. M. (2005). Mechanisms of, and barriers to, horizontal gene transfer between bacteria. *Nat. Rev. Microbiol.* 3, 711–721. doi: 10.1038/nrmicro1234

Tolker-Nielsen, T., Brinch, U. C., Ragas, P. C., Andersen, J. B., Jacobsen, C. S., and Molin, S. (2000). Development and dynamics of *Pseudomonas* sp. *Biofilms J. Bacteriol.* 182, 6482–6489. doi: 10.1128/jb.182.22.6482-6489.2000

Tolker-Nielsen, T., and Molin, S. (2000). Spatial organization of microbial biofilm communities. *Microb. Ecol.* 40, 75–84.

Trevors, J. T., Elsas, J. D. V., Starodub, M. E., and Overbeek, L. S. V. (1989). Survival of and plasmid stability in *Pseudomonas* and *Klebsiella* spp. introduced into agricultural drainage water. *Can. J. Microbiol.* 35, 675–680. doi: 10.1139/m89-110

Turner, P. E., Cooper, V. S., and Lenski, R. E. (1998). Tradeoff between horizontal and vertical modes of transmission in bacterial plasmids. *Evolution* 52, 315–329. doi: 10.1111/j.1558-5646.1998.tb01634.x

UNEP (2017). *Frontiers 2017 Emerging Issues of Environmental Concern*. Nairobi: United Nations Environment Programme.

Wang, Q., Lu, Q., Mao, D., Cui, Y., and Luo, Y. (2015a). The horizontal transfer of antibiotic resistance genes is enhanced by ionic liquid with different structure of varying alkyl chain length. *Front. Microbiol.* 6:864. doi: 10.3389/fmicb.2015.00864

Wang, Q., Mao, D., and Luo, Y. (2015b). Ionic liquid facilitates the conjugative transfer of antibiotic resistance genes mediated by plasmid RP4. *Environ. Sci. Technol.* 49, 8731–8740. doi: 10.1021/acs.est.5b01129

Willetts, N., and Wilkins, B. (1984). Processing of plasmid DNA during bacterial conjugation. *Microbiol. Rev.* 48, 24–41.

Willey, J., Sherwood, L. M., and Woolverton, C. (2008). *Prescott/Harley/Klein's Microbiology*, Seventh Edn. Cardiff: Colin Wheatley/Janice Roerig-Blong.

Williams-Nguyen, J., Sallach, J. B., Bartelt-Hunt, S., Boxall, A. B., Durso, L. M., McLain, J. E., et al. (2016). Antibiotics and antibiotic resistance in agroecosystems: state of the science. *J. Environ. Qual.* 45, 394–406. doi: 10.2134/jeq2015.07.0336

Yano, H., Garruto, C. E., Sota, M., Ohtsubo, Y., Nagata, Y., Zylstra, G. J., et al. (2007). Complete sequence determination combined with analysis of transposition/site-specific recombination events to explain genetic organization of IncP-7 TOL Plasmid pWW53 and related mobile genetic elements. *J. Mol. Biol.* 369, 11–26. doi: 10.1016/j.jmb.2007.02.098

Yano, H., Rogers, L. M., Knox, M. G., Heuer, H., Smalla, K., Brown, C. J., et al. (2013). Host range diversification within the IncP-1 plasmid group. *Microbiology* 159(Pt 11), 2303–2315. doi: 10.1099/mic.0.068387-0

Zhou, J., Wu, L., Deng, Y., Zhi, X., Jiang, Y. H., Tu, Q., et al. (2011). Reproducibility and quantitation of amplicon sequencing-based detection. *ISME J.* 5, 1303–1313. doi: 10.1038/ismej.2011.11

Zhu, Y. G., Gillings, M., Simonet, P., Stekel, D., Banwart, S., and Penuelas, J. (2018). Human dissemination of genes and microorganisms in Earth's critical zone. *Glob. Change Biol.* 24, 1488–1499. doi: 10.1111/gcb.14003

Zhu, Y. G., Johnson, T. A., Su, J. Q., Qiao, M., Guo, G. X., Stedtfeld, R. D., et al. (2013). Diverse and abundant antibiotic resistance genes in Chinese swine farms. *Proc. Natl. Acad. Sci. U.S.A.* 110, 3435–3440. doi: 10.1073/pnas.1222743110

Zhu, Y. G., Zhao, Y., Li, B., Huang, C. L., Zhang, S. Y., Yu, S., et al. (2017). Continental-scale pollution of estuaries with antibiotic resistance genes. *Nat. Microbiol.* 2:16270. doi: 10.1038/nmicrobiol.2016.270

Conflict of Interest Statement: The authors declare that the research was conducted in the absence of any commercial or financial relationships that could be construed as a potential conflict of interest.

Advantages of publishing in Frontiers

OPEN ACCESS
Articles are free to read for greatest visibility and readership

FAST PUBLICATION
Around 90 days from submission to decision

HIGH QUALITY PEER-REVIEW
Rigorous, collaborative, and constructive peer-review

TRANSPARENT PEER-REVIEW
Editors and reviewers acknowledged by name on published articles

Frontiers
Avenue du Tribunal-Fédéral 34
1005 Lausanne | Switzerland

Visit us: www.frontiersin.org
Contact us: info@frontiersin.org | +41 21 510 17 00

REPRODUCIBILITY OF RESEARCH
Support open data and methods to enhance research reproducibility

DIGITAL PUBLISHING
Articles designed for optimal readership across devices

FOLLOW US
@frontiersin

IMPACT METRICS
Advanced article metrics track visibility across digital media

EXTENSIVE PROMOTION
Marketing and promotion of impactful research

LOOP RESEARCH NETWORK
Our network increases your article's readership